PB88-238357

Development of Sorbent Injection Criteria for Sulfur Oxides Control from Tangentially Fired Coal Boilers

Combustion Engineering, Inc., Windsor, CT

Prepared for

Environmental Protection Agency
Research Triangle Park, NC

Aug 88

U.S. Department of Commerce
National Technical Information Service
NTIS

TECHNICAL REPORT DATA

(Please read Instructions on the reverse before completing)

1. REPORT NO.
EPA/600/7-88/013

2.

3. RECIPIENT'S ACCESSION NO.
PB88 238357/AS

4. TITLE AND SUBTITLE
Development of Sorbent Injection Criteria for Sulfur Oxides Control from Tangentially Fired Coal Boilers

5. REPORT DATE
August 1988

6. PERFORMING ORGANIZATION CODE

7. AUTHOR(S)
R.W. Koucky, J.L. Marion, and D.K. Anderson

8. PERFORMING ORGANIZATION REPORT NO.

9. PERFORMING ORGANIZATION NAME AND ADDRESS
Combustion Engineering, Inc.
P.O. Box 500
Windsor, Connecticut 06095-0500

10. PROGRAM ELEMENT NO.

11. CONTRACT/GRANT NO.
68-02-4224

12. SPONSORING AGENCY NAME AND ADDRESS
EPA, Office of Research and Development
Air and Energy Engineering Research Laboratory
Research Triangle Park, NC 27711

13. TYPE OF REPORT AND PERIOD COVERED
Final Report; 7/85 - 8/87

14. SPONSORING AGENCY CODE
EPA/600/13

15. SUPPLEMENTARY NOTES AEERL project officer is Samuel L. Rakes, Mail Drop 63, 919/541-2828.

16. ABSTRACT
The report describes a program to develop design criteria for injecting dry sorbents into tangentially fired coal furnaces for the control of SOx emissions. The program included aerodynamic cold-flow testing and mathematical modeling of sorbent injection, demonstration testing of SOx emissions control in a 14.7 MW thermal (50 million Btu/hr) tangentially fired Boiler Simulation Facility (BSF), and development of recommendations for sorbent injection in a tangentially fired boiler demonstration of the process. The isothermal flow modeling led to development of sorbent injection systems for tangentially fired furnaces which provide high levels of sorbent dispersion. A sorbent dispersion mathematical modeling technique was developed to support flow modeling in identifying and optimizing sorbent injection locations and methods. Sorbent injection tests in the BSF investigated the following variables: sorbent type, injection location, injector tilt, injection velocity, number of injectors, and carrier air flow rate. Sulfur capture efficiency up to 50% was achieved at a Ca/S molar ratio of 2/1 with calcium hydroxide sorbent treated with calcium lignosulfonate. A procedure was developed for specifying sorbent injection locations and methods for a full-scale demonstration of the sorbent injection process in a tangentially fired utility boiler.

17. KEY WORDS AND DOCUMENT ANALYSIS

a. DESCRIPTORS		b. IDENTIFIERS/OPEN ENDED TERMS	c. COSATI Field/Group
Pollution	Calcium Hydroxides	Pollution Control	13B
Sorbents		Stationary Sources	11G
Sulfur Oxides		Dry Sorbent Injection	07B
Boilers		Tangential Firing	13A
Coal		Calcium Lignosulfonate	21D
Mathematical Models			12A

18. DISTRIBUTION STATEMENT
Release to Public

19. SECURITY CLASS *(This Report)*
Unclassified

20. SECURITY CLASS *(This page)*
Unclassified

21. NO. OF PAGES
333

22. PRICE

EPA Form 2220-1 (9-73)

PB88-238357

EPA/600/7-88/013
August 1988

DEVELOPMENT OF SORBENT INJECTION CRITERIA FOR SULFUR OXIDES CONTROL FROM TANGENTIALLY FIRED COAL BOILERS

By

R. W. Koucky
J. L. Marion
D. K. Anderson

COMBUSTION ENGINEERING, INC.
Windsor, Connecticut 06095

EPA Contract 68-02-4224

Project Officer

Samuel L. Rakes
U.S. ENVIRONMENTAL PROTECTION AGENCY
Air and Energy Engineering Research Laboratory
Research Triangle Park, North Carolina 27711

AIR AND ENERGY ENGINEERING RESEARCH LABORATORY
OFFICE OF RESEARCH AND DEVELOPMENT
U.S. ENVIRONMENTAL PROTECTION AGENCY
RESEARCH TRIANGLE PARK, NC 27711

NOTICE

This document has been reviewed in accordance with U.S. Environmental Protection Agency policy and approved for publication. Mention of trade names or commercial products does not constitute endorsement or recommendation for use.

ABSTRACT

Combustion Engineering, Inc. conducted a program under Environmental Protection Agency sponsorship to develop design criteria for injection of dry sorbents into tangentially fired furnaces for the control of sulfur oxides emissions. The program included aerodynamic cold-flow testing and mathematical modeling of sorbent injection, demonstration testing of sulfur oxides emissions control in a 14.7 MW thermal (50 million Btu per hour) tangentially fired Boiler Simulation Facility (BSF), and development of recommendations for sorbent injection in a tangentially fired boiler demonstration of the process. The isothermal flow modeling led to development of sorbent injection systems for tangentially fired furnaces which provide high levels of sorbent dispersion. A sorbent dispersion mathematical modeling technique was developed to support flow modeling in identifying and optimizing sorbent injection locations and methods. Sorbent injection tests in the BSF investigated the following variables: sorbent type, injection location, injector tilt, injection velocity, number of injectors, and carrier air flow rate. Sulfur capture efficiency up to 50% was achieved at a Ca/S molar ratio of 2:1 with calcium hydroxide sorbent treated with calcium lignosulfonate. A procedure was developed for specifying sorbent injection locations and methods for a full-scale demonstration of the sorbent injection process in a tangentially fired utility boiler.

CONTENTS

Page

Abstract iii
Figures vi
Tables xv
Abbreviations and Symbols (Metric Equivalents) xvi
Acknowledgements xviii

1. Introduction 1-1
2. Conclusions 2-1
3. Recommendations 3-1
4. Isothermal Flow Modeling Studies 4-1
    Project Description 4-1
    Facility Description 4-2
    Results 4-20
    Summary of Results 4-110
5. Mathematical Modeling Studies 5-1
    Thermal Modeling 5-1
    Sorbent Dispersion Modeling 5-1
    Sulfur Capture Performance Modeling 5-22
    Summary 5-35
6. Combustion Testing 6-1
    Objectives 6-1
    Project Description 6-2
    Experimental Approach and Facilities Description 6-5
    Combustion Test Matrix 6-28
    Coal and Sorbent Analyses 6-38
    Combustion Testing Results 6-48
    Summary of Combustion Test Results 6-121
7. Sorbent Injection System Design Recommendations 7-1
    Approach 7-1
    Description of Design Procedure 7-1
    Summary 7-8

References R-1

Appendix

A. Quality Assurance Procedures A-1
    Summary of Quality Assurance Procedures A-1
    Discussion of Data Quality A-2
    Audits and Corrective Action A-10

FIGURES

Number		Page
1-1	Furnace sorbent injection	1-2
4-1	Cross flow injector test facility schematic	4-3
4-2	Typical cross flow injection test	4-4
4-3	Large scale furnace aerodynamics test facility	4-6
4-4	LSFATF instrument traversing system	4-7
4-5	Flow model sorbent injection nozzle	4-10
4-6	Flow model injection nozzle details	4-11
4-7	Five hole pitot tube details	4-13
4-8	Automatic probe traversing device	4-15
4-9	Laser absorption spectrophotometer schematic	4-17
4-10	Residence time distribution instrumentation setup	4-18
4-11	Idealized RTD test results	4-19
4-12	Predicted BSF gas temperatures	4-24
4-13	Flow model sorbent injection locations	4-26
4-14	Predicted BSF sorbent jet penetrations	4-27
4-15	CFITF gas-solids jet	4-30
4-16	CFITF gas only jet	4-30
4-17	Upper furnace streak lines observed during flow visualization tests	4-36
4-18	BASF flow model test plane locations	4-39
4-19	Baseline furnace velocity vectors: Test Plane 1	4-40
4-20	Normalized axial velocities: Test Plane 1	4-41
4-21	Baseline furnace velocity vectors: Test Plane 2	4-42

FIGURES
(Continued)

Number		Page
4-22	Normalized axial velocities: Test Plane 2	4-43
4-23	Baseline furnace normalized velocity profiles: Test Plane 2	4-44
4-24	Normalized axial isovelocity plot and velocity contour plot: Test Plane 2	4-45
4-25	Baseline furnace velocity vectors: Test Plane 3	4-46
4-26	Normalized axial velocities: Test Plane 3	4-47
4-27	Baseline furnace normalized velocity profiles: Test Plane 3	4-48
4-28	Normalized axial isovelocity plot and velocity contour plot: Test Plane 3	4-49
4-29	Baseline furnace velocity vectors: Test Plane 4	4-50
4-30	Normalized axial velocities: Test Plane 4	4-51
4-31	Baseline furnace normalized velocity profiles: Test Plane 4	4-52
4-32	Normalized axial isovelocity plot and velocity contour plot: Test Plane 4	4-53
4-33	Baseline furnace velocity vectors: Test Plane 5	4-54
4-34	Normalized axial velocities: Test Plane 5	4-55
4-35	Baseline furnace normalized velocity profiles: Test Plane 5	4-56
4-36	Normalized axial isovelocity plot and velocity contour plot: Test Plane 5	4-57
4-37	Baseline furnace velocity vectors: Test Plane 6	4-58
4-38	Normalized axial velocities: Test Plane 6	4-59
4-39	Baseline furnace normalized velocity profiles: Test Plane 6	4-60
4-40	Normalized axial isovelocity plot and velocity contour plot: Test Plane 6	4-61

FIGURES
(Continued)

Number		Page
4-41	Baseline furnace velocity vectors: Test Plane 7	4-62
4-42	Normalized axial velocities: Test Plane 7	4-63
4-43	Baseline furnace normalized velocity profiles: Test Plane 7	4-64
4-44	Normalized axial isovelocity plot and velocity contour plot: Test Plane 7	4-65
4-45	Typical visualization test of front wall injection	4-68
4-46	0° tilt front wall injection flow visualization results	4-69
4-47	-20° tilt front wall injection flow visualization results	4-69
4-48	Rearward facing lance flow visualization results	4-72
4-49	Frontward facing lance flow visualization results	4-72
4-50	Gas mixing isoconcentration plot: Test No. 201: Plane 5	4-76
4-51	Gas mixing isoconcentration plot: Test No. 201: Plane 6	4-77
4-52	Gas mixing isoconcentration plot: Test No. 202: Plane 5	4-78
4-53	Gas mixing isoconcentration plot: Test No. 202: Plane 6	4-79
4-54	Gas mixing isoconcentration plot: Test No. 203: Plane 5	4-80
4-55	Gas mixing isoconcentration plot: Test No. 203: Plane 6	4-81
4-56	Gas mixing isoconcentration plot: Test No. 204: Plane 5	4-82
4-57	Gas mixing isoconcentration plot: Test No. 204: Plane 6	4-83
4-58	Gas mixing isoconcentration plot: Test No. 205: Plane 5	4-84

FIGURES
(Continued)

Number		Page
4-59	Gas mixing isoconcentration plot: Test No. 205: Plane 6	4-85
4-60	Gas mixing isoconcentration plot: Test No. 206: Plane 4	4-86
4-61	Gas mixing isoconcentration plot: Test No. 206: Plane 5	4-87
4-62	Gas mixing isoconcentration plot: Test No. 206: Plane 6	4-88
4-63	Gas mixing isoconcentration plot: Test No. 207: Plane 4	4-90
4-64	Gas mixing isoconcentration plot: Test No. 207: Plane 5	4-91
4-65	Gas mixing isoconcentration plot: Test No. 208: Plane 4	4-92
4-66	Gas mixing isoconcentration plot: Test No. 208: Plane 5	4-93
4-67	Gas mixing isoconcentration plot: Test No. 209: Plane 5	4-94
4-68	Gas mixing isoconcentration plot: Test No. 209: Plane 6	4-95
4-69	Gas mixing isoconcentration plot: Test No. 210: Plane 5	4-96
4-70	Gas mixing isoconcentration plot: Test No. 210: Plane 6	4-97
4-71	Gas mixing isoconcentration plot: Test No. 211: Plane 5	4-98
4-72	Gas mixing isoconcentration plot: Test No. 211: Plane 6	4-99
4-73	Second screening level variances	4-101
4-74	Flow model RTD test setup	4-105
4-75	Idealized RTD test results	4-106
4-76	Residence time distribution study test results	4-107

FIGURES
(Continued)

Number		Page
5-1	LSTATF flow model and the boundary of the control volume used in the 3-D flow simulation	5-3
5-2	Calculated Plane 5 isovelocity plot	5-4
5-3	Calculated Plane 5 velocity vectors	5-6
5-4	Calculated Plane 6 isovelocity plot	5-7
5-5	Calculated Plane 6 velocity vectors	5-8
5-6	Calculated velocity vectors in Lane 1	5-10
5-7	Calculated velocity vectors in Lane 2	5-11
5-8	Calculated velocity vectors in Lane 3	5-12
5-9	Calculated velocity vectors in Lane 4	5-13
5-10	Calculated isoconcentration plot for Test No. 201 at Plane 5	5-15
5-11	Calculated isoconcentration plot for Test No. 201 at Plane 6	5-16
5-12	Calculated concentration contours in Lane 1 for Test No. 201	5-17
5-13	Calculated concentration contours in Lane 2 for Test No. 201	5-18
5-14	Calculated concentration contours in Lane 3 for Test No. 201	5-19
5-15	Calculated concentration contours in Lane 4 for Test No. 201	5-20
5-16	Calculated isoconcentration plot for Test No. 204 at Plane 5	5-21
5-17	Calculated isoconcentration plot for Test No. 204 at Plane 6	5-23
5-18	Calculated concentration contours in Lane 1 for Test No. 204	5-24
5-19	Calculated concentration contours in Lane 2 for Test No. 204	5-25

FIGURES
(Continued)

Number		Page
5-20	Calculated concentration contours in Lane 3 for Test No. 204	5-26
5-21	Calculated concentration contours in Lane 4 for Test No. 204	5-27
5-22	SO_2 capture modeling	5-29
5-23	SO_2 capture for fully mixed sorbent and uniform velocity	5-30
5-24	Measured and calculated SO_2 capture	5-32
5-25	Applications of SO_2 capture modeling	5-34
6-1	Combustion testing approach	6-3
6-2	Typical modern C-E designed tangentially fired boiler	6-6
6-3	Combustion Engineering's Boiler Simulation Facility (BSF)	6-8
6-4a	BSF in operation	6-9
6-4b	BSF outlet duct and back-end equipment	6-10
6-5	Calculated gas temperature/residence time profile for the BSF	6-12
6-6	View from ash pit towards upper furnace of BSF	6-14
6-7	Firing System Development Complex	6-16
6-8	Suction pyrometer temperature measurement at elevation 35'-3" on BSF	6-17
6-9	Stack flyash sampling	6-18
6-10	Boiler Simulation Facility control room	6-19
6-11	Sootblowers located in convective pass	6-21
6-12	Variation of SO_2 capture with sootblowing cycle	6-22
6-13	Sorbent storage and supply system	6-24
6-14	Sorbent feed system	6-25
6-15	Sorbent supply system	6-26

FIGURES
(Continued)

Number		Page
6-16	Sorbent injectors and conveying lines on the front wall at Location A	6-29
6-17	Sorbent injectors prior to installation on BSF	6-30
6-18	Definition of injector angles	6-32
6-19	Definition of Location D injector angles	6-33
6-20	Tested injector locations	6-35
6-21	Coal particle size data	6-43
6-22	Sorbent particle size data	6-47
6-23	Carbon conversion efficiency vs. excess O_2, Phase I test data	6-72
6-24	Carbon conversion efficiency vs. excess O_2, Phase II test data	6-73
6-25	NO_x emissions vs. excess O_2, Phase I test data	6-74
6-26	NO_x emissions vs. excess O_2, Phase II test data	6-75
6-27	SO_2 emissions vs. excess O_2, Phase I test data	6-78
6-28	SO_2 emissions vs. excess O_2, Phase II test data	6-79
6-29	BSF temperature profile data (°F)	6-81
6-30	BSF time/temperature profile	6-82
6-31	BSF's thermal topography (°F) shown as an isometric view of main furnace	6-84
6-32	BSF thermal topography (°F) shown as an isometric view of convective pass from behind	6-85
6-33	Temperature data from plane at elevation 37'-9" at the furnace arch	6-87
6-34	Temperature data in upper furnace, elevation 48'	6-88
6-35	Temperature data in upper furnace, elevation 43'	6-88
6-36	Temperature data at vertical outlet plane	6-89

FIGURES
(Continued)

Number Page

6-37 Temperature data from plane at elevation 44'-6" below the rear pass cavity 6-90

6-38 SO_2 capture vs. Ca/S ratio, Location A, front wall injection, -45° tilt, 100 ft/sec 6-94

6-39 SO_2 capture vs. Ca/S ratio, Phase I, -45° injection angle, 100 ft/sec 6-96

6-40 SO_2 capture vs. Ca/S ratio, Location D 6-98

6-41 SO_2 capture vs. injector tilt, front wall injection, Sorbent A 6-99

6-42 SO_2 capture vs. injection velocity, Phase I, front wall injection, Sorbent A 6-101

6-43 SO_2 capture vs. injector tilt, Location A, front wall injection, vel = 100-145 ft/sec 6-102

6-44 SO_2 capture vs. injector tilt, Location A, vel = 160-220 ft/sec 6-103

6-45 Flow visualization results for Location A injection at various tilts 6-104

6-46 SO_2 capture vs. injection velocity, Location A, 0° tilt, Sorbent C 6-106

6-47 SO_2 capture vs. injection velocity, Location A, -45° tilt, front wall injection 6-107

6-48 SO_2 capture vs. injection velocity, Location A, -90° tilt, Sorbent C 6-108

6-49 Flow visualization results for Location D injection, countercurrent vs. co-current injection 6-110

6-50 Flow visualization results for Location D injection as a function of injection velocity 6-111

6-51 Flow visualization results for Location D injection as a function of injector tilt 6-112

6-52 SO_2 capture vs. injector tilt at Location D 6-113

6-53 SO_2 capture vs. injector velocity at Location D 6-114

FIGURES
(Continued)

Number		Page
6-54	SO_2 capture vs. injection velocity with eight injectors as a function of carrier air flow	6-116
6-55	SO_2 capture vs. injection velocity with eight injectors	6-117
6-56	SO_2 capture vs. injection velocity with six injectors	6-118
6-57	Comparison of SO_2 capture vs. injection velocity for 8, 6, and 4 injectors	6-120

TABLES

Number		Page
4-1	Injector locations	4-23
4-2	First screening level test configurations	4-25
4-3	Jet penetration correlations	4-32
4-4	Summary of scaling calculations	4-35
4-5	Second screening level test configurations	4-74
4-6	Second screening level coefficients of variation	4-100
4-7	Third screening level configurations	4-103
4-8	Sorbent injector recommendations	4-109
6-1	Injection velocities	6-31
6-2	Phase I test matrix	6-36
6-3	Phase II test matrix	6-37
6-4	Pittsburgh No. 8 coal analyses	6-39
6-5	Pittsburgh No. 8 coal particle size analyses	6-42
6-6	Sorbent properties	6-45
6-7	Task C combustion test data - Phase I	6-49
6-8	Task C combustion test data - Phase II	6-57
A-1	Calibration Gases	A-3
A-2	Analyses of Coal and Ash Standard Reference Materials	A-7
A-3	Analyses of Sorbent Standard Reference Materials	A-8
A-4	Ash Fusibility Precision Data	A-9
A-5	Coal Sieving Precision Example	A-9

ABBREVIATIONS AND SYMBOLS

Symbol	
A	--Area, m^2 (ft^2)
d	--Diameter, m (ft)
J	--Momentum ratio, dimensionless
m	--Mass flow rate, Kg/sec (lb/sec)
n	--Number of injectors, dimensionless
Q	--Volumetric flow rate, m^3/sec (ft^3/sec)
SF	--Model scale factor
V	--Velocity, m/sec (ft/sec)
X	--Distance axially from jet face m, (ft)
Y	--distance traverse from jet centerline, m (ft)
ρ	--density, Kg/m^3 (lb/ft^3)

Subscripts	
c	--crossflow
j	--jet
mix	--mixture
m	--model
p	--prototype

TABLE OF METRIC EQUIVALENTS

1.0 Btu = 1054.8 joules

°C = 5/9 (°F -32)

°F = 9/5 °C + 32

1.0 ft = 0.3048m

1.0 in = 0.02540m

1.0 lb = 0.4536kg

1.0 psi = 6.894 kPa

ACKNOWLEDGEMENTS

The authors wish to acknowledge the guidance and support of the management and staff of EPA's Air and Energy Engineering Research Laboratory. In particular, we acknowledge the contributions and suggestions of Samuel L. Rakes, the Project Officer and Charles C. Masser, the former Project Officer.

The authors wish to thank the management of Combustion Engineering, Inc. for their encouragement and support. Construction of the Boiler Simulation Facility was a major C-E commitment in support of this program. C-E management personnel who provided guidance and suggestions for the program include A. Stathoplos, M. Rao Gogineni, and J. D. Bianca. We thank D. P. Towle for his technical support in construction and operation of the Boiler Simulation Facility and Angelos Kokkinos, formerly manager of the Firing Systems Development Group at C-E, for his technical guidance during the program.

The authors also wish to thank the personnel at Kreisinger Development Laboratory's Firing System Development Complex and Mechanical Systems Engineering Group for their skillful operation of these facilities for the experimental portions of this program. The authors would also like to acknowledge the excellent support of KDL's Chemical Analytical Services Laboratory for fuel, sorbent, and ash analyses.

SECTION 1

INTRODUCTION

Increasing concern for the environmental effects of acid rain has led to a reexamination of the fossil fuel burning electric utility industry. Previously, only new plants were mandated to install pollution control equipment for gaseous emissions under federal New Source Performance Standards (NSPS), although some existing plants were retrofitted with equipment due to local requirements. However, proposed legislation in response to the acid rain question may require at least a portion of existing oil- and coal-burning plants to limit emissions of sulfur dioxide (SO_2).

Furnace sorbent injection is under development as an approach for SO_2 control for coal-burning utility boilers. The process is attractive for retrofit of existing boilers since the capital equipment requirements are less than for other options such as flue gas desulfurization, and the estimated overall sulfur reduction cost per ton of sulfur removed from flue gas is less than for these options, Clark et al. (1986). The principles of furnace sorbent injection are shown in Figure 1-1. The sorbent, usually calcium hydroxide ($Ca(OH)_2$) or limestone ($CaCO_3$), is injected above the flame zone and mixes with flue gas containing sulfur dioxide (SO_2). The SO_2 reacts chemically in the upper furnace with lime (CaO), formed from the sorbent, to make solid calcium sulfate ($CaSO_4$). The $CaSO_4$ is removed with fly ash in particulate control equipment.

A review of earlier furnace sorbent injection investigations by Clark et al. (1986) indicated that important requirements for SO_2 capture are effective mixing of sorbent across the furnace, effective calcination of sorbent to

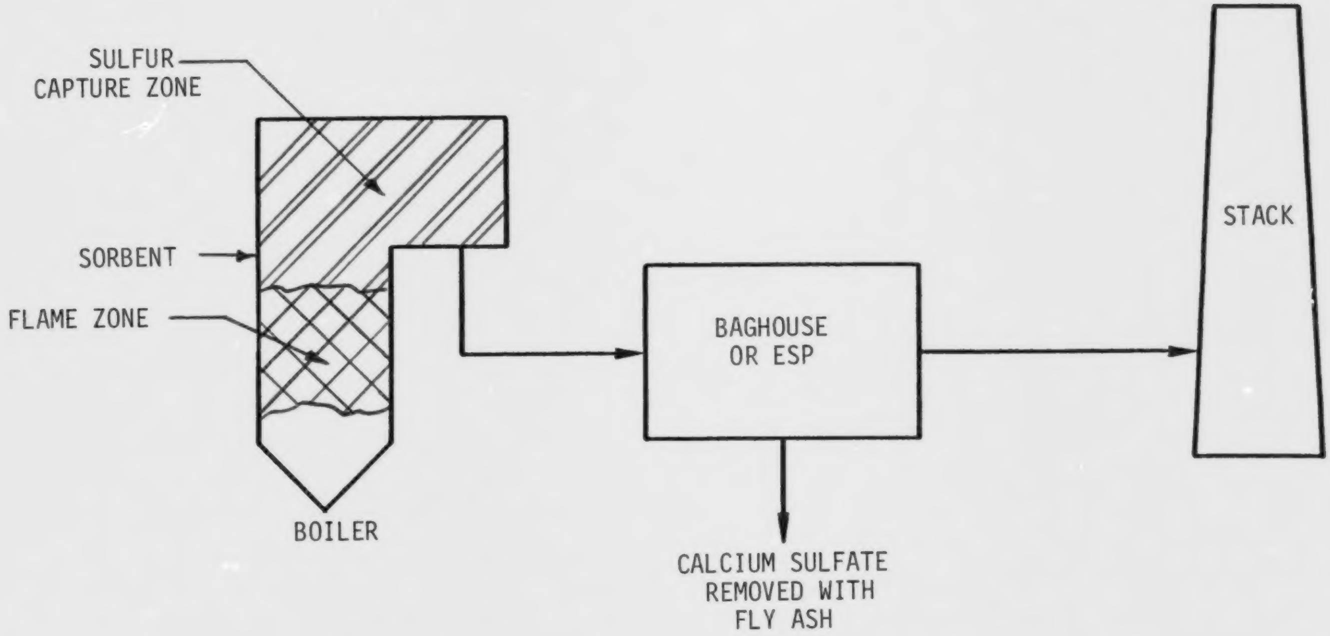
SULFUR CAPTURE ZONE
SORBENT
FLAME ZONE
BOILER
BAGHOUSE OR ESP
CALCIUM SULFATE REMOVED WITH FLY ASH
STACK

Figure 1-1. Furnace sorbent injection.

facilitate sulfur capture, minimum deactivation of sorbent pore structure due to unfavorably high gas temperatures, and maximum gas and sorbent residence time in the region of the furnace where temperatures are favorable for the sorbent - SO_2 chemical reaction. These requirements, in turn, depend upon the design of the sorbent injection system, including both the sorbent injection locations and the injection method.

Chemical equilibrium, chemical kinetics, sorbent deactivation, and furnace design considerations all play important roles in defining the temperature limits and residence time for SO_2 capture, Gullett and Kramlich (1987). Equilibrium considerations set an upper limit temperature for formation of the $CaSO_4$ product of about 1200°C (2192°F). Below 900°C (1652°F) the reaction becomes too slow for practical application. These two temperatures define the sulfation temperature boundaries of the process, commonly termed the "sulfation temperature window." The residence time in this temperature window is determined by the temperature/time gradient of the flue gas and is established by furnace heat transfer design considerations. A typical temperature/time gradient, or "quench rate," through the sulfation temperature window is 275°C/sec (527°F/sec). The residence time in the sulfation window is therefore typically about one second. The optimum furnace gas temperature at the point of sorbent injection depends upon both sorbent mixing and sorbent deactivation considerations. This temperature is typically between 1200°C to 1300°C (2200°F to 2400°F), Overmoe et al. (1986), Stern (1987), and Beittel et al. (1986). For a quench rate of 275°C/sec a sorbent mixing time of about 0.36 sec. is therefore available before the SO_2 capture reaction begins. This short time emphasizes the importance of effective mixing.

A significant fraction of the existing boilers in the United States that would be candidates for retrofit with sorbent injection technology are tangentially fired utility boilers, Clark et al. (1986) and Stern (1987). Tangential firing introduces special considerations for the design of sorbent injection systems due to the unique aerodynamics in the sorbent mixing region of tangentially fired furnaces. Therefore, a program was established to address the criteria for the location and method of sorbent injection for tangentially fired coal-burning furnaces in order to provide the most cost-effective removal of sulfur oxides. This program was conducted under EPA Contract No. 68-02-4224 by Combustion Engineering, Inc. The program includes screening a variety of injection locations and injection method variables in a tangentially fired cold flow facility, application of mathematical techniques to translate the cold flow results into injection locations and injector designs for testing in combustion facilities, testing of these alternative injection locations and methods in a large pilot-scale boiler simulation combustion facility, and the development of recommendations for the design of sorbent injectors for a demonstration of furnace sorbent injection in a tangentially fired utility boiler. This report summarizes the results, conclusions, and recommendations of the investigations conducted in the program.

The program included four tasks. These tasks were as follows:

TASK A - Cold flow modeling of sorbent injection systems.

TASK B - Mathematical modeling of sorbent injection systems, SO_2 capture performance, and furnace thermal performance.

TASK C - Combustion testing of sorbent injection location/injector design combinations in the pitot scale (14.7 MW thermal) (50 MBtu/hr) Boiler Simulation Facility (BSF).

TASK D - Sorbent injection system design recommendations for a full-scale tangentially fired boiler demonstration.

The Conclusions and Recommendations developed from these tasks are given in Section 2 and 3, respectively. Following these sections the methods used and work accomplished in each of the four tasks are discussed in detail in Sections 4, 5, 6, and 7. References and a discussion of quality assurance and quality control methods are included in separate sections.

SECTION 2

CONCLUSIONS

Each of the tasks of this program led to significant conclusions. This section summarizes the major results of the program and lists the major conclusions.

1. Isothermal flow modeling led to development of sorbent injection systems for tangentially fired furnaces which provide high levels of sorbent dispersion for a wide range of sulfation temperature windows and corresponding sorbent injection locations. Specific designs were selected and tested in the 50×10^6 Btu/hr Boiler Simulation Facility (BSF).

2. For furnaces in which the beginning of the sulfation temperature window is located at or near the arch elevation, injection from a position low in the front wall provides effective sorbent dispersion.

3. For furnaces in which the beginning of the sulfation temperature window is located below the arch, tangential injection from the corners of the unit provides very effective sorbent penetration and dispersion across the furnace plan area.

4. At any injection location, angling the sorbent injection nozzles such that the resulting jet flow is in the direction opposite of the bulk gas flow significantly increases sorbent dispersion.

5. The trajectory and dispersion of a two-phase jet can be predicted by a gas-only jet correlation if the size of the particles in the jet are small (approximately 20 micron or smaller) and the mixture density of the jet is used in the trajectory calculations.

6. Thermal modeling using proprietary C-E design codes provided significant support to the program for the design of the BSF, selection of injector locations for both the isothermal flow studies and BSF combustion testing, and in interpretation of BSF test results.

7. Computational fluid dynamic (CFD) modeling provides an effective simulation of the flow patterns and mixing in the upper furnace of tangentially fired furnaces. CFD simulation in combination with cold flow modeling can be used to identify and optimize sorbent injector locations and operating conditions for dry sorbent injection systems for SO_2 control in tangentially fired furnaces.

8. A model was developed to predict SO_2 capture as a function of furnace geometry, furnace temperature profile, operating conditions, sorbent injection parameters, and the inherent SO_2 capture performance of the sorbent by application of a proprietary C-E computer code. The model will be applied in scaling up results of this program for a demonstration of dry sorbent injection technology in a tangentially fired utility boiler.

9. The BSF was found to be representative of a large utility boiler in terms of operation, volumetric heat release, gas time/temperature history, carbon burnout, and NO_x/SO_2 emissions.

10. The BSF horizontal furnace outlet plane gas temperature (temperature at the furnace arch) averaged 2200°F. The convective pass quench rate was 500-600°F/sec.

11. Three sorbents were tested. Sorbent A was untreated Black River hydrated lime, Sorbent B was untreated Marblehead hydrated lime, and

Sorbent C was Marblehead hydrated lime treated with calcium lignosulfonate. SO_2 capture varied with sorbent type. Typical SO_2 capture performance results at a calcium/sulfur molar ratio of 2:1 were as follows:

Sorbent A	25% - 30%
Sorbent B	30% - 40%
Sorbent C	35% - 50%

Specific differences in the percent SO_2 capture performance for sorbents were:

Sorbent A vs. B:
Sorbent B was better than A in SO_2 capture by nine (9) to fifteen (15) percent (average of thirteen (13) percent).

Sorbent B vs. C:
Sorbent C was better than B in SO_2 capture by seven (7) to thirty (30) percent (average of eighteen (18) percent).

12. With Sorbent C, SO_2 capture efficiency of up to 50% was obtained with a Ca/S molar ratio of 2:1 for selected test conditions.

13. Although most sorbent injection tests were run for a constant twenty (20) minute time interval, longer duration tests showed that SO_2 capture could be increased by 10 to 20 percent by extending the sorbent injection to one hour. This was due to deposition of reactive sorbent on heat transfer surfaces.

14. Optimum SO_2 capture was obtained by injection into the region between Locations A and D where furnace gas temperatures ranged from 2250°F to 2350°F. Location A was front wall injection from a position opposite the arch. Location D was tangential injection from the four corners at a location below the arch.

15. Injection into the optimum region was accomplished by upward injection at Location D, downward injection at Location A, or

simultaneous injection at both locations. Tilt was demonstrated to be an effective approach for injecting sorbent into the optimum location.

16. At Location D, where injection was into the swirling lower furnace flow field, increasing injection air velocity either by reducing the size of the injector nozzles or by increasing injection air flow rate improved SO_2 capture.

17. A step-by-step procedure was developed for specifying sorbent injection locations and methods for a full-scale demonstration of the sorbent injection process in a tangentially fired utility boiler.

SECTION 3

RECOMMENDATIONS

This program led to specific recommendations for sorbent injection designs for tangentially fired boilers, recommendations for experimental and analytical methods for developing these designs, and recommendations for future work. These recommendations are summarized in this section.

1. Sorbent injector designs, including injection method, location, and operating conditions, for field demonstration of in-furnace sorbent injection in tangentially fired boilers should be based upon isothermal flow modeling supported by mathematical modeling and pilot scale combustion testing.

2. Injection locations on the front wall or tangential injection below the arch are the prime candidates for injection locations for tangentially fired furnaces. Specific recommendations depend upon the thermal topography of the candidate boiler.

3. In-furnace injection of hydrated lime sorbents should be into regions where furnace gases are in the 1200°C to 1300°C (2200°F to 2400°F) range. Injection into this temperature range is critical for optimizing SO_2 capture.

4. Computational fluid dynamics (CFD) should continue to be developed for modeling sorbent dispersion since this method readily provides great detail concerning mixing and flow patterns and has the potential for permitting the study of a wide range of geometries and operating conditions.

5. Sulfur capture performance modeling should be further developed. A logical approach is to add a SO_2 capture kinetics module to a CFD code. This approach would permit detailed SO_2 capture predictions within the sorbent mixing zone and in this way would reduce the dependency of SO_2 capture modeling upon empirical mixedness parameters.

6. SO_2 capture was found to vary with sorbent type. The relative SO_2 capture was highest with the finest sorbent and lowest with the coarsest sorbent. The SO_2 capture performance was also highest with lignosulfonate-modified sorbent. It is not clear what the relative contributions were of the finer particle sizing of the sorbent and the treatment. A future test is warranted where performance of identically classified particle sizes of both treated and untreated sorbent are compared.

7. The sorbent injection process for SO_2 capture takes place in the upper furnace and does not affect lower furnace operation. Therefore, sorbent injection is compatible with NO_x emissions control technologies that involve combustion system modifications. The use of low-NO_x firing systems in combination with in-furnace sorbent injection should be investigated for a combined NO_x/SO_2 control process.

SECTION 4

ISOTHERMAL FLOW MODELING STUDIES

4.1 PROJECT DESCRIPTION

Isothermal flow modeling experiments were conducted as Task A of this program to develop and evaluate sorbent injection locations and methods for tangentially fired furnaces. In support of these experiments, a study was conducted to develop criteria by which the cold-flow air-only flow modeling experiments could simulate the penetration and mixing of cold gas-solid jets with furnace gases at temperatures of about 1315°C (2400°F). The results of these analytical and experimental studies were used to provide recommendations for sorbent injectors for Task C combustion testing at the Boiler Simulation Facility (BSF) and guidelines for sorbent injector designs for a field demonstration of the dry sorbent injection process in a tangentially fired furnace.

Task A was divided into four subtasks. The objectives of these subtasks were to:

1. Identify candidate sorbent injector location/method combinations to provide effective sorbent penetration and dispersion within the furnace.

2. Develop modeling techniques by which isothermal, single phase, gas-only jets can be used to accurately simulate the trajectory and dispersion of cold two-phase gas-solid sorbent jets into hot furnace gases.

3. Screen, through a multi-level test program, the proposed configurations developed during Subtask 1 with application of the jet modeling techniques developed during Subtask 2 in a large scale aerodynamic test facility.

4. Recommend, on the basis of Subtask 3, injector configurations to provide the required level of sorbent penetration, dispersion and residence time within the test furnace's sulfation temperature window to yield optimal SO_2 removal efficiency for Task C combustion testing and to recommend sorbent injector design guidelines for a field demonstration of the dry sorbent injection process.

The following subsections discuss the aerodynamic test facilities, the testing performed, and the conclusions and recommendations of the isothermal flow modeling studies.

4.2 FACILITY DESCRIPTION

Two test facilities were used during the Task A project. This section describes these and the instrumentation and procedures used to make the experimental measurements.

4.2.1 Crossflow Injector Test Facility

The Crossflow Injection Test Facility (CFITF) was designed and built to study sorbent injection jet performance under controlled conditions. From these studies, jet modeling correlations were developed for use in the tests performed in Subtask 3. The CFITF is shown in Figure 4-1. It consists of a 3.65 m (12 ft.) tall test cell with a 0.304 m x 0.9144 m (1 ft x 3 ft) cross-sectional area. A single circular injection nozzle was placed at the side of the facility 0.609 m (2 ft) downstream from the inlet bellmouth. This assured a uniform flow profile of ambient air drawn up to the point of injection. The facility operated under induced draft using a high pressure fan. A baghouse was provided at the fan inlet to collect the solids that were injected during the two-phase jet evaluations.

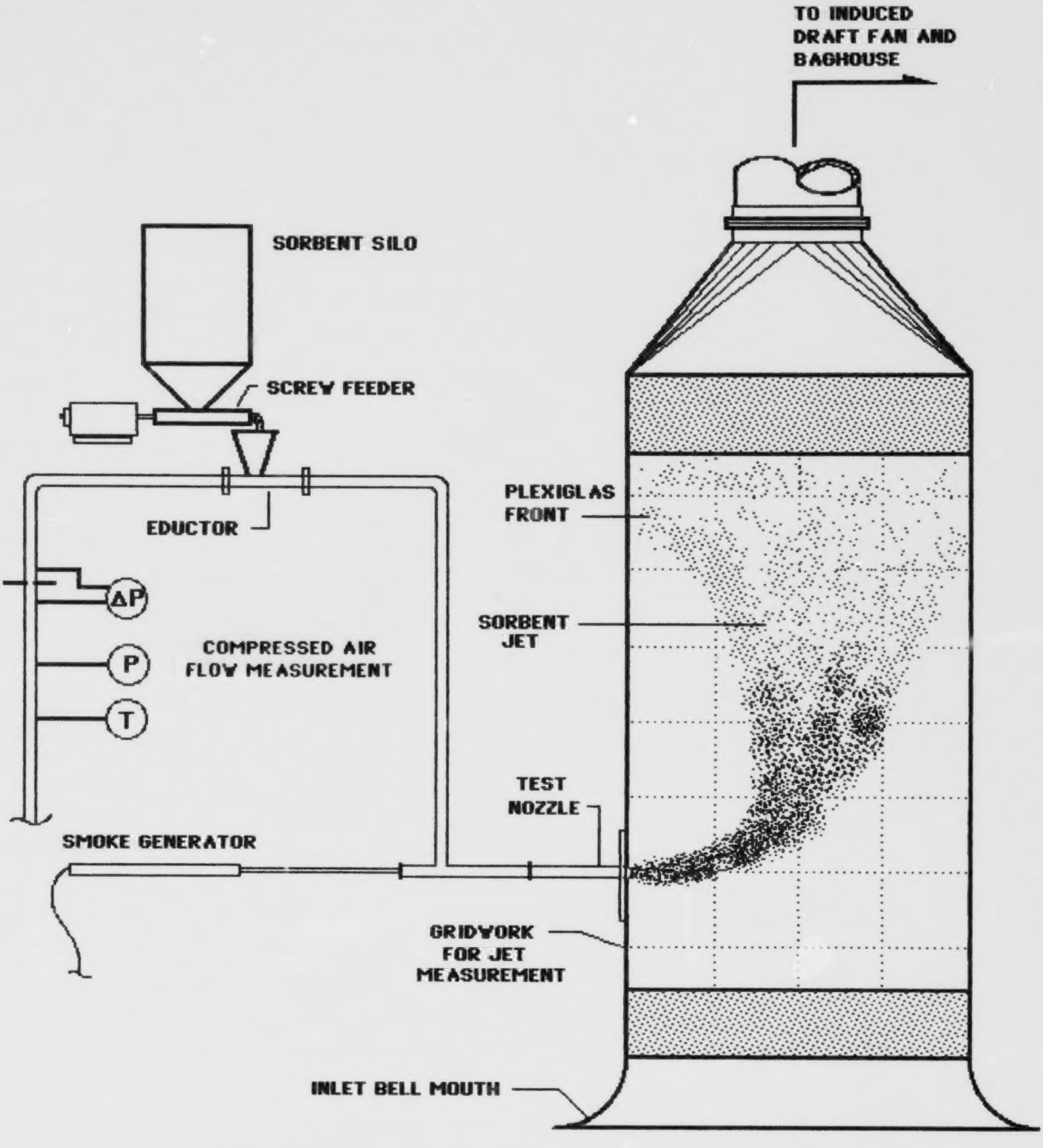
TO INDUCED
DRAFT FAN AND
BAGHOUSE
SORBENT SILO
SCREW FEEDER
PLEXIGLAS
FRONT
EDUCTOR
ΔP
P
T
COMPRESSED AIR
FLOW MEASUREMENT
SORBENT
JET
TEST
NOZZLE
SMOKE GENERATOR
GRIDWORK
FOR JET
MEASUREMENT
INLET BELL MOUTH

Figure 4-1. Cross flow injection test facility schematic.

Reproduced from
best available copy.

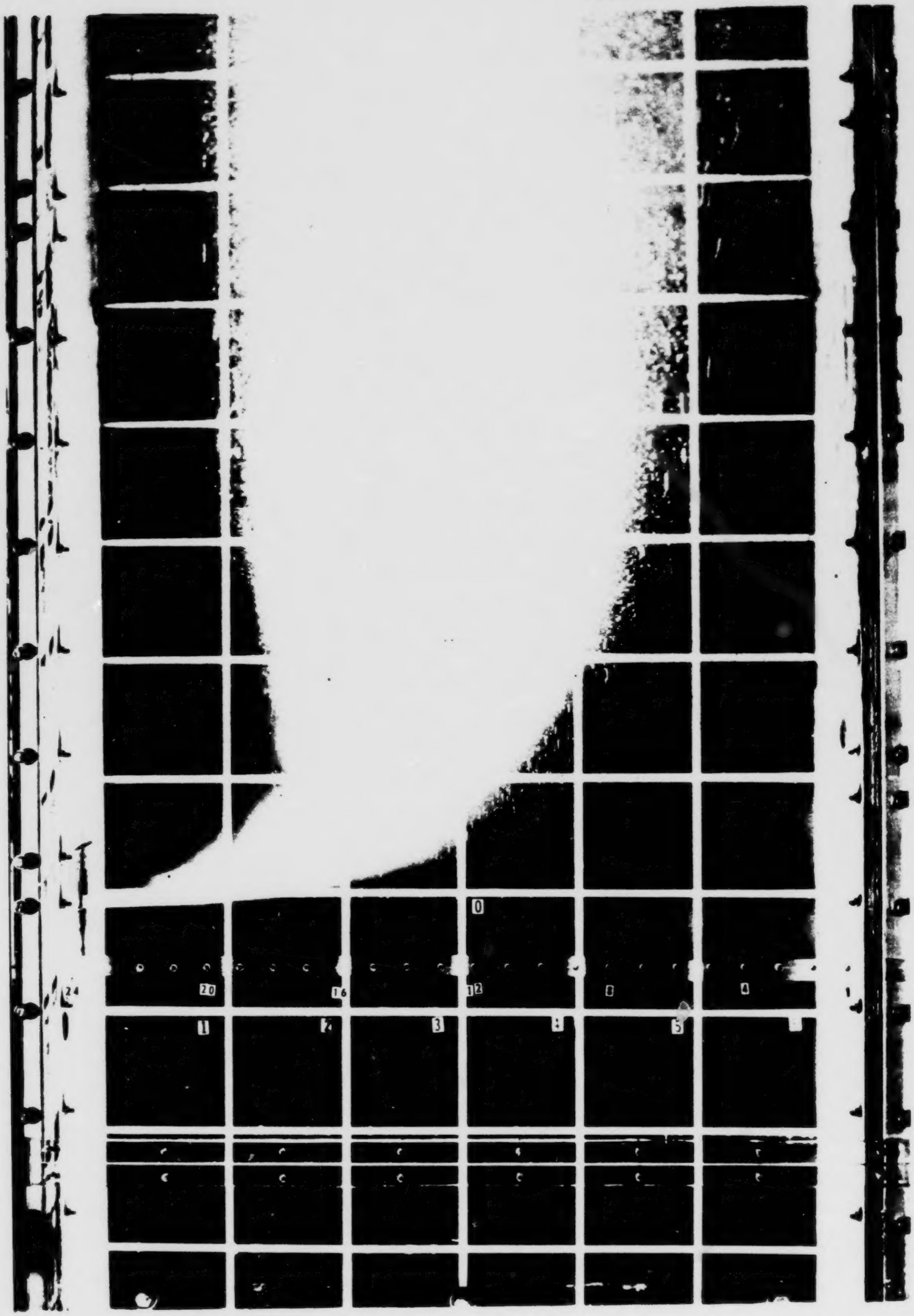
0
20
16
12
8
4
1
2
3
5

Figure 4-2. Typical cross flow injection test.

The test nozzle consisted of a circular tube that was 0.0158 m (0.622 in) in diameter and supplied by compressed air. A jet injection velocity of 45.72 m/sec (150 ft/sec) was used for all crossflow tests. To evaluate two-phase operation, fly ash was introduced to the jet at a rate of 54.43 kg/hr (120 lb/hr) through a rotary valve and eductor arrangement. Solids mass flow was measured with a calibrated screwfeeder and weigh hopper.

Changes in the jet to crossflow velocity and momentum ratio were obtained by changing the crossflow air velocity. Momentum ratios ranged from 100 to 534. This translated to crossflow velocities ranging from 4.5 to 1.98 m/sec (15 to 6.5 ft/sec), respectively.

To aid flow visualization, the front of the facility was constructed of plexiglas. The back wall of the test cell was painted black with a 0.152 m x 0.152 m (6 in x 6 in) white grid for tracking the position of the jet within the test cell. (See Figure 4-2). Still photographs and color video were used to record the penetration and dispersion performance of the injection jet. The injected solids permitted visualization of two-phase operation. Smoke, generated by a commercially available smoke fluid was used to visualize the gas-only jet. The smoke was injected into the jet air stream far enough upstream from the nozzle exit to be fully mixed and to minimize any effects on the jet's exit parameters.

4.2.2 Large Scale Furnace Aerodynamics Test Facility

The Large Scale Furnace Aerodynamics Test Facility (LSFATF) was used extensively in this program. The LSFATF is a tool for C-E's ongoing study of furnace aerodynamics and represents part of C-E's continued commitment to the improvement of coal burning technologies, Koucky, et al. (1986) and Anderson, et al. (1986). The LSFATF is shown in Figure 4-3. For this program, the facility was modified to simulate C-E's Boiler Simulation Facility (BSF) used in the Task C combustion tests.

The LSFATF model was geometrically scaled (0.46 scale factor) to encompass the entire BSF furnace from the hopper bottom to the economizer outlet. Because the penetration and dispersion performance of the sorbent

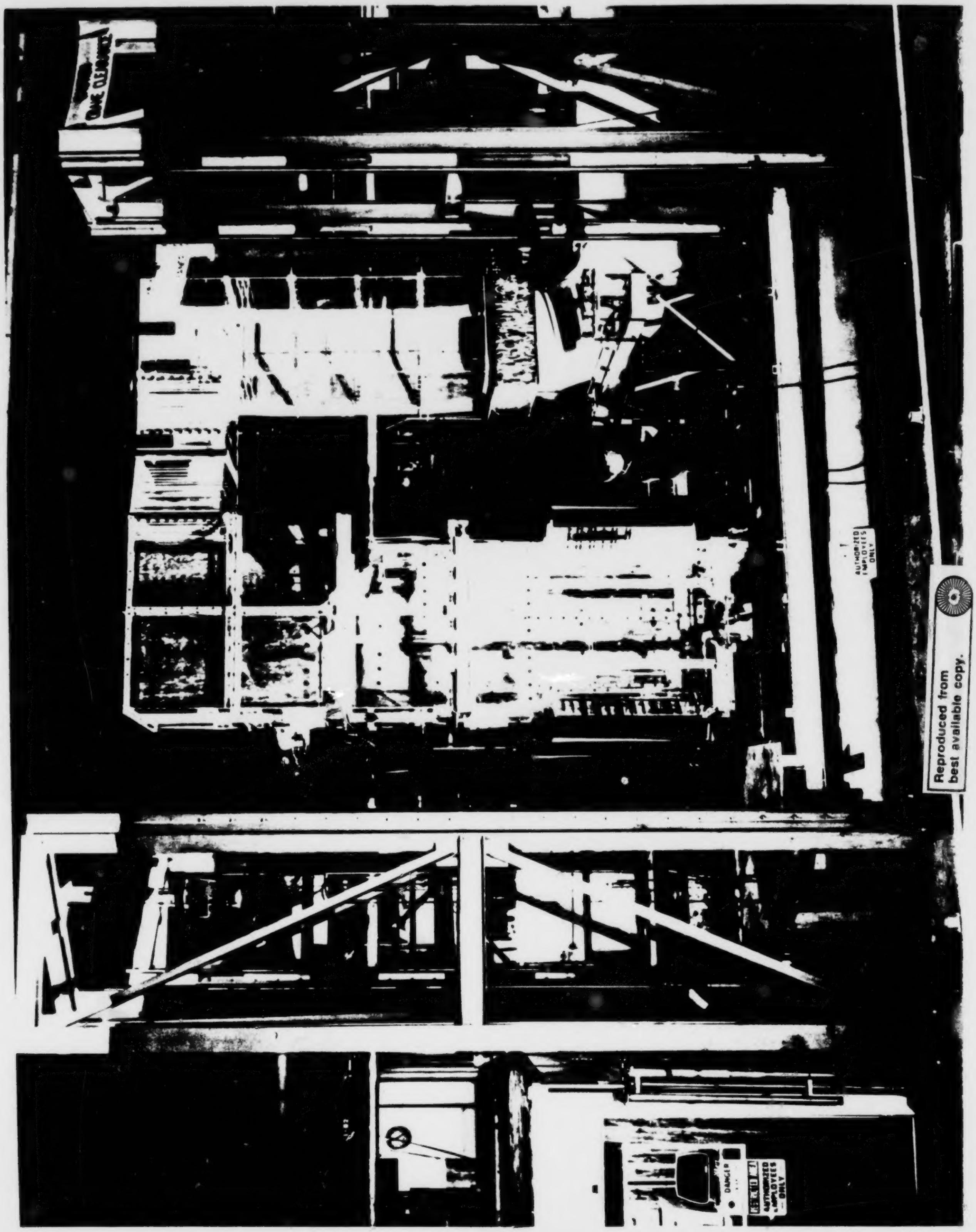
CRANE CLEARANCE
AUTHORIZED EMPLOYEES ONLY
DANGER
AUTHORIZED EMPLOYEES ONLY

Reproduced from best available copy.

Figure 4-3. Large scale furnace aerodynamics test facility.

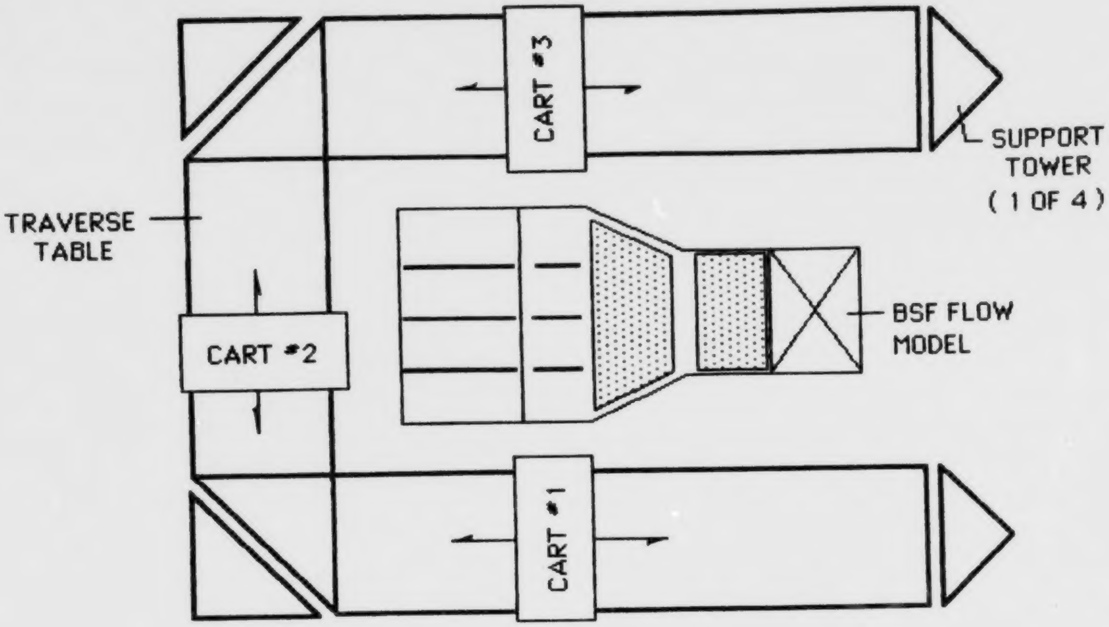
CART #3
SUPPORT TOWER
(1 OF 4)
TRAVERSE TABLE
CART #2
BSF FLOW MODEL
CART #1

**TRAVERSING SYSTEM
PLAN VIEW**

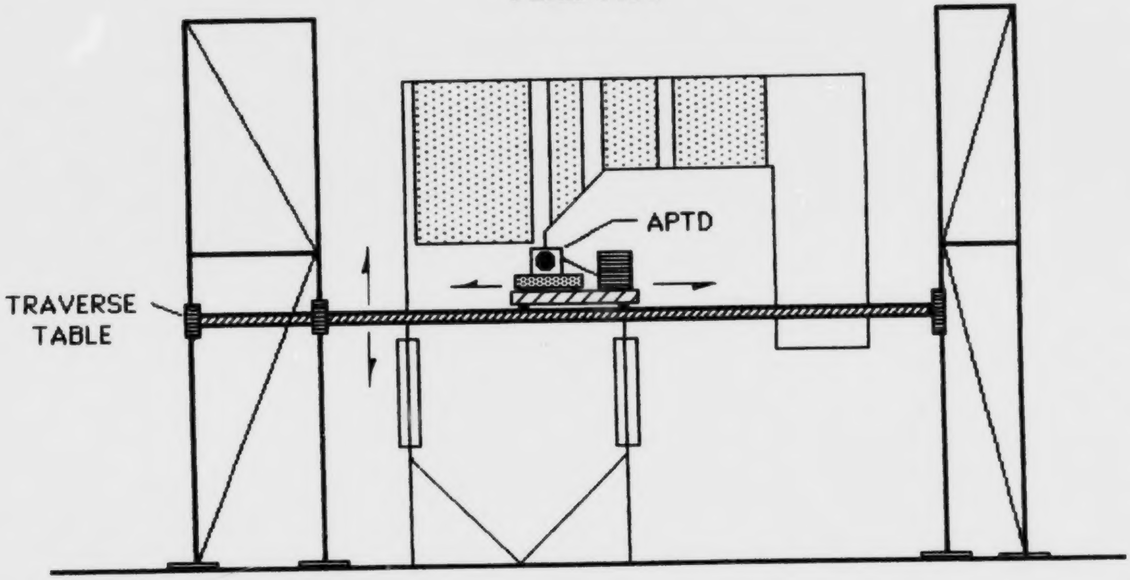
APTD
TRAVERSE TABLE

**TRAVERSING SYSTEM
ELEVATIONAL VIEW**

Figure 4-4. LSFATF instrument traversing system.

injection jet is a function of the furnace flow patterns, the detailed lower furnace section was modeled. Particular attention was paid to the simulated fuel admission assemblies. The free areas of the nozzles were adjusted according to the Thring-Newby criteria to account for the change in gas density that occurs as a result of combustion within the furnace. In the model, the height of the fuel admission assemblies were held constant while the width was increased by the ratio of the isothermal to prototype gas densities. Thring-Newby criteria insured that the furnace flow patterns were accurately modeled. The lower furnace section was also designed for easy changeover and/or adjustment of the primary/secondary fuel and air firing angles, the air flow or velocity ratio, the overfire air mass flow, and the distribution of fuel to and within the various firing elevations.

The flow model was built primarily of plexiglas to permit flow visualization. Sheet metal was used to fabricate the inlet and outlet ductwork, the fuel admission assemblies, and the inlet bellmouths. All radiant and convective heat transfer surfaces in the upper furnace were accurately modeled. Upper furnace heat transfer surfaces were fabricated from masonite and wood dowels. All scaled dimensions of the BSF were maintained to a tolerance of +/-0.00159 m (1/16 in) in the flow model. A large FD fan (849.6 m^3/min, 30,000 CFM) provides air to operate the flow model. The fan is equipped with a control damper and flow measurement instrumentation.

Real time display of model operating parameters and instrumentation status assures that proper test conditions are maintained. Test data, obtained via the facilities data acquisition computer, is automatically downloaded to a central processing computer. From here, the data is reduced to engineering units and presented in a format specified by the project engineer.

Surrounding the furnace model is a three-axis instrument traversing system, shown in Figure 4-4. This system allows the placement of instrument packages around or within the furnace model. Three-dimensional instrument traversing is controlled by the facility operator and computer. For ease in placing the instrumentation, a targeting TV camera is provided for the operator so that probe positioning can be performed without the operator leaving the control room. This camera is attached to the instrument carriage and hence moves with the entire unit. Traversing is also automated.

4.2.2.1 Sorbent Injection System

Studies conducted at C-E indicate that the preferred method for injecting sorbent into the furnace is by pneumatic transport of dry sorbent powder. In full scale utility applications the sorbent may be transported to the furnace by either of two methods. In the first method, the sorbent is transported from the bottom of the sorbent feed hopper with only a portion of the injection air. The sorbent, sorbent transport air, and remainder of the injection air mix upstream of the furnace. This method would typify dense-phase sorbent transport. In the second method, the sorbent is transported from the bottom of the feed hopper using the entire sorbent injection airflow. This typifies dilute-phase transport. The second method was used in the Task A cold flow modeling tests and in the Task C combustion tests.

Figure 4-5 shows one of the sorbent injection nozzles used in Task A. The nozzles were cast from an epoxy polymer. The required inside diameters were formed by using the appropriately sized cores during the casting process. Figure 4-6 presents a cross-sectional view of a typical nozzle. A compressed air header system was used to feed the injection nozzles. Compressed air flow rate was established through two flow control valves and measured using an ASME orifice.

Methane gas used as a tracer in the gas mixing studies was fed to the compressed air header at a point far upstream of the nozzle exit to ensure that the tracer gas was fully mixed with the injection air before the mixture entered the flow model. Taps were also provided in the sorbent air heater for the introduction of smoke for flow visualization. One smoke injection tap was located before the header branches to each injector and was used for seeding all of the injectors. Additional taps were located in each branch for seeding single nozzles for specific tests. Perforated plates were attached to the upstream end of each sorbent nozzle to establish equal injection velocities for each of the nozzles in service.

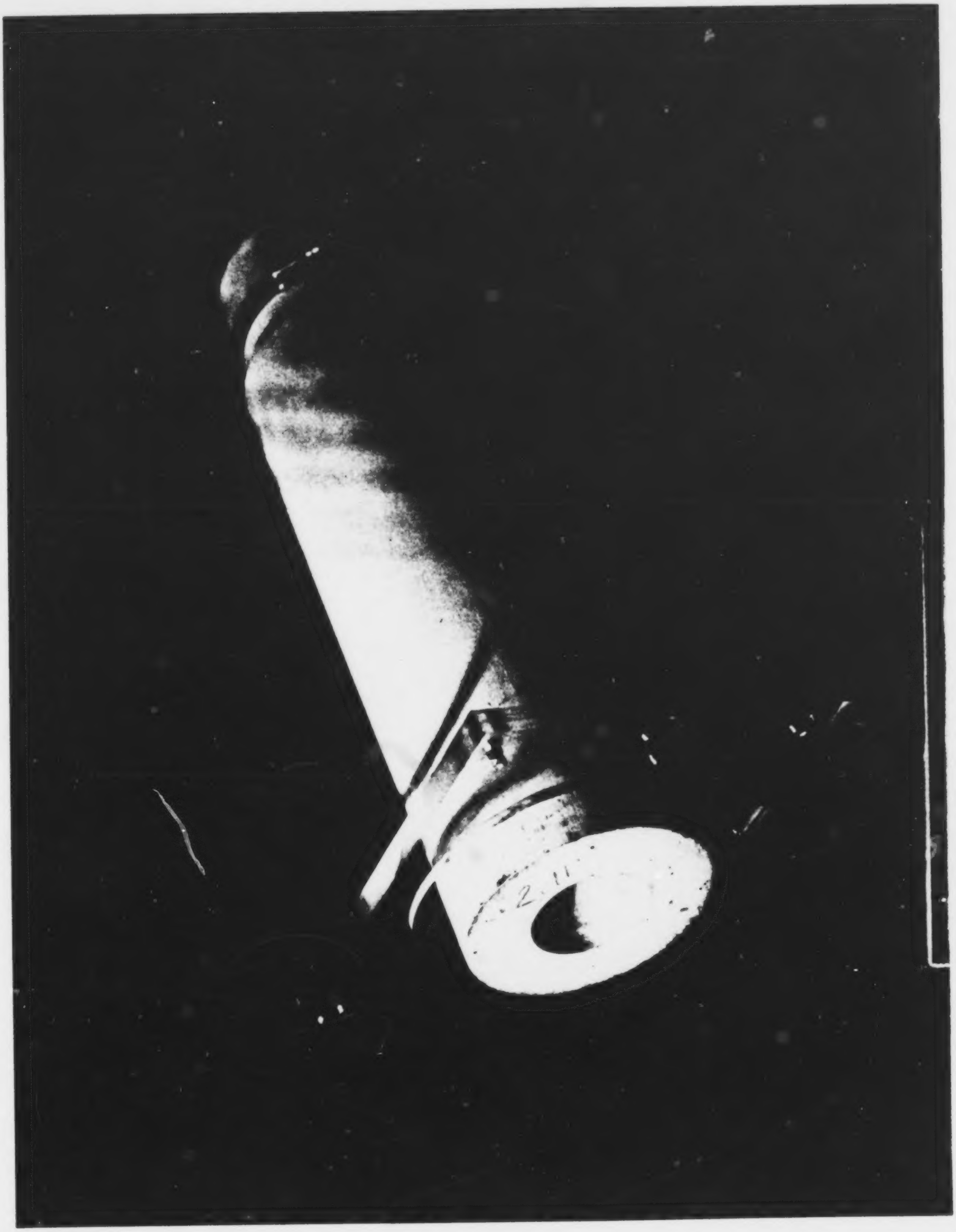

Figure 4-5. Flow model sorbent injection nozzle.

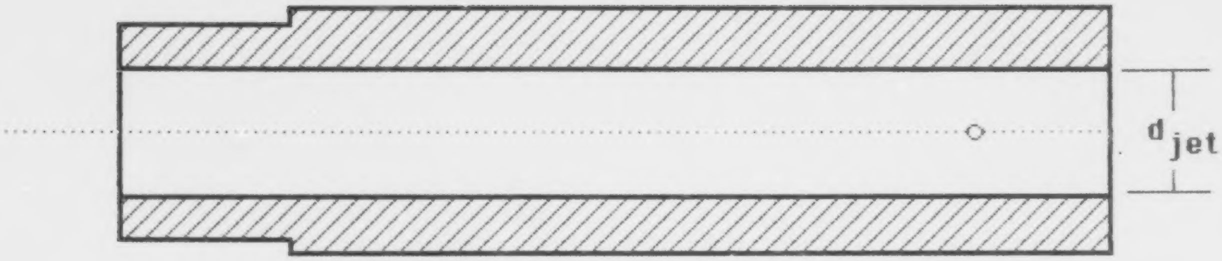

NOZZLE CROSS SECTION

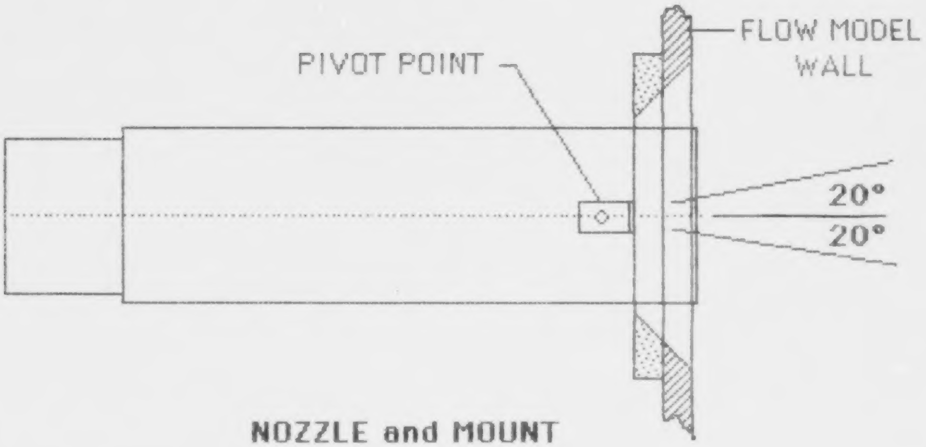
PIVOT POINT
FLOW MODEL WALL
20°
20°

NOZZLE and MOUNT ELEVATIONAL VIEW

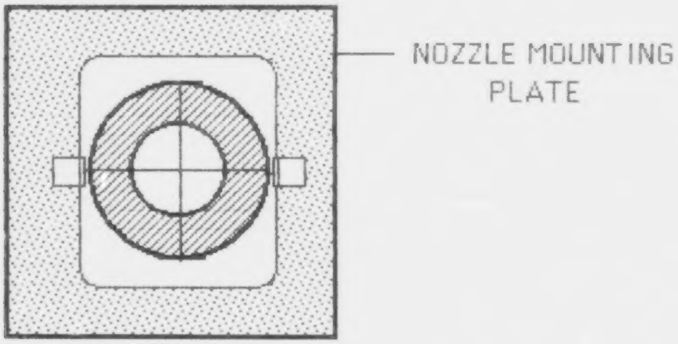
NOZZLE MOUNTING PLATE

NOZZLE and MOUNT FRONT VIEW

Figure 4-6. Flow model injection nozzle details.

4.2.2.2 Test Instrumentation

A number of instrumentation systems were used during the Task A test program. These included automatically controlled three-dimensional pitot probes and laser based gas concentration measurement systems. Each instrumentation system was calibrated before and after each test series. These systems and the equipment used in the flow visualization experiments are discussed briefly.

Three-Dimensional Pitot Tube Probe -- A commercially available five-hole directional sensing pitot tube probe, shown schematically in Figure 4-7, was used. The probe has five pressure measuring holes located at its tip. The centrally located pressure hole, P1, measures the total or impact pressure of the fluid, while the two lateral pressure holes, P2 and P3, measure the static pressure. If the probe is rotated around its axis until P2=P3, the plane of flow can be identified and measured. However, since the condition of P2=P3 can give two separate planes 180° apart, the correct vector plane is identified when P2=P3 and P1 has its highest positive value with respect to P2 and P3. An angular encoder is attached to the probe at its base so that the angle of this vector plane, commonly called the yaw angle, can be measured. The yaw angle indicates the plane of the flow but does not give the flow angle within this place. This flow angle, known as the pitch angle, is determined by the differential pressure P4-P5.

In actual practice, four (4) differential pressure readings are required to fully define the flow at a particular point in the flow field of interest. These pressure differentials are:

P1-Pat = Indicated total pressure with respect to atmosphere
P1-P2 = Indicated velocity pressure
P2-P3 = Yaw angle pressure
P4-P5 = Pitch angle pressure

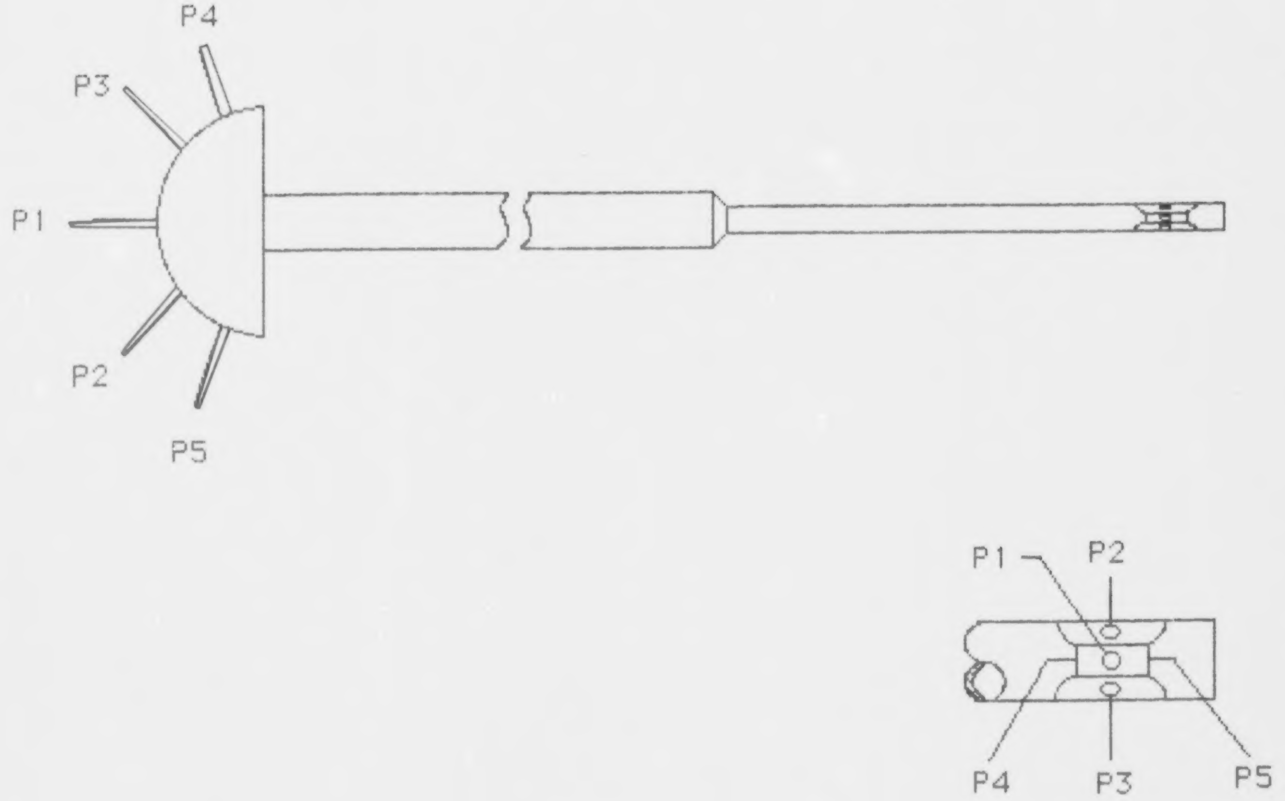
P4
P3
P1
P2
P5
P1
P2
P4
P3
P5

Figure 4-7. Five hole pitot tube details.

Calibration curves are used to relate these pressure differentials to the actual pressures and pitch angles. These curves are generated, through detailed probe calibrations, at the beginning and end of each test series. These curves enable the experimenter to determine the actual velocity head and the pitch angle of the flow at each measuring point. Knowing this data and the yaw angle, the x, y, and z or the normal, radial, and tangential velocity vectors are determined using simple geometric relationships

Automated Probe Traversing Device -- All quantitative three-dimensional velocity and pressure mapping within the test facilities was obtained with a calibrated five-hole pitot tube coupled to a computer controlled traversing and data acquisition system. This system, which was developed and built at KDL, is called the Automatic Probe Traversing Device or APTD.

The APTD is a programmable data acquisition system which automatically positions and nulls the five-hole pitot tube, and then records all the pressure readings on the laboratory's central computer system. Figure 4-8 shows the five-hole pitot tube, probe positioning robot, and local programmable controller/electronic manometer cabinet. The motion of the probe is controlled by the system's local processor. This processor is programmed by the facilities operator at the start of each instrumentation traverse by entering the appropriate operational parameters for the particular test. These parameters include; instrument type and serial number (for accessing the most recent calibrations), test number, test plane, the number of data points to be obtained, the distance between each test point, and the maximum distance of probe travel (a safety feature). Once these operational parameters have been entered, the traverse can be started by indicating the desired automatic operational mode.

The processor controls stepping motors which move the probe to the preprogrammed test point location and rotates it until the direction of flow is obtained. The outputs of the four pressure transmitters, measuring the pressure differentials listed above, are then recorded along with the probe position, angle, test number, test plane, etc. by the central data acquisition computer.

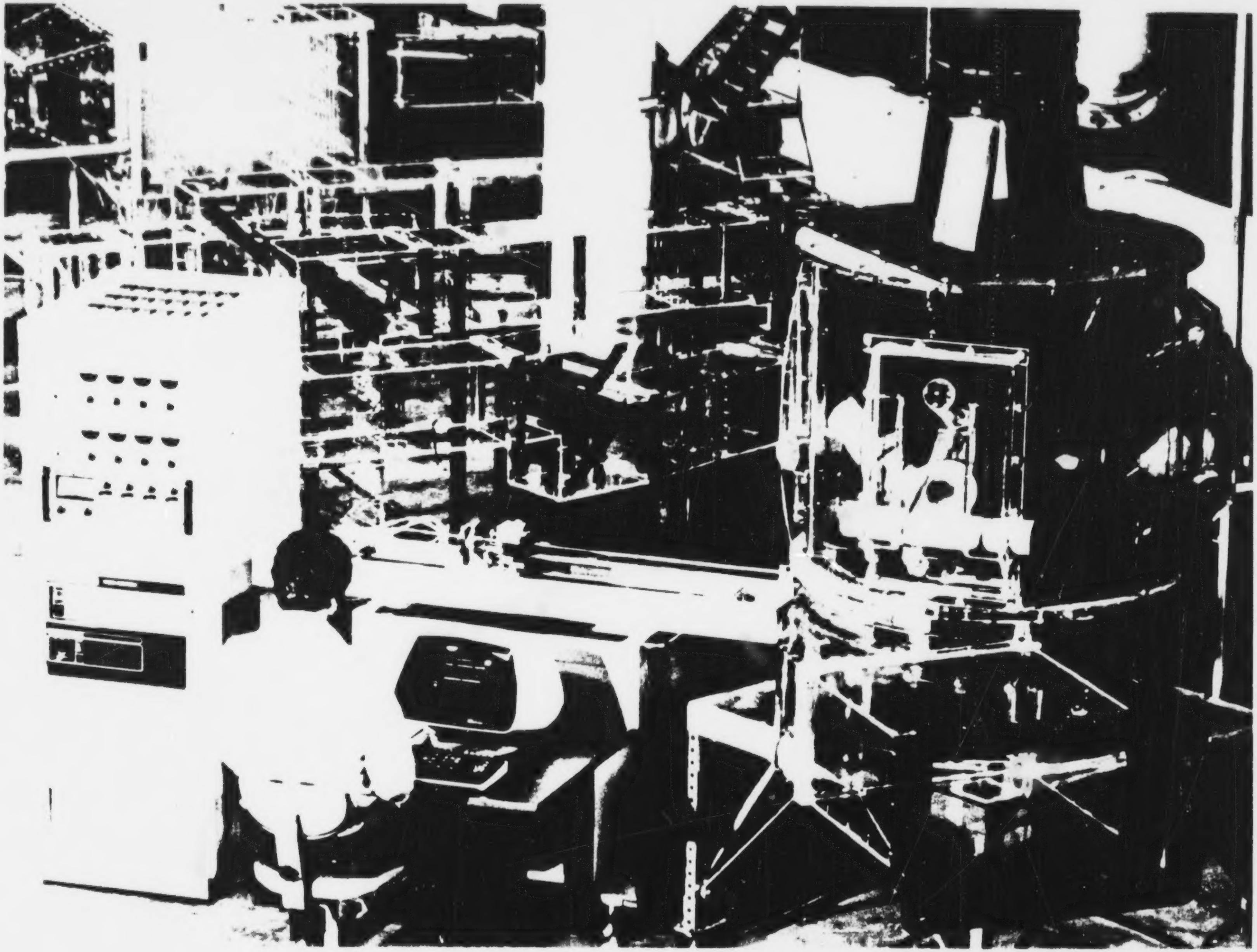

Figure 4-8. Automatic probe traversing device.

Laser Absorption Spectrophotometer -- All sorbent mixing studies performed during the Task A evaluations were performed with an in-house developed gas tracer system. This system is sometimes referred to as the Laser-Methane System because it relies on methane as the seed or tracer medium. This system is shown schematically in Figure 4-9.

During steady state operation of the instrument, the gas sample from the furnace model was drawn from the test point via the P1-Pat tap of the five-hole pitot tube. The tube from this tap was replaced with one that runs to the gas tracer instrument in order to measure methane tracer gas concentration. The other four (4) pressure taps were sealed. Configured in this manner, the computer controlled APTD positioning mechanisms were utilized for gas mixing traverses.

Before and after each traverse into the flow model, the system was zeroed. At each test point, the data obtained was down loaded to the laboratory's central data acquisition computer. Full calibrations of the instrument were performed at the beginning and end of the test series.

The Laser Methane system was also used to obtain sorbent residence times within the sulfation temperature window of the flow model. During transient operation of this instrument, the system was modified as detailed in Figure 4-10. One of the laser beams from the instrument was directed through the flow model instead of to a remote sample cell. In this configuration, with the simulated sorbent jet being tagged with methane, the integrated average concentration along the line of sight of the laser beam was measured. The flow of tracer gas was then abruptly terminated and the decay in the methane concentration recorded. The slope, shape and length of the decay curve is a measure of the residence time and evacuation rate of the tracer gas within the furnace. A typical transient methane output plot is shown in Figure 4-11.

Smoke Generator -- A commercially available smoke generator was utilized during the flow visualization tests. The system consisted of a power supply, smoke fluid reservoir, and smoke generation wand. Resistance heating is used to flash the fluid into a dense white stream of smoke, which is then injected into the flow model.

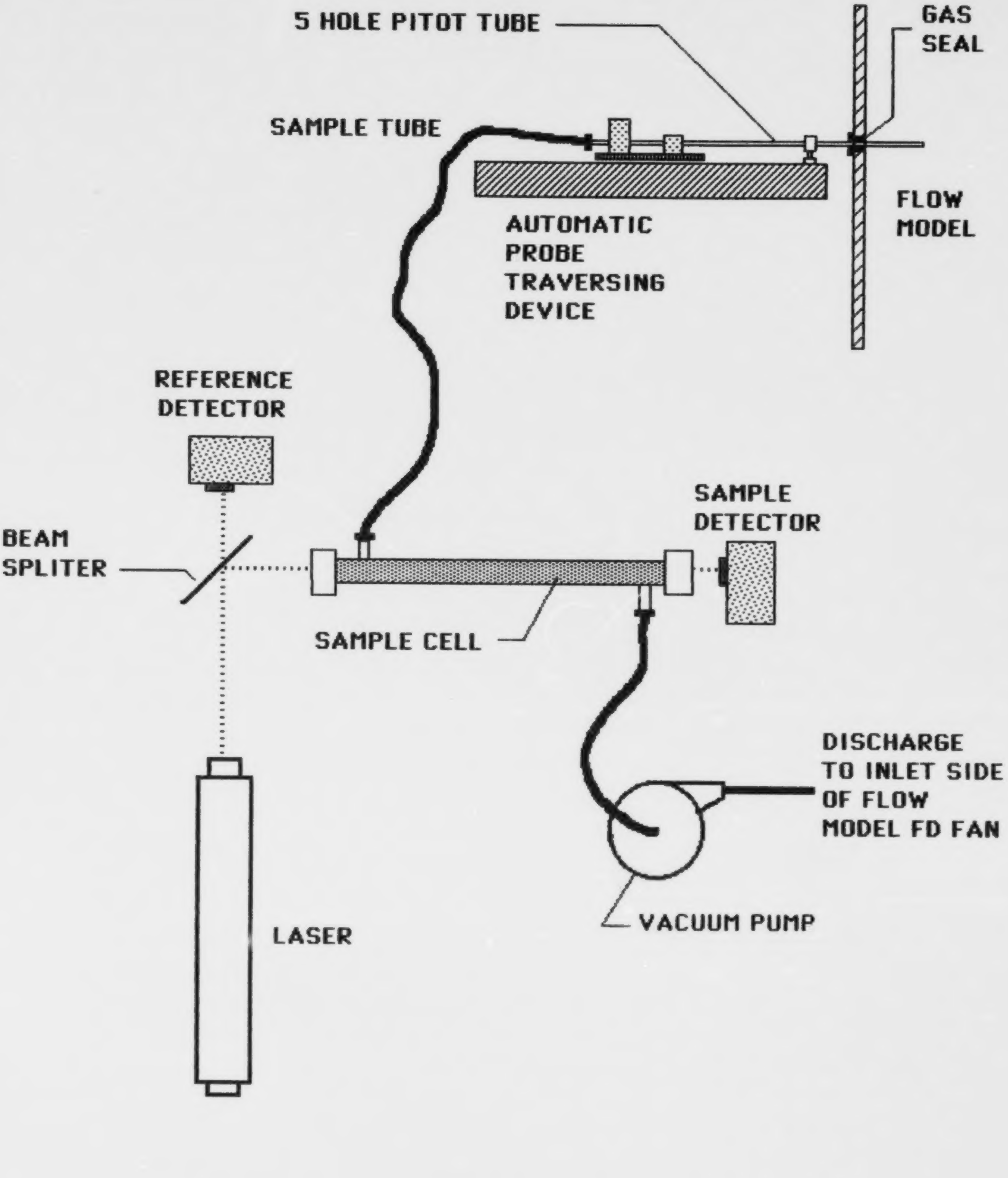
5 HOLE PITOT TUBE
GAS SEAL
SAMPLE TUBE
FLOW MODEL
AUTOMATIC PROBE TRAVERSING DEVICE
REFERENCE DETECTOR
SAMPLE DETECTOR
BEAM SPLITER
SAMPLE CELL
DISCHARGE TO INLET SIDE OF FLOW MODEL FD FAN
VACUUM PUMP
LASER

Figure 4-9. Laser absorption spectrophotometer schematic.

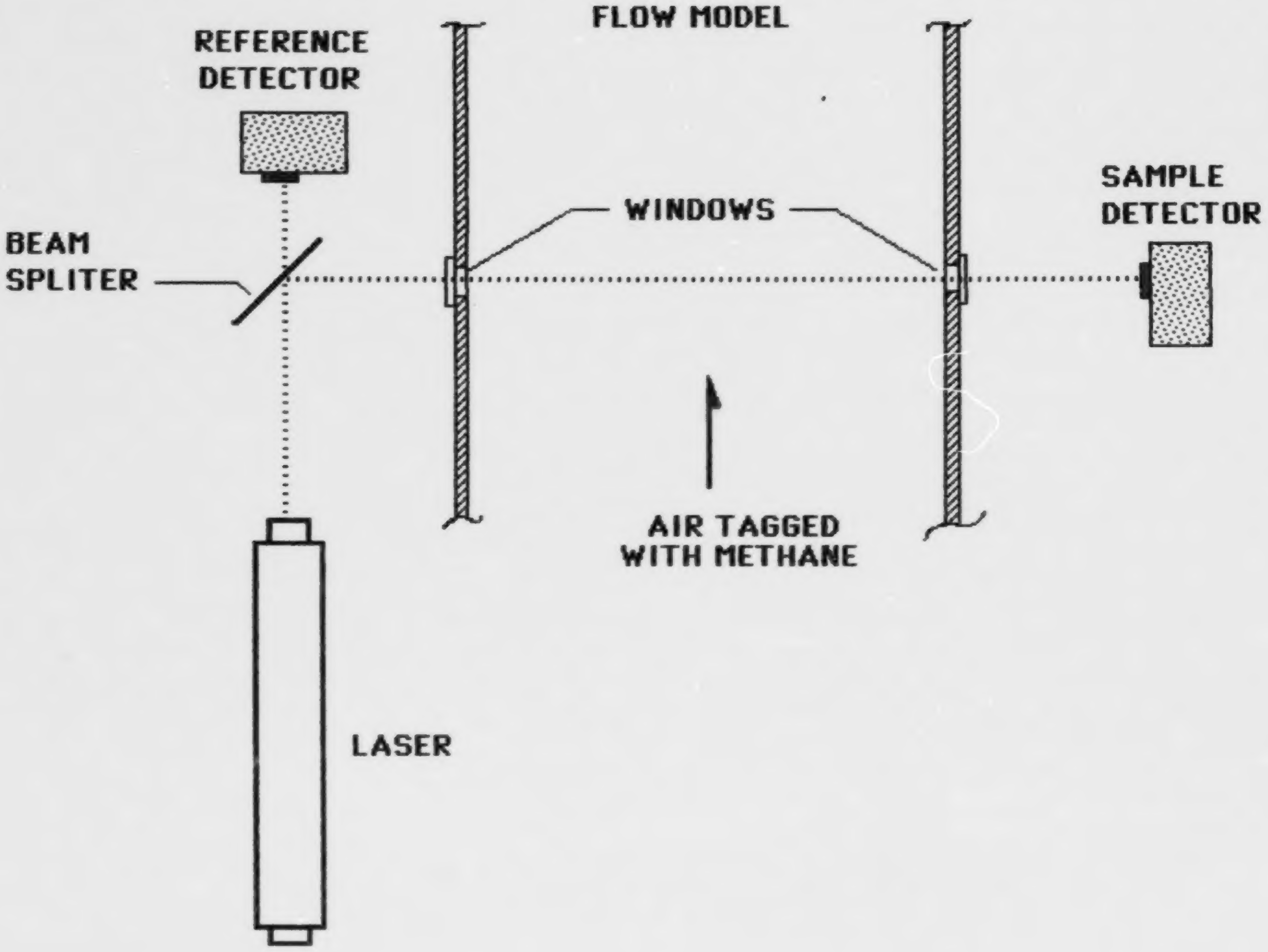
FLOW MODEL
REFERENCE DETECTOR
WINDOWS
SAMPLE DETECTOR
BEAM SPLITER
AIR TAGGED WITH METHANE
LASER

Figure 4-10. Residence time distribution instrumentation setup.

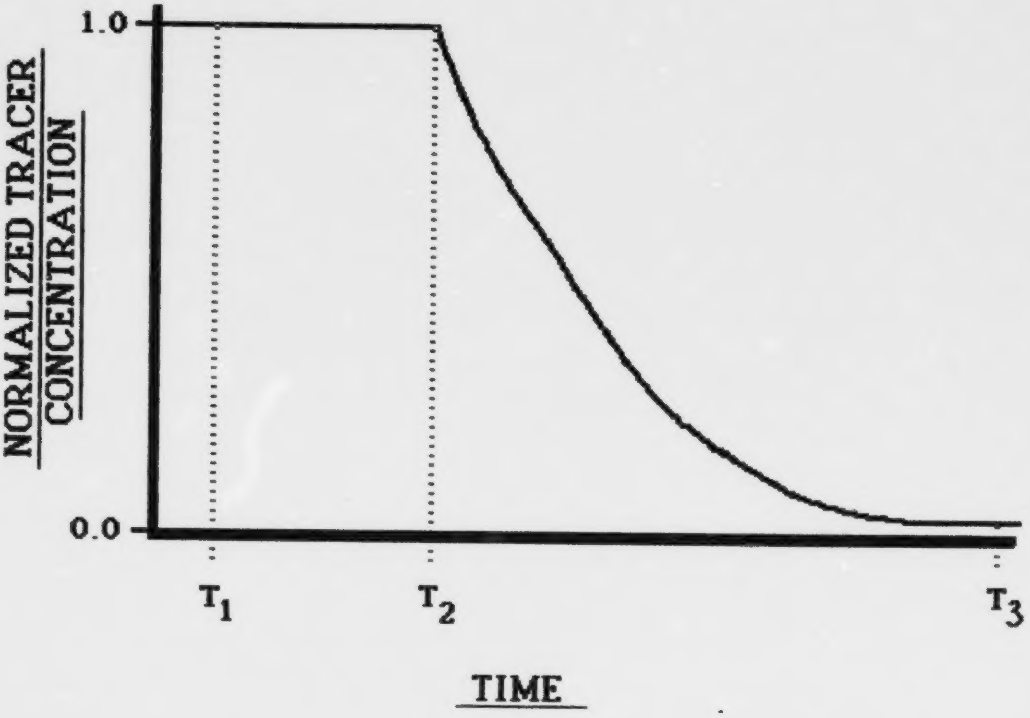

T_1	TRACER GAS FLOW TERMINATED
T_1-T_2	PLUG FLOW REGION
T_2-T_3	WELL MIXED REGION

Figure 4-11. Idealized RTD test result.

Color Video Tape System -- The flow visualization test results were documented using a commercially available closed circuit VHS color video tape system. The variable speed, stop action and color reversal capabilities of the system during playback proved to be a very useful tool. Also, the ability to evaluate the test results for the various designs, which were obtained over a period of several days, together in one session improved interpretation of design comparisons.

4.3 RESULTS

To achieve the objectives of the isothermal flow modeling task, the following subtasks were conducted:

1. Identification of candidate injection configurations.
2. Development of jet modeling criteria.
3. Evaluation, through a multi-leveled flow modeling effort, sorbent injector location/design combinations for their penetration, dispersion and mixing performance for a wide range of conditions.
4. Identification of injection systems with the highest levels of dispersion and mixing performance and recommendation of those systems for combustion testing at the BSF.

These subtasks and the results obtained are discussed in the following sections.

4.3.1 Identification of Candidate Injection Configurations

Selection of candidate sorbent injection configurations for the BSF required two types of specifications - injection location and injector carrier air operating conditions, including both airflow and velocity. Both types of specifications are discussed in this section.

Pilot-scale sulfation experiments sponsored by the EPA and others suggest that the optimum location for sorbent injection is a location where the flue gas temperature is in the range between 1300°C (2375°F) and 1200°C (2200°F), Beittle, et al. (1986). The optimum injection temperature varies with sorbent type, furnace quench rate, and other parameters. In addition, the optimum temperature varies from boiler to boiler. The optimum temperature window for the sulfation reaction is in the range from 1200°C to 900°C (2192°F to 1652°F). In some units the entrance to this window may be below the arch or be far back in the unit's reheater section. For these reasons the injection locations selected for the initial cold flow modeling efforts were not limited to the expected BSF thermal topography (Figure 4-12), but included configurations that would provide generalized injector performance data for the full range of tangentially fired utility boilers.

A number of factors were considered in the choice of the injector locations for the Task A cold flow modeling. These included (1) C-E's data base and predictions of furnace temperature profiles, (2) the results of jet injection calculations, and, (3) the geometry of the combustion test facility. Eight (8) possible injection locations, each consisting of four injection points, were selected. These are detailed in Table 4-1 as Locations A through H. Injector configurations tested consisted of injection at these individual locations (4 injectors) plus combinations of locations (8 injectors) and various injection velocities and angles. The sorbent injection configurations which made up the Task A first level test matrix are listed in Table 4-2, and are shown in Figure 4-13.

Test Configurations 1, 2, and 3 evaluated front wall injection at three elevations above the arch. Configurations 4, 5, and 6 evaluated combinations of these elevations. Configuration 7 evaluated an arrangement to provide deep penetration from Location A in combination with wide dispersion and low penetration at Location B. Configurations 8, 9, 10, and 11 evaluated injection below the arch. Co-current and countercurrent tangential injection of sorbent were evaluated in configurations 8 and 9. Configuration 10 evaluated injection from the rear wall below the arch. Configuration 11 evaluated injection from below the arch in combination with front wall injection at Location B. Configurations 12, 13, 14, 15, and 16 evaluated various roof mounted sorbent injection schemes. Configuration 13 evaluated four roof mounted injectors in combination with front wall injection. Configurations 14 and 15 evaluated lances mounted from the roof and hanging into the sulfation temperature window. At the end of each lance a 45° or 90° angles injection nozzle was installed to direct the sorbent jets. The advantage of a lance based injection system is that the sorbent material can be introduced exactly at the desired location. Configuration 16 evaluated lances in combination with front wall injection.

4.3.2 Identification of Sorbent Carrier Flow Rate and Injection Velocities

Carrier air mass flow rate and the injection velocity required to achieve effective sorbent penetration within the furnace were determined through a parametric study based on empirical jet penetration equations. The jet penetration equation developed by Patrick (1967) was used, although equations are also available from several other investigators, Ivanov (1972), Kamotani and Greber (1971), Rudinger (1975), Salzman and Schwartz (1978), and Shandovov (1972). Jet penetrations were calculated for the BSF as a function of injector diameter, mass flow rate, and injection velocity. Furnace gas temperature was assumed to be constant at 1315°C (2400°F). Jet penetrations were calculated for solid loadings of zero to as high as 975 kg/hr (2144 lbs/hr) which corresponds to a 4:1 Ca/S mole ratio, 3% sulfur coal, and the use of calcium carbonate as the sorbent. Average sorbent supply rate for Task C was 600 lbs/hr based on 2:1 Ca/S using $Ca(OH)_2$ and 3% sulfur Pittsburgh #8 seam coal.

The results of the jet calculations are summarized in Figure 4-14. Based on these calculations, preliminary sorbent injection guidelines, including sorbent carrier air flow rate and velocity, were developed for the BSF. These BSF injector guidelines were scaled to cold-flow testing at the LSFATF using modeling criteria discussed in the next subsection. The preliminary guidelines were that, under the hot operating conditions at the BSF, adequate penetration could be obtained with a cold, 37.7°C (100°F), sorbent jet with injection velocities of between 7.6 and 22.9 m/sec (25 and 75 ft/sec) for a carrier air mass flow rate equal to 5% of the BSF's combustion air flow at 100% load and 25% excess air. This translates to injection at the BSF using either four (4) injectors with nominal diameters between 10.26 and 5.92 cm (4.04 and 2.33 inches) or eight (8) injectors with nominal diameters of between 7.23 and 4.19 cm (2.85 and 1.65 inches). These sorbent injection design guidelines were evaluated during the Task C combustion testing, and revisions were made to the guidelines. These revisions are discussed as part of the combustion test results in Section 6.

TABLE 4-1. INJECTOR LOCATION

Location	Description
A	Above arch, low, on front wall
B	Above arch, mid, on front wall
C	Above arch, high, on front wall
D	Under arch, T-Fired from corners
E	Under arch along back wall
F	Roof mounted between superheater panels
G	Roof mounted hanging lance, mid position, 45° downward tilt
H	Roof mounted hanging lance, low position, 90° tilt

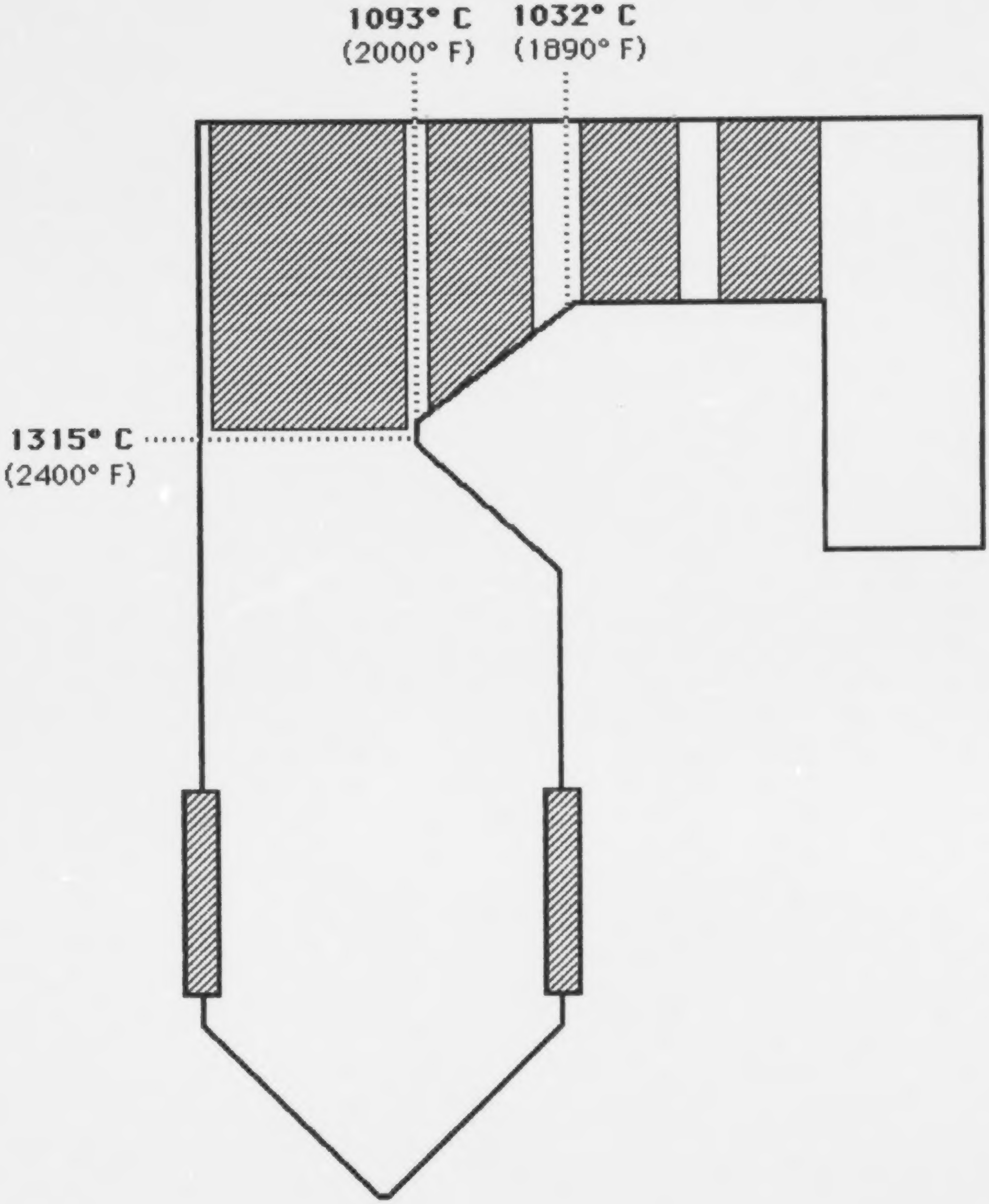
1093° C
(2000° F)
1032° C
(1890° F)
1315° C
(2400° F)

Figure 4-12. Predicted BSF gas temperatures.

TABLE 4-2. FIRST SCREENING LEVEL TEST CONFIGURATIONS

Configuration*	Location	Description
1	A	Above arch, low, along front wall
2	B	Above arch, mid, along front wall
3	C	Above arch, high, along front wall, -45° tilt
4	A,B	Combination of Configurations 1 & 2
5	B,C	Combination of Configurations 2 & 3
6	A,C	Combination of Configurations 1 & 3
7	A,B	Combination of Configurations 1 & 2 Location A with high velocity Location B with low velocity
8	D	Under arch, T-fired corotational
9	D	Under arch, T-fired counter-rotational
10	E	Under arch, along back wall
11	E,B	Under arch, along back wall combined with above the arch, along front wall
12	F	Roof mounted
13	A,F	Four above arch, low, along front wall with four roof mounted
14	H	Roof mounted, single port, vertical hanging lance, low position, and 90° tilt
15	G	Roof mounted, hanging lance, high position, and -45° tilt
16	H	Roof mounted, single port, vertical hanging lance, combined with front wall, high

* Each configuration was evaluated at three injector velocities simulating BSF injection conditions of 5% of total air for sorbent transport flow and injection velocities of 7.6, 15.2, and 22.9 m/sec (25, 50, and 75 ft/sec). Jet velocity was changed through changes in the jet diameters. Furnace flow was held constant at the condition representing 100% load and 25% excess air.

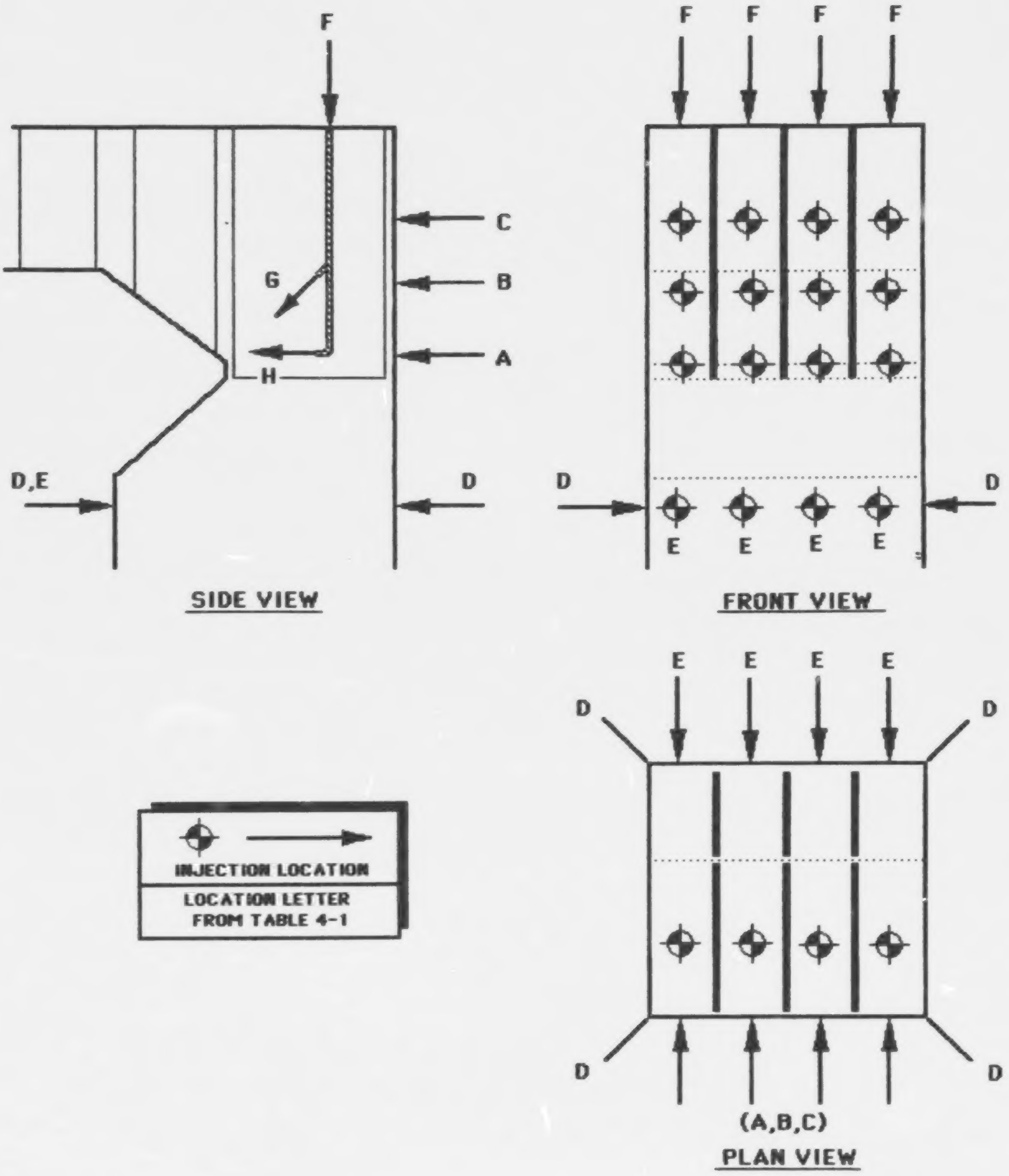
F
C
B
A
G
H
D,E
D
SIDE VIEW
F F F F
D
D
E E E E
FRONT VIEW
INJECTION LOCATION
LOCATION LETTER FROM TABLE 4-1
E E E E
D D
D D
(A,B,C)
PLAN VIEW

Figure 4-13. Flow model sorbent injection locations.

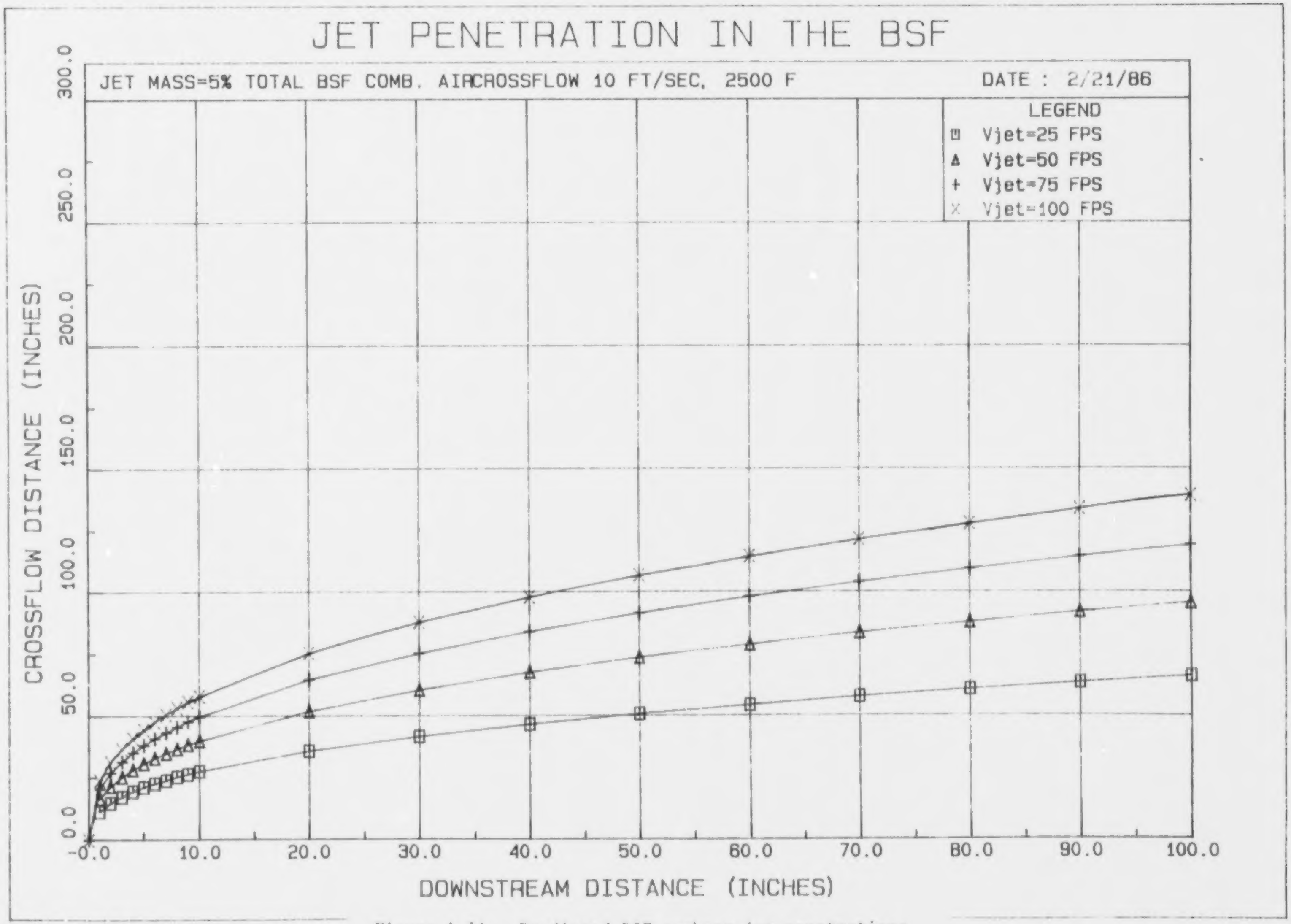

Figure 4-14. Predicted BSF sorbent jet penetrations.

4.3.3 Development of Jet Modeling Criteria

The aerodynamic modeling tests used isothermal, air-only jets to simulate the injection of cold gas-solid jets into hot 1315°C (2400°F) furnace gases. The objective of this subtask was to develop the method by which a scaled isothermal simulation of the sorbent injection and dispersion process could be performed.

This subtask consisted of two efforts:

1. Develop and validate a penetration correlation between gas-only jets and 2-phase (gas/solids) sorbent loaded jets.

2. Develop a modeling correlation to isothermally simulate at reduced scale the nonisothermal injection of sorbent into a boiler.

A series of tests were performed in the Crossflow Injection Test Facility (CFITF). These tests determined how the penetration of a two-phase jet could be predicted using single phase gas-only jet penetration correlations. A criteria was developed for jets whose particulate component has a mass mean diameter of less than 20 microns, which is applicable to typical sorbents. The criteria uses the mixture density of the two-phase stream in place of the gas density. That is, the density term in the jet penetration correlations was adjusted according to the equation:

$$\rho\Big|_{mix} = \frac{\dot{m}_{solids} + \dot{m}_{air}}{Q} \qquad (4\text{-}1)$$

A list of Abbreviations and Symbols is given in the front matter of this report.

For this investigation, tests were run in the CFITF at three (3) different solid-gas mass ratios, 0, 0.7, and 1.4. The jet velocity for each test was held constant at 45.8 m/sec (150 ft/sec), and three (3) crossflow velocities were utilized, 4.57, 3.85, and 3.0 m/sec (15, 12.66, and 10.06

ft/sec). Using equation (4-1) for the mixture density of a two-phase stream and the gas-only jet penetration correlation of Patrick (1967), crossflow velocities were then calculated for the gas-only jet such that the resulting jet to crossflow momentum ratios matched those of the two-phase tests. Using these crossflow velocities, gas-only jet injection tests were run in the CFITF. Still and video recordings were made for each test. For the gas-only injection tests, smoke was introduced into the jet for visualization.

Figure 4-15 shows a typical two-phase jet operating at a 0.7 solids-gas ratio and injecting at 3.05 m/sec (10 ft/sec). Figure 4-16 shows the single phase complement in which the cross flow velocity was adjusted so that the resulting momentum flux ratio was equal to that calculated for the two-phase jet using the mixture density. The jet penetrations are essentially the same. Overall jet dispersion was also matched, but is slightly underestimated in the gas-only case. As a result of these tests, it was determined that the technique of using a single phase representation of a two-phase jet is valid if the mixture density of the two-phase stream is utilized in the jet penetration calculations.

The second phase of this subtask dealt with the development of sorbent injection nozzle scaling criteria and development of an isothermal modeling technique for nonisothermal sorbent injection. Much information is available in the literature detailing the performance of a jet injecting into a uniform crossflow. (Several references are listed in the previous subsection.) Typically, however, the same fluid was used for both the jet and crossflow and they were also the same temperature. Because most flow model investigations are performed at reduced scale and isothermally, adjustments must be made to the size and operating conditions of the injection nozzle if the resulting jet performance is to be correctly simulated within the model. This is typically accomplished by adjusting the nozzle diameter according to the model scale, and then matching the jet to crossflow momentum ratio of the prototype system. If the prototype situation is one of a cold jet injecting into a hot environment (as is the case with most isothermal furnace systems) establishing the correct momentum ratio can only be obtained through changes to the flow conditions of either the jet or crossflow. In general, the jet injection

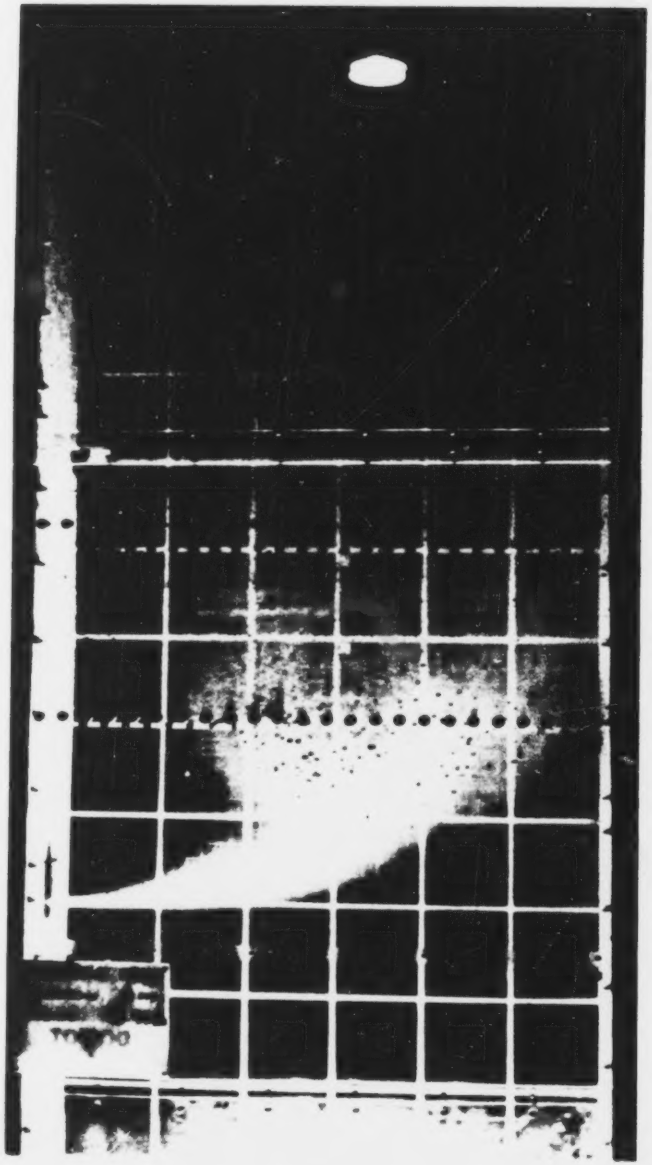

Figure 4-15. CFITF gas-solids jet.

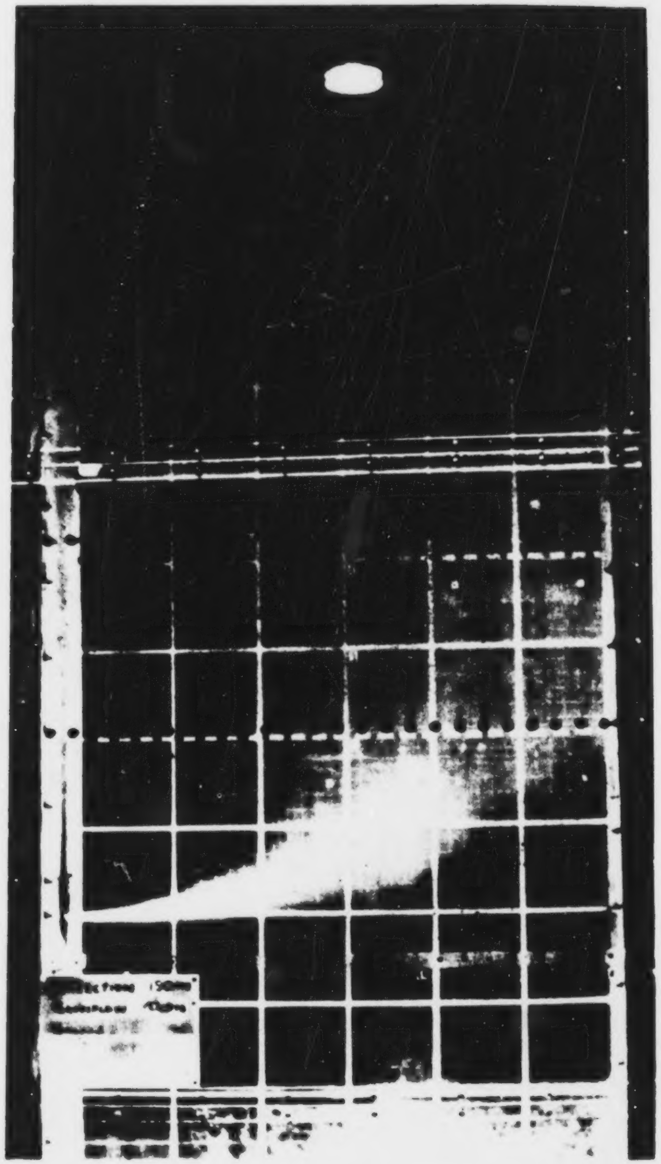

Figure 4-16. CFITF gas only jet.

velocity must be either increased or the crossflow velocity decreased. This type of adjustment, however, results in a lack of similarity between the model and prototype in that the mass flow ratio between the jet and crossflow would be higher. As the quantity of material entrained into the jet from the surrounding fluid is a function of this parameter, simulations which ignore it will overestimate the dispersion and mixing of the jet with the surrounding fluid.

As part of Task A, a new jet modeling technique was developed to model both the penetration and mixing performance of an isothermal jet injected into a crossflow at reduced scale. The technique is derived below with the following variables being held equal in the model and the prototype.

1) $\dot{m}$ jet/$\dot{m}$ crossflow
2) jet centerline trajectory

As detailed in Table 4-3 the correlation of Patrick (1967) is very similar to that used by many researchers, and gives similar numerical results. Thus, the scaling criteria was based upon Patrick's correlation, which is:

$$\frac{Y}{d_{jet}} = (1.0)\, J^{0.425} \left(\frac{X}{d_{jet}}\right)^{0.38} \qquad (4\text{-}2)$$

For trajectory similarity, y/x in the model and in the prototype must be equal. Rearranging Eq. (4-2) yields the following equation for y/x:

$$\frac{Y}{X} = J^{0.425}\, d_{jet}^{\;0.62}\, X^{-0.62} \qquad (4\text{-}3)$$

This equation can be reduced to a single expression in terms of $\dot{m}$ jet/$\dot{m}$ crossflow by use of the definition of J:

$$J = \frac{(\rho V^2)_{jet}}{(\rho V^2)_{crossflow}} \qquad (4\text{-}4)$$

TABLE 4-3. JET PENETRATION CORRELATIONS

INVESTIGATOR (REFERENCE)	FLUIDS	FORM OF CORRELATION	LOCATION OF JET PATH	MOMENTUM RATIO, J
Patrick (1967)	Gas Jets	$\frac{Y}{d_{jet}} = (1.0)\ J^{0.425}\left(\frac{X}{d_{jet}}\right)^{0.38}$	Center of mass concentration profile	45.2
Kamotani and Greber (1971, 1972)	Gas Jets	$\frac{Y}{d_{jet}} = (0.89)\ J^{0.49}\left(\frac{X}{d_{jet}}\right)^{0.36}$	Velocity centerline	15-60
Ivanov (Mohr, 1972)	Gas Jets	$\frac{Y}{d_{jet}} = (1.0)\ J^{0.433}\left(\frac{X}{d_{jet}}\right)^{0.33}$	Velocity Centerline	1.25-1000
Shandorov (Mohr, 1972)	Gas Jets	$\frac{Y}{d_{jet}} = (1.0)\ J^{0.392}\left(\frac{X}{d_{jet}}\right)^{0.392}$	Velocity Centerline	2 - 21.7
Rudinger (1975)	Gas Jets	$\frac{Y}{d_{jet}} = (1.39) J^{0.4}\left(\frac{X}{d_{jet}}\right)^{0.29}$	Velocity Centerline	summary of other invesitgators data
Salzman & Schwartx (1978)	Gas/Solids Jets	$\frac{Y}{d_{jet}} = (1.92)\ J^{0.325}\left(\frac{X}{d_{jet}}\right)^{0.33}$	Mass Concentration Centerline	?
Rudinger (1975)	Gas/Solids Jets	$\frac{Y}{d_{jet}} = C\left(\frac{\dot{m}_{solids}}{\dot{m}_{gas}}\right) J^{0.3}\left(\frac{X}{d_{jet}}\right)^{0.3}$	Mass Concentration Centerline	1-10

and:

$$\dot{m} = \rho V A \tag{4-5}$$

this results in the expression:

$$\frac{y}{x} = \left[\left[\frac{\dot{m}_{jet}}{\dot{m}_{crossflow}}\right]^2 \frac{A^2_{crossflow}}{\pi^2/16}\left[\frac{\rho_{crossflow}}{\rho_{jet}}\right]\right]^{0.425}\left[\frac{1}{d_{jet}}\right]^{1.08}\left[\frac{1}{x}\right]^{0.62} \tag{4-6}$$

For equal trajectories:

$$\left.\frac{y}{x}\right|_{prototype} = \left.\frac{y}{x}\right|_{model} \tag{4-7}$$

Also equating mass flow ratios:

$$\left.\frac{\dot{m}_{jet}}{\dot{m}_{crossflow}}\right|_{prototype} = \left.\frac{\dot{m}_{jet}}{\dot{m}_{crossflow}}\right|_{model} \tag{4-8}$$

and utilizing a linear scaling factor defined as:

$$SF = \frac{x_{prototype}}{x_{model}} \tag{4-9}$$

Results in a relation for the model jet nozzle diameter:

$$\frac{d_{jet}\big|_{model}}{d_{jet}\big|_{prototype}} = SF\left[\left.\frac{\rho_{crossflow}}{\rho_{jet}}\right|_{model}\left.\frac{\rho_{jet}}{\rho_{crossflow}}\right|_{prototype}\right]^{0.394} \tag{4-10}$$

In the isothermal model ρjet = ρ crossflow, therefore:

$$d_{jet}\Big|_{model} = \frac{d_{jet}\Big|_{prototype}}{SF}\left[\frac{\rho_{jet}}{\rho_{crossflow}}\Bigg|_{prototype}\right]^{0.393} \qquad (4\text{-}11)$$

With the jet scaling criteria developed above, injection nozzles were sized for use in the 0.46 scale isothermal flow model of the BSF. Table 4-4 gives a summary of these scaling calculations.

The jet velocities shown where calculated by the equation below with d_{jet} from equation 4-11, $\dot{m}_{jet}$ from equation 4-8, and $\dot{m}$ crossflow set to the test facilities capacities.

$$V_{jet}\Big|_{model} = \frac{\dot{m}_{jet}\,4}{d_{jet}^{\,2}\,\pi} \qquad (4\text{-}12)$$

4.3.4 Isothermal Flow Model Tests

4.3.4.1 Baseline Flow Field Characterization

Flow modeling tests were performed in the LSFATF modified to match the BSF. The first series of tests was a baseline evaluation of the furnace aerodynamics with no injectors in operation. This evaluation included both flow visualization and quantitative three-dimensional velocity profiling.

Figure 4-17 shows observations made during the flow visualization tests, detailing the flow fields in the four lanes formed by the three simulated pendant superheater panels. Note, the region within the superheater panels is felt to be the most favorable location for sorbent injection at the BSF. The front to back gas flow distributions were found to be closely tied to the swirling flow field of the lower furnace. In general, the counterclockwise rotating flow established in the lower furnace was maintained until the pendant superheater panels were encountered. At this point the gases were

TABLE 4-4. SUMMARY OF SCALING CALCULATIONS

BSF Jet Velocity (Hot) m/sec (ft/sec)	BSF Crossflow Velocity m/sec (ft/sec)	No. of Jets	BSF Jet Dia. (Hot) m (in)	BSF Jet Vel. (Cold) m/sec (ft/sec)	BSF Jet Dia. (Cold) m (in)	Flow Model Jet m (in)	Momentum Ratio BSF (Hot)	Momentum Ratio Model (Cold)
7.6 (25)	3.1 (10)	4	0.1 (4.04)	11.1 (36.4)	0.2 (8.04)	0.09 (3.7)	35.25	13.2
15.2 (50)	3.1 (10)	4	0.07 (2.85)	22.1 (72.4)	0.14 (5.67)	0.066 (2.61)	141	52.1
22.9 (75)	3.1 (10)	4	0.06 (2.33)	33.25 (109.1)	0.11 (4.63)	0.05 (2.13)	317	119
7.6 (25)	3.1 (10)	8	0.07 (2.85)	11.1 (36.4)	0.14 (5.67)	0.066 (2.61)	35.25	13.2
15.2 (50)	3.1 (10)	8	0.055 (2.20)	22.1 (72.4)	0.10 (4.02)	0.046 (1.85)	141	52.1
22.9 (75)	3.1 (10)	8	0.042 (1.65)	33.25 (109.1)	0.08 (3.29)	0.038 (1.51)	317	119
7.6/22.9 (25/75)	3.1 (10)	8	0.07 (2.85) 0.042 (1.65")	11.1 (36.4) 33.25 (1.09.1)	0.14 (5.67) 0.08 (3.29")	0.066 (2.61) 0.038 (1.51)	35.25 317	13.2 119

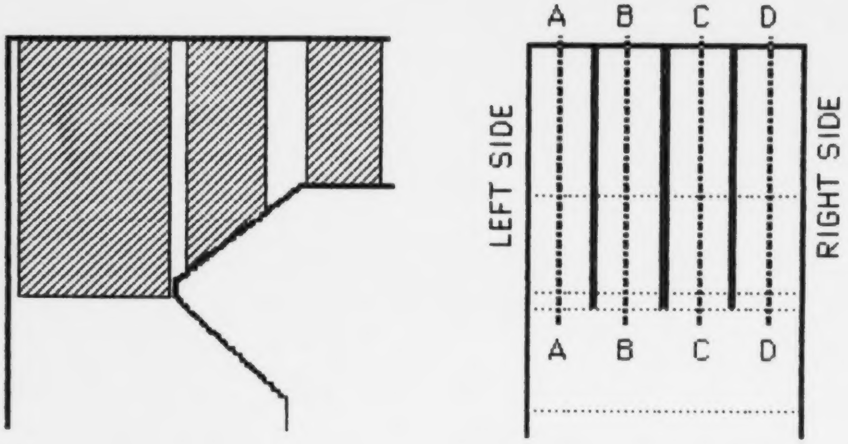
A
B
C
D
LEFT SIDE
RIGHT SIDE
A
B
C
D

SIDE VIEW FRONT VIEW

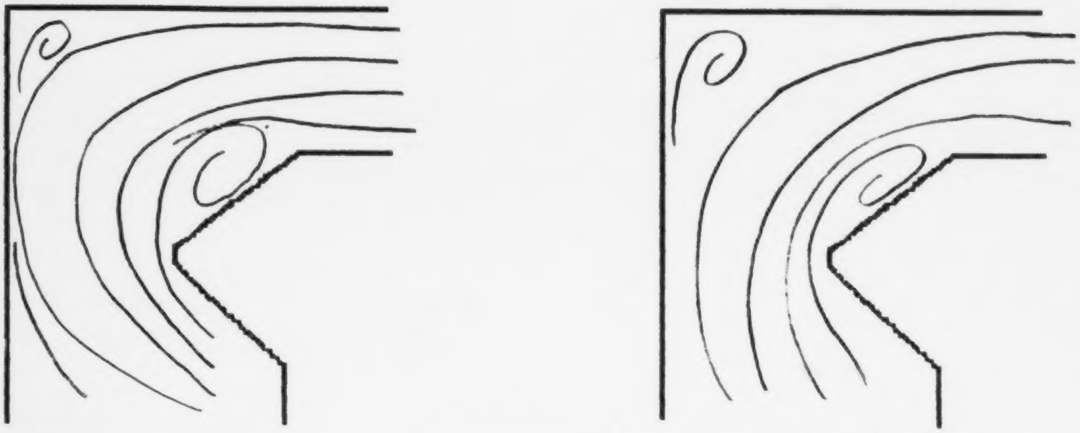

SECTION AA - LANE 4 SECTION BB - LANE 3

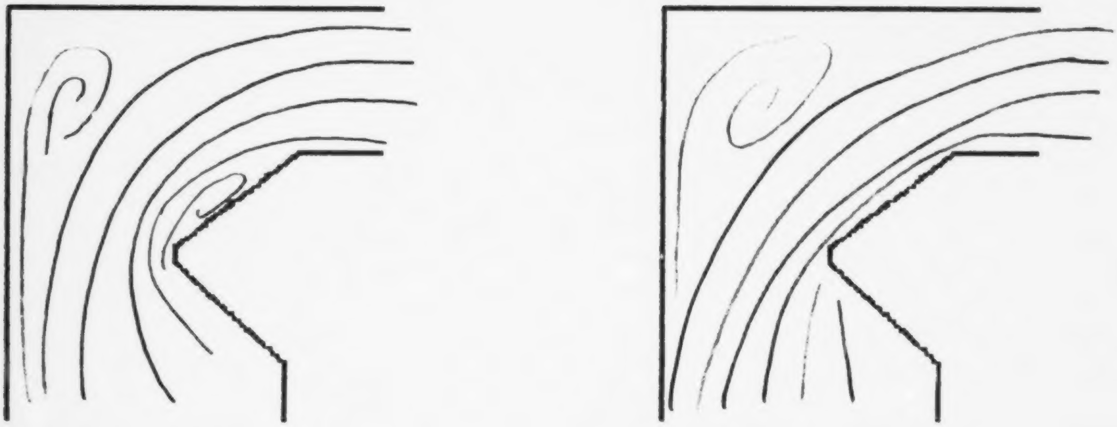

SECTION CC - LANE 2 SECTION DD - LANE 1

Figure 4-17. Upper furnace streak lines observed during flow visualization tests.

sliced into four independent flow streams (lanes) with little redistribution between the lanes until well back into the unit. The distribution of flow within the four lanes formed by the panels is not uniform. In the right hand channel, Lane 1, between the panel and the outer wall, the tangential component of flow was directed towards the rear of the unit. Between the left wall and panel the flow is directed towards the front. Because of this, the flow within the right channel is directed out of the unit smoothly over the arch eliminating recirculation above the arch. Because the bulk of the flow in the right channel leaves near the arch, the volume of the upper furnace is not effectively utilized and a large recirculation pattern is created near the upper corner of the front wall and roof. Front wall sorbent injection systems mounted within this right most channel would therefore encounter a stagnant recirculation zone.

A different flow pattern is encountered within the channel along the left side of the unit, Lane 4. Within this channel, the gas flow impacts the front wall of the furnace and turns 180 degrees before exiting the unit. In the process of turning, the gases flow vertically along the front wall of the unit before exiting the unit with most of the flow near the roof. Accordingly, sorbent injection from the front wall into this channel will encounter a higher crossflow than injection into the other three channels. It was also observed that because of the reversed nature of flow in this channel a large recirculation zone is formed above the nose of the arch. The flow behavior in the center lanes is a proportional mix between the flow behavior in the right and left lanes.

Velocity profiles were measured at the planes shown in Figure 4-18. Figures 4-19 through 4-44 present the results of these evaluations. This quantitative data verified the flow visualization evaluation. Of particular interest to sorbent injection studies are the flow fields at the beginning of the sulfation temperature window within the upper furnace. In the case of the BSF, the beginning of this window is located at the bottom of the pendant superheater panels at the horizontal furnace outlet plane (Test Plane 4). At this location, the flow field swirls counterclockwise. The highest tangential velocities and highest axial mass flows were found along the walls of the unit. When the flow encounters the superheater panels, the two outer channels

THIS PAGE WAS INTENTIONALLY LEFT BLANK TO
PERMIT FIGURES FOR THE SAME TEST PLANE TO APPEAR
ON OPPOSITE PAGES

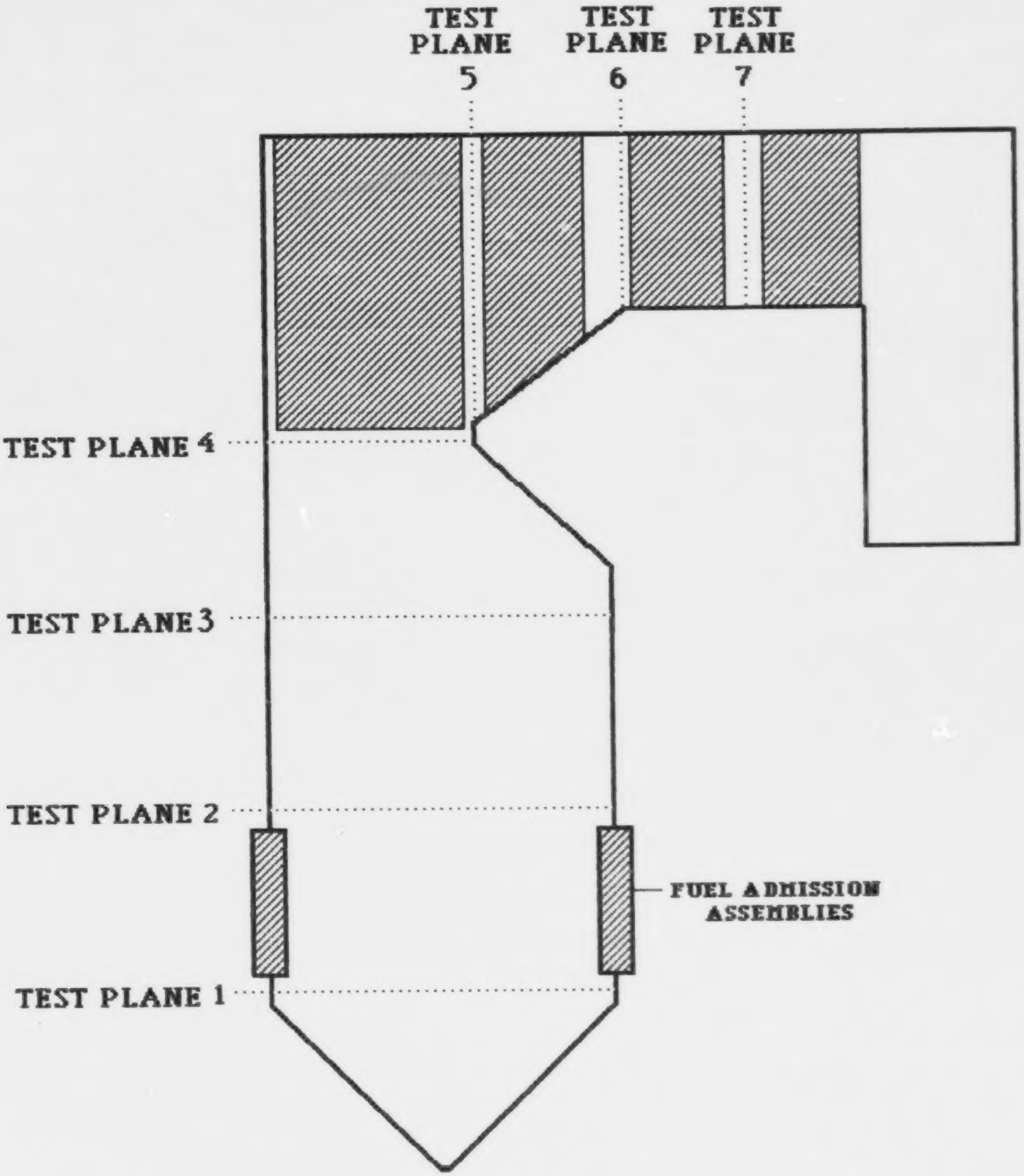
TEST PLANE 5
TEST PLANE 6
TEST PLANE 7
TEST PLANE 4
TEST PLANE 3
TEST PLANE 2
FUEL ADMISSION ASSEMBLIES
TEST PLANE 1

Figure 4-18. BSF flow model test plane locations.

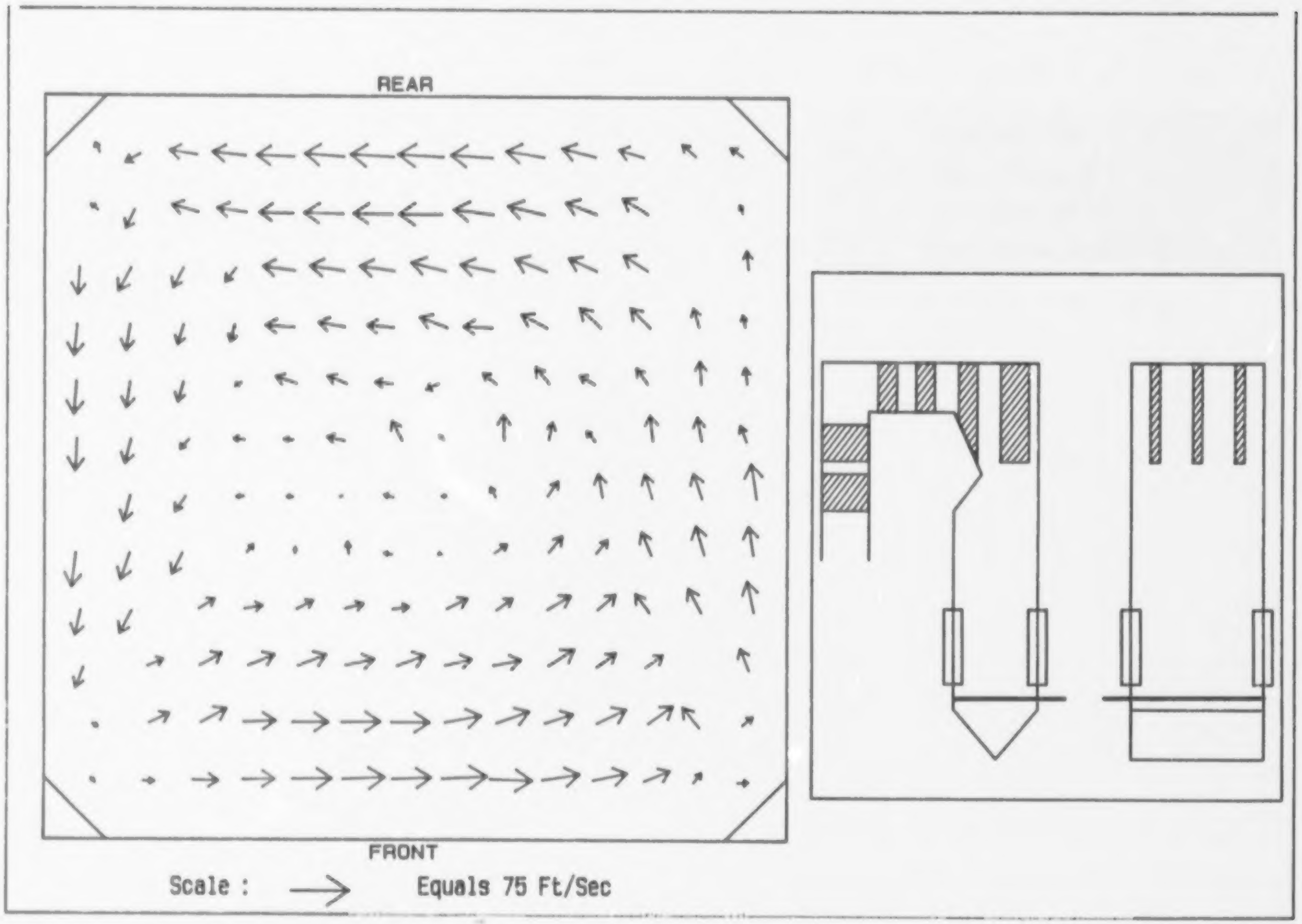

Figure 4-19. Baseline furnace velocity vectors: Test Plane 1.

Average Velocity = 1.69 Ft/Sec
RMS DEVIATION = 1067.84 %

REAR

-8.75	-14.70	-11.28	-8.46	-8.83	-5.58	-5.86	-8.84	-7.14	-5.91	-7.68	-8.28	-7.69	-4.81
-14.21	-12.21	-5.06	-2.37	1.66	-0.69	3.86	1.57	3.15	3.41	0.58	0.07		-8.44
-10.27	-8.03	-6.58	-3.46	3.27	4.58	6.50	8.66	7.50	8.29	8.54	5.67	0.58	-7.17
12.77	13.32	10.46	8.18	10.49	13.65	12.84	10.32	11.77	8.38	7.37	5.65	-14.12	-20.06
17.56	14.34	10.84	13.06	8.61	11.39	18.07	15.84	12.28	11.08	11.66	12.74	-12.98	-22.46
17.48	15.31	13.26	8.68	12.70	14.72	16.56	25.00	2.24	13.16	13.10	-8.96	-14.70	-24.53
15.18	17.06	10.48	10.84	14.47	18.41	17.42	21.65	18.23	11.97	-6.13	-8.81	-12.82	-2.30
-8.87	-6.27	-0.39	7.86	12.50	13.77	14.12	20.16	18.81	11.58	13.17	9.00	6.04	-1.67
-10.18	-4.31	-2.48	-0.88	1.07	6.06	7.65	10.55	13.81	8.50	6.15	6.43	1.65	-2.56
-10.71	-12.13	-6.97	-3.58	-4.22	-0.75	-0.48	-0.77	-0.44	2.23	1.31	-0.74	-2.28	-2.04
-18.53	-14.06	-8.65	-8.28	-8.58	-6.07	-4.84	-4.40	-5.82	-3.55	-3.66	-4.65	-5.13	-7.80
-8.51	-16.24	-13.40	-12.35	-12.60	-15.53	-13.43	-11.63	-12.21	-10.72	-10.37	-8.34	-12.28	-2.34

FRONT

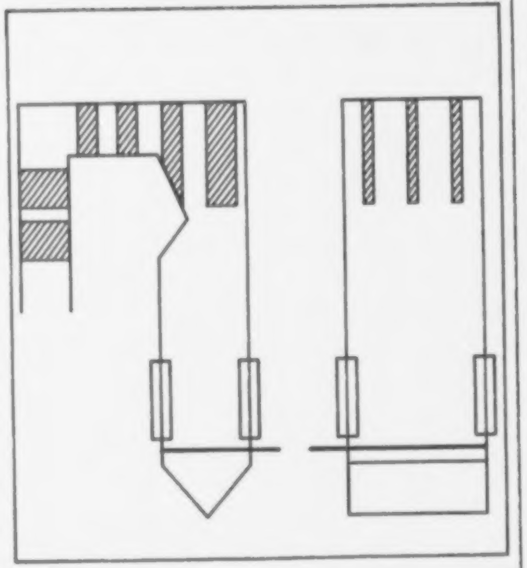

Figure 4-20. Normalized axial velocities: Test Plane 1.

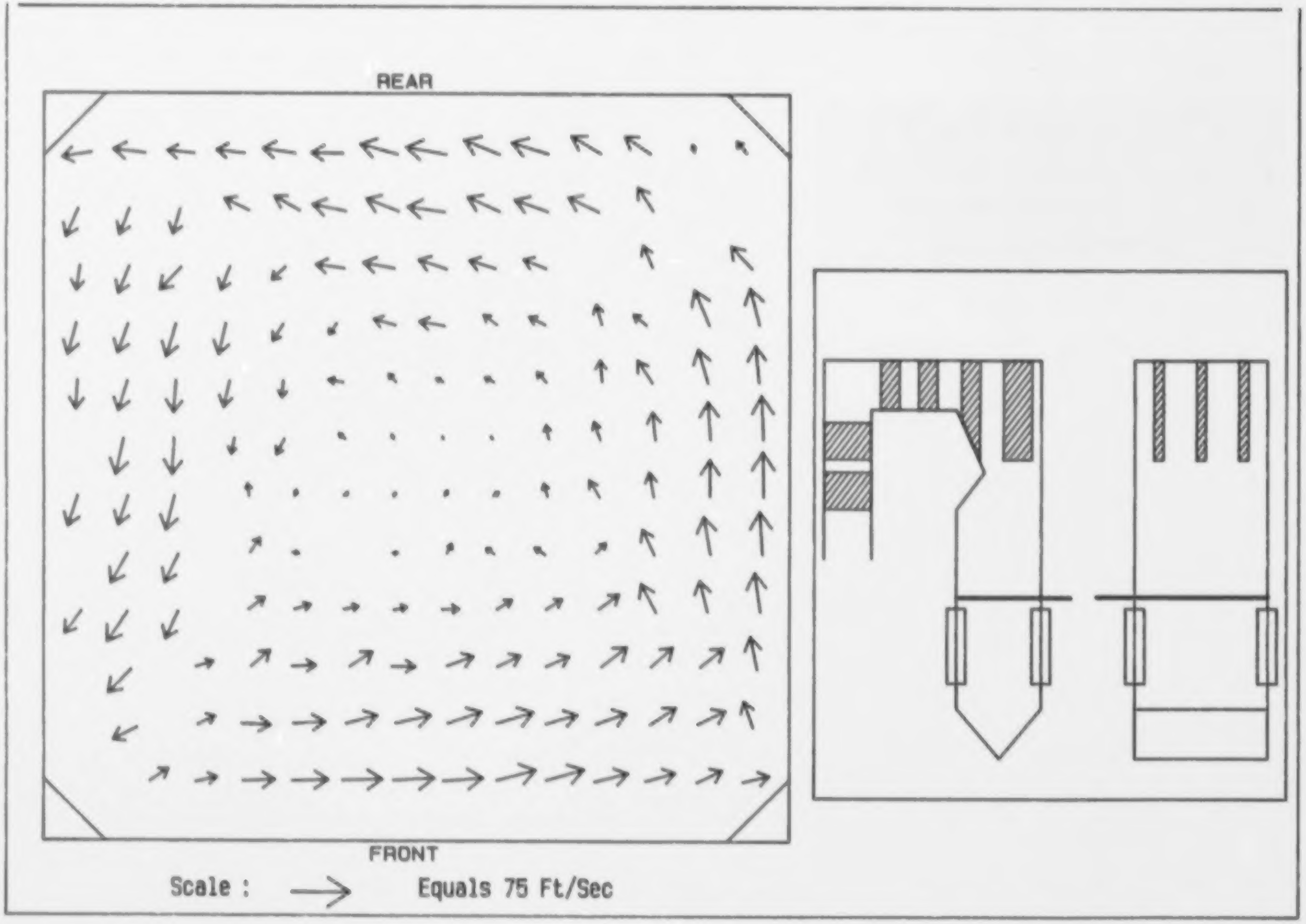

Figure 4-21. Baseline furnace velocity vectors: Test Plane 2.

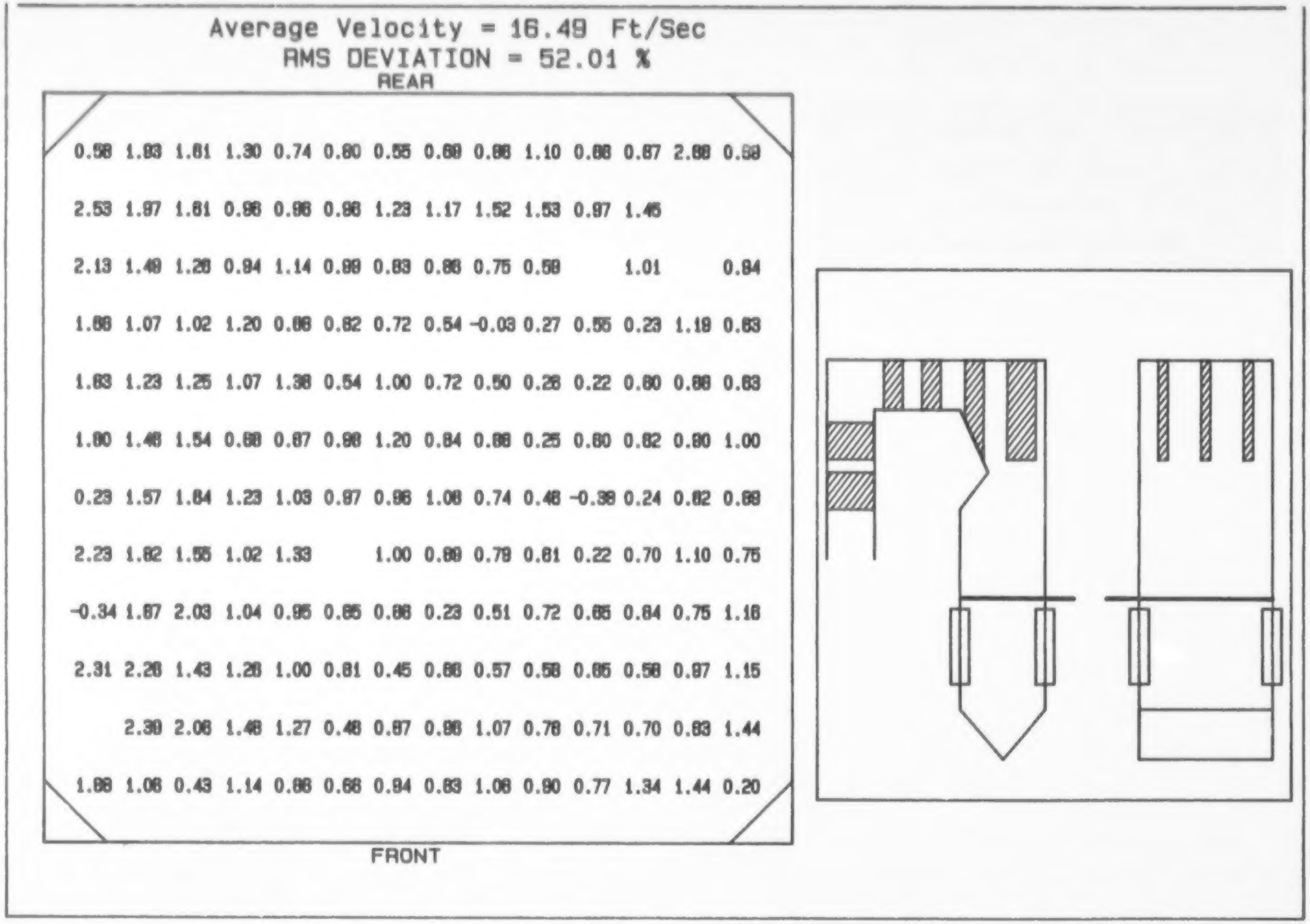

0.58	1.93	1.81	1.30	0.74	0.80	0.55	0.69	0.86	1.10	0.88	0.87	2.88	0.58
2.53	1.97	1.81	0.98	0.96	0.98	1.23	1.17	1.52	1.53	0.97	1.45		
2.13	1.49	1.28	0.94	1.14	0.99	0.83	0.86	0.75	0.58		1.01		0.84
1.88	1.07	1.02	1.20	0.88	0.82	0.72	0.54	-0.03	0.27	0.55	0.23	1.19	0.63
1.63	1.23	1.25	1.07	1.38	0.54	1.00	0.72	0.50	0.28	0.22	0.80	0.88	0.63
1.80	1.48	1.54	0.68	0.87	0.98	1.20	0.84	0.86	0.25	0.80	0.82	0.90	1.00
0.23	1.57	1.84	1.23	1.03	0.97	0.96	1.08	0.74	0.48	-0.38	0.24	0.82	0.89
2.23	1.82	1.55	1.02	1.33		1.00	0.89	0.79	0.81	0.22	0.70	1.10	0.75
-0.34	1.87	2.03	1.04	0.95	0.85	0.86	0.23	0.51	0.72	0.65	0.84	0.75	1.16
2.31	2.28	1.43	1.28	1.00	0.81	0.45	0.68	0.57	0.58	0.65	0.58	0.97	1.15
	2.39	2.06	1.48	1.27	0.48	0.87	0.98	1.07	0.78	0.71	0.70	0.83	1.44
1.88	1.06	0.43	1.14	0.86	0.68	0.94	0.83	1.06	0.90	0.77	1.34	1.44	0.20

Figure 4-22. Normalized axial velocities: Test Plane 2.

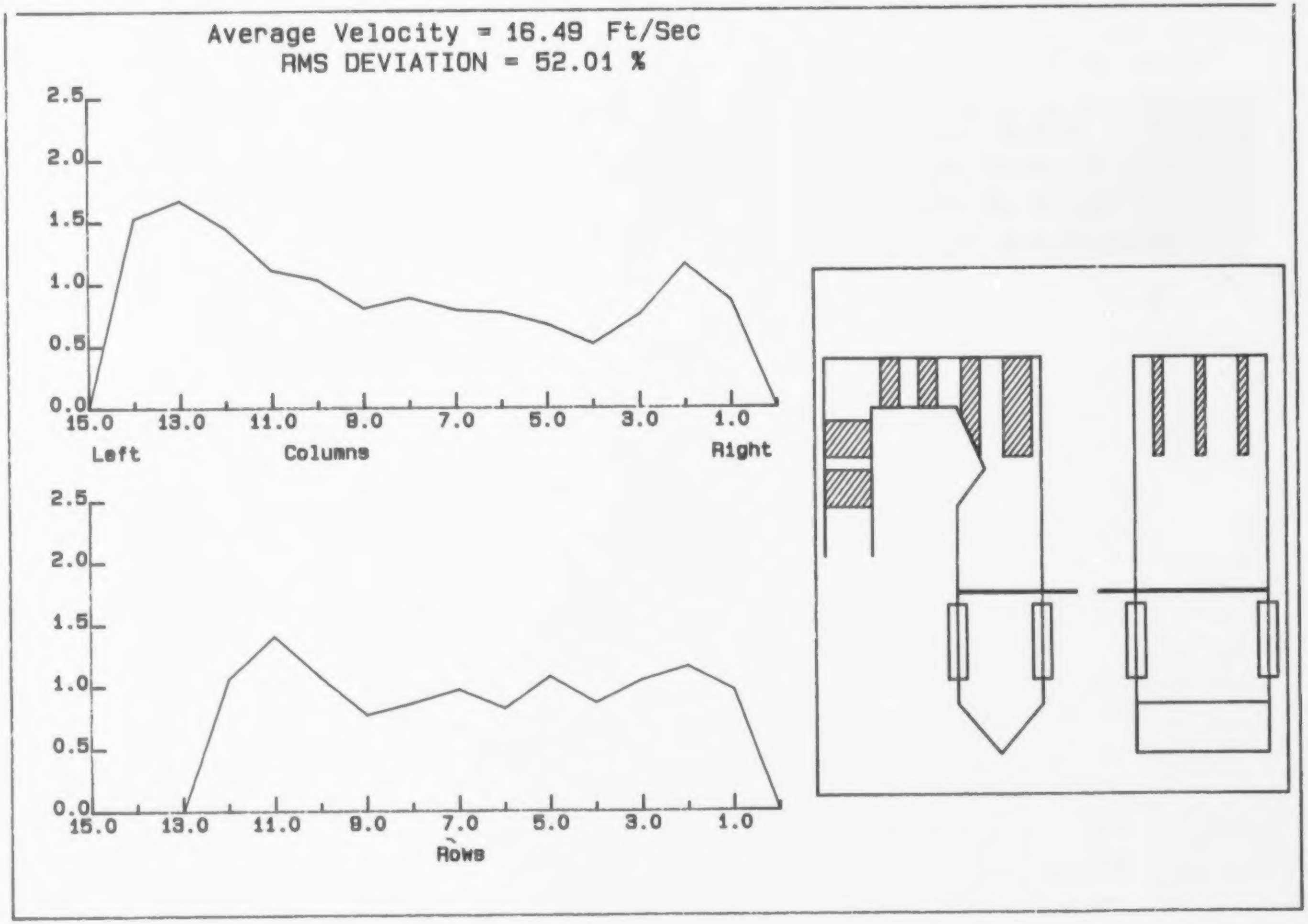

Figure 4-23. Baseline furnace normalized velocity profiles: Test Plane 2.

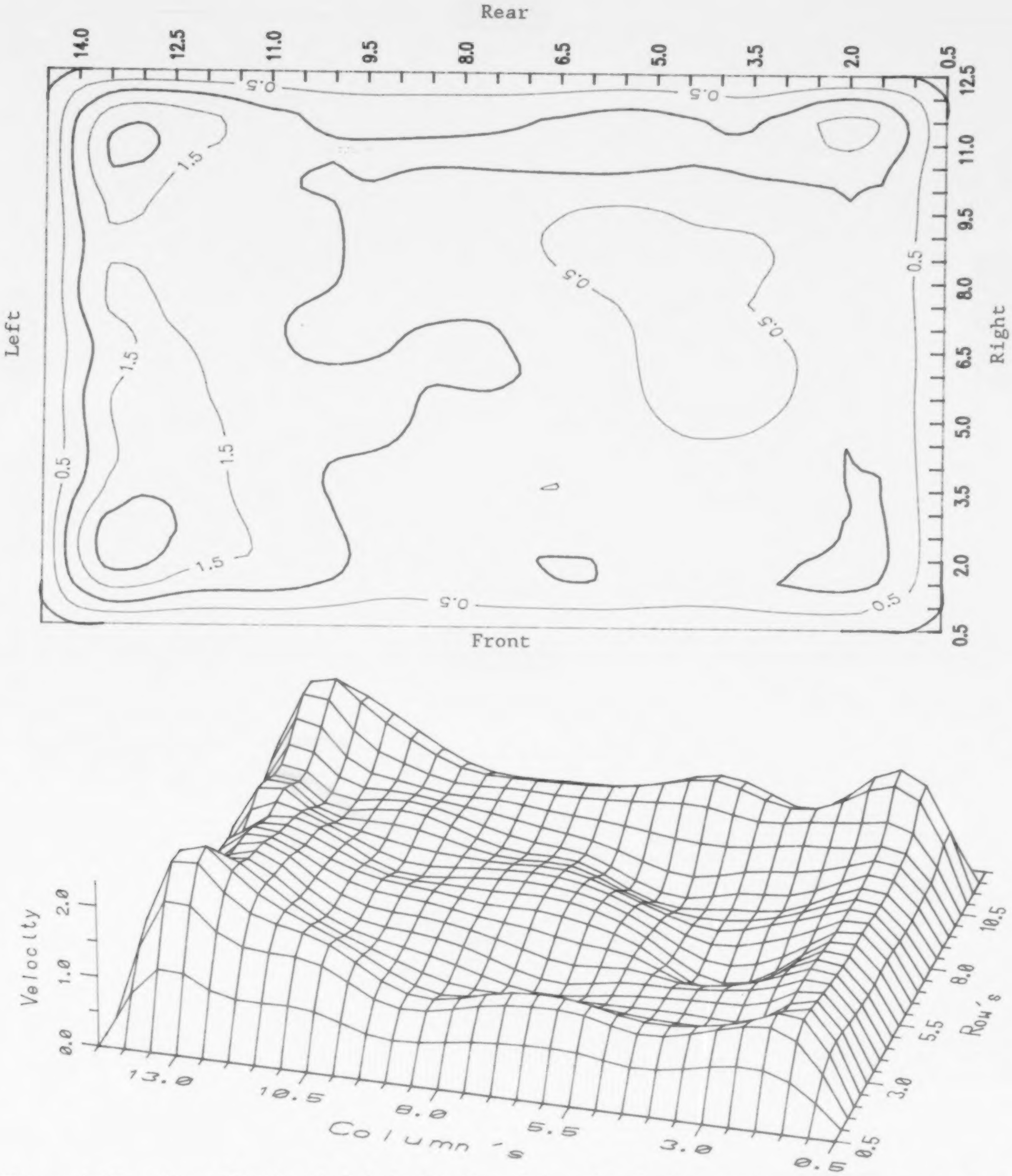

Figure 4-24. Normalized axial isovelocity plot and velocity contour plot: Test Plane 2.

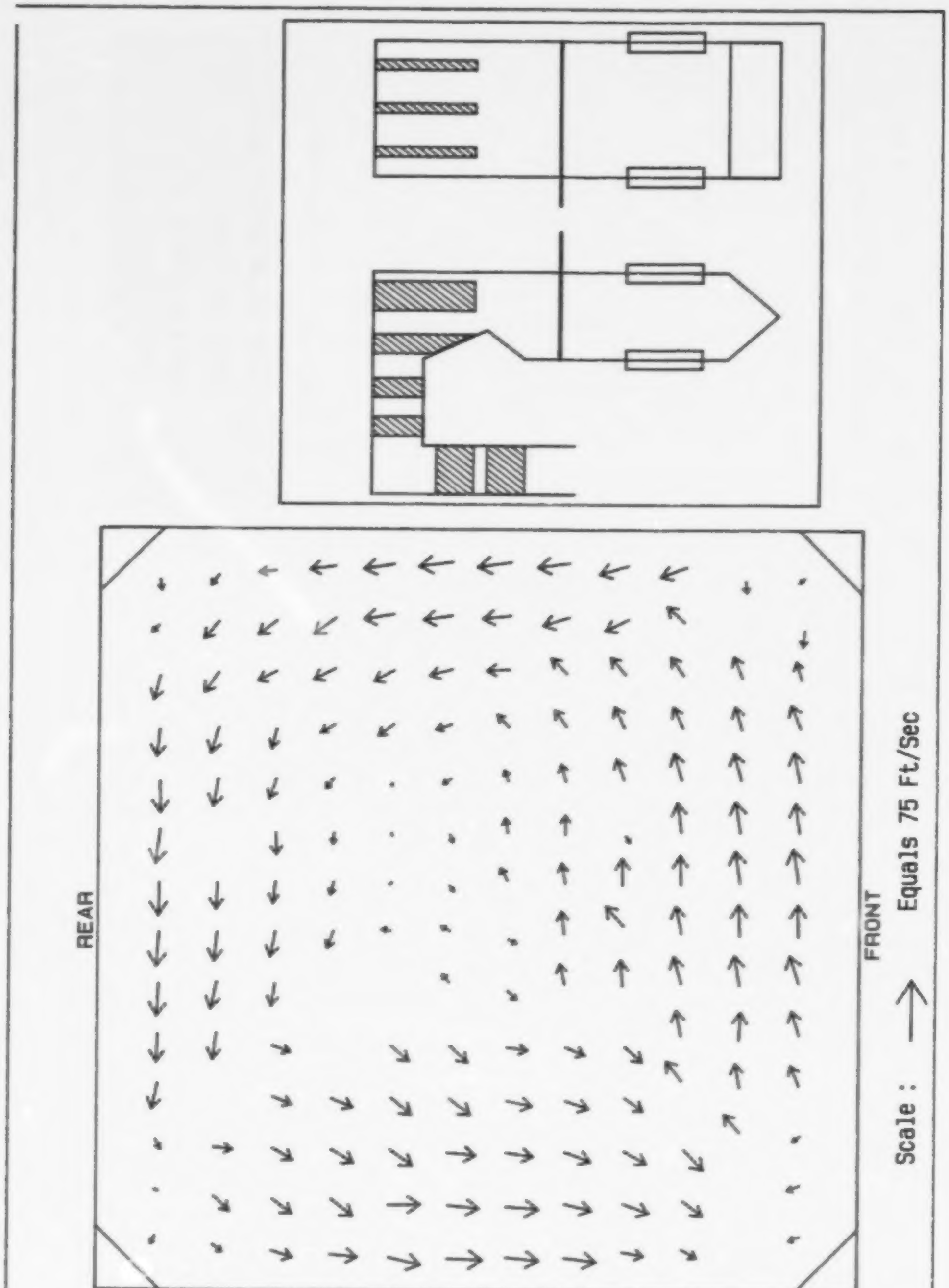

Figure 4-25. Baseline furnace velocity vectors: Test Plane 3.

Average Velocity = 12.13 Ft/Sec
RMS DEVIATION = 93.98 %
REAR

2.81	2.78	2.57	1.51	1.75	1.48	1.42	1.31	1.61	1.47	1.81	1.60	2.41	2.20
2.05	1.65	1.63		1.28	0.87	0.81	1.03	-1.22	1.08	1.33	1.31	1.88	1.82
1.82	1.40	1.35	0.79	0.78	0.58	0.77	0.87	0.88	1.03	0.48	1.51	1.51	2.33
1.88	0.86	0.95	0.88			0.08	1.49	0.86	0.78	1.48	1.28	1.32	1.49
1.61	1.13	0.11	0.34	-0.15		1.15	1.84	1.45	1.21	1.15	0.84	1.37	1.59
1.63	1.08	0.38	0.03	-0.05	1.14	1.16	1.63	1.40	1.69	1.26	0.89	1.01	1.84
1.84	1.06	0.26	-0.02	0.28	0.88	1.58	0.86	1.04	1.05	0.85	0.83	1.08	1.71
1.83	0.98	0.55	0.25	0.15	0.37	0.42	0.43	0.38	0.86	0.66	0.72	0.87	1.59
2.22	1.40	0.83	0.44	0.44	0.14	0.13	0.59	1.14	0.45	0.51	0.87	1.10	1.78
2.13	1.28	1.06	0.66	0.81	0.67	0.20	0.69	0.79	0.76	1.02	1.20	1.24	1.45
-2.19	-1.06	1.05	1.42	1.03	1.27	1.19	0.70	1.05	1.20	1.12	1.45	-1.86	-1.64
-3.07	-2.59	-1.55	2.01	2.35	2.40	1.49	1.51	1.83	1.91	1.92	1.49	-2.88	1.85

FRONT

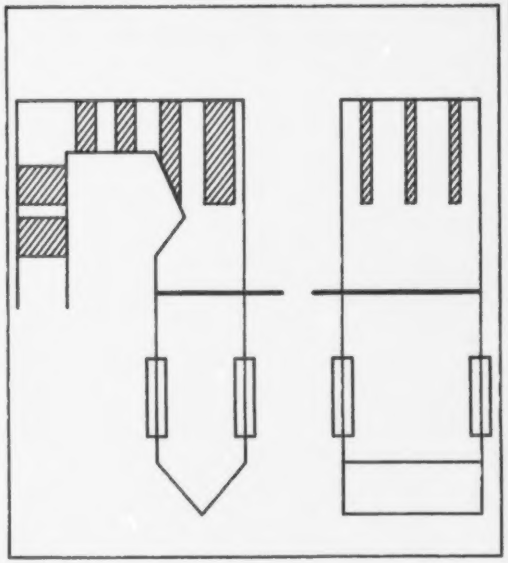

Figure 4-26. Normalized axial velocities: Test Plane 3.

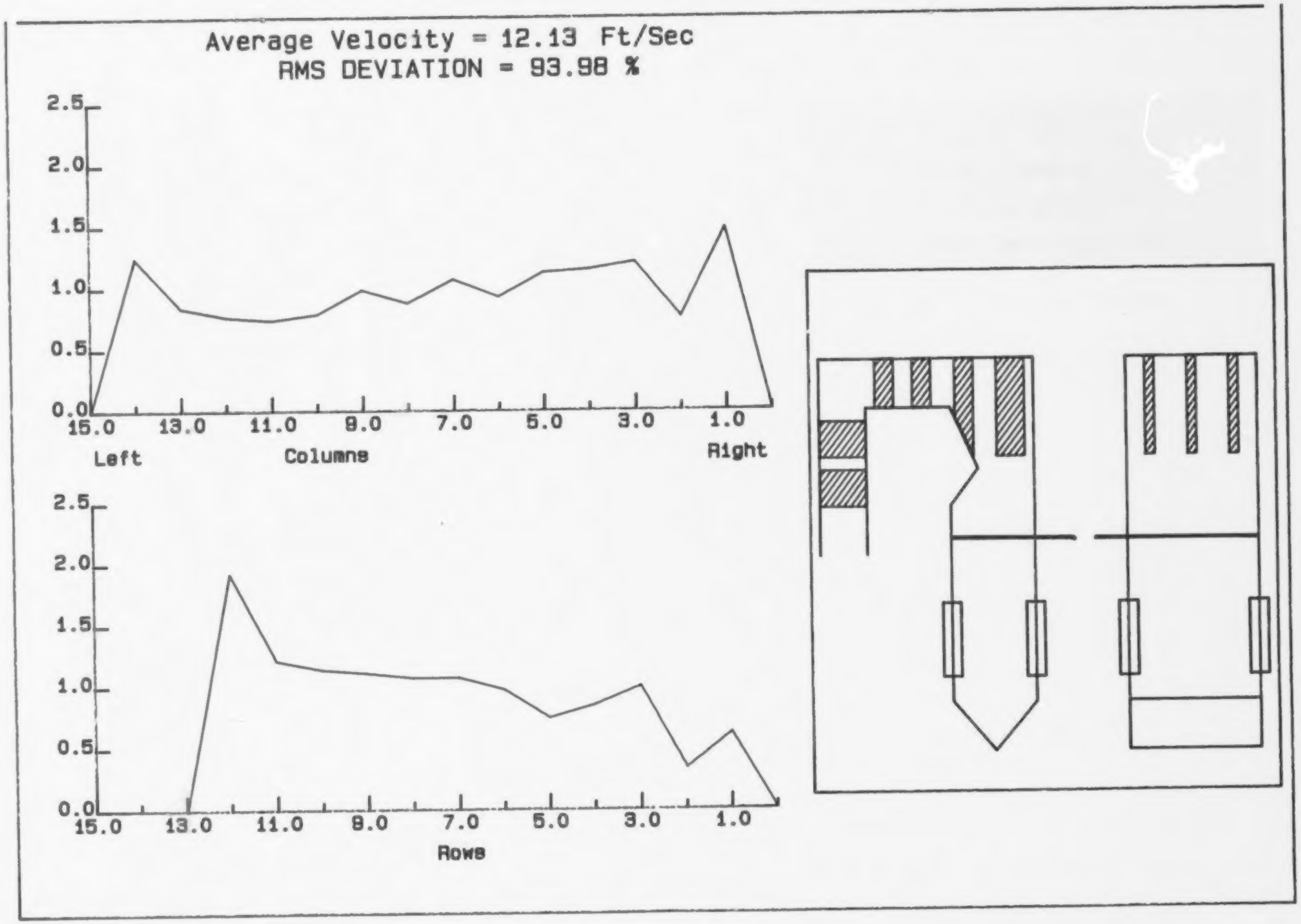

Figure 4-27. Baseline furnace normalized velocity profiles: Test Plane 3.

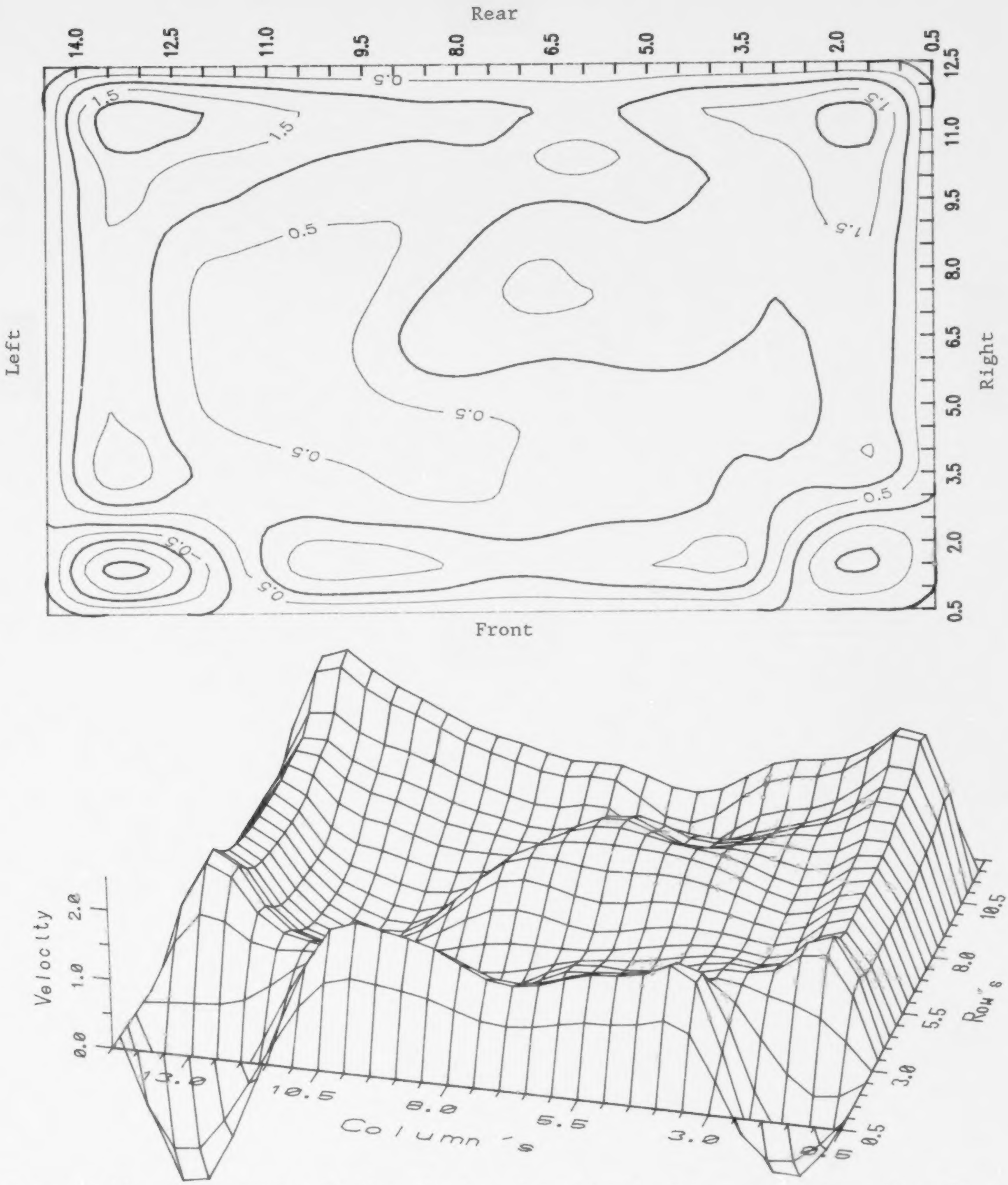

Figure 4-28. Normalized axial isovelocity plot and velocity contour plot: Test Plane 3.

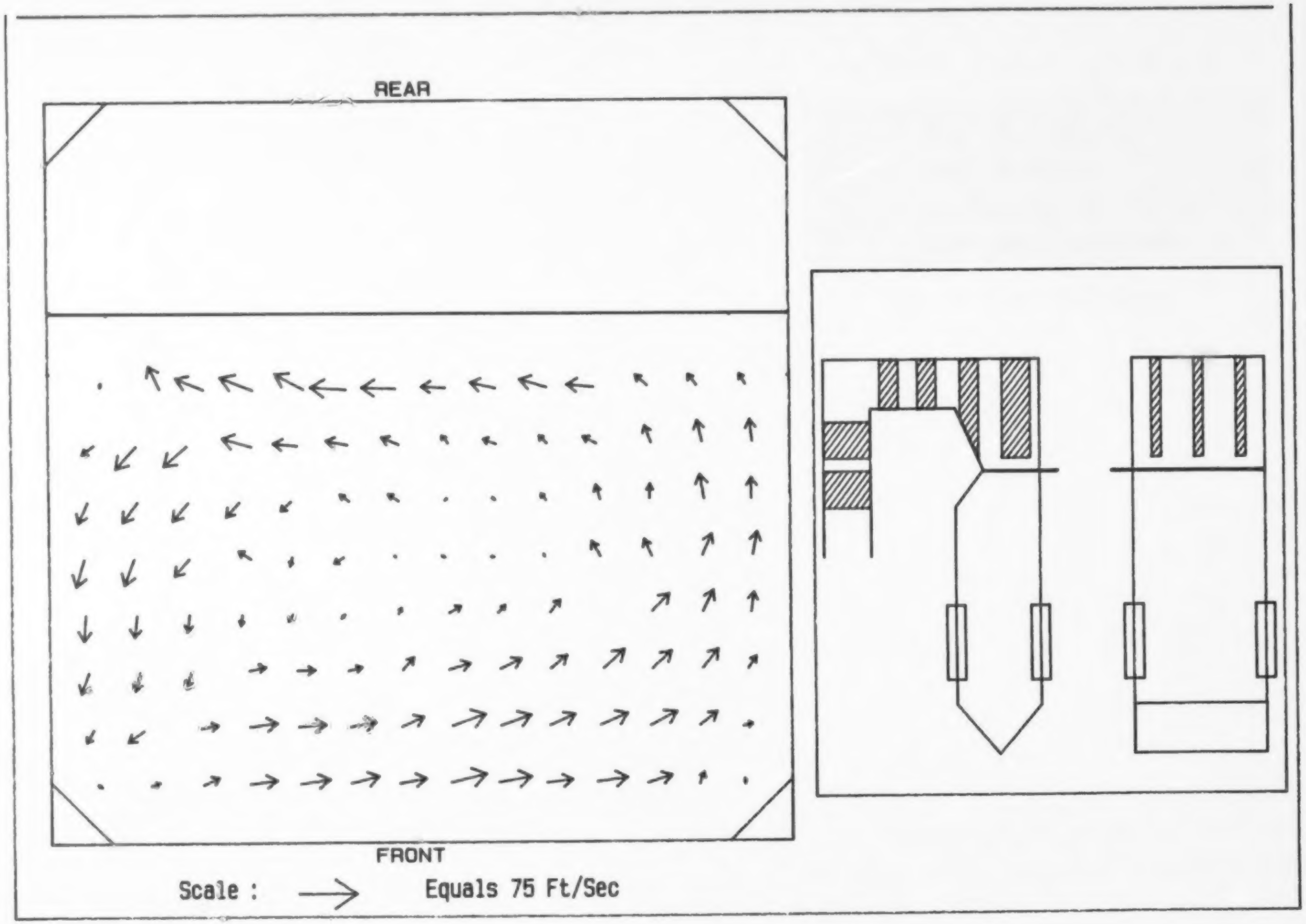

Figure 4-29. Baseline furnace velocity vectors: Test Plane 4.

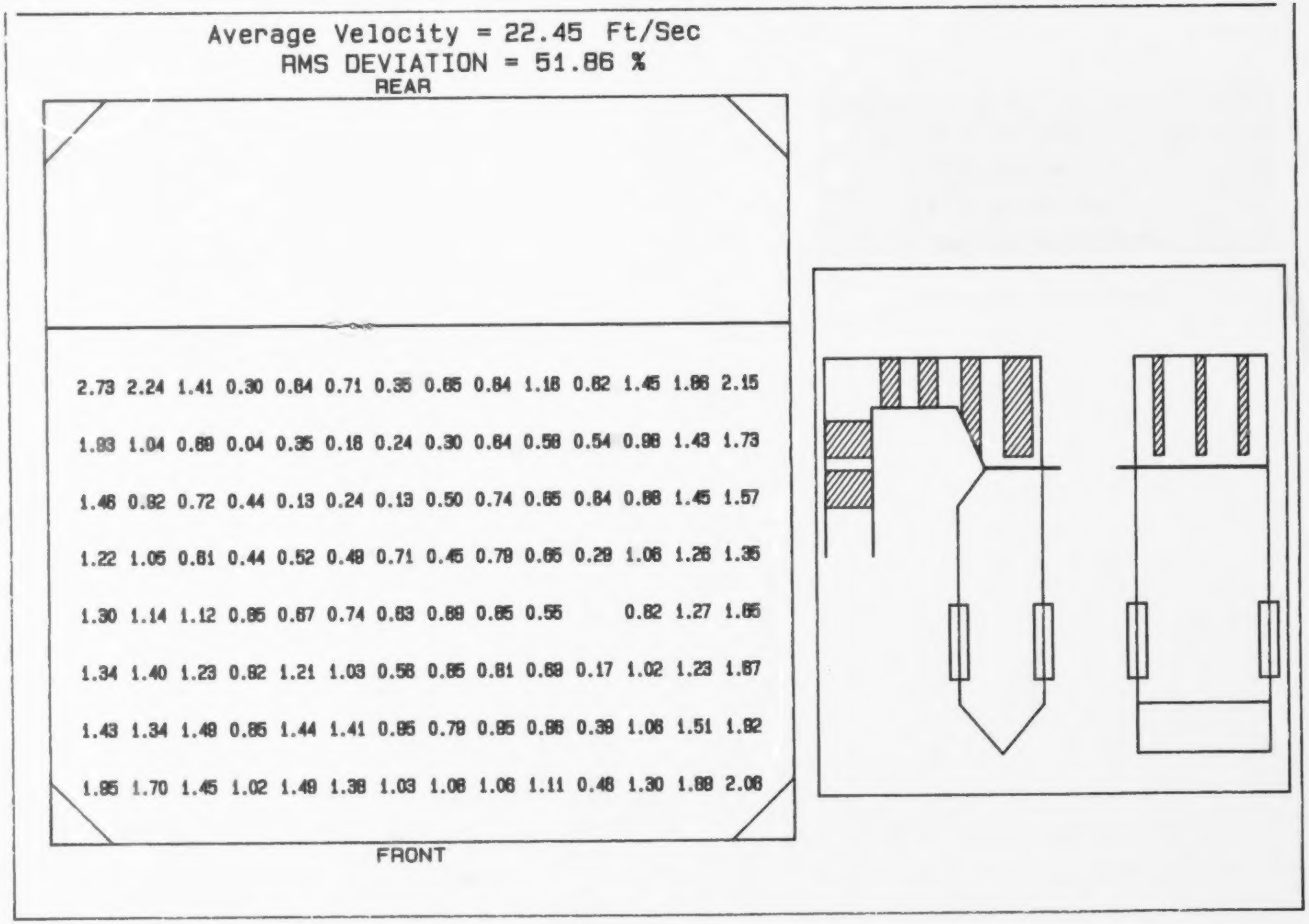

2.73	2.24	1.41	0.30	0.84	0.71	0.35	0.65	0.84	1.18	0.82	1.45	1.88	2.15
1.83	1.04	0.89	0.04	0.35	0.18	0.24	0.30	0.84	0.58	0.54	0.98	1.43	1.73
1.46	0.92	0.72	0.44	0.13	0.24	0.13	0.50	0.74	0.65	0.84	0.88	1.45	1.57
1.22	1.05	0.81	0.44	0.52	0.49	0.71	0.45	0.79	0.65	0.29	1.06	1.26	1.35
1.30	1.14	1.12	0.85	0.67	0.74	0.63	0.89	0.85	0.55		0.82	1.27	1.65
1.34	1.40	1.23	0.92	1.21	1.03	0.58	0.85	0.81	0.69	0.17	1.02	1.23	1.87
1.43	1.34	1.49	0.85	1.44	1.41	0.95	0.79	0.95	0.86	0.39	1.06	1.51	1.92
1.95	1.70	1.45	1.02	1.49	1.38	1.03	1.08	1.06	1.11	0.48	1.30	1.88	2.08

Figure 4-30. Normalized axial velocities: Test Plane 4

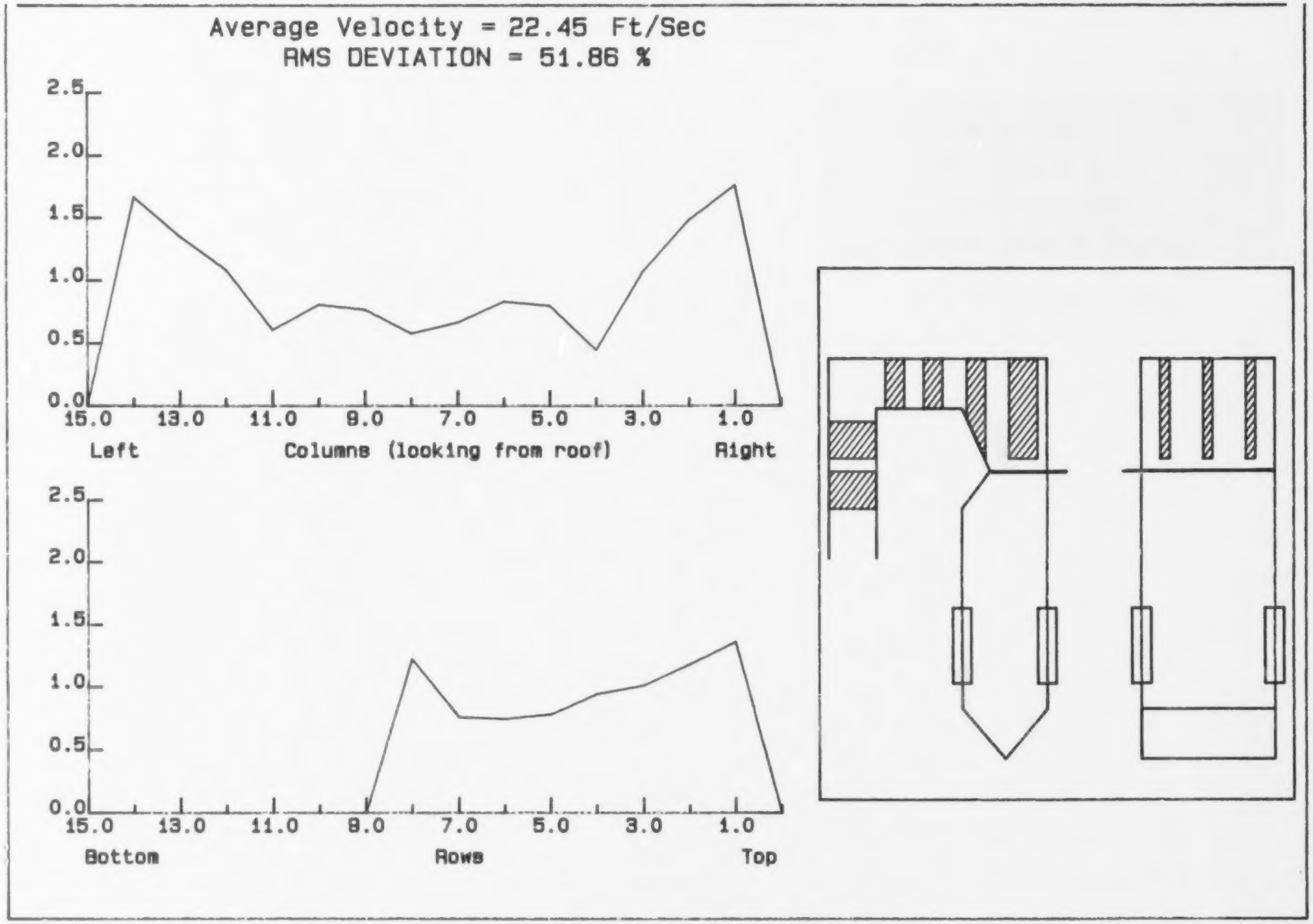

Figure 4-31. Baseline furnace normalized velocity profiles: Test Plane 4.

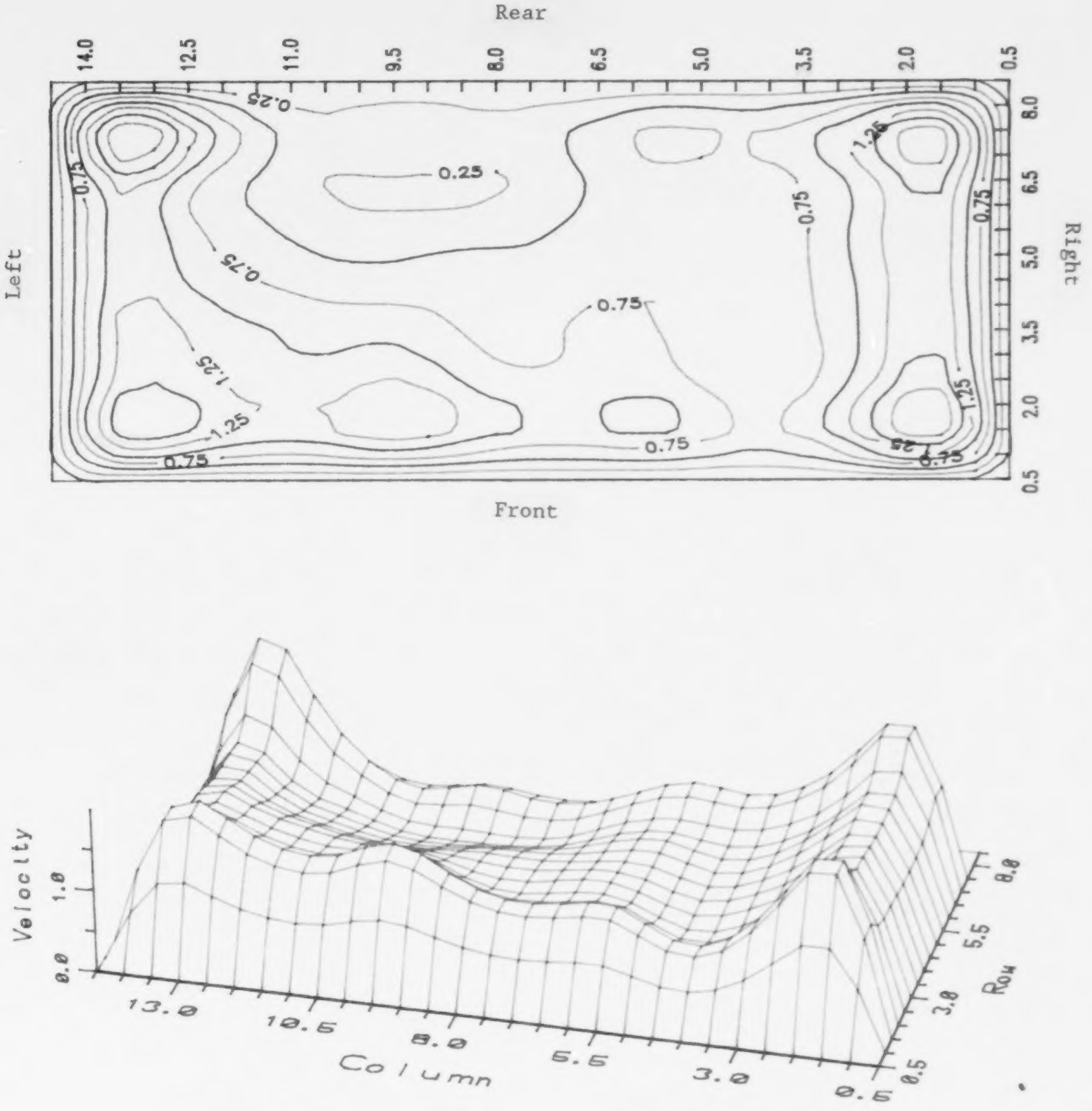

Figure 4-32. Normalized axial isovelocity plot and velocity contour plot: Test Plane 4.

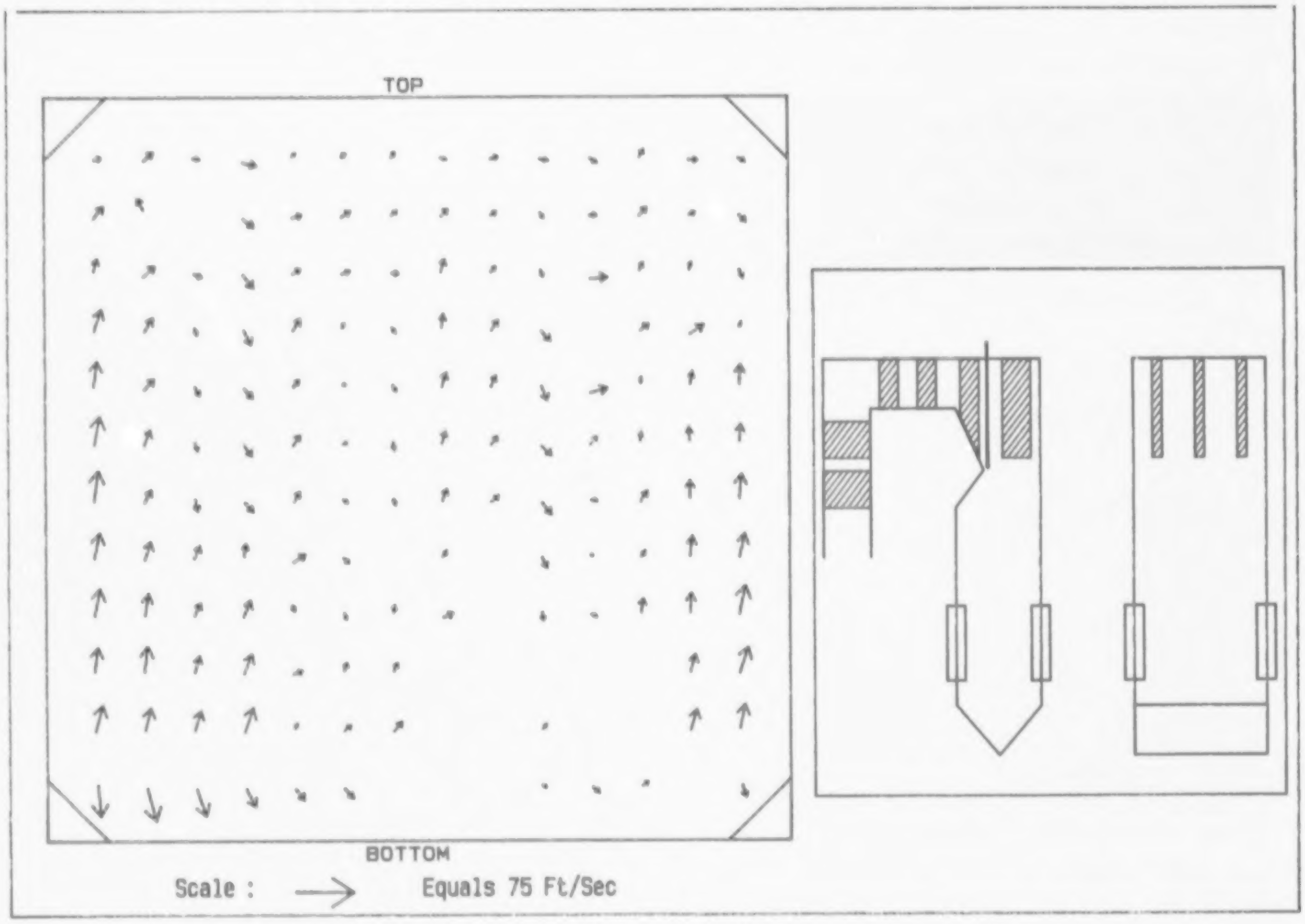

Figure 4-33. Baseline furnace velocity vectors: Test Plane 5.

Average Velocity = 16.73 Ft/Sec
RMS DEVIATION = 55.48 %
TOP

0.86	1.15	0.88	1.41	1.04	1.15	1.18	1.67	1.80	1.78	1.71	2.07	2.18	2.30
0.78	0.81		1.30	1.01	1.06	1.28	1.37	1.14	1.32	1.54	1.80	2.17	2.00
0.48	0.70	0.84	1.27	1.07	0.98	1.15	0.98	0.87	1.06	1.38	1.85	1.67	1.84
0.79	0.58	0.81	1.03	0.85	0.80	0.89	0.87	0.81	0.68		1.54	1.28	1.81
1.21	0.43	0.47	0.73	0.48	0.73	0.83	0.98	0.23	0.72	1.42	1.79	1.28	1.17
0.98	0.53	1.07	0.50	0.36	0.84	0.89	1.10	0.44	0.34	1.67	1.47	1.10	1.17
1.19	0.88	0.33	0.71	0.86	0.62	0.75	1.28	0.35	0.39	1.45	0.90	0.88	0.74
1.71	0.54	0.78	0.98	0.67	0.23		0.75		0.15	1.04	0.98	0.18	0.28
1.81	1.89	1.11	0.87	0.72	-0.17	0.24	0.79		0.02	0.50	0.50	0.25	0.55
1.97	1.92	1.13	0.96	0.84	0.57	0.20						0.51	0.84
1.78	2.01	1.57	1.24	0.87	0.85	0.48			-0.18			0.84	0.78
2.27	2.27	2.08	1.70	0.31	0.70				0.57	0.38	-0.31		0.70

BOTTOM

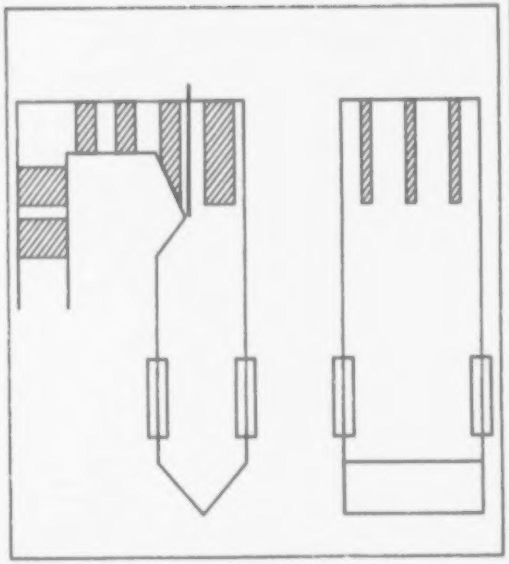

Figure 4-34. Normalized axial velocities: Test Plane 5.

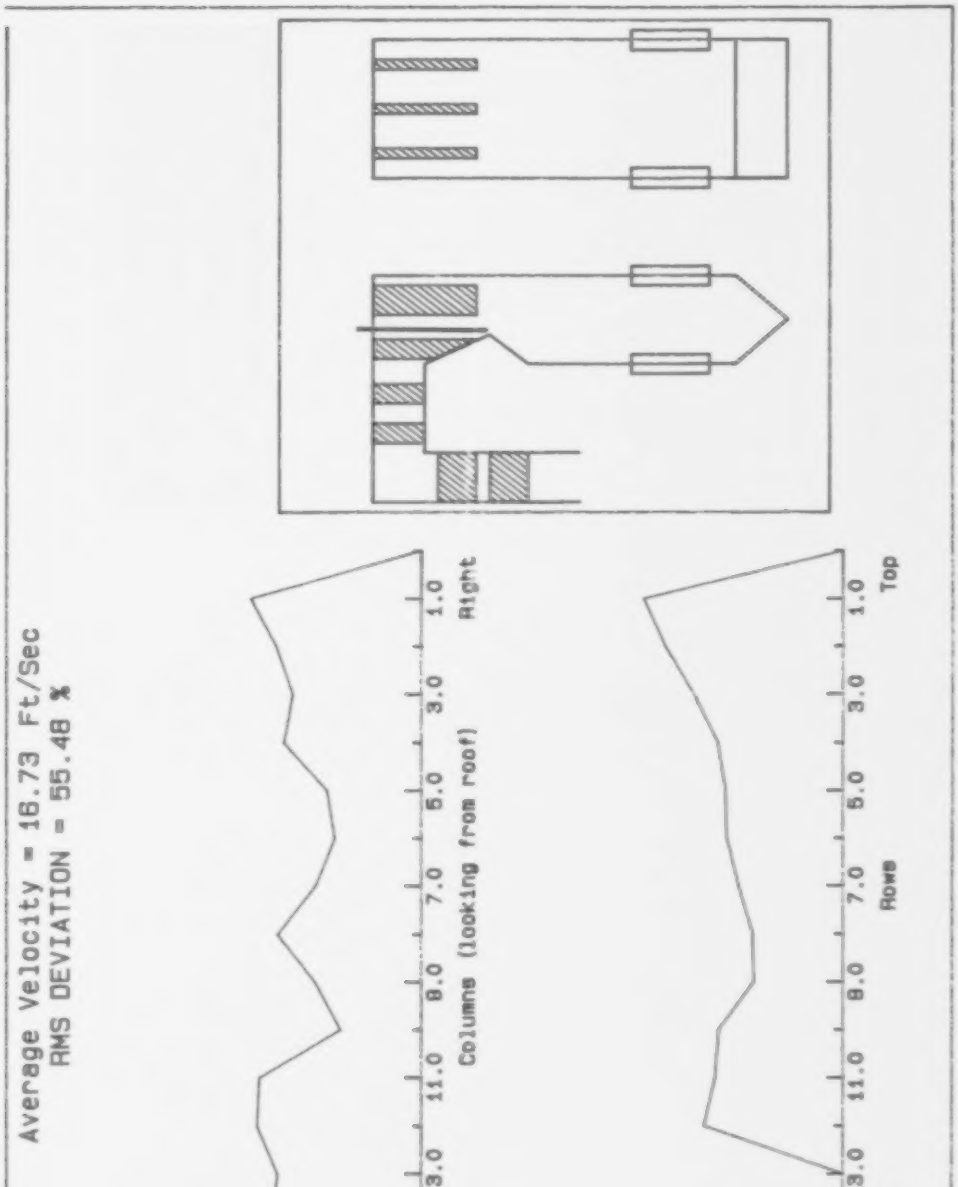

Figure 4-35. Baseline furnace normalized velocity profiles: Test Plane 5.

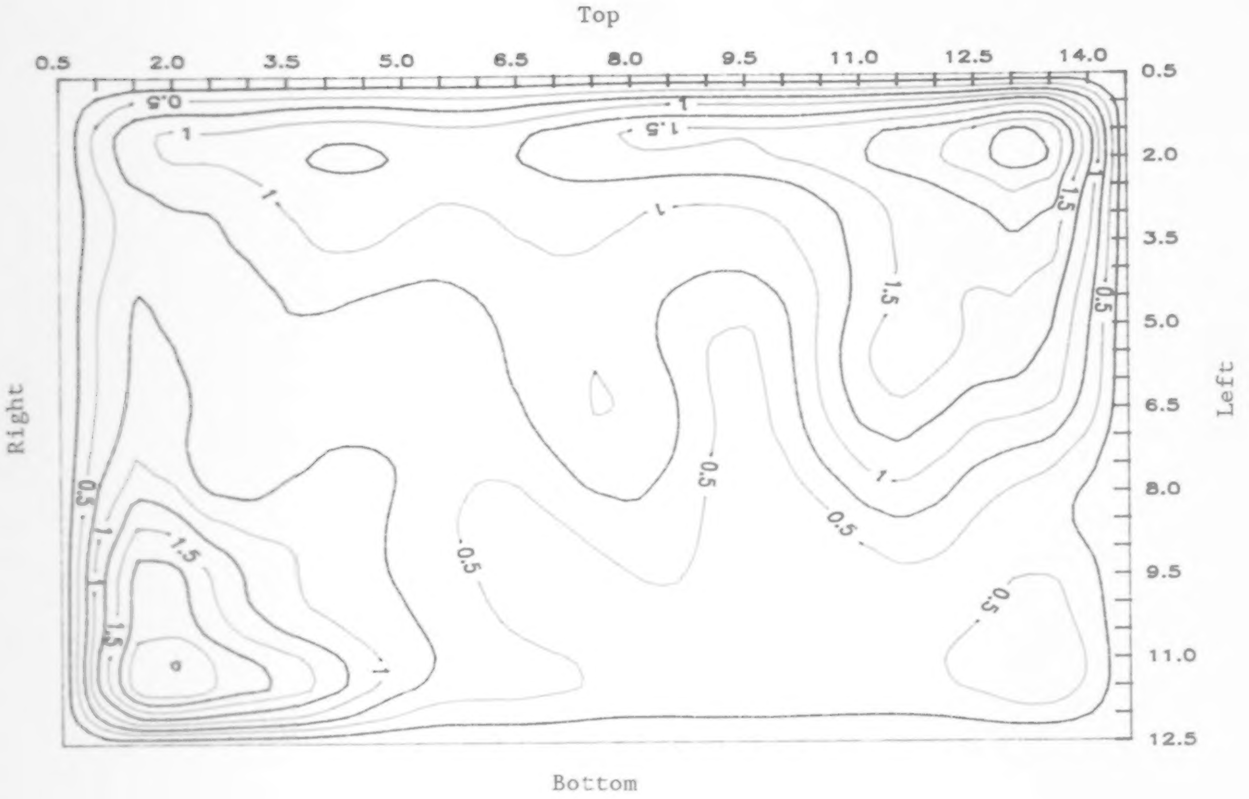

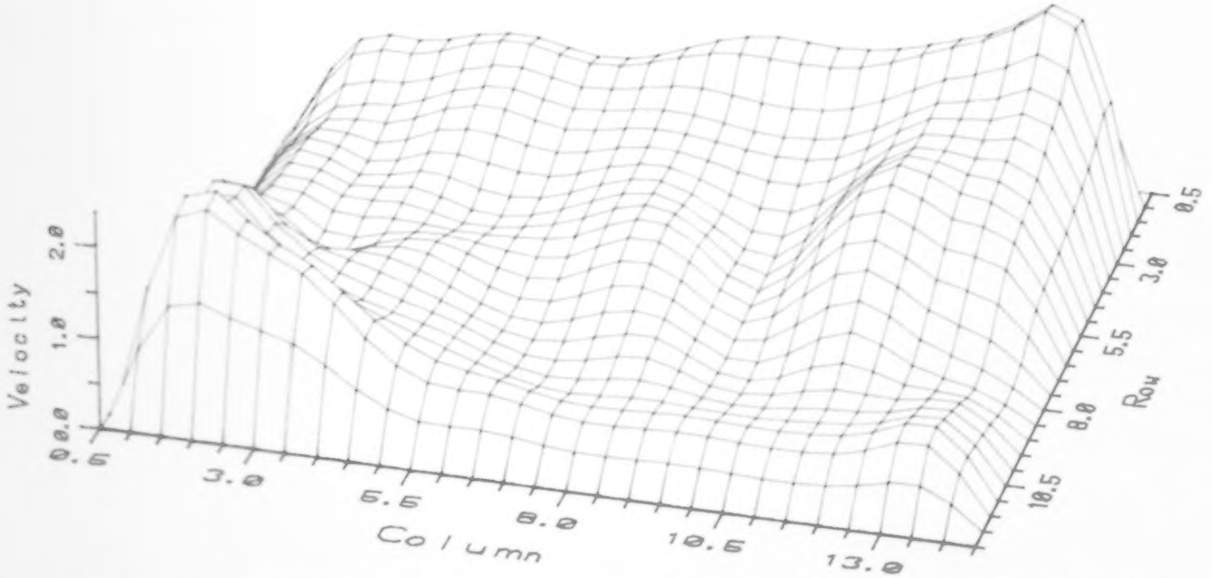

Figure 4-36. Normalized axial isovelocity plot and velocity contour plot: Test Plane 5.

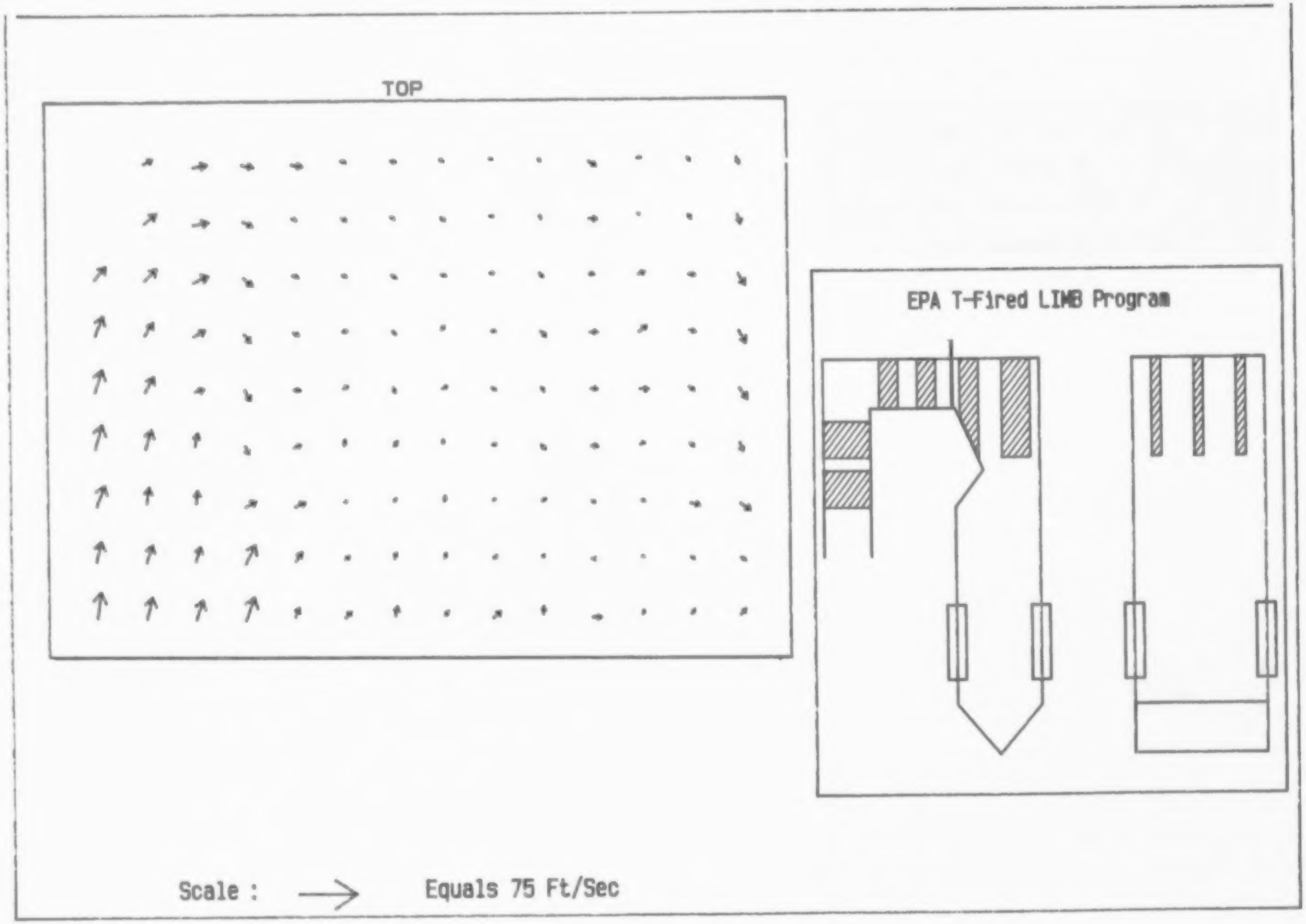

Figure 4-37. Baseline furnace velocity vectors: Test Plane 6.

Average Velocity = 25.49 Ft/Sec
RMS DEVIATION = 22.88 %
TOP

	0.78	0.82	1.25	0.80	1.05	1.09	1.31	1.18	1.21	1.50	1.38	1.43	1.28
	0.83	0.77	1.16	0.82	0.98	1.08	1.01	1.03	1.15	1.24	1.52	1.32	1.26
0.41	0.71	0.88	1.02	0.79	0.94	1.03	0.90	0.90	1.04	1.28	1.29	1.38	1.46
0.84	0.71	0.82	1.08	0.78	0.80	0.83	0.84	1.04	1.08	1.20	1.28	1.30	1.34
0.85	0.83	0.90	0.98	0.78	0.88	0.91	0.75	0.83	0.88	1.25	1.17	1.18	1.17
0.83	1.00	0.97	0.94	0.71	0.87	0.90	0.85	0.88	0.81	1.17	1.18	1.05	0.94
1.08	1.18	1.06	0.98	0.75	0.90	0.82	0.85	0.83	0.82	1.04	1.03	0.77	0.88
1.18	1.34	1.28	1.36	0.84	0.98	0.85	0.75	0.80	0.77	0.88	0.82	0.86	0.81
1.34	1.44	1.38	1.43	0.85	0.86	0.86	0.83	0.76	0.83	0.87	0.98	0.87	0.35

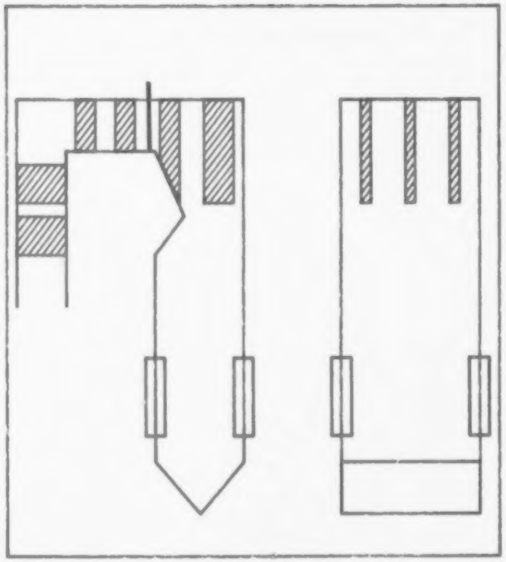

Figure 4-38. Normalized axial velocities: Test Plane 6.

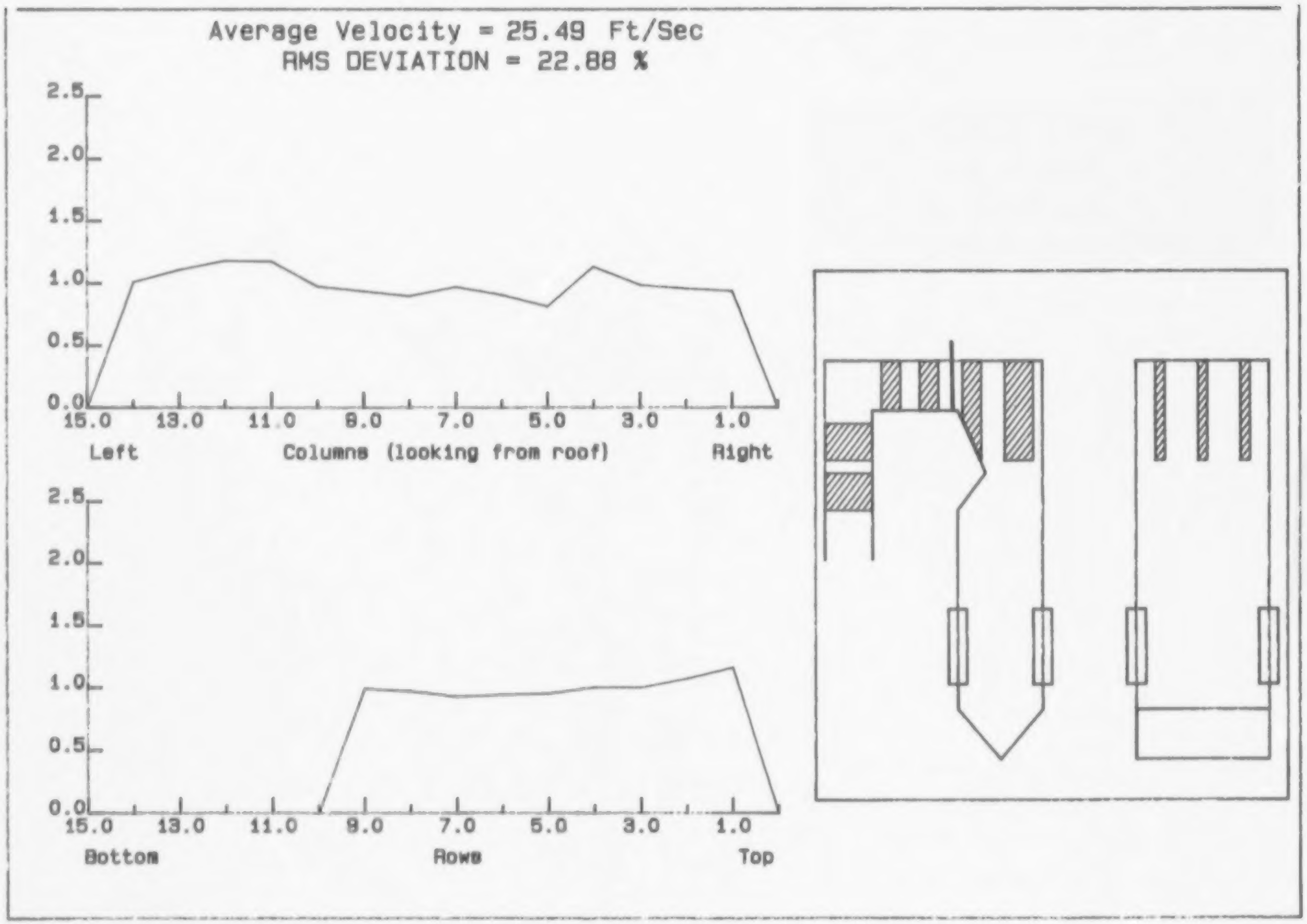

Figure 4-39. Baseline furnace normalized velocity profiles: Test Plane 6.

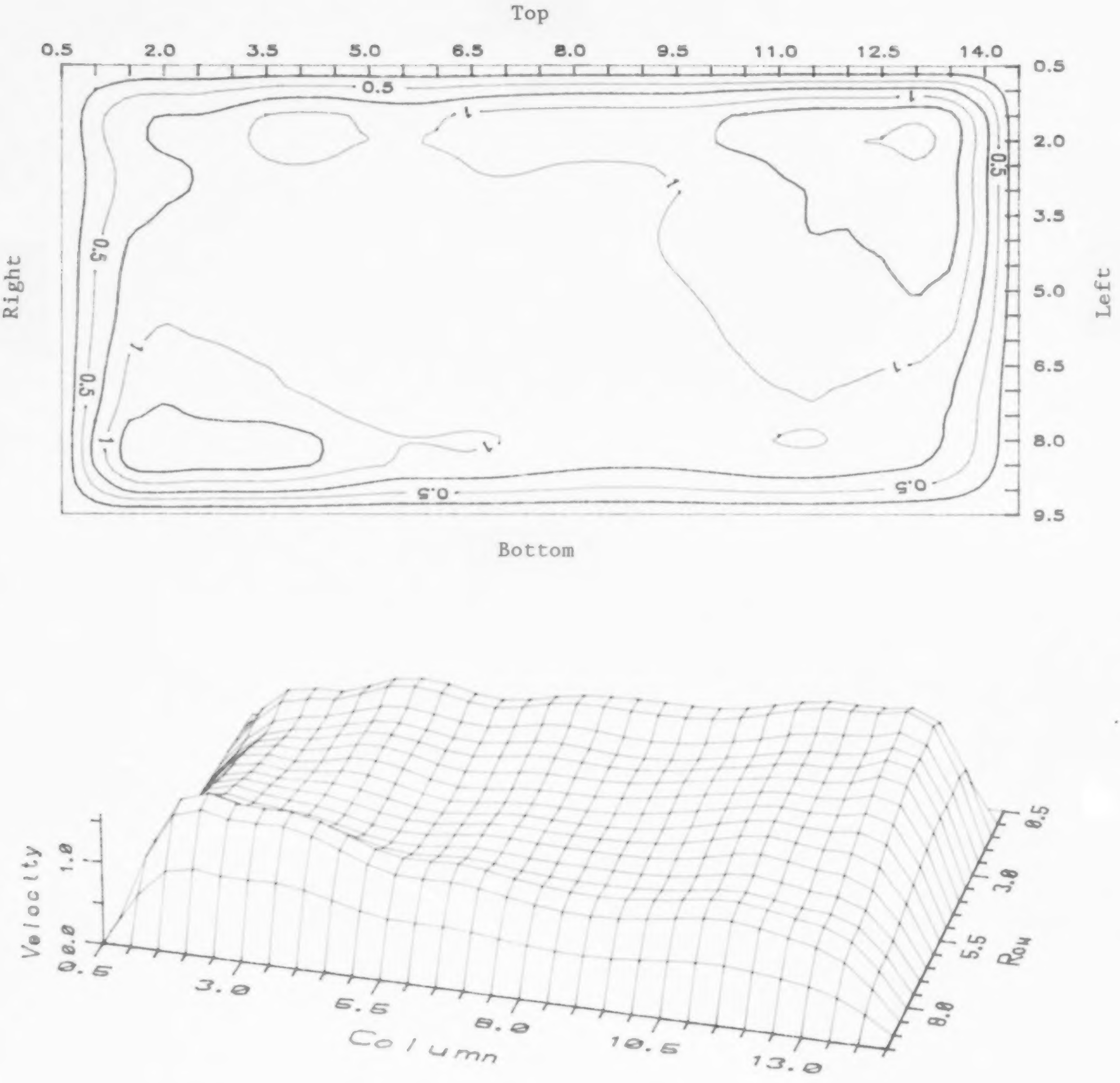

Figure 4-40. Normalized axial isovelocity plot and velocity contour plot: Test Plane 6.

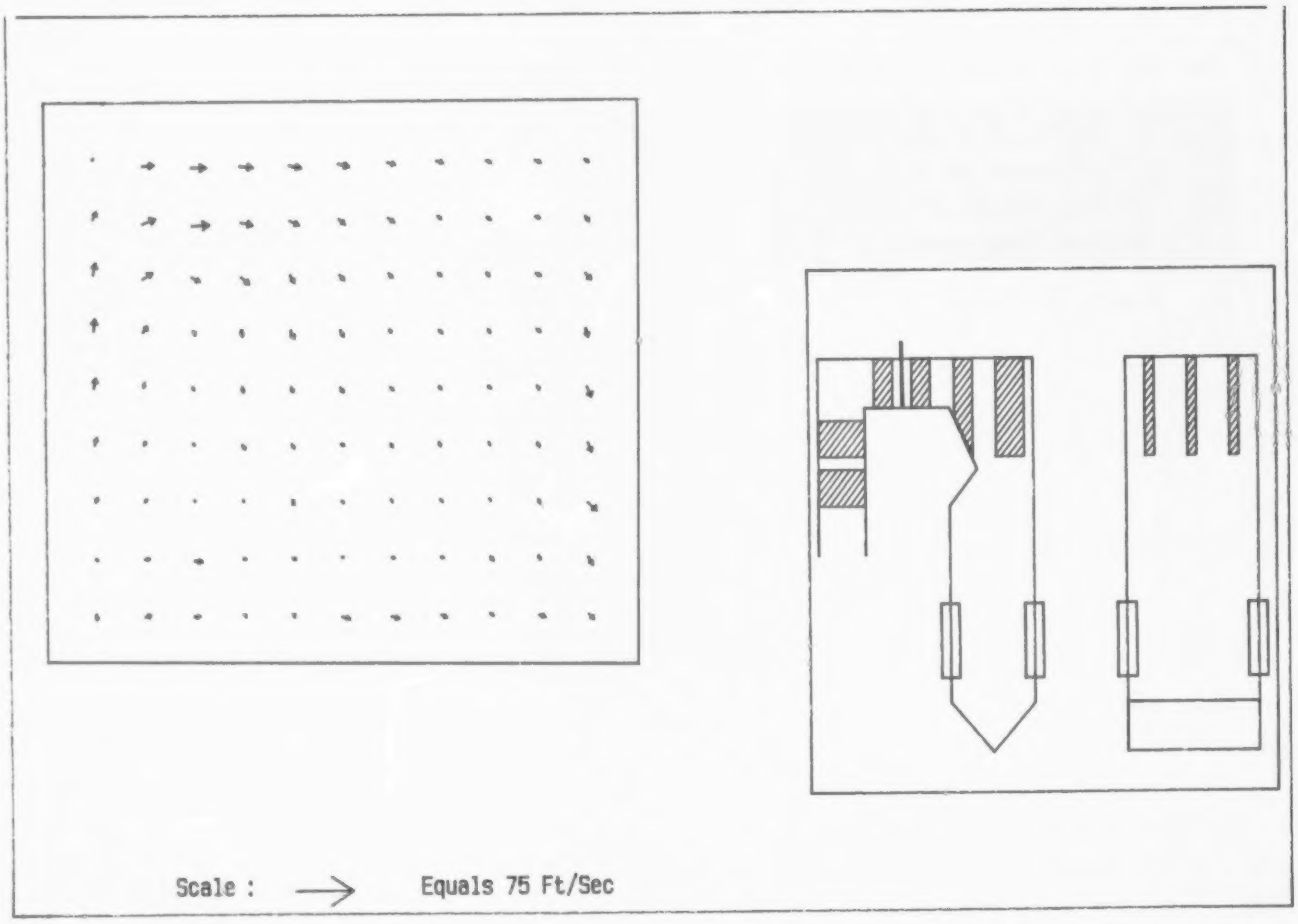

Figure 4-41. Baseline furnace velocity vectors: Test Plane 7.

Average Velocity = 46.85 Ft/Sec
RMS DEVIATION = 7.97 %
TOP

0.86	1.01	0.82	0.81	0.88	0.82	0.83	0.88	0.87	1.11	1.14
0.88	1.02	0.82	0.92	0.92	0.93	0.96	0.97	1.02	1.10	1.10
0.89	1.03	1.02	0.97	0.87	0.98	0.89	0.84	0.96	1.07	1.11
1.11	1.07	1.07	1.02	0.86	0.96	1.00	0.93	1.00	1.04	1.13
1.14	1.07	1.06	1.00	0.86	0.93	0.91	0.90	1.01	1.04	1.08
1.20	1.12	1.10	0.88	0.84	0.93	0.93	0.97	0.88	1.07	1.11
1.20	1.13	1.03	1.01	0.89	0.93	0.86	0.93	1.04	1.05	1.13
1.10	1.02	0.98	1.01	0.87	0.93	0.93	0.84	0.86	1.06	1.05
1.01	1.01	0.92	0.98	0.86	0.89	0.80	0.82	0.98	1.00	1.00

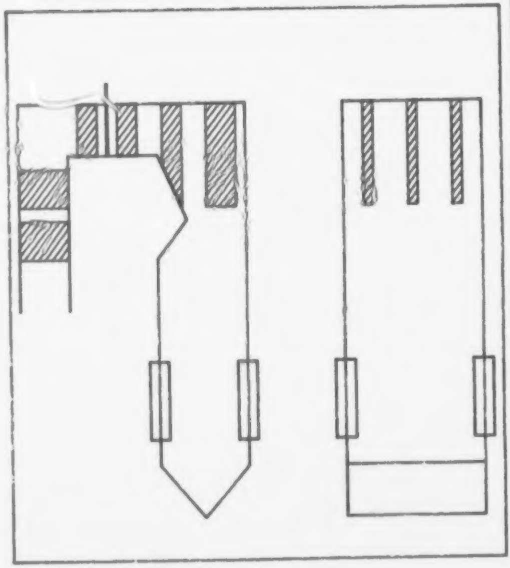

Figure 4-42. Normalized axial velocities: Test Plane 7.

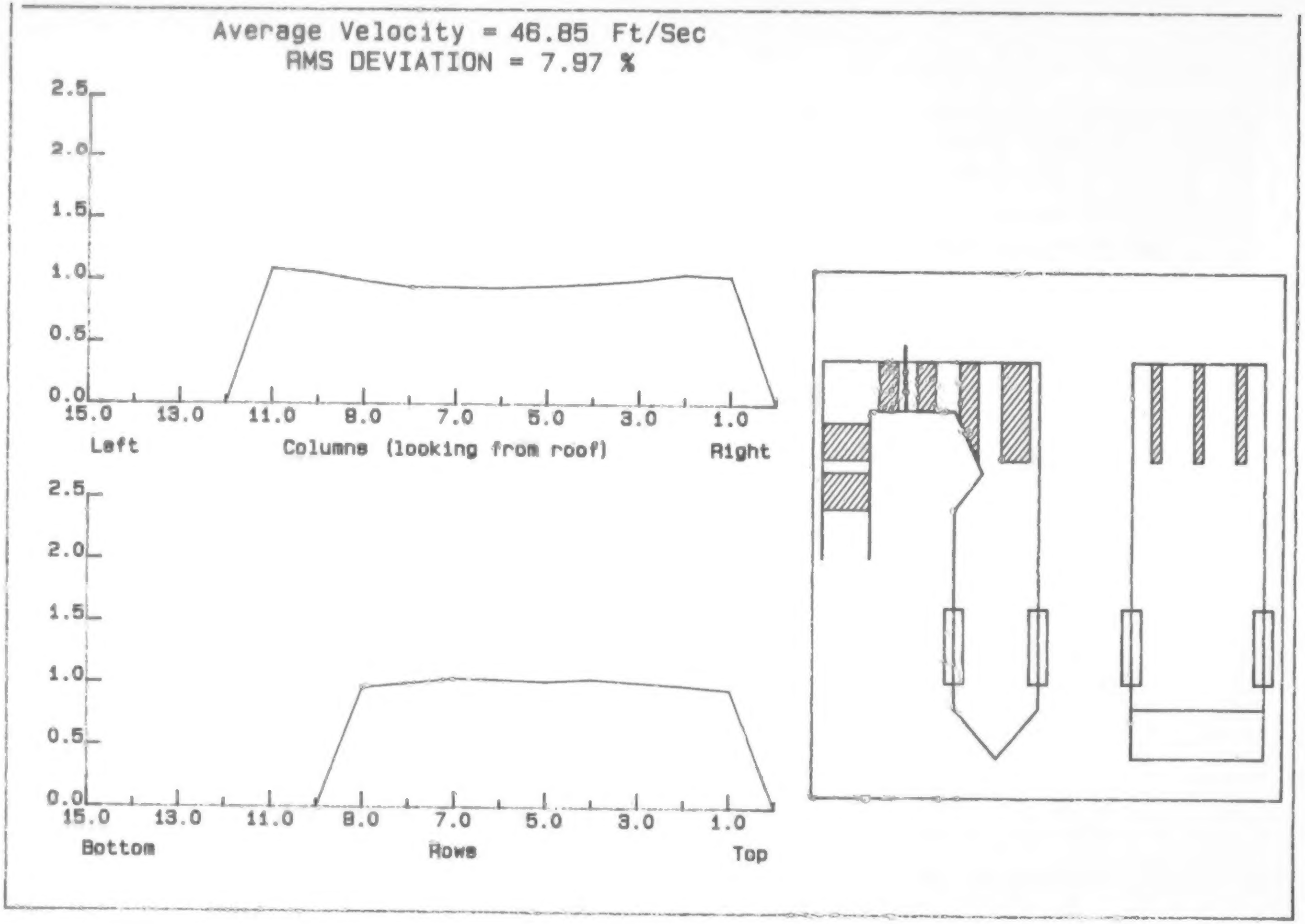

Figure 4-43. Baseline furnace normalized velocity profiles: Test Plane 7.

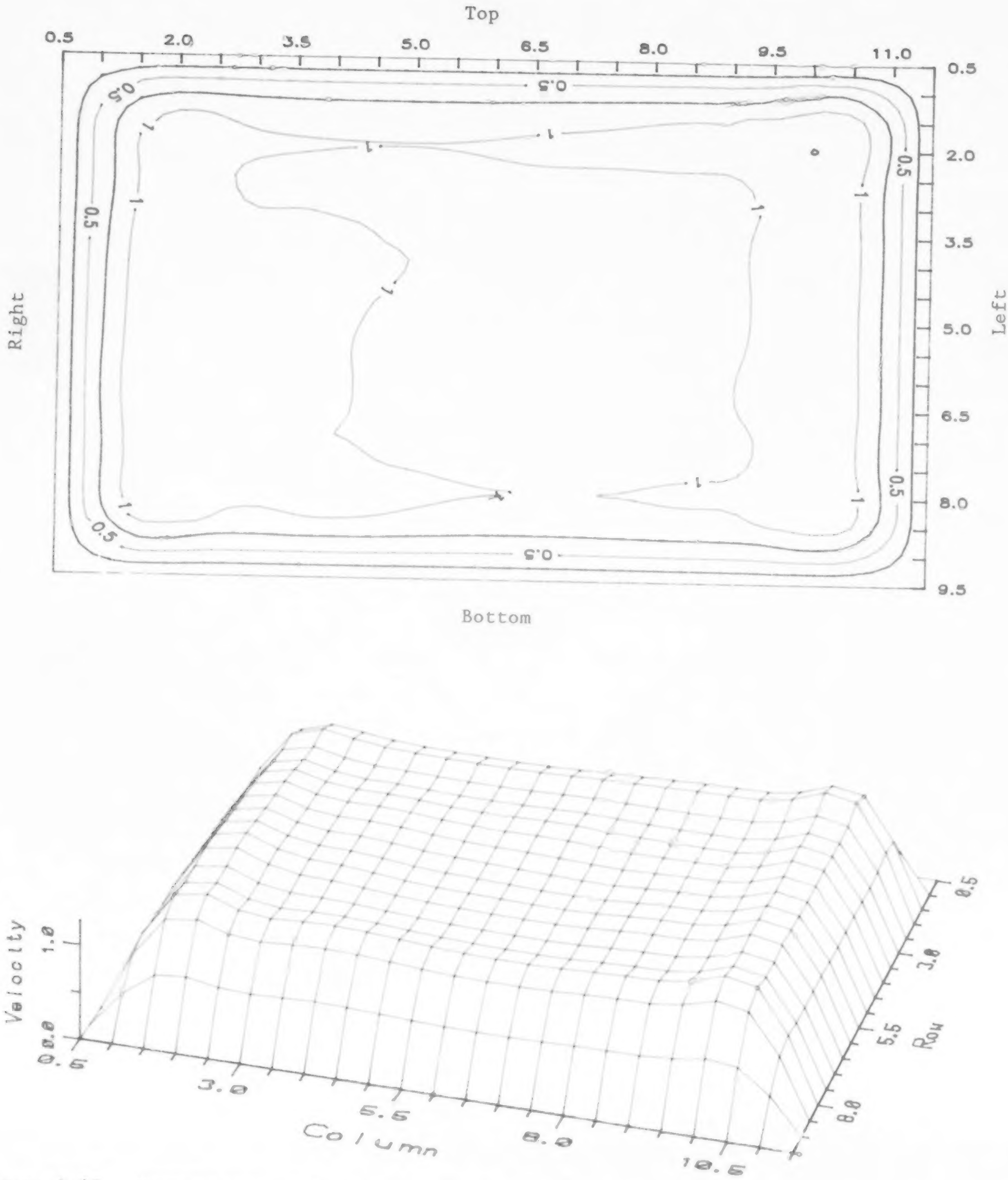

Figure 4-44. Normalized axial isovelocity plot and velocity contour plot: Test Plane 7.

obtained higher flue gas mass flow than the inner two. This phenomenon can be observed in Figures 4-29 through 4-32. It can be seen that the outer two lanes received approximately 40% more mass flow than the inner two.

4.3.4.2 Injector Screening

Using the jet modeling criteria discussed earlier, simulated sorbent injection nozzles were fabricated and installed on the LSFATF flow model of the BSF. The flow rates through each injection nozzle were measured and balanced so that each injector had identical outlet velocities and mass flow. For each test the air flow rate through the furnace model was held constant at the level required to make the injector air flow rate 5% of that entering the model through the windboxes. Sorbent injector configurations were tested in three screening levels designed to lead progressively to the selection of sorbent injector design/location combinations for Task C combustion testing. In the first screening level, flow visualization tests utilizing smoke as the tracer medium were performed for the sixteen (16) initial injection configurations (Table 4-2) at simulated full load furnace operating conditions. Each injection configuration was evaluated at three carrier air velocities and three injector tilts. The results of these tests are discussed in this section.

The eleven (11) best injector configurations from the first screening level were then evaluated in the second screening level which consisted of steady state mixing studies using methane as the tracer gas. From the results of these eleven (11) tests, five (5) were advanced to the third screening level in which transient residence time distribution (RTD) studies were also performed. Velocity traverses were performed for these third screening level configurations to assess the impact of sorbent injection on upper furnace aerodynamics. The three (3) injection configurations that provided the best tracer gas distribution and retained the tracer gas for the greatest length of time in the RTD studies were then identified as candidate injection systems for Task C combustion testing. An additional series of tests were then performed. These tests evaluated injector performance for upward and downward furnace burner tilts and were performed to aid in the interpretation of the Task C combustion test results. Burner tilts are used for steam temperature control in tangentially fired boilers and the aerodynamic impact of this on injector performance was quantified during these trials.

First screening level; flow visualizations -- To aid in the discussion of the test results, the flow visualization tests have been broken down into six classes representing injection into different aerodynamic zones within the furnace. These classes are:

1) Injection from the front wall into the lanes between the superheater panels. (Configurations 1, 2, 3, 4, 5, 6, and 7)
2) Injection from the roof between the superheater panels. (Configuration 12)
3) Lance injection between the superheater panels. (Configurations 14 and 15)
4) Injection from the rear furnace wall into the main furnace volume. (Configuration 10)
5) Injection from the corners (T-fired injection) into the main furnace volume. (Configurations 8 and 9)
6) Combinations of the previous five (5) classes. (Configurations 11, 13, and 16)

Figure 4-45 is a photograph of a typical flow visualization test for injection from the front wall (Location A) into the lanes between the superheater panels. At higher injection velocities, injection from this elevation on the front wall gave good sorbent penetration and mixing within the upper furnace. However, the region above the arch was not adequately seeded. This was corrected somewhat by tilting the nozzles downward 20°. This is shown in Figures 4-46 and 4-47.

Dispersion was further improved by increasing the injection velocity to a value greater than the simulated BSF injection velocity of 22.9 m/sec (75 ft/sec). For the injection locations higher on the front wall of the furnace (Locations B and C), mixing was not as good as that observed for the lowest front wall location. Downward tilts from the upper injection locations improved sorbent penetration and dispersion, but did not achieve the performance observed by injection from the lowest front wall position. However, for furnaces in which the sulfation temperature window begins after the first set of superheater panels, injection from the intermediate front wall (Location B) might be attractive.

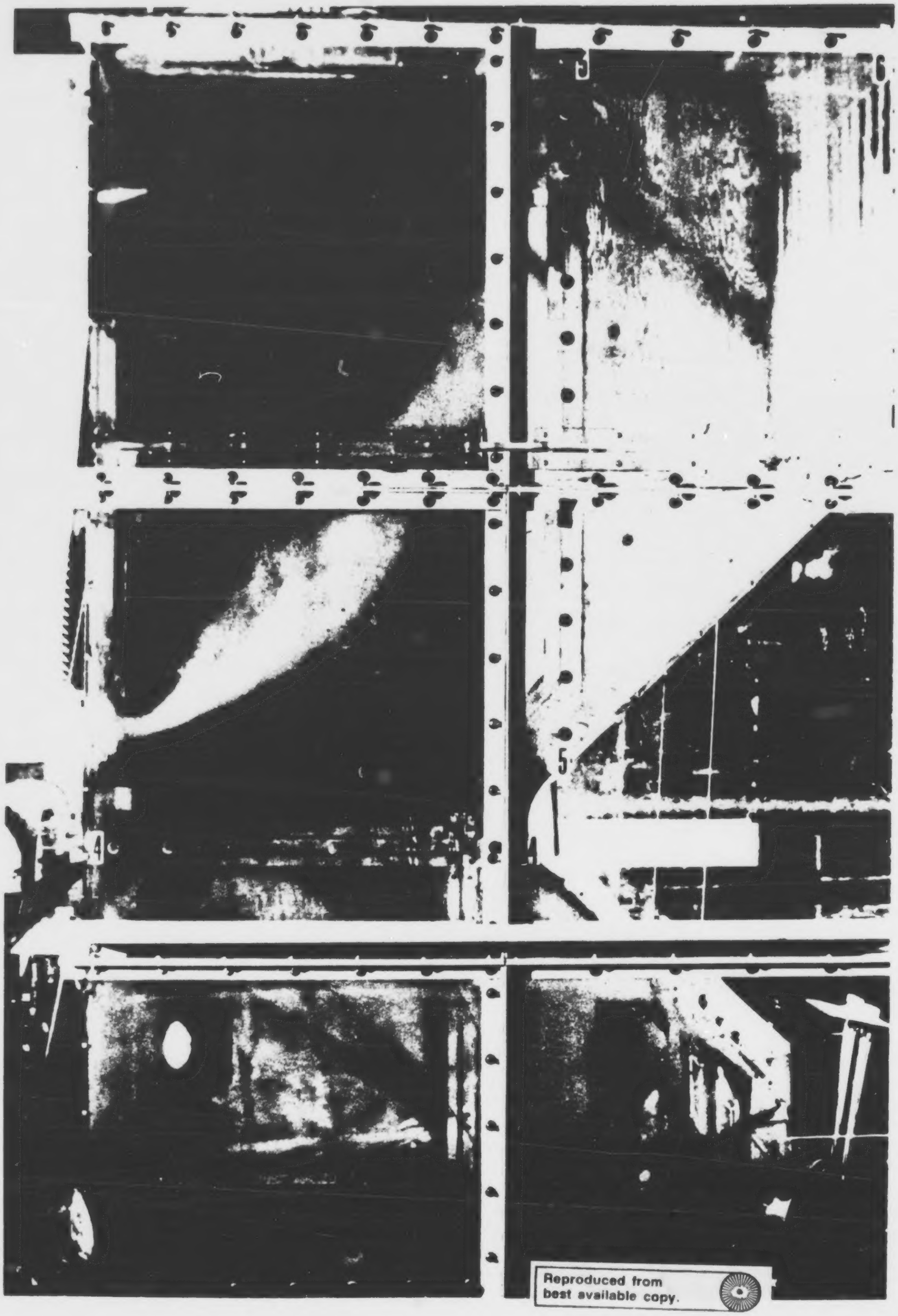

Reproduced from
best available copy.

Figure 4-45. Typical flow visualization test of front wall injection.

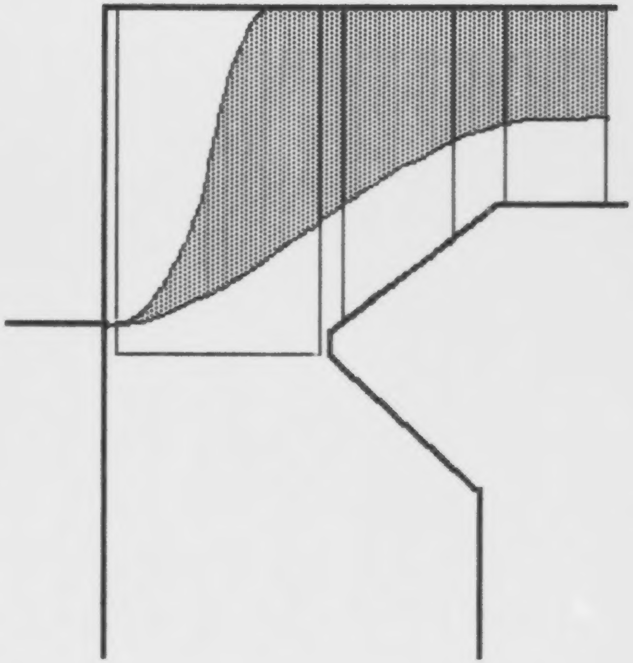

Figure 4-46. No tilt front wall injection flow visualization results.

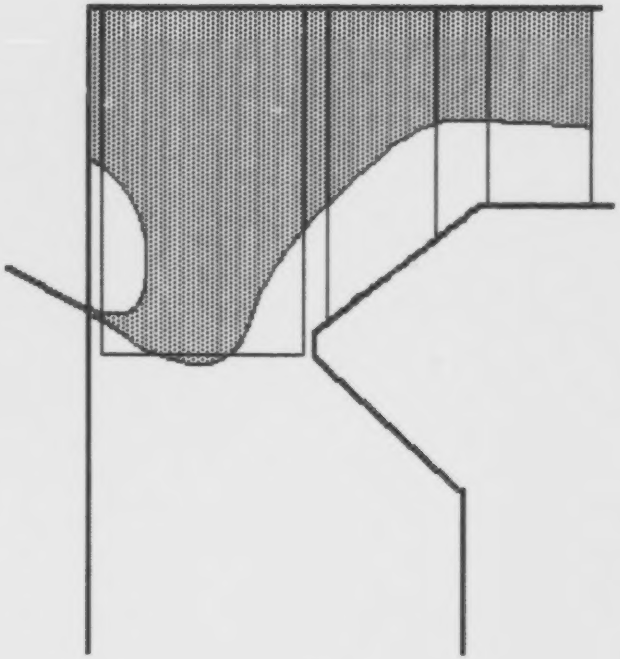

Figure 4-47. -20° tilt front wall injection flow visualization results.

When the lower furnace gas encounters the superheater panels it is split into the four (4) channels or lanes between the panels of the BSF. Because of the rotational nature of the furnace flow field in the lower furnace, the tangential component of flow along the right wall of the unit is towards the back of the unit while along the left wall is towards the front. This means that for injection systems mounted low on the front wall the nozzle in the lane at the far right is injecting into an axial flow field while the one injecting into the left lane is injecting into a counterflow. This effect was found to be reversed for injectors mounted high on the front wall since the horizontal flow is strong high on the left side and relatively weak high on the right side.

The second class of injection was vertically downward from the roof of the furnace. This type of injection gave good sorbent penetration and dispersion ahead of the second set of superheater panels. Angling the injectors toward the front of the unit increased the overall sorbent dispersion, but at the expense of reduced penetration. Angling the injectors towards the rear of the unit increased the overall penetration, but sorbent dispersion occurred too far downstream to make such a scheme desirable. As with front wall injection, higher injection velocities gave greater jet penetration and dispersion.

The third injection class involved the use of lances. The lances were installed vertically from the roof and had a single tiltable injection nozzle at their ends. With the lance injection nozzles aimed towards the back of the boiler (i.e., with the direction of furnace gas flow) lance injection did not provide adequate dispersion as shown in Figure 4-48. Rotation of the injection nozzle 180 degrees into the direction of the flue gases significantly enhanced sorbent dispersion, Figure 4-49. Two lance injection nozzles were evaluated. These were 45° and 90° elbows attached to the end of the injection pipe. Of the two, the 45° elbow resulted in the highest levels of furnace dispersion. This was because by angling the jet flow downward, counter to the direction of the flow, dispersion was increased. Lance injection was found to yield the most favorable performance of all configurations tested.

The fourth class of injection was from the rear wall of the unit below the arch. During these tests increased injection velocities and/or downward tilts increased sorbent jet penetration and dispersion. Low injection velocities resulted in limited sorbent penetration. This, in combination with the tangential flow field, forced the injected material to remain along the walls of the unit thus limiting dispersion. Because the sorbent material was flowing tangentially around the perimeter of the unit in the lower furnace, uneven levels of sorbent flow between the superheater panels were created. It was found that the outer two channels became overseeded while the inner two were underseeded. This result was consistent with the baseline velocity traverses performed at the horizontal and vertical furnace outlet planes. These data indicated that the bulk of the furnace gas flow is similarly nonuniform. The best injection configuration evaluated of this fourth class had the highest injection velocity, 22.9 m/sec (75 ft/sec), and the most downward tilt, and counter-rotational injection. Injection in this manner resulted in a high level of sorbent dispersion throughout the furnace cross section and the expected sulfation temperature window of the BSF. It should be noted, however, that injection below the furnace area in most tangentially fired boiler applications would be into excessively higher temperatures (i.e., greater than 1315°C (2400°F)).

The fifth class was tangential injection from the four corners, co-current and countercurrent to the swirling flow field. For a given injection velocity and/or tilt, it was found that countercurrent injection gave better dispersion and uniformity of sorbent over the furnace cross section below the arch and within the lanes between the superheater panels. As with rear wall injection, increases in the injection velocity and/or downward tilt resulted in improved dispersion within the furnace.

A number of injection configurations were evaluated which were combinations of those discussed above. It was found, with few exceptions, that injection with eight (8) injectors rather than four (4) resulted in reduced sorbent jet penetration and dispersion for the injection velocities tested. The reduced penetration was caused by the required reduction in nozzle diameter and the individual injector air mass flow rates when the number of injection nozzles was doubled while maintaining the overall sorbent

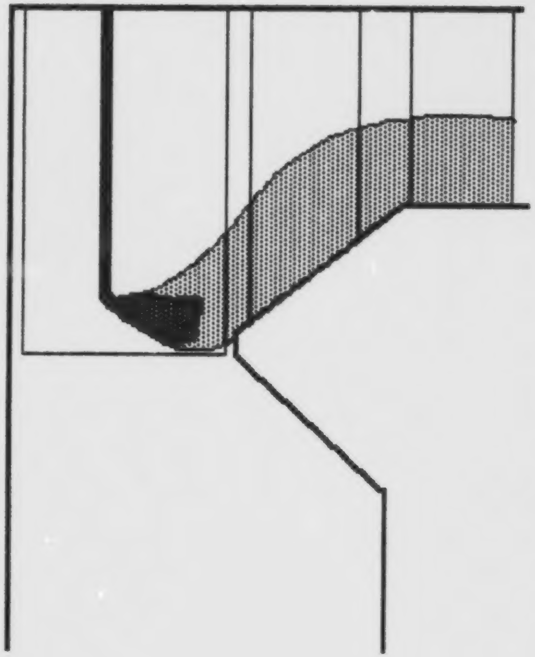

Figure 4-48. Rearward facing lance flow visualization results.

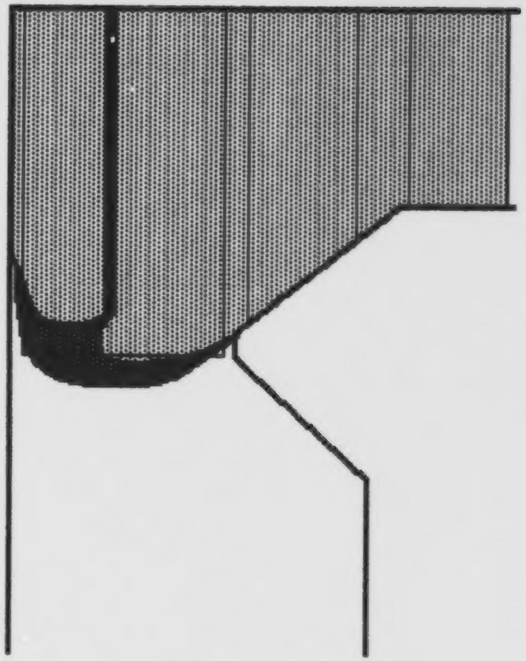

Figure 4-49. Frontward facing lance flow visualization results.

carrier air mass flow constant at 5% of total combustion air. The best cases were those combinations which included injection below the arch. However, as stated earlier, injection in this region is not appropriate for many boilers.

In summary, the flow visualization testing showed that 5% of the total BSF combustion air flow for sorbent carrier air is sufficient, and that higher injection velocities are preferred. For a given injection velocity, injection counter to the local flow field provided better sorbent dispersion than perpendicular or co-directional injection because of the enhanced turbulent mixing such an injection scheme offers. Lances were found to provide precise positioning of the injection of sorbents and also the highest observed levels of dispersion when injected against the direction of the local flow field. While the nonsymetric nature of the aerodynamics within the upper furnace did not greatly affect the observed performance of the injection systems tested, its effect was greatest for injection schemes involving injectors mounted on the front wall of the unit. Lastly, injection with eight (8) injectors rather than four (4) resulted in an overall reduction in sorbent dispersion for a given injection carrier air mass flow rate.

The location of the entrance to the sulfation temperature window within a furnace depends on the unit's design and operating conditions. The location of the appropriate temperature window for the full range of tangentially fired boilers can be envisioned as being located within three (3) zones of the upper furnace; (1) below the nose (2), the area between the horizontal and vertical furnace outlet planes (HFOP and VFOP), and (3) downstream of the VFOP. The final choice of configurations for advancement to the second screening level addresses each of these zones. The sulfation temperature window in the BSF is within zone (2). Table 4.5 details the eleven (11) injection configurations that, based on the flow visualization tests, provided the best overall sorbent penetration and dispersion within each of these three (3) zones. For two (2) of the configurations, Test Numbers (TN) 205 and 211, jet velocity was increased from 22.9 m/sec (75 ft/sec) to 30.5 m/sec (100 ft/sec). This was done since flow visualization tests indicated that increased jet velocity may improve sorbent penetration and dispersion within the sulfation temperature window.

TABLE 4-5. SECOND SCREENING LEVEL TEST CONFIGURATIONS

Test No.	Injectors	Location	BSF Injection Velocity m/sec (ft/sec)	Tilt	Description
201	4	F	22.9 (75)	0^o	Roof Straight Down
202	4	G	22.9 (75)	-45^o	Front Facing Lance
203	4	B	22.9 (75)	-20^o	Front Wall
204	4	A	22.9 (75)	-20^o	Front Wall
205	4	A	30.5 (100)	0^o	Front Wall
206	4	D	22.9 (75)	-20^o	T-fired (counter)
207	4	E	22.9 (75)	-20^o	Rear Wall
208	8	B/E	22.9/22.9 (75/75)	$-20^o/-20^o$	Front and Rear Wall
209	8	A/F	22.9/22.9 (75/75)	$-20^o/-20^o$	Front Wall and Roof
210	8	B/G	22.9/22.9 (75/75)	$0^o/0^o$	Front Wall and Roof Lance
211	4	C	30.5 (100)	-20^o	Front Wall

Second screening level; steady state gas mixing tests -- The purpose of the second screening level was to quantify the level of "sorbent" penetration and dispersion for the eleven (11) best configurations selected from the first screening level. Two (2) planes of steady state gas mixing data were obtained for each of the eleven (11) injection schemes. The planes evaluated were the two (2) closest test planes downstream of the actual point of injection. (See Figure 4-18 for locations of LSFATF test planes). Mixing of solid sorbent particles was characterized by a tracer gas using the scaling relationships discussed previously in this report. The tracer gas was introduced to the injector air flow at a point far enough upstream to assure a uniform tracer gas concentration at the exit of the injector. Using a sampling probe attached to the Automatic Probe Traversing Device (APTD), the concentrations of tracer gas at a specific locations within the furnace flow model were determined. Using the APTD to traverse the sample probe through the model, tracer gas concentration profiles were generated.

Figures 4-50 through 4-72 present the results of each injection configuration in the form of contour plots and isoconcentration plots. The numerical values on the isoconcentration plots correspond to lines of constant concentration equal to 0.5, 1.0, 1.5, 2.0, etc. times the well-mixed tracer gas concentration as measured at the outlet of the flow model. The thoroughness of mixing for the concentration profiles shown in these figures has been characterized in terms of tracer gas concentration coefficients of variation. This coefficient is defined as the average RMS deviation of the concentrations measured at the test plane divided by the well mixed concentration of tracer gas as measured at the exit of the flow model multiplied by 100. These coefficients present a measure of how well the tracer gas representing sorbent is mixed across the test plane. The lower the coefficient, the better mixed the sorbent is across the test plane. The coefficients for each of the traverses for each test plane are summarized in Table 4-6 and Figure 4-73.

As with the tests of the first screening level, the injection configurations listed in Table 4-5 and Table 4-6 fall into six classifications: rear wall below the arch, lower furnace tangential injection, front wall, roof, lances installed from the roof, and combinations of the previous five classifications.

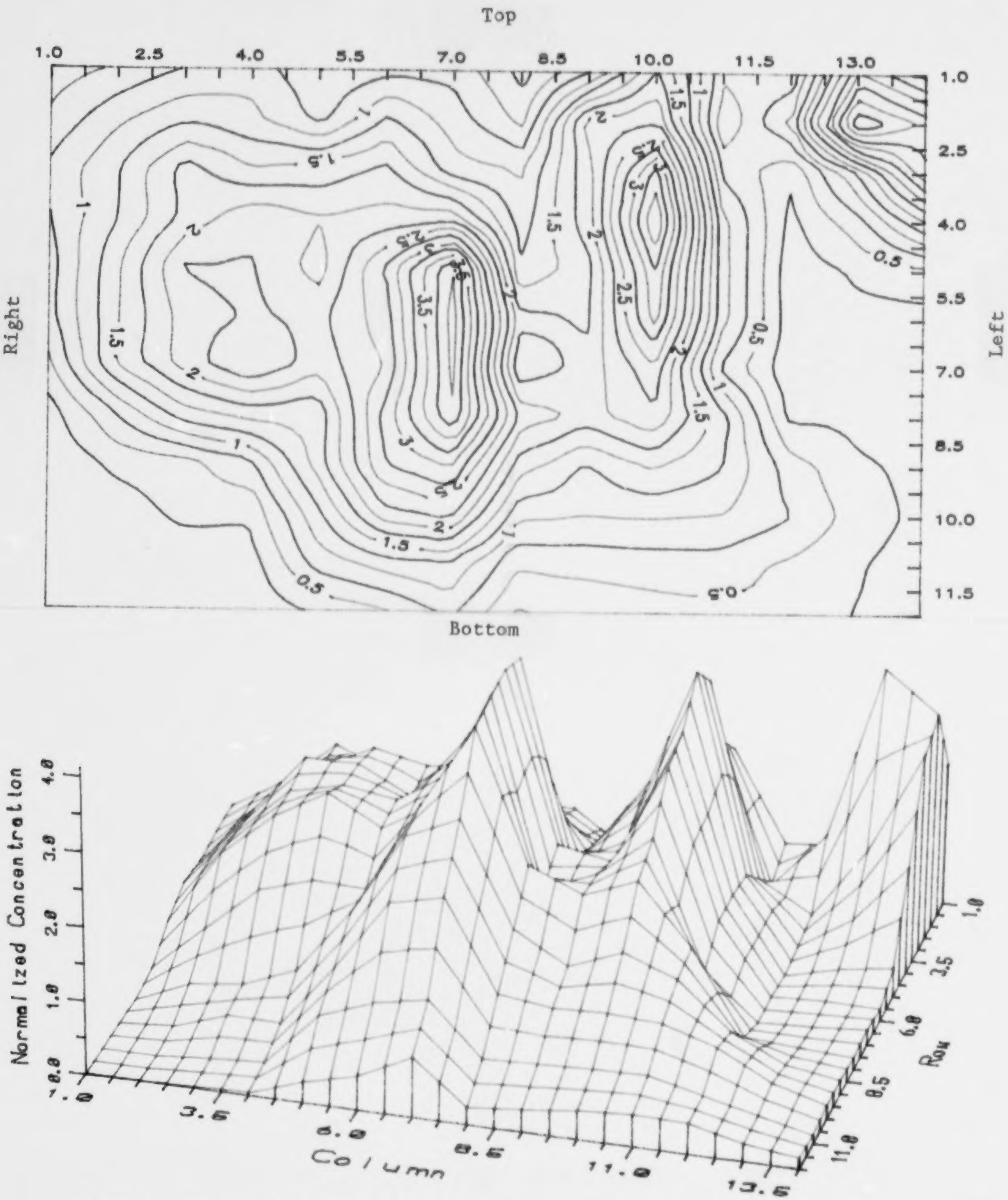

Figure 4-50. Gas mixing isoconcentration plot: Test No. 201: Plane 5.

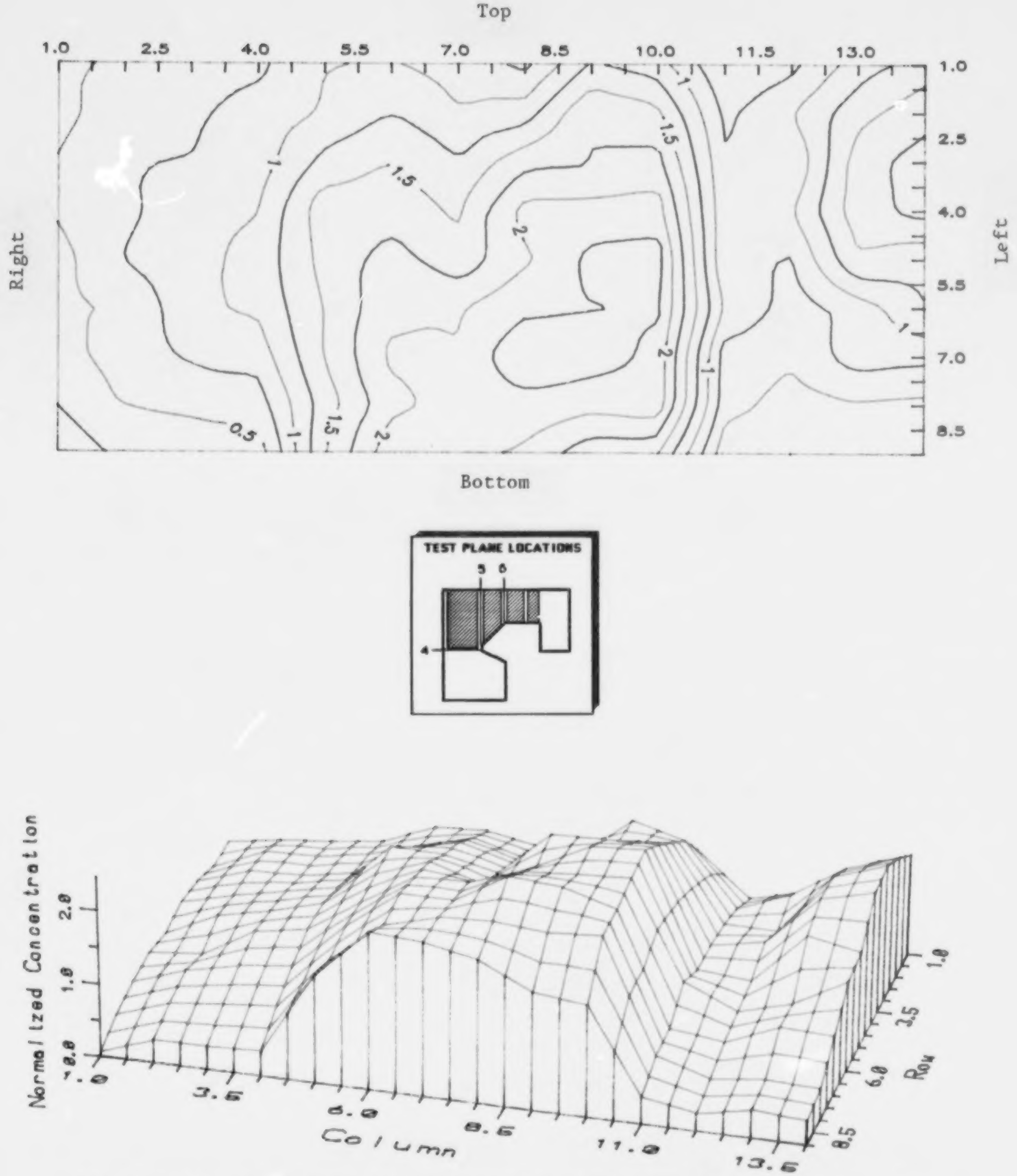

Figure 4-51. Gas mixing isoconcentration plot: Test No. 201: Plane 6.

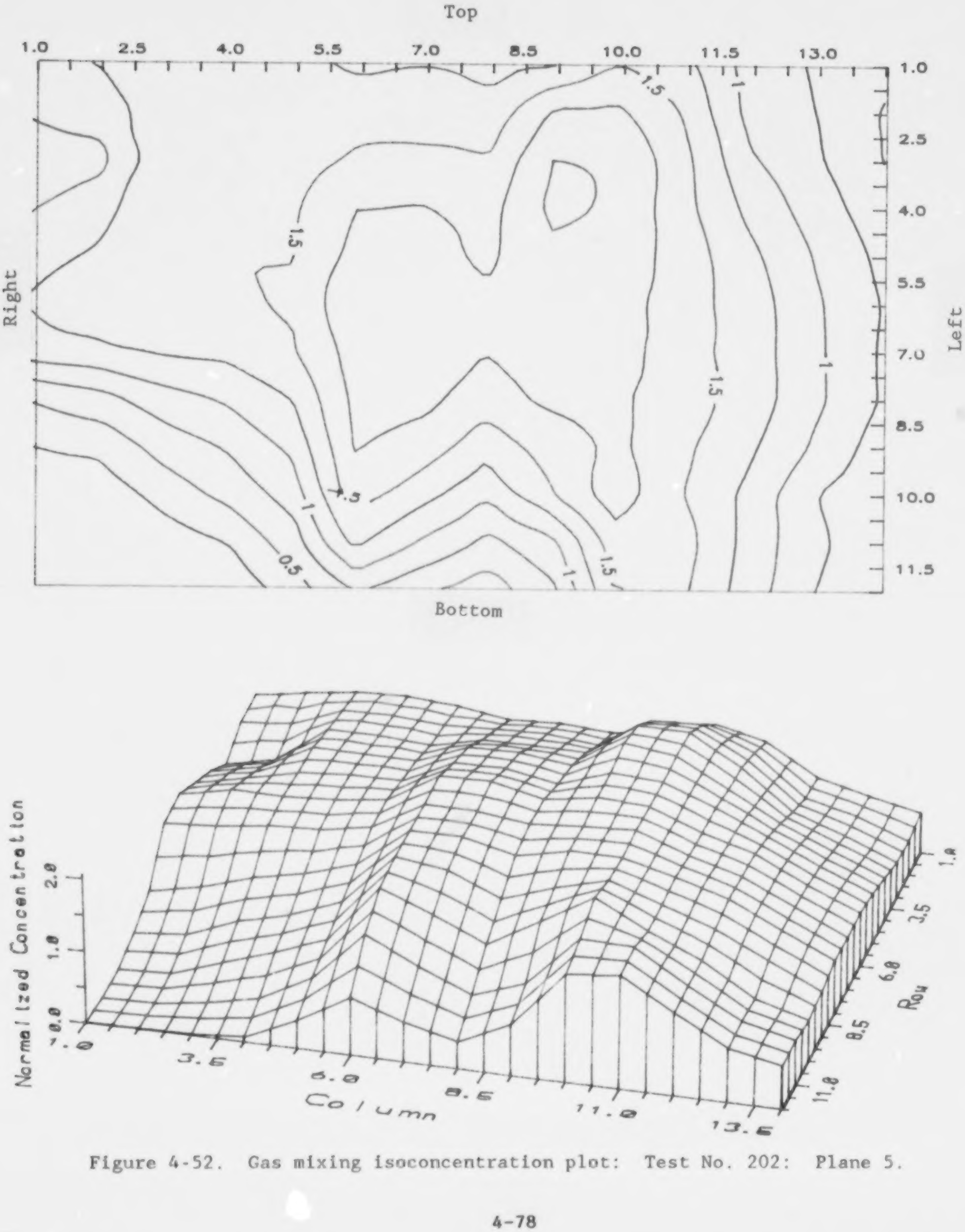

Figure 4-52. Gas mixing isoconcentration plot: Test No. 202: Plane 5.

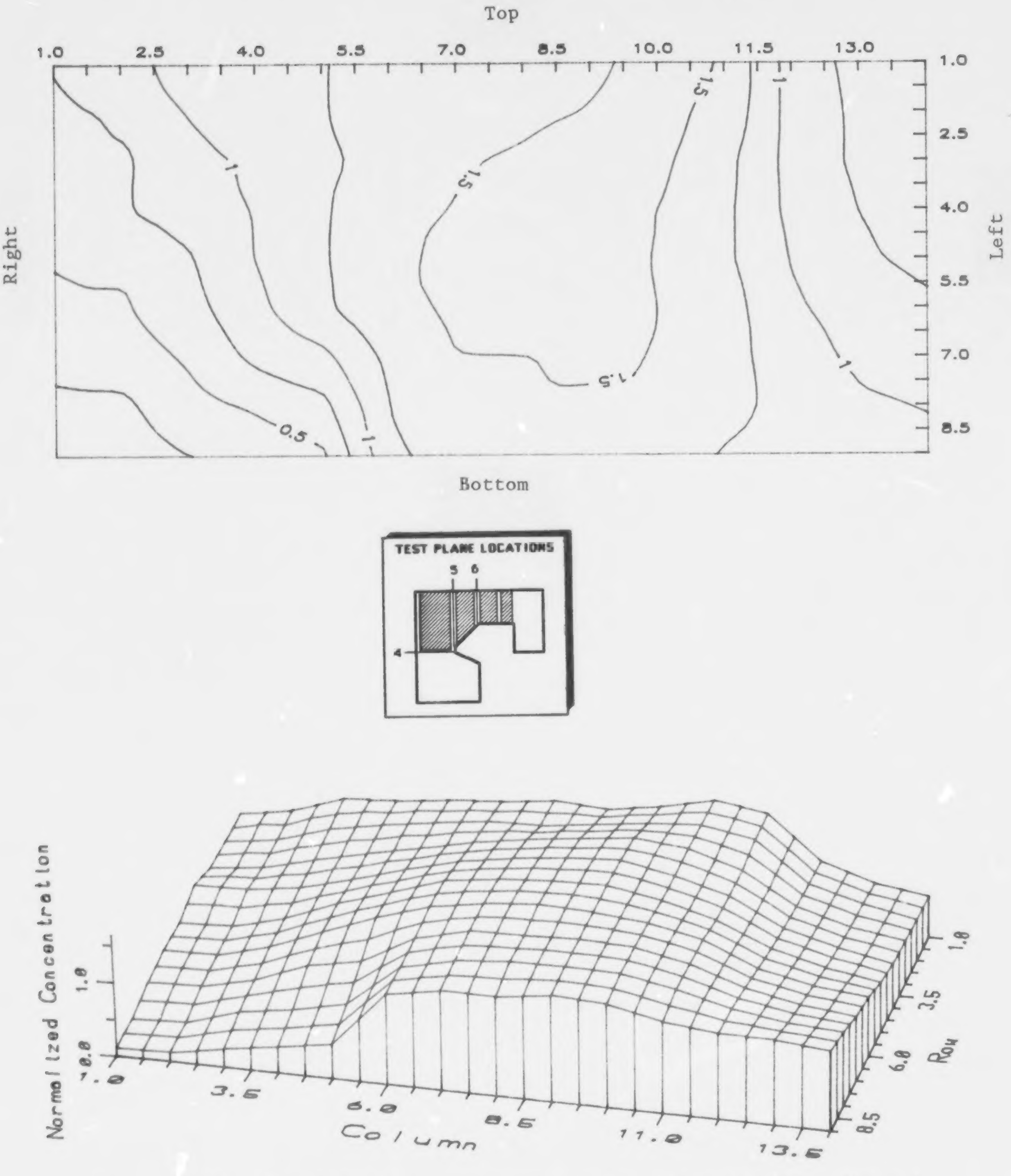

Figure 4-53. Gas mixing isoconcentration plot: Test No. 202: Plane 6.

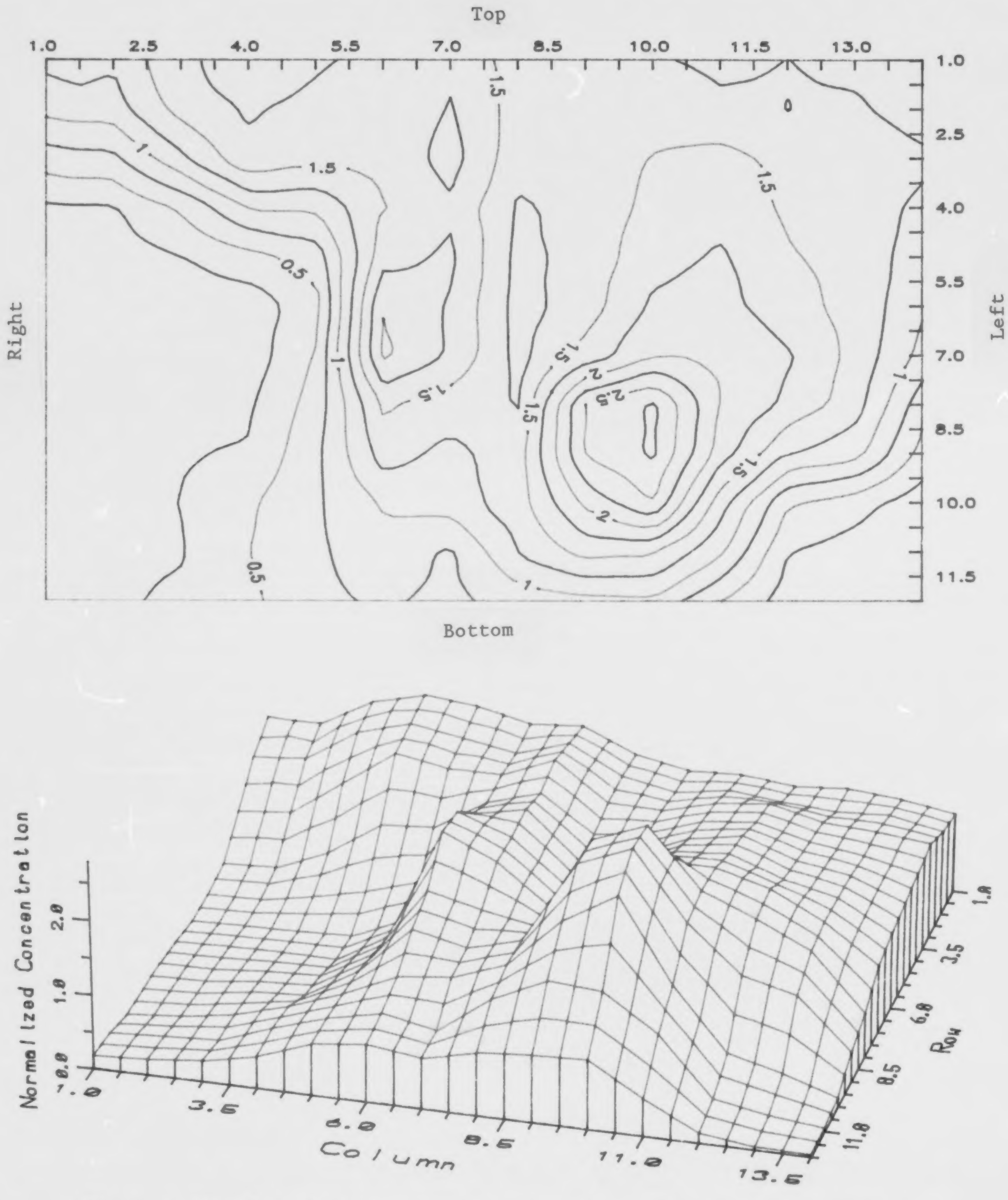

Figure 4-54. Gas mixing isoconcentration plot: Test No. 203: Plane 5.

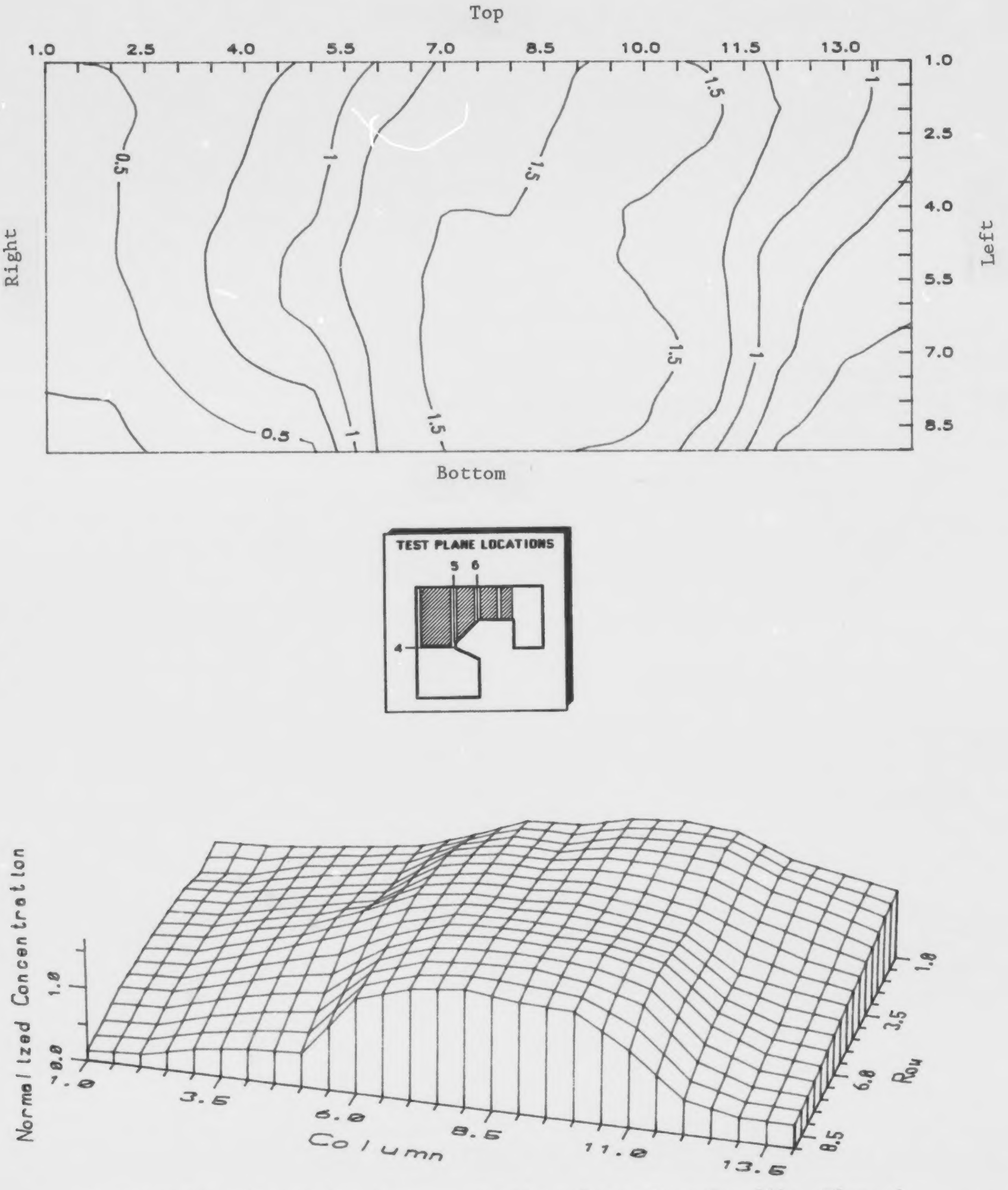

Figure 4-55. Gas mixing isoconcentration plot: Test No. 203: Plane 6.

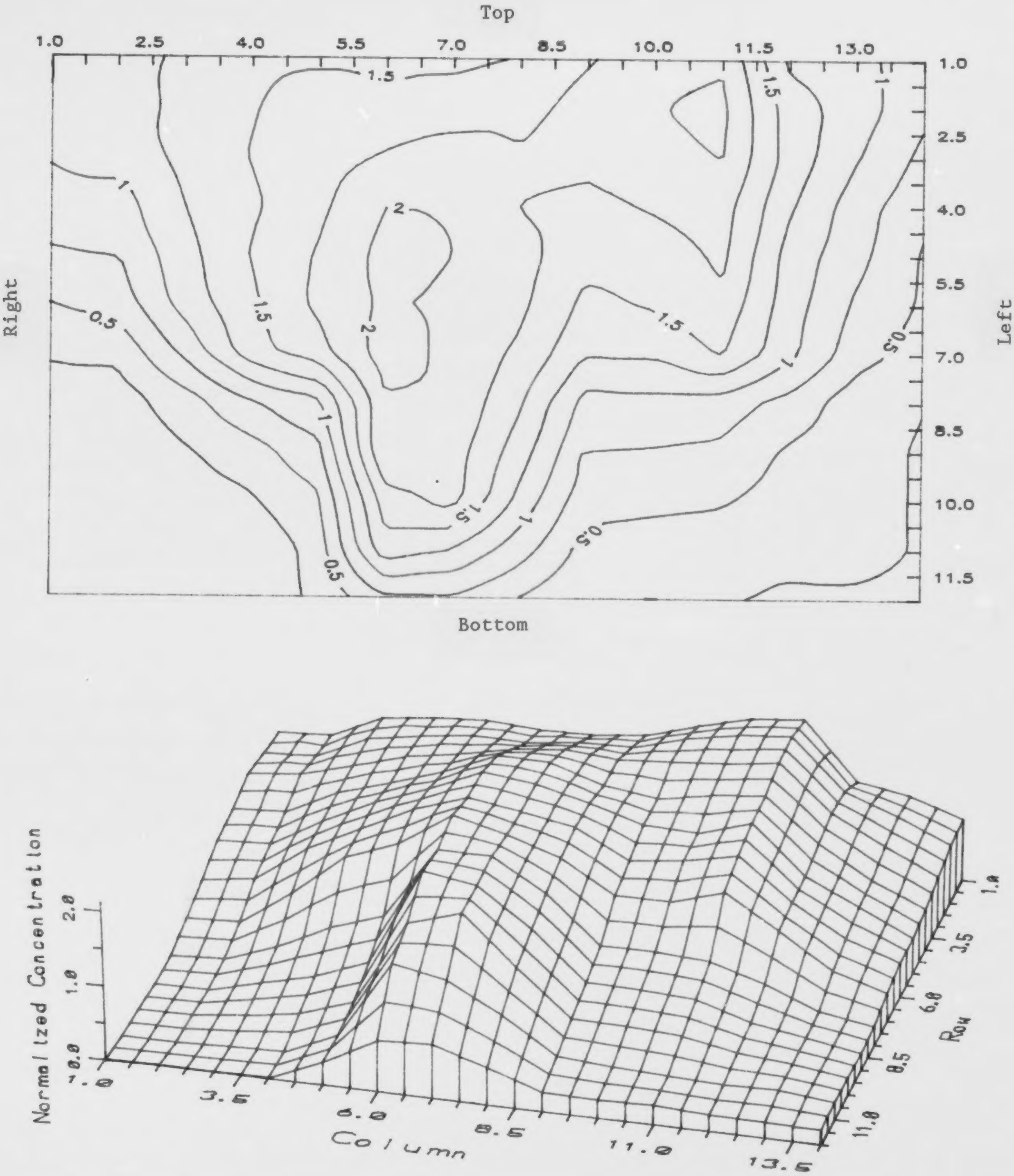

Figure 4-56. Gas mixing isoconcentration plot: Test No. 204: Plane 5.

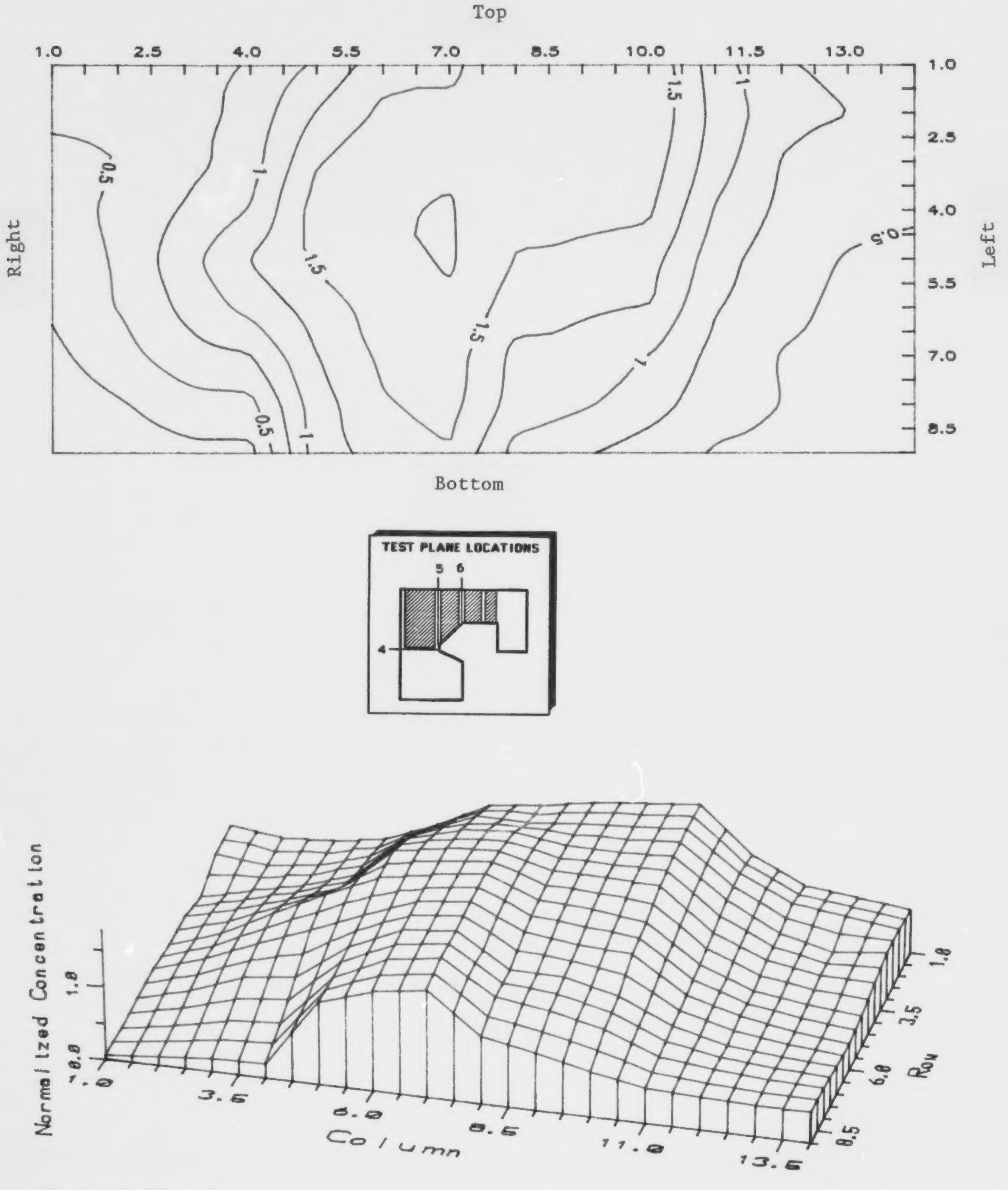

Figure 4-57. Gas mixing isoconcentration plot: Test No. 204: Plane 6.

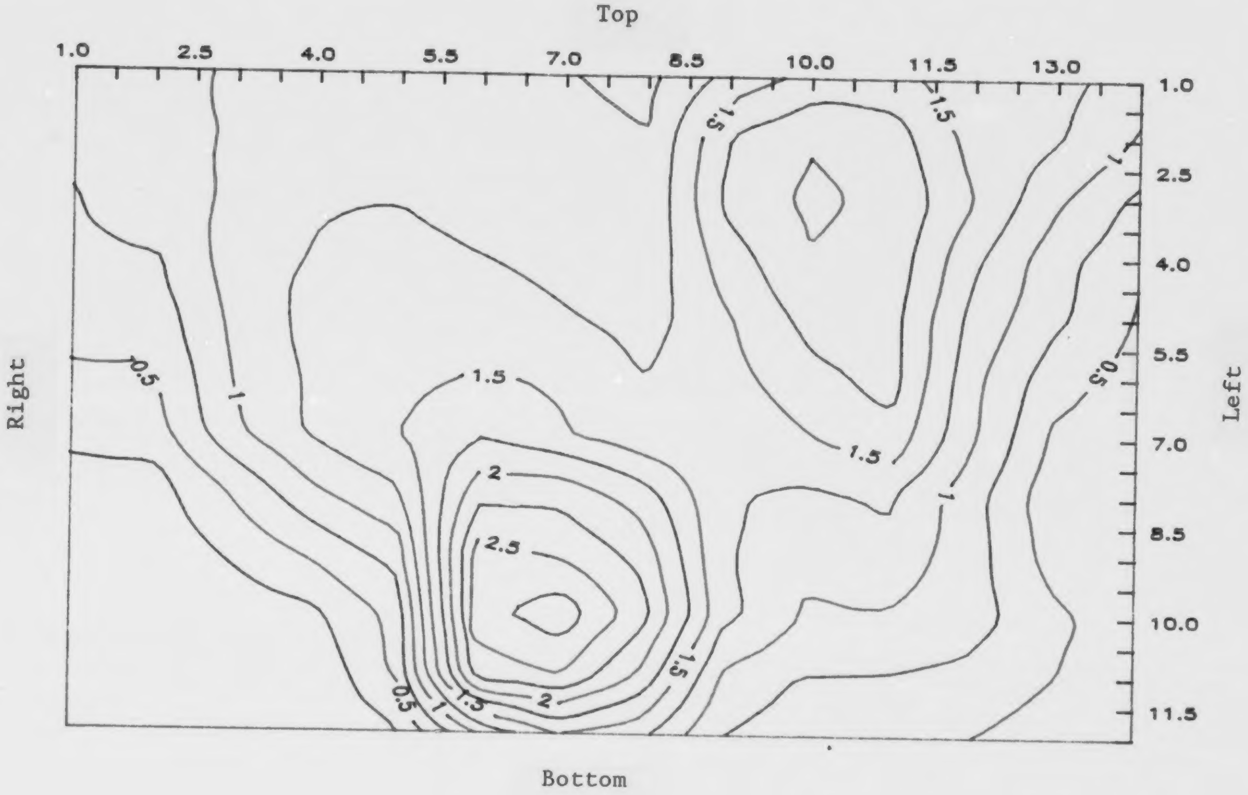

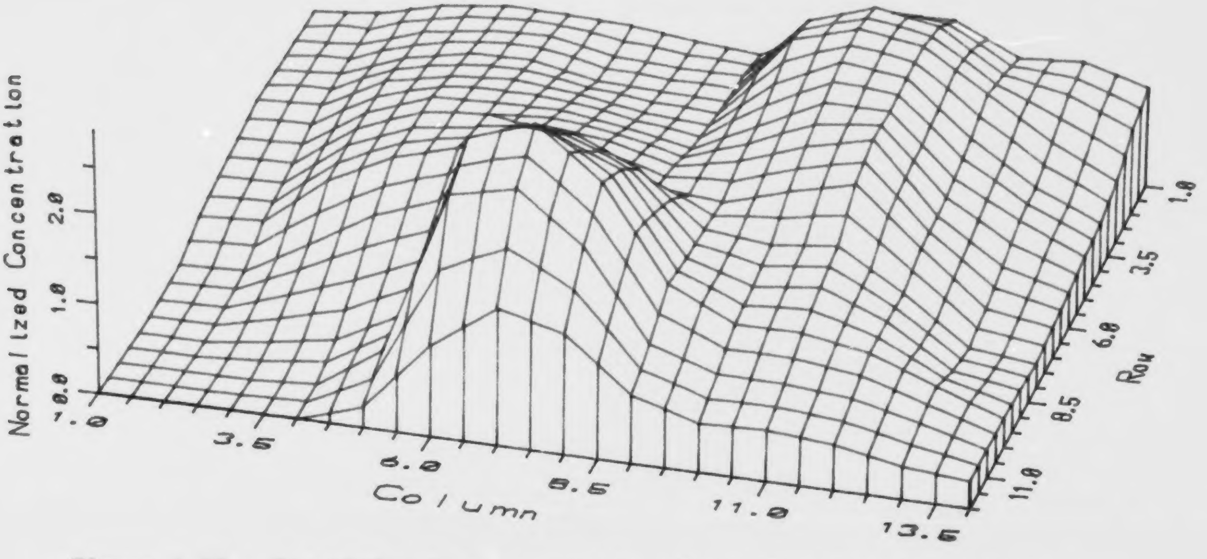

Figure 4-58. Gas mixing isoconcentration plot: Test No. 205: Plane 5.

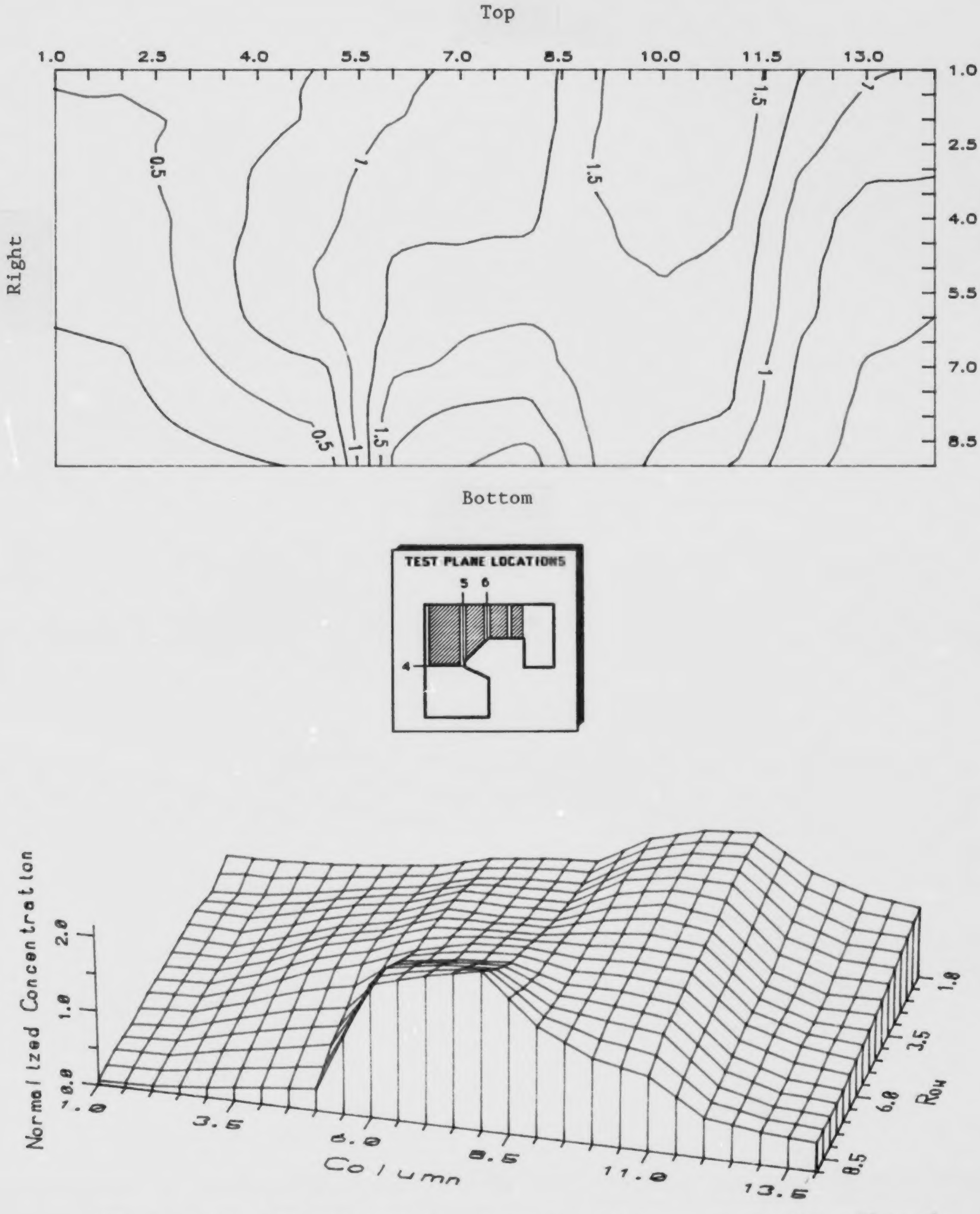

Figure 4-59. Gas mixing isoconcentration plot: Test No. 205: Plane 6.

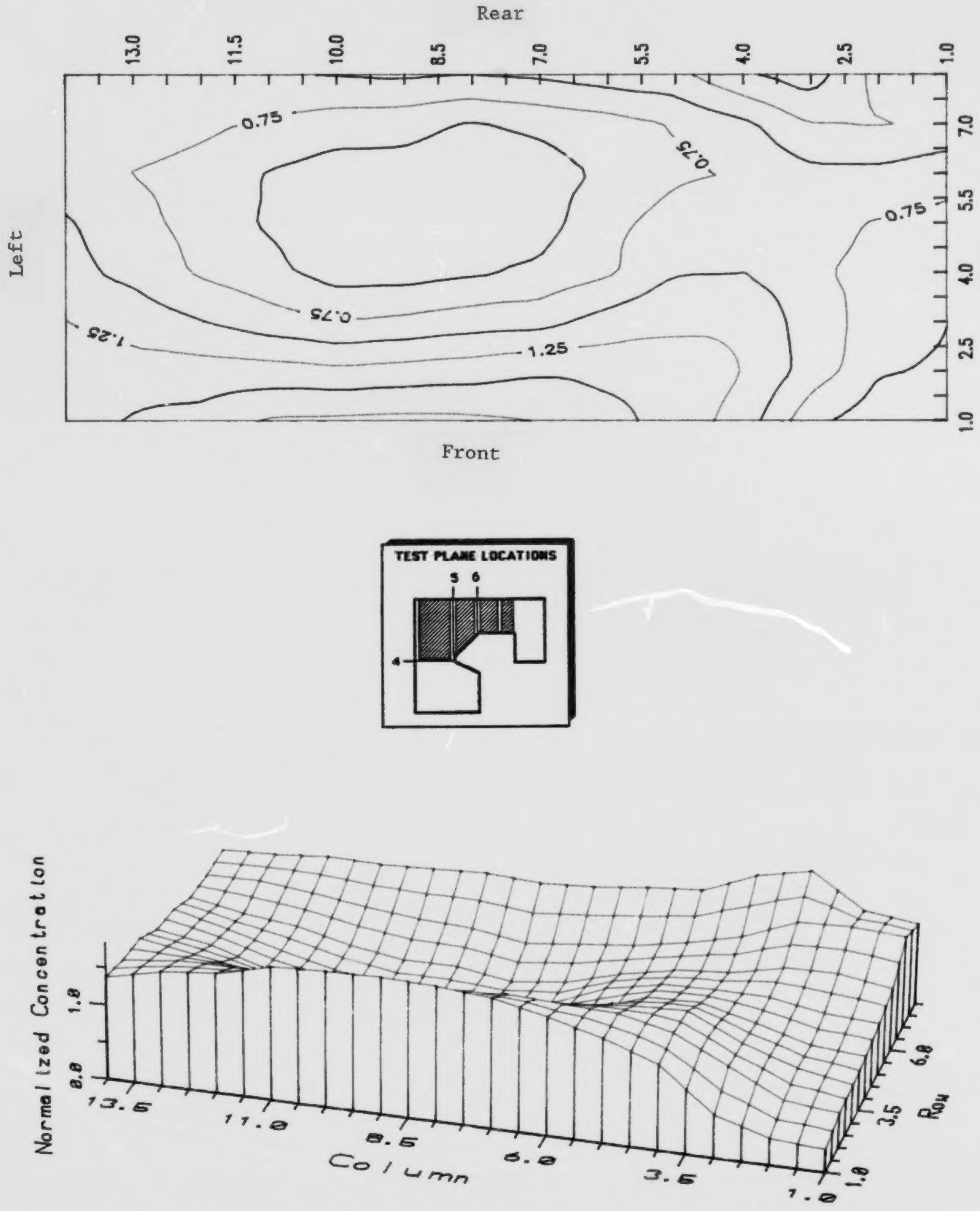

Figure 4-60. Gas mixing isoconcentration plot: Test No. 206: Plane 4.

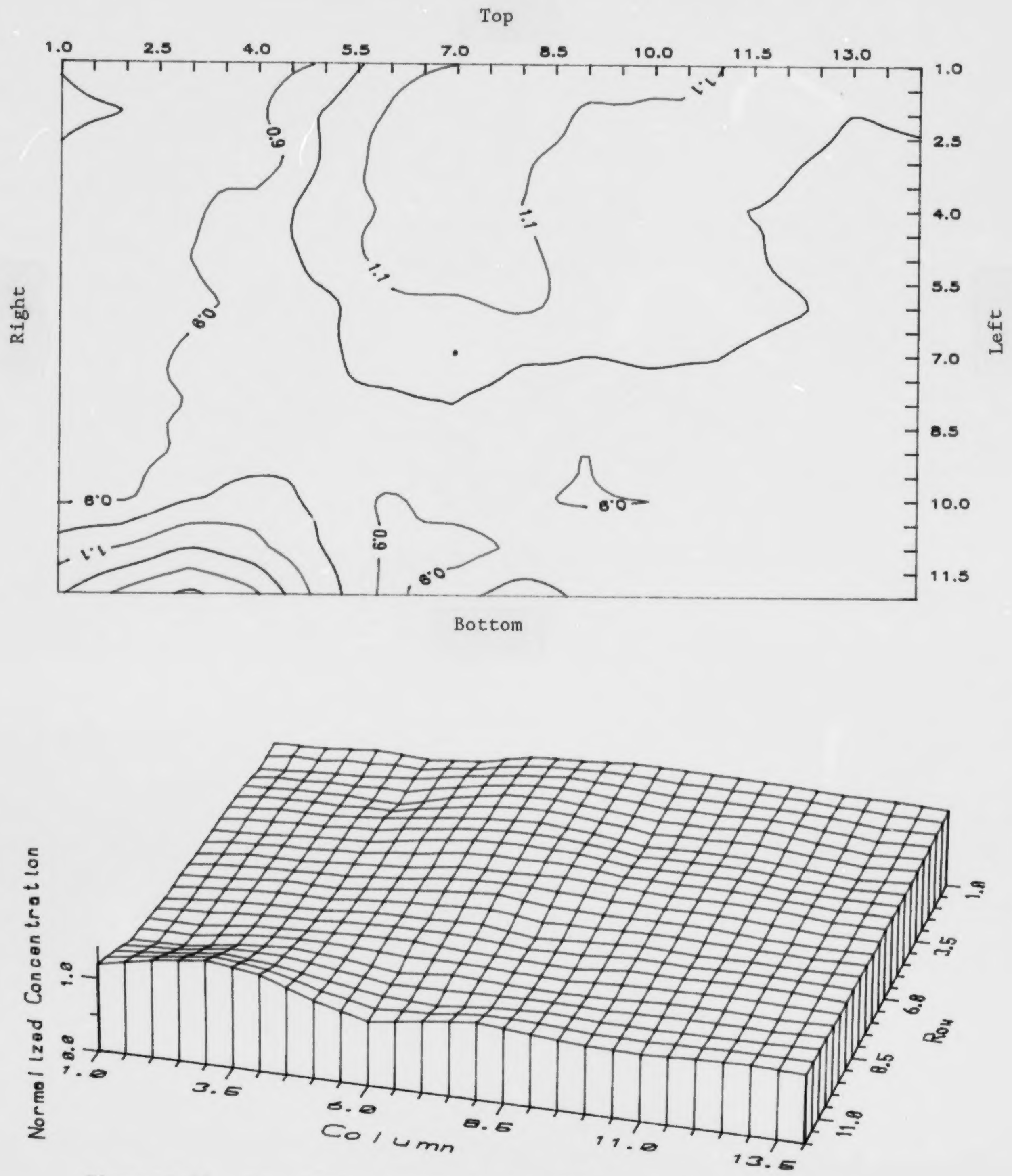

Figure 4-61. Gas mixing isoconcentration plot: Test No. 206: Plane 5.

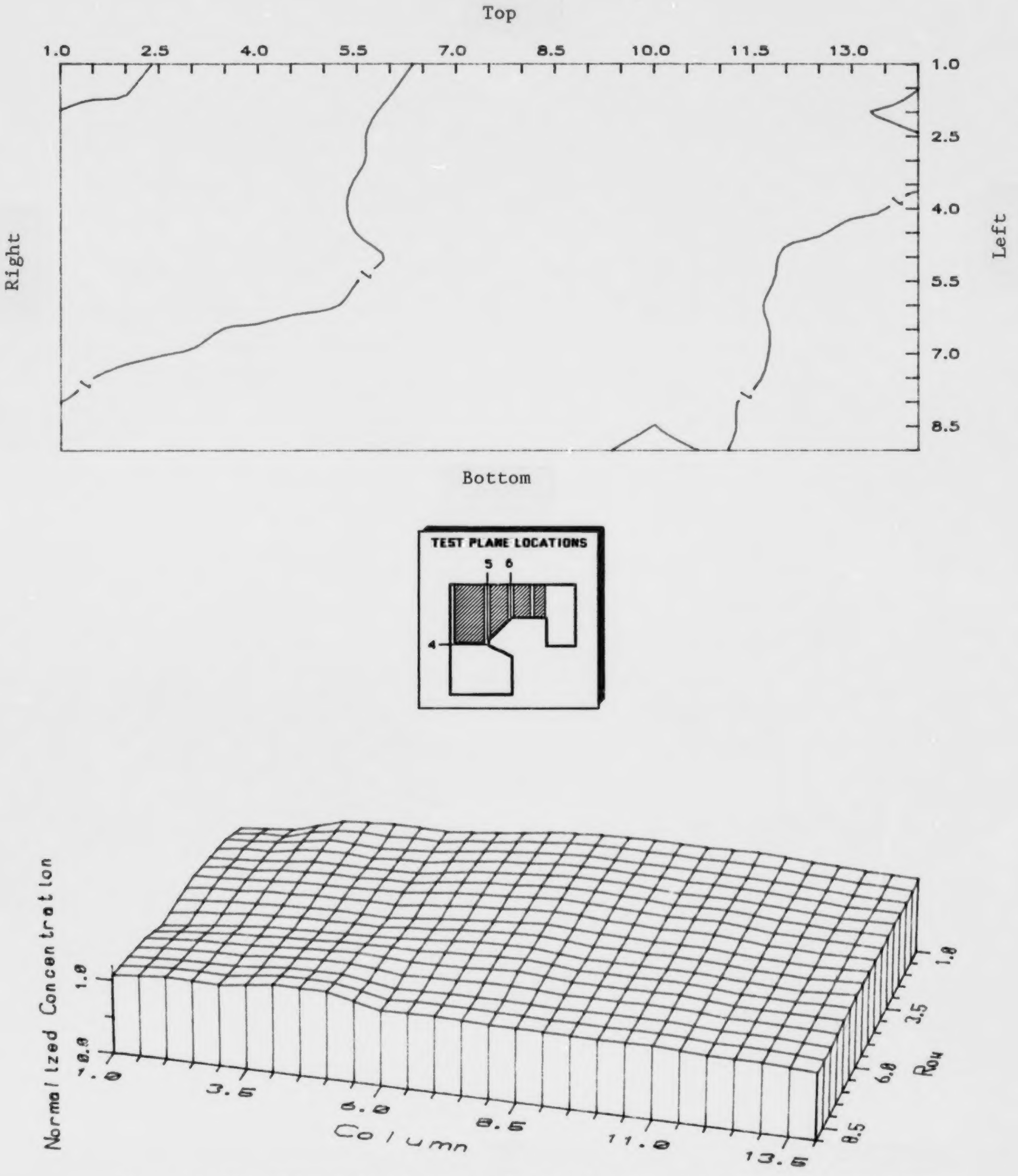

Figure 4-62. Gas mixing isoconcentration plot: Test No. 206: Plane 6.

THIS PAGE WAS INTENTIONALLY LEFT BLANK TO
PERMIT FIGURES FOR THE SAME TEST NO. TO APPEAR
ON OPPOSITE PAGES

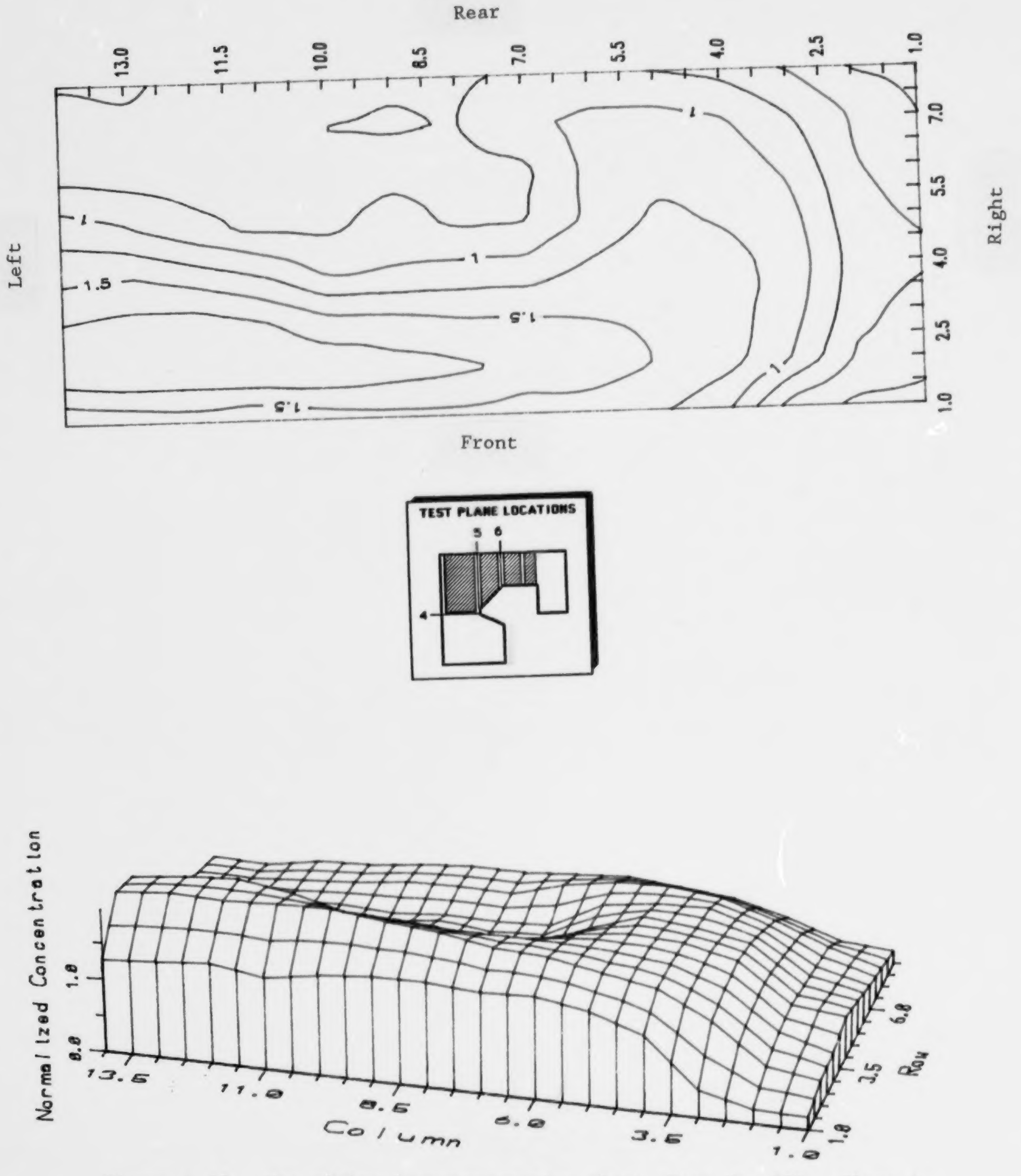

Figure 4-63. Gas mixing isoconcentration plot: Test No. 207: Plane 4.

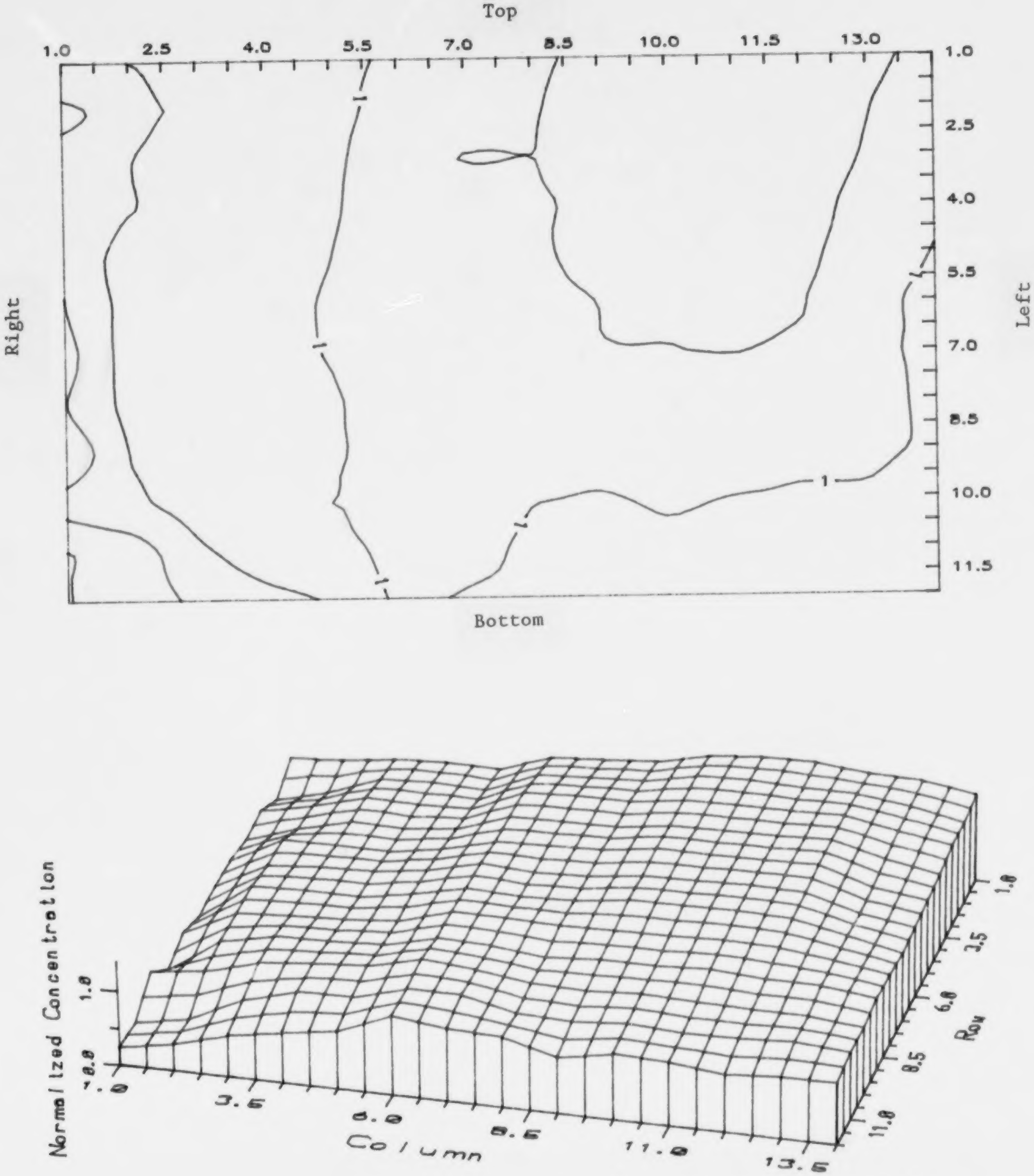

Figure 4-64. Gas mixing isoconcentration plot: Test No. 207: Plane 5.

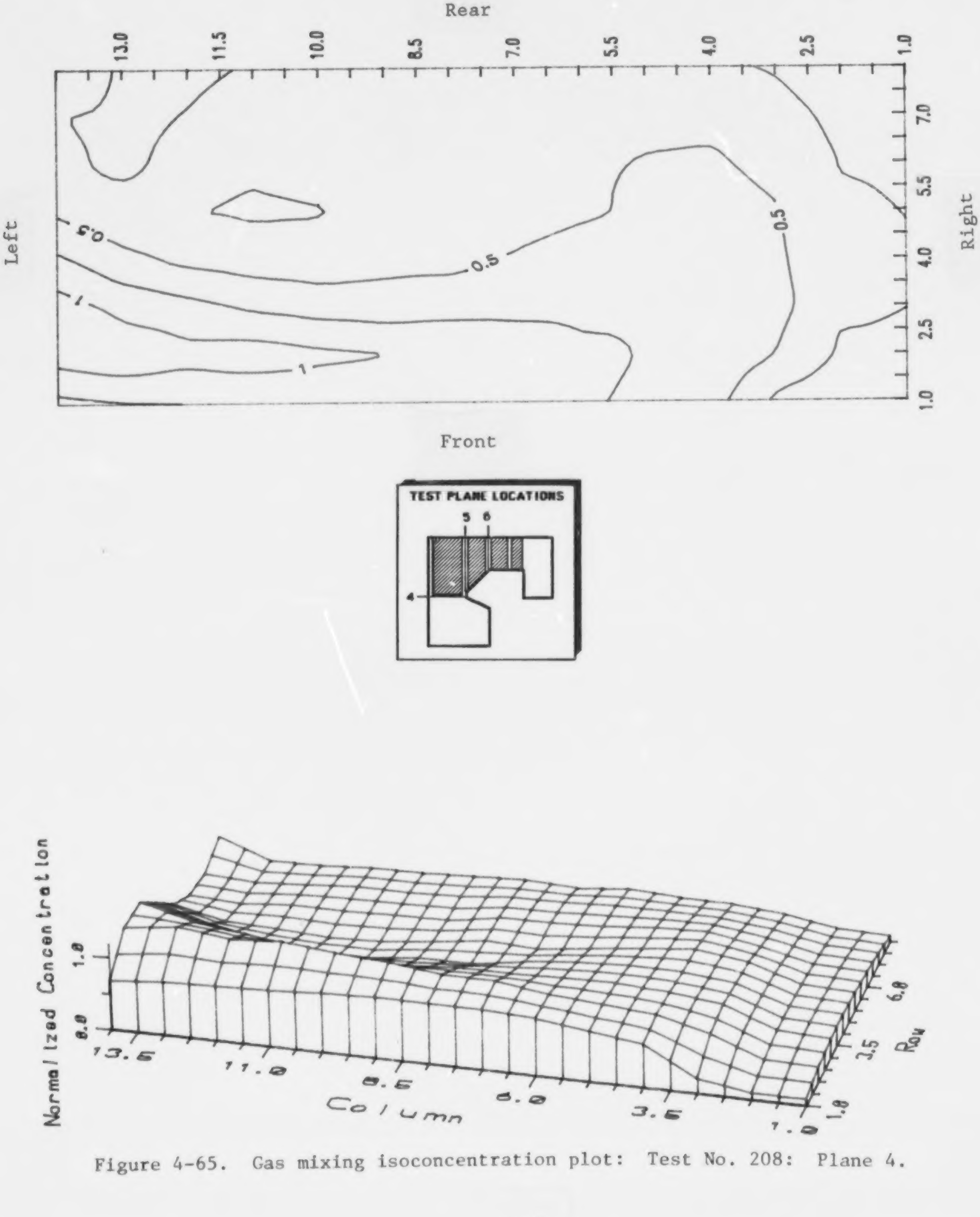

Figure 4-65. Gas mixing isoconcentration plot: Test No. 208: Plane 4.

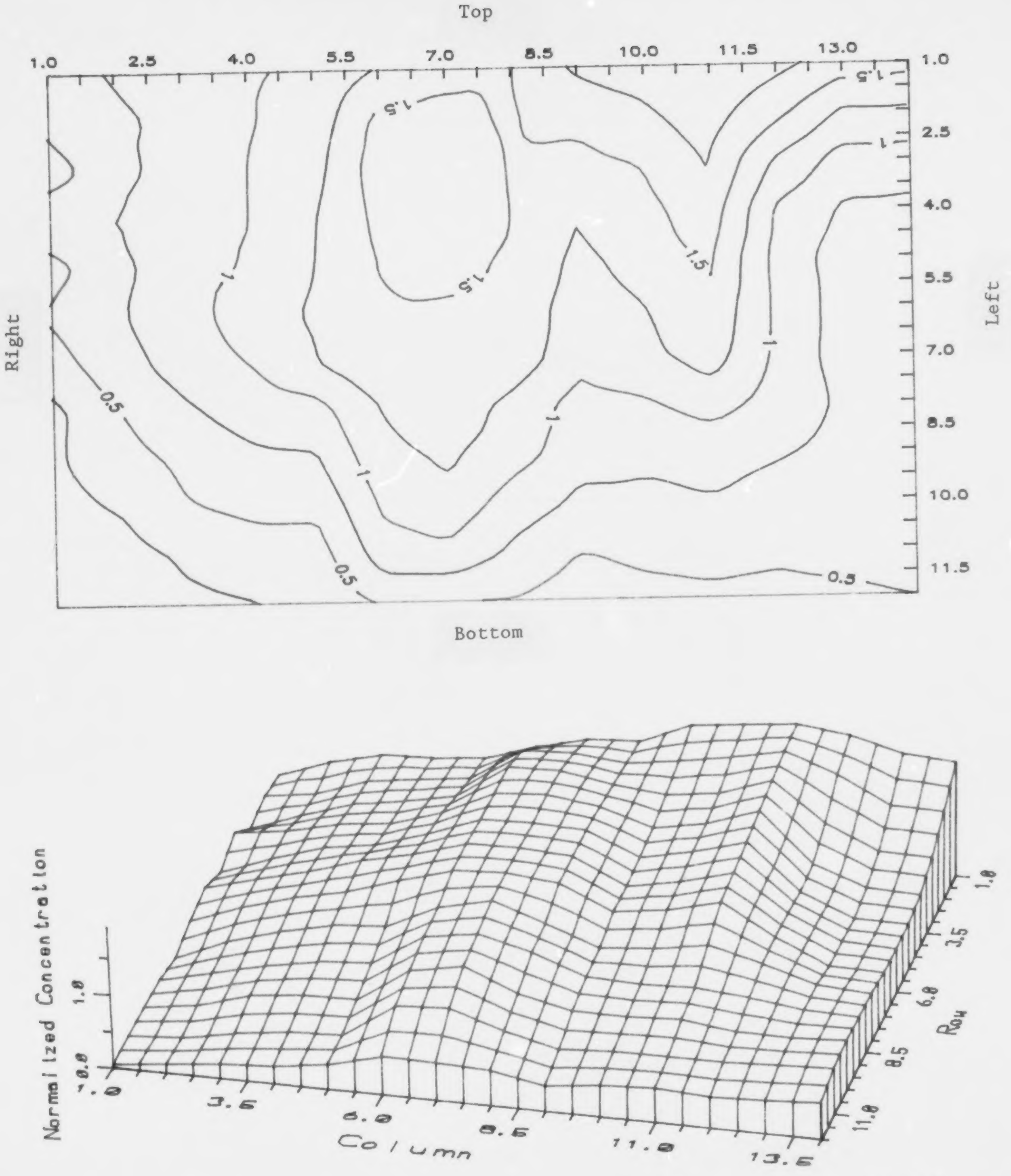

Figure 4-66. Gas mixing isoconcentration plot: Test No. 208: Plane 5.

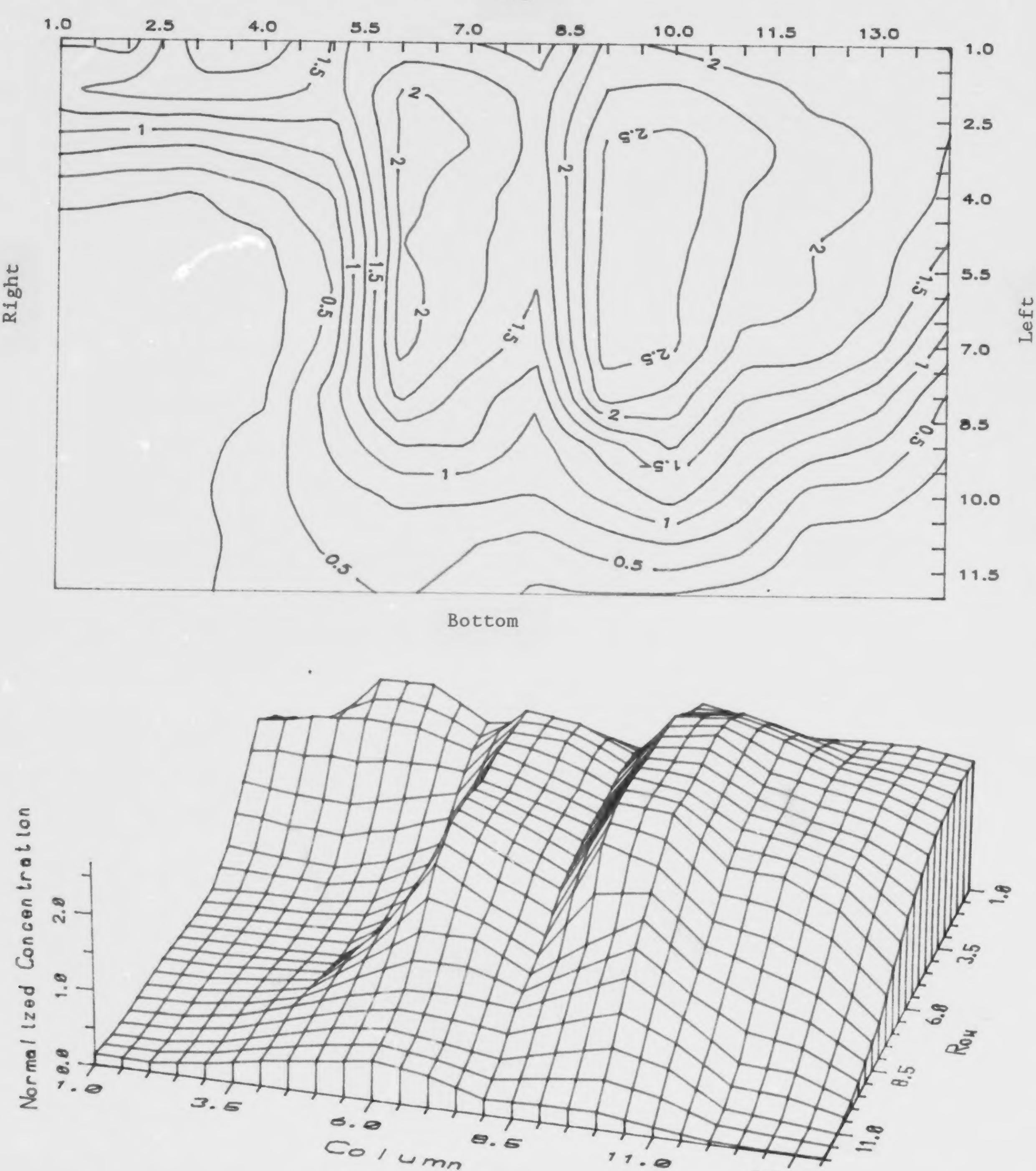

Figure 4-67. Gas mixing isoconcentration plot: Test No. 209: Plane 5.

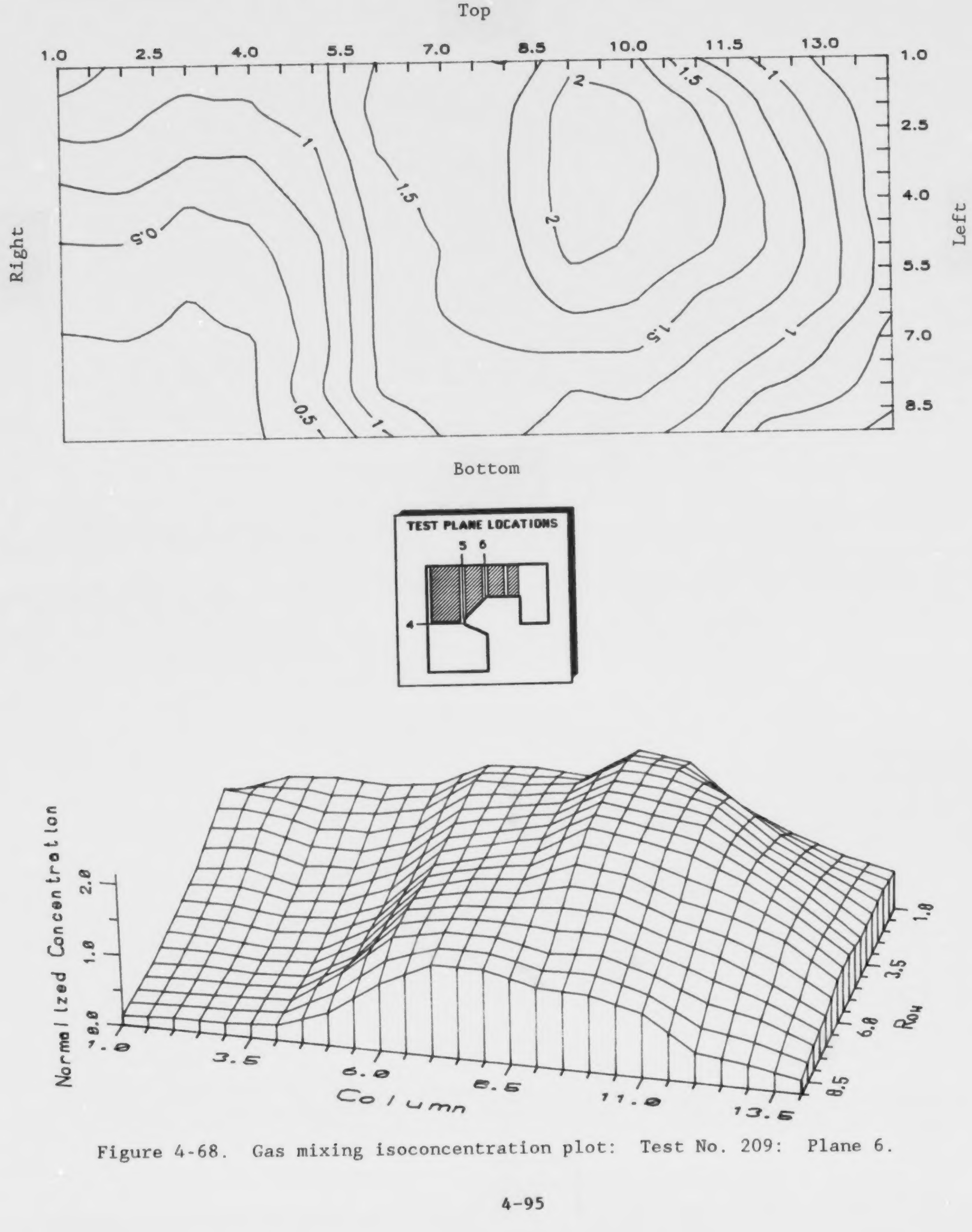

Figure 4-68. Gas mixing isoconcentration plot: Test No. 209: Plane 6.

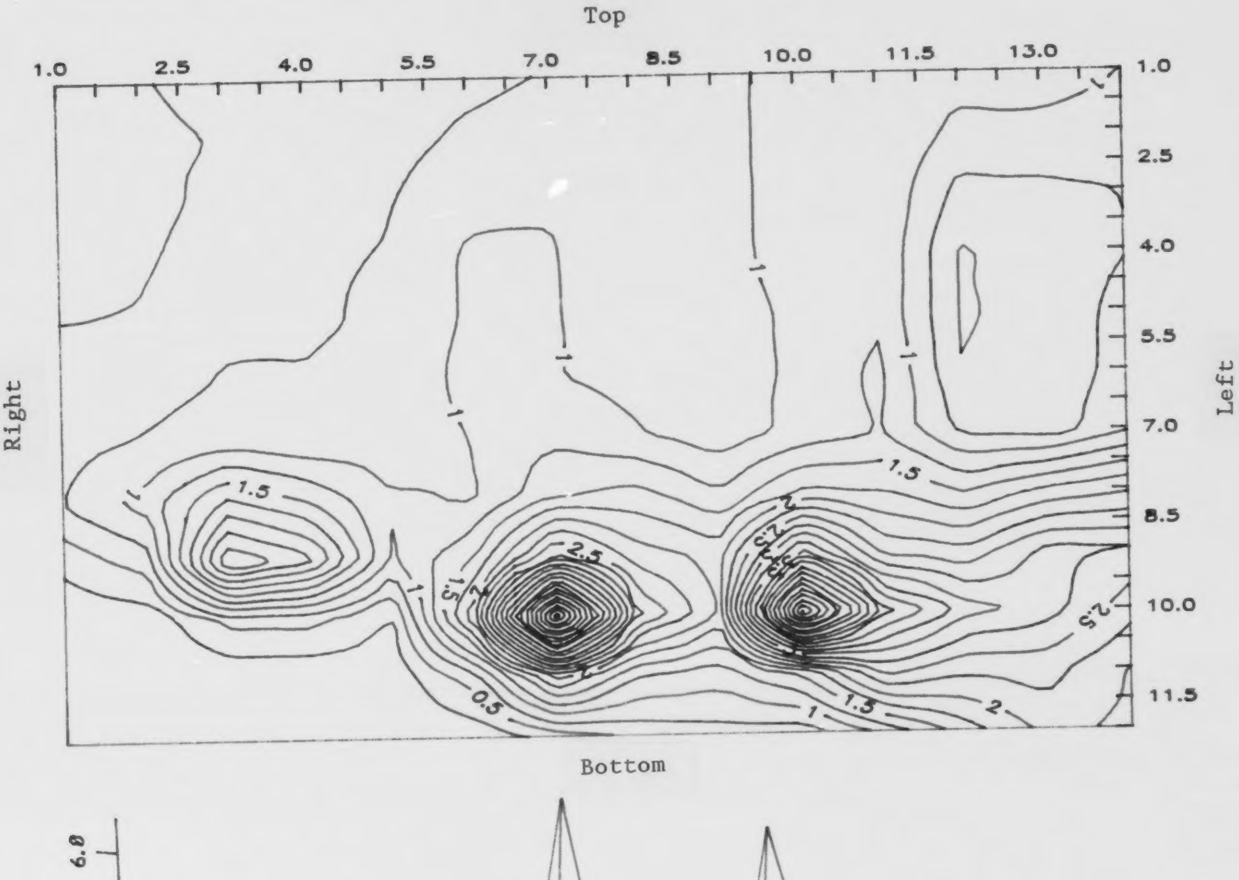

Figure 4-69. Gas mixing isoconcentration plot: Test No. 210: Plane 5.

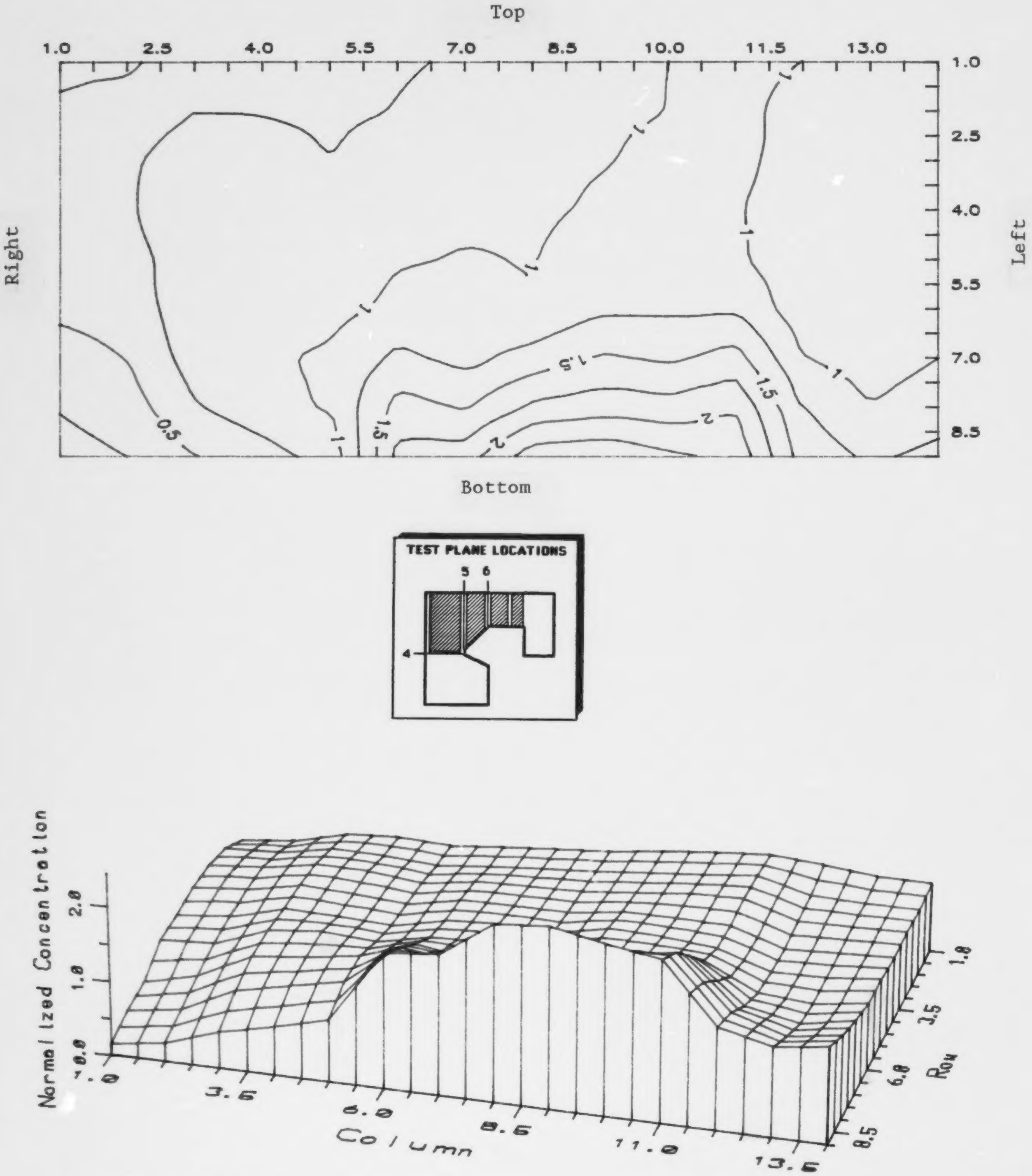

Figure 4-70. Gas mixing isoconcentration plot: Test No. 210: Plane 6.

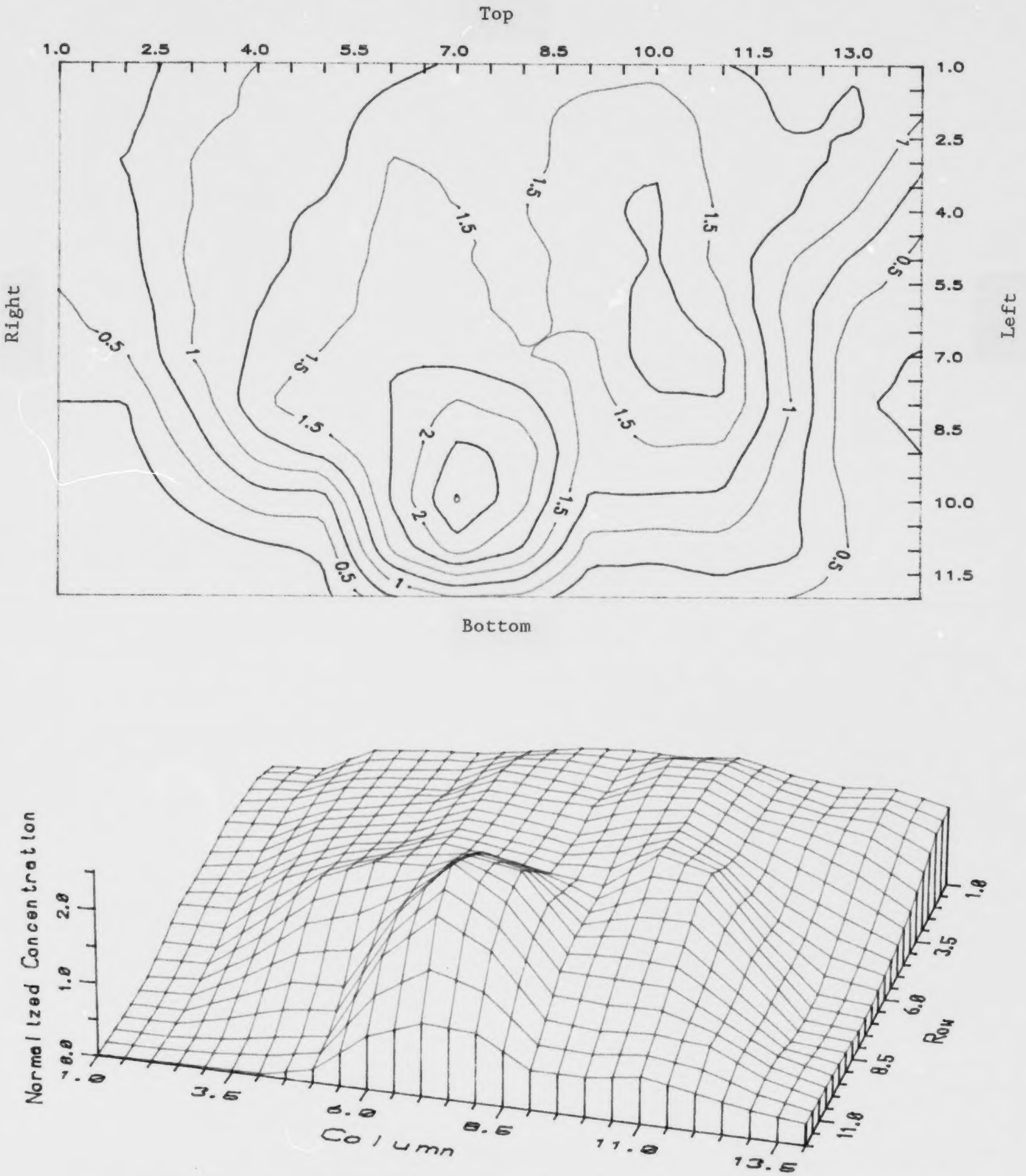

Figure 4-71. Gas mixing isoconcentration plot: Test No. 211: Plane 5.

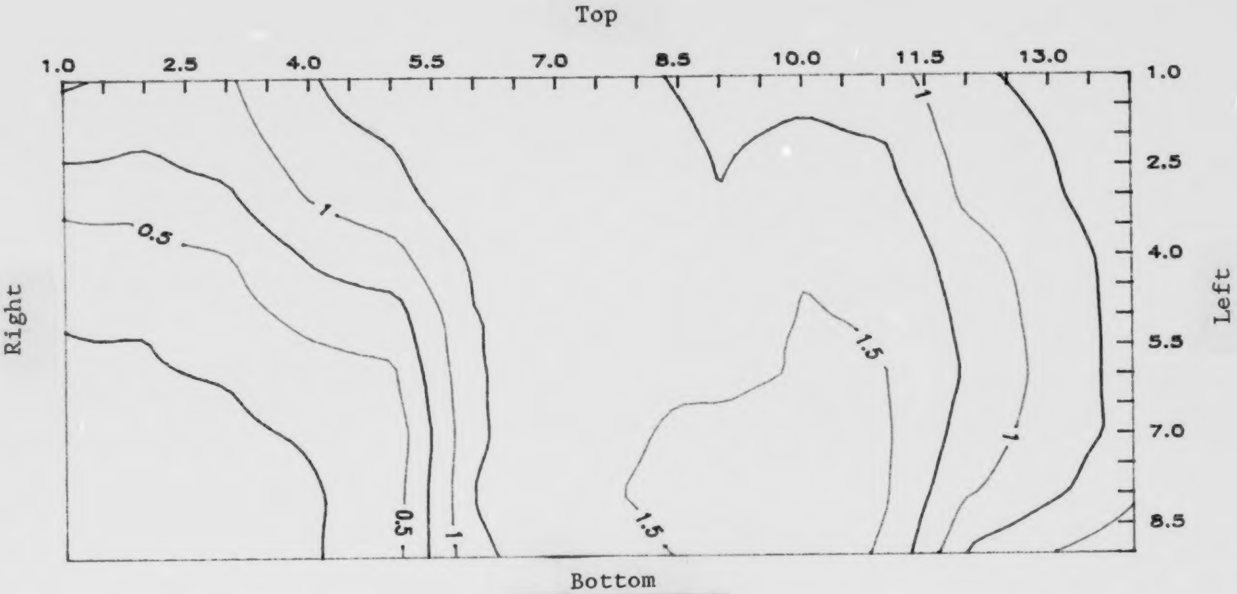

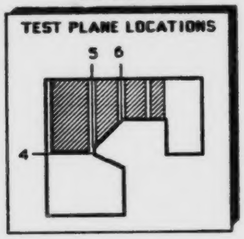
TEST PLANE LOCATIONS
5
6
4

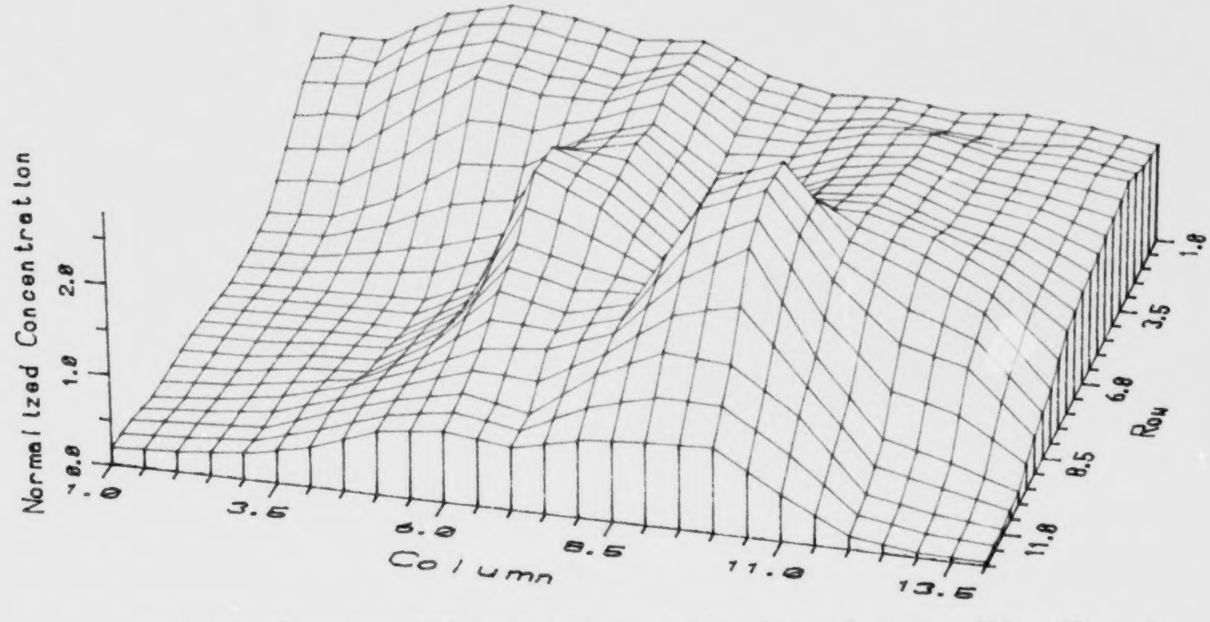

Figure 4-72. Gas mixing isoconcentration plot: Test No. 211: Plane 6.

TABLE 4-6. SECOND SCREENING LEVEL COEFFICIENTS OF VARIATION

TN	Location	Tilt	Plane 4 Cov, %	Plane 5 Cov, %	Plane 6 Cov, %	Description
201	F	0°	--	81	65	Roof
202	G	-45°	--	43	38	Front facing lance
203	B	-20°	--	54	45	Front wall
204	A	-20°	--	62	51	Front wall
205	A	0°	--	59	50	Front wall 30.5 m/sec (100 ft/sec)
206	D	-20°	39	11	--	Counter 'T' Fired
207	E	-20°	46	25	--	Rear wall
208	B/E	-20°/-20°	58	47	--	Front wall/rear wall
209	A/F	-20°/-20°	--	72	56	Front wall/roof
210	B/G	0°/0°	--	84	40	Front wall/roof lance
211	C	-20°	--	61	47	Front wall 30.5 m/sec (100 ft/sec)

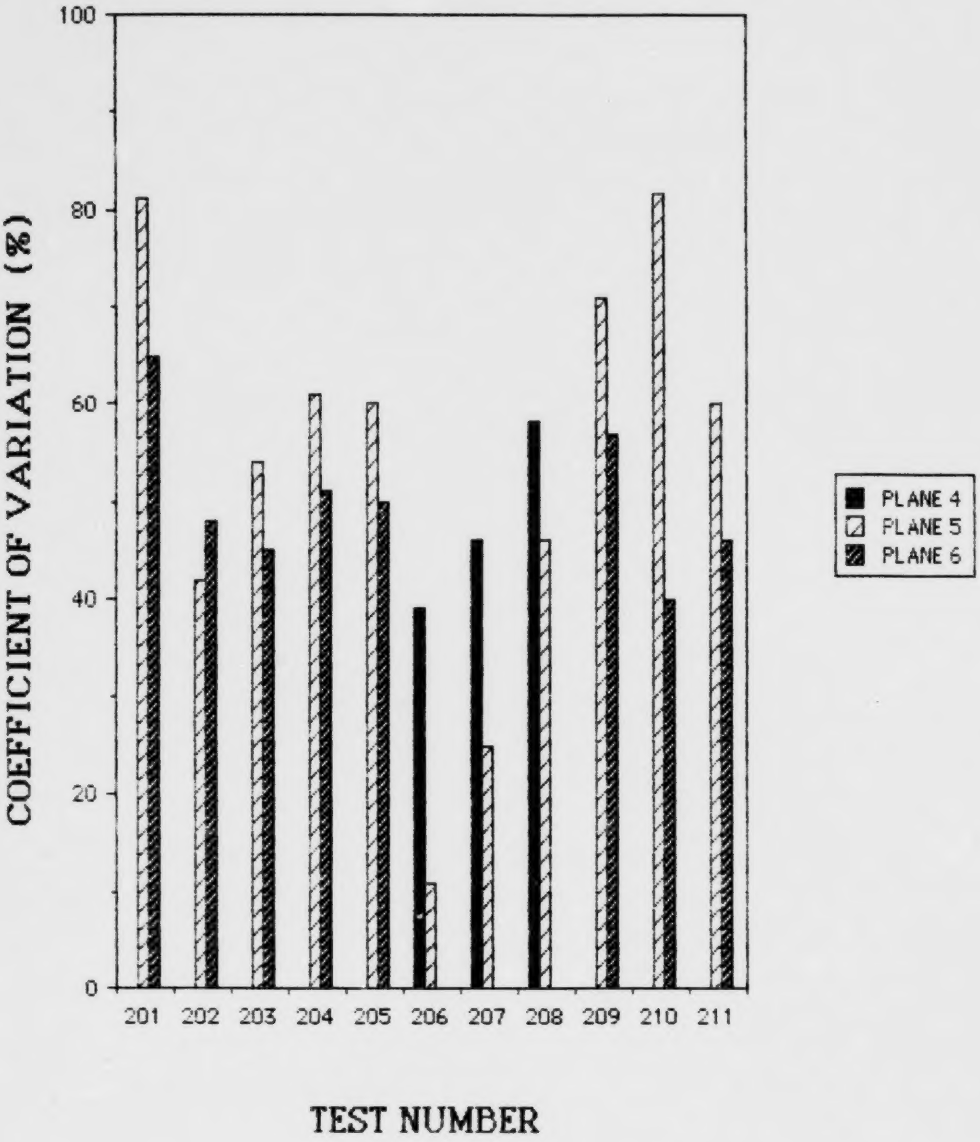

Figure 4-73. Second screening level variances.

Injection below the arch, TN 206 and 207, provided a long residence time for the injected sorbent to mix before the flow was biased by the presence of the superheater panels. Injection locations below the arch provided very effective levels of mixing at both the horizontal furnace outlet plane (HFOP), Plane 4 and at Plane 5. Since a temperature of 1315°C (2400°F) was anticipated at the arch in the Boiler Simulation Facility, sorbent injection locations below the arch were not evaluated further during Task A. However, flue gas temperatures were lower than anticipated during Task C testing at the BSF, and sorbent injection below the arch was being successfully applied during this testing. The combustion test results are discussed in Section 6.

Sorbent injection from the front wall generally provided effective penetration and mixing although the effect of the nonsymetric upper furnace flow patterns and mass flow distributions were evident. For example, for TN 205, injection from Location A, the region of highest concentration in the left hand lane was along the roof, while in the right lane the region of highest concentration just above the arch. In the two (2) intermediate lanes the effect was also observable but less pronounced. Three (3) front wall injection configurations were chosen for advancement to the third screening level. These are detailed in Table 4-7.

The flow visualization tests in the first screening level indicated that sorbent injected through lances directed counter to the local flow environment gave very high levels of dispersion. This was confirmed by the favorable results of the tracer gas traverses for TN 202. The coefficient of variation at Plane 5 was the lowest of all the configurations tested with the exception of injection schemes below the arch. This configuration was advanced to the third screening level and is listed in Table 4-7.

The use of eight (8) injectors rather than four (4) did not increase the effectiveness of penetration, dispersion, and mixing of the simulated sorbent within the upper furnace. The reason for this is that when the mass flow of sorbent transport air is held constant, as was specified during these tests, using eight (8) injectors in place of four (4) necessitated a reduction in the open area of each injector by one-half and its diameter to $1/\sqrt{2}$ of the original. This leads to lower jet penetration as shown by the empirical equations given in Table 4-4.

TABLE 4-7. THIRD SCREENING LEVEL CONFIGURATIONS

TN	Location	Tilt	Description
201	F	0^0	Roof
202	G	180^0	Front facing lance
204	A	-20^0	Front wall low
205	A,G	0^0	Front wall low, 30.5 m/sec (100ft/sec)
211	C	-20^0	Front wall high 30.5 m/sec (100ft/sce)

The steady state gas mixing tests have quantified the observations made during the first screening level tests. Five (5) injection configurations were chosen for advancement to the third screening level based on the steady state gas mixing test results and the expected location of the sulfation temperature window within the BSF during the Task C combustion tests. These configurations are listed in Table 4-7.

Third screening level tests; residence time distribution studies -- For each of the five (5) configurations detailed in Table 4-7 the residence time distribution of the tracer gas within the flow model was measured. These measurements were obtained using the same laser system as was used for the steady state gas mixing tests, but configured quite differently. Figure 4-74 shows the arrangement. To perform a test, methane was first injected into the furnace at steady state. The resultant intensity of the laser beam directed through the flow model was reduced in proportion to the quantity of methane the beam passed through. The methane tracer gas flow was then terminated and the resulting concentration decay over the line of sight was recorded by the data acquisition computer. Figure 4-75 presents an idealized representation of the resulting concentration versus time plot or Residence Time Distribution (RTD).

For each configuration tested, nine (9) of these RTD measurements were obtained at Test Plane No. 6. The results of these tests are summarized in Figure 4-76. On this figure the length of the horizontal line in the upper left corner of the plot is proportional to the plug flow residence time from the sorbent injection point to the test plane location. The exponential decay of tracer concentration has been linearized by plotting in logarithmic format. The slope of the line indicates the rate at which the sorbent material is evacuated from this volume. The lower the value of the negative slope, the longer the time required to evacuate the tracer gas and therefore the longer the residence time in the sulfation temperature window. They intercept at a long residence time such as six seconds represents overall residence time. The greater its value, the greater the overall residence time. By evaluating the RTD results this way, the following observations were made.

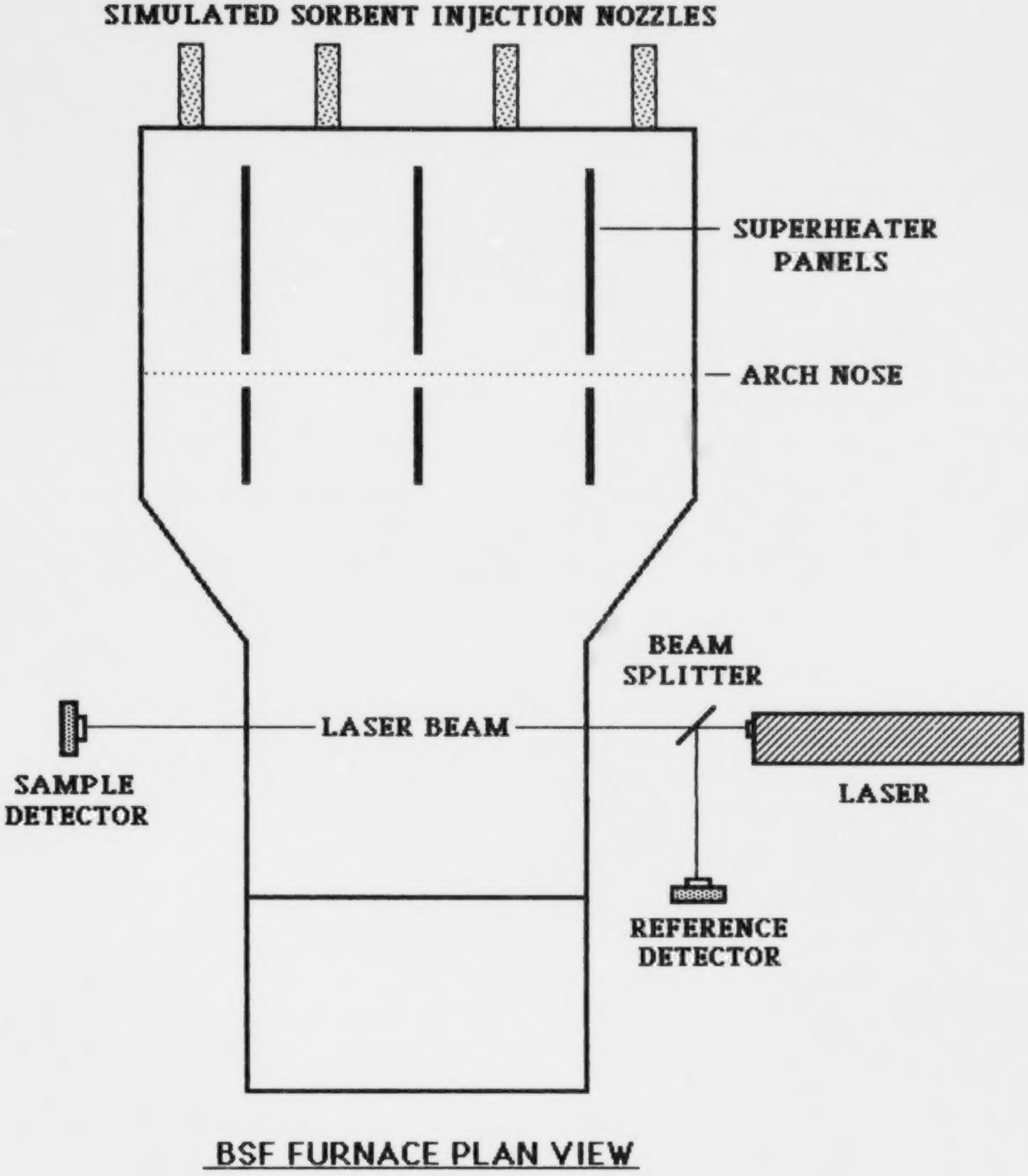
SIMULATED SORBENT INJECTION NOZZLES
SUPERHEATER PANELS
ARCH NOSE
BEAM SPLITTER
LASER BEAM
SAMPLE DETECTOR
LASER
REFERENCE DETECTOR
BSF FURNACE PLAN VIEW

Figure 4-74. Flow model RTD test setup.

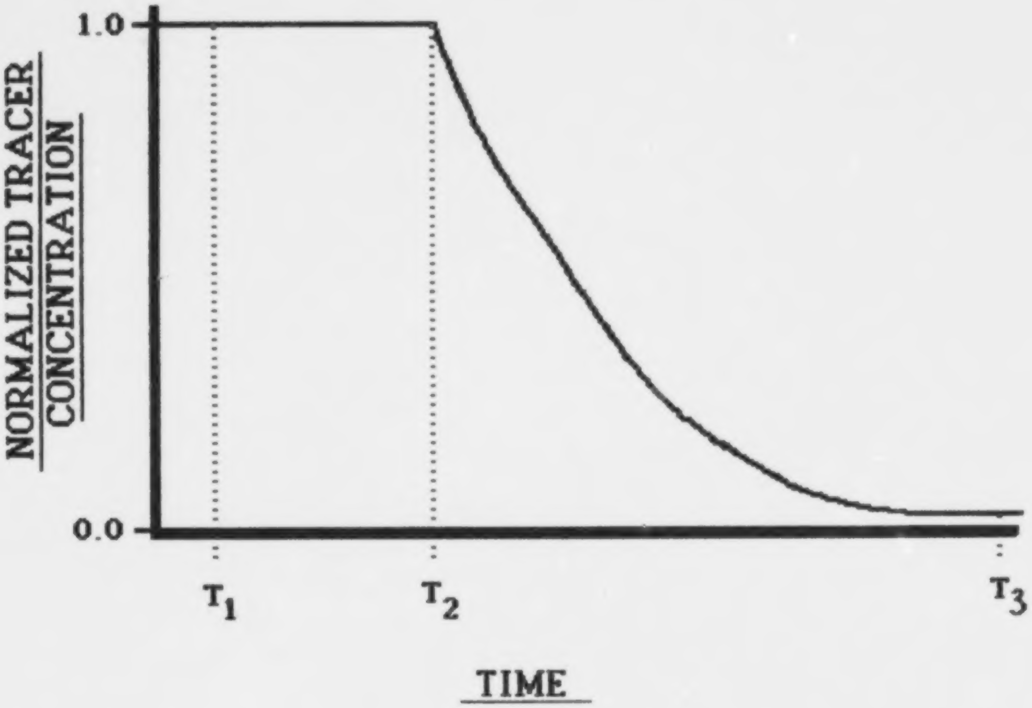

T_1 TRACER GAS FLOW TERMINATED

T_1-T_2 PLUG FLOW REGION

T_2-T_3 WELL MIXED REGION

Figure 4-75. Idealized RTD test result.

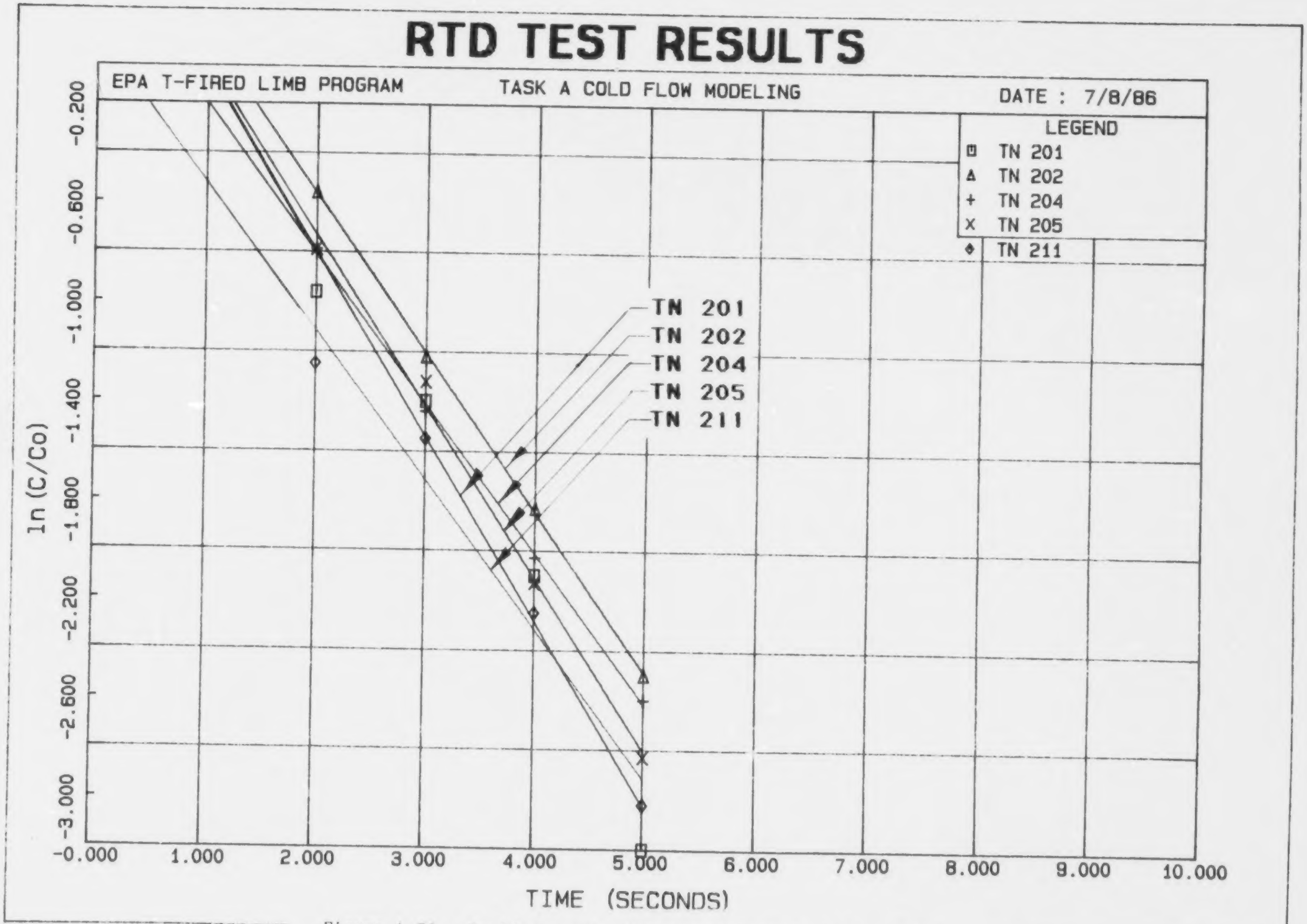

Figure 4-76. Residence time distribution study test results.

The roof mounted front facing lance, TN202 provided the longest sorbent residence time within the BSF's expected sulfation temperature window as well as one of the slowest evacuation rates. TN211, front wall injection at Point C, had the quickest overall evacuation rate. This was due to the fact that the injection nozzles were aimed towards the back of the unit and were injecting into an almost coaxial flow environment. Injection in this manner, had good penetration, but poor dispersion.

While the configuration involving roof mounted injectors (TN201), had the closest actual injection point to the test plane, the counterflow injection enhanced the dispersion process. This configuration, while having a comparatively long plug flow time, had the shortest overall total residence time of all the configurations tested. While not a good candidate for an effective BSF sorbent injection system, injection from this location would be desirable for furnaces whose thermal topography would place the sulfation temperature window at a point past the superheater sections of the furnace.

Based on the results of Task A tests, five (5) injection schemes have been identified capable of providing high levels of sorbent dispersion and residence time within the expected sulfation window of the BSF. These configurations, listed in Table 4-8, were recommended for hot testing during the Task C combustion tests.

Additional tests were performed during the third level screening tests to evaluate the effect of fuel admission assembly tilt and the resulting changes to the upper furnace aerodynamics on the penetration and dispersion performance of the injection system. The tests consisted of additional three-dimensional velocity traverses and steady state gas-mixing tests. In general, it was found that tilting the fuel admission assemblies either up or down 20° had little or no significant effect on the penetration and dispersion performance of the sorbent injection system.

TABLE 4-8. SORBENT INJECTOR RECOMMENDATIONS

Location	Tilt	Velocity m/sec(ft/sec)	Corresponding Task A Test No.	Description
G	180°	22.9 (75)	202	Front facing lance
B	-20°	22.9 (75)	203	Front wall middle
A	-20°	22.9 (75)	204	Front wall low
A	0°	30.5 (100)	205	Front wall low
C	-20°	30.5 (100)	211	Front wall high

4.4 SUMMARY OF RESULTS

Isothermal flow modeling, supported by mathematical modeling, was used to develop sorbent injector locations and methods for combustion testing at C-E's BSF and to develop injector design guidelines for field testing of the furnace sorbent injection process in a tangentially fired utility boiler. From these studies the following conclusions and design guidelines were developed:

1. Sorbent injection systems were developed which provide high levels of sorbent dispersion for a wide range of sulfation temperature windows and corresponding sorbent injection locations. Specific designs selected for the BSF temperature window and tested at the BSF are discussed in Section 6.

2. As an initial design guideline for the BSF, pneumatic transport and injection of sorbent using air at a flow rate equivalent to 5% of the full load combustion air flow and injection velocities of between 22.9 and 30.5 m/sec (75 and 100 ft/sec) were recommended. These guidelines were adjusted by experience gained by testing at the BSF.

3. The trajectory and dispersion of a two-phase jet can be predicted by a gas-only jet correlation if the size of the particles in the jet are small (approximately 20 micron or smaller) as is typical of most sorbents and the mixture density of the jet is used in the trajectory calculations. The mixture density is defined by:

$$\rho\Big|_{mix} = \frac{\dot{m}_{solids} + \dot{m}_{air}}{Q}$$

4. For furnaces in which the beginning of the sulfation temperature window is located at or near the arch elevation, injection from a position low on the front wall is effective.

5. For furnaces in which the beginning of the sulfation temperature window is located below the arch, tangential injection from the corners of the unit provides very effective sorbent penetration and dispersion across the furnace plan area.

6. Lance injection provides an effective method for injecting sorbent precisely into the desired location in the furnace and demonstrated excellent dispersion performance. Although practical considerations limit the applicability of lance injection, this design should be considered where feasible.

7. For the BSF, four (4) sorbent injection jets were found to provide better overall sorbent penetration and dispersion than eight (8) for a constant sorbent and carrier air mass flow rate. This result was attributed to more effective jet penetration when using the larger nozzle size which corresponds to the fewer nozzles.

8. At any injection location, angling the sorbent injection nozzles such that the resulting jet flow is in the direction opposite of the bulk gas flow significantly increased sorbent dispersion.

SECTION 5

MATHEMATICAL MODELING STUDIES

5.1 THERMAL MODELING

Proprietary Combustion Engineering thermal modeling computer programs were used to calculate heat transfer rates and gas temperature distributions for selection of candidate sorbent injector locations both for the flow model testing and BSF combustion testing. Gas temperature and heat transfer calculations were used in the design of the BSF and in interpreting BSF test results to permit further optimization of SO_2 capture performance at the BSF. Thermal modeling will also be used in developing recommendations for sorbent injection locations for field demonstrations of sorbent injection technology. These specific applications of thermal modeling are discussed in Sections 4, 6, and 7.

5.2 SORBENT DISPERSION MODELING

Computational fluid dynamic (CFD) modeling studies were initiated under this program and continued under C-E funding for calculating dispersion of sorbent. The purpose of this modeling was to supplement the cold-flow testing conducted within Task A and to provide additional detail and insight concerning the mixing process. This section describes the modeling approach, discusses validation of the CFD model, and identifies areas where CFD modeling can provide information which is not readily available from physical modeling.

5.2.1 Modeling Approach

Sorbent dispersion modeling was performed using the TEMPEST CFD code. TEMPEST is a proprietary CFD code similar to the code described by Boysan et al. (1982). The code solves the fundamental equations governing fluid flow, including the continuity, three-dimensional momentum, and energy equations in steady state with a finite difference numerical algorithm. Additional equations such as the k-ε turbulence model and the conservation equations for chemical species are also solved simultaneously by a similar approach.

CFD analysis was applied to the upper furnace of the LSFATF discussed in Section 4. Comparison of calculated results to LSFATF test data was used to validate CFD modeling as a method for studying sorbent mixing in tangentially fired furnaces. The boundary of the control volume used in the TEMPEST simulation is shown in Figure 5-1. Linear dimensions of the LSFATF were modeled full scale. Although TEMPEST can calculate temperature distributions by activating the energy balance module, the calculations for this study were isothermal at ambient temperature using the same hot flow to isothermal flow scaling criteria as were used in the cold flow modeling studies. The three-dimensional domain of the calculation includes the space between Test Plane 4 and the roof, the front wall and Test Plane 6, and the side walls of the LSFATF.

5.2.2 Calculated Results and Comparison with Experiments

The TEMPEST simulation of the LSFATF was evaluated by comparing measured and calculated velocities at Planes 5 and 6 for Test 101, by comparing calculated upper furnace velocity data to LSFATF flow visualization experiments, and by comparing measured and calculated concentrations for two sorbent tracer experiments (Tests 201 and 204).

5.2.2.1 Upper Furnace Velocities

Two types of velocity measurement were used to compare calculated results to LSFATF data. The first is axial velocities normal to the traverse planes. The second is velocity vectors (both magnitude and direction) in the traverse planes. Study of velocity vectors is important for tangential flow since the swirl indicated by these vectors has a significant influence on the axial velocity distribution. Study of the velocity vectors therefore is valuable to evaluate the effectiveness of the calculated flow simulations.

Figures 4-36 and 5-2 give the measured and calculated velocities at Plane 5. The contour lines in Figure 5-2 were calculated by a plotting routine in TEMPEST from the complete matrix of TEMPEST axial velocity data. The numbers

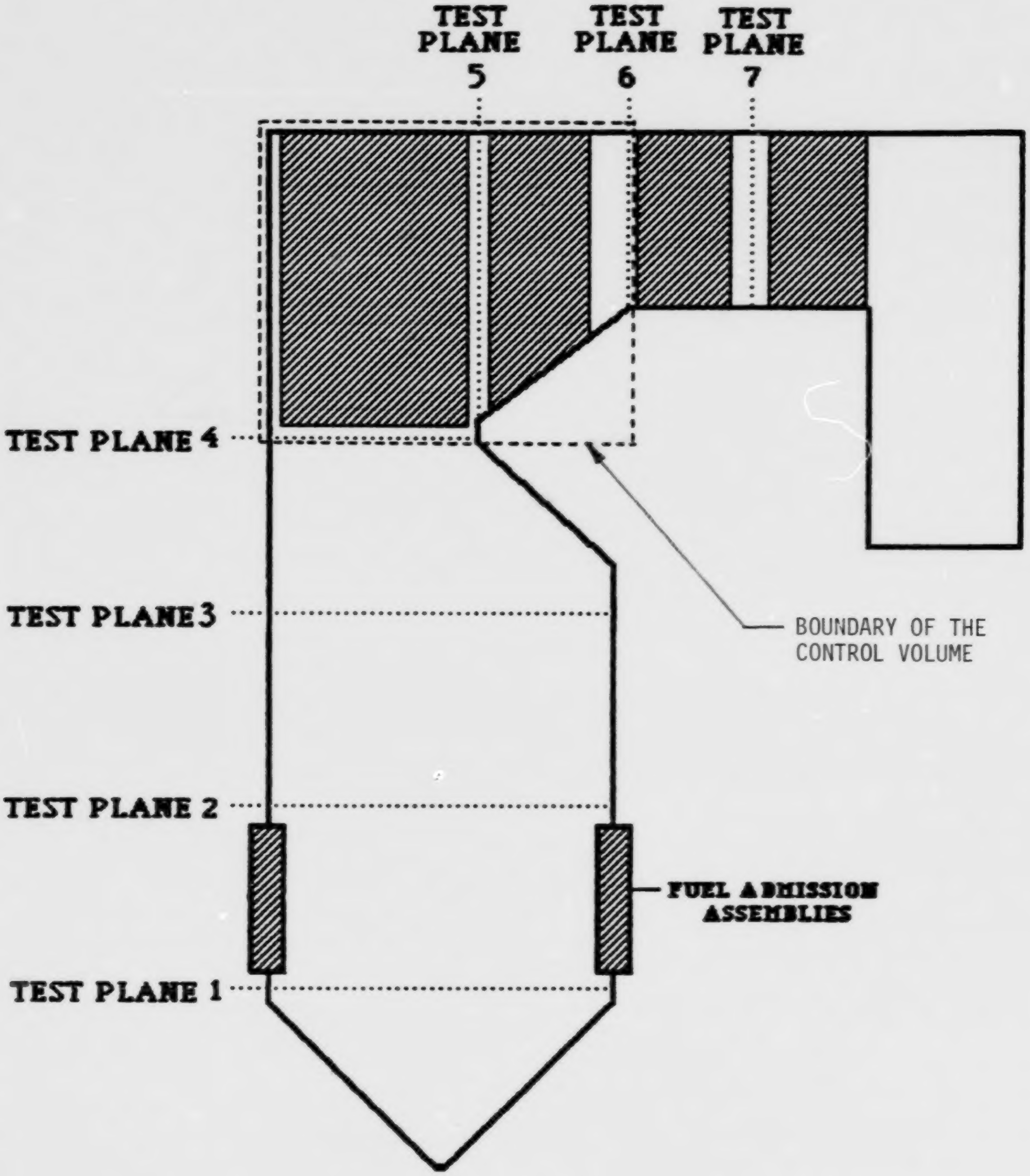
TEST PLANE 5
TEST PLANE 6
TEST PLANE 7
TEST PLANE 4
TEST PLANE 3
TEST PLANE 2
TEST PLANE 1
BOUNDARY OF THE CONTROL VOLUME
FUEL ADMISSION ASSEMBLIES

Figure 5-1. LSTATF flow model and the boundary of the control volume used in the 3-D flow simulation.

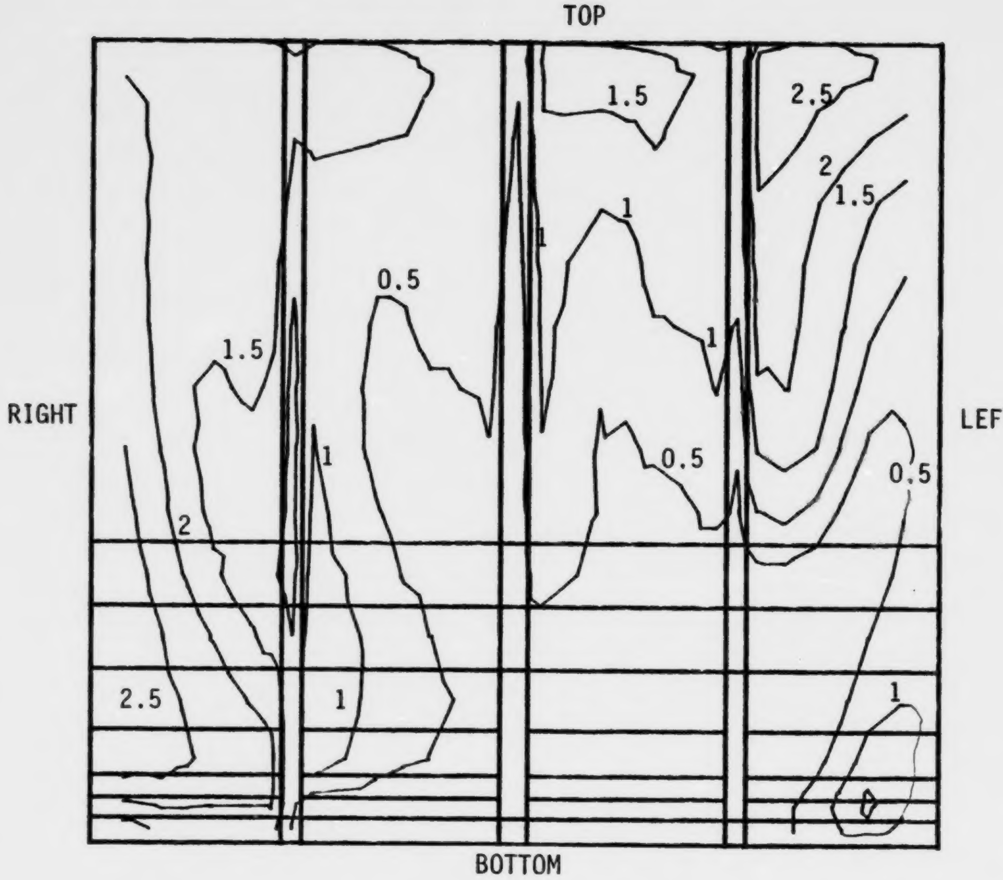

Figure 5-2. Calculated Plane 5 isovelocity plot.

indicate velocities 0.5, 1.0, 1.5, 2.0, etc. times the average velocity at the plane. The figure shows all of the physical features of the model that would be visible if viewed from downstream of Plane 6. Therefore, the panels and horizontal lines corresponding to the steps of the arch are visible in the figure even though these features do not exist at Plane 5.

The measured velocities are highest in the lower right corner and upper left corner in Figure 4-36. The same trend is seen in the calculated results in Figure 5-2. However, one difference is that the calculated maxima in the corners are greater than the measured maxima and the calculated mass flow in the center two lanes is less than the measured flow in the center lanes. This is due to less calculated "spreading" of flow through the gap between the front wall and the first row of panels and through the gap between the first and second row of panels. This discrepancy may be due to the nonuniform mesh sizes which were used in the CFD simulation to describe the panels. This can be corrected by using a finer mesh throughout the calculation. However, such an approach would increase the overall size of the computation grid and the corresponding computer time.

Figures 4-33 and 5-3 show the measured and calculated velocity vectors at Plane 5. Both figures show strong upward movement of flow along both sidewalls and circulating flow within the lanes. The velocity vector agreement is very good.

Figures 4-40 and 5-4 show the measured and calculated normal velocities at Plane 6. At this plane the measured flow continues to show maxima in the upper left and lower right corners. The calculated flow shows a higher maximum in the upper left corner but does not show a maximum at the bottom right. While the overall trend is reasonable, it is possible that better agreement at Plane 6 could be achieved by extending the calculation domain further downstream so that Plane 6 would be farther away from the outlet boundary condition location.

The measured and calculated velocity vectors at Plane 6 are shown in Figures 4-37 and 5-5. The figures show that recirculation still exists within each lane and that the flows are generally similar. One difference can be

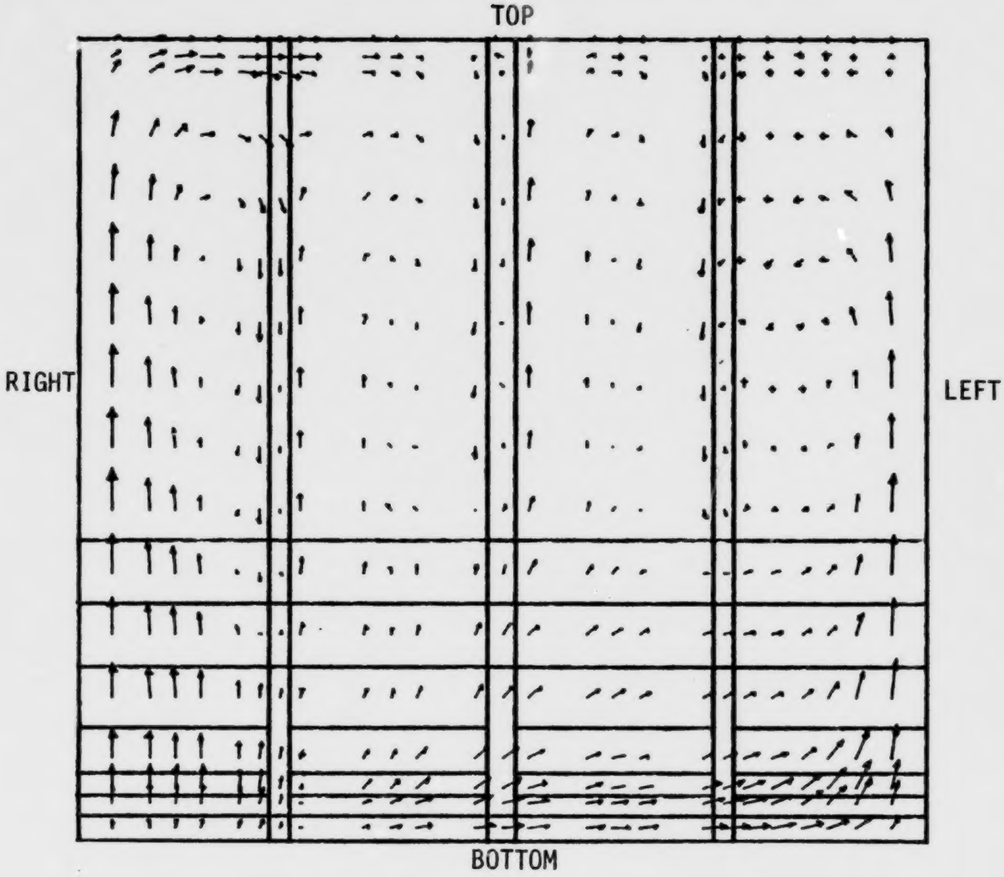

Figure 5-3. Calculated Plane 5 velocity vectors.

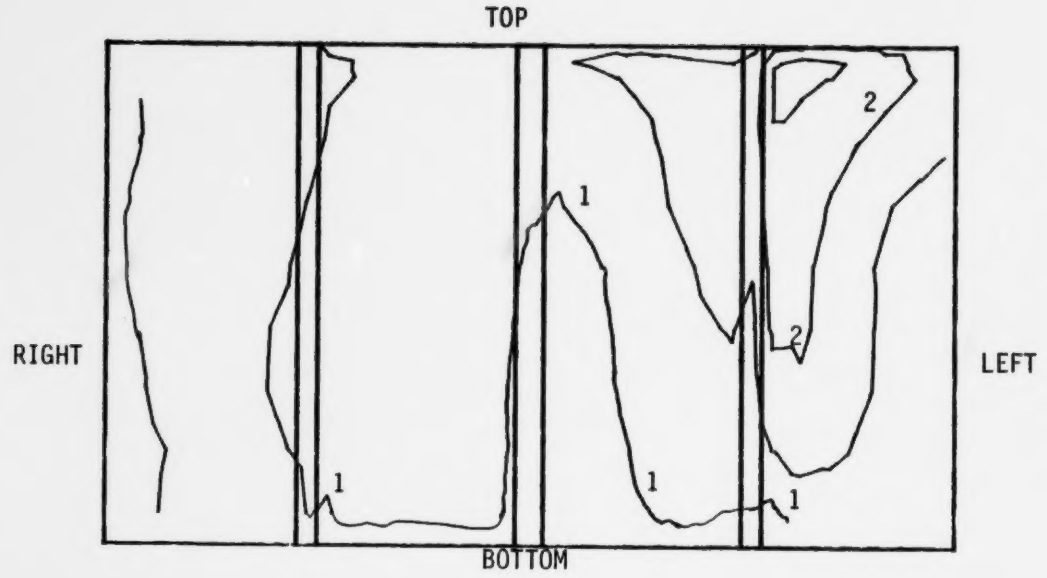

Figure 5-4. Calculated Plane 6 isovelocity plot.

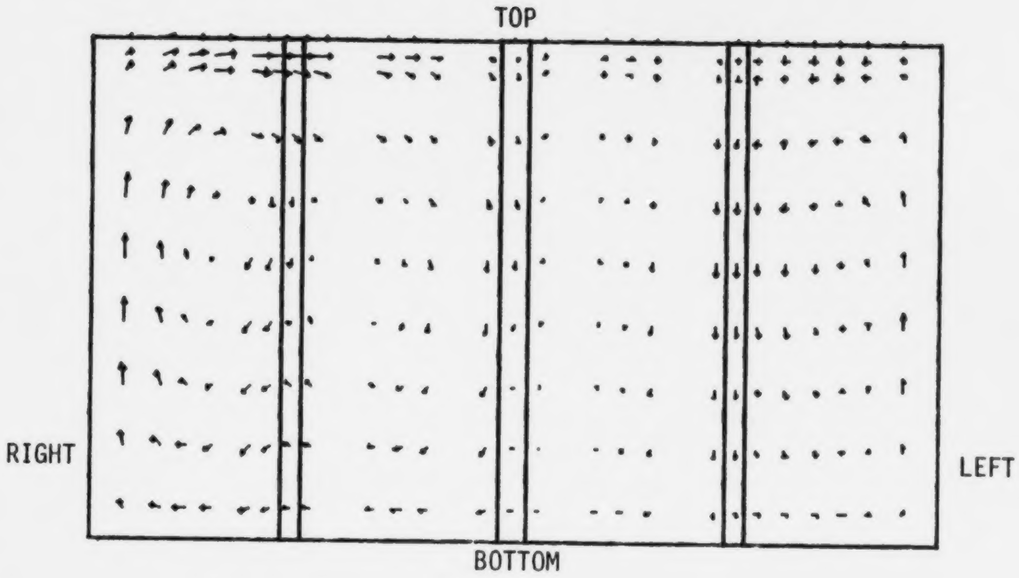

Figure 5-5. Calculated Plane 6 velocity vectors.

noted in the flow in Lane 4 (the lane at the far left). The calculated flow along the left wall is upward whereas the measured flow along the left wall is downward. This discrepancy might not have occurred if the calculation had been extended beyond Plane 6 as discussed above.

One additional evaluation of the calculated velocity data was a study of velocity vectors in vertical planes through the upper furnace. Vector plots for the velocities at the centerlines of Lanes 1, 2, 3, and 4 are given in Figures 5-6 through 5-9. Velocity measurements were not made within the upper furnace. However, flow visualization experiments with a smoke tracer gas were conducted during baseline testing at the LSFATF. The flow visualization results can be used as a basis for comparing the calculated vectors to test results. Streak-line sketches of the flow visualization tests are given in Figure 4-17. The flow is strong and angled directly along the arch but is weak and recirculating at the top front in Lane 1 in both the vector plot and flow visualization sketch. The flow is strong next to the front wall but weak along the arch in Lane 4 for both the calculation and flow visualization results. Flow in the two intermediate lanes has intermediate behavior in both the calculated vector plots and flow visualization sketches. Comparison of the vector plots and flow visualization sketches provides further qualitative confirmation of the effectiveness of the CFD simulation of the upper furnace. In addition, the calculations provide quantitative data which would be very tedious and expensive to obtain experimentally.

5.2.2.2 Upper Furnace Sorbent Dispersion

The second CFD evaluation was a comparison of measured and calculated sorbent tracer mixing. Two mixing tests were studied, Test 201 and Test 204. These tests were selected to identify how successful CFD would be in distinguishing between an injector configuration which gave poor mixing performance (Test 201) and a configuration which gave good mixing performance (Test 204). The Test 201 configuration consisted of injection from the roof directly downward into each of the four lanes at a BSF injection air velocity of 22.9 m/sec (75 ft/sec). The Test 204 configuration was four injectors low on the front wall (Location A) with a BSF injection air velocity of 22.9 m/sec (75 ft/sec) and -20° tilt. The injector configurations are specified in Table

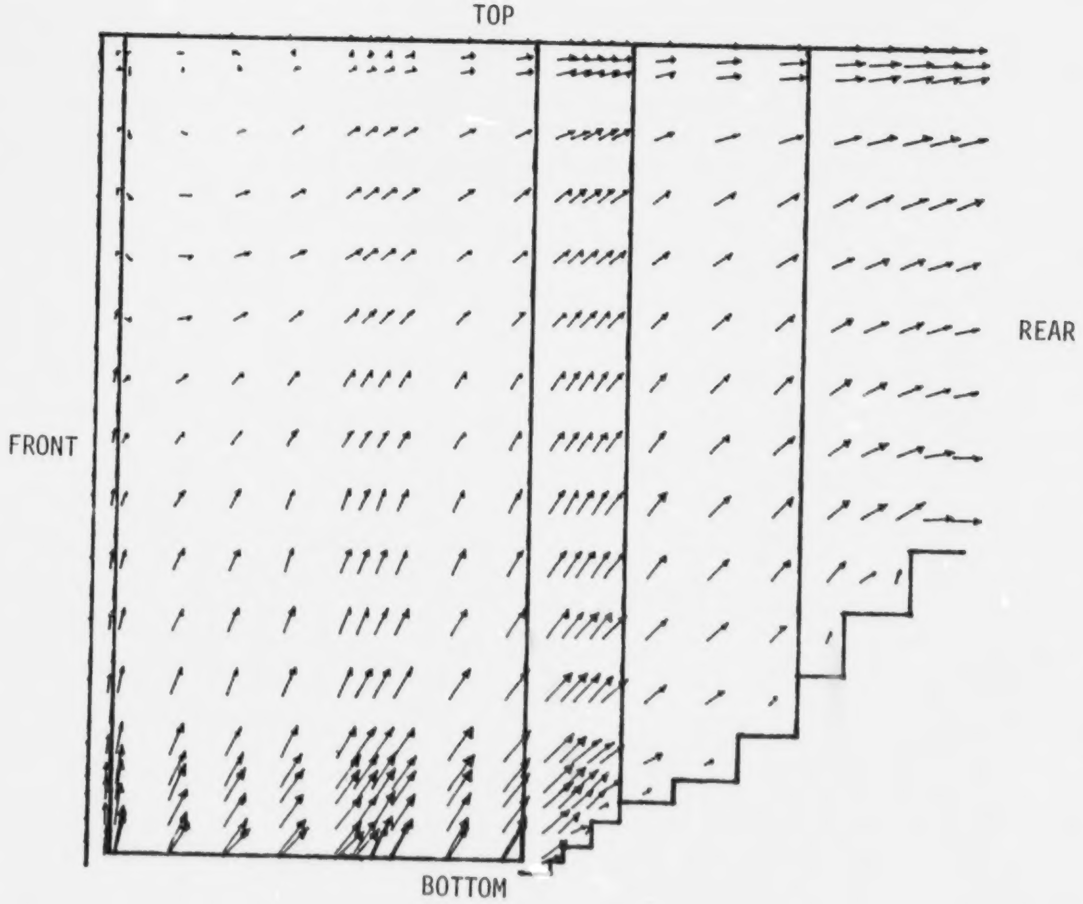

Figure 5-6. Calculated velocity vectors in Lane 1.

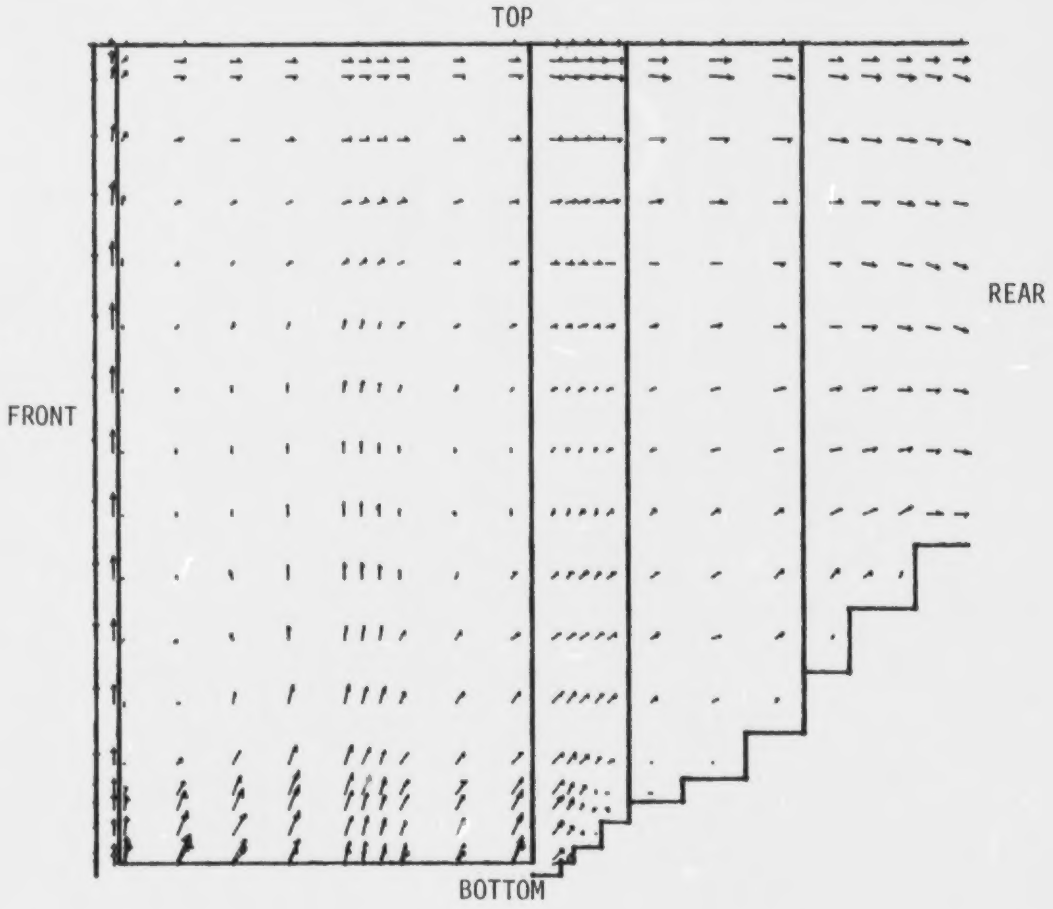

Figure 5-7. Calculated velocity vectors in Lane 2.

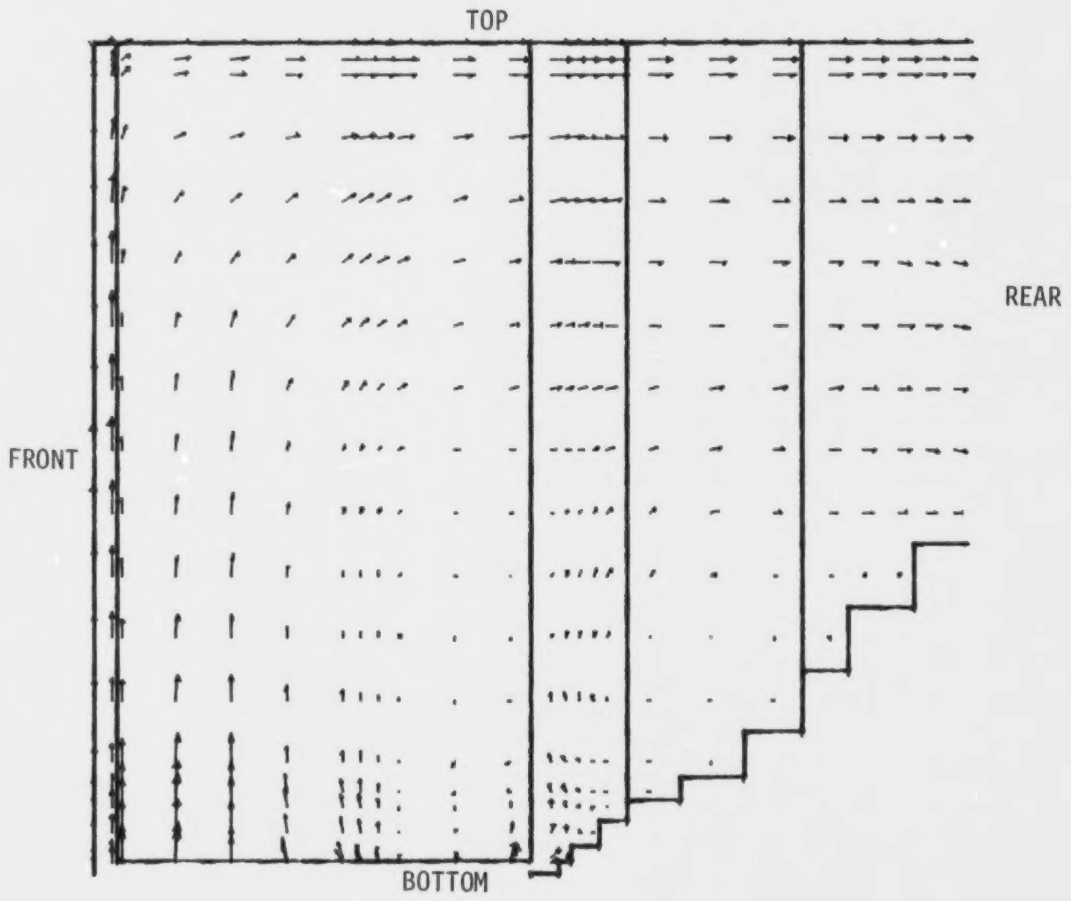

Figure 5-8. Calculated velocity vectors in Lane 3.

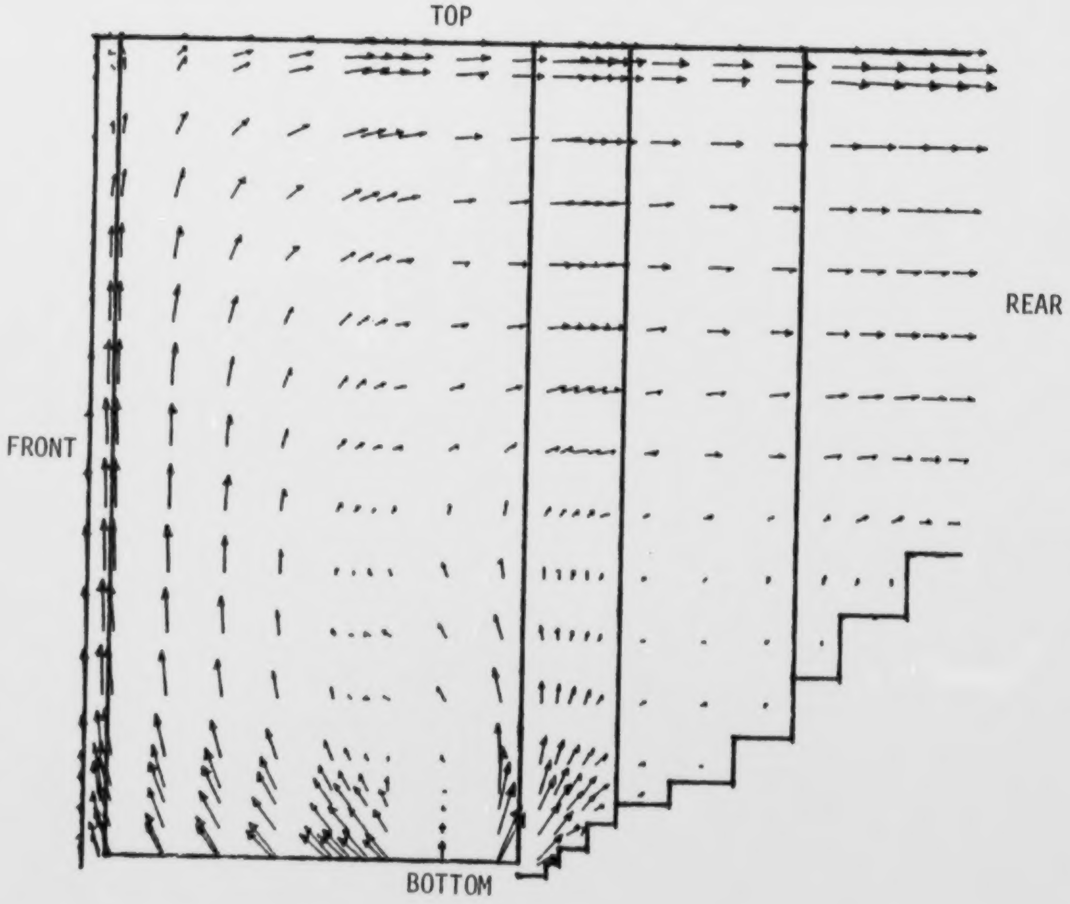

Figure 5-9. Calculated velocity vectors in Lane 4.

4-5. Injector locations and carrier air to mainstream air velocity ratio in the CFD calculations duplicated LSFATF test conditions. The CFD injectors were square and had the same area as the circular injectors at the LSFATF. The CFD model calculates the sorbent concentration distribution by use of an additional conservation equation for the quantity designated "Species F." The measured and calculated sorbent tracer concentrations for Test 201 at Plane 5 are shown in Figures 4-50 and 5-10. The plots are made by computer-generated interpolation routines from the measured and calculated matrices of data plots. In both cases the numbers on the isoconcentration plots indicate concentrations 0.5, 1.0, 1.5, 2.0, etc. times the fully mixed concentration. The measured data plot also includes a contour plot. The tracer is highly concentrated in both the measured and calculated data plots. The only discrepancy is that there is less dispersion of tracer in the upper part of the right lane for the calculation than for the measured data.

The measured and calculated concentrations for Test 201 at Plane 6 are shown in Figures 4-51 and 5-11. In both cases the tracer is highly concentrated in the lower part of the middle lanes with low tracer concentrations at the lower corners and along the top. In general, the comparison between the two figures shows good agreement except in the upper right corner.

Figures 5-12 through 5-15 show contours of concentration for Test 201 in vertical planes through the centerline of Lanes 1, 2, 3, and 4 of the upper furnace. Comparable test data were not available due to the cost that would be required to obtain such detailed traverse data. The figures show that there is little or no tracer in the front half of the upper furnace and that there are large areas with very high concentrations (greater than four times the average). The figures show very deep penetration in Lanes 2 and 3 due to the low mainstream gas velocity in these lanes.

Figures 4-56 and 5-16 show measured and calculated contours of tracer gas at Plane 5 for Test 204. The mixing behavior is significantly better than for Test 201 at Plane 5. The agreement between the measured and calculated contours is good. Both show higher tracer concentrations in the middle lanes

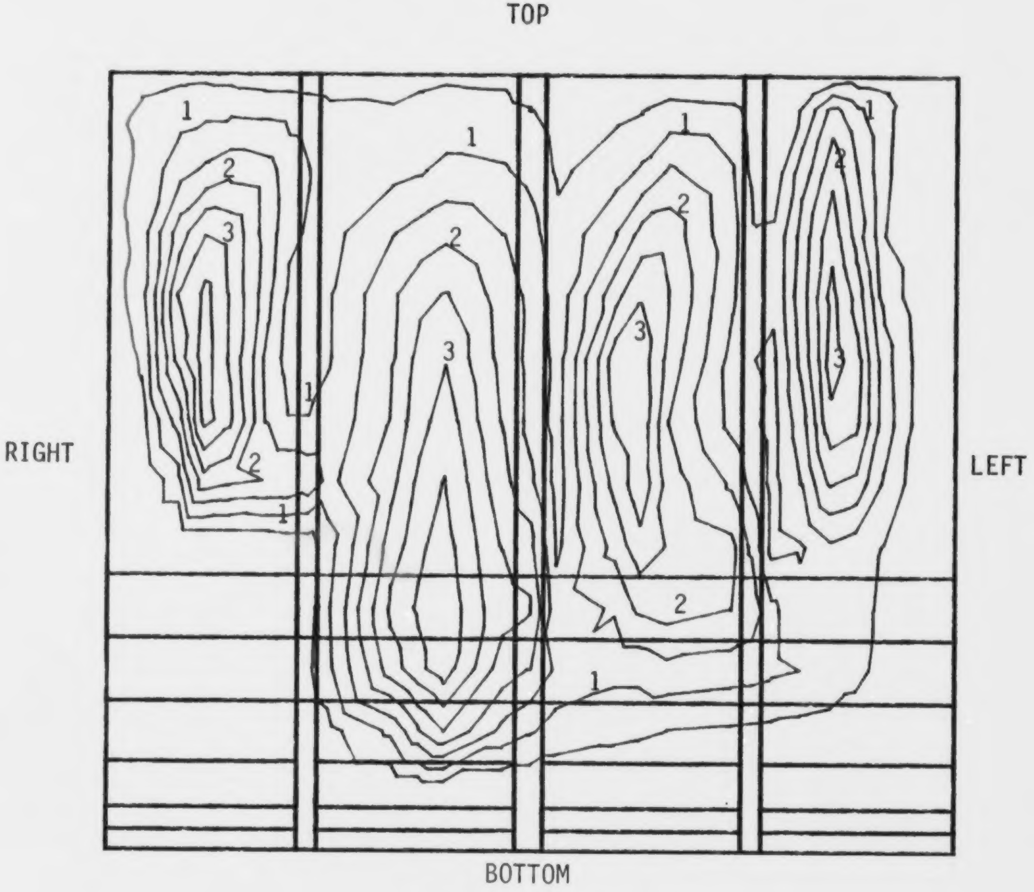

Figure 5-10. Calculated isoconcentration plot for Test No. 201 at Plane 5.

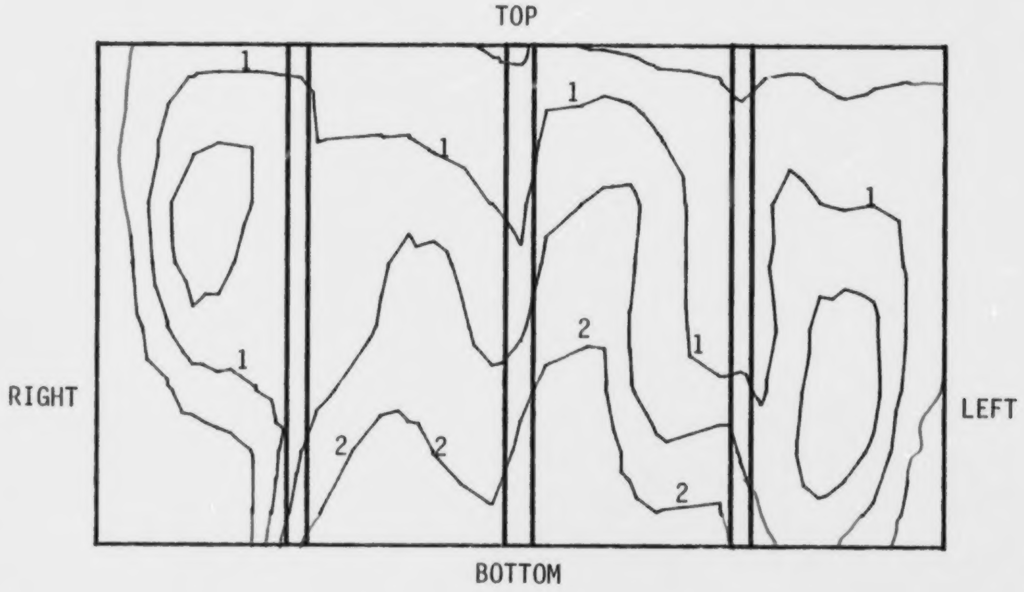

Figure 5-11. Calculated isoconcentration plot for Test No. 201 at Plane 6.

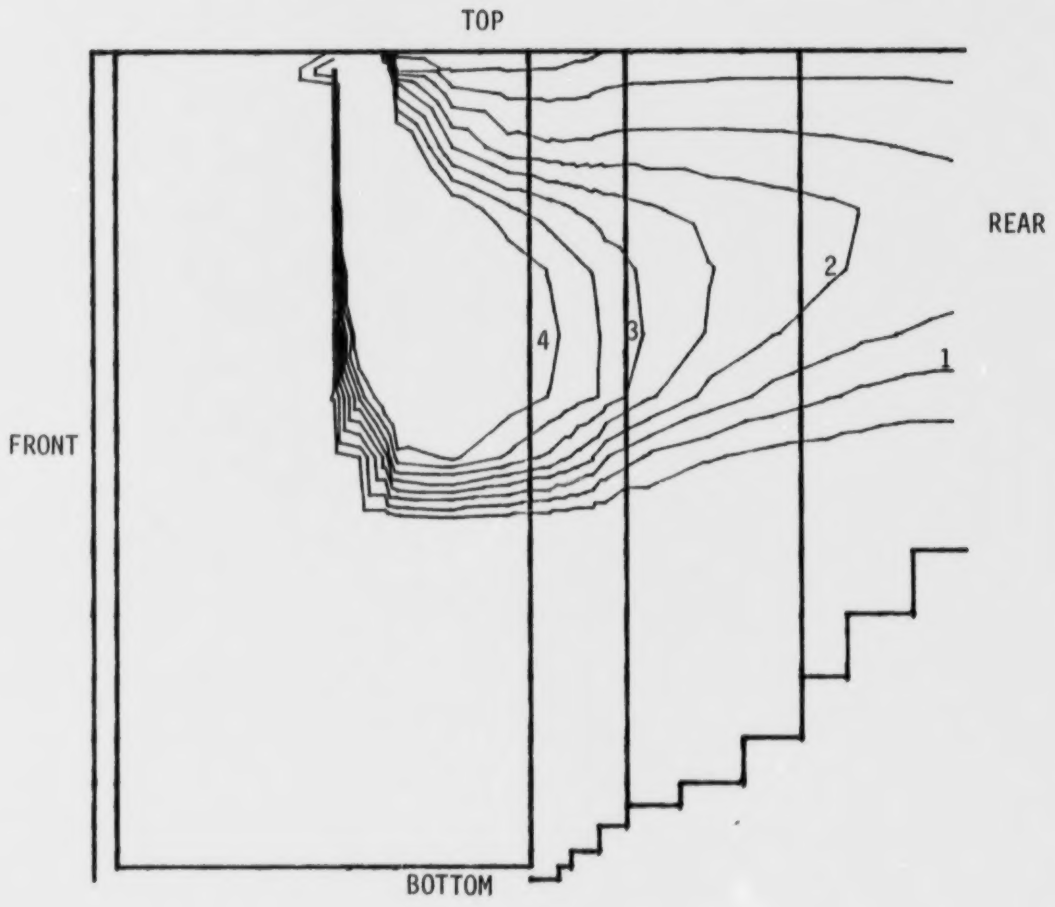

Figure 5-12. Calculated concentration contours in Lane 1 for Test No. 201.

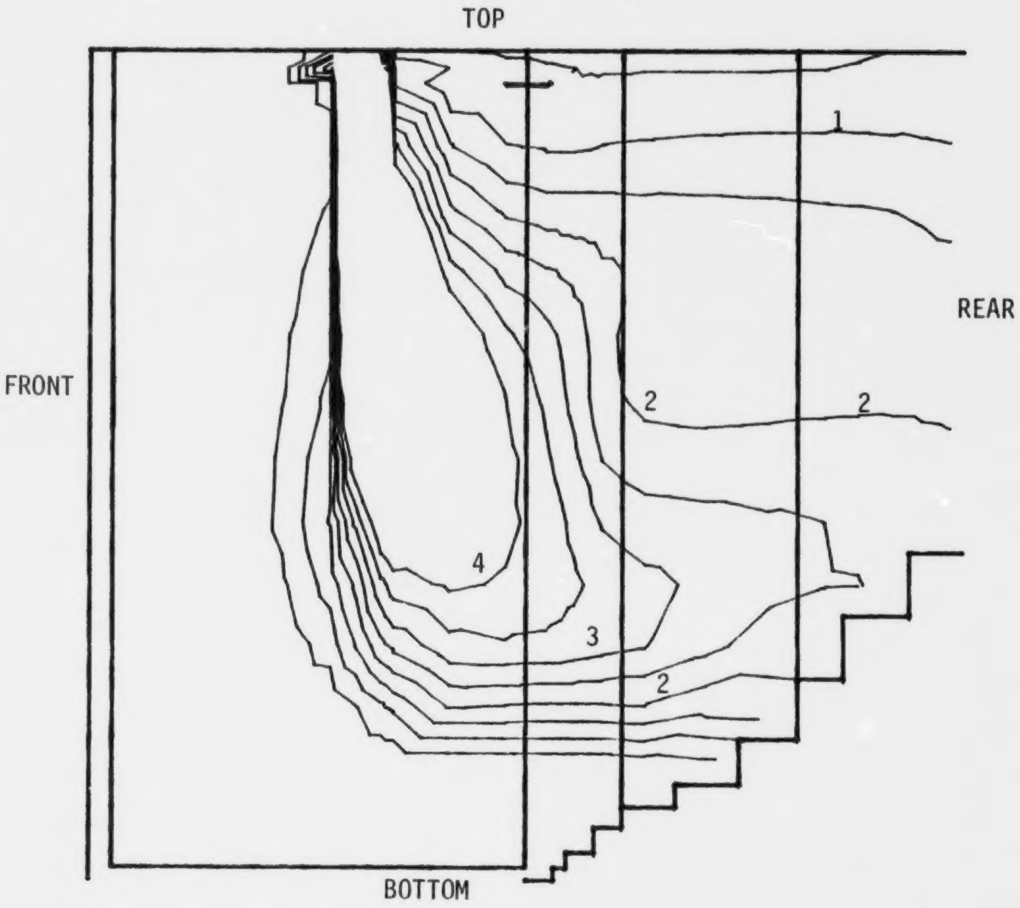

Figure 5-13. Calculated concentration contours in Lane 2 for Test No. 201.

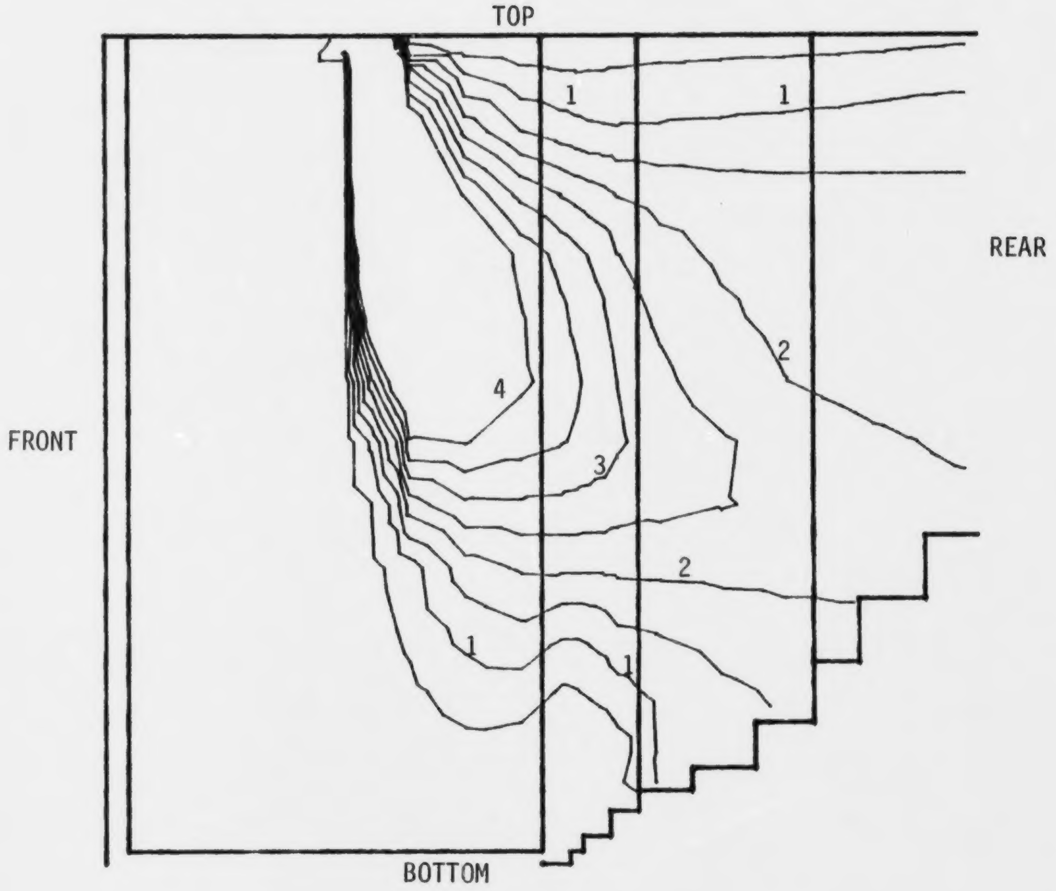

Figure 5-14. Calculated concentration contours in Lane 3 for Test No. 201.

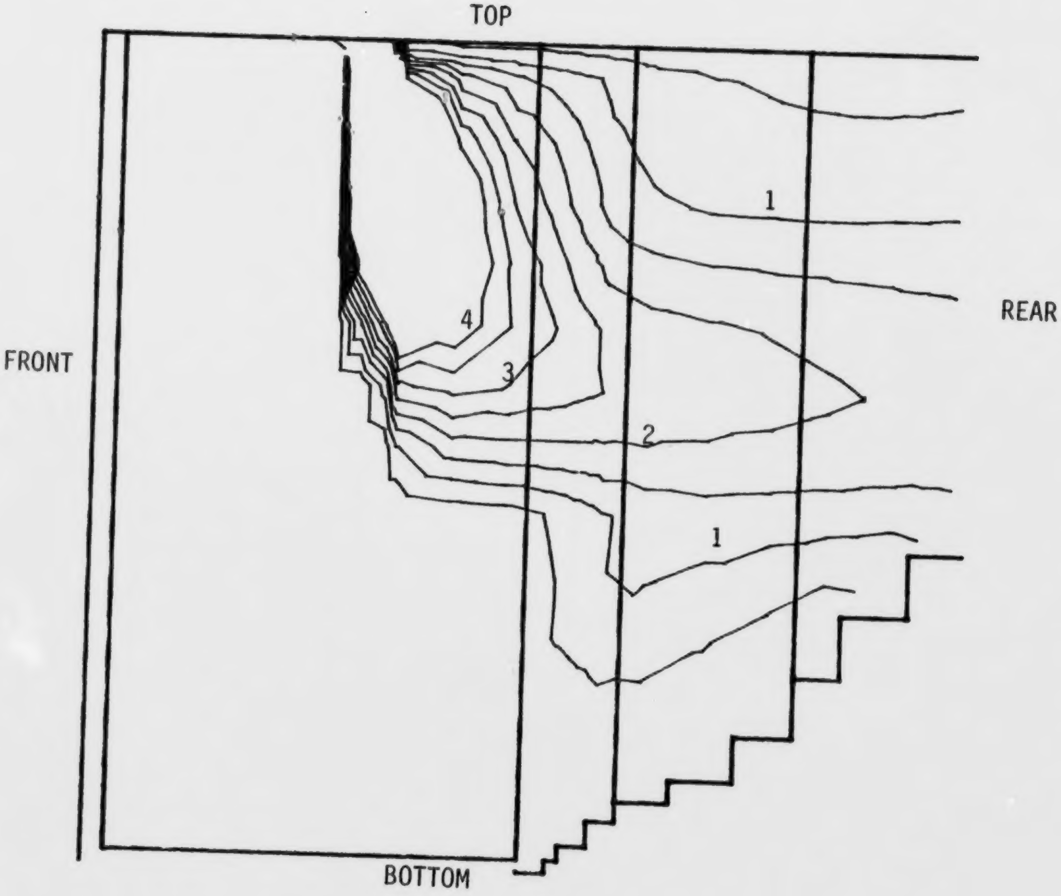

Figure 5-15. Calculated concentration contours in Lane 4 for Test No. 201.

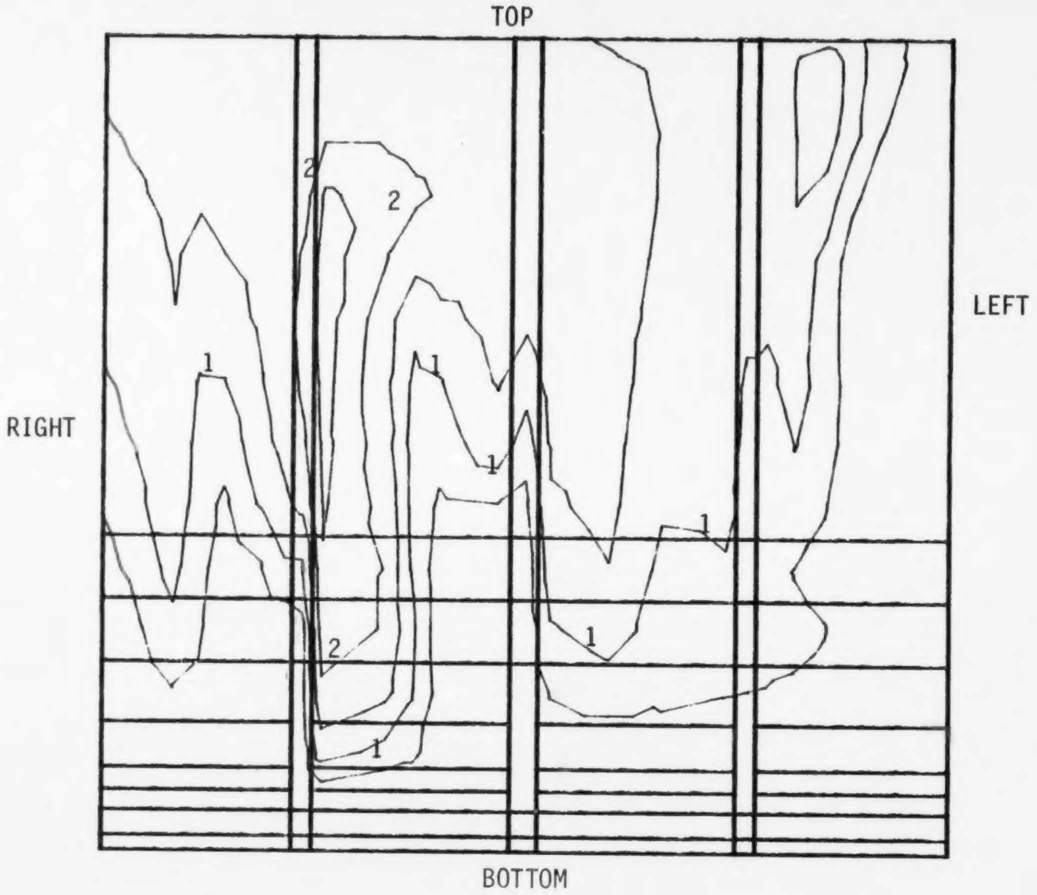

Figure 5-16. Calculated isoconcentration plot for Test No. 204 at Plane 5.

and lower concentrations at the lower corners, but the concentration gradients are more extreme for the calculated case. The higher calculated concentrations in the middle lanes are due to the lower calculated spread of air to the middle lanes as discussed in the section on upper furnace velocities.

Figures 4-57 and 5-17 give the measured and calculated concentration contours for the tracer gas at Plane 6 for Test 204. The results generally show good agreement. The higher maximum concentration for the calculated case is again shown and is due to the lower spread of air to the middle lanes as discussed above. The figures clearly show the improved mixing for Test 204 compared to Test 201.

Figures 5-18 through 5-21 show contours of concentration in vertical planes through the centerlines of Lanes 1, 2, 3, and 4 for Test 204. The improved mixing of Test 204 compared to Test 201 can be seen by comparing these figures to Figures 5-12 through 5-15. The data shown in these figures gives information concerning the mixing process which could be obtained experimentally only with large effort and expense. The calculated results illustrate the effectiveness of CFD for simulating the flow patterns and sorbent mixing in the upper furnace of the tangential furnace aerodynamic flow model. The results also show the effectiveness of CFD for identifying and optimizing sorbent injector designs. Approaches were suggested by which further improvements can be made to the CFD simulation of sorbent dispersion.

5.3 SULFUR CAPTURE PERFORMANCE MODELING

A SO_2 capture performance model was developed to interpret test results from the BSF and to serve as the basis for evaluating SO_2 capture in the sorbent injector design procedure for tangentially fired furnaces described in Section 7. The model predicts SO_2 capture as a function of furnace operating parameters, sorbent injection parameters, and the inherent SO_2 capture performance of the sorbent. The model is described using SO_2 capture performance calculations for the BSF as an example.

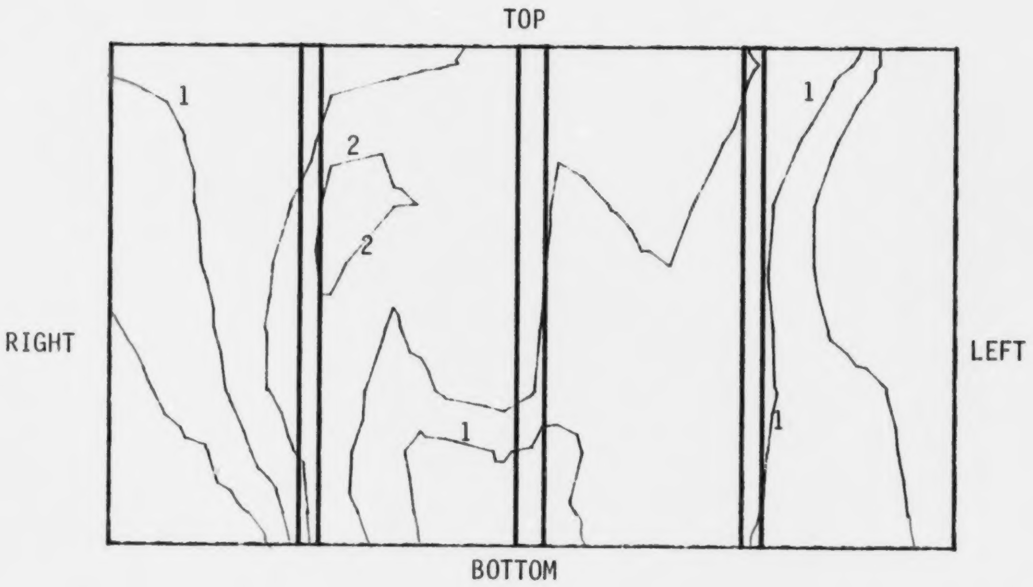

Figure 5-17. Calculated isoconcentration plot for Test No. 204 at Plane 6.

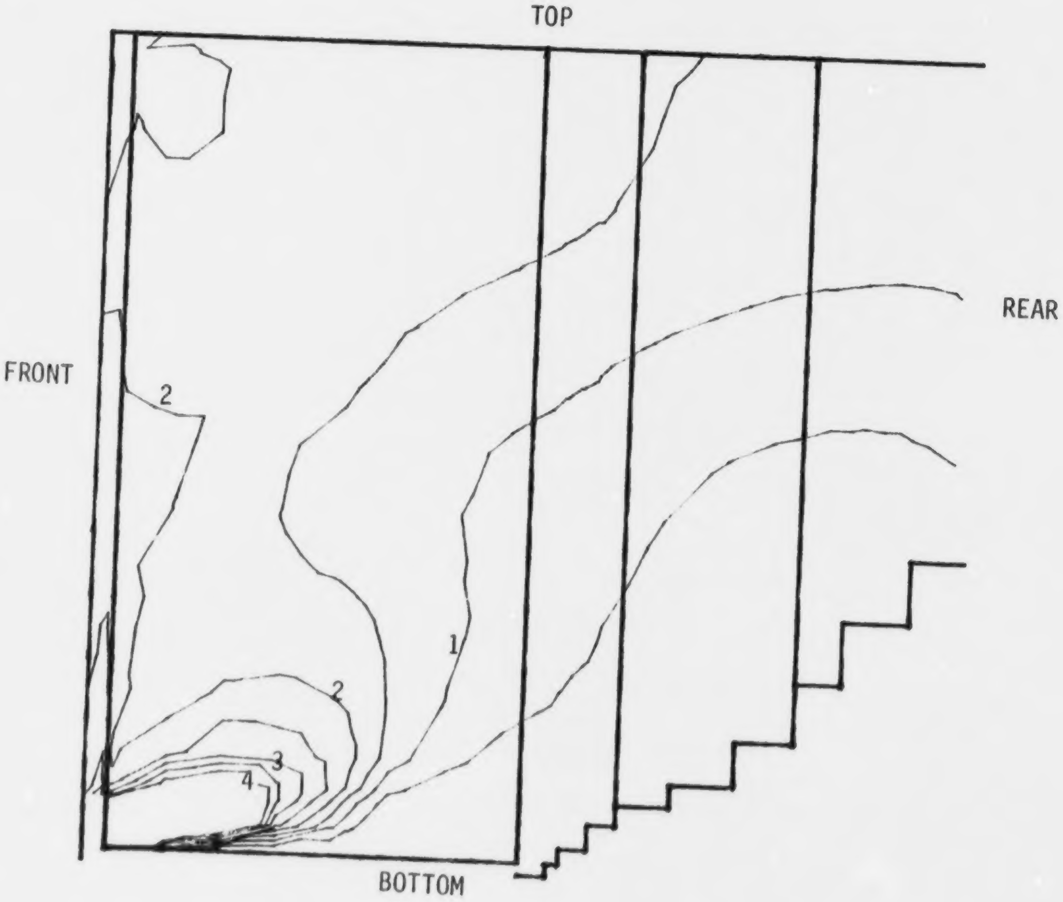

Figure 5-18. Calculated concentration contours in Lane 1 for Test No. 204.

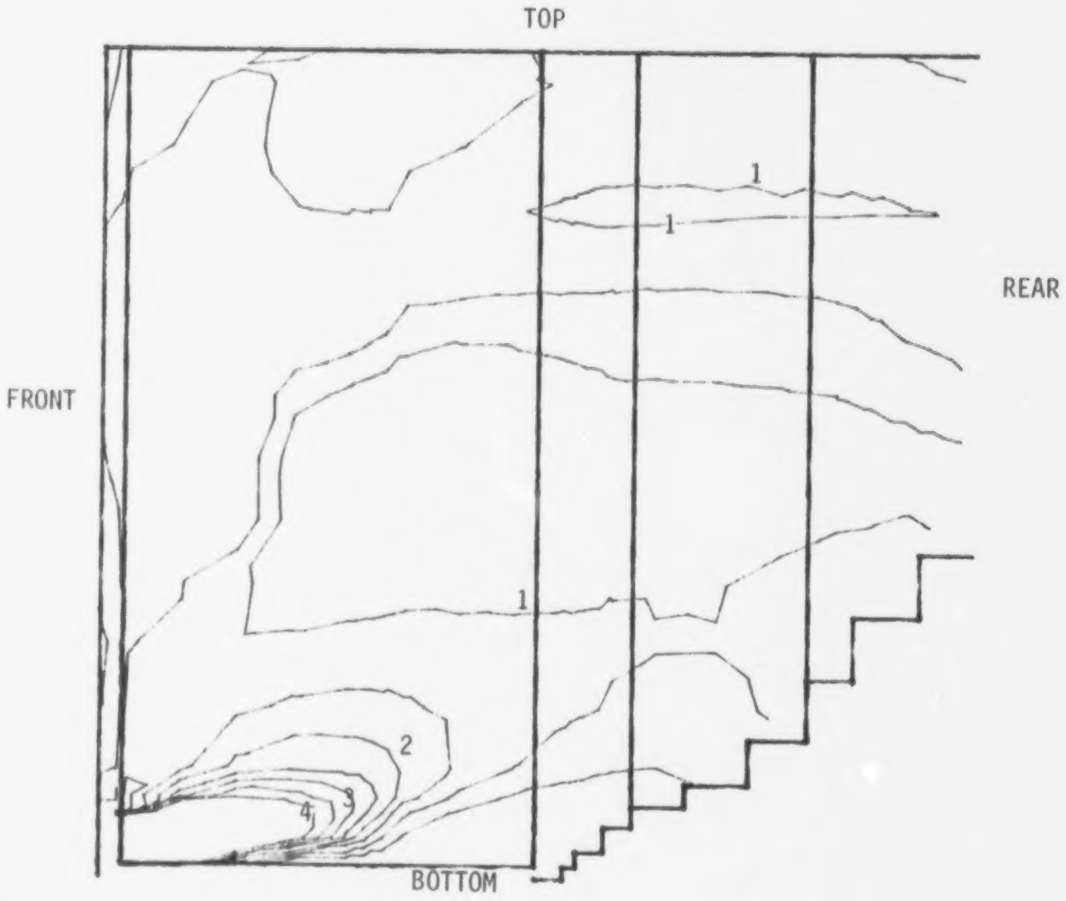

Figure 5-19. Calculated concentration contours in Lane 2 for Test No. 204.

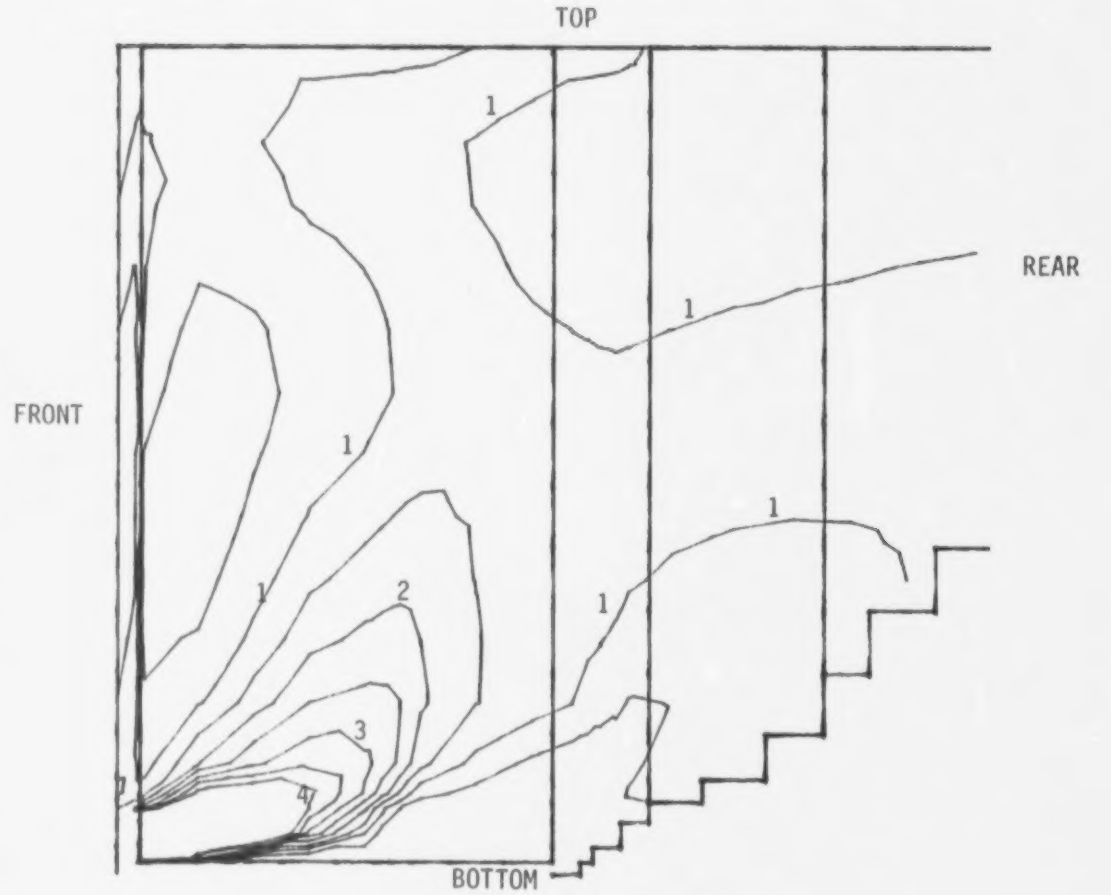

Figure 5-20. Calculated concentration contours in Lane 3 for Test No. 204.

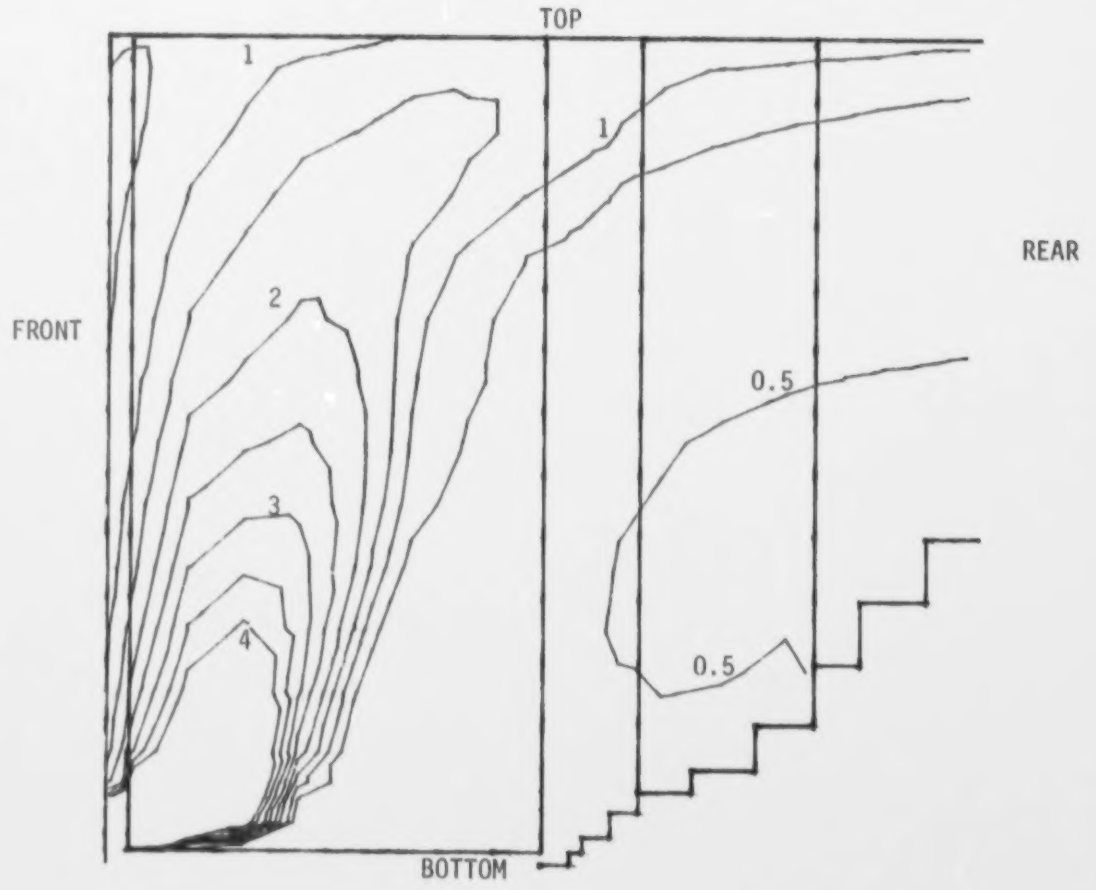

Figure 5-21. Calculated concentration contours in Lane 4 for Test No. 204.

Features of the model as applied to the BSF are summarized in Figure 5-22. The flow through the SO_2 capture window of the furnace is divided into 168 stream tubes corresponding to the 12 by 14 traverse probe matrix used in the LSFATF testing at the furnace vertical outlet plane (VFOP), Plane 5 on Figure 4-18. It is assumed that no mixing takes place between stream tubes. The SO_2 capture is calculated for each of the stream tubes, and the overall SO_2 capture is calculated as the mass flow weighted SO_2 capture for all of the stream tubes.

Inputs for the model include laboratory and/or pilot plant SO_2 capture data, the time/temperature profile of the furnace, LSFATF velocity and concentration profile data for Plane 5, and limited SO_2 capture performance data from the BSF. The SO_2 capture performance is predicted as a function of Ca/S ratio, time/temperature profile, sorbent injector design, and the inherent SO_2 capture performance of the sorbent.

Using LSFATF concentration profile data for Plane 5 for the sorbent injection configuration of interest, expressed as the local concentration divided by the mean concentration, and the specified overall mean Ca/S ratio, the local Ca/S ratio is calculated for each stream tube. Similarly, using the ratio of local velocity to mean velocity measured in the LSFATF for Plane 5 and the furnace overall time/temperature profile, the time/temperature profile for each stream tube can be calculated.

Capture of SO_2 is calculated for each stream tube as a function of Ca/S ratio, time/temperature profile, and initial SO_2 concentration in the gas by DESULF, a proprietary computer code developed by C-E in 1985. The DESULF model is matched to SO_2 capture data for tests with fully mixed sorbent and uniform velocity, such as data from laboratory or small-scale pilot plants, by adjusting the chemical kinetics rate constant in the DESULF model. Figure 5-23 shows a composite of SO_2 capture data from EPA-sponsored investigations for three sorbents and a quench rate of 500°F/sec., typical of the BSF. The dashed line shows the SO_2 capture calculation for DESULF using calcitic atmospheric hydrated lime sorbent.

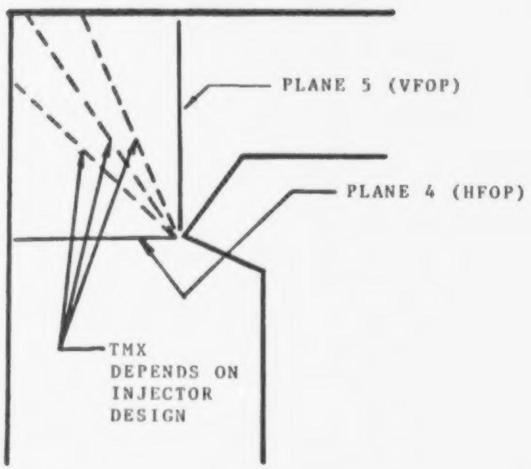
PLANE 5 (VFOP)
PLANE 4 (HFOP)
TMX
DEPENDS ON
INJECTOR
DESIGN

OBJECTIVES

- SO_2 CAPTURE AS A FUNCTION OF Ca/S
- SO_2 CAPTURE AS A FUNCTION OF FOT
- SO_2 CAPTURE FOR OTHER INJECTION LOCATIONS

INPUTS

- LABORATORY/PILOT PLANT SO_2 CAPTURE DATA
- TIME/TEMPERATURE PROFILE
- COLD FLOW VELOCITY AND CONCENTRATION DATA
- SOME SO_2 CAPTURE DATA FROM THE BSF

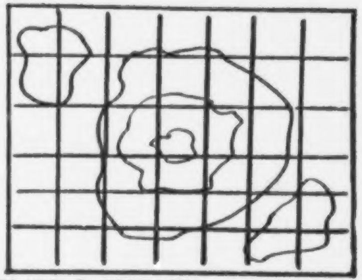

PLANE 5 VELOCITY AND SORBENT PROFILE DATA FROM THE LSFATF

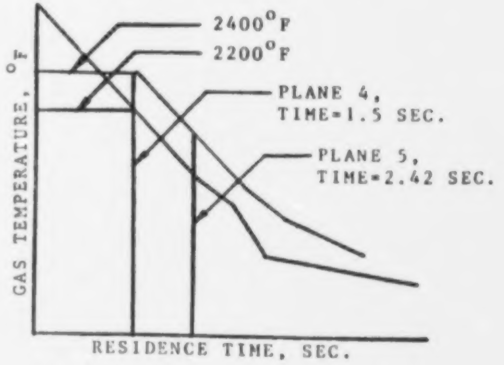

BSF TIME/TEMPERATURE PROFILE

Figure 5-22. SO_2 capture modeling.

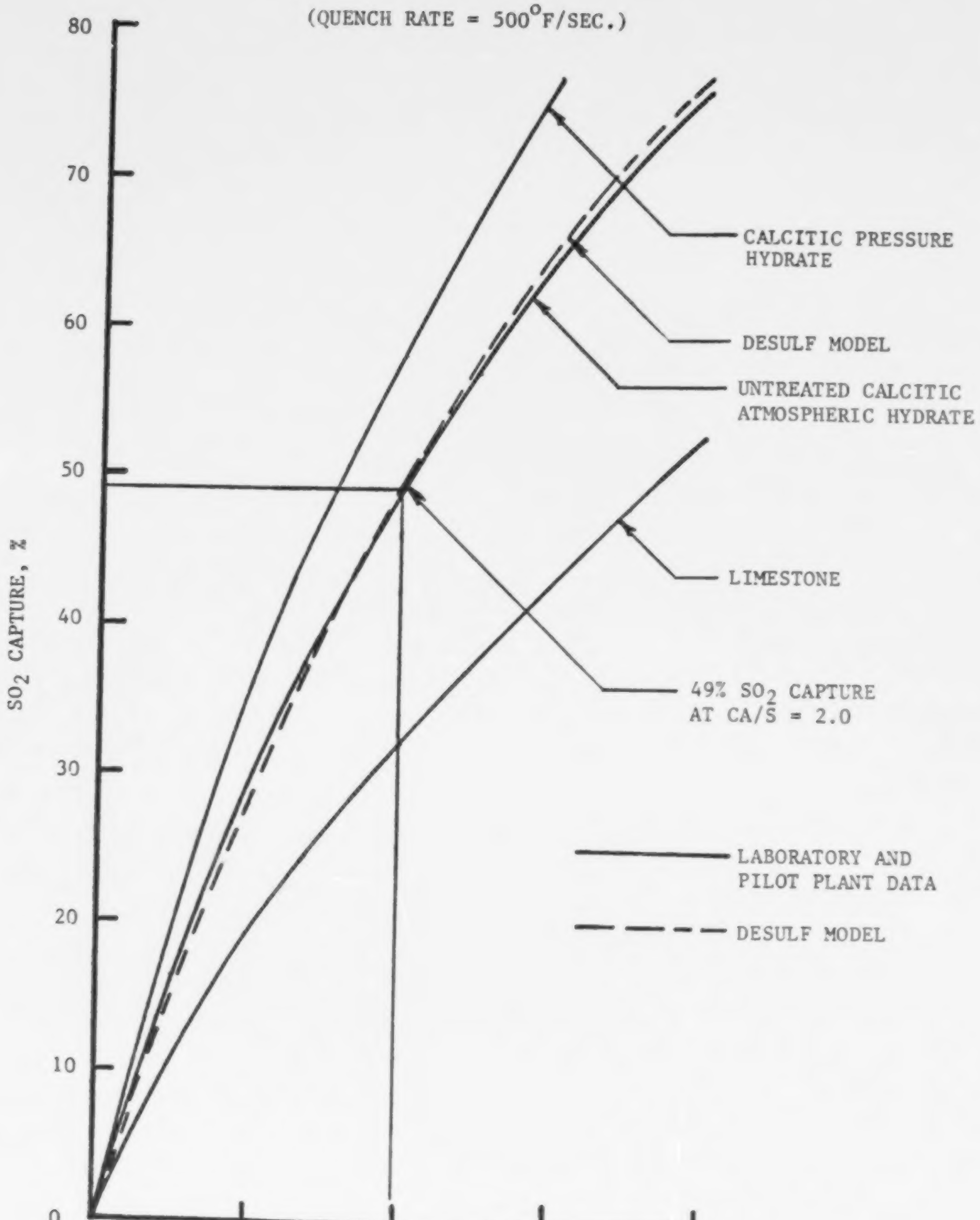

Figure 5-23. SO_2 capture for fully mixed sorbent and uniform velocity.

To make SO_2 capture predictions for the BSF, one additional factor must be considered. This is the effectiveness of sorbent mixing in the upper furnace. The mixing effectiveness is treated by an additional quantity in the model, TMX. The quantity TMX is the time when the gas and sorbent have mixed sufficiently well for the SO_2 capture process to begin. Computationally, it is assumed that prior to the time TMX the SO_2 capture rate is zero and after TMX the SO_2 capture takes place with the Ca/S ratio which exists at Plane 5 as calculated by the method described above. This corresponds to a situation where the sorbent is completely unmixed before TMX and completely mixed to the Plane 5 level of mixing immediately after TMX.

The SO_2 capture model was verified by applying it to BSF data for Phase I Test 26 shown in Figure 5-24. For this test, sorbent was fed through four injectors tilted downward at Location A with a carrier air velocity of 150 ft/sec. The quantity TMX was calculated for the test point at Ca/S = 1.84 by running the model for a range of values of TMX with Ca/S = 1.84 and the measured time/temperature profile to find the value of TMX where the calculated SO_2 capture matched the measured SO_2 capture of 28.4%. These calculations gave TMX = 1.95 sec. This indicates that the SO_2 capture is delayed by incomplete mixing until 0.45 sec. after the gas passes across Plane 4 in Figure 5-22. Using this value of TMX, SO_2 capture was calculated for a range of Ca/S ratios and is shown in the figure. The measured values of SO_2 capture for Ca/S = 3.01 and 4.11 are also plotted on the figure. The agreement between calculated and measured SO_2 capture is excellent for these two data points verifying the applicability of the model for this injector design.

The quantity TMX is therefore an empirical quantity which is determined or calculated in order to apply this method for predicting SO_2 capture. Before discussing the application of the SO_2 capture prediction method for the BSF, a brief discussion is given of methods for evaluating TMX for other furnace designs so that the SO_2 capture prediction method described here can have general applicability to tangentially fired furnaces. The sketch on the left in Figure 5-22 suggests that TMX depends upon the time that the sorbent must mix between Plane 4 and Plane 5 before the SO_2 capture begins. The degree of mixing along the diagonals shown in Figure 5-22 is related to the

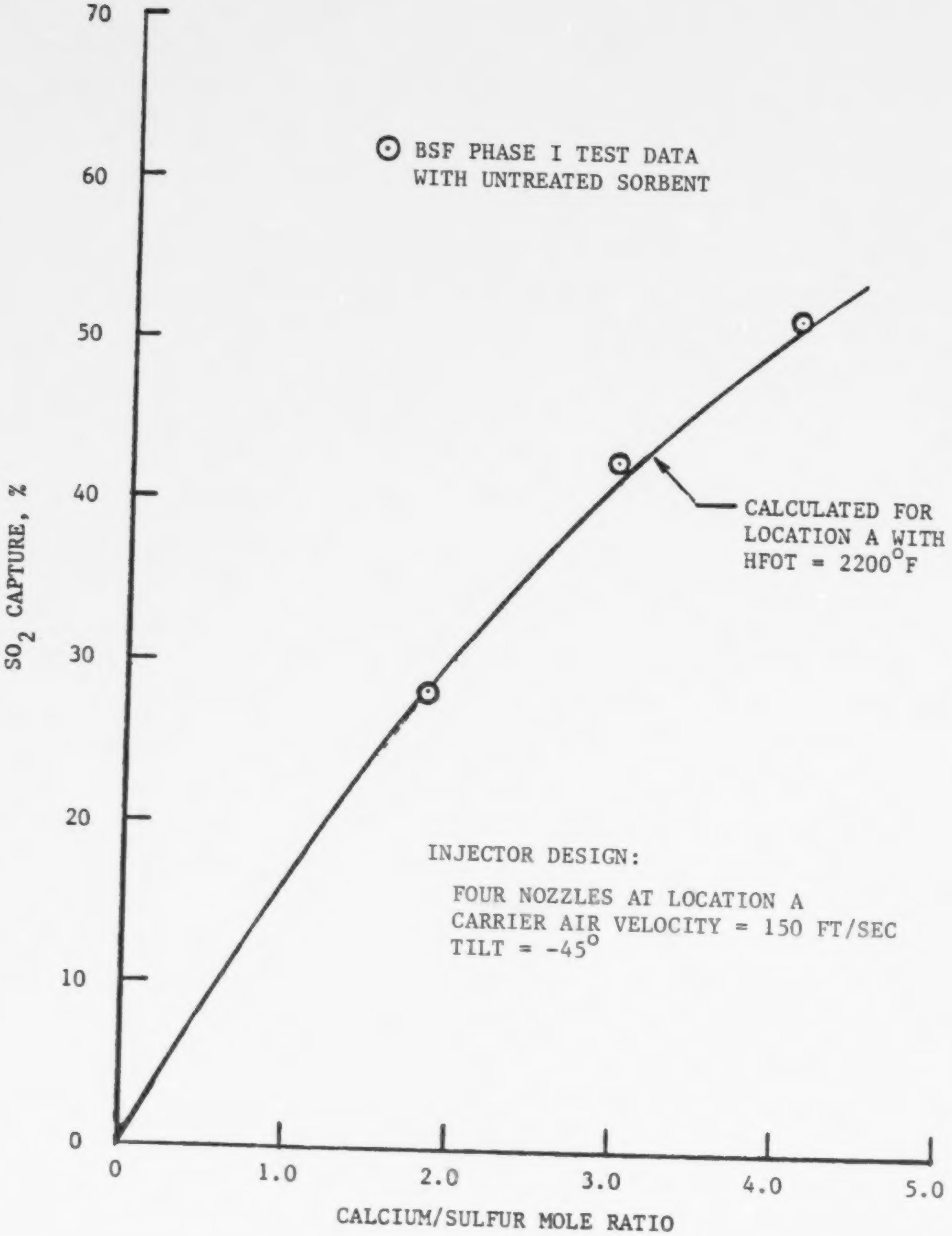

Figure 5-24. Measured and calculated SO_2 capture.

degree of mixing at Plane 5. The Plane 5 concentration profiles given in Section 4 and the corresponding coefficients of variation given for Plane 5 in Figure 4-73 characterize the quality of mixing at Plane 5 and, therefore, at the intermediate diagonal planes between Plane 4 and Plane 5. The quality of mixing between Planes 4 and 5 can also be characterized by CFD calculations as shown in Figures 5-12 through 5-15 and Figures 5-18 through 5-21. Top to bottom variation of gas temperature and gas mass flow rate are additional important factors since sorbent injector designs with similar mixedness performance (characterized by the coefficient of variation) can have significantly different SO_2 capture performance. An effective method for characterizing TMX for other furnace designs is therefore in terms of measured mixing coefficient of variation at Plane 5, sorbent concentration distribution between Plane 4 and Plane 5 calculated by CFD, and an adjustment for the top to bottom gas temperature gradient.

Returning to the discussion of the application of the SO_2 capture model to BSF test data, two applications are shown in Figure 5-25. The first is a calculation of expected SO_2 capture at the BSF for the sorbent injection design used in Phase I, Test 26 for a potential time/temperature profile with a horizontal furnace outlet temperature (HFOT) of 2400°F. Using the value TMX = 1.95 sec. and the corresponding time/temperature profile, sulfur capture was calculated for a range of Ca/S ratios. At Ca/S = 2.0 a SO_2 capture of 41% would be expected for untreated hydrate sorbent with a HFOT of 2400°F and injection of Location A.

The second application of the SO_2 capture model is for tangential injection at Location D with a BSF HFOT of 2200°F. As will be discussed in Section 6 of this report, injection at a lower location at the BSF was recommended with a 2200°F HFOT in order to provide more gas residence time in the SO_2 capture window. In addition, injection at Location D gave excellent mixing in the LSFATF tests performed in Task A. Because of the excellent mixing for Location D in the LSFATF tests, a value of TMX = 1.5 sec. was used to calculate SO_2 capture performance for this injector location. The calculated results for a range of Ca/S ratios are shown in Figure 5-25. Sulfur capture of 43.3% is predicted for Ca/S = 2.0 for the BSF with HFOT = 2200°F and untreated atmospheric pressure hydrated lime.

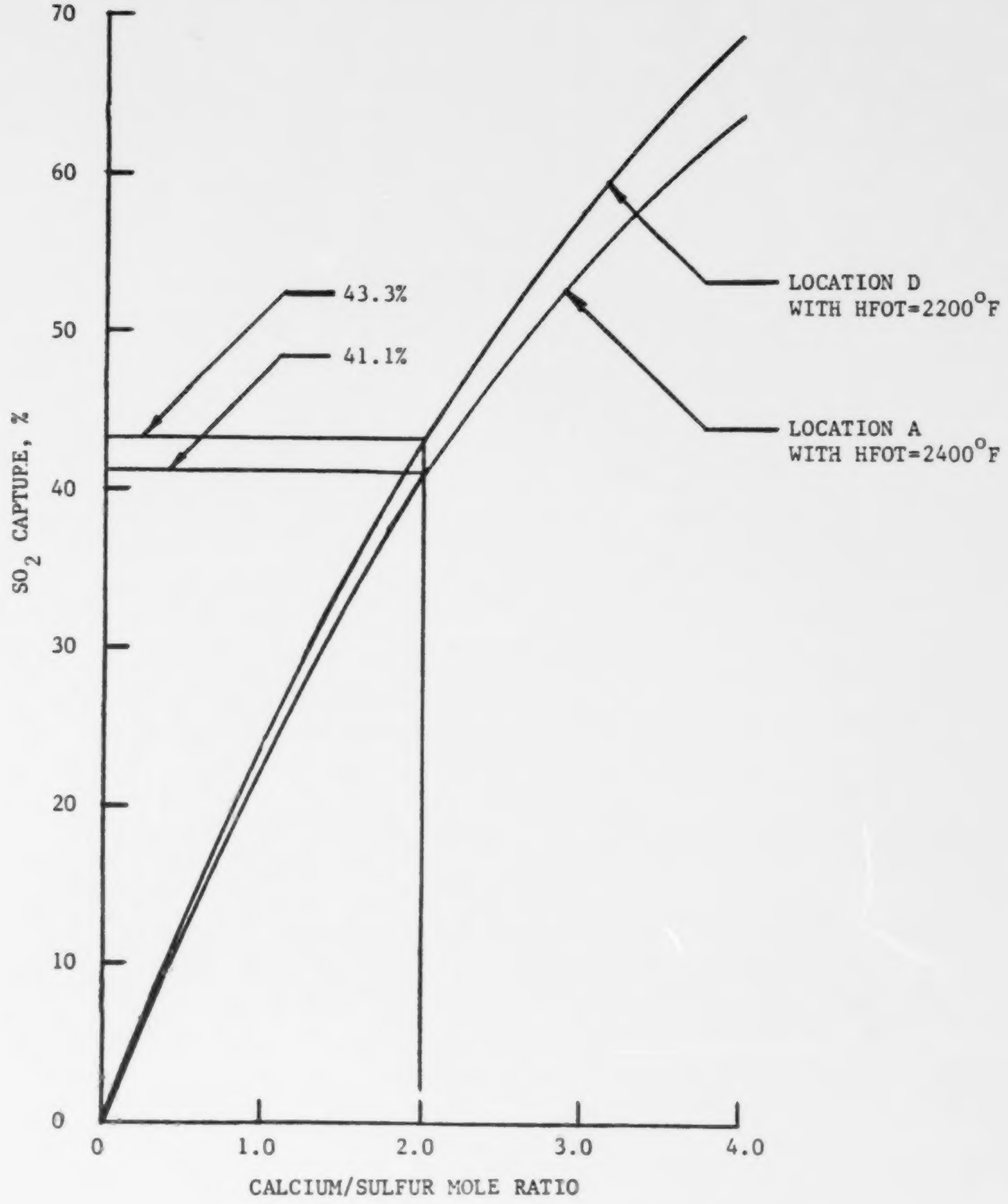

Figure 5-25. Applications of SO_2 capture modeling.

5.4 SUMMARY

Three applications of mathematical modeling studies are discussed in this section. These are thermal modeling, sorbent dispersion modeling, and SO_2 capture modeling. These studies are in addition to the analysis performed in Task A to specify sorbent injector designs for the isothermal flow modeling studies and the analysis of BSF test results performed in Task C. Thermal modeling was conducted to design the BSF and to select candidate sorbent injector locations for both the isothermal flow studies and the combustion testing at the BSF. Sorbent dispersion modeling was conducted using a CFD code. Calculated results show that CFD can effectively simulate sorbent mixing in the upper furnace of a tangential furnace flow model. CFD can therefore be an effective design tool for selecting and optimizing sorbent injector locations and methods. A SO_2 capture performance model was described. The model predicts SO_2 capture as a function of furnace geometry, furnace temperature profile and operating conditions, sorbent injection parameters, and the inherent SO_2 capture performance of the sorbent.

SECTION 6

COMBUSTION TESTING

6.1 OBJECTIVES

The purpose of this task was to evaluate and optimize sorbent injection concepts developed from Isothermal Modeling Studies (Section 4) and Mathematical Modeling Studies (Section 5) in a large scale tangentially fired test furnace.

A number of injection design/location combinations were tested over a range of furnace and injector operating conditions. Three sorbents were studied. Specific test objectives were to:

1) Evaluate SO_2 capture performance for various injection locations, designs, and operating conditions.

2) Evaluate three hydrated lime sorbents, including a hydrated lime treated with calcium lignosulfonate.

3) Optimize SO_2 capture performance.

4) Refine the sorbent injector design guidelines developed in Tasks A and B for sorbent injection at the BSF.

5) Create a data-base for sorbent injection system design guidelines for tangentially fired boilers.

6.2 PROJECT DESCRIPTION

Combustion testing was performed in C-E's new $50x10^6$ Btu/hr Boiler Simulation Facility (BSF). This facility was designed and built by C-E specifically to support this program and represents a significant contribution by C-E towards the EPA's goal of commercializing the in-furnace sorbent injection technology for SO_2 control. This facility accurately models the time/temperature history, heat release rate, heat absorption, and aerodynamic characteristics of a large utility boiler. Both the lower and upper furnaces are modeled so that the region of the boiler where SO_2 capture reactions take place are properly represented. A detailed discussion of the BSF's design and operation is given in the following sections.

The combustion testing task involved a series of steps which are shown in flow chart form on Figure 6-1. The test plan was developed on the basis of Task A and B results. The plan is organized to study and optimize sorbent injection in the BSF. The test plan specified BSF design features to insure that the tests would be representative of the expected combustion performance and furnace gas time/temperature profile of a typical C-E designed tangentially fired utility boiler.

Combustion test preparation was extensive and was performed in parallel with C-E's own efforts to design and construct the BSF. Specific items accomplished were:

- Design, fabrication, and installation of sorbent injectors specified under tasks A and B.

- Design, construction, and installation of a sorbent supply, metering, and distribution system.

- Fabrication and installation of three pendant-type simulated superheater panels.

- Selective refractory insulation of the test furnace water walls. C-E's proprietary furnace simulation code was utilized to specify

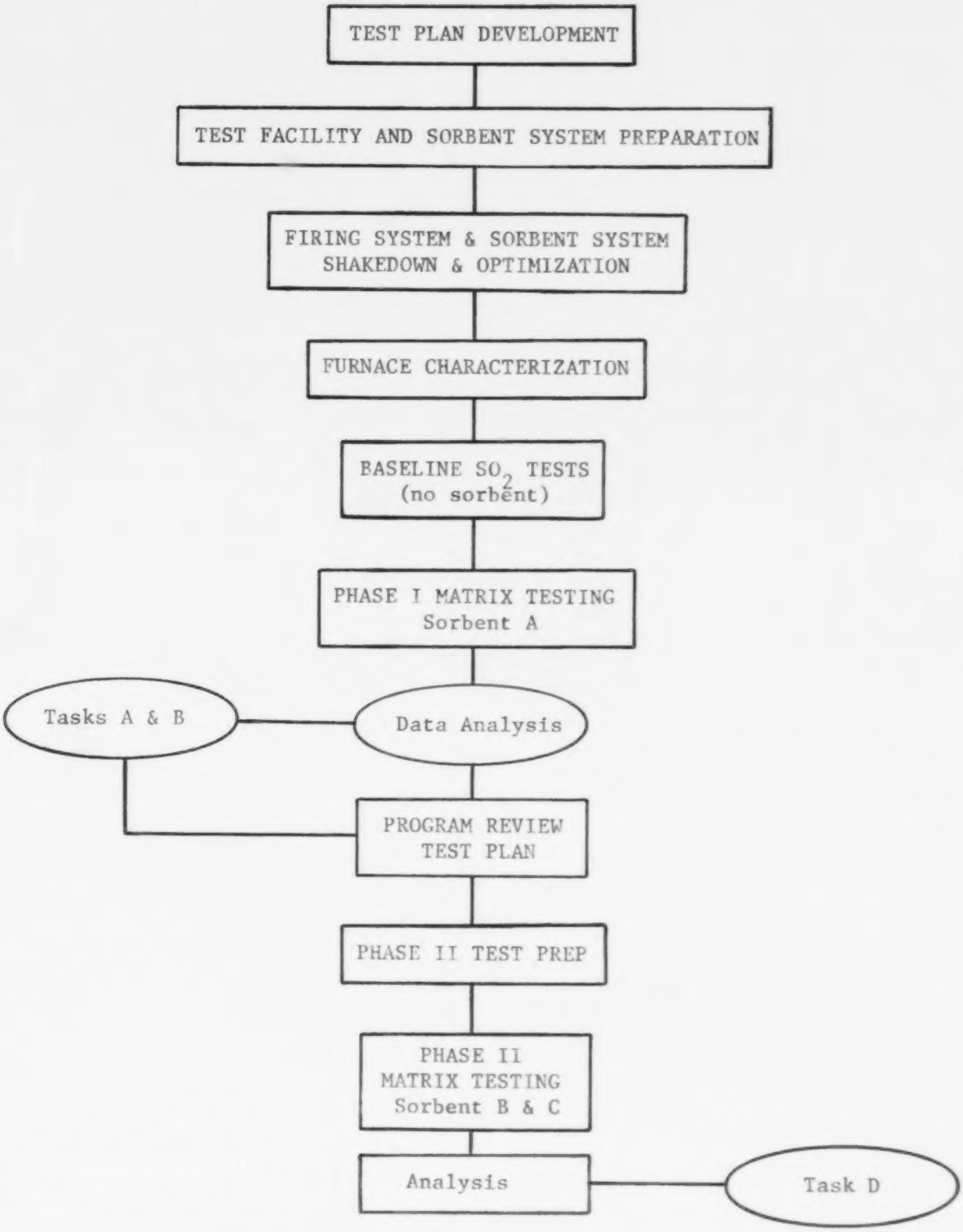
TEST PLAN DEVELOPMENT
TEST FACILITY AND SORBENT SYSTEM PREPARATION
FIRING SYSTEM & SORBENT SYSTEM SHAKEDOWN & OPTIMIZATION
FURNACE CHARACTERIZATION
BASELINE SO2 TESTS (no sorbent)
PHASE I MATRIX TESTING Sorbent A
Tasks A & B
Data Analysis
PROGRAM REVIEW TEST PLAN
PHASE II TEST PREP
PHASE II MATRIX TESTING Sorbent B & C
Analysis
Task D

Figure 6-1. Combustion testing approach.

refractory insulation in the BSF to achieve the gas time/temperature history of a typical 'T'-fired utility boiler.

- Procurement, storage, analysis, and preparation (pulverization) of the required 400+ tons of Pittsburgh #8 seam coal.

- Procurement, storage, and analysis of the three different hydrated lime sorbents. A total of about 30-35 tons was utilized.

- Procurement of miscellaneous test supplies

- Installation and calibration of test instrumentation.

Following the completion of these efforts, the test facility, the sorbent injection system, and related instrumentation and auxiliaries were systematically shaken down. Attention was given to defining the operability range of these systems and to insure that they would perform as required over the conditions specified in the test plan. Reworking of some components was performed followed by further verification tests before actual combustion testing began.

Initial tests were performed with no sorbent injection to measure baseline SO_2 emissions and gas time/temperature characteristics. Parametric tests were then performed (Phase I) with sorbent injection (Sorbent A) to investigate the effect of injector location, tilt, velocity, and sorbent carrier air on SO_2 capture performance. Phase I results were extensively analyzed. This included further review of Task A results and additional math modeling efforts under Task B. The output of these analyses were presented to the EPA during two working meetings (one in Windsor, CT and one in Research Triangle Park, N.C.). During these meetings a Phase II test plan was developed.

Phase II testing included further parametric testing of injection variables for the goal of optimizing SO_2 capture. An SO_2 reduction of

50% over baseline levels was sought and achieved for selected test conditions. Phase II testing utilized the same coal as Phase I but studied two additional sorbents. These sorbents were a hydrated lime with and without an additive (lignosulfonate) that had been shown in small scale tests to enhance SO_2 capture performance.

Finally, all combustion test results were analyzed and are reported in the following sections. These results were incorporated with Task A and Task B results to provide guidelines for in-furnace sorbent injection designs for tangentially fired boilers. The application of these results is discussed in Section 7.

6.3 EXPERIMENTAL APPROACH AND FACILITIES DESCRIPTION

6.3.1 Boiler Simulation Facility

Experimental testing was performed to create a data base from which design guidelines for field application of in-furnace sorbent injection for SO_2 capture on tangentially fired boilers could be developed. In order to meet this objective, testing was performed under conditions which were representative of typical tangentially-fired utility boilers. Combustion Engineering designed and built a new large scale combustion test facility which accurately models a C-E designed utility boiler. A description of this facility including its design, construction, auxiliary components, and instrumentation is given here. Also the sorbent injection, supply and storage systems which were designed, built and utilized during this test program are detailed.

Of equal importance to having representative experimental facilities, was that furnace and sorbent injection test conditions were also representative. The coal, sorbents and test conditions were carefully selected with EPA guidance for the purpose of meeting that criteria. These are discussed in the next section (Section 6.4.2).

Combustion Engineering reviewed U.S. utility boilers it has designed and identified a unit which was felt to be representative of a "typical" modern

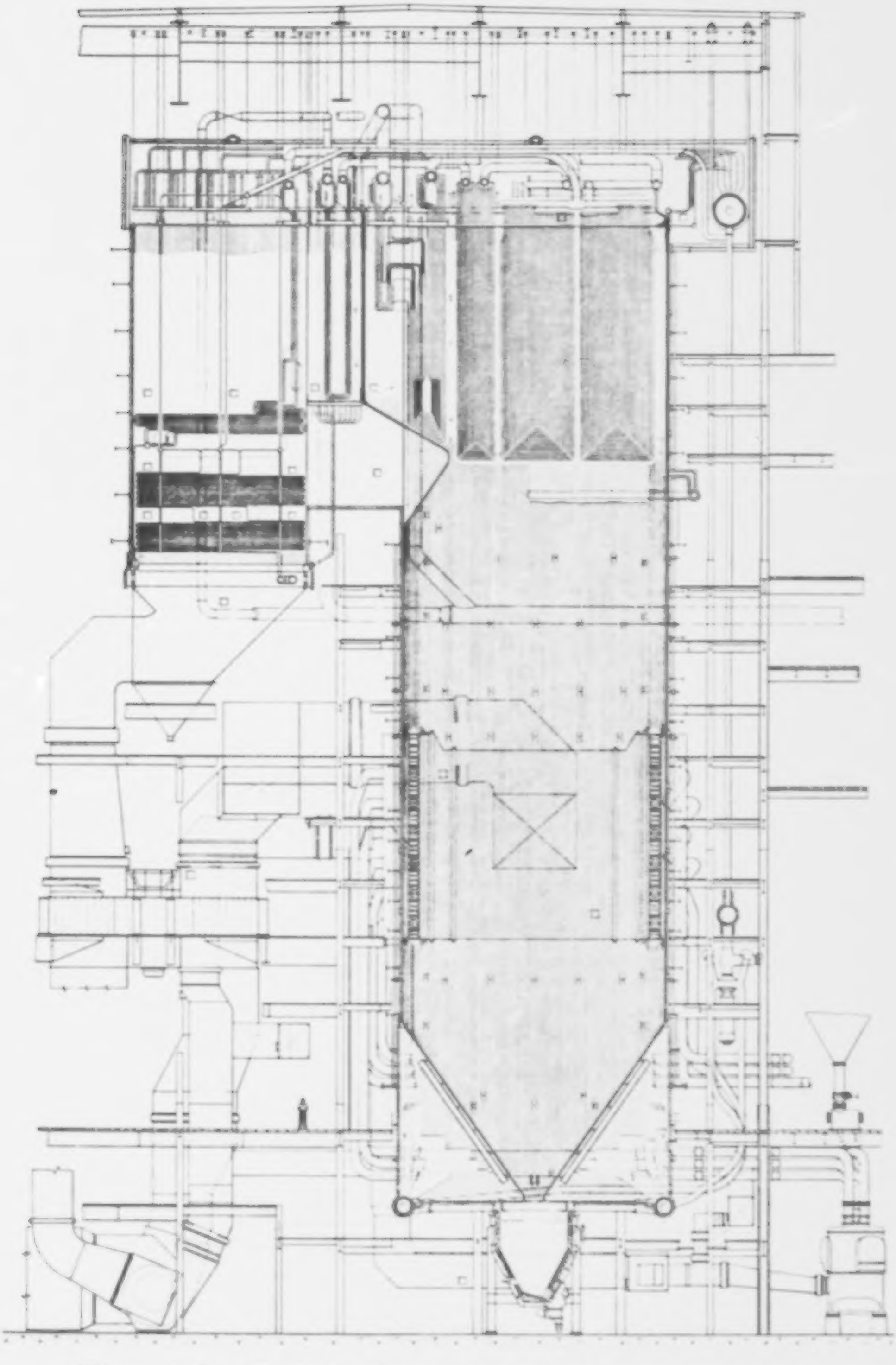

Figure 6-2. Typical modern C-E designed tangentially fired coal-burning boiler.

tangentially-fired boiler. This 560 MW unit is shown in Figure 6-2 and is representative of post 1961, eastern and midwestern, high volatile, bituminous or subbituminous coal fired boilers. The unit has multiple elevations of tilting tangential fuel admission assemblies which include overfire air ports for NO_x control. The upper furnace is segregated from the lower furnace by an arch. The upper furnace includes pendant-type superheater panels and reheater and economizer sections.

C-E's new Boiler Simulation Facility (BSF) was designed to model this specific unit. Key design considerations were:

- Time/Temperature Profile in the Sulfation Temperature Window
- Combustor Swirl and Other Aerodynamic Features
- Geometric Similarity to Typical 'T'-Fired Utility Boiler
- Carbon Burnout
- Residence Time in the Combustor
- Absence of Particle Settling in the Combustor
- Axial Velocity in the Combustor
- Acceptable Coal/Primary Air and Secondary Air Injection Velocities
- Flexibility; including adjustable heat absorption, adjustable to wall or stoker firing, and staged air and fuel ports

All major aspects of the utility boiler are duplicated in the BSF (Figures 6-3, 6-4a, and 6-4b) including the lower furnace, the ash hopper, multiple burners, the arch section, superheater panels, and the convective heat transfer surfaces. The furnace walls and heat transfer surfaces are cooled by a surrounding water jacket as shown in Figure 6-3. Steam generated is not utilized but is vented off at atmospheric pressure so that a constant

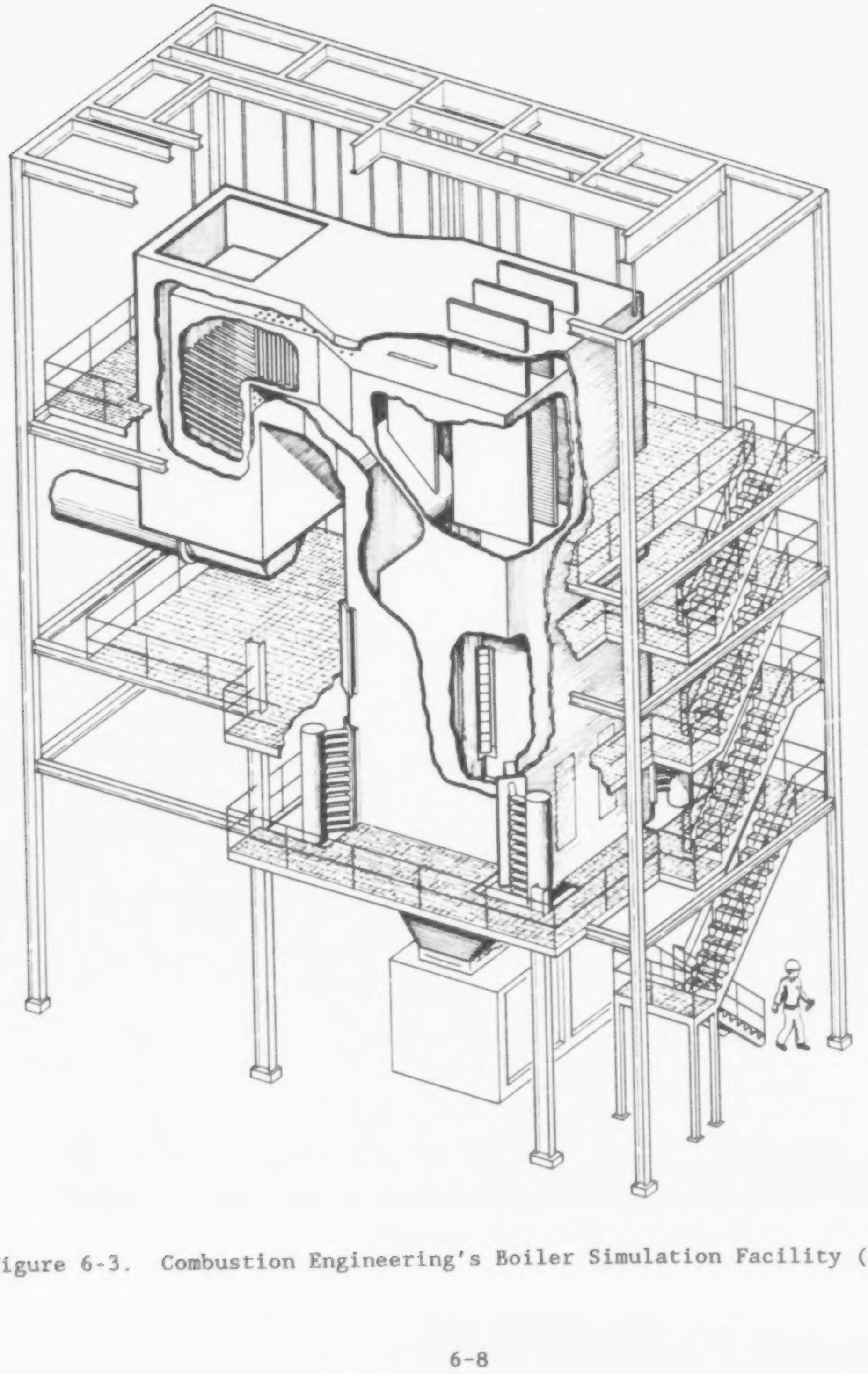

Figure 6-3. Combustion Engineering's Boiler Simulation Facility (BSF).

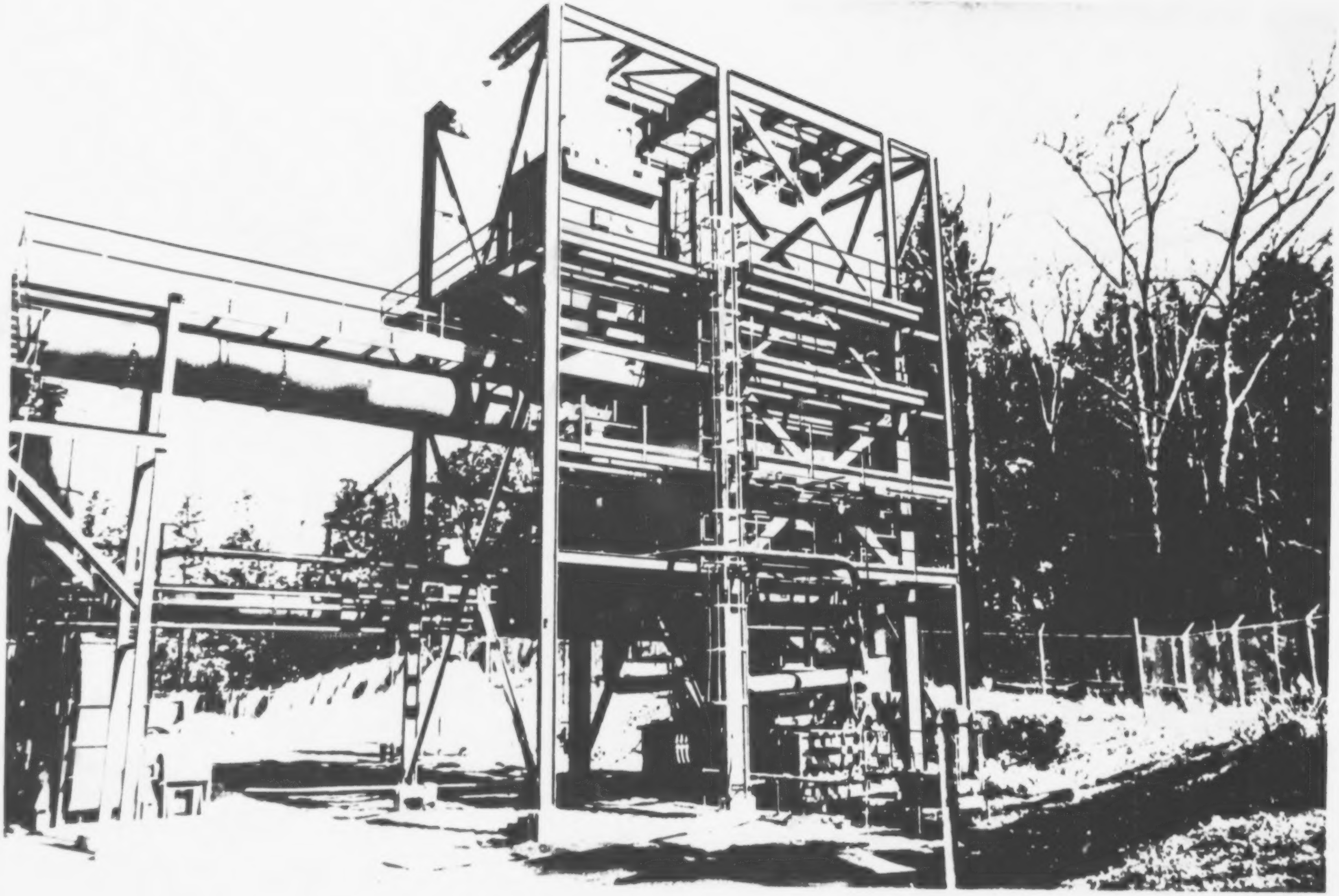

Figure 6-4a. BSF in operation.

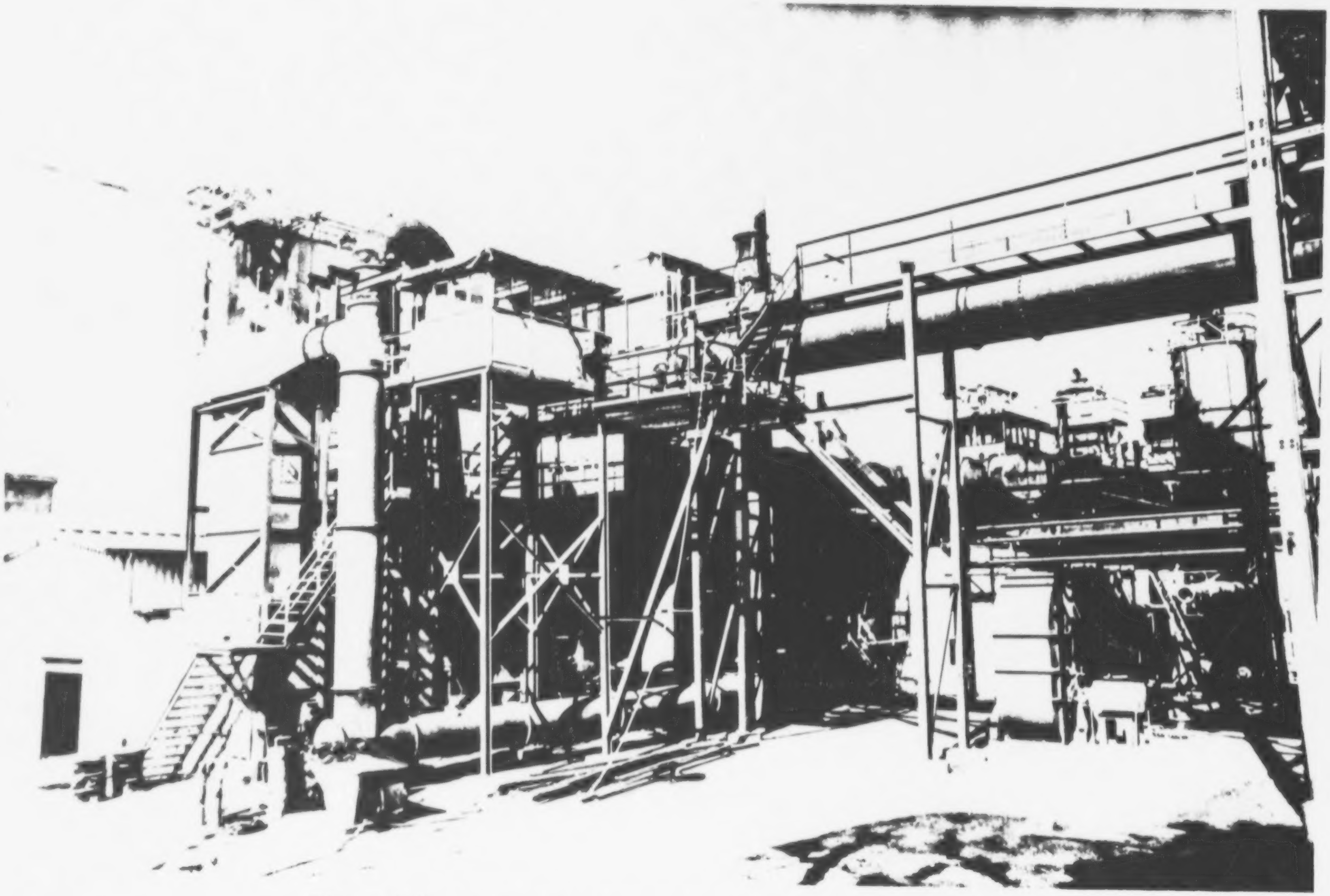

Figure 6-4b. BSF outlet duct and back-end equipment.

sink temperature of 212°F is maintained. The lower furnace water walls are selectively refractory lined to maintain furnace gas temperatures. Refractory is required because the walls are cooler than those of a typical boiler and the surface-to-volume ratio of the BSF is greater than that of a utility boiler.

As a part of the Task B effort discussed in Section 5, refractory specification was made using two proprietary C-E analysis codes. The first calculated heat transfer rates and gas temperatures in the lower furnace (up to the horizontal furnace outlet plane, HFOP) and the second calculated gas temperature and heat transfer rates in the upper furnace (above the HFOP). Input variables to these codes are firing rate, gas properties, furnace dimensions, and heat transfer surface conductance expressed as slag and/or refractory thermal conductivity divided by the thickness of this material. Lower furnace program calculations indicated that gas temperatures between 2400 to 2600° could be achieved at the HFOP with the furnace operated at firing rates of $50\text{x}10^6$ Btu/hr to $70\text{x}10^6$ Btu/hr if the lower furnace was covered with the appropriate thickness of castable refractory. The corresponding calculated time/temperature profiles for the BSF upper furnace are shown in Figure 6-5. Residence times in this figure are referenced to time of zero at the HFOP. The two profiles for BSF firing rate of $50\text{x}10^6$ Btu/hr have time/temperature profile slopes (quench rates) of 485 to 585°F/sec in the temperature range between 2400°F to 1600°F. The quench rate for the $70\text{x}10^6$ Btu/hr firing rate is 750°F/sec. The selection of design HFOT and quench rate was influenced by the need to relate the BSF operation to performance parameters for boilers being tested in other LIMB programs and the general population of utility boilers in the U.S. After considerable deliberation including discussions with EPA, it was decided to design the BSF lower furnace refractory for a HFOP temperature of 2400°F with a firing rate of $50\text{x}10^6$ Btu/hr.

The gas temperatures measured at the HFOP with the furnace operating at $50\text{x}10^6$ Btu/hr were less than 2400°F. This difference was probably due to the fact that the heat transfer codes were calibrated by field test data from slag covered utility boilers cooled by high pressure boiling water (at temperatures up to 1000°F) while our application of the code was to the refractory covered

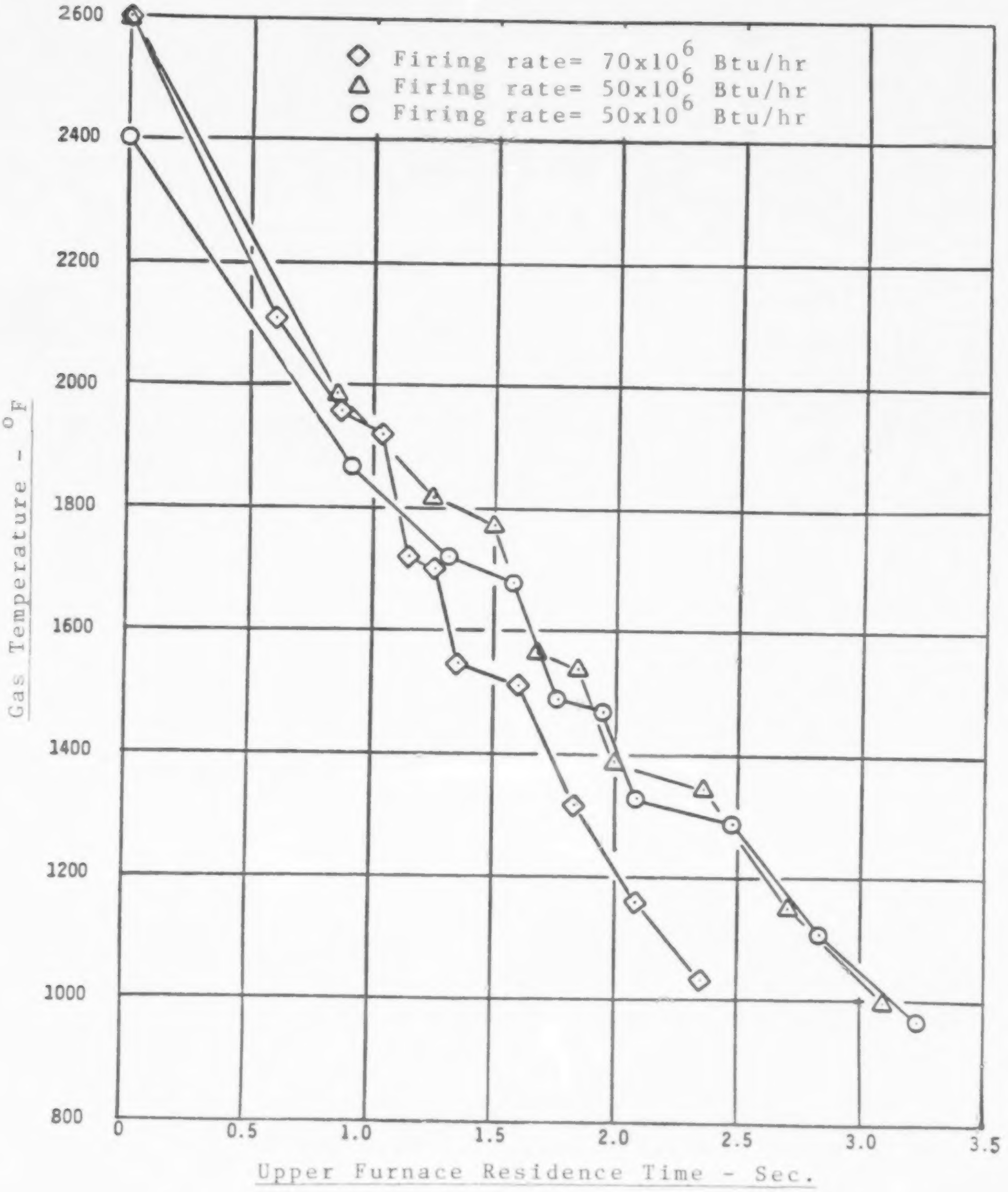

Figure 6-5. Calculated gas temperature/residence time profile for the BSF.

BSF walls cooled by boiling water at 212°F. The lower than expected gas temperature at the HFOP influenced the selection of the sorbent injection test matrix for Phase II testing at the BSF. This is discussed in a later portion of this report.

Aerodynamic characteristics were also modeled. The BSF incorporates three elevations of tilting tangential coal admission assemblies (a total of twelve coal burners). These fuel admission assemblies are of standard C-E design. However, the firing rate was adjusted to match the lower furnace swirl number (an aerodynamic parameter defined as the ratio of angular to axial momentum). Burner stability and fuel burnout were excellent during testing.

The aerodynamics of the upper furnace are as important for the study of sorbent injection as those of the lower furnace. In the case unit, the swirling flow of the lower furnace is straightened as it passes through lanes formed between the pendant superheater panels. Panels were included in the BSF as shown in Figures 6-3 and 6-6. As the furnace gases enter the convective pass they travel through a series of tube bundles which are similar to an actual boiler's convective pass.

Figure 6-6 is a photograph of the BSF from the inside standing in the ash hopper and looking upwards at the three (3) simulated superheater panels at the top of the furnace. The eight (8) square objects to either side of the panels are explosion relief vents. The furnace arch is to the right of the panels and the convective section passes behind it and to the right out of view. Refractory insulation covers the lower furnace water walls up to the elevation of the superheater panels (i.e. the furnace arch elevation). Lastly, two of the multi-elevation corner-located tangential fuel admission assemblies can be observed.

The BSF was fired at 50×10^6 Btu/hr for this program which required about 2.25 tons/hr of coal. Coal was crushed, pulverized, and stored in two 30 ton silos prior to testing. Pulverized coal was metered by a gravimetric feeder (weigh belt) and supplied to the BSF pneumatically at an air/fuel ratio and temperature typical of utility practice.

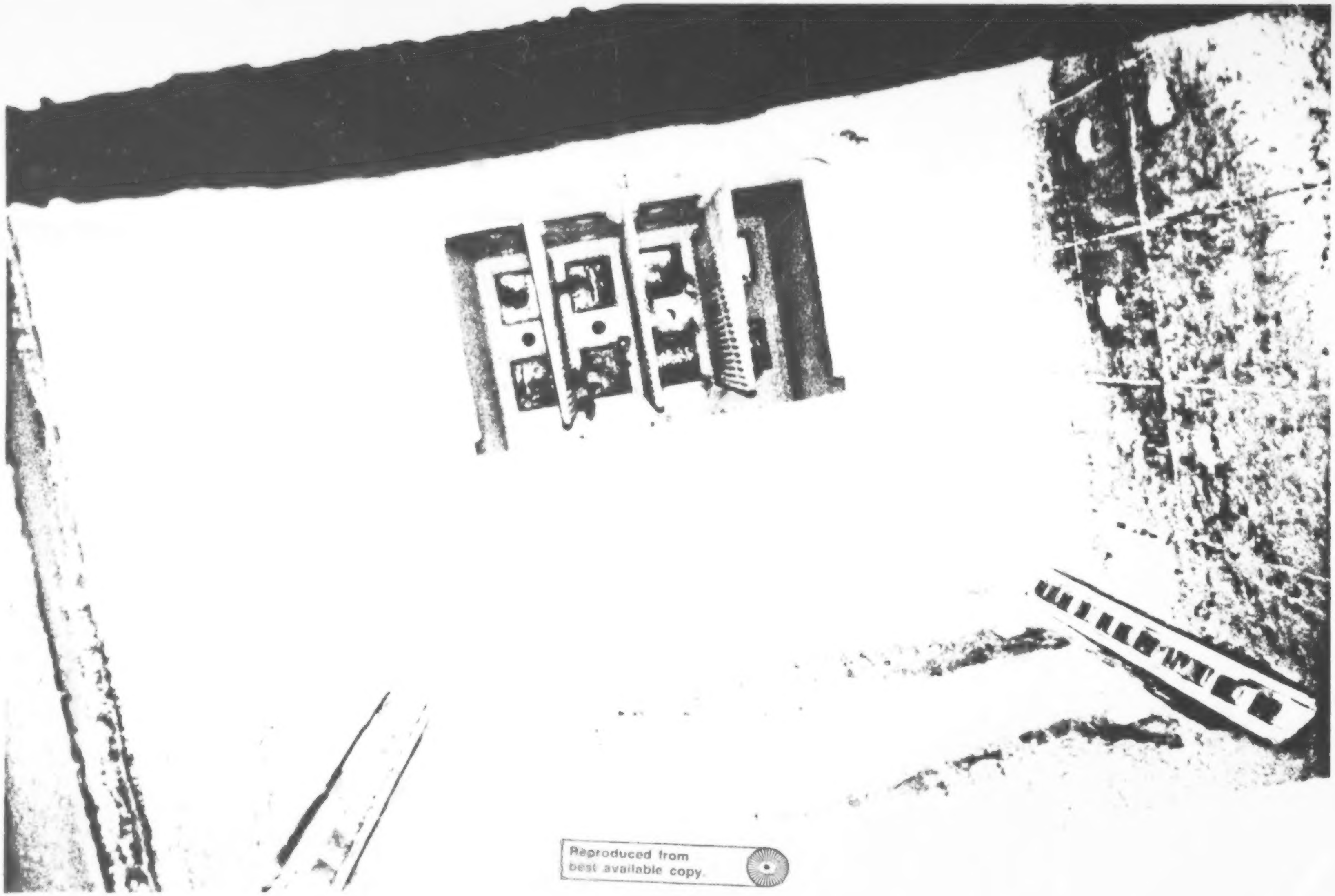

Reproduced from
best available copy.

Figure 6-6. View from ash hopper towards upper furnace of ESF.

The BSF is part of C-E's Firing Systems Development Complex at KDL (Figure 6-7) which includes the coal preparation and storage facilities. This complex also includes auxiliary equipment to permit all types of pulverized fuels and liquid fuels ranging from No. 2 distillate to heavy residual oils, plus coal-oil, coal-water or petroleum coke-oil slurries to be fired. The complex includes two other large scale furnaces, the Full Scale Burner Test Facility and the Sub-Scale Burner Test Facility, for performing burner development work up to firing rates of 200×10^6 Btu/hr. The BSF shares ancillary equipment with these facilities including the F.D. and I.D. fans, air preheat system, fuel preparation and supply systems and emission control system. A venturi-rod scrubber is utilized for local SO_2 and particulate emissions compliance.

The BSF is fully instrumented to monitor combustion phenomena. Access ports are located throughout the furnace and convective sections for temperature and velocity measurements, and for particulate and flue gas sampling. Figure 6-8 shows a test crew taking in-furnace suction pyrometer gas temperature measurements through one of the many access ports. Suction pyrometer measurements were taken with a water cooled probe and a shielded Platinum 30% Rhodium/Platinum 6% Rhodium thermocouple. Aspiration equipment and water cooling provisions are located on each BSF deck level to facilitate measurements.

Stack flyash sampling is shown in Figure 6-9. Here a technician is performing isokinetic sampling with an EPA method 5 sample train. The BSF is in the background. In the foreground at the left, a cyclone sampler was located for high volume flyash sampling. In the same vicinity continuous flue gas sampling was performed utilizing a phase discrimination system to preclude further alkali/SO_2 reactions. Flue gas was transferred via heated sample line to continuous analyzers located in the facility control room (Figure 6-10).

Critical furnace operating and test measurements were recorded by a data acquisition computer. Operations data were reduced on-line and presented to the facility operator at the terminals shown in Figure 6-10. The flue gas analysis system is to the right of the terminals in this figure.

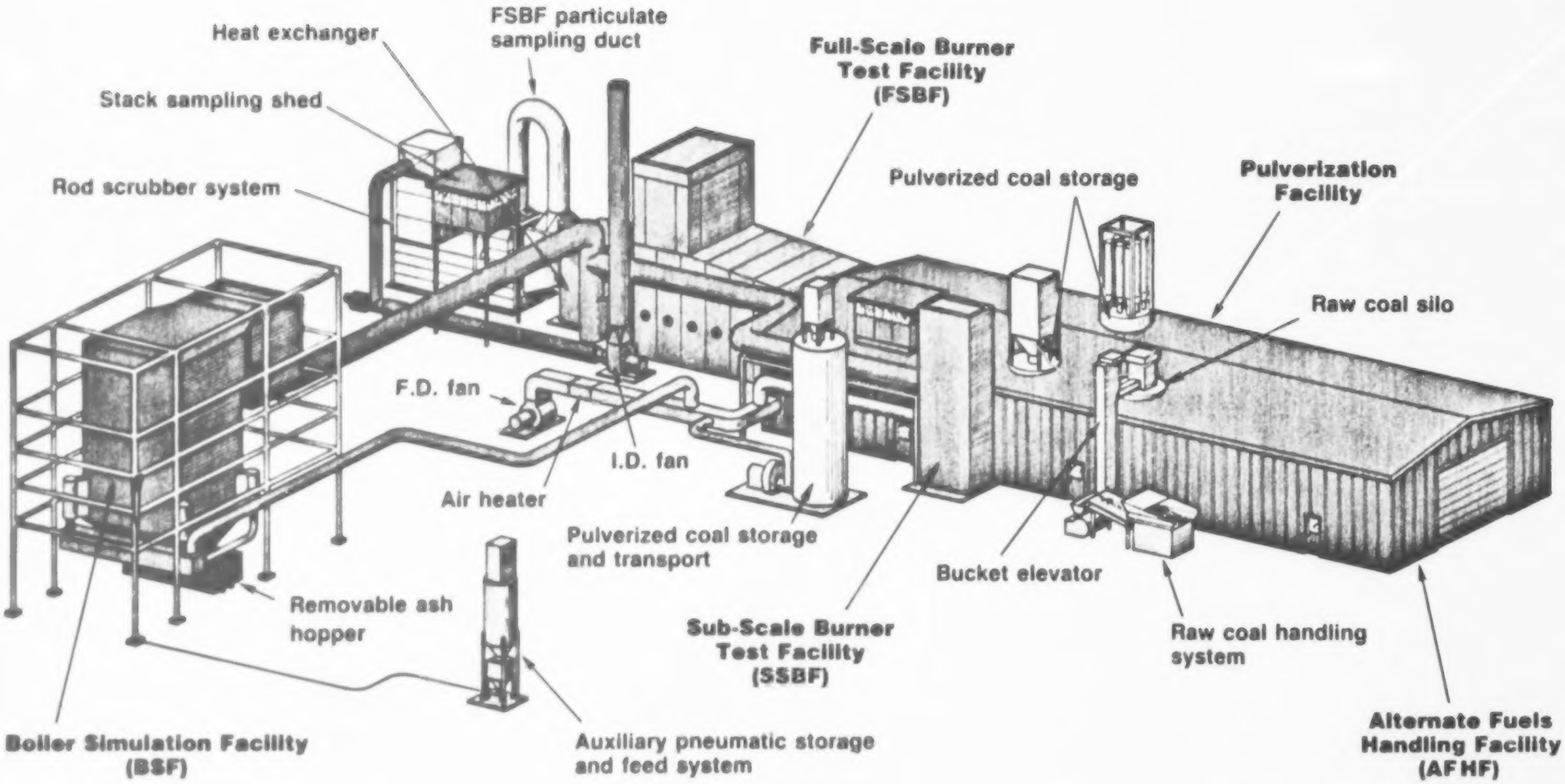
Heat exchanger
FSBF particulate sampling duct
Full-Scale Burner Test Facility (FSBF)
Stack sampling shed
Rod scrubber system
Pulverized coal storage
Pulverization Facility
Raw coal silo
F.D. fan
I.D. fan
Air heater
Pulverized coal storage and transport
Bucket elevator
Removable ash hopper
Sub-Scale Burner Test Facility (SSBF)
Raw coal handling system
Boiler Simulation Facility (BSF)
Auxiliary pneumatic storage and feed system
Alternate Fuels Handling Facility (AFHF)

Figure 6-7. Firing system development complex.

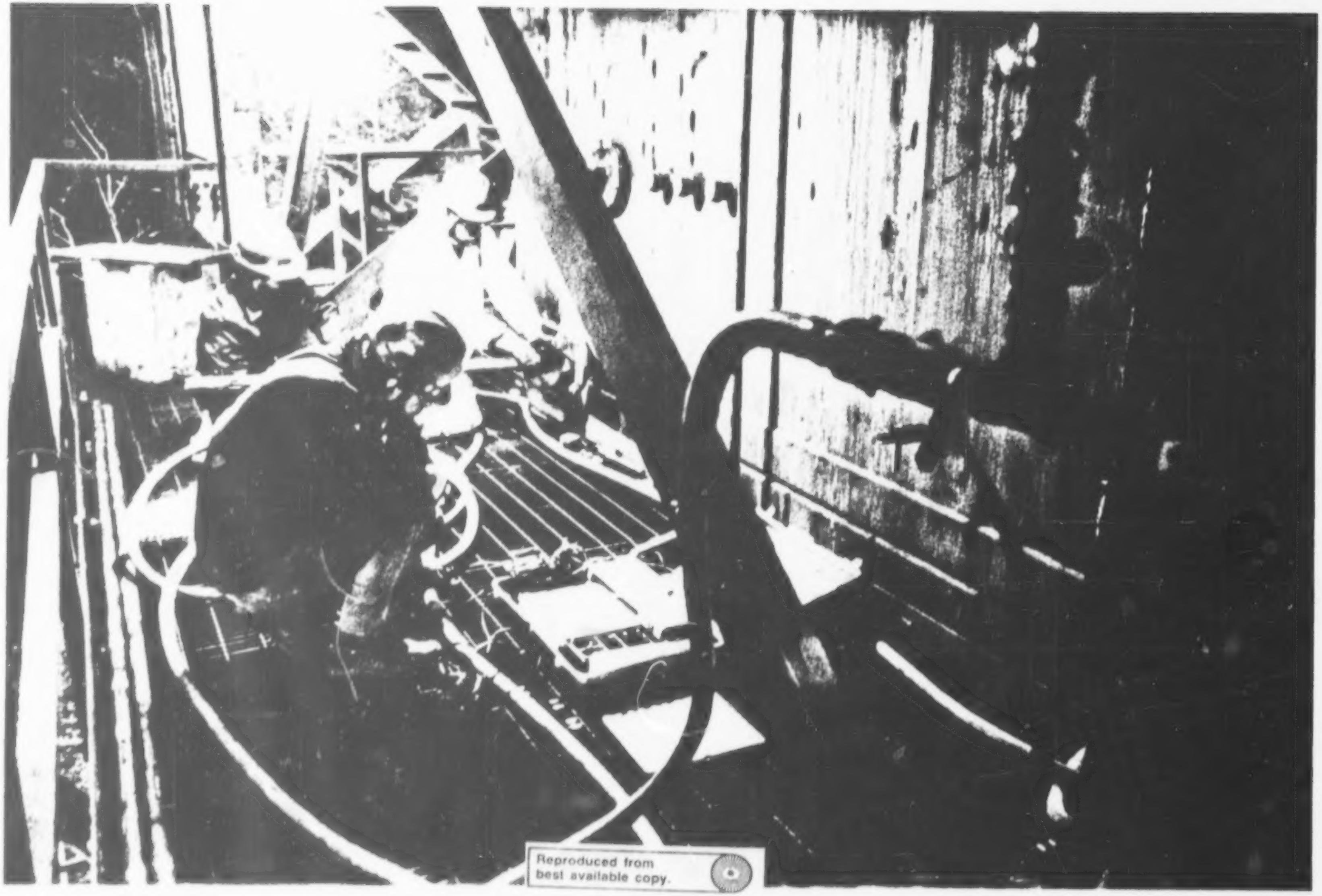

Reproduced from best available copy.

Figure 6-8. Suction pyrometer temperature measurement at elevation 35'-3" on BSF.

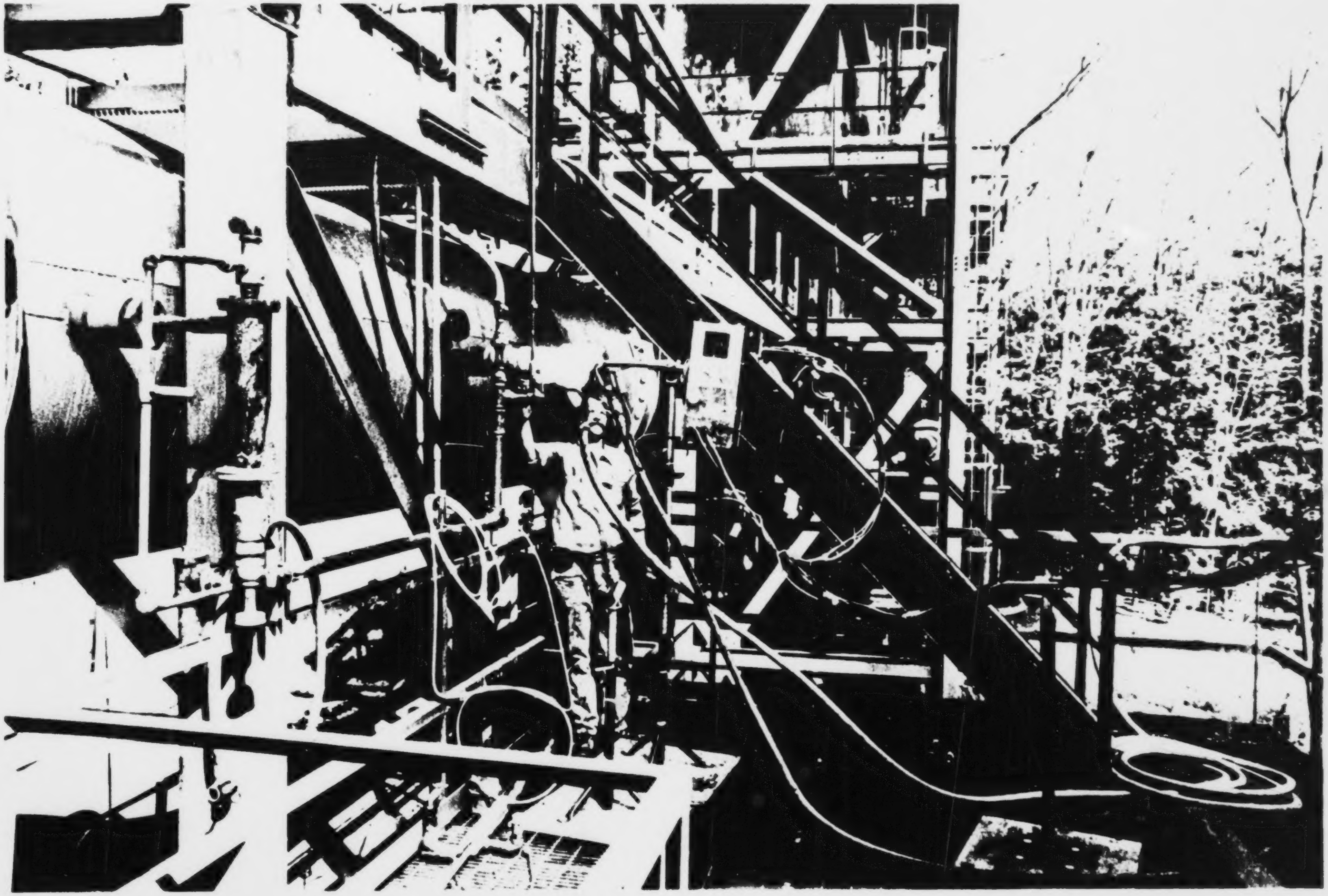

Figure 6-9. Stack flyash sampling.

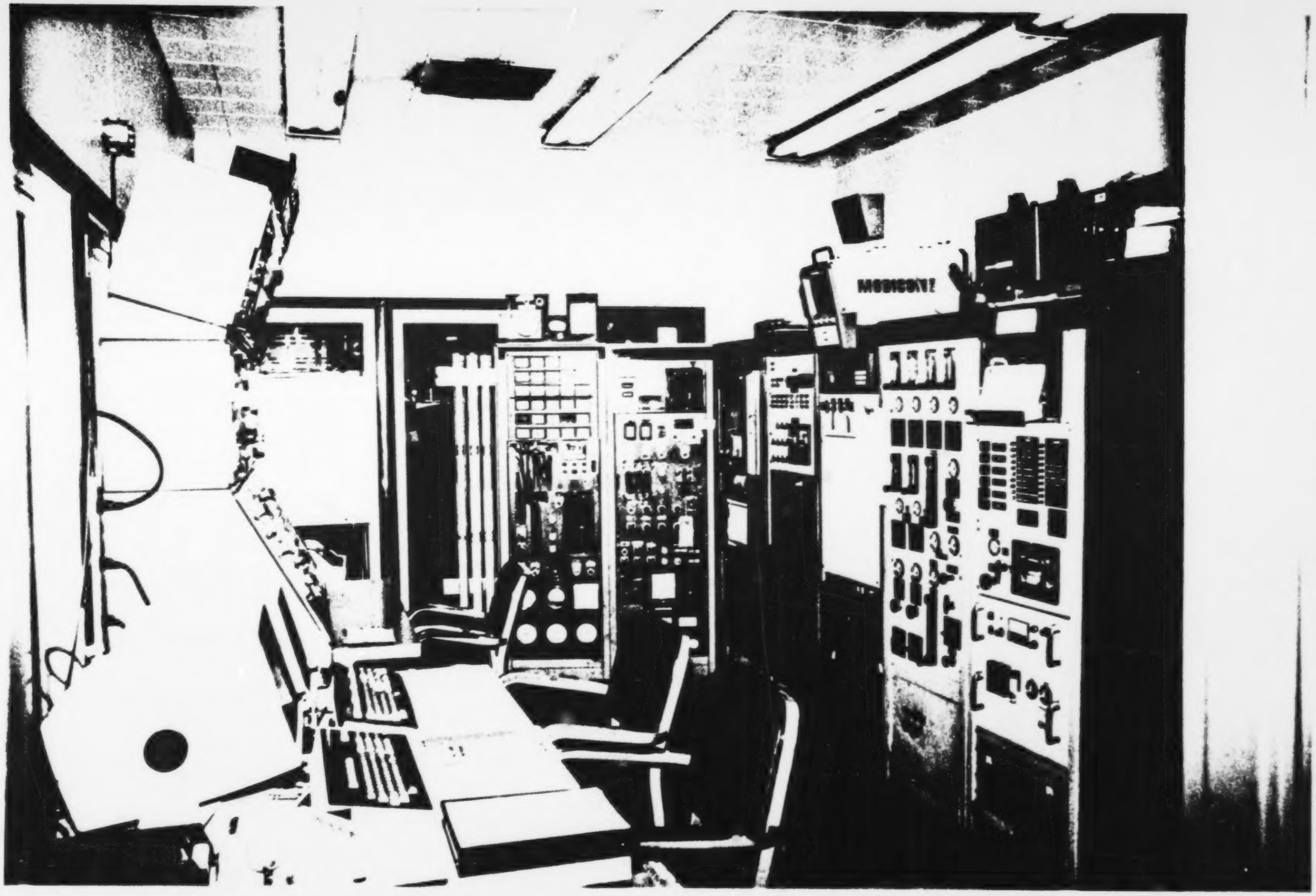

Figure 6-10. Boiler Simulation Facility control room.

The BSF also includes sootblowers for keeping the convective heat transfer surfaces clean. Two of the BSF sootblowers are shown in Figure 6-11. Sootblowing was important so that furnace gas temperatures (quench rate, etc.) remained constant during testing as this has been shown to influence SO_2 capture (Beittel, 1986). A more important effect though is due to the accumulation of reactive sorbent. Over time it would produce an apparent improvement in SO_2 capture as shown in Figure 6-12. While some tests investigated this improvement, most tests were performed over a constant time interval of sorbent injection, followed by sootblowing and a return to baseline SO_2 emission levels.

6.3.2 Sorbent Supply System

As part of the combustion testing effort, a sorbent storage, metering, and supply system was designed, built and utilized. The system's capabilities centered around the design guidelines developed during cold flow modeling (i.e., number of injectors, their location, 5% of the BSF combustion air flow rate, etc.). The actual capabilities extended beyond these to provide flexibility to the system for different sorbents and test operating conditions. The sorbent supply system had the following capabilities:

- Sorbent carrier air supply ranging from 1600 to 3500 lb/hr at ambient temperature (This represents dilute phase transport with 4% to 7% additional air over the BSF's nominal full load, 20% excess air combustion air flow rate).

- Wide feed range of Ca/S molar ratios (2800 lb/hr - 80 lb/hr) for a range of sorbent types from $CaCO_3$ to $Ca(OH)_2$ (i.e., bulk densities of 60 to 20 lbs/ft^3).

- Measurement of feed accuracy better than 1% for the conditions tested.

- Sorbent and transport air flows recorded by data acquisition computer.

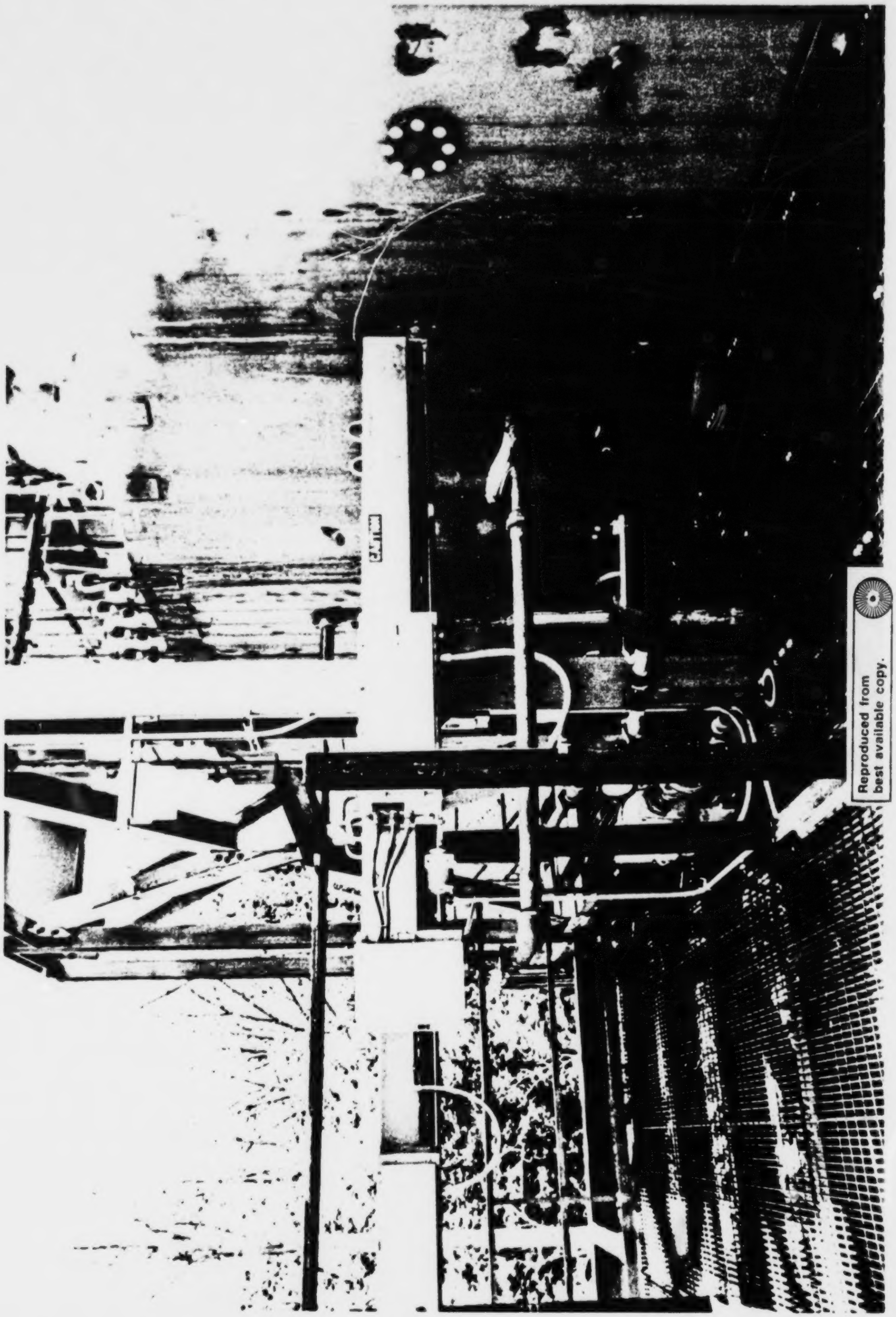

Reproduced from best available copy.

Figure 6-11. Sootblowers located in convective pass.

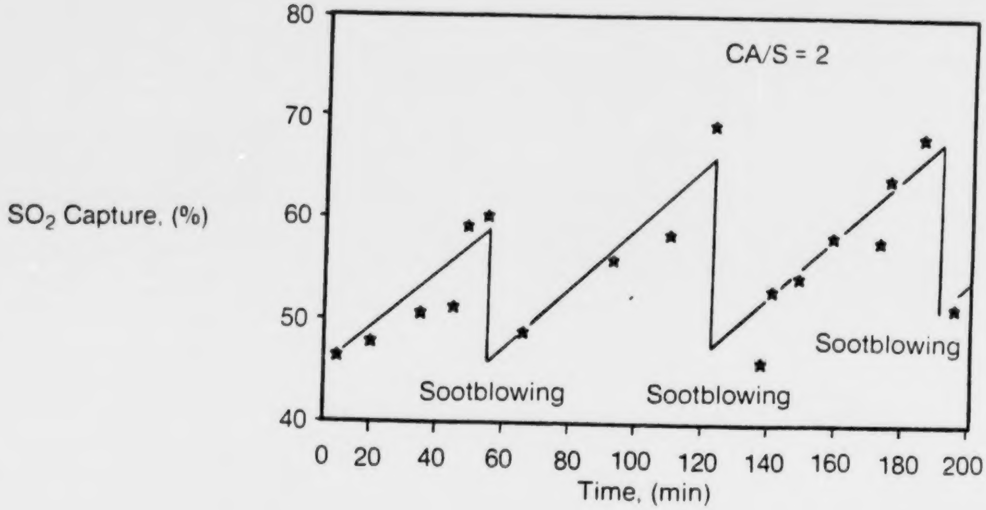

Figure 6-12. Variation of SO_2 capture with sootblowing cycle. (from Offen et al, 1985)

- Distribution system capable of four-, six-, or eight-way splitting and adjustable during testing.

- Injection velocities of 50 to 300 ft/sec and adjustable during testing.

- Multiple injection locations and adjustable during testing.

- Bulk sorbent storage of 20 tons.

An overall schematic of the sorbent storage and supply system is shown in Figure 6-13. An existing silo with a capacity of 20 tons of hydrated lime was utilized for bulk sorbent storage. This silo was equipped with a mass-flow style bin bottom to facilitate feeding. This prevented flooding and bridging which are common problems with hydrated limes. From this silo, material was periodically fed by dense phase to a small intermediate "test-bin." This test-bin was the heart of the sorbent feed system and had special features to ensure accurate and even sorbent feed. The test-bin could also be fed directly from bulk transport trucks as was done during Phase II testing when two sorbents were tested back-to-back.

The test-bin and additional details of the sorbent feed system are shown schematically in Figure 6-14. Figure 6-15 is a photograph of the test-bin. This bin was small in order to minimize potential feeding problems. It incorporated a live-bin bottom and a remotely actuated pneumatically operated gate valve which, when activated, very rapidly refilled an Acrison loss-in-weight feeder located directly below. Bin discharge flooding was promoted to insure rapid refill of the Acrison feeder. Effective isolation of the test-bin and the feeder was accomplished between refills of the Acrison feeder by the pneumatic gate valve discussed above.

The Acrison loss-in-weight feeder was selected after an extensive search, because its special characteristics made it the most accurate dry sorbent metering device available. Accurate and uniform sorbent feed was felt by the investigators to be critical for insuring that the best quality data possible

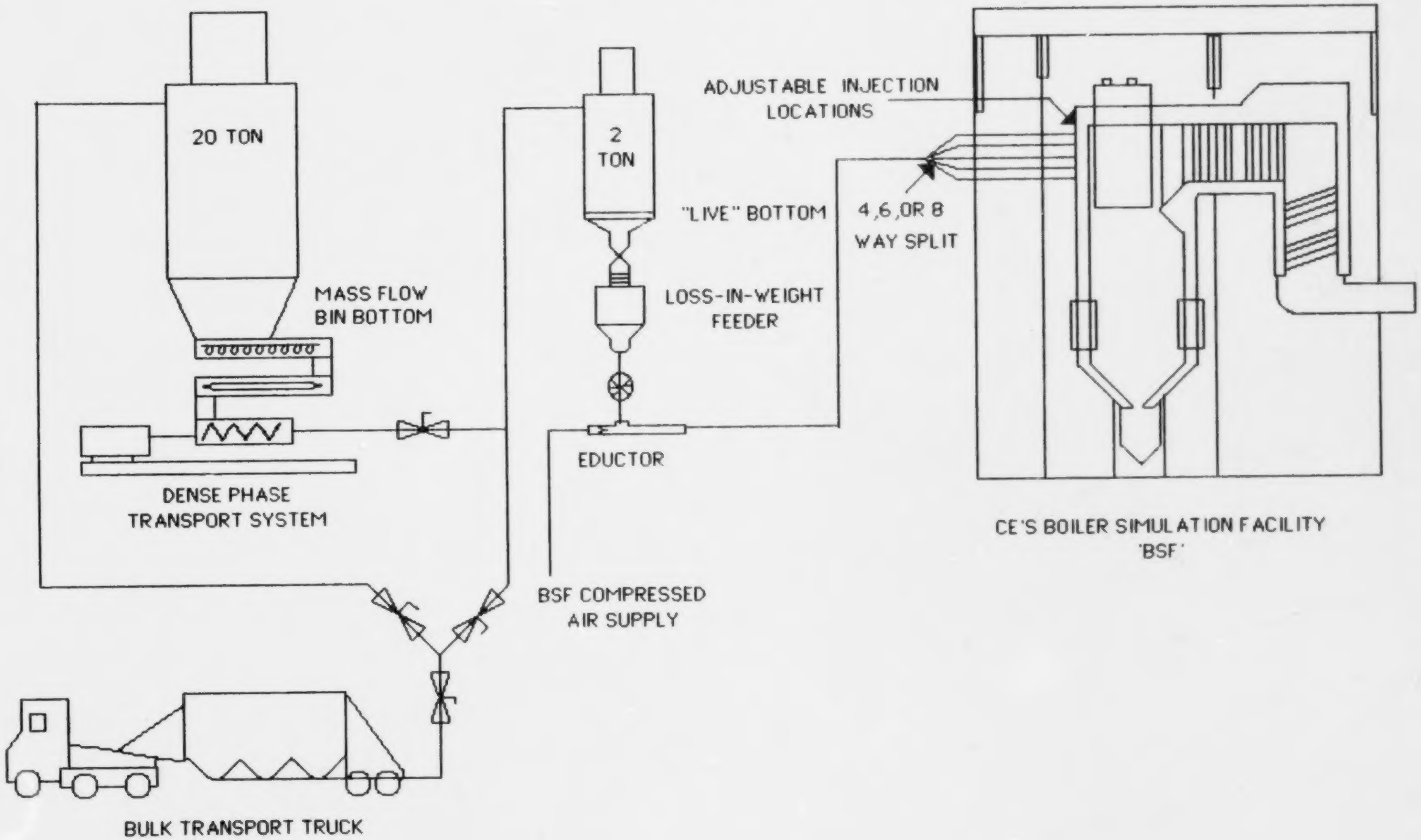
20 TON
MASS FLOW
BIN BOTTOM
DENSE PHASE
TRANSPORT SYSTEM
BULK TRANSPORT TRUCK
2
TON
"LIVE" BOTTOM
LOSS-IN-WEIGHT
FEEDER
EDUCTOR
BSF COMPRESSED
AIR SUPPLY
ADJUSTABLE INJECTION
LOCATIONS
4,6,OR 8
WAY SPLIT
CE'S BOILER SIMULATION FACILITY
'BSF'

Figure 6-13. Sorbent storage and supply system.

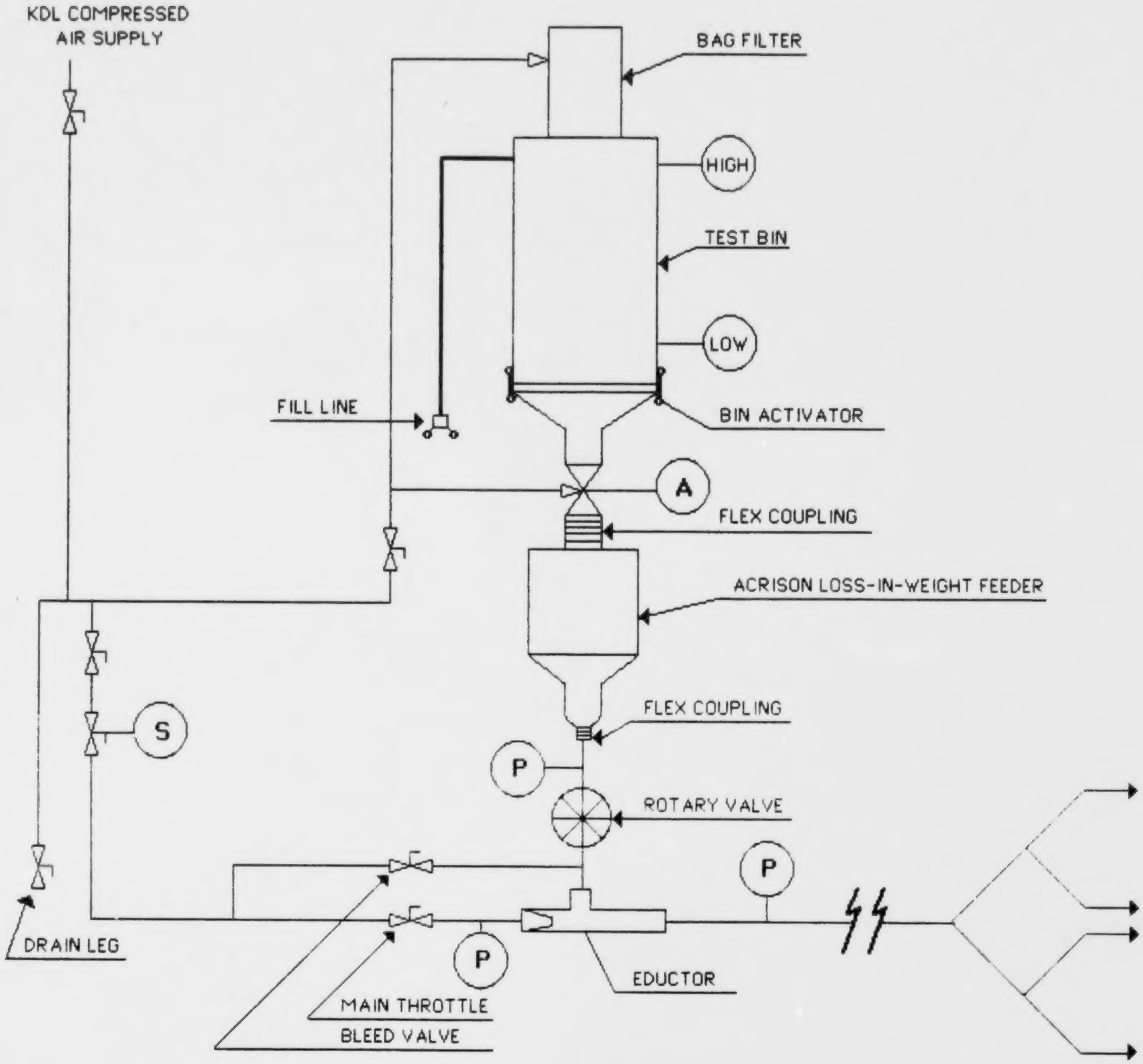
KDL COMPRESSED AIR SUPPLY
BAG FILTER
HIGH
TEST BIN
LOW
FILL LINE
BIN ACTIVATOR
A
FLEX COUPLING
ACRISON LOSS-IN-WEIGHT FEEDER
S
FLEX COUPLING
P
ROTARY VALVE
P
DRAIN LEG
P
EDUCTOR
MAIN THROTTLE
BLEED VALVE

Figure 6-14. Sorbent Feed System

Figure 6-15. Sorbent supply system.

was obtained during combustion testing. The principle of the loss-in-weight feeder is simple. The feeder incorporates a small bin from which product is discharged by a variable speed screw auger. The rate of product discharge is controlled by sensing the rate of weight loss in the bin and appropriately modulating the screw auger speed. When the bin is nearly depleted the screw "locks" into a constant rpm and the silo above is activated to rapidly refill the bin (only a few seconds were normally required). Once refilled the feeder returns to the gravimetric mode.

The Acrison feeder utilized during testing was calibration checked both at the factory (with the investigators present) and during testing at Combustion Engineering's Kreisinger Development Laboratory. The feeder was found to be better than 1% accurate over the range required for combustion matrix testing.

Because of the loss-in-weight principle, the feeder had to be carefully isolated from the storage silo and conveying lines. This included use of vented flexible couplings as shown in Figure 6-14. These isolated static vibration and pressure loads from the weigh bin. Wind and weather protection of the feeder were also required and can be seen in Figure 6-15. Sorbent discharged from the feeder's screw auger passed through a flexible coupling, then through a rotary air lock and into a venturi eductor. This eductor was specifically designed for solids conveying and incorporated a bleed valve to control eductor vacuum to eliminate undesirable pressure forces on the loss-in-weight feeder. Eductor transport air supply capacity was sized by use of a C-E developed pneumatic transport design code which estimated the sorbent feed system pressure drop.

The eductor transport air was supplied by the laboratory compressed air system. A drain leg was included to drain condensed moisture from the supply line before startup (this was an outdoor installation) and to thus avoid line pluggage by moistened sorbent. The compressed air supply was not dried but included several standard mechanical liquid moisture separators. Moisture in the conveying lines was not observed nor were any related feed problems encountered during testing

From the eductor, sorbent was conveyed pneumatically by dilute phase a total of about 200 feet including a 50 foot vertical section to various sorbent injection locations on the BSF. Four-, six-, and eight-way splitting of the sorbent feed was performed by an adjustable distribution system located on the single vertical section. The four-way distribution system was calibrated and found to be within +/-10%.

From the four-, six-, or eight-way distribution system, sorbent was conveyed through flexible tubing to the multiple injection points discussed in the next section. Figure 6-16 shows the sorbent conveying lines connected up to injectors on the front wall of the furnace. The flexible conveying lines included a grounded copper wire which prevented static charge build-up commonly encountered in pneumatic transport.

The sorbent injectors were quite simple and are shown in Figure 6-17. They were fabricated from different pipe sizes and schedules to produce the various desired sorbent injection velocities. The injection velocities and injector pipe dimensions are listed in Table 6-1. Injection tilt was accomplished by utilizing pipe elbows and nipples as shown in Figures 6-18 and 6-19. The injectors were flanged to fit the 6" diameter ports on the BSF. This also permitted injector tilt adjustment upwards, downwards or any desired angle. The flanges also permitted quick change-over of injectors (i.e., sizes, tilts, etc.) during testing. The flexible sorbent transport lines were connected to these injectors by quick connect fittings to further expedite change-overs.

6.4 COMBUSTION TEST MATRIX

Combustion testing was performed parametically to investigate the effects of the following variables on SO_2 capture:

- sorbent type
- sorbent injection location
- sorbent injection velocity
- sorbent injection angle
- sorbent carrier air flow rate

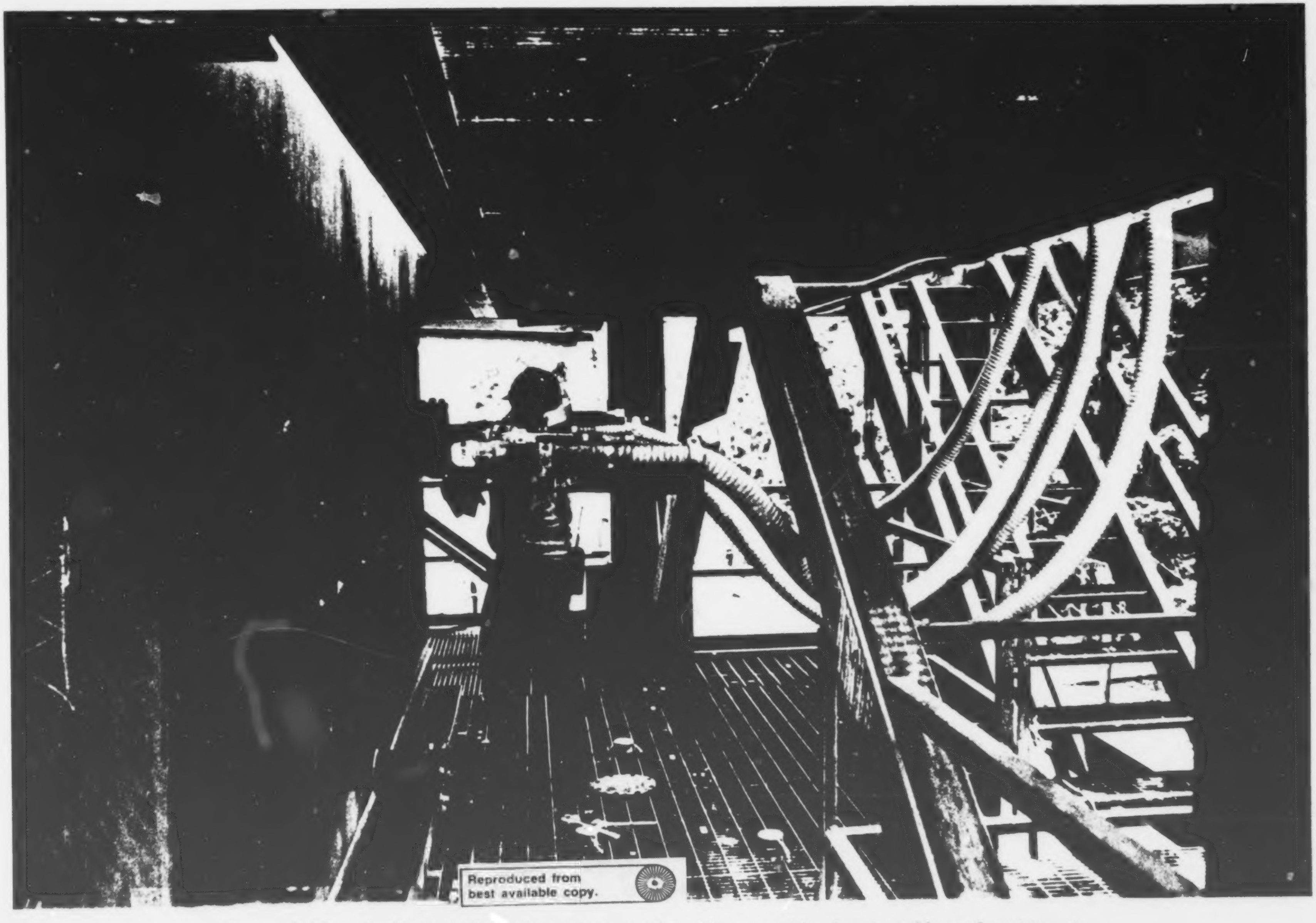

Reproduced from
best available copy.

Figure 6-16. Sorbent injectors and conveying lines on the front wall at location A.

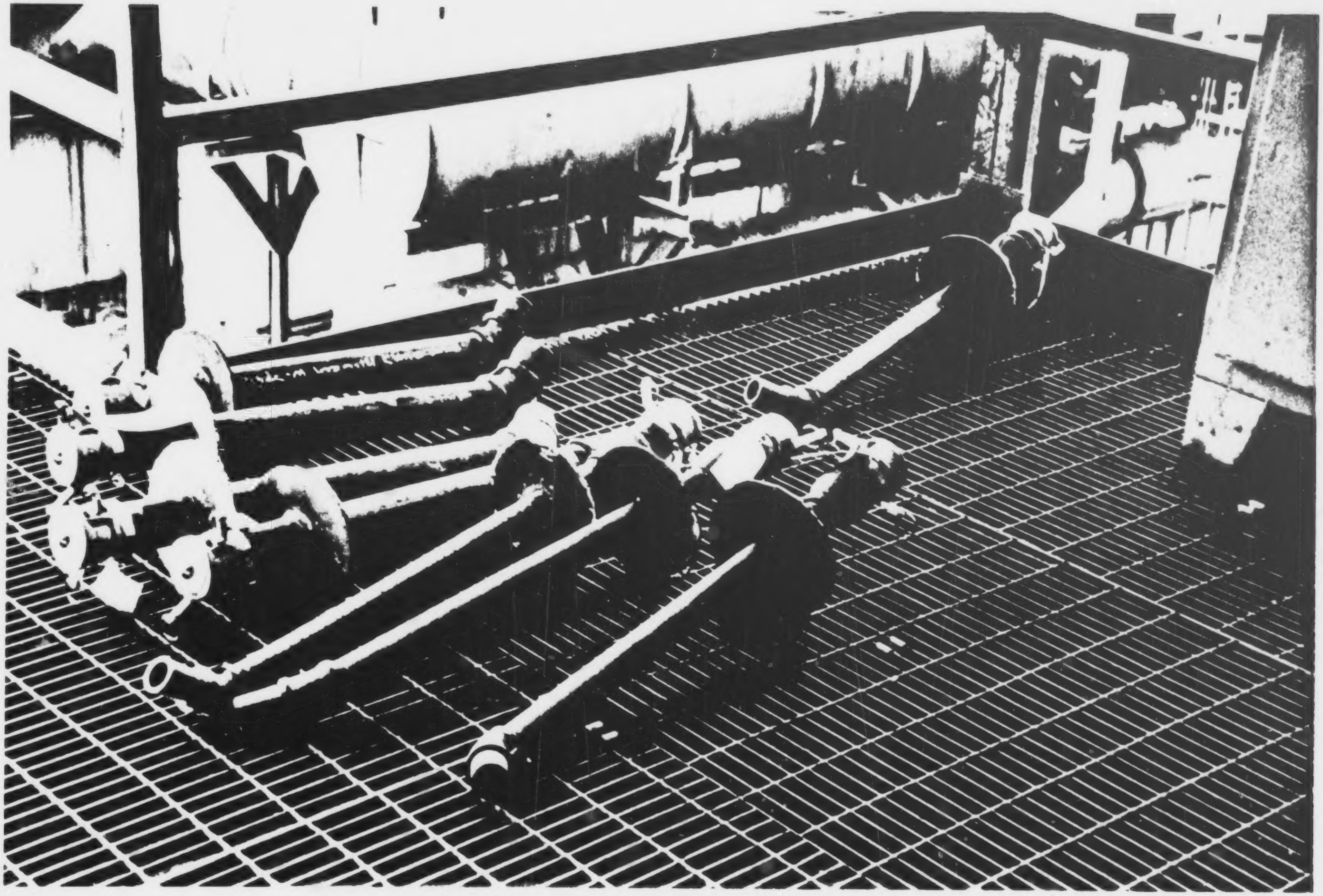

Figure 6-17. Sorbent injectors prior to installation on BSF.

Table 6-1

INJECTION VELOCITIES

For 2000 lbs/hr sorbent air flow:

For Four Way Injection

75 ft/sec = Sch. 80 2-1/2" Pipe; ID = 2.31"
100 ft/sec = Sch. 80 2" Pipe; ID = 1.94"
150 ft/sec = Sch. 40 1-1/2" Pipe; ID = 1.61"

For Eight Way Injection:

75 ft/sec = Sch. 40 1-1/2" Pipe; ID = 1.61"
100 ft/sec = Sch. 40 1-1/4" Pipe; ID = 1.38"
150 ft/sec = Sch. 160 1-1/4" Pipe; ID = 1.16"

NOTE: Higher and lower sorbent carrier flow rates were also tested. For each test actual injection velocities were calculated based on flow rate, injection diameter, and number of injectors.

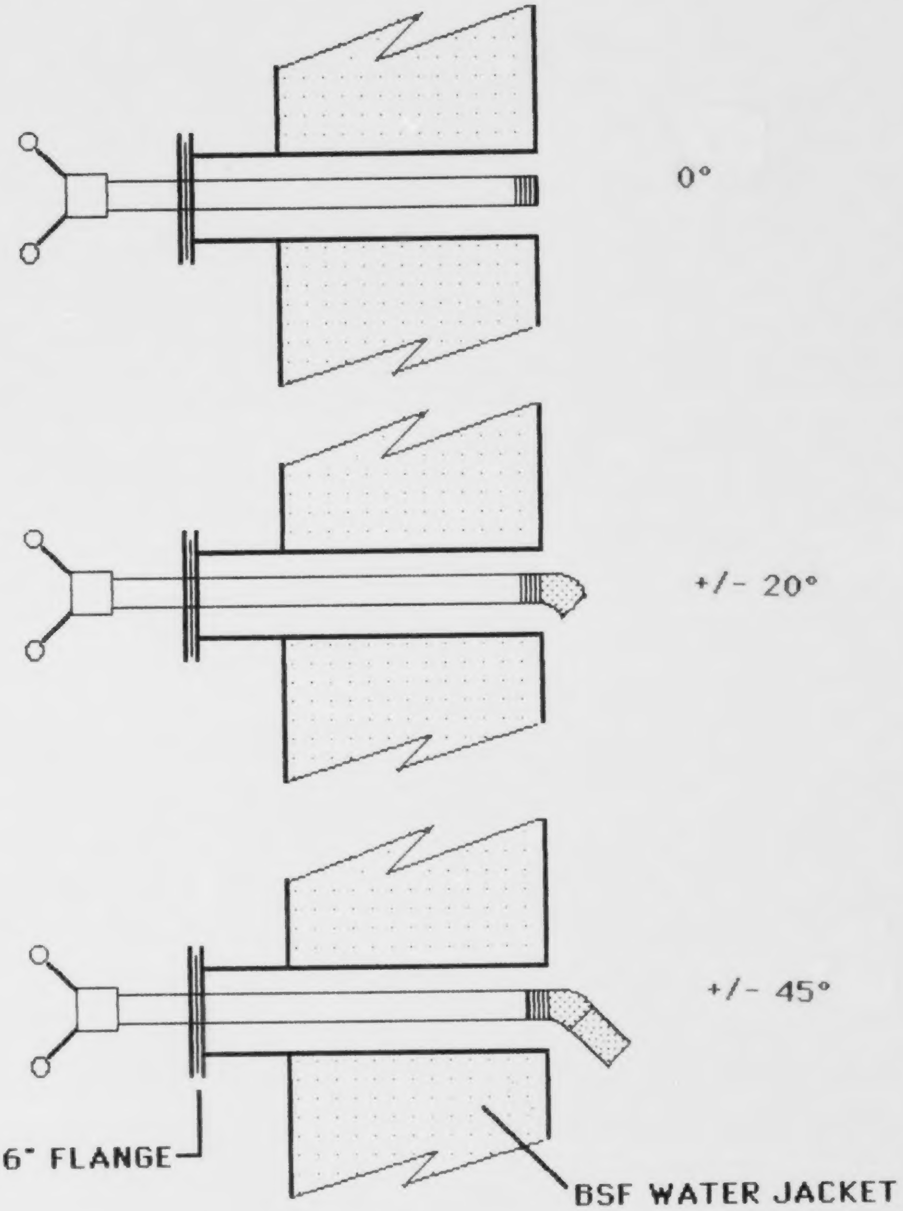
0°
+/- 20°
+/- 45°
6" FLANGE
BSF WATER JACKET

Figure 6-18. Definition of injector angles (shown are front wall type injectors).

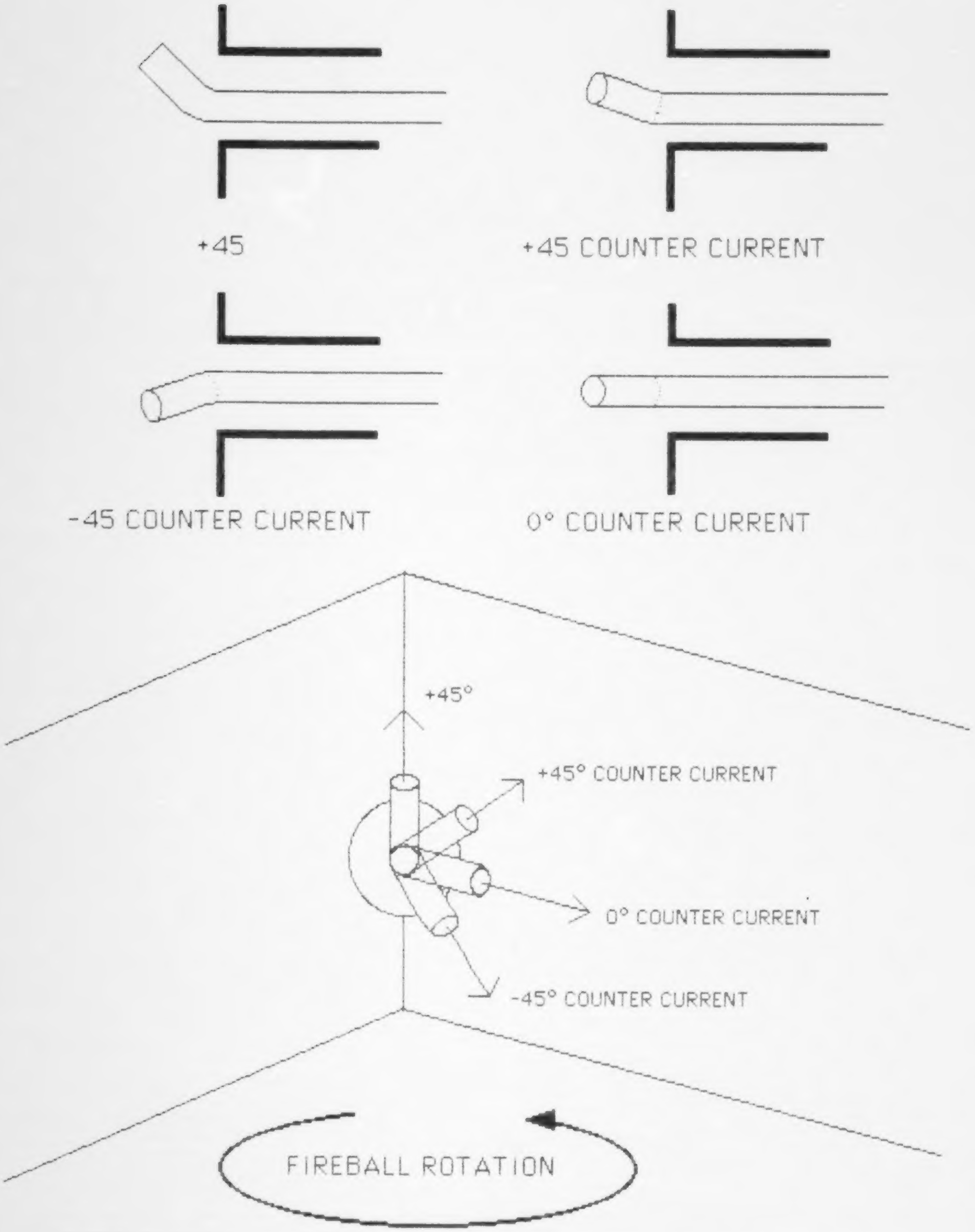
+45
+45 COUNTER CURRENT
-45 COUNTER CURRENT
0° COUNTER CURRENT
+45°
+45° COUNTER CURRENT
0° COUNTER CURRENT
-45° COUNTER CURRENT
FIREBALL ROTATION

Figure 6-19. Definition of location D injector angles (one corner shown, injector tip includes 45° elbow).

Tests were performed in two discrete phrases. During Phase I, initial tests were performed with no sorbent injection to measure baseline SO_2 and NO_x emissions, carbon conversion efficiency, and the furnace gas temperature distribution. Tests were then performed with sorbent injection to investigate the effect of injection parameters on SO_2 capture performance. During Phase I only one sorbent was studied (Referred to as Sorbent A). This sorbent was an untreated hydrated line obtained from Dravo Lime Company's Black River Plant. Sorbent characteristics are presented in Section 6.5. Also, during Phase I, only front wall injection at locations A, B, or C with four injectors were studied (See Figure 6-20). The Phase I test matrix is Table 6-2. Of the twenty-two (22) tests specified, all but a few were performed, but additional tests and repeat test conditions were performed yielding a total of fifty (50) Phase I test points.

Phase I test results were extensively analyzed. This included review of Task A Cold Flow Modeling results and additional math modeling efforts under Task B. The output of these analyses were presented to the EPA Program management during two working meetings during which a Phase II test matrix was developed (Table 6-3). Phase I test results showed that the furnace gas temperatures in the range of 2200-2400°F, assumed optimum for sorbent injection were located lower in the furnace than expected and as a consequence an additional and lower injection location (Location D on Figure 6-20) was studied during Phase II. Also during Phase II, two additional sorbents were studied, referred to as Sorbents B and C. These were Marblehead Lime Co. hydrated limes with and without lignosulfonate additive treatment (Sorbent C and Sorbent B, respectively).

Of the twenty tests (20) specified in the Phase II test matrix all were performed plus many additional tests and repeat conditions for a total of one hundred and twelve (112) individual Phase II test points. In addition, the goal of 50% SO_2 capture with a Ca/S molar ratio of 2:1 was achieved. Section 6.6 presents the results obtained during Phase I and Phase II testing.

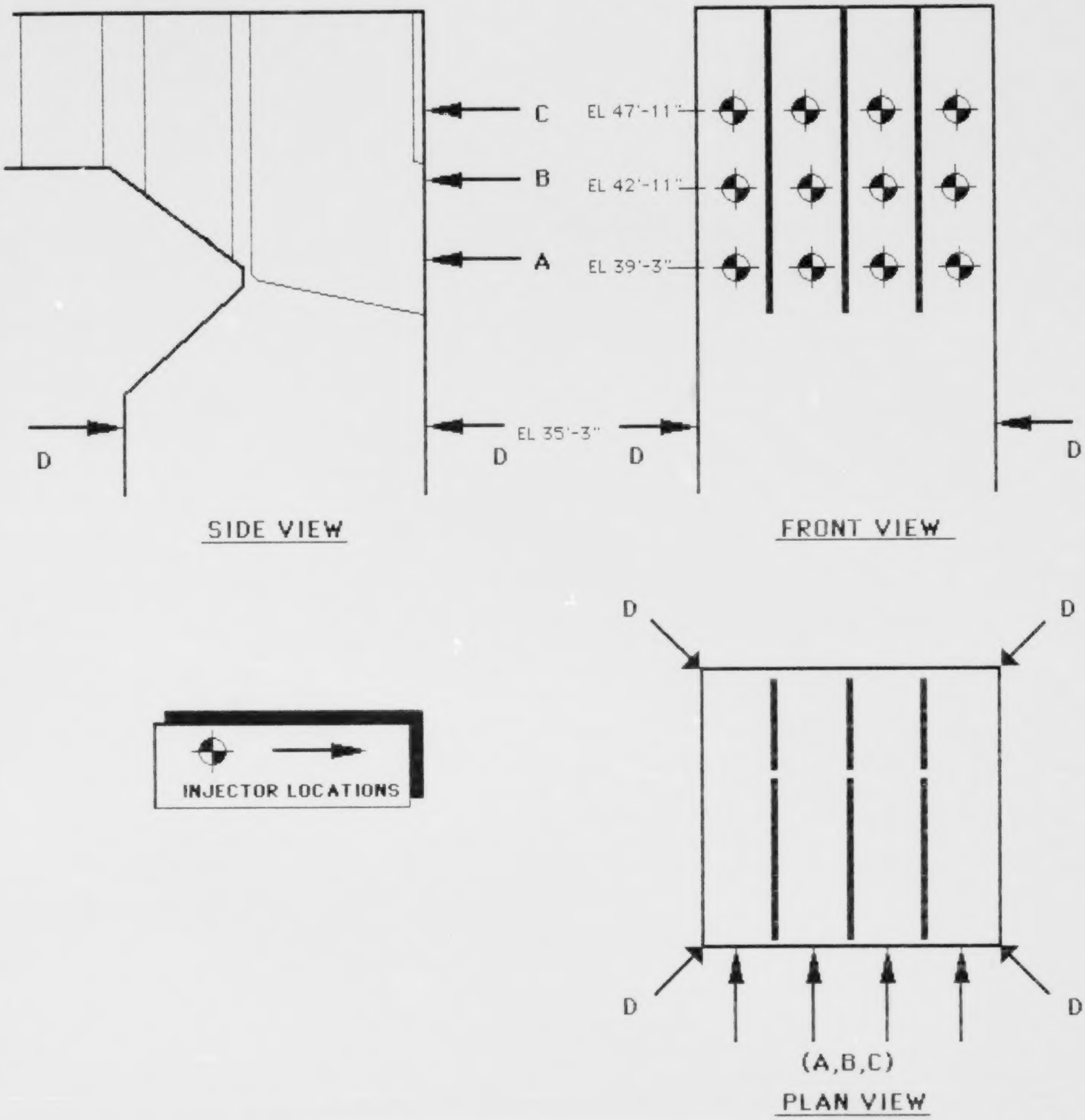
C
B
A
D
D
SIDE VIEW
EL 47'-11"
EL 42'-11"
EL 39'-3"
EL 35'-3"
D
D
FRONT VIEW
INJECTOR LOCATIONS
D
D
D
D
(A,B,C)
PLAN VIEW

Figure 6-20. Tested injector locations.

Table 6-2
PHASE I TEST MATRIX

PURPOSE	BASELINE TESTS					EFFECT OF INJECTION VARIABLES																
TEST NO.	1	2	3	4	5	6	7	8	9	10	11	12	13	14	15	16	17	18	19	20	21	22
TYPE OF COAL	A	A	A	A	A	A	A	A	A	A	A	A	A	A	A	A	A	A	A	A	A	A
FURNACE LOAD	100	100	100	100	50	100	100	100	100	100	100	100	100	100	100	100	100	100	100	100	100	100
EXCESS OXYGEN	3.5	4.25	5.5	3.5	OPT	3.5	3.5	3.5	3.5	3.5	3.5	3.5	3.5	3.5	3.5	3.5	3.5	3.5	3.5	3.5	3.5	3.5
OFA	15	15	15	0	OPT	15	15	15	15	15	15	15	15	15	15	15	15	15	15	15	15	15
BURNER TILT	0	0	0	0	0	0	0	0	0	0	0	0	0	0	0	0	0	0	0	0	0	0
SORBENT TYPE	-	-	-	-	-	A	A	A	A	A	A	A	A	A	A	A	A	A	A	A	A	A
Ca/S MOLAR RATIO	0	0	0	0	0	2:1	2:1	2:1	2:1	2:1	2:1	2:1	2:1	2:1	2:1	2:1	2:1	2:1	2:1	2:1	2:1	2:1
SORBENT INJECTION LOCATION (1)	-	-	-	-	-	A	A	A	B	B	B	B	B	B	B	C	C	C	C	C	C	REPEAT
NO. OF SORBENT INJECTORS	-	-	-	-	-	4	4	4	4	4	4	4	4	4	4	4	4	4	4	4	4	
SORBENT INJECTION VELOCITY (2)	-	-	-	-	-	75	100	150	100	75	100	150	75	100	150	75	100	150	75	100	150	
SORBENT INJECTION ANGLE (3)	-	-	-	-	-	0	0	0	0	-20	-20	-20	-45	-45	-45	-20	-20	-20	-45	-45	-45	
TEST MEASUREMENTS:																						
CO EMISSIONS	X	X	X	X	X	X	X	X	X	X	X	X	X	X	X	X	X	X	X	X	X	X
CO2 EMISSIONS	X	X	X	X	X	X	X	X	X	X	X	X	X	X	X	X	X	X	X	X	X	X
O2 EMISSIONS	X	X	X	X	X	X	X	X	X	X	X	X	X	X	X	X	X	X	X	X	X	X
SO2 EMISSIONS	X	X	X	X	X	X	X	X	X	X	X	X	X	X	X	X	X	X	X	X	X	X
NOX EMISSIONS	X	X	X	X	X	X	X	X	X	X	X	X	X	X	X	X	X	X	X	X	X	X
FURNACE OUTLET TEMPERATURE	X	X	X	X	X	X	X	X	X	X	X	X	X	X	X	X	X	X	X	X	X	X
FURNACE GAS TEMPERATURE	X	X	X	X	X	X	X	X	X	X	X	X	X	X	X	X	X	X	X	X	X	X
HEAT FLUX PROFILE	X	X	X	X	X	X	X	X	X	X	X	X	X	X	X	X	X	X	X	X	X	X
STACK SOLIDS SAMPLING	X	X	X	X	X	X	X	X	X	X	X	X	X	X	X	X	X	X	X	X	X	X
EPA 5 STACK SOLIDS SAMPLING	X	-	-	-	X	-	X	-	X	-	X	-	-	-	-	-	-	-	-	X	-	X
SULFUR CAPTURE	X	X	X	X	X	X	X	X	X	X	X	X	X	X	X	X	X	X	X	X	X	X
FURNACE OPERATING PARAMETERS	X	X	X	X	X	X	X	X	X	X	X	X	X	X	X	X	X	X	X	X	X	X
SORBENT INJECTION OPERATING PARAMETERS	X	X	X	X	X	X	X	X	X	X	X	X	X	X	X	X	X	X	X	X	X	X

(1) refer to Figure 6-20 for definition of locations
(2) sorbent injection velocity is ft/sec
(3) sorbent injection angle is degrees from axis of furnace penetration, refer to Figures 6-18 and 6-19
(4) OPT (optimum) defined qualitatively during testing

TABLE 6-3
PHASE II TEST MATRIX

PURPOSE	BASELINE TESTS		EFFECT OF INJECTION VARIABLES																	
TEST NO.	1	2	3	4	5	6	7	8	9	10	11	12	13	14	15	16	17	18	19	20
TYPE OF COAL	A	A	A	A	A	A	A	A	A	A	A	A	A	A	A	A	A	A	A	A
FURNACE LOAD	100	100	100	100	100	100	100	100	100	100	100	100	100	100	100	100	100	100	100	100
EXCESS OXYGEN	3.5	3.25	3.5	3.5	3.5	3.5	3.5	3.5	3.5	3.5	3.5	3.5	3.5	3.5	3.5	3.5	3.5	3.5	3.5	3.5
OFA	15	15	15	15	15	15	15	15	15	15	15	15	15	15	15	15	15	15	15	15
BURNER TILT	0	0	0	0	0	0	0	0	0	0	0	0	0	0	0	0	0	0	0	0
SORBENT TYPE	-	-	C	C	C	C	C	B	C	C	C	C	C	C	B	B	B	OPT	OPT	REPEAT TEST
Ca/S MOLAR RATIO	0	0	2:1	2:1	2:1	2:1	2:1	2:1	2:1	2:1	3:1	2:1	2:1	3:1	2:1	2:1	2:1	2:1	2:1	
SORBENT INJECTION LOCATION (1)	-	-	D	D	D	A	D	D	A/D	A/D	A/D	A/D	A/D	A/D	A	D	A/D	OPT	OPT	
NO. OF SORBENT INJECTORS	-	-	4	4	4	4	4	4	8	8	8	6	6	6	4	4	OPT	OPT	OPT	
SORBENT INJECTION VELOCITY (2)	-	-	100	100	100	100	150	150	OPT	OPT	OPT	OPT	OPT	OPT	100	OPT	OPT	LOW	HIGH	
SORBENT INJECTION ANGLE (3)	-	-	+45 COUNT	-45 COUNT	0 COUNT	-45	OPT D	OPT D	OPT	OPT	OPT	OPT	OPT	OPT	-45	OPT	OPT	OPT	OPT	
SORBENT CARRIER AIR FLOW	-	-	2000	2000	2000	2000	2000	2000	2000	2500	OPT	2000	2500	OPT	2000	2000	OPT	LOW	HIGH	
TEST MEASUREMENTS:																				
CO EMISSIONS	X		X	X	X	X	X	X	X	X	X	X	X	X	X	X	X	X	X	X
CO2 EMISSIONS	X		X	X	X	X	X	X	X	X	X	X	X	X	X	X	X	X	X	X
O2 EMISSIONS	X		X	X	X	X	X	X	X	X	X	X	X	X	X	X	X	X	X	X
SO2 EMISSIONS	X		X	X	X	X	X	X	X	X	X	X	X	X	X	X	X	X	X	X
NOX EMISSIONS	X		X	X	X	X	X	X	X	X	X	X	X	X	X	X	X	X	X	X
FURNACE OUTLET TEMPERATURE	X		X	X	X	X	X	X	X	X	X	X	X	X	X	X	X	X	X	X
FURNACE GAS TEMPERATURE	X		X	X	X	X	X	X	X	X	X	X	X	X	X	X	X	X	X	X
HEAT FLUX PROFILE	X		X	X	X	X	X	X	X	X	X	X	X	X	X	X	X	X	X	X
STACK SOLIDS SAMPLING	X		X	X	X	X	X	X	X	X	X	X	X	X	X	X	X	X	X	X
SULFUR CAPTURE	X		X	X	X	X	X	X	X	X	X	X	X	X	X	X	X	X	X	X
FURNACE OPERATING PARAMETERS	X		X	X	X	X	X	X	X	X	X	X	X	X	X	X	X	X	X	X
SORBENT INJECTION OPERATING PARAMETERS	X		X	X	X	X	X	X	X	X	X	X	X	X	X	X	X	X	X	X

(1) refer to Figure 6-20 for definition of locations
(2) sorbent injection velocity is in ft/sec
(3) sorbent injection angle is degrees from axis of furnace penetration, refer to Figures 6-18 and 6-19
(4) OPT (optimum) defined qualitatively during testing

6.5 COAL AND SORBENT ANALYSES

6.5.1 Coal Properties

A Pittsburgh #8 seam coal was utilized exclusively during all combustion tests. A total of about 450 tons was procured from Boich Mining Co. in Bloomingdale, Ohio. This coal had been characterized in previous EPA sorbent injection studies and was to be used in the Ohio Edison Edgewater unit demonstration.

Numerous coal samples were collected and analyzed during the course of this project. These are presented in Table 6-4. These analyses indicate that this coal is typical of a high sulfur Eastern Bituminous coal. Coal analyses were by ASTM procedures in C-E's Analytical Laboratory (See Appendix A).

The coal sulfur content on an "as received" basis was initially 2.9%. On a moisture free basis it was 3.1%. However during the course of testing the sulfur content dropped slightly due to exposure (outdoor storage). During Phase I testing it was about 3.0% and by Phase II testing, about 2.8% on a moisture free basis. This small drop should not affect SO_2 capture performance data since coal analyses specific to each test day were utilized for data analysis. The small drop in sulfur content does appear however when comparing the baseline SO_2 emissions measurements from Phases I and II. Baseline tests are defined as tests without sorbent injection.

Coal particle sizing is shown in Table 6-5 and Figures 6-21a, b, and c. All coal was prepulverized under controlled conditions in a standard C-E Raymond bowl mill and stored in silos prior to testing. Average coal particle sizing based on many samples was 70% minus 200 mesh. This grind is typical of that utilized at most power plants. On the basis of a Rosin-Rammler distribution, the mass median particle size was slightly less than 40 microns. Coal particle sizing was performed by Tyler mesh screening.

Table 6-4
PITTSBURGH #8 COAL ANALYSES
(as received)

	PRETEST SAMPLES						PRETEST
	1	2	3	4	5	6	AVE
HHV (Btu/lb)	11805.00	-	-	11755.00	-	-	11780.00
ULTIMATE ANALYSIS:							
MOISTURE %	5.40	5.80	7.80	5.80	6.60	8.80	6.70
H %	4.80	-	-	4.70	-	-	4.75
C %	66.90	-	-	67.80	-	-	67.35
S %	3.00	2.90	2.90	2.90	2.90	-	2.92
N %	1.20	-	-	1.20	-	-	1.20
O %	5.40	-	-	4.30	-	-	4.85
ASH %	13.30	11.80	13.10	13.30	11.90	12.60	12.67
TOTAL	100.00	-	-	100.00	-	-	100.00
ASH COMPOSITION (% IN ASH):							
S102	53.90	-	-	56.00	-	-	54.95
A1203	18.60	-	-	19.40	-	-	19.00
Fe203	21.50	-	-	19.80	-	-	20.65
Ca0	2.50	-	-	1.70	-	-	2.10
Mg0	0.50	-	-	0.50	-	-	0.50
Na20	TRACE	-	-	TRACE	-	-	TRACE
K20	1.10	-	-	1.30	-	-	1.20
T102	1.00	-	-	1.10	-	-	1.05
P205	NA	-	-	NA	-	-	NA
S03	1.90	-	-	1.30	-	-	1.60
TOTAL	101.00	-	-	101.20	-	-	101.10
SCREEN SIZE ANALYSIS:							
MESH SIZE							
+16	-	-	-	-	-	-	
+30	-	-	-	-	-	-	
+50	-	-	-	-	-	-	
+100	-	-	-	-	-	-	
+200	-	-	-	-	-	-	
+325	-	-	-	-	-	-	
-325	-	-	-	-	-	-	
ASH FUSIBILITY:							
I.T.(DEG F)	1900.00	-	-	1900.00	-	-	1900.00
S.T.	2050.00	-	-	2160.00	-	-	2150.00
H.T.	2160.00	-	-	2200.00	-	-	2180.00
F.T.	2200.00	-	-	2240.00	-	-	2220.00
DELTA T (FT-IT)	300.00	-	-	340.00	-	-	320.00

TABLE 6-4 (continued)
PITTSBURGH #8 COAL ANALYSES
(as received)

	PHASE I-A			PHASE I-B		PHASE I
	I-21A	I-1A	I-15	I-14E	I-15C	AVE
HHV (Btu/lb)	12395.00	12440.00	12235.00	12400.00	12300.00	12354.00
ULTIMATE ANALYSIS:						
MOISTURE %	1.20	1.40	1.30	1.50	1.60	1.40
H %	4.80	4.90	4.80	4.80	4.70	4.80
C %	69.60	69.90	69.00	69.60	69.40	69.50
S %	3.20	2.90	2.90	2.80	3.10	2.98
N %	1.40	1.40	1.40	1.30	1.30	1.36
O %	7.40	7.60	7.80	7.70	7.50	7.60
ASH %	12.40	11.90	12.80	12.30	12.40	12.36
TOTAL	100.00	100.00	100.00	100.00	100.00	100.00
ASH COMPOSITION (% IN ASH):						
S102	48.90	-	-	52.50	50.40	50.60
A1203	19.20	-	-	21.70	21.20	20.70
Fe203	25.30	-	-	21.40	25.50	24.07
Ca0	1.50	-	-	1.70	1.50	1.57
Mg0	0.60	-	-	0.60	0.60	0.60
Na20	0.40	-	-	0.20	0.40	0.33
K20	1.60	-	-	1.50	1.50	1.53
T102	1.10	-	-	0.80	0.00	0.63
P205	NA	-	-	NA	NA	0.00
S03	1.30	-	-	0.50	1.20	1.00
TOTAL	99.90	-	-	100.90	103.20	101.33
SCREEN SIZE ANALYSIS:						
MESH SIZE						
+16	0.20	0.00	0.00	0.00	0.00	0.04
+30	0.80	0.10	TRACE	0.00	0.00	0.18
+50	1.90	0.80	0.20	0.90	0.80	0.92
+100	11.30	7.30	3.90	7.20	7.70	7.48
+200	24.80	20.50	15.50	19.40	21.60	20.36
+325	15.30	15.00	13.30	15.50	15.10	14.84
-325	45.70	56.30	67.10	57.00	54.80	56.18
ASH FUSIBILITY:						
I.T.(DEG F)	-	-	-	1980.00	-	1980.00
S.T.	-	-	-	2170.00	-	2170.00
H.T.	-	-	-	2340.00	-	2340.00
F.T.	-	-	-	2450.00	-	2450.00
DELTA T (FT-IT)	-	-	-	470.00	-	470.00

TABLE 6-4 (conclusion)
PITTSBURGH #8 COAL ANALYSES
(as received)
PHASE II TEST SAMPLES

	II-24	II-30	II-PRE.	II-17	II-88	PHASE II AVE
HHV (Btu/lb)	12355.00	12330.00	12415.00	12397.00	12227.00	12344.80
ULTIMATE ANALYSIS:						
MOISTURE %	1.30	1.45	1.40	1.42	1.50	1.41
H %	4.70	-	4.50	-	-	4.60
C %	69.60	-	66.10	-	-	67.85
S %	2.90	2.74	2.70	2.69	2.70	2.75
N %	1.30	-	1.30	-	-	1.30
O %	7.90	-	12.10	-	-	10.00
ASH %	12.30	12.02	11.90	12.07	12.75	12.21
TOTAL	100.00	-	100.00	-	-	100.00
ASH COMPOSITION (% IN ASH):						
S102	47.50	-	50.30	-	-	48.90
A1203	20.40	-	21.60	-	-	21.00
Fe203	25.60	-	22.70	-	-	24.15
Ca0	1.40	-	1.40	-	-	1.40
Mg0	0.50	-	0.50	-	-	0.50
Na20	0.40	-	0.40	-	-	0.40
K20	1.30	-	1.30	-	-	1.30
T102	0.80	-	0.90	-	-	0.85
P205	NA	-	NA	-	-	0.00
S03	1.80	-	1.60	-	-	1.70
TOTAL	99.70	-	100.70	-	-	100.20
SCREEN SIZE ANALYSIS:						
MESH SIZE						
+16	0.00	-	TRACE	-	-	0.00
+30	0.20	-	0.30	-	-	0.25
+50	1.40	-	1.40	-	-	1.40
+100	9.70	-	8.80	-	-	9.25
+200	24.30	-	22.20	-	-	23.25
+325	15.20	-	15.10	-	-	15.15
-325	49.20	-	52.20	-	-	50.70
ASH FUSIBILITY:						
I.T.(DEG F)	-	-	-	-	-	-
S.T.	-	-	-	-	-	-
H.T.	-	-	-	-	-	-
F.T.	-	-	-	-	-	-
DELTA T (FT-IT)	-	-	-	-	-	-

TABLE 6-5
PITTSBURGH #8 COAL PARTICLE SIZE ANALYSES

PHASE I-A

MESH SIZE	1	3	2	AVE	MICRONS	% LESS THAN
+16	0.20	0.00	0.00	0.07	1180>	99.93
+30	0.80	TRACE	0.10	0.30	600>	99.63
+50	1.90	0.20	0.80	0.97	300>	98.67
+100	11.30	3.90	7.30	7.50	150>	91.17
+200	24.80	15.50	20.50	20.27	75>	70.90
+325	15.30	13.30	15.00	14.53	45>	56.37
-325	45.70	67.10	56.30	56.37		

PHASE I-B

MESH SIZE	27	28	AVE	MICRONS	% LESS THAN
+16	0.00	0.00	0.00	1180>	100.00
+30	0.00	0.00	0.00	600>	100.00
+50	0.90	0.80	0.85	300>	99.15
+100	7.20	7.70	7.45	150>	91.70
+200	19.40	21.60	20.50	75>	71.20
+325	15.50	15.10	15.30	45>	55.90
-325	57.00	54.80	55.90		

PHASE II

MESH SIZE	COAL PRETEST 94	COAL 24 97	AVE	MICRONS	% LESS THAN
+16	TRACE	0.00	0.00	1180>	100.00
+30	0.30	0.20	0.25	600>	99.75
+50	1.40	1.40	1.40	300>	98.35
+100	8.80	9.70	9.25	150>	89.10
+200	22.20	24.30	23.25	75>	65.85
+325	15.10	15.20	15.15	45>	50.70
-325	52.20	49.20	50.70		

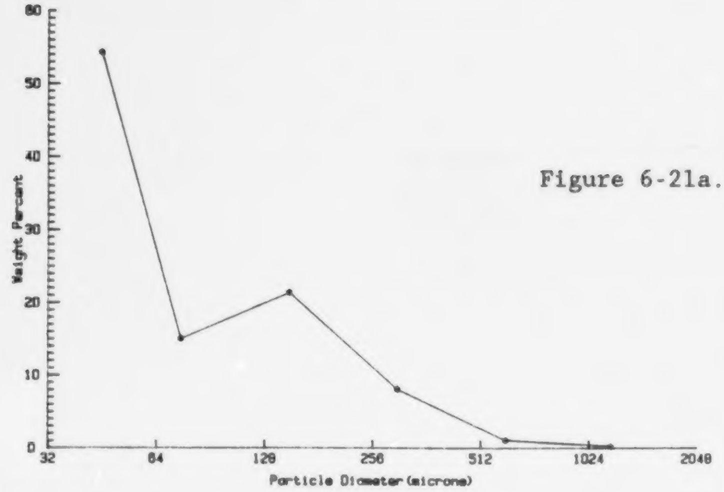

Figure 6-21a. Gaussian distribution of coal particle size data.

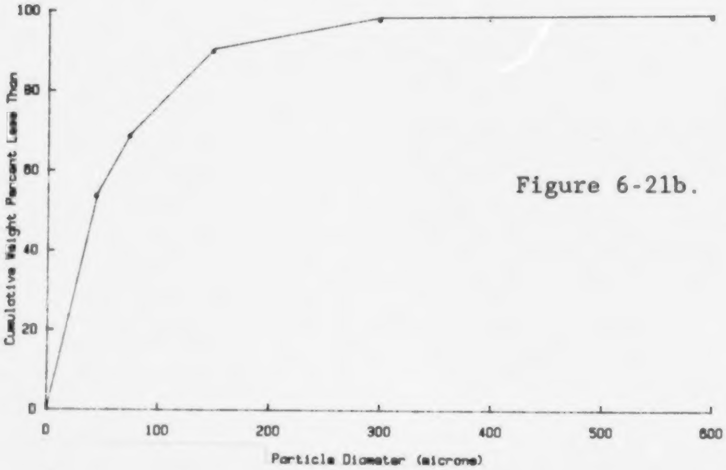

Figure 6-21b. Cumulative distribution of coal particle size data.

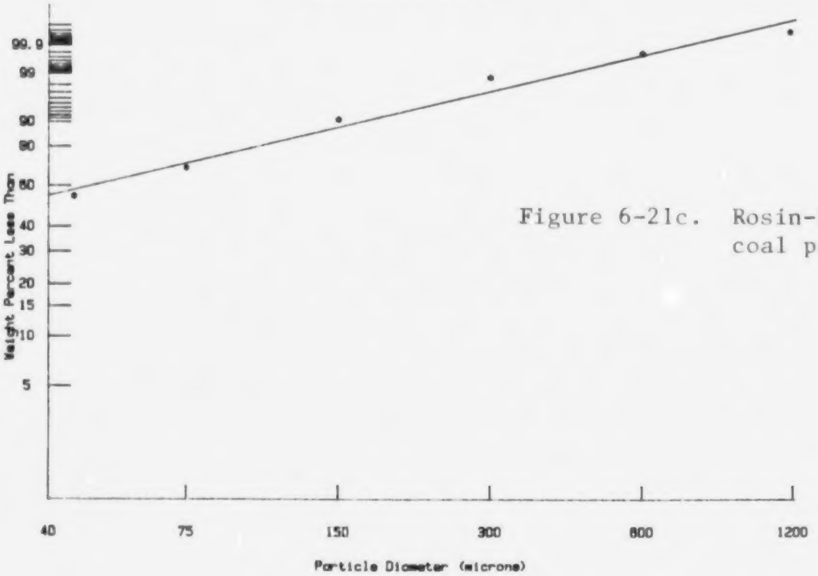

Figure 6-21c. Rosin-Rammler curve fit of coal particle size data.

6.5.2 Sorbent Properties

Three sorbents where studied during combustion testing. All were hydrated limes ($Ca(OH)_2$) and each was a candidate for use at the Ohio Edison Edgewater unit demonstration. Analyses of these sorbents are presented in Table 6-6. These sorbents will be referred to here and in the presentation of the combustion test results as Sorbents A, B, and C.

Sorbent A was an untreated hydrated lime produced by Dravo Lime Co.'s Black River facility in Carntown, Kentucky. Sorbents B and C were hydrated limes produced by Marblehead Lime Co.'s Detroit, Michigan Plant. Sorbent B was untreated. Sorbent C was treated with lignosulfonate which was added to the water of hydration during sorbent production. Lignosulfonate-modified calcium hydroxide was developed by the EPA and showed promise in small scale combustion investigations as an enhanced sorbent for SO_2 capture (Kirchgessner and Lorrain, 1987). Combustion tests presented here in C-E's Boiler Simulation Facility were the largest scale tests performed at the time. The production of lignosulfonate-modified calcium hydroxide and postulated mechanisms for enhanced SO_2 capture performance are discussed in Kirchgessner and Lorrain, 1987.

Comparison of the chemical properties of sorbents A, B, and C in Table 6-6 shows little differences. All can be characterized as high calcium hydrates. The most significant differences between the sorbents are physical. In Table 6-6 the BET apparent surface area (m^2/gm) is listed and shows average values of:

Sorbent A	12.38 m^2/gm
Sorbent B	15.85 m^2/gm
Sorbent C	11.80 m^2/gm

In general, we would assume that the greater the BET surface area, with all other factors constant, the greater the reactivity of the sorbent for SO_2 capture. Recent investigations, however, have been unable to demonstrate a correlation between surface area and SO_2 capture reactivity for hydrated limes (Gooch, et al., 1986).

TABLE 6-6
SORBENT PROPERTIES

TEST	BLACK RIVER CO. UNTREATED Ca(OH)2 (SORBENT A)					MARBLEHEAD CO. UNTREATED Ca(OH)2 (SORBENT B)			MARBLEHEAD CO. TREATED Ca(OH)2 (SORBENT C)			
	PHASE 1A SORBENTS		PHASE 1B SORBENTS			PHASE II			PHASE II			
	14B	18B	14E	30B	AVE	8B UNTREATED	10A UNTREATED	AVE	17A TREATED	24E TREATED	30C TREATED	AVE
	WEIGHT PERCENTS					WEIGHT PERCENTS			WEIGHT PERCENTS			
CALCIUM	40.20	51.10	50.30	51.00	50.40	50.50	51.00	50.75	50.60	50.90	50.60	50.70
MAGNESIUM	0.99	0.98	2.60	1.20	1.44	1.50	1.40	1.45	1.00	0.80	0.90	0.90
FREE H20	0.50	0.90	0.70	0.80	0.73	1.20	1.20	1.20	1.40	1.20	1.20	1.27
Mg(OH)2	2.40	2.40	6.20	2.90	3.48	2.50	2.30	2.40	1.60	1.30	1.50	1.47
Ca(OH)2	73.30	84.80	90.00	91.50	84.90	88.20	88.10	88.15	87.00	88.00	87.00	87.33
CaCO3	10.90	4.30	-	-	7.60	5.00	5.30	5.15	7.20	6.40	7.20	6.93
CaO	7.30	4.90	2.20	2.10	4.13	1.10	1.80	1.45	0.80	1.00	1.00	0.93
TOTAL	94.40	97.30	-	-	95.85	98.00	98.70	98.35	98.00	97.90	97.90	97.93
BET m^2/gm	11.70	12.32	12.20	13.30	12.38	15.20	16.50	15.85	11.80	12.40	11.20	11.80
L.O.I.	23.10	22.00	20.30	17.00	20.60	-	-		-	-	-	
MOISTURE	0.26	0.22	0.20	0.20	0.22	0.20	0.20	0.20	0.40	0.30	0.40	0.37
HYDROGEN	2.43	2.28	-	-	2.36	2.40	2.30	2.35	2.40	2.30	2.30	2.33
CARBON	2.45	0.40	-	-	1.43	0.40	0.50	0.45	0.90	0.70	0.90	0.83
NITROGEN	0.76	<.1	-	-	0.38	0.20	0.20	0.20	0.10	0.20	0.20	0.17
ASH	76.86	78.00	79.67	83.00	79.38	76.70	76.80	76.75	75.70	76.00	75.90	75.87
HYDROXIDE AS H20	18.50	21.30	-	-	19.90	-	-		-	-	-	
CARBONATE AS CO2	4.80	1.90	-	-	3.35	-	-		-	-	-	
ASH COMPOSITION:												
SiO2	-	-	2.50	1.20	1.85	-	-		-	-	-	
Al203	-	-	0.60	0.60	0.60	-	-		-	-	-	
Fe203	-	-	<.1	0.30	0.15	-	-		-	-	-	
Na20	-	-	<.1	<.1	0.00	-	-		-	-	-	
K20	-	-	0.10	0.10	0.10	-	-		-	-	-	
TiO2	-	-	<.1	<.1	0.00	-	-		-	-	-	
MnO	-	-	<.1	<.1	0.00	-	-		-	-	-	
S03	-	-	<.1	<.1	0.00	-	-		-	-	-	

A significant physical property of the sorbents is particle size distribution which is presented in Figures 6-22a, b, and c. Each of these plots shows a comparison of the three sorbents. Through careful review it can be noted that sorbent C is the finest, then sorbent B, and sorbent A is the coarsest. Based on a Rosin-Rammler distribution fit, the mass median particle sizes for each were:

Sorbent A	15.5 microns
Sorbent B	12.8 microns
Sorbent C	7.0 microns

All other factors being equal, one would expect enhanced SO_2 capture performance as sorbent particle size decreases (Cole, et al, 1986 and Kirchgessner, et al., 1986). There is disagreement, however, on the effect of particle size (Gooch, et al., 1986). Sorbent particle sizing reported here was measured by a granulometer. This device measures the particle size optically by analyzing a suspension of particles in acetone.

In addition to these quantitative measurements of sorbent properties, the relative handling properties of each were noted during testing. All sorbents were readily off-loaded from silos and bulk storage trucks and were also readily transported. No transfer line pluggage occurred during the project and non-uniform sorbent feed (pulsed flow) was encountered only once. This occurred with six injectors and was believed to be caused by poor sorbent flow splitting. Increased sorbent carrier air flow rate corrected the situation.

While all sorbents were handled without incident, sorbent C (the lignosulfonate-treated Marblehead hydrate) was noticeably easier to handle and feed. Most noteable was that the Acrison feeder screw speed varied little and less frequently then it did with sorbents A and B as it controlled mass feed rate.

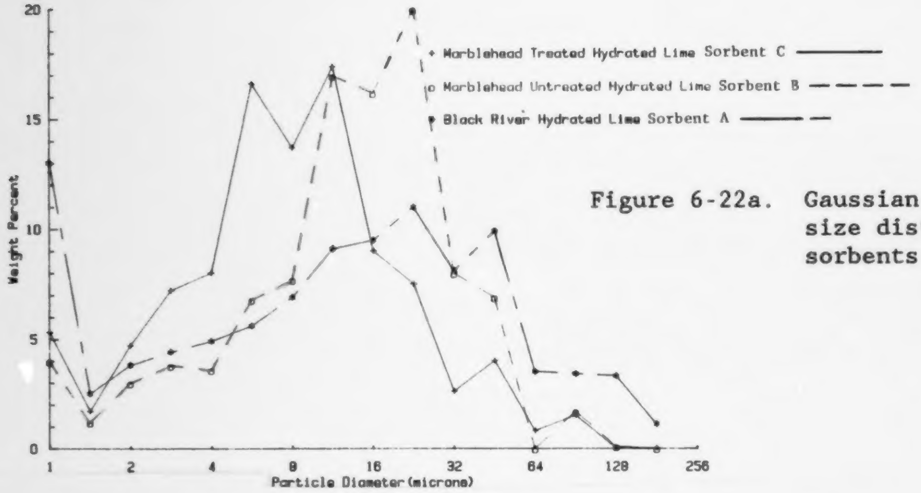

Figure 6-22a. Gaussian particle size distribution of sorbents investigated.

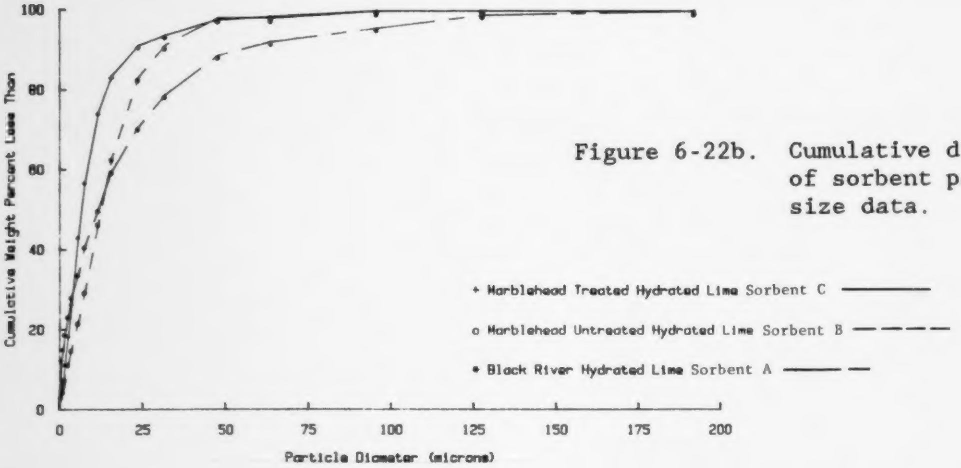

Figure 6-22b. Cumulative distribution of sorbent particle size data.

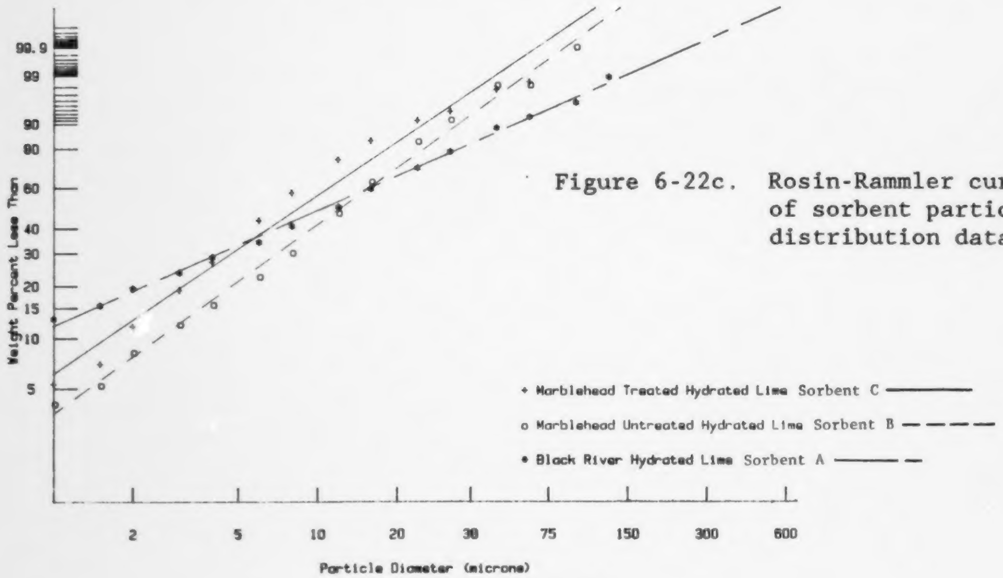

Figure 6-22c. Rosin-Rammler curve fit of sorbent particle size distribution data.

6.6 COMBUSTION TESTING RESULTS

6.6.1 Introduction

The emissions and sulfur capture results obtained during Phase I and II matrix testing are tabulated in Tables 6-7 and 6-8 respectively. A total of over one hundred and sixty (160) data points were obtained and are presented. Table 6-7 page 8, gives an explanation of the terms by which the Phase I data is presented. Table 6-8 page 14, gives the same for Phase II data presentation.

Gaseous emissions (CO_2, CO, NO_x, and SO_2) have been corrected to a constant reference level O_2 of 3% by the following formula (Steam, 1979):

example SO_2 emissions:

$$SO_2 \ @ \ 3\% \ O_2 = SO_2 \ @\text{measured} \ O_2 \left[\frac{18}{21 - O_2 \text{ measured}} \right]$$

6.6.2 Baseline Combustion Efficiency and Emissions Performance

Baseline emissions are presented here to show the representativeness of the BSF to the performance of typical C-E tangentially-fired boilers. Tests were performed to characterize the facility's combustion behavior including flame stability and operability, as well as, combustion efficiency and emissions levels of SO_2 and NO_x without sorbent injection. Another important consideration for sorbent injection performance is the location of furnace gas temperatures in the critical SO_2 capture window between 2300°F and 1600°F. Furnace gas temperature data is presented in the next section (Section 6.6.3). Combustion efficiency and emissions results from tests without sorbent injection (baseline) are discussed here.

The presence of sorbent injection carrier air was a variable during these baseline tests. The BSF was operated at nominally twenty percent (20%) excess air, or about 3.5% excess O_2. Sorbent carrier air was nominally an additional 5% of the total combustion air (2000 lbs/hr) which increased the overall excess air to twenty-six percent (26%) or about 4.5% excess O_2. Higher and

Table 6-7
TASK C COMBUSTION TEST DATA - PHASE I

PURPOSE	BASELINE TESTS							
TEST NO.	1	1	1	2	3	3	4	5
TYPE OF COAL	A	A	A	A	A	A	A	A
FURNACE LOAD	100	100	100	100	100	100	100	50
EXCESS OXYGEN	3.30	3.50	3.75	4.60	5.40	5.25	-	-
OFA	15	15	15	15	15	15	0	OPT
BURNER TILT	0	0	0	0	0	0	0	0
SORBENT TYPE	-	-	-	-	-	-	-	-
Ca/S MOLAR RATIO (NOMINAL)	0	0	0	0	0	0	0	0
SORBENT INJECTION LOCATION (1)	-	-	-	-	-	-	-	-
NO. OF SORBENT INJECTORS	-	-	-	-	-	-	-	-
INJECTOR DIA. (IN)	-	-	-	-	-	-	-	-
SORBENT INJECTION VELOCITY (2)	-	-	-	-	-	-	-	-
SORBENT INJECTION ANGLE (3)	-	-	-	-	-	-	-	-
TEST IDENTIFIER	1A	1B	1E	1D	3A	1C	-	-
DATE	3/18/87	3/18/87	4/13/87	4/13/87	4/13/87	3/18/87	-	-
TIME-HRS	1130	1207	1340	1152	1515	1343	-	-
SORBENT FEED LB/HR	0.00	0.00	0.00	0.00	0.00	0.00	-	-
SORBENT AIR LB/HR	0.00	0.00	0.00	0.00	0.00	0.00	-	-
O2 EMISSIONS, %	3.30	3.50	3.75	4.60	5.40	5.25	-	-
CO2 EMISSIONS AT 3% O2, %	14.80	14.80	15.10	15.30	15.00	15.10	-	-
CO EMISSIONS AT 3% O2, PPM	53.00	57.00	51.00	46.00	54.00	51.00	-	-
NOX EMISSIONS AT 3% O2, PPM	295.00	293.00	319.00	357.00	352.00	377.00	-	-
SO2 EMISSIONS AT 3% O2,PPM	2150.00	2110.00	2240.00	2190.00	2180.00	2030.00	-	-
CARBON CONV. BY PARTICULATE	-	-	99.71	99.88	99.76	99.88	-	-
SO2 AT 3% O2 (C)	2146.00	2109.00	2238.00	2190.00	2181.00	2035.00	-	-
AVE BASELINE SO2 (A)	2100.00	2100.00	2200.00	2200.00	2200.00	2100.00	-	-
UPDATED BASELINE SO2 (B)	-	-	-	-	-	-	-	-
CA/S RATIO (ACTUAL)	0.00	0.00	0.00	0.00	0.00	0.00	-	-
SO2 CAPTURE BY G.A.S.- A vs C	NA	NA	NA	NA	NA	NA	-	-
SO2 CAPTURE BY G.A.S.- B vs C	NA	NA	NA	NA	NA	NA	-	-
SO2 CAPTURE BY G.A.S.- NEXT B vs C	NA	NA	NA	NA	NA	NA	-	-
SO2 CAPTURE BY G.A.S.- AVERAGE	NA	NA	NA	NA	NA	NA	-	-
SO2 CAPTURE BY FLYASH BAL	NA	NA	NA	NA	NA	NA	-	-
SO2 CAPTURE BY FLYASH CA UT.	NA	NA	NA	NA	NA	NA		
CA UTILIZATION	NA	NA	NA	NA	NA	NA		
SO2 CAPTURE- OVERALL AVERAGE	0.00	0.00	0.00	0.00	0.00	0.00	-	-

Table 6-7 (continued)

TASK C COMBUSTION TEST DATA - PHASE I

PURPOSE	EFFECT OF INJECTION VARIABLES								
TEST NO.	6	6	7	8	9	10	10	11	11
TYPE OF COAL	A	A	A	A	A	A	A	A	A
FURNACE LOAD	100	100	100	100	100	100	100	100	100
EXCESS OXYGEN	3.90	3.50	-	-	-	4.05	3.60	3.85	3.30
OFA	15	15	15	15	15	15	15	15	15
BURNER TILT	0	0	0	0	0	0	0	0	0
SORBENT TYPE	A	A	A	A	A	A	A	A	A
Ca/S MOLAR RATIO (NOMINAL)	0	2:1	2:1	2:1	2:1	0	2:1	0	2:1
SORBENT INJECTION LOCATION (1)	A	A	A	A	B	B	B	B	B
NO. OF SORBENT INJECTORS	4.00	4.00	4.00	4.00	4.00	4.00	4.00	4.00	4.00
INJECTOR DIA. (IN)	2.31	2.31	1.94	1.61	1.94	2.31	2.31	1.94	1.94
SORBENT INJECTION VELOCITY (2)	62	68	100	150	100	60	66	91	87
SORBENT INJECTION ANGLE (3)	0	0	0	0	0	-20	-20	-20	-20
TEST IDENTIFIER	6A	6B	-	-	-	10A	10B	11A	11B
DATE	4/16/87	4/16/87	-	-	-	4/15/87	4/15/87	4/15/87	4/16/87
TIME-HRS	0108	0121	-	-	-	2100	2109	2345	0001
SORBENT FEED LB/HR	0.00	608.00	-	-	-	0.00	603.00	0.00	602.00
SORBENT AIR LB/HR	1980.00	2174.00	-	-	-	1924.00	2125.00	2051.00	1965.00
O2 EMISSIONS, %	3.90	3.50	-	-	-	4.05	3.60	3.85	3.30
CO2 EMISSIONS AT 3% O2, %	15.20	15.10	-	-	-	15.20	15.10	15.20	15.20
CO EMISSIONS AT 3% O2, PPM	28.00	34.00	-	-	-	37.00	38.00	34.00	43.00
NOX EMISSIONS AT 3% O2, PPM	-	-	-	-	-	-	-	-	-
SO2 EMISSIONS AT 3% O2,PPM	2150.00	1740.00	-	-	-	2090.00	1780.00	2160.00	1740.00
CARBON CONV. BY PARTICULATE	-	99.39	-	-	-	-	99.36	-	99.29
SO2 AT 3% O2 (C)	2147.00	1743.00	-	-	-	2087.00	1784.00	2157.00	1739.00
AVE BASELINE SO2 (A)	2200.00	2200.00	-	-	-	2200.00	2200.00	2200.00	2200.00
UPDATED BASELINE SO2 (B)	-	2147.00	-	-	-	-	2087.00	-	2157.00
CA/S RATIO (ACTUAL)	0.00	2.08	-	-	-	0.00	2.03	0.00	2.05
SO2 CAPTURE BY G.A.S.- A vs C	NA	20.80	-	-	-	NA	18.90	NA	21.00
SO2 CAPTURE BY G.A.S.- B vs C	NA	18.80	-	-	-	NA	14.50	NA	19.40
SO2 CAPTURE BY G.A.S.- NEXT B vs C	NA	-	-	-	-	NA	17.40	NA	19.00
SO2 CAPTURE BY G.A.S.- AVERAGE	NA	19.80	-	-	-	NA	16.90	NA	19.80
SO2 CAPTURE BY FLYASH BAL	NA	20.44	-	-	-	NA	20.38	NA	18.58
SO2 CAPTURE BY FLYASH CA UT.	NA	22.79				NA	19.05	NA	17.86
CA UTILIZATION	NA	10.97				NA	9.27	NA	8.72
SO2 CAPTURE- OVERALL AVERAGE	0.00	21.01	-	-	-	0.00	18.78	0.00	18.75

Table 6-7 (continued)
TASK C COMBUSTION TEST DATA - PHASE I

PURPOSE	EFFECT OF INJECTION VARIABLES									
TEST NO.	12	13	13	13	14	14	14	14	14	14
TYPE OF COAL	A	A	A	A	A	A	A	A	A	A
FURNACE LOAD	100	100	100	100	100	100	100	100	100	100
EXCESS OXYGEN	-	4.70	4.45	4.15	5.30	5.50	5.35	3.30	4.25	4.85
OFA	15	15	15	15	15	15	15	15	15	15
BURNER TILT	0	0	0	0	0	0	0	0	0	0
SORBENT TYPE	A	A	A	A	A	A	A	A	A	A
Ca/S MOLAR RATIO (NOMINAL)	2:1	0	2:1	2:1	2:1	0	2:1	0	0	2:1
SORBENT INJECTION LOCATION (1)	B	B	B	B	B	B	B	B	B	B
NO. OF SORBENT INJECTORS	4.00	4.00	4.00	4.00	4.00	4.00	4.00	4.00	4.00	4.00
INJECTOR DIA. (IN)	1.61	2.31	2.31	2.31	1.94	1.94	1.94	1.94	1.94	1.94
SORBENT INJECTION VELOCITY (2)	150	64	64	60	90	0	90	0	87	89
SORBENT INJECTION ANGLE (3)	-20	-45	-45	-45	-45	-45	-45	-45	-45	-45
TEST IDENTIFIER	-	13A	13B	13C	14A	14Ab	14B	14C	14D	14E
DATE	-	3/19/87	3/19/87	3/19/87	3/18/87	3/18/87	3/18/87	4/15/87	4/15/87	4/15/87
TIME-HRS	-	0535	0542	0614	1926	2013	2030	1657	1712	1716
SORBENT FEED LB/HR	-	0.00	587.00	664.00	602.00	0.00	596.00	0.00	0.00	600.00
SORBENT AIR LB/HR	-	2045.00	2043.00	1937.00	2037.00	0.00	2043.00	0.00	1975.00	2000.00
O2 EMISSIONS, %	-	4.70	4.45	4.15	5.30	5.50	5.35	3.30	4.25	4.85
CO2 EMISSIONS AT 3% O2, %	-	15.00	14.90	15.10	15.00	15.20	15.20	15.10	15.00	15.90
CO EMISSIONS AT 3% O2, PPM	-	50.00	54.00	53.00	77.00	60.00	75.00	38.00	42.00	48.00
NOX EMISSIONS AT 3% O2, PPM	-	337.00	321.00	310.00	355.00	372.00	357.00	-	-	-
SO2 EMISSIONS AT 3% O2,PPM	-	2090.00	1750.00	1730.00	1650.00	2250.00	1660.00	2120.00	2100.00	1770.00
CARBON CONV. BY PARTICULATE	-	-	99.25	99.36	99.27	-	-	-	-	99.36
SO2 AT 3% O2 (C)	-	2087.00	1746.00	1731.00	1651.00	2253.00	1656.00	2120.00	2096.00	1772.00
AVE BASELINE SO2 (A)	-	2100.00	2100.00	2100.00	2100.00	2100.00	2100.00	2200.00	2200.00	2200.00
UPDATED BASELINE SO2 (B)	-	-	2087.00	2087.00	2253.00	-	2253.00	-	-	2096.00
CA/S RATIO (ACTUAL)	-	0.00	1.94	2.19	1.74	0.00	1.90	0.00	0.00	2.03
SO2 CAPTURE BY G.A.S.- A vs C	-	NA	16.90	17.60	21.40	NA	21.10	NA	NA	19.50
SO2 CAPTURE BY G.A.S.- B vs C	-	NA	16.30	17.10	26.70	NA	26.50	NA	NA	15.50
SO2 CAPTURE BY G.A.S.- NEXT B vs C	-	NA	15.10	15.80	25.50	NA	25.20	NA	NA	14.60
SO2 CAPTURE BY G.A.S.- AVERAGE	-	NA	16.10	16.80	24.50	NA	24.30	NA	NA	16.50
SO2 CAPTURE BY FLYASH BAL	-	NA	16.17	20.71	18.96	NA	-	NA	NA	19.34
SO2 CAPTURE BY FLYASH CA UT.		NA	19.14	25.13	20.78	NA	-	NA	NA	22.05
CA UTILIZATION		NA	9.85	11.50	11.97	NA	-	NA	NA	10.87
SO2 CAPTURE- OVERALL AVERAGE	-	0.00	17.14	20.88	21.41	0.00	24.30	0.00	0.00	19.30

Table 6-7 (continued)

TASK C COMBUSTION TEST DATA - PHASE I

PURPOSE	EFFECT OF INJECTION VARIABLES								
TEST NO.	15	15	15	15	15	15	15	15	15
TYPE OF COAL	A	A	A	A	A	A	A	A	A
FURNACE LOAD	100	100	100	100	100	100	100	100	100
EXCESS OXYGEN	5.15	4.85	4.65	4.30	4.25	-	3.20	4.00	3.65
OFA	15	15	15	15	15	15	15	15	15
BURNER TILT	0	0	0	0	0	0	0	0	0
SORBENT TYPE	A	A	A	A	A	A	A	A	A
Ca/S MOLAR RATIO (NOMINAL)	0	0	2:1	2:1	0	2:1	0	0	2:1
SORBENT INJECTION LOCATION (1)	B	B	B	B	B	B	B	B	B
NO. OF SORBENT INJECTORS	4.00	4.00	4.00	4.00	4.00	4.00	4.00	4.00	4.00
INJECTOR DIA. (IN)	1.61	1.61	1.61	1.61	1.61	1.61	1.61	1.61	1.61
SORBENT INJECTION VELOCITY (2)	131	0	131	128	0	130	0	75	125
SORBENT INJECTION ANGLE (3)	-45	-45	-45	-45	-45	-45	-45	-45	-45
TEST IDENTIFIER	15A	15AA	15B	15C	15Cb2	15C2	15D1	15D2	15D3
DATE	3/19/87	3/19/87	3/19/87	3/19/87	4/13/87	4/13/87	4/15/87	4/15/87	4/15/87
TIME-HRS	0236	0350	0400	0422	1411	1411	1224	1231	1237
SORBENT FEED LB/HR	0.00	OFF	598.00	602.00	OFF	574.00	OFF	0.00	593.00
SORBENT AIR LB/HR	2032.00	OFF	2031.00	1987.00	OFF	2024.00	OFF	1172.00	1948.00
O2 EMISSIONS, %	5.15	4.85	4.65	4.30	4.25	-	3.20	4.00	3.65
CO2 EMISSIONS AT 3% O2, %	15.10	15.10	15.00	14.90	15.00	-	15.30	15.30	15.20
CO EMISSIONS AT 3% O2, PPM	51.00	50.00	57.00	54.00	53.00	-	43.00	46.00	54.00
NOX EMISSIONS AT 3% O2, PPM	352.00	340.00	325.00	307.00	306.00	-	-	-	-
SO2 EMISSIONS AT 3% O2,PPM	2140.00	2120.00	1680.00	1680.00	2220.00	-	2200.00	2190.00	1760.00
CARBON CONV. BY PARTICULATE	-	-	99.01	-	-	-	-	-	-
SO2 AT 3% O2 (C)	2135.00	2123.00	1684.00	1681.00	2224.00	-	2199.00	2192.00	1759.00
AVE BASELINE SO2 (A)	2100.00	2100.00	2100.00	2100.00	2200.00	-	2200.00	2200.00	2200.00
UPDATED BASELINE SO2 (B)	-	-	2123.00	2123.00	-	-	-	-	2192.00
CA/S RATIO (ACTUAL)	0.00	0.00	1.98	1.94	0.00	-	0.00	0.00	2.02
SO2 CAPTURE BY G.A.S.- A vs C	NA	NA	19.80	20.00	NA	-	NA	NA	20.00
SO2 CAPTURE BY G.A.S.- B vs C	NA	NA	20.70	20.80	NA	-	NA	NA	19.80
SO2 CAPTURE BY G.A.S.- NEXT B vs C	NA	NA	19.30	19.50	NA	-	NA	NA	20.30
SO2 CAPTURE BY G.A.S.- AVERAGE	NA	NA	19.90	20.10	NA	-	NA	NA	20.00
SO2 CAPTURE BY FLYASH BAL	NA	NA	15.67	-	NA	-	NA	NA	-
SO2 CAPTURE BY FLYASH CA UT.	NA	NA	17.71	-	NA		NA	NA	-
CA UTILIZATION	NA	NA	8.96	-	NA		NA	NA	-
SO2 CAPTURE- OVERALL AVERAGE	0.00	0.00	17.76	20.10	0.00	-	0.00	0.00	20.00

Table 6-7 (continued)

TASK C COMBUSTION TEST DATA - PHASE I

PURPOSE	EFFECT OF INJECTION VARAIBLES								
TEST NO.	16	17	18	18	18	18	19	19	19
TYPE OF COAL	A	A	A	A	A	A	A	A	A
FURNACE LOAD	100	100	100	100	100	100	100	100	100
EXCESS OXYGEN	-	-	5.25	5.00	4.75	4.45	5.15	5.05	5.05
OFA	15	15	15	15	15	15	15	15	15
BURNER TILT	0	0	0	0	0	0	0	0	0
SORBENT TYPE	A	A	A	A	A	A	A	A	A
Ca/S MOLAR RATIO (NOMINAL)	2:1	2:1	0	2:1	0	3:1	0	2:1	2:1
SORBENT INJECTION LOCATION (1)	C	C	C	C	C	C	C	C	C
NO. OF SORBENT INJECTORS	4.00	4.00	4.00	4.00	4.00	4.00	4.00	4.00	4.00
INJECTOR DIA. (IN)	2.31	1.94	1.61	1.61	1.61	1.61	2.31	2.31	2.31
SORBENT INJECTION VELOCITY (2)	75	100	136	130	0	129	0	60	60
SORBENT INJECTION ANGLE (3)	-20	-20	-20	-20	-20	-20	-45	-45	-45
TEST IDENTIFIER	-	-	18A1	18A2	18B1	18B2	19A	19B	19C
DATE	-	-	3/19/87	3/19/87	3/19/87	3/19/87	3/18/87	3/18/87	3/19/87
TIME-HRS	-	-	0800	0830	0852	0855	2328	2333	0008
SORBENT FEED LB/HR	-	-	0.00	599.00	OFF	890.00	OFF	584.00	600.00
SORBENT AIR LB/HR	-	-	2116.00	2017.00	OFF	2010.00	OFF	1924.00	1911.00
O2 EMISSIONS, %	-	-	5.25	5.00	4.75	4.45	5.15	5.05	5.05
CO2 EMISSIONS AT 3% O2, %	-	-	15.10	15.00	15.00	14.80	15.10	15.00	15.60
CO EMISSIONS AT 3% O2, PPM	-	-	54.00	59.00	55.00	60.00	53.00	85.00	72.00
NOX EMISSIONS AT 3% O2, PPM	-	-	371.00	366.00	349.00	332.00	352.00	344.00	360.00
SO2 EMISSIONS AT 3% O2,PPM	-	-	2060.00	1840.00	2040.00	1750.00	2220.00	1930.00	1930.00
CARBON CONV. BY PARTICULATE	-	-	-	99.07	-	98.81	-	99.08	-
SO2 AT 3% O2 (C)	-	-	2057.00	1839.00	2044.00	1746.00	2215.00	1930.00	1930.00
AVE BASELINE SO2 (A)	-	-	2100.00	2100.00	2100.00	2100.00	2100.00	2100.00	2100.00
UPDATED BASELINE SO2 (B)	-	-	-	2057.00	-	2044.00	-	2215.00	2215.00
CA/S RATIO (ACTUAL)	-	-	0.00	1.99	0.00	2.94	0.00	1.69	1.92
SO2 CAPTURE BY G.A.S.- A vs C	-	-	NA	12.40	NA	16.90	NA	8.10	8.10
SO2 CAPTURE BY G.A.S.- B vs C	-	-	NA	10.60	NA	14.60	NA	12.90	12.90
SO2 CAPTURE BY G.A.S.- NEXT B vs C	-	-	NA	10.00	NA	-	NA	9.10	9.10
SO2 CAPTURE BY G.A.S.- AVERAGE	-	-	NA	11.00	NA	15.80	NA	10.00	10.00
SO2 CAPTURE BY FLYASH BAL	-	-	NA	13.32	NA	15.30	NA	14.62	-
SO2 CAPTURE BY FLYASH CA UT.			NA	13.36	NA	17.62	NA	15.81	-
CA UTILIZATION			NA	6.72	NA	5.99	NA	9.35	-
SO2 CAPTURE- OVERALL AVERAGE	-	-	0.00	12.56	0.00	16.24	0.00	13.48	10.00

Table 6-7 (continued)
TASK C COMBUSTION TEST DATA - PHASE I

PURPOSE	EFFECT OF INJECTION VARIABLES					EXTRA TESTS		
TEST NO.	20	20	21	21	22	23	24	
TYPE OF COAL	A	A	A	A	A	A	A	A
FURNACE LOAD	100	100	100	100	100	50	100	100
EXCESS OXYGEN	4.00	3.65	4.20	4.30	P	-	4.15	3.75
OFA	15	15	15	15	15	15	15	15
BURNER TILT	0	0	0	0	0	0	0	0
SORBENT TYPE	A	A	A	A	A	A	A	A
Ca/S MOLAR RATIO (NOMINAL)	0	2:1	2:1	0	2:1	2:1	0	2:1
SORBENT INJECTION LOCATION (1)	C	C	C	C		OPT (4)	A	A
NO. OF SORBENT INJECTORS	4.00	4.00	4.00	4.00		4	4.00	4.00
INJECTOR DIA. (IN)	1.94	1.94	1.61	1.61			1.94	1.94
SORBENT INJECTION VELOCITY (2)	91	88	126	0		OPT (4)	86	104
SORBENT INJECTION ANGLE (3)	-45	-45	-45	-45		OPT (4)	+45	+45
TEST IDENTIFIER	20A	20B	21A	21B	S	-	24A	24B
DATE	4/15/87	4/15/87	3/18/87	3/18/87	E	-	4/15/87	4/15/87
TIME-HRS	2204	2217	1725	1745	E	-	1520	1531
SORBENT FEED LB/HR	0.00	600.00	593.00	OFF		-	0.00	593.00
SORBENT AIR LB/HR	2066.00	1986.00	1953.60	OFF	R	-	1952.00	2354.00
					E			
O2 EMISSIONS, %	4.00	3.65	4.20	4.30	P	-	4.15	3.75
CO2 EMISSIONS AT 3% O2, %	15.00	15.20	15.00	15.10	E	-	15.20	14.90
CO EMISSIONS AT 3% O2, PPM	37.00	42.00	118.00	54.00	A	-	43.00	49.00
NOX EMISSIONS AT 3% O2, PPM	-	-	295.00	296.00	T	-	-	-
SO2 EMISSIONS AT 3% O2,PPM	2160.00	1880.00	1880.00	2250.00	S	-	2200.00	1860.00
CARBON CONV. BY PARTICULATE	-	98.98	98.80	-		-	-	98.93
SO2 AT 3% O2 (C)	2160.00	1883.00	1875.00	2253.00		-	2195.00	1863.00
AVE BASELINE SO2 (A)	2200.00	2200.00	2100.00	2100.00		-	2200.00	2200.00
UPDATED BASELINE SO2 (B)	-	2160.00	2253.00	-		-	-	2195.00
CA/S RATIO (ACTUAL)	0.00	2.03	1.72	0.00		-	0.00	2.06
SO2 CAPTURE BY G.A.S.- A vs C	NA	14.40	10.70	NA		-	NA	15.30
SO2 CAPTURE BY G.A.S.- B vs C	NA	12.80	16.80	NA		-	NA	15.10
SO2 CAPTURE BY G.A.S.- NEXT B vs C	NA	12.70	16.80	NA		-	NA	11.10
SO2 CAPTURE BY G.A.S.- AVERAGE	NA	13.30	14.80	NA			NA	13.80
SO2 CAPTURE BY FLYASH BAL	NA	16.35	13.07	NA		-	NA	13.70
SO2 CAPTURE BY FLYASH CA UT.	NA	14.34	16.81	NA			NA	13.49
CA UTILIZATION	NA	7.05	9.79	NA			NA	6.53
SO2 CAPTURE- OVERALL AVERAGE	0.00	14.66	14.89	0.00		-	0.00	13.66

Table 6-7 (continued)
TASK C COMBUSTION TEST DATA - PHASE I

PURPOSE	EXTRA INJECTION TEST						
TEST NO.	25	25	26	26	26	26	26
TYPE OF COAL	A	A	A	A	A	A	A
FURNACE LOAD	100	100	100	100	100	100	100
EXCESS OXYGEN	4.25	3.80	3.60	3.95	3.60	4.00	3.35
OFA	15	15	15	15	15	15	15
BURNER TILT	0	0	0	0	0	0	0
SORBENT TYPE	A	A	A	A	A	A	A
Ca/S MOLAR RATIO (NOMINAL)	0	2:1	2:1	0	3:1	0	4:1
SORBENT INJECTION LOCATION (1)	A	A	A	A	A	A	A
NO. OF SORBENT INJECTORS	4.00	4.00	4.00	4.00	4.00	4.00	4.00
INJECTOR DIA. (IN)	1.94	1.94	1.61	1.61	1.61	1.61	1.61
SORBENT INJECTION VELOCITY (2)	89	113	151	119	129	129	119
SORBENT INJECTION ANGLE (3)	-45	-45	-45	-45	-45	-45	-45
TEST IDENTIFIER	25Ab	25A	26A	26Ab	26B	26Bb	26C
DATE	4/15/87	4/15/87	4/15/87	4/15/87	4/15/87	4/15/87	4/15/87
TIME-HRS	1325	1338	1823	1800	1907	1900	1920
SORBENT FEED LB/HR	0.00	544.00	540.00	0.00	889.00	0.00	1202.00
SORBENT AIR LB/HR	2000.00	2554.00	2352.00	1850.00	2000.00	2000.00	1850.00
O2 EMISSIONS, %	4.25	3.80	3.60	3.95	3.60	4.00	3.35
CO2 EMISSIONS AT 3% O2, %	15.20	15.10	14.90	15.00	15.00	15.10	15.00
CO EMISSIONS AT 3% O2, PPM	48.00	54.00	47.00	42.00	48.00	-	48.00
NOX EMISSIONS AT 3% O2, PPM	-	-	-	-	-	-	-
SO2 EMISSIONS AT 3% O2,PPM	2210.00	1490.00	1470.00	2070.00	1240.00	2080.00	1030.00
CARBON CONV. BY PARTICULATE	-	99.43	99.57	-	99.63	-	-
SO2 AT 3% O2 (C)	2055.00	1491.00	1474.00	2074.00	1241.00	2081.00	1025.00
AVE BASELINE SO2 (A)	2200.00	2200.00	2200.00	2200.00	2200.00	2200.00	2200.00
UPDATED BASELINE SO2 (B)	-	2208.00	2074.00	-	2081.00	-	2081.00
CA/S RATIO (ACTUAL)	0.00	1.85	1.84	0.00	3.01	0.00	4.11
SO2 CAPTURE BY G.A.S.- A vs C	NA	32.20	33.00	NA	43.60	NA	53.40
SO2 CAPTURE BY G.A.S.- B vs C	NA	32.50	28.90	NA	40.40	NA	50.70
SO2 CAPTURE BY G.A.S.- NEXT B vs C	NA	32.10	29.20	NA	40.40	NA	50.90
SO2 CAPTURE BY G.A.S.- AVERAGE	NA	32.30	30.40	NA	41.50	NA	51.70
SO2 CAPTURE BY FLYASH BAL	NA	28.24	26.40	NA	36.30	NA	-
SO2 CAPTURE BY FLYASH CA UT.	NA	26.04	22.86	NA	34.55	NA	-
CA UTILIZATION	NA	14.07	12.42	NA	11.49	NA	-
SO2 CAPTURE- OVERALL AVERAGE	0.00	28.86	26.55	0.00	37.45	0.00	51.70

Table 6-7 (concluded)
TASK C COMBUSTION TEST DATA - PHASE I

PURPOSE	EXPLANATIONS OF DATA PRESENTATION
TEST NO.	AS SPECIFIED IN TEST MATRIX
TYPE OF COAL	PITTS. # 8 FOR ALL PHASE I TESTS
FURNACE LOAD	100% FOR ALL PHASE I
EXCESS OXYGEN	@STACK
OFA	% THROUGH OVERFIRE AIR PORTS
BURNER TILT	DEGREES FROM HORIZONTAL
SORBENT TYPE	DRAVO BLACK RIVER HYDRATE - PHASE I
Ca/S MOLAR RATIO (NOMINAL)	-
SORBENT INJECTION LOCATION (1)	SEE ATTACHED FIGURE
NO. OF SORBENT INJECTORS	FOUR AT GIVEN INJECTION LEVEL FOR PHASE I
INJECTOR DIA. (IN)	
SORBENT INJECTION VELOCITY (2)	SPECIFIED IN FT/SEC.
SORBENT INJECTION ANGLE (3)	DEGREES FROM HORIZONTAL
TEST IDENTIFIER	SPECIFIC TO EACH TEST RUN
DATE	-
TIME-HRS	-
SORBENT FEED LB/HR	ZERO IS A BASELINE TEST
SORBENT AIR LB/HR	AIR WAS ON DURING SOME BASELINE TESTS
O_2 EMISSIONS, %	@STACK
CO_2 EMISSIONS AT 3% O_2, %	CORRECTED EMISSIONS @STACK
CO EMISSIONS AT 3% O_2, PPM	CORRECTED EMISSIONS @STACK
NOX EMISSIONS AT 3% O_2, PPM	CORRECTED EMISSIONS @STACK
SO_2 EMISSIONS AT 3% O_2,PPM	CORRECTED EMISSIONS @STACK
CARBON CONV. BY PARTICULATE	% CARBON BURNOUT
SO_2 AT 3% O_2 (C)	SO_2 @ GIVEN TEST
AVE BASELINE SO_2 (A)	SO_2 MEASURED DURING INITIAL BASELINE TESTS
UPDATED BASELINE SO_2 (B)	SO_2 MEASURED BEFORE SORBENT TURNED ON FOR GIVEN TEST
CA/S RATIO (ACTUAL)	FROM MEASURED FEED RATES
SO_2 CAPTURE BY G.A.S.- A vs C	% SO_2 REMOVAL COMPARING AVE. BASELINE SO_2 (A) VS. C
SO_2 CAPTURE BY G.A.S.- B vs C	% SO_2 REMOVAL COMPARING UPDATED SO_2 (B) vs. C
SO_2 CAPTURE BY G.A.S.- NEXT B vs C	% SO_2 REMOVAL COMPARING THE NEXT TEST'S B TO C
SO_2 CAPTURE BY G.A.S.- AVERAGE	AVE. OF THREE SO_2 CAPTURE RESULTS BY G.A.S. ABOVE
SO_2 CAPTURE BY FLYASH BAL	% SO_2 REMOVAL MEASURED BY FLYASH ANALYSIS; S MASS BALANCE
SO_2 CAPTURE BY FLYASH CA UT.	% SO_2 REMOVAL MEASURED BY FLYASH CA UTILIZATION
CA UTILIZATION	% UTILIZATION OF CA FOR S CAPTURE BY FLYASH ANALYSIS
SO_2 CAPTURE- OVERALL AVERAGE	AVE. OF % SO_2 REMOVAL BY FLYASHS MASS BALANCE, CA UTILIZATION AND G.A.S.

Table 6-8
TASK C COMBUSTION TEST DATA - PHASE II

PURPOSE	BASELINE TESTS					
TEST NO.	1	1	1	1	1	1
TYPE OF COAL	A	A	A	A	A	A
FURNACE LOAD	100	100	100	100	100	100
EXCESS OXYGEN	3.5	3.6	2.75	3.5	3.6	3.6
OFA	15	15	15	15	15	15
BURNER TILT	0	0	0	0	0	0
SORBENT TYPE	NA	NA	NA	NA	NA	NA
Ca/S MOLAR RATIO (NOMINAL)	0	0	0	0	0	0
SORBENT INJECTION LOCATION (1)	NA	NA	NA	NA	A	A
NO. OF SORBENT INJECTORS	NA	NA	NA	NA	4.00	4.00
INJECTOR DIA. (IN.)	NA	NA	NA	NA	1.61	1.61
SORBENT INJECTION VELOCITY (2)	NA	NA	NA	NA	199	199
SORBENT INJECTION ANGLE (3)	NA	NA	NA	NA	-90	-90
TEST IDENTIFIER	1F	1G	1H	1I	1J	1K
DATE	7/14/87	7/14/87	7/14/87	7/14/87	7/17/87	7/17/87
TIME -HRS	0430	0900	1000	1048	0450	0500
SORBENT FEED (LB/HR)	0.00	0.00	0.00	0.00	0.00	0.00
SORBENT AIR (LB/HR)	0.00	0.00	0.00	0.00	3096.00	3098.00
O2 EMISSIONS, %	3.50	3.50	2.75	3.50	3.60	3.60
CO2 EMISSIONS AT 3% O2, %	16.05	15.22	15.26	15.16	15.56	15.51
CO EMISSIONS AT 3% O2, PPM	54.54	46.38	47.64	47.18	44.92	44.71
NOX EMISSIONS AT 3% O2, PPM	319.00	316.00	296.00	319.00	250.00	250.00
SO2 EMISSIONS AT 3% O2,PPM	1929.00	1986.00	2042.00	2006.00	1860.00	1860.00
CARBON CONV. BY PARTICULATE	-	99.69	-	-	-	-
AVG BASELINE SO2 (A) 3%O2	1983.00	1983.00	1983.00	1983.00	1983.00	1983.00
UPDATED BASELINE SO2 (B) 3%O2	2055.00	2042.00	2006.00	1946.00	1861.00	NA
BASELINE SO2 PRIOR (C) 3%O2	NA	2077.00	1986.00	2042.00	1945.00	1945.00
CA/S RATIO (ACTUAL)	0.00	0.00	0.00	0.00	0.00	0.00
SO2 CAPTURE BY G.A.S.- A vs C	NA	NA	NA	NA	NA	NA
SO2 CAPTURE BY G.A.S.- B vs C	NA	NA	NA	NA	NA	NA
SO2 CAPTURE BY G.A.S.-PRIOR B vs C	NA	NA	NA	NA	NA	NA
SO2 CAPTURE BY G.A.S.- AVERAGE	NA	NA	NA	NA	NA	NA
SO2 CAPTURE BY FLYASH CA UT.	NA	NA	NA	NA	NA	NA
PERCENT CA UTILIZATION	NA	NA	NA	NA	NA	NA
SO2 CAPTURE- OVERALL AVERAGE	0.00	0.00	0.00	0.00	0.00	0.00

Table 6-8 (continued)

TASK C COMBUSTION TEST DATA - PHASE II

PURPOSE	EFFECT OF INJECTION VARIABLES						
TEST NO.	6	6	7	7	7	7	7
TYPE OF COAL	A	A	A	A	A	A	A
FURNACE LOAD	100	100	100	100	100	100	100
EXCESS OXYGEN	4.1	4.2	4.0	4.1	3.8	4.0	3.8
OFA	15	15	15	15	15	15	15
BURNER TILT	0	0	0	0	0	0	0
SORBENT TYPE	-	B	C	C	C	C	C
Ca/S MOLAR RATIO (NOMINAL)	0	2:1	0	0	2:1	2:1	3:1
SORBENT INJECTION LOCATION (1)	A	A	A	A	A	A	A
NO. OF SORBENT INJECTORS	4.00	4.00	4.00	4.00	4.00	4.00	4.00
INJECTOR DIA. (IN.)	1.94	1.94	1.94	1.94	1.94	1.94	1.94
SORBENT INJECTION VELOCITY (2)	87	90	103	103	102	102	103
SORBENT INJECTION ANGLE (3)	-45	-45	-45	-45	-45	-45	-45
TEST IDENTIFIER	6A1	6A2	7A1	7A2	7B1	7B2	7C
DATE	7/14/87	7/14/87	7/14/87	7/14/87	7/14/87	7/14/87	7/14/87
TIME -HRS	1849	1851	0540	0540	0550	0550	0621
SORBENT FEED (LB/HR)	0.00	601.43	0.00	0.00	599.04	599.04	902.05
SORBENT AIR (LB/HR)	1961.00	2031.00	2320.00	2320.00	2313.00	2313.00	2318.00
O2 EMISSIONS, %	4.10	4.20	4.00	4.10	3.80	4.00	3.80
CO2 EMISSIONS AT 3% O2, %	15.20	15.22	15.18	-	15.26	-	15.23
CO EMISSIONS AT 3% O2, PPM	41.87	45.39	50.36	-	55.74	-	57.42
NOX EMISSIONS AT 3% O2, PPM	309.00	311.00	303.00	303.00	302.00	302.00	-
SO2 EMISSIONS AT 3% O2,PPM	1997.00	1334.00	2033.00	2077.00	1130.00	1270.00	942.00
CARBON CONV. BY PARTICULATE	-	-	-	-	-	-	-
AVG BASELINE SO2 (A) 3%O2	1983.00	1983.00	1983.00	1983.00	1983.00	1983.00	1983.00
UPDATED BASELINE SO2 (B) 3%O2	1938.00	1938.00	1986.00	1986.00	1986.00	1986.00	1986.00
BASELINE SO2 PRIOR (C) 3%O2	1973.00	1997.00	1929.00	2033.00	2077.00	2077.00	2077.00
CA/S RATIO (ACTUAL)	0.00	2.14	0.00	0.00	2.10	2.10	3.15
SO2 CAPTURE BY G.A.S.- A vs C	NA	32.73	NA	NA	43.02	35.96	52.50
SO2 CAPTURE BY G.A.S.- B vs C	NA	31.17	NA	NA	43.10	36.05	52.57
SO2 CAPTURE BY G.A.S.-PRIOR B vs C	NA	33.20	NA	NA	45.59	38.85	54.65
SO2 CAPTURE BY G.A.S.- AVERAGE	NA	32.36	NA	NA	43.90	36.95	53.24
SO2 CAPTURE BY FLYASH CA UT.	NA	33.11	NA	NA	-	-	-
PERCENT CA UTILIZATION	NA	15.47	NA	NA	-	-	-
SO2 CAPTURE- OVERALL AVERAGE	0.00	32.74	0.00	0.00	43.90	36.95	53.24

Table 6-8 (continued)
TASK C COMBUSTION TEST DATA - PHASE II

PURPOSE	EFFECT OF INJECTION VARIABLES										
TEST NO.	8	8	8	8	9	9	9	9	9	10	10
TYPE OF COAL	A	A	A	A	A	A	A	A	A	A	A
FURNACE LOAD	100	100	100	100	100	100	100	100	100	100	100
EXCESS OXYGEN	3.6	3.6	4.1	3.9	4.0	4.0	3.7	3.65	3.5	4.3	4.25
OFA	15	15	15	15	15	15	15	15	15	15	15
BURNER TILT	0	0	0	0	0	0	0	0	0	0	0
SORBENT TYPE	-	B	-	B	-	C	-	C	C	-	B
Ca/S MOLAR RATIO (NOMINAL)	0	2:1	0	2:1	0	2:1	0	2:1	3:1	0	2:1
SORBENT INJECTION LOCATION (1)	A	A	A	A	A	A	A	A	A	D	D
NO. OF SORBENT INJECTORS	4.00	4.00	4.00	4.00	4.00	4.00	4.00	4.00	4.00	4.00	4.00
INJECTOR DIA. (IN.)	1.61	1.61	1.61	1.61	1.61	1.61	1.61	1.61	1.61	1.94	1.94
SORBENT INJECTION VELOCITY (2)	143	143	213	209	223	222	145	144	145	90	88
SORBENT INJECTION ANGLE (3)	-45	-45	-45	-45	-45	-45	-45	-45	-45	+45	+45
										COUNTER	COUNTER
TEST IDENTIFIER	8A	8B	8C	8D	9A	9B	9C	9D	9E	10A1	10A2
DATE	7/15/87	7/15/87	7/15/87	7/15/87	7/15/87	7/15/87	7/15/87	7/15/87	7/15/87	7/14/87	7/14/87
TIME -HRS	0431	0438	0454	0517	0242	0245	0319	0325	0350	1730	0350
SORBENT FEED (LB/HR)	0.00	605.60	0.00	606.11	0.00	604.25	0.00	604.85	901.45	0.00	607.66
SORBENT AIR (LB/HR)	2224.00	2229.00	3317.00	3243.00	3466.00	3457.00	2249.00	2241.00	2252.00	2025.00	1991.00
O2 EMISSIONS, %	3.60	3.60	4.10	3.90	4.00	4.00	3.70	3.65	3.50	4.30	4.25
CO2 EMISSIONS AT 3% O2, %	15.35	15.40	15.39	15.40	15.27	15.30	15.32	15.35	15.29	15.27	15.24
CO EMISSIONS AT 3% O2, PPM	41.40	46.33	41.40	48.06	44.76	47.14	40.92	46.77	48.66	41.75	46.56
NOX EMISSIONS AT 3% O2, PPM	259.00	259.00	243.00	247.00	270.00	270.00	265.00	265.00	262.00	318.00	317.00
SO2 EMISSIONS AT 3% O2,PPM	1924.00	1241.00	1924.00	1295.00	1938.00	1144.00	1945.00	1183.00	833.00	1973.00	1386.00
CARBON CONV. BY PARTICULATE	-	99.68	-	-	-	-	-	99.70	-	-	99.55
AVG BASELINE SO2 (A) 3%O2	1983.00	1983.00	1983.00	1983.00	1983.00	1983.00	1983.00	1983.00	1983.00	1983.00	1983.00
UPDATED BASELINE SO2 (B) 3%O2	1924.00	1924.00	NA	NA	1945.00	1945.00	1924.00	1924.00	1924.00	1997.00	1997.00
BASELINE SO2 PRIOR (C) 3%O2	1945.00	1924.00	1924.00	1924.00	NA	1938.00	1938.00	1945.00	1945.00	1996.00	1973.00
CA/S RATIO (ACTUAL)	0.00	2.16	0.00	2.16	0.00	2.16	0.00	2.14	3.15	0.00	2.14
SO2 CAPTURE BY G.A.S.- A vs C	NA	37.42	NA	34.69	NA	42.31	NA	40.34	57.99	NA	30.11
SO2 CAPTURE BY G.A.S.- B vs C	NA	35.50	NA	-	NA	41.18	NA	38.51	56.70	NA	30.60
SO2 CAPTURE BY G.A.S.-PRIOR B vs C	NA	35.50	NA	32.69	NA	40.97	NA	39.18	57.17	NA	29.75
SO2 CAPTURE BY G.A.S.- AVERAGE	NA	36.14	NA	33.69	NA	41.49	NA	39.34	57.29	NA	30.15
SO2 CAPTURE BY FLYASH CA UT.	NA	32.12	NA	-	NA	37.83	NA	34.33	-	NA	30.04
PERCENT CA UTILIZATION	NA	14.86	NA	-	NA	17.51	NA	16.07	-	NA	14.04
SO2 CAPTURE- OVERALL AVERAGE	0.00	34.13	0.00	33.69	0.00	39.66	0.00	36.84	57.29	0.00	30.10

Table 6-8 (continued)
TASK C COMBUSTION TEST DATA - PHASE II

PURPOSE	EFFECT OF INJECTION VARIABLES									
TEST NO.	11	11	11	11	11	13	13	13	13	13
TYPE OF COAL	A	A	A	A	A	A	A	A	A	A
FURNACE LOAD	100	100	100	100	100	100	100	100	100	100
EXCESS OXYGEN	4.5	4.5	4.5	4.5	4.5	4.5	4.35	4.2	4.2	4.25
OFA	15	15	15	15	15	15	15	15	15	15
BURNER TILT	0	0	0	0	0	0	0	0	0	0
SORBENT TYPE	-	C	C	C	C	-	C	-	C	C
Ca/S MOLAR RATIO (NOMINAL)	0	2:1	2:1	3:1	4:1	0	2:1	0	2:1	2:1
SORBENT INJECTION LOCATION (1)	D	D	D	D	D	D	D	D	D	D
NO. OF SORBENT INJECTORS	4.00	4.00	4.00	4.00	4.00	4.00	4.00	4.00	4.00	4.00
INJECTOR DIA. (IN.)	1.94	1.94	1.94	1.94	1.94	1.94	1.94	1.94	1.94	1.94
SORBENT INJECTION VELOCITY (2)	87	90	90	89	89	86	89	109	110	130
SORBENT INJECTION ANGLE (3)	-45	-45	-45	-45	-45	+45	+45	+45	+45	+45
	COUNTER	COUNTER	COUNTER	COUNTER	COUNTER	COUNTER	COUNTER	COUNTER	COUNTER	COUNTER
TEST IDENTIFIER	11A1	11A2	11A3	11B	11C	13A1	13A2	13B1	13B2	13C
DATE	7/14/87	7/14/87	7/14/87	7/14/87	7/14/87	7/14/87	7/14/87	7/14/87	7/14/87	7/14/87
TIME -HRS	1516	1528	1528	1405	1416	1345	1348	1415	1422	1444
SORBENT FEED (LB/HR)	0.00	602.71	602.71	900.00	1200.00	0.00	604.83	0.00	604.57	605.27
SORBENT AIR (LB/HR)	1959.00	2037.00	2037.00	2000.00	2000.00	1938.00	2014.00	2467.00	2482.00	2946.00
O2 EMISSIONS, %	4.50	4.50	4.50	4.50	4.50	4.50	4.35	4.20	4.20	4.25
CO2 EMISSIONS AT 3% O2, %	15.12	15.14	-	-	-	15.14	15.20	15.14	15.15	15.02
CO EMISSIONS AT 3% O2, PPM	46.82	52.23	-	-	-	41.18	46.34	44.14	50.62	52.93
NOX EMISSIONS AT 3% O2, PPM	338.00	338.00	338.00	338.00	338.00	322.00	319.00	311.00	311.00	312.00
SO2 EMISSIONS AT 3% O2,PPM	1996.00	1472.00	1407.00	1244.00	998.00	1964.00	1297.00	1929.00	1286.00	1225.00
CARBON CONV. BY PARTICULATE	-	-	-	-	-	-	99.68	-	-	-
AVG BASELINE SO2 (A) 3%O2	1983.00	1983.00	1983.00	1983.00	1983.00	1983.00	1983.00	1983.00	1983.00	1983.00
UPDATED BASELINE SO2 (B) 3%O2	1973.00	1973.00	1973.00	1973.00	1973.00	1929.00	1929.00	1996.00	1996.00	1996.00
BASELINE SO2 PRIOR (C) 3%O2	1929.00	1996.00	1996.00	1996.00	1996.00	1946.00	1964.00	1964.00	1929.00	1929.00
CA/S RATIO (ACTUAL)	0.00	2.14	2.14	3.20	4.26	0.00	2.14	0.00	2.12	2.12
SO2 CAPTURE BY G.A.S.- A vs C	NA	25.77	29.05	37.27	49.67	NA	34.59	NA	35.15	38.22
SO2 CAPTURE BY G.A.S.- B vs C	NA	25.39	28.69	36.95	49.42	NA	32.76	NA	35.57	38.63
SO2 CAPTURE BY G.A.S.-PRIOR B vs C	NA	26.25	29.51	37.68	50.00	NA	33.96	NA	33.33	36.50
SO2 CAPTURE BY G.A.S.- AVERAGE	NA	25.80	29.08	37.30	49.70	NA	33.77	NA	34.68	37.78
SO2 CAPTURE BY FLYASH CA UT.	NA	26.37	-	-	-	NA	30.95	NA	30.96	-
PERCENT CA UTILIZATION	NA	12.35	-	-	-	NA	14.46	NA	14.58	-
SO2 CAPTURE- OVERALL AVERAGE	0.00	26.09	29.08	37.30	49.70	0.00	32.36	0.00	32.82	37.78

Table 6-8 (continued)

TASK C COMBUSTION TEST DATA - PHASE II

PURPOSE	EFFECT OF INJECTION VARAIBLES									
TEST NO.	14	14	14	14	14	15	15	15	15	15
TYPE OF COAL	A	A	A	A	A	A	A	A	A	A
FURNACE LOAD	100	100	100	100	100	100	100	100	100	100
EXCESS OXYGEN	4.15	4.1	4.1	4.4	4.4	4.0	4.0	4.6	4.65	4.6
OFA	15	15	15	15	15	15	15	15	15	15
BURNER TILT	0	0	0	0	0	0	0	0	0	0
SORBENT TYPE	-	C	C	-	C	-	C	-	C	C
Ca/S MOLAR RATIO (NOMINAL)	0	2:1	2:1	0	2:1	0	2:1	0	2:1	2:1
SORBENT INJECTION LOCATION (1)	D	D	D	D	D	D	D	D	D	D
NO. OF SORBENT INJECTORS	4.00	4.00	4.00	4.00	4.00	4.00	4.00	4.00	4.00	4.00
INJECTOR DIA. (IN.)	1.61	1.61	1.61	1.61	1.61	1.61	1.61	1.61	1.61	1.61
SORBENT INJECTION VELOCITY (2)	138	139	139	196	196	129	136	223	206	206
SORBENT INJECTION ANGLE (3)	+45	+45	+45	+45	+45	+45	+45	+45	+45	+45
	COUNTER	COUNTER	COUNTER	COUNTER	COUNTER					
TEST IDENTIFIER	14A	14B1	14B2	14C	14D	15E	15F	15G	15H1	15H2
DATE	7/14/87	7/14/87	7/14/87	7/14/87	7/14/87	7/14/87	7/15/87	7/15/87	7/15/87	7/15/87
TIME -HRS	2135	2143	2143	2225	2232	2331	2400	0034	0038	0125
SORBENT FEED (LB/HR)	0.00	605.84	605.84	0.00	605.53	0.00	604.60	0.00	600.00	600.00
SORBENT AIR (LB/HR)	2149.00	2157.00	2157.00	3053.00	3046.00	2000.00	2112.00	3466.00	3200.00	3200.00
O2 EMISSIONS, %	4.15	4.10	4.10	4.40	4.40	4.00	4.20	4.60	4.65	4.60
CO2 EMISSIONS AT 3% O2, %	15.30	15.43	-	15.43	15.49	15.58	15.66	15.63	-	-
CO EMISSIONS AT 3% O2, PPM	43.15	48.12	-	42.71	46.28	40.47	44.99	39.69	-	-
NOX EMISSIONS AT 3% O2, PPM	310.00	309.00	309.00	304.00	304.00	307.00	307.00	291.00	292.00	291.00
SO2 EMISSIONS AT 3% O2,PPM	1955.00	1374.00	1278.00	1952.00	1193.00	1906.00	1189.00	1877.00	1040.00	922.00
CARBON CONV. BY PARTICULATE	-	-	-	-	-	-	-	-	99.60	99.73
AVG BASELINE SO2 (A) 3%O2	1983.00	1983.00	1983.00	1983.00	1983.00	1983.00	1983.00	1983.00	1983.00	1983.00
UPDATED BASELINE SO2 (B) 3%O2	1952.00	1952.00	1952.00	1906.00	1906.00	1877.00	1877.00	1938.00	1938.00	1938.00
BASELINE SO2 PRIOR (C) 3%O2	1938.00	1955.00	1955.00	1955.00	1952.00	1952.00	1906.00	1906.00	1877.00	1877.00
CA/S RATIO (ACTUAL)	0.00	2.13	2.13	0.00	2.13	0.00	2.12	0.00	2.09	2.09
SO2 CAPTURE BY G.A.S.- A vs C	NA	30.71	35.55	NA	39.84	NA	40.04	NA	47.55	53.50
SO2 CAPTURE BY G.A.S.- B vs C	NA	29.61	34.53	NA	37.41	NA	36.65	NA	46.34	52.43
SO2 CAPTURE BY G.A.S.-PRIOR B vs C	NA	29.72	34.63	NA	38.88	NA	37.62	NA	44.59	50.88
SO2 CAPTURE BY G.A.S.- AVERAGE	NA	30.01	34.90	NA	38.71	NA	38.10	NA	46.16	52.27
SO2 CAPTURE BY FLYASH CA UT.	NA	34.29	34.29	NA	58.84	NA	32.62	NA	38.54	37.44
PERCENT CA UTILIZATION	NA	16.13	16.13	NA	27.66	NA	15.42	NA	18.40	17.87
SO2 CAPTURE- OVERALL AVERAGE	0.00	32.15	34.60	0.00	48.78	0.00	35.36	0.00	42.35	44.85

Table 6-8 (continued)
TASK C COMBUSTION TEST DATA - PHASE II

PURPOSE	EFFECT OF INJECTION VARAIBLES									
TEST NO.	17	17	17	17	19	19	24	24	24	24
TYPE OF COAL	A	A	A	A	A	A	A	A	A	A
FURNACE LOAD	100	100	100	100	100	100	100	100	100	100
EXCESS OXYGEN	4.35	4.0	4.6	4.6	4.0		4.1	4.0	4.0	4.2
OFA	15	15	15	15	15	15	15	15	15	15
BURNER TILT	0	0	0	0	0	0	0	0	0	0
SORBENT TYPE	-	C	C	C	-	C	-	C	C	-
Ca/S MOLAR RATIO (NOMINAL)	0	2:1	2:1	2:1	0	2:1	0	2:1	2:1	0
SORBENT INJECTION LOCATION (1)	D	D	D	D	D	D	A,D	A,D	A,D	A,D
NO. OF SORBENT INJECTORS	4.00	4.00	4.00	4.00	4.00	4.00	8.00	8.00	8.00	8.00
INJECTOR DIA. (IN.)	1.94	1.94	1.94	1.94	1.61	1.61	1.16	1.16	1.16	1.16
SORBENT INJECTION VELOCITY (2)	88	76	111	111	139	140	135	133	133	159
SORBENT INJECTION ANGLE (3)	0	0	0	0	0	0	-45,+45	-45,+45	-45,+45	-45,+45
	COUNTER	COUNTER	COUNTER	COUNTER	COUNTER	COUNTER				
TEST IDENTIFIER	17A1	17A2	17B1	17B2	19A	19B	24A	24B1	24B2	24C1
DATE	7/14/87	7/14/87	7/14/87	7/14/87	7/14/87	7/14/87	7/16/87	7/16/87	7/16/87	7/16/87
TIME -HRS	1135	1141	1216	1216	2038	2051.00	0630	0639	0639	0900
SORBENT FEED (LB/HR)	0.00	605.90	618.57	618.57	0.00	609.58	0.00	592.12	592.12	0.00
SORBENT AIR (LB/HR)	1989.00	1725.00	2499.00	2499.00	2161.00	2177.00	2188.00	2152.00	2152.00	2571.00
O2 EMISSIONS, %	4.35	4.00	4.60	4.60	4.00	4.00	4.10	4.00	4.00	4.20
CO2 EMISSIONS AT 3% O2, %	15.19	15.13	15.11	-	15.43	15.33	15.23	15.23	-	15.29
CO EMISSIONS AT 3% O2, PPM	50.24	52.42	55.84	-	44.32	51.54	45.83	56.31	-	44.71
NOX EMISSIONS AT 3% O2, PPM	314.00	312.00	318.00	318.00	307.00	307.00	300.00	295.00	295.00	285.00
SO2 EMISSIONS AT 3% O2,PPM	1946.00	1509.00	1317.00	1482.00	1938.00	1429.00	2080.00	1175.00	953.00	2075.00
CARBON CONV. BY PARTICULATE	-	-	-	-	-	-	-	99.72	-	-
AVG BASELINE SO2 (A) 3%O2	1983.00	1983.00	1983.00	1983.00	1983.00	1983.00	1983.00	1983.00	1983.00	1983.00
UPDATED BASELINE SO2 (B) 3%O2	1964.00	1964.00	1964.00	1964.00	1955.00	1955.00	2075.00	2075.00	2075.00	2025.00
BASELINE SO2 PRIOR (C) 3%O2	2006.00	1946.00	1946.00	1946.00	1997.00	1938.00	1924.00	2080.00	2080.00	2080.00
CA/S RATIO (ACTUAL)	0.00	2.15	2.18	2.18	0.00	2.15	0.00	2.09	2.09	0.00
SO2 CAPTURE BY G.A.S.- A vs C	NA	23.90	33.59	25.26	NA	27.94	NA	40.75	51.94	NA
SO2 CAPTURE BY G.A.S.- B vs C	NA	23.17	32.94	24.54	NA	26.91	NA	43.37	54.07	NA
SO2 CAPTURE BY G.A.S.-PRIOR B vs C	NA	22.46	32.32	23.84	NA	26.26	NA	43.51	54.18	NA
SO2 CAPTURE BY G.A.S.- AVERAGE	NA	23.18	32.95	24.55	NA	27.04	NA	42.54	53.40	NA
SO2 CAPTURE BY FLYASH CA UT.	NA	-	-	-	NA	38.53	NA	33.38	-	NA
PERCENT CA UTILIZATION	NA	-	-	-	NA	17.88	NA	15.98	-	NA
SO2 CAPTURE- OVERALL AVERAGE	0.00	23.18	32.95	24.55	0.00	32.78	0.00	37.96	53.40	0.00

Table 6-8 (continued)

TASK C COMBUSTION TEST DATA - PHASE II

PURPOSE	EFFECT OF INJECTION VARAIBLES										
TEST NO.	24	24	24	24	24	24	24	24	24	24	24
TYPE OF COAL	A	A	A	A	A	A	A	A	A	A	A
FURNACE LOAD	100	100	100	100	100	100	100	100	100	100	100
EXCESS OXYGEN	4.0	4.0	4.2	4.0	4.0	3.7	3.5	3.8	4.1	4.0	4.0
OFA	15	15	15	15	15	15	15	15	15	15	15
BURNER TILT	0	0	0	0	0	0	0	0	0	0	0
SORBENT TYPE	C	C	-	C	C	-	C	C	-	C	C
Ca/S MOLAR RATIO (NOMINAL)	2:1	2:1	0	2:1	2:1	0	2:1	2:1	0	2:1	2:1
SORBENT INJECTION LOCATION (1)	A,D	A,D	A,D	A,D	A,D	A,D	A,D	A,D	A,D	A,D	A,D
NO. OF SORBENT INJECTORS	8.00	8.00	8.00	8.00	8.00	8.00	8.00	8.00	8.00	8.00	8.00
INJECTOR DIA. (IN.)	1.16	1.16	1.16	1.16	1.16	1.16	1.16	1.16	1.16	1.16	1.16
SORBENT INJECTION VELOCITY (2)	157	157	186	186	186	125	124	124	157	157	157
SORBENT INJECTION ANGLE (3)	-45,+45	-45,+45	-45,+45	-45,+45	-45,+45	-45,+45	-45,+45	-45,+45	-45,+45	-45,+45	-45,+45
TEST IDENTIFIER	24C2	24C3	24D1	24D2	24D3	24E1	24E2	24E3	24F1	24F2	24F3
DATE	7/16/87	7/16/87	7/16/87	7/16/87	7/16/87	7/16/87	7/16/87	7/16/87	7/16/87	7/16/87	7/16/87
TIME -HRS	0905	0905	942.00	0946	0946	1545	1550	1550	1719	1722	1722
SORBENT FEED (LB/HR)	602.82	602.82	0.00	600.52	600.52	0.00	602.19	602.19	0.00	602.50	602.50
SORBENT AIR (LB/HR)	2533.00	2533.00	2997.00	3001.00	3001.00	2023.00	2009.00	2009.00	2537.00	2537.00	2537.00
O2 EMISSIONS, %	4.00	4.00	4.20	4.00	4.00	3.70	3.50	3.80	4.10	4.00	4.00
CO2 EMISSIONS AT 3% O2, %	15.11	-	15.17	15.07	-	15.13	15.16	-	15.11	15.17	-
CO EMISSIONS AT 3% O2, PPM	50.12	-	43.37	52.37	-	43.34	53.86	-	45.94	52.65	-
NOX EMISSIONS AT 3% O2, PPM	285.00	285.00	285.00	280.00	280.00	285.00	285.00	300.00	305.00	295.00	295.00
SO2 EMISSIONS AT 3% O2,PPM	1175.00	1110.00	2025.00	1145.00	1110.00	2125.00	1398.00	1162.00	2075.00	1335.00	1270.00
CARBON CONV. BY PARTICULATE	-	-	-	-	-	-	-	-	-	-	-
AVG BASELINE SO2 (A) 3%O2	1983.00	1983.00	1983.00	1983.00	1983.00	1983.00	1983.00	1983.00	1983.00	1983.00	1983.00
UPDATED BASELINE SO2 (B) 3%O2	2025.00	2025.00	2035.00	2035.00	2035.00	2075.00	2075.00	2075.00	2110.00	2110.00	2110.00
BASELINE SO2 PRIOR (C) 3%O2	2075.00	2075.00	2075.00	2025.00	2025.00	2095.00	2125.00	2125.00	2125.00	2075.00	2075.00
CA/S RATIO (ACTUAL)	2.13	2.13	0.00	2.11	2.11	0.00	2.12	2.12	0.00	2.13	2.13
SO2 CAPTURE BY G.A.S.- A vs C	40.75	44.02	NA	42.26	44.02	NA	29.50	41.40	NA	32.68	35.96
SO2 CAPTURE BY G.A.S.- B vs C	41.98	45.19	NA	43.73	45.45	NA	32.63	44.00	NA	36.73	39.81
SO2 CAPTURE BY G.A.S.-PRIOR B vs C	43.37	46.51	NA	43.46	45.19	NA	34.21	45.32	NA	35.66	38.80
SO2 CAPTURE BY G.A.S.- AVERAGE	42.03	45.24	NA	43.15	44.89	NA	32.11	43.57	NA	35.02	38.19
SO2 CAPTURE BY FLYASH CA UT.	-	-	NA	37.85	-	NA	-	-	NA	-	-
PERCENT CA UTILIZATION	-	-	NA	17.93	-	NA	-	-	NA	-	-
SO2 CAPTURE- OVERALL AVERAGE	42.03	45.24	0.00	40.50	44.89	0.00	32.11	43.57	0.00	35.02	38.19

Table 6-8 (continued)

TASK C COMBUSTION TEST DATA - PHASE II

PURPOSE	EFFECT OF INJECTION VARAIBLES										
TEST NO.	25	25	25	25	25	25	26	26	26	26	26
TYPE OF COAL	A	A	A	A	A	A	A	A	A	A	A
FURNACE LOAD	100	100	100	100	100	100	100	100	100	100	100
EXCESS OXYGEN	4.3	4.4	4.4	4.8	4.6	4.6	4.4	4.0	4.4	4.2	4.2
OFA	15	15	15	15	15	15	15	15	15	15	15
BURNER TILT	0	0	0	0	0	0	0	0	0	0	0
SORBENT TYPE	-	C	C	-	C	C	-	C	-	C	C
Ca/S MOLAR RATIO (NOMINAL)	0	2:1	2:1	0	2:1	2:1	0	2:1	0	2:1	2:1
SORBENT INJECTION LOCATION (1)	A,D	A,D	A,D	A,D	A,D	A,D	A,D	A,D	A,D	A,D	A,D
NO. OF SORBENT INJECTORS	6.00	6.00	6.00	6.00	6.00	6.00	6.00	6.00	6.00	6.00	6.00
INJECTOR DIA. (IN.)	1.16	1.16	1.16	1.16	1.16	1.16	1.16	1.16	1.16	1.16	1.16
SORBENT INJECTION VELOCITY (2)	167	166	166	248	247	247	165	165	252	248	248
SORBENT INJECTION ANGLE (3)	-45INR2 +45ALL4	-45INR2 +45ALL4	-45INR2 +45ALL4	-45INR2 +45ALL4	-45INR2 +45ALL4	-45INR2 +45ALL4	-45OUT2 +45ALL4	-45OUT2 +45ALL4	-45OUT2 +45ALL4	-45OUT2 +45ALL4	-45OUT2 +45ALL4
TEST IDENTIFIER	25A1	25A2	25A3	25B1	25B2	25B3	26A	26B	26C1	26C2	26C3
DATE	7/16/87	7/16/87	7/16/87	7/16/87	7/16/87	7/16/87	7/16/87	7/16/87	7/16/87	7/16/87	7/16/87
TIME -HRS	1048	1053	1053	1123	1128	1128	1223	1228	1255	1258	1258
SORBENT FEED (LB/HR)	0.00	600.52	600.52	0.00	599.93	599.93	0.00	599.73	0.00	600.51	600.51
SORBENT AIR (LB/HR)	2017.00	2016.00	2016.00	3009.00	2997.00	2997.00	2004.00	2002.00	3050.00	3005.00	3005.00
O2 EMISSIONS, %	4.30	4.40	4.40	4.80	4.60	4.60	4.40	4.00	4.40	4.20	4.20
CO2 EMISSIONS AT 3% O2, %	15.14	15.12	-	15.09	15.12	-	15.26	15.28	15.29	15.34	-
CO EMISSIONS AT 3% O2, PPM	45.86	49.22	-	48.13	54.70	-	47.21	52.38	45.42	52.55	-
NOX EMISSIONS AT 3% O2, PPM	295.00	300.00	300.00	295.00	290.00	290.00	300.00	290.00	275.00	275.00	275.00
SO2 EMISSIONS AT 3% O2,PPM	2035.00	1270.00	1205.00	1950.00	1085.00	1055.00	2015.00	1240.00	1980.00	1125.00	1095.00
CARBON CONV. BY PARTICULATE	-	-	-	-	-	-	-	-	-	-	-
AVG BASELINE SO2 (A) 3%O2	1983.00	1983.00	1983.00	1983.00	1983.00	1983.00	1983.00	1983.00	1983.00	1983.00	1983.00
UPDATED BASELINE SO2 (B) 3%O2	1950.00	1950.00	1950.00	2015.00	2015.00	2015.00	1950.00	1950.00	2150.00	2150.00	2150.00
BASELINE SO2 PRIOR (C) 3%O2	2025.00	2035.00	2035.00	2035.00	1950.00	1950.00	1950.00	2015.00	2015.00	1980.00	1980.00
CA/S RATIO (ACTUAL)	0.00	2.14	2.14	0.00	2.11	2.11	0.00	2.11	0.00	2.12	2.12
SO2 CAPTURE BY G.A.S.- A vs C	NA	35.96	39.23	NA	45.28	46.80	NA	37.47	NA	43.27	44.78
SO2 CAPTURE BY G.A.S.- B vs C	NA	34.87	38.21	NA	46.15	47.64	NA	36.41	NA	47.67	49.07
SO2 CAPTURE BY G.A.S.-PRIOR B vs C	NA	37.59	40.79	NA	44.36	45.90	NA	38.46	NA	43.18	44.70
SO2 CAPTURE BY G.A.S.- AVERAGE	NA	36.14	39.41	NA	45.27	46.78	NA	37.45	NA	44.71	46.18
SO2 CAPTURE BY FLYASH CA UT.	NA	35.40	-	NA	36.40	-	NA	-	NA	-	-
PERCENT CA UTILIZATION	NA	16.56	-	NA	17.25	-	NA	-	NA	-	-
SO2 CAPTURE- OVERALL AVERAGE	0.00	36.14	39.41	0.00	40.83	46.78	0.00	37.45	0.00	44.71	46.18

Table 6-8 (continued)

TASK C COMBUSTION TEST DATA - PHASE II

PURPOSE	EFFECT OF INJECTION VARAIBLES				
TEST NO.	27	27	27	27	27
TYPE OF COAL	A	A	A	A	A
FURNACE LOAD	100	100	100	100	100
EXCESS OXYGEN	3.9	3.6	3.6	4.1	3.9
OFA	15	15	15	15	15
BURNER TILT	0	0	0	0	0
SORBENT TYPE	-	C	C	-	C
Ca/S MOLAR RATIO (NOMINAL)	0	2:1	2:1	0	2:1
SORBENT INJECTION LOCATION (1)	A,D	A,D	A,D	A,D	A,D
NO. OF SORBENT INJECTORS	6.00	6.00	6.00	6.00	6.00
INJECTOR DIA. (IN.)	1.16	1.16	1.16	1.16	1.16
SORBENT INJECTION VELOCITY (2)	164	164	164	251	250
SORBENT INJECTION ANGLE (3)	-45 (4), +45 (2)	-45 (4), +45 (2)	-45 (4), +45 (2)	-45 (4), +45 (2)	-45 (4), +45 (2)
TEST IDENTIFIER	27A1	27A2	27A3	27B1	27B2
DATE	7/16/87	7/16/87	7/16/87	7/16/87	7/16/87
TIME -HRS	1354	1400	1412	1423	1429
SORBENT FEED (LB/HR)	0.00	599.53	599.53	0.00	600.22
SORBENT AIR (LB/HR)	1984.00	1988.00	1988.00	3038.00	3026.00
O2 EMISSIONS, %	3.90	3.60	3.65	4.10	3.90
CO2 EMISSIONS AT 3% O2, %	15.32	15.30	-	15.34	15.32
CO EMISSIONS AT 3% O2, PPM	46.34	53.03	-	44.15	54.19
NOX EMISSIONS AT 3% O2, PPM	295.00	285.00	285.00	275.00	280.00
SO2 EMISSIONS AT 3% O2,PPM	2150.00	1490.00	1320.00	2095.00	1295.00
CARBON CONV. BY PARTICULATE	-	-	-	-	-
AVG BASELINE SO2 (A) 3%O2	1983.00	1983.00	1983.00	1983.00	1983.00
UPDATED BASELINE SO2 (B) 3%O2	2095.00	2095.00	2095.00	2125.00	2125.00
BASELINE SO2 PRIOR (C) 3%O2	1980.00	2150.00	2150.00	2150.00	2095.00
CA/S RATIO (ACTUAL)	0.00	2.11	2.11	0.00	2.14
SO2 CAPTURE BY G.A.S.- A vs C	NA	24.86	33.43	NA	34.69
SO2 CAPTURE BY G.A.S.- B vs C	NA	28.88	36.99	NA	39.06
SO2 CAPTURE BY G.A.S.-PRIOR B vs C	NA	30.70	38.60	NA	38.19
SO2 CAPTURE BY G.A.S.- AVERAGE	NA	28.15	36.34	NA	37.31
SO2 CAPTURE BY FLYASH CA UT.	NA	-	-	NA	-
PERCENT CA UTILIZATION	NA	-	-	NA	-
SO2 CAPTURE- OVERALL AVERAGE	0.00	28.15	36.34	0.00	37.31

Table 6-8 (continued)

TASK C COMBUSTION TEST DATA - PHASE II

PURPOSE	EFFECT OF INJECTION VARAIBLES								
TEST NO.	28	28	28	28	28	28	28	28	28
TYPE OF COAL	A	A	A	A	A	A	A	A	A
FURNACE LOAD	100	100	100	100	100	100	100	100	100
EXCESS OXYGEN	4.1	3.9	3.9	4.0	4.0	4.0	4.2	4.1	4.1
OFA	15	15	15	15	15	15	15	15	15
BURNER TILT	0	0	0	0	0	0	0	0	0
SORBENT TYPE	-	C	C	-	C	C	-	C	C
Ca/S MOLAR RATIO (NOMINAL)	0	2:1	2:1	0	2:1	2:1	0	2:1	2:1
SORBENT INJECTION LOCATION (1)	A,D	A,D	A,D	A,D	A,D	A,D	A,D	A,D	A,D
NO. OF SORBENT INJECTORS	8.00	8.00	8.00	8.00	8.00	8.00	8.00	8.00	8.00
INJECTOR DIA. (IN.)	1.38	1.38	1.38	1.38	1.38	1.38	1.38	1.38	1.38
SORBENT INJECTION VELOCITY (2)	90	92	92	108	114	114	138	139	139
SORBENT INJECTION ANGLE (3)	-45,+45	-45,+45	-45,+45	-45,+45	-45,+45	-45,+45	-45,+45	-45,+45	-45,+45
TEST IDENTIFIER	28A1	28A2	28A3	28B1	28B2	28B3	28C1	28C2	28C3
DATE	7/16/87	7/16/87	7/16/87	7/16/87	7/16/87	7/16/87	7/16/87	7/16/87	7/16/87
TIME -HRS	1824	1827	1827	1914	1919	1919	1954	1959	1959
SORBENT FEED (LB/HR)	0.00	599.17	599.17	0.00	600.60	600.60	0.00	599.79	599.79
SORBENT AIR (LB/HR)	2059.00	2096.00	2096.00	2465.00	2612.00	2612.00	3157.00	3167.00	3167.00
O2 EMISSIONS, %	4.10	3.90	3.90	4.00	4.00	4.00	4.20	4.10	4.10
CO2 EMISSIONS AT 3% O2, %	15.30	15.24	-	15.37	15.29	-	15.29	15.29	-
CO EMISSIONS AT 3% O2, PPM	45.61	51.45	-	45.11	53.09	-	44.93	54.69	-
NOX EMISSIONS AT 3% O2, PPM	305.00	295.00	295.00	300.00	295.00	295.00	295.00	295.00	295.00
SO2 EMISSIONS AT 3% O2,PPM	2110.00	1325.00	1230.00	2035.00	1270.00	1205.00	2025.00	1245.00	1180.00
CARBON CONV. BY PARTICULATE	-	-	-	-	-	-	-	-	-
AVG BASELINE SO2 (A) 3%O2	1983.00	1983.00	1983.00	1983.00	1983.00	1983.00	1983.00	1983.00	1983.00
UPDATED BASELINE SO2 (B) 3%O2	2035.00	2035.00	2035.00	2025.00	2025.00	2025.00	2035.00	2035.00	2035.00
BASELINE SO2 PRIOR (C) 3%O2	2075.00	2110.00	2110.00	2110.00	2035.00	2035.00	2035.00	2025.00	2025.00
CA/S RATIO (ACTUAL)	0.00	2.11	2.11	0.00	2.12	2.12	0.00	2.15	2.15
SO2 CAPTURE BY G.A.S.- A vs C	NA	33.18	37.97	NA	35.96	39.23	NA	37.22	40.49
SO2 CAPTURE BY G.A.S.- B vs C	NA	34.89	39.56	NA	37.28	40.49	NA	38.82	42.01
SO2 CAPTURE BY G.A.S.-PRIOR B vs C	NA	37.20	41.71	NA	37.59	40.79	NA	38.52	41.73
SO2 CAPTURE BY G.A.S.- AVERAGE	NA	35.09	39.75	NA	36.94	40.17	NA	38.19	41.41
SO2 CAPTURE BY FLYASH CA UT.	NA	31.97	-	NA	-	-	NA	38.25	-
PERCENT CA UTILIZATION	NA	15.15	-	NA	-	-	NA	17.78	-
SO2 CAPTURE- OVERALL AVERAGE	0.00	33.53	39.75	0.00	36.94	40.17	0.00	38.22	41.41

Table 6-8 (continued)

TASK C COMBUSTION TEST DATA - PHASE II

PURPOSE	EFFECT OF INJECTION VARAIBLES								
TEST NO.	29	29	29	29	29	29	29	29	29
TYPE OF COAL	A	A	A	A	A	A	A	A	A
FURNACE LOAD	100	100	100	100	100	100	100	100	100
EXCESS OXYGEN	4.0	3.8	3.8	3.8	3.8	3.8	3.8	3.7	3.7
OFA	15	15	15	15	15	15	15	15	15
BURNER TILT	0	0	0	0	0	0	0	0	0
SORBENT TYPE	-	C	C	-	C	C	-	C	C
Ca/S MOLAR RATIO (NOMINAL)	0	2:1	2:1	0	2:1	2:1	0	2:1	2:1
SORBENT INJECTION LOCATION (1)	A	A	A	A	A	A	A	A	A
NO. OF SORBENT INJECTORS	4.00	4.00	4.00	4.00	4.00	4.00	4.00	4.00	4.00
INJECTOR DIA. (IN.)	1.61	1.61	1.61	1.61	1.61	1.61	1.61	1.61	1.61
SORBENT INJECTION VELOCITY (2)	190	189	189	162	162	162	133	132	132
SORBENT INJECTION ANGLE (3)	-90	-90	-90	-90	-90	-90	-90	-90	-90
TEST IDENTIFIER	29A1	29A2	29A3	29B1	29B2	29B3	29C1	29C2	29C3
DATE	7/16/87	7/16/87	7/16/87	7/16/87	7/16/87	7/16/87	7/16/87	7/16/87	7/16/87
TIME -HRS	2115	2121	2121	2159	2205	2205	2235	2239	2239
SORBENT FEED (LB/HR)	0.00	600.40	600.40	0.00	599.09	599.09	0.00	599.94	599.94
SORBENT AIR (LB/HR)	2957.00	2942.00	2942.00	2525.00	2513.00	2513.00	2064.00	2049.00	2049.00
O2 EMISSIONS, %	4.00	3.80	3.80	3.80	3.80	3.80	3.80	3.70	3.70
CO2 EMISSIONS AT 3% O2, %	15.39	15.48	-	15.52	15.48	-	15.53	15.50	-
CO EMISSIONS AT 3% O2, PPM	45.78	52.52	-	45.61	51.57	-	45.74	51.12	-
NOX EMISSIONS AT 3% O2, PPM	285.00	275.00	275.00	275.00	285.00	285.00	275.00	285.00	285.00
SO2 EMISSIONS AT 3% O2,PPM	2035.00	1475.00	1415.00	2025.00	1475.00	1445.00	2025.00	1530.00	1465.00
CARBON CONV. BY PARTICULATE	-	-	-	-	-	-	-	99.67	99.67
AVG BASELINE SO2 (A) 3%O2	1983.00	1983.00	1983.00	1983.00	1983.00	1983.00	1983.00	1983.00	1983.00
UPDATED BASELINE SO2 (B) 3%O2	2025.00	2025.00	2025.00	2025.00	2025.00	2025.00	1850.00	1850.00	1850.00
BASELINE SO2 PRIOR (C) 3%O2	2025.00	2035.00	2035.00	2035.00	2025.00	2025.00	2025.00	2025.00	2025.00
CA/S RATIO (ACTUAL)	0.00	2.13	2.13	0.00	2.11	2.11	0.00	2.11	2.11
SO2 CAPTURE BY G.A.S.- A vs C	NA	25.62	28.64	NA	25.62	27.13	NA	22.84	26.12
SO2 CAPTURE BY G.A.S.- B vs C	NA	27.16	30.12	NA	27.16	28.64	NA	17.30	20.81
SO2 CAPTURE BY G.A.S.-PRIOR B vs C	NA	27.52	30.47	NA	27.16	28.64	NA	24.44	27.65
SO2 CAPTURE BY G.A.S.- AVERAGE	NA	26.77	29.74	NA	26.65	28.14	NA	21.53	24.86
SO2 CAPTURE BY FLYASH CA UT.	NA	-	30.37	NA	-	-	NA	45.02	45.02
PERCENT CA UTILIZATION	NA	-	14.26	NA	-	-	NA	21.32	21.32
SO2 CAPTURE- OVERALL AVERAGE	0.00	26.77	30.06	0.00	26.65	28.14	0.00	33.27	34.94

Table 6-8 (continued)
TASK C COMBUSTION TEST DATA - PHASE II

PURPOSE	EFFECT OF INJECTION VARAIBLES								
TEST NO.	30	30	30	30	30	30	30	30	30
TYPE OF COAL	A	A	A	A	A	A	A	A	A
FURNACE LOAD	100	100	100	100	100	100	100	100	100
EXCESS OXYGEN	3.5	3.5	3.5	3.6	3.7	3.7	3.9	3.7	3.7
OFA	15	15	15	15	15	15	15	15	15
BURNER TILT	0	0	0	0	0	0	0	0	0
SORBENT TYPE	-	C	C	-	C	C	-	C	C
Ca/S MOLAR RATIO (NOMINAL)	0	2:1	2:1	0	2:1	2:1	0	2:1	2:1
SORBENT INJECTION LOCATION (1)	A	A	A	A	A	A	A	A	A
NO. OF SORBENT INJECTORS	4.00	4.00	4.00	4.00	4.00	4.00	4.00	4.00	4.00
INJECTOR DIA. (IN.)	1.61	1.61	1.61	1.61	1.61	1.61	1.61	1.61	1.61
SORBENT INJECTION VELOCITY (2)	133	132	132	162	162	162	199	199	199
SORBENT INJECTION ANGLE (3)	0	0	0	0	0	0	0	0	0
TEST IDENTIFIER	30A1	30A2	30A3	30B1	30B2	30B3	30C1	30C2	30C3
DATE	7/17/87	7/17/87	7/17/87	7/17/87	7/17/87	7/17/87	7/17/87	7/17/87	7/17/87
TIME -HRS	0057	0103	0103	0134	0141	0141	0222	0227	0227
SORBENT FEED (LB/HR)	0.00	599.74	599.74	0.00	599.86	599.86	0.00	598.54	598.54
SORBENT AIR (LB/HR)	2066.00	2055.00	2055.00	2512.00	2523.00	2523.00	3096.00	3095.00	3095.00
O2 EMISSIONS, %	3.50	3.50	3.50	3.60	3.70	3.70	3.90	3.70	3.70
CO2 EMISSIONS AT 3% O2, %	15.35	15.38	-	15.44	15.40	-	15.45	15.42	-
CO EMISSIONS AT 3% O2, PPM	43.82	50.65	-	44.26	50.05	-	45.46	55.40	-
NOX EMISSIONS AT 3% O2, PPM	255.00	255.00	255.00	255.00	260.00	260.00	260.00	250.00	250.00
SO2 EMISSIONS AT 3% O2,PPM	1850.00	1200.00	1140.00	1895.00	1250.00	1185.00	1960.00	1215.00	1095.00
CARBON CONV. BY PARTICULATE	-	99.42	99.42	-	-	-	-	-	-
AVG BASELINE SO2 (A) 3%O2	1983.00	1983.00	1983.00	1983.00	1983.00	1983.00	1983.00	1983.00	1983.00
UPDATED BASELINE SO2 (B) 3%O2	1895.00	1895.00	1895.00	1960.00	1960.00	1960.00	1945.00	1945.00	1945.00
BASELINE SO2 PRIOR (C) 3%O2	2025.00	1850.00	1850.00	1850.00	1895.00	1895.00	1895.00	1960.00	1960.00
CA/S RATIO (ACTUAL)	0.00	2.10	2.10	0.00	2.11	2.11	0.00	2.10	2.10
SO2 CAPTURE BY G.A.S.- A vs C	NA	39.49	42.51	NA	36.96	40.24	NA	38.73	44.78
SO2 CAPTURE BY G.A.S.- B vs C	NA	36.68	39.84	NA	36.22	39.54	NA	37.53	43.70
SO2 CAPTURE BY G.A.S.-PRIOR B vs C	NA	35.14	38.38	NA	34.04	37.47	NA	38.01	44.13
SO2 CAPTURE BY G.A.S.- AVERAGE	NA	37.10	40.24	NA	35.74	39.08	NA	38.09	44.21
SO2 CAPTURE BY FLYASH CA UT.	NA	58.54	58.54	NA	49.70	49.70	NA	43.13	-
PERCENT CA UTILIZATION	NA	27.87	27.87	NA	23.59	23.59	NA	20.52	-
SO2 CAPTURE- OVERALL AVERAGE	0.00	47.82	49.39	0.00	42.72	44.39	0.00	40.61	44.21

Table 6-8 (continued)

TASK C COMBUSTION TEST DATA - PHASE II

PURPOSE	EFFECT OF INJECTION VARAIBLES		
TEST NO.	31	31	31
TYPE OF COAL	A	A	A
FURNACE LOAD	100	100	100
EXCESS OXYGEN	3.8	3.6	3.6
OFA	15	15	15
BURNER TILT	0	0	0
SORBENT TYPE	-	B	B
Ca/S MOLAR RATIO (NOMINAL)	0	2:1	2:1
SORBENT INJECTION LOCATION (1)	A	A	A
NO. OF SORBENT INJECTORS	4.00	4.00	4.00
INJECTOR DIA. (IN.)	1.61	1.61	1.61
SORBENT INJECTION VELOCITY (2)	200	200	200
SORBENT INJECTION ANGLE (3)	0	0	0
TEST IDENTIFIER	31A1	31A2	31A3
DATE	7/17/87	7/17/87	7/17/87
TIME -HRS	0334	0340	0340
SORBENT FEED (LB/HR)	0.00	602.41	602.41
SORBENT AIR (LB/HR)	3108.00	3105.00	3105.00
O_2 EMISSIONS, %	3.80	3.60	3.60
CO_2 EMISSIONS AT 3% O_2, %	15.43	15.42	-
CO EMISSIONS AT 3% O_2, PPM	44.31	54.91	-
NOX EMISSIONS AT 3% O_2, PPM	245.00	250.00	250.00
SO_2 EMISSIONS AT 3% O_2,PPM	1945.00	1270.00	1085.00
CARBON CONV. BY PARTICULATE	-	-	-
AVG BASELINE SO_2 (A) 3%O_2	1983.00	1983.00	1983.00
UPDATED BASELINE SO_2 (B) 3%O_2	1860.00	1860.00	1860.00
BASELINE SO_2 PRIOR (C) 3%O_2	1960.00	1945.00	1945.00
CA/S RATIO (ACTUAL)	0.00	2.12	2.12
SO_2 CAPTURE BY G.A.S.- A vs C	NA	35.96	45.28
SO_2 CAPTURE BY G.A.S.- B vs C	NA	31.72	41.67
SO_2 CAPTURE BY G.A.S.-PRIOR B vs C	NA	34.70	44.22
SO_2 CAPTURE BY G.A.S.- AVERAGE	NA	34.13	43.72
SO_2 CAPTURE BY FLYASH CA UT.	NA	-	44.49
PERCENT CA UTILIZATION	NA	-	20.96
SO_2 CAPTURE- OVERALL AVERAGE	0.00	34.13	44.11

Table 6-8 (concluded)
TASK C COMBUSTION TEST DATA - PHASE II

PURPOSE	EXPLANATIONS OF DATA PRESENTATION
TEST NO.	AS SPECIFIED IN TEST MATRIX
TYPE OF COAL	PITTS. # 8 FOR ALL PHASE I TESTS
FURNACE LOAD	100% FOR ALL PHASE I
EXCESS OXYGEN	@ STACK
OFA	% THROUGH OVERFIRE AIR PORTS
BURNER TILT	DEGREES FROM HORIZONTAL
SORBENT TYPE	A= BLACK RIVER; B= UNTREATED; C= TREATED
Ca/S MOLAR RATIO (NOMINAL)	NOMINAL VALUE
SORBENT INJECTION LOCATION (1)	SEE ATTACHED FIGURE FOR DEFINITIONS
NO. OF SORBENT INJECTORS	FOUR, SIX, OR EIGHT INJECTORS USED
INJECTOR DIA. (IN.)	INNER DIAMETER OF INJECTOR NOZZLES
SORBENT INJECTION VELOCITY (2)	SPECIFIED IN FT/SEC.
SORBENT INJECTION ANGLE (3)	DEGREES FROM HORIZONTAL UNLESS OTHERWISE SPECIFIED
TEST IDENTIFIER	SPECIFIC TO EACH TEST RUN
DATE	-
TIME -HRS	-
SORBENT FEED (LB/HR)	ZERO IS BASELINE TEST
SORBENT AIR (LB/HR)	AIR WAS ON DURING SOME BASELINE TESTS
O2 EMISSIONS, %	@STACK
CO2 EMISSIONS AT 3% O2, %	CORRECTED EMISSIONS @STACK
CO EMISSIONS AT 3% O2, PPM	CORRECTED EMISSIONS @STACK
NOX EMISSIONS AT 3% O2, PPM	CORRECTED EMISSIONS @STACK
SO2 EMISSIONS AT 3% O2,PPM	CORRECTED EMISSIONS @STACK
CARBON CONV. BY PARTICULATE	% CARBON BURNOUT MEASURED FORM FLYASH SAMPLE
AVG BASELINE SO2 (A) 3%O2	SO2 MEASURED DURING INITIAL BASELINE TESTS
UPDATED BASELINE SO2 (B) 3%O2	SO2 MEASURED AFTER SORBENT TURNED OFF FOR GIVEN TEST
BASELINE SO2 PRIOR (C) 3%O2	SO2 MEASURED BEFORE SORBENT TURNED ON FOR GIVEN TEST
CA/S RATIO (ACTUAL)	FROM MEASURED SORBENT AND COAL FEED RATES
SO2 CAPTURE BY G.A.S.- A vs C	% SO2 REMOVAL COMPARING SO2 VS. BASELINE (A) AVE
SO2 CAPTURE BY G.A.S.- B vs C	% SO2 REMOVAL COMPARING SO2 VS. BASELINE OF NEXT TEST (B)
SO2 CAPTURE BY G.A.S.-PRIOR B	% SO2 REMOVAL COMPARING SO2 VS. BASELINE (C) PRIOR TEST
SO2 CAPTURE BY G.A.S.- AVERAGE	AVE. OF THREE SO2 CAPTURE RESULTS BY GAS ANALYSIS ABOVE
SO2 CAPTURE BY FLYASH CA UT.	% SO2 REMOVAL MEASURED BY CA UTILIZATION FROM FLYASH
PERCENT CA UTILIZATION	% CALCIUM UTILIZATION FOR SULFUR CAPTURE
SO2 CAPTURE- OVERALL AVERAGE	AVE. OF % SO2 REMOVAL BY FLYASH AND BY GAS ANALYSIS

lower sorbent carrier airflows were also tested. The actual carrier airflows for each test are shown in Tables 6-7 and 6-8. The baseline data presented here includes all tests without sorbent injection.

Carbon conversion efficiency as a function of excess O_2 for Phase I and II are shown in Figures 6-23 and 6-24, respectively. Carbon conversion efficiency is defined as the percent conversion of fuel carbon to CO_2 via the combustion process. Carbon conversion efficiency correlates with, but is slightly lower than "combustion efficiency" which is the conversion of all combustibles including volatile components. Carbon conversion efficiency was determined by a mass balance of carbon utilizing stack flyash samples.

Figures 6-23 and 6-24 show that for both Phase I and II, carbon conversion was greater than 99% for all tests and it was not a function of excess O_2 over the range tested. These data are typical in C-E's experience of tangentially fired boilers burning similar rank coals (Kokkinos et al, 1985).

Baseline NO_x emissions are presented as a function of flue O_2 concentration in Figures 6-25 and 6-26, for Phase I and II tests respectively. NO_x emissions data presented have all been corrected to the reference 3% O_2 level. Although tests spanned a fairly narrow band of excess air levels (i e. excess O_2 emissions), a clear trend of increased NO_x emissions with increased excess air is demonstrated. The magnitude of the NO_x emissions ranged from 275 ppm to 375 ppm (corrected to 3% O_2), equivalent to 0.30 to 0.40 lbs per million Btu fired. These emission levels and the trends observed are typical of full scale pre NSPS tangentially-fired boilers (Kelly, et al., 1981, Collette, 1985, and Kokkinos, et al. 1985).

It is interesting to note that the magnitude of the Phase II emissions are slightly lower than those of Phase I; approximately 300 ppm at 3.5% O_2 in Phase I and 275 ppm at 3.5% O_2 in Phase II (both data corrected to 3% O_2 reference). This difference is likely due to combustion air staging from sorbent carrier airflow and is explained below.

Figure 6-23

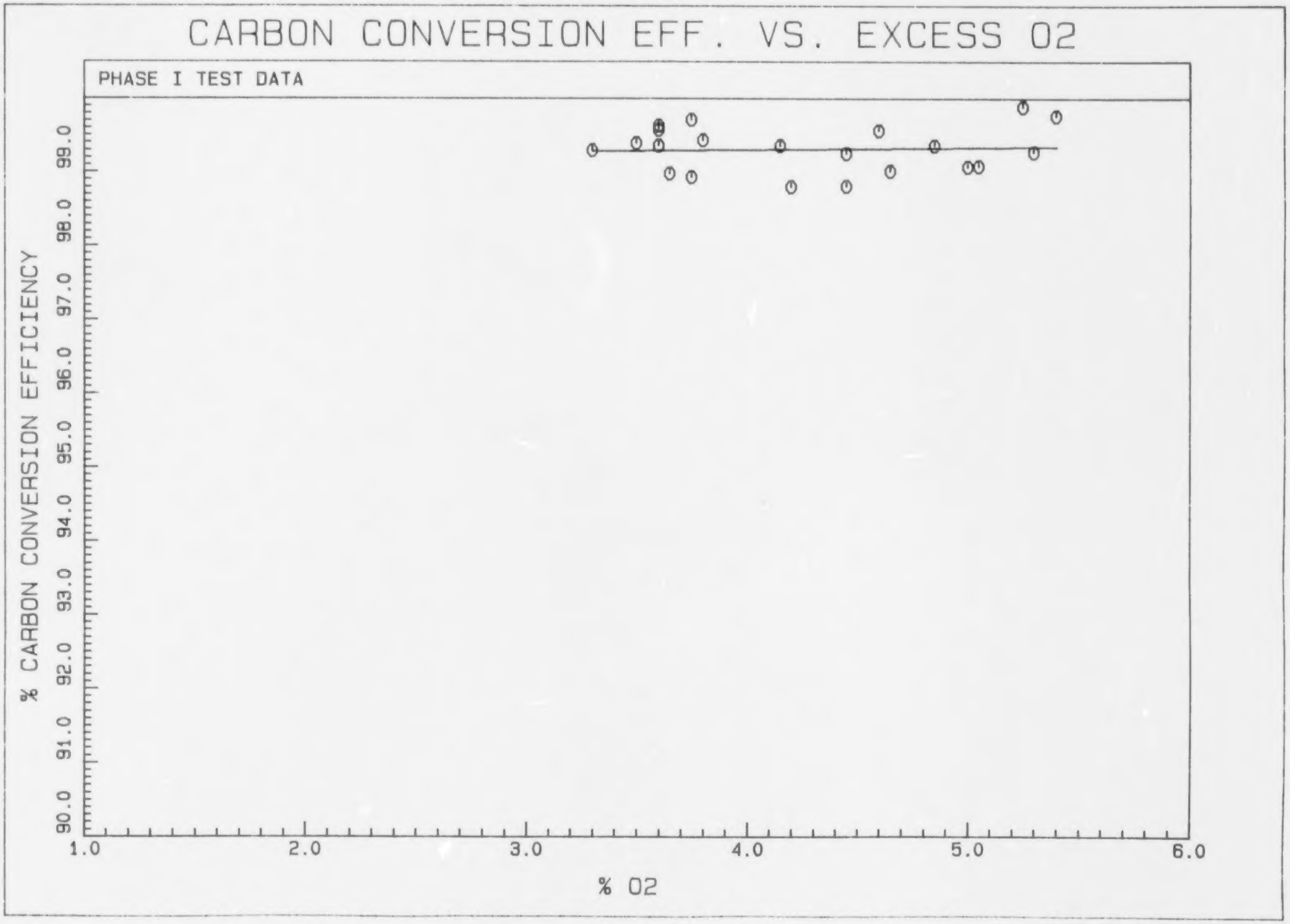
CARBON CONVERSION EFF. VS. EXCESS O2
PHASE I TEST DATA
% CARBON CONVERSION EFFICIENCY
90.0
91.0
92.0
93.0
94.0
95.0
96.0
97.0
98.0
99.0
1.0
2.0
3.0
4.0
5.0
6.0
% O2

Figure 6-24

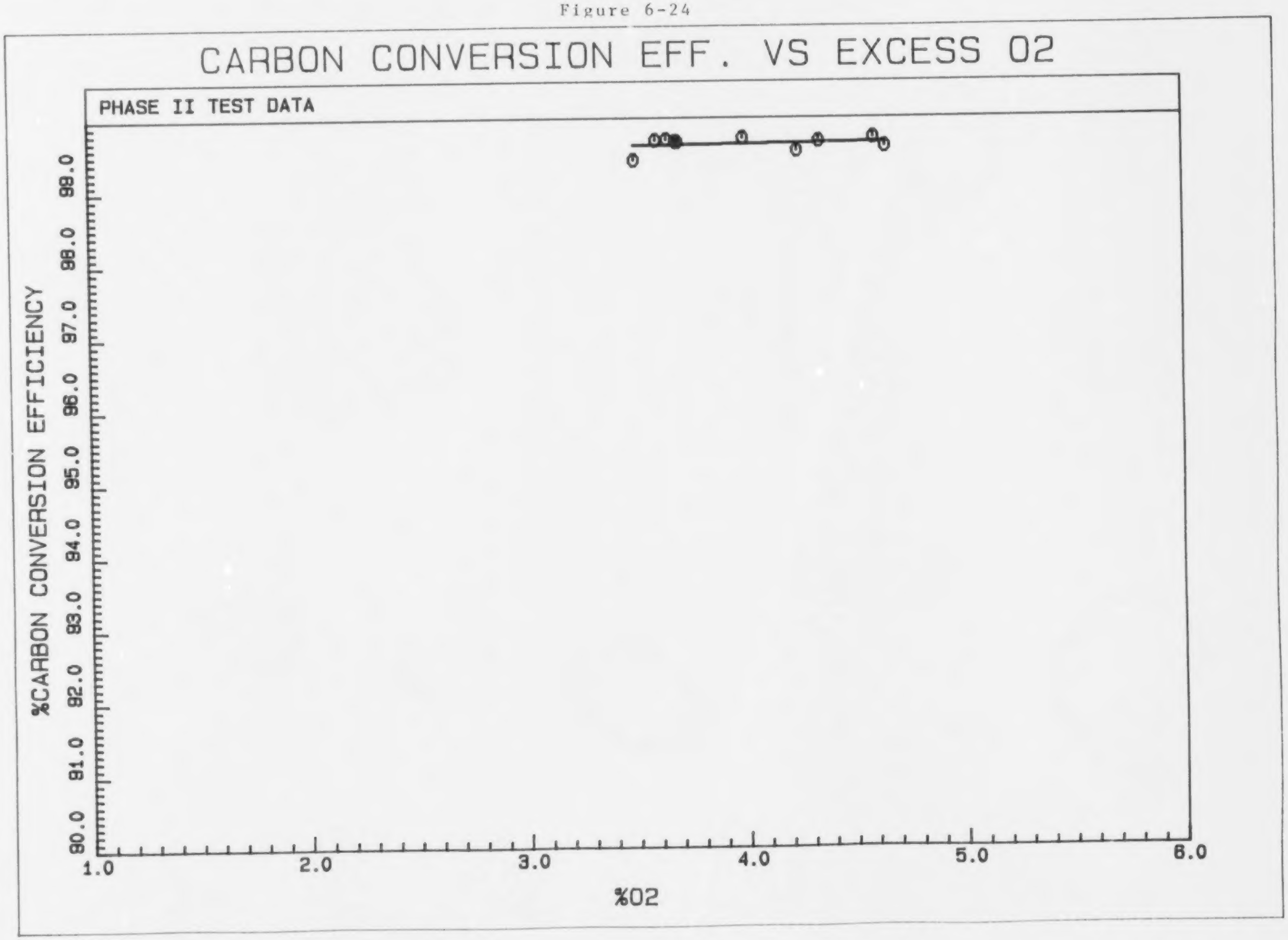
CARBON CONVERSION EFF. VS EXCESS 02
PHASE II TEST DATA
%CARBON CONVERSION EFFICIENCY
90.0
91.0
92.0
93.0
94.0
95.0
96.0
97.0
98.0
99.0
1.0
2.0
3.0
4.0
5.0
6.0
%02

Figure 6-25

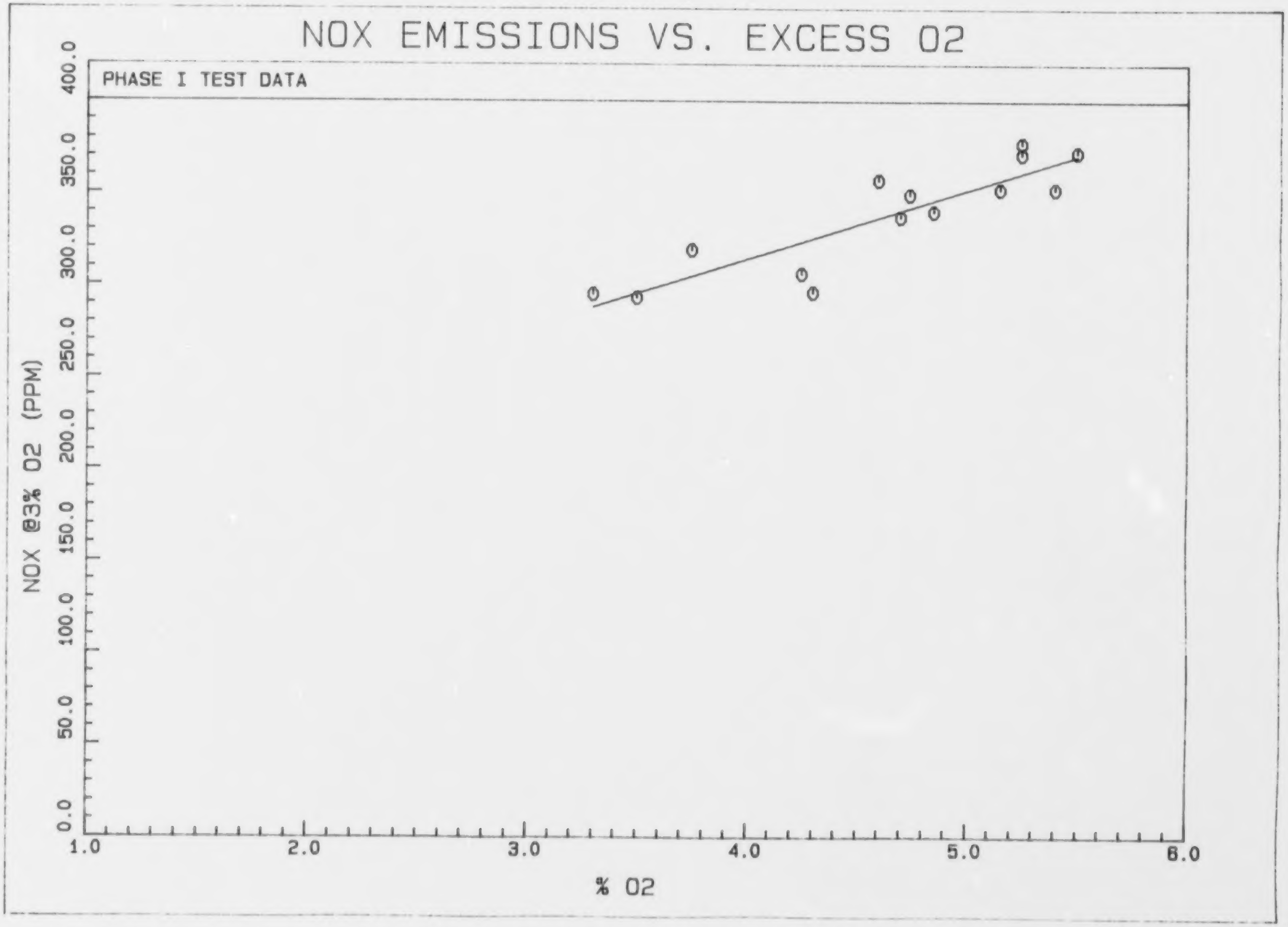
NOX EMISSIONS VS. EXCESS O2
PHASE I TEST DATA
NOX @3% O2 (PPM)
0.0
50.0
100.0
150.0
200.0
250.0
300.0
350.0
400.0
% O2
1.0
2.0
3.0
4.0
5.0
6.0

Figure 6-26

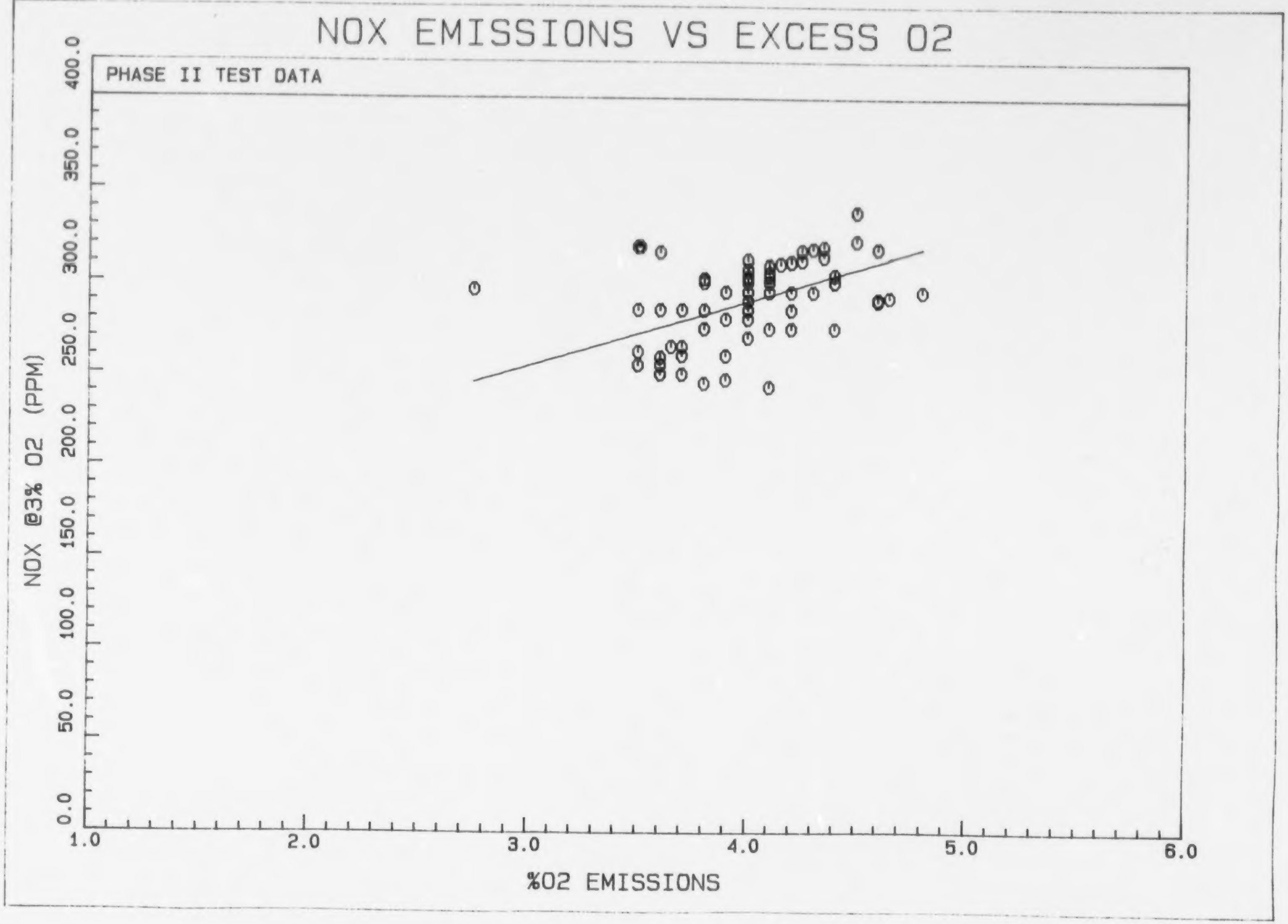
NOX EMISSIONS VS EXCESS O2
PHASE II TEST DATA
NOX @3% O2 (PPM)
0.0
50.0
100.0
150.0
200.0
250.0
300.0
350.0
400.0
1.0
2.0
3.0
4.0
5.0
6.0
%O2 EMISSIONS

It is well documented that NO_x production during combustion results from two primary mechanisms (Singer, 1981, Levy et al, 1978, Wendt & Schulze, 1976 and Zeldovich 1947). The Zeldovich mechanism describes one route for the formation of NO_x which is via thermal fixation of atmospheric nitrogen (sometimes referred to as "thermal NO_x"). NO_x is also formed during combustion from oxidation of organically bound fuel nitrogen (referred to as "fuel NO_x"). Although only a small fraction of the fuel nitrogen maybe converted to NO_x, "fuel NO_x" usually represents the largest fraction of total NO_x emissions, especially when firing a fuel with a high nitrogen content. While the mechanisms of "fuel NO_x" are not yet fully understood, it has been shown that "fuel NO_x" emissions can be reduced by controlling the stoichiometric history of the fuel particles through firing system design. This is achieved by regulating the rates of fuel and combustion air mixing. Specifically for low NO_x combustion, one wants to promote fast devolatization of nitrogen species (fuel bound) in an oxygen depleted environment. This maximizes the total production of volatile nitrogen species and subsequent conversion of these volatile nitrogen species to molecular nitrogen rather than NO by introducing the air required to complete combustion downstream and at lower temperatures. Overfire air is one method of achieving these conditions in a utility boiler (Kelly et al, 1981, Collette 1985, and Kokkinos et al., 1985).

During baseline tests the presence of sorbent carrier (its magnitude and location) were variables. The NO_x data presented includes conditions with and without carrier air and at various locations. This is one reason for some of the data scatter, particular with the Phase II data. During Phase I tests, sorbent injection was only performed at locations on the front wall at elevations above the horizontal furnace outlet plane (defined as a horizontal plane located at the centerline of the furnace arch). In particular, Locations A, B, and C in Figure 6-20. Since these locations were significantly downstream from the combustion zone and the gas temperatures were rapidly quenched in this region, it is unlikely that the introduction of the sorbent carrier air at these locations would affect any combustion processes including NO_x formation.

During Phase II however, most of the injection tests were performed at a location in the lower furnace below the furnace arch (location D, Figure 6-20). Here the presence of sorbent carrier air acted as staged air or overfire air. For some test conditions only the carrier air was modulated and for these a reduction in NO_x emissions with increased carrier air flowrate was observed. This result is consistent with full scale tangentially-fired boiler experience. In particular, that of the C-E Canada and Saskatchewan Power Corporation demonstration of in-furnace sorbent injection for SO_2 control and combustion modification for NO_x control at the Boundary Dam Generating Station Unit 4 (Feindel, R. G. and Gass, D., 1986). In this demonstration the presence of sorbent injection carrier air at a similar location in the boiler was also found to reduce NO_x emissions.

Baseline SO_2 emissions are presented as a function of flue O_2 concentration in Figures 6-27 and 6-28, for Phase I and II tests respectively. SO_2 emissions presented have all been corrected to the reference 3% O_2 level. No trend of SO_2 emissions to excess air level (i.e. O_2 concentration) was obtained. This result is consistent with the carbon conversion data which showed complete combustion during all tests (i.e. 99+% combustion efficiency). A reduction in baseline SO_2 emissions can be seen in the Phase II results as compared with the Phase I results. This is consistent with the slightly lower fuel sulfur content during Phase II.

6.6.3 Furnace Gas Temperature Distribution Results

Furnace gas temperatures were extensively measured by suction pyrometer. During both Phase I and II a complete mapping of gas temperatures was performed from just above the fuel admission assemblies to the furnace stack outlet. Additionally, periodic measurements were taken at the horizontal furnace outlet plane (elevation 37'-9") and at elevation 35'-3" to verify consistent furnace conditions. Measured temperature variations over time at those locations were less than or equal to +/- 100°F.

Furnace gas temperature data is presented here in several forms (Figures 6-29 to 6-37). These data are important to the dry sorbent SO_2 capture process since gas temperature is a critical factor in optimizing the location

Figure 6-27

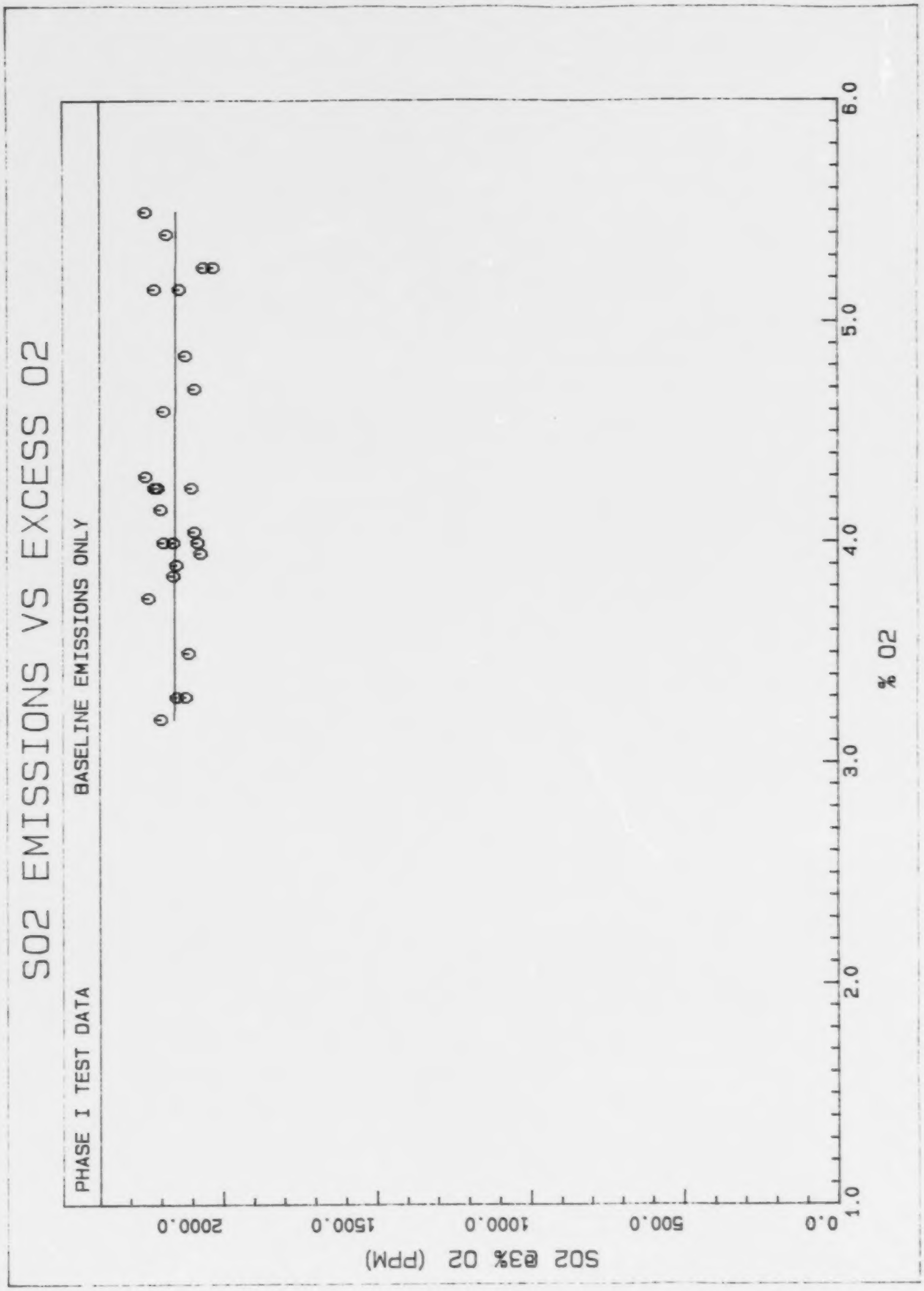

SO2 EMISSIONS VS EXCESS O2

Figure 6-28

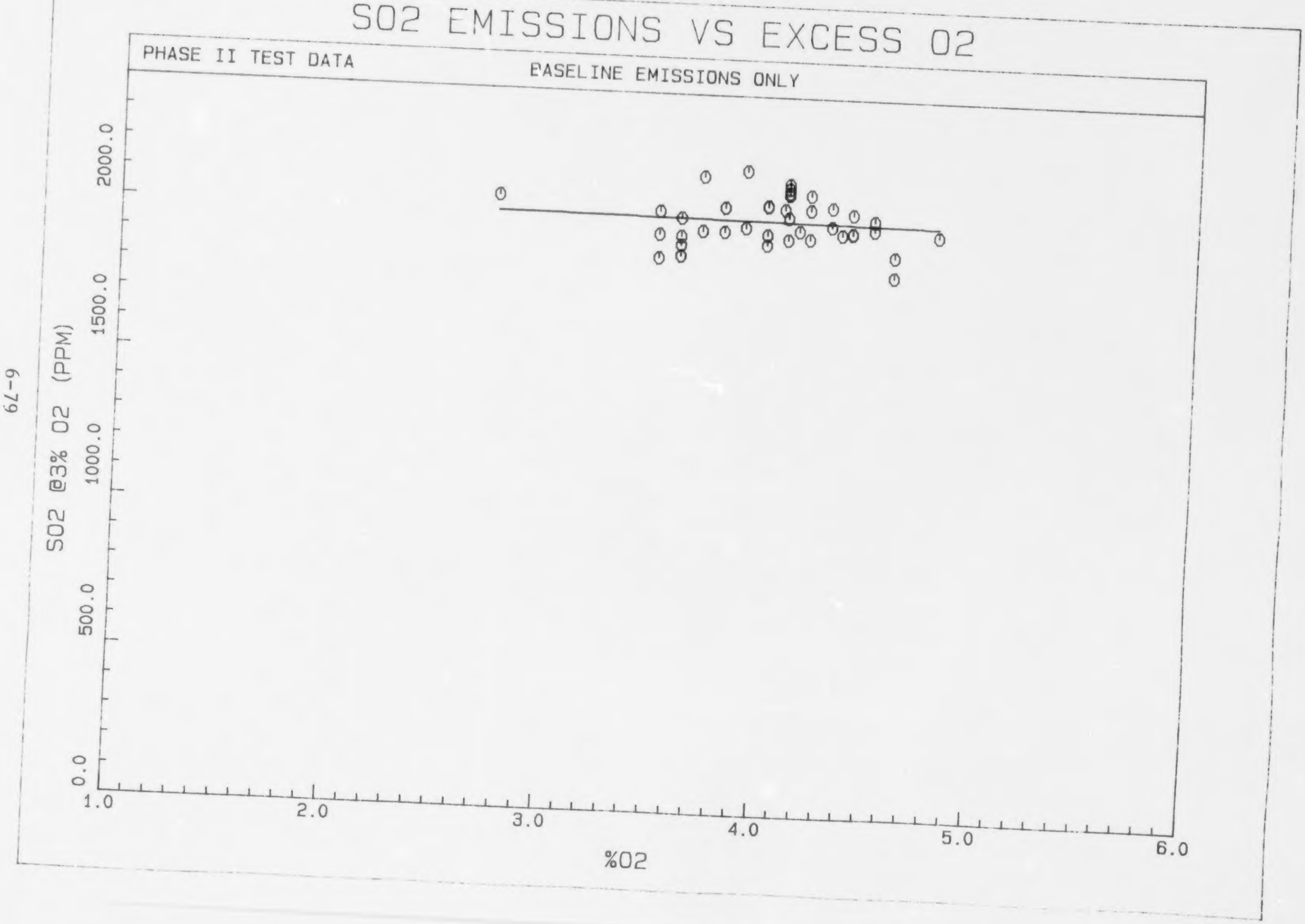
SO2 EMISSIONS VS EXCESS O2
PHASE II TEST DATA
BASELINE EMISSIONS ONLY
SO2 @3% O2 (PPM)
0.0
500.0
1000.0
1500.0
2000.0
%O2
1.0
2.0
3.0
4.0
5.0
6.0

for injection of sorbent. The sulfur capture process proceeds most rapidly in the temperature region of 1200°C (2192°F) to 900°C (1652°F), Gullett and Kramlich (1987) and Beittel et al. (1986). In the chemical reaction

$$CaSO_4 \rightleftarrows SO_2 + CaO + \frac{1}{2} O_2$$

$CaSO_4$ disassociates above 1200°C (2192°F) and below 900°C (1652°F) the reaction proceeds too slowly to have significance in suspension fired boilers. The optimum temperature for sorbent injection varies with the sorbent and the boiler. At temperatures above 1260°C (2300°F) the sorbent is "dead burned", that is the sorbent particle surface is sintered and it loses its porosity and reactivity for SO_2. For hydrated limes ($Ca(OH)_2$) optimum injection temperatures ranging from 1200°C (2200°F) to 1260°C (2300°F), have been found (Stern, 1987 and Beittel, 1986).

Figure 6-29 is a side view of the BSF and gives the measured high, low, and average temperature at each of the measurement planes. The average values shown are the combined average for each of the planes from both Phase I and Phase II. On the basis of Figure 6-29, one might hypothesize an optimum injection location (temperature 2300-2200°F) at or just below the furnace outlet plane. (i.e. elevations 35'-3" to 37'-9"). This region represents injection at or somewhere between injection Locations A and D shown on Figure 6-20. Extensive injection tests were performed at these locations and are discussed in the next report section.

Of significance to sulfur capture is not only the furnace gas temperature at the point of sorbent injection, but also the gas temperature history to which the sorbent particle is exposed after injection. Figure 6-30 presents both measured and calculated gas time/temperature history profiles. These plots are based on an average gas temperature value for the traverse planes (i.e. cross sectional plane through flow field at a given elevation) and the plug flow residence between planes. Time zero (0) seconds is at a plane located through the centerline of the fuel admission assemblies. Time 4.5 to 5.0 seconds (the last data points) are located at the furnace stack outlet. Various other intermediate BSF locations and corresponding residence times are shown.

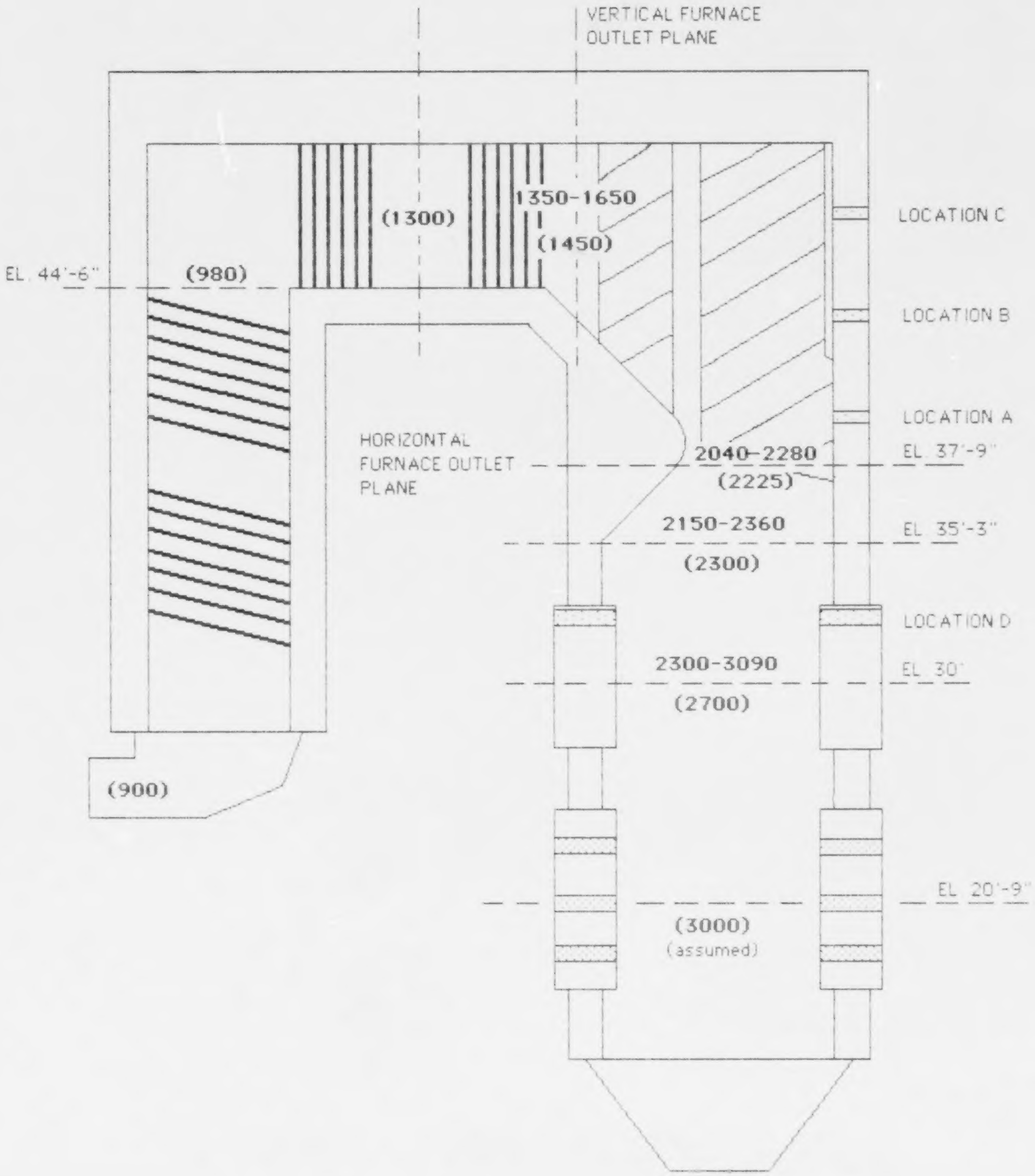
VERTICAL FURNACE OUTLET PLANE
1350-1650
(1300)
(1450)
LOCATION C
EL. 44'-6"
(980)
LOCATION B
LOCATION A
HORIZONTAL FURNACE OUTLET PLANE
2040-2280
EL. 37'-9"
(2225)
2150-2360
EL. 35'-3"
(2300)
LOCATION D
2300-3090
EL. 30'
(2700)
(900)
EL. 20'-9"
(3000)
(assumed)

Figure 6-29. BSF temperature profile data (°F).

Figure 6-30

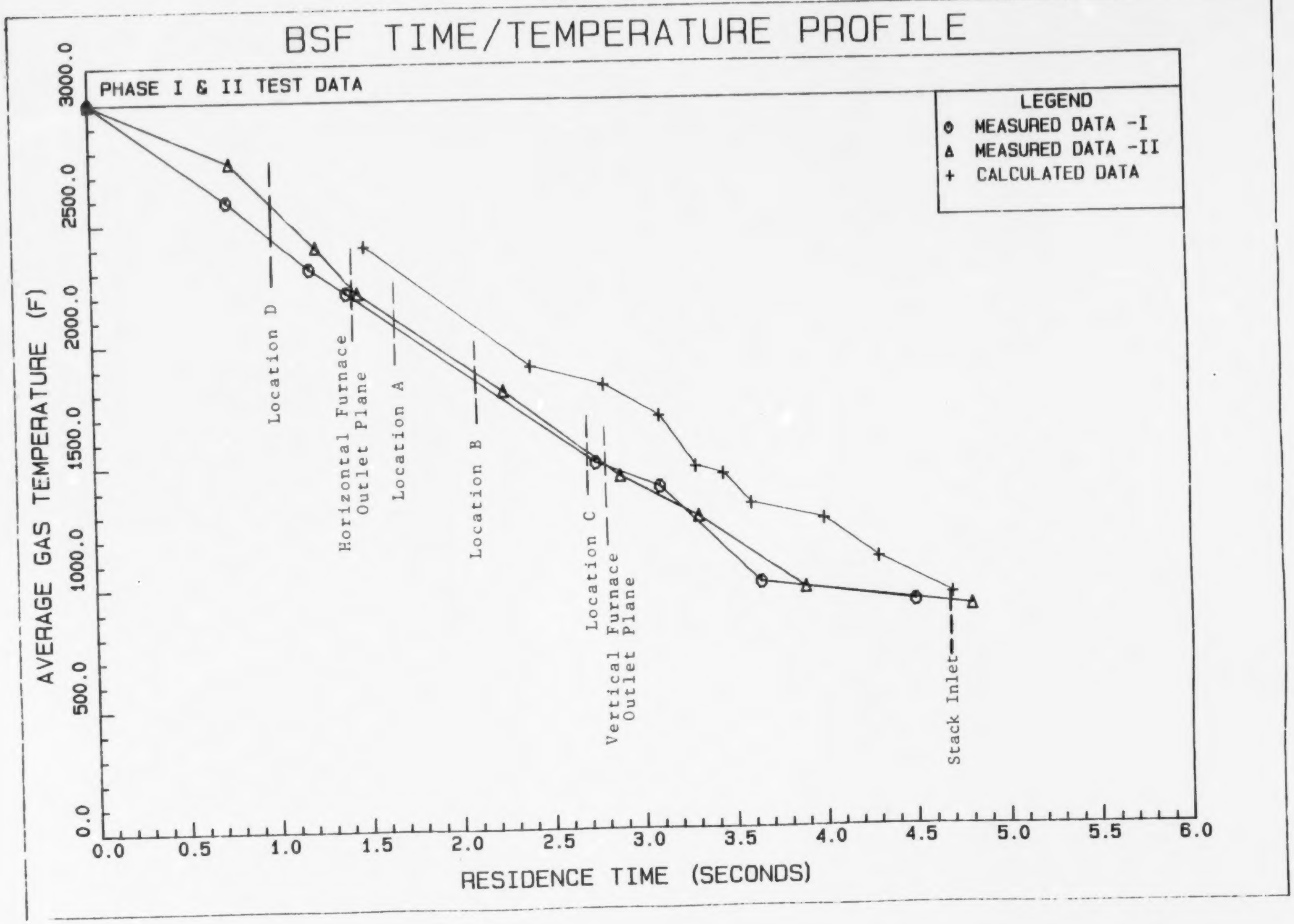
BSF TIME/TEMPERATURE PROFILE
PHASE I & II TEST DATA
LEGEND
○ MEASURED DATA -I
△ MEASURED DATA -II
+ CALCULATED DATA
AVERAGE GAS TEMPERATURE (F)
0.0
500.0
1000.0
1500.0
2000.0
2500.0
3000.0
RESIDENCE TIME (SECONDS)
0.0
0.5
1.0
1.5
2.0
2.5
3.0
3.5
4.0
4.5
5.0
5.5
6.0
Location D
Horizontal Furnace Outlet Plane
Location A
Location B
Location C
Vertical Furnace Outlet Plane
Stack Inlet

Figure 6-30 includes a time/temperature history profile plot for both Phase I and II measurements. These plots show little difference and demonstrate consistent furnace conditions between the two test phases. A calculated gas time/temperature profile is also presented. This predicted gas temperature history was made with a proprietary C-E analysis code as was discussed in Section 6.3.1. The actual measured temperatures are about 200°F lower than predicted. Although additional refractory could have been installed to increase furnace temperatures this was not done because the furnace temperatures obtained were consistent with recent planned and performed full scale sorbent injection demonstrations.

Although the predicted gas temperatures where about 200°F higher than measured temperatures, the predicted design quench rate through the 2400°F-1300°F temperature "window" of 500-550°F/sec was obtained. The resultant gas time/temperature profile at the BSF was typical of many utility boilers. The measured profile (Figure 6-30) shows that the lower furnace residence time is about 1.5 seconds and that the residence time through the postulated sulfur capture "window" of 2300°F to 1600°F is about 1.2 seconds. It is not clear that all 1.2 seconds are available for sulfur capture reactions, however. Other investigations have shown that product layer formation on the sorbent particle surface limits further reaction usually only after two or three hundred microseconds (.2-.3 seconds). This emphasizes the importance of selecting an optimum injection location. The optimum location must include not only consideration of furnace gas temperatures but also mixing performance. Furthermore, identification of the location of the optimum injection temperature is not straight forward in a large furnace.

Figures 6-29 and 6-30 presented only average gas temperature data for a given measurement plane. Actual gas temperatures were not uniform. This must be factored into selection of the optimum sorbent injection location. Figures 6-31 through 6-37 show the spatial variation of gas temperatures within the furnace. Figure 6-31 is an isometric view of the main furnace. The view is from the front left side of the BSF. Figure 6-32 an isometric view of the convective pass as it would appear from behind the boiler. The view is from the left rear of the BSF.

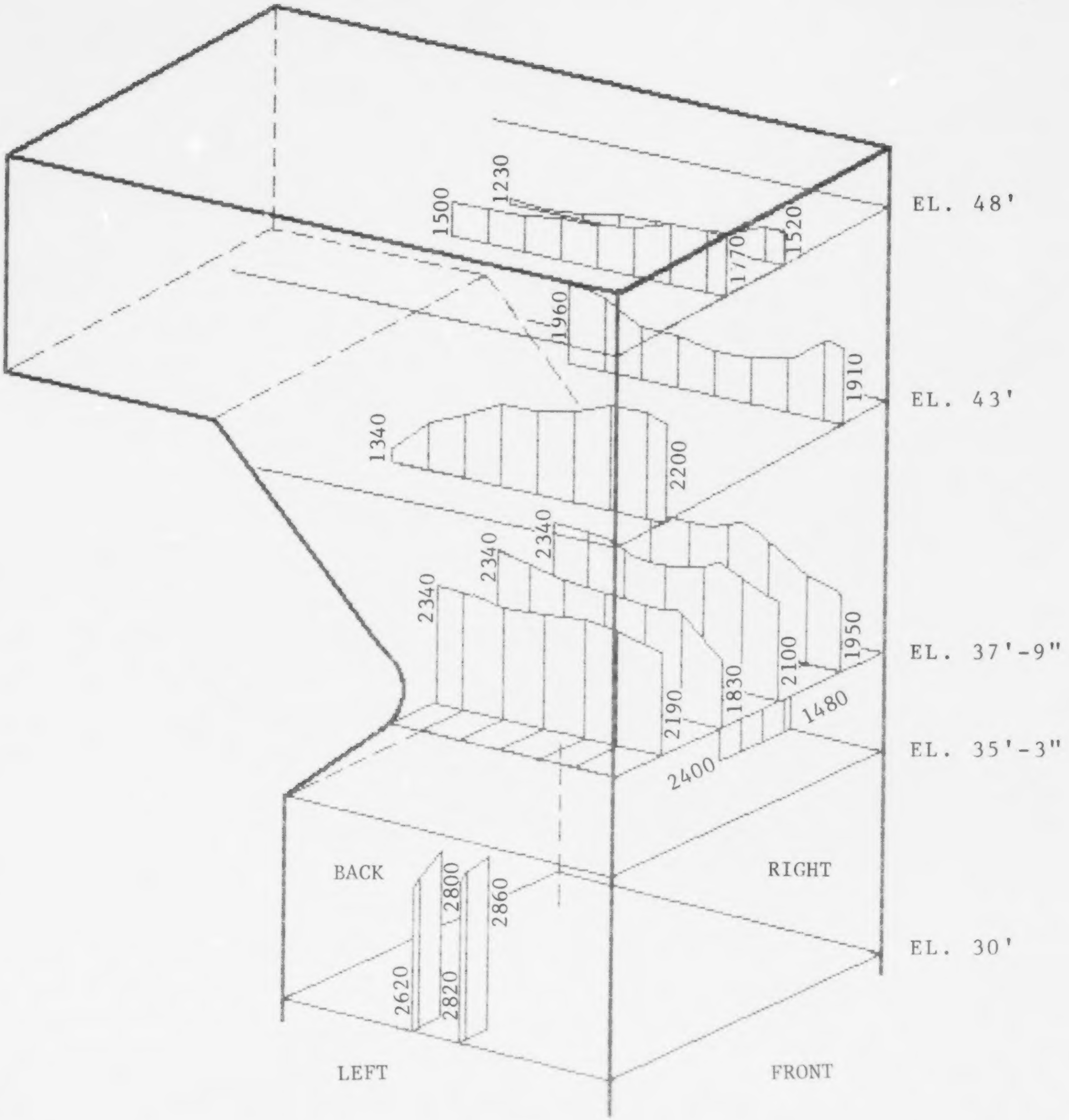
1230
1500
1520
1770
1960
EL. 48'
1910
EL. 43'
1340
2200
2340
2340
2340
1950
2100
1830
2190
EL. 37'-9"
1480
2400
EL. 35'-3"
BACK
2800
2860
RIGHT
EL. 30'
2620
2820
LEFT
FRONT

Figure 6-31. BSF's thermal topography (°F) shown as an isometric view of main furnace.

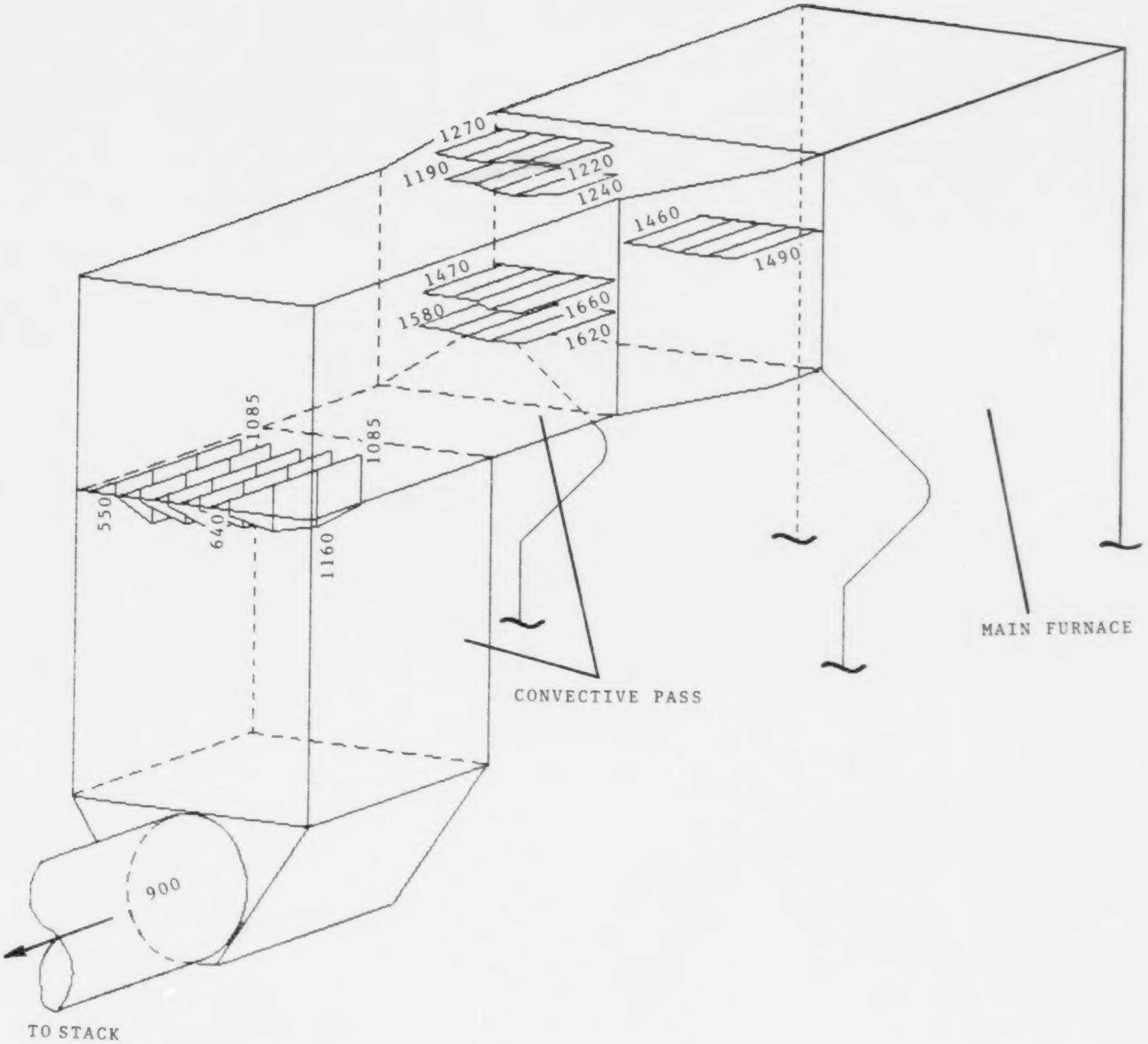
1270
1190
1220
1240
1460
1490
1470
1580
1660
1620
1085
1085
550
640
1160
MAIN FURNACE
CONVECTIVE PASS
900
TO STACK

Figure 6-32. BSF's thermal topography (°F) shown as an isometric view of convective pass from behind.

Figures 6-33a, b, and c show the spatial variation of temperature for elevation 37'-9" (the horizontal furnace outlet plane). Contour plotting shows that the gas temperatures along the front wall are cooler than those at the rear. The rear wall at this plane is the furnace arch.

Figures 6-34 and 6-35 are of gas temperature data taken between the superheat panels. The temperature data taken at elevation 43' (Figure 6-34) was taken through the Location B injection ports and data at elevation 48' (Figure 35) was taken through the Location C injector ports. Missing lanes of data were due to external structural steel members which obstructed the use of the suction pyrometer probe.

Figures 6-36a, b, and c are contour plotted temperature data obtained at the vertical furnace outlet plane defined as a vertically oriented plane just above the furnace arch (see Figure 6-29). Figures 3-37a, b, and c are data obtained across a horizontal plane located at elevation 44'-6" in the convective pass just below the rear cavity.

6.6.4 Sorbent Injection Test Results

6.6.4.1 Method of SO_2 Capture Analysis

SO_2 capture data was presented in Tables 6-7 and 6-8 as percent SO_2 capture by three different approaches. These approaches were; 1) by gas analysis measurements, 2) by mass balance of sulfur utilizing flyash samples, and 3) by measurement of calcium utilization in flyash samples. Each approach is discussed below.

All sorbent injection tests were performed in an "off/on/off" mode. That is, for every test with sorbent injection on, a baseline with no sorbent injection was performed both before and after. During these baseline tests attention was made to insure that SO_2 emissions levels returned to an average baseline value before further injection tests proceeded. This process included a high pressure air purge of the gas sampling probe, and cycling of the sootblowers in the BSF's convective pass. Furthermore, to insure the comparability of sorbent injection tests, each was run for a constant time

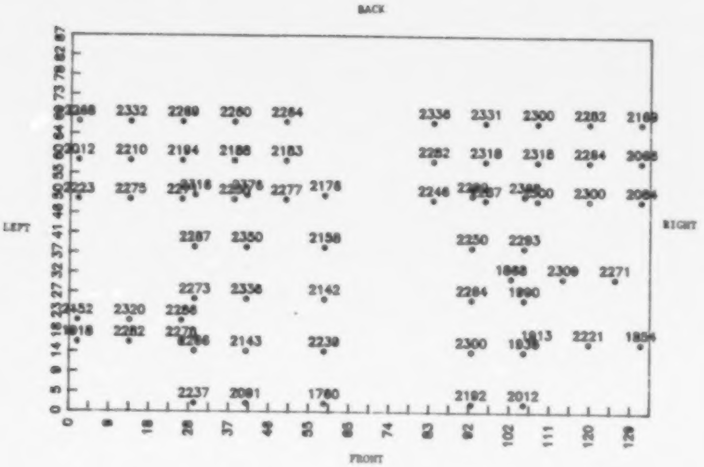

Figure 6-33a.

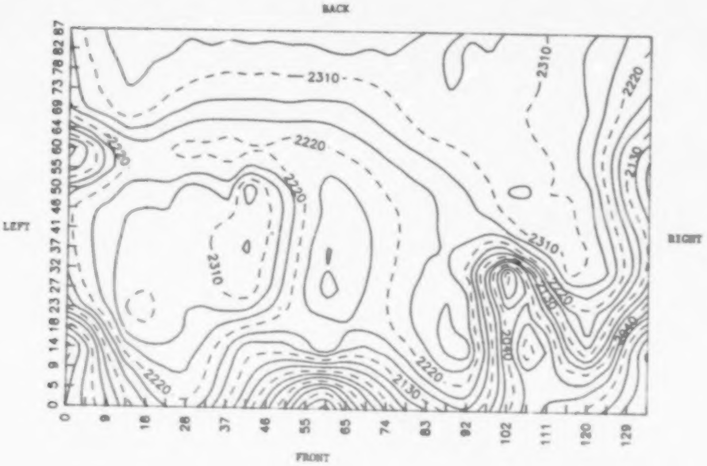

Figure 6-33b.

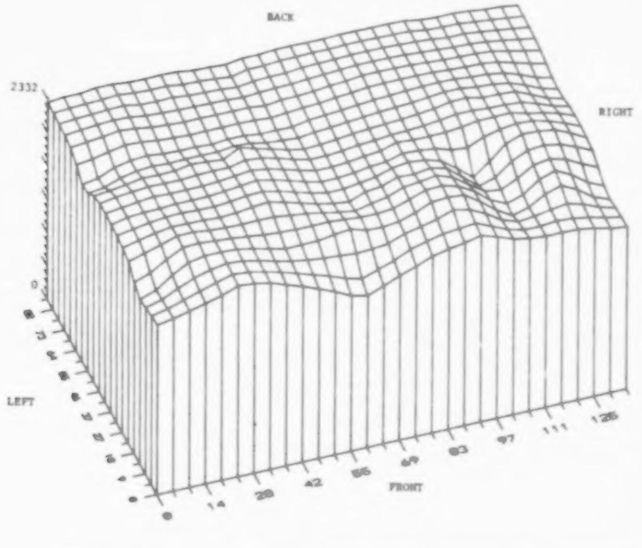

Figure 6-33c.

Temperature data from plane at elevation 37'-9" at the furnace arch (temperatures are in F, X & Y axis scale is in inches).

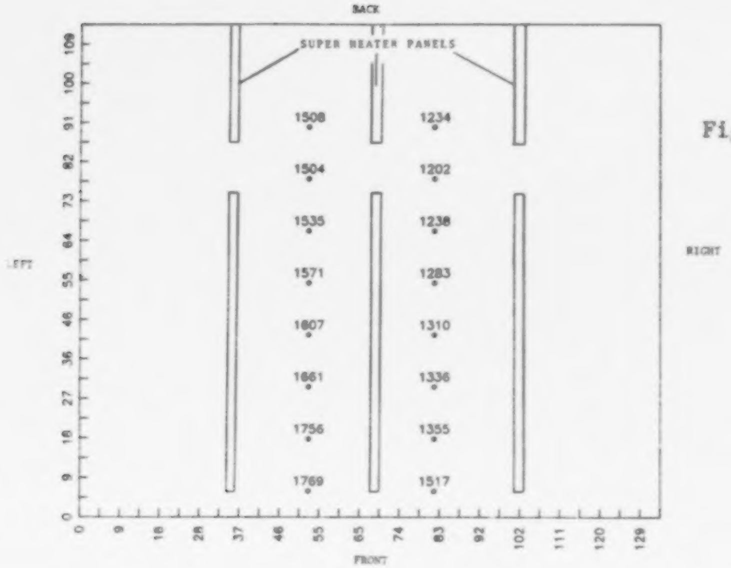

Figure 6-34. Elevation 48'

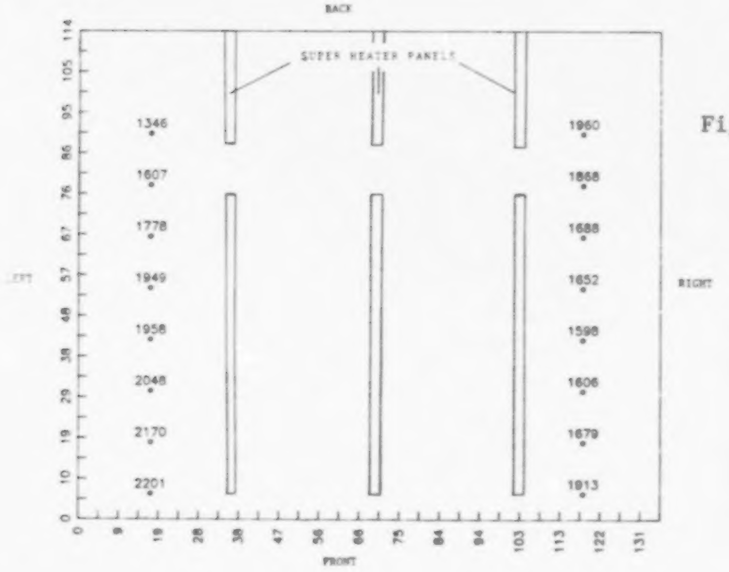

Figure 6-35. Elevation 43'

Temperature data in upper furnace measured in the lanes between superheater panels. (temperatures are in F, X & Y axis scale is in inches)

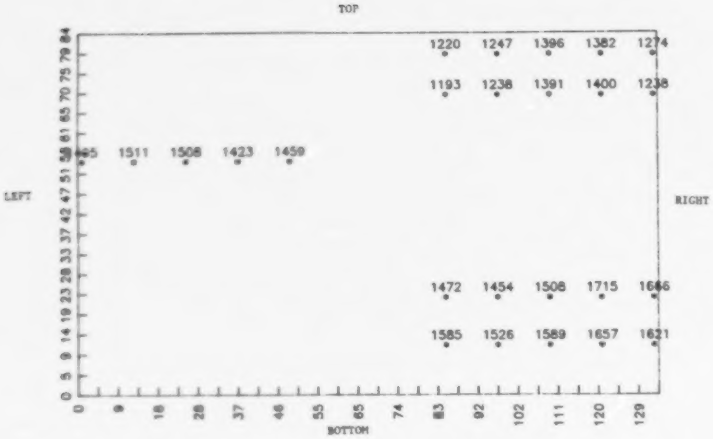

Figure 6-36a.

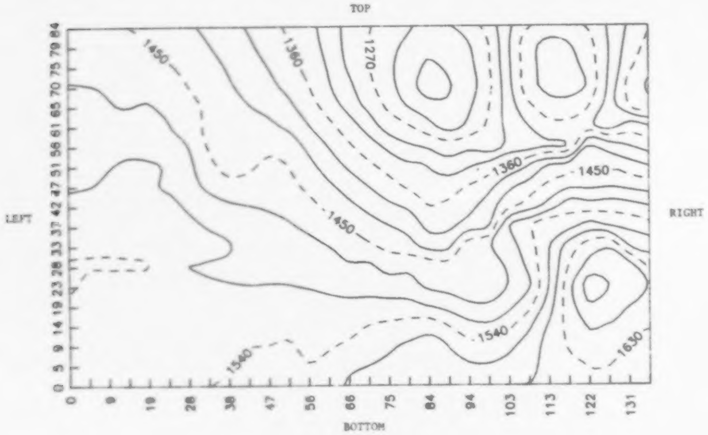

Figure 6-36b.

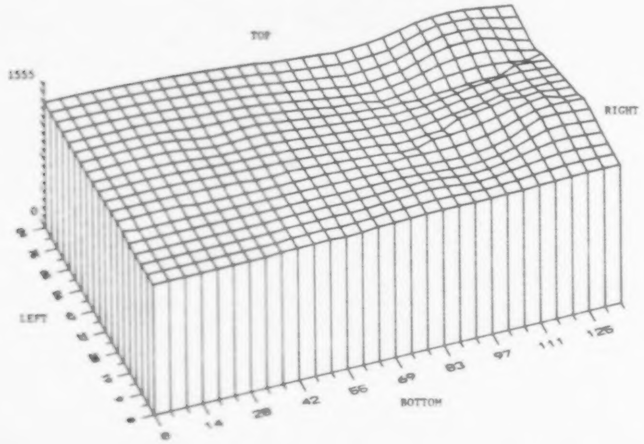

Figure 6-36c.

Temperature data at vertical furnace outlet plane. (temperatures are in F, X & Y axis scale is in inches)

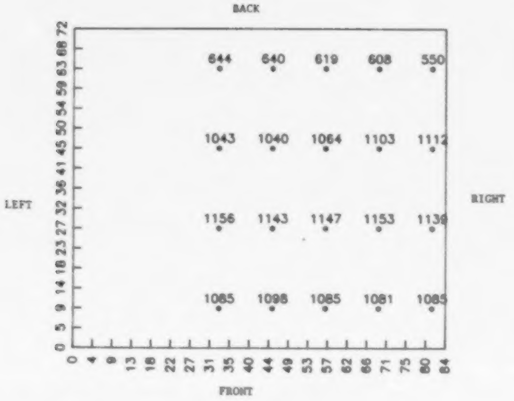

Figure 6-37a.

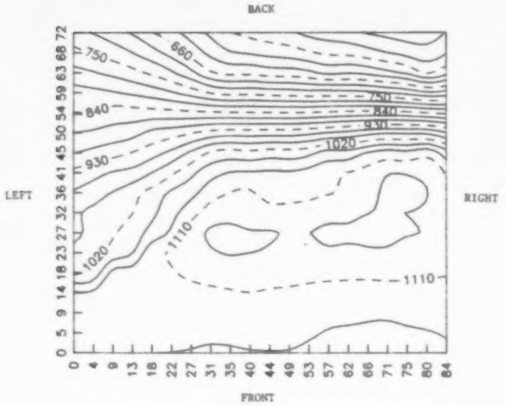

Figure 6-37b.

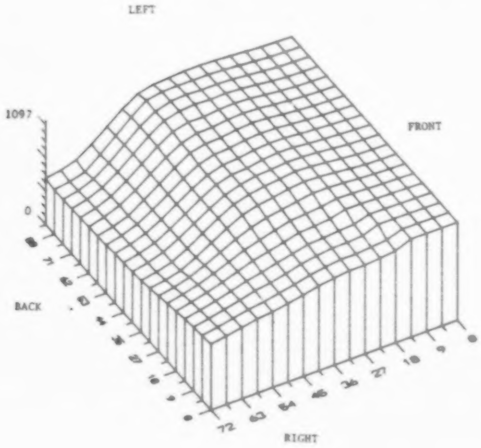

Figure 6-37c.

Temperature data from plane at elevation 44'-6" below the rear pass cavity. (temperatures are in F, X & Y axis scale is in inches) interval of twenty (20) minutes. During Phase II, specific longer duration tests were performed to assess the effect on SO_2 capture of deposited sorbent on the BSF's heat transfer surfaces. These tests showed that SO_2 capture could be increased by 10 to 20 percent (or 4 to 10 percentage points) by extending the sorbent injection duration to one hour. Since deposition of reactive sorbent in an actual boiler is likely over the time frames noted, the results presented here may be slightly conservative. The major objective here however was to obtain comparable data that would lead to design guidelines for optimization of SO_2 capture in a tangentially fired boiler demonstration.

SO_2 capture based on gas analysis system (G.A.S) measurements was calculated as follows:

$$\% \ SO_2 \ \underset{\text{(by G.A.S)}}{\text{CAPTURE}} = 100 \times \left[\frac{SO_{2 \text{ Without Sorbent}} - SO_{2 \text{ With Sorbent}}}{SO_{2 \text{ Without Sorbent}}}\right]$$

where:

$SO_{2 \text{ Without Sorbent}}$ = baseline SO_2 emissions

and:

all SO_2 values are corrected to 3% O_2

SO_2 capture by gas analysis measurements was calculated by this formula for three different baseline SO_2 values; 1) an average baseline SO_2 emissions value for the test series, 2) the baseline SO_2 emission measured prior to sorbent injection, and 3) the baseline SO_2 emission obtained after sorbent injection was stopped. Each of these three values are presented in Tables 6-7 and 6-8 along with the average of the three.

SO_2 capture was also determined from flyash samples which were obtained during most test conditions. These samples were obtained by a high sampling rate cyclone sampler. During Phase I testing, EPA method 5 isokinetic sampling was also performed and found to correlate closely with the samples obtained in the cyclone sampler. Flyash samples were analyzed for carbon, sulfur, calcium, magnesium, and ash. From these data SO_2 capture was determined two ways:

1) By Ca UTILIZATION:

$$\%\ \text{Ca UTILIZATION} = \underset{\text{in flyash}}{\left(\frac{\text{wt \% S}}{\text{wt \% Ca}}\right)} \times \left(\frac{40.08}{32.064}\right) \times 100.$$

and

$$\%\ SO_2\ \text{CAPTURE} = \%\ \text{Ca UTILIZATION} \times \text{Ca/S molar ratio}$$

where:

Ca/S molar ratio is determined from fuel and sorbent chemical analysis and measured feed rates

2) By Sulfur MASS BALANCE:

$$\%\ SO_2\ \text{CAPTURE} = \left[1 - \left[\frac{S_{in} - S_{out}}{S_{in}}\right]\right] \times 100$$

where:

S = Lbs/hr of sulfur into and out of furnace

S_{in} = (% S in coal/100) x (Lbs/hr coal)

S_{out} = is calculated by an ash tracer method:

$$S_{out} = \left(\frac{\text{\% S in flyash}}{\text{\% ASH in flyash}}\right) \times (\text{ASH in})$$

where:

ASH in = (Lbs/hr coal x % ASH in coal/100) +
(Lbs/hr sorbent x % ASH in sorbent/100)

SO_2 capture determined by these approaches is tabulated in Tables 6-7 and 6-8 for each test condition. For those tests where no flyash sample was obtained the SO_2 capture by G.A.S. only is reported. For baseline tests, SO_2, capture is reported as NA (not applicable). An overall average SO_2 capture is also reported for each test which is an average of the value calculated by the three methods discussed. The overall average percent SO_2 capture value has been used for all plots presenting the effects of injector variables on capture performance.

6.6.4.2 Capture Results

Figures 6-38 through 6-57 present SO_2 capture results obtained by in-furnace sorbent injection. These results show that SO_2 capture performance varies widely with the following sorbent injection operating and design variables:

- sorbent type
- injection location
- injector tilt
- injection velocity
- number of injectors
- carrier air flowrate

Sorbent type -- Figure 6-38 compares the performance of the three sorbents tested. This comparison is made for injection at Location A, with four injectors, -45° tilt, and an injection velocity of 100 ft/sec. It can be readily seen that sorbent A was the poorest performer in terms of SO_2 capture, sorbent B was better, and sorbent C had the best performance. This ranking of sorbent performance was consistent for all other injection locations tested but the magnitude of the improvements was not. Although the data is limited, it suggests that less difference in sorbent performance was obtained at the

Figure 6-38

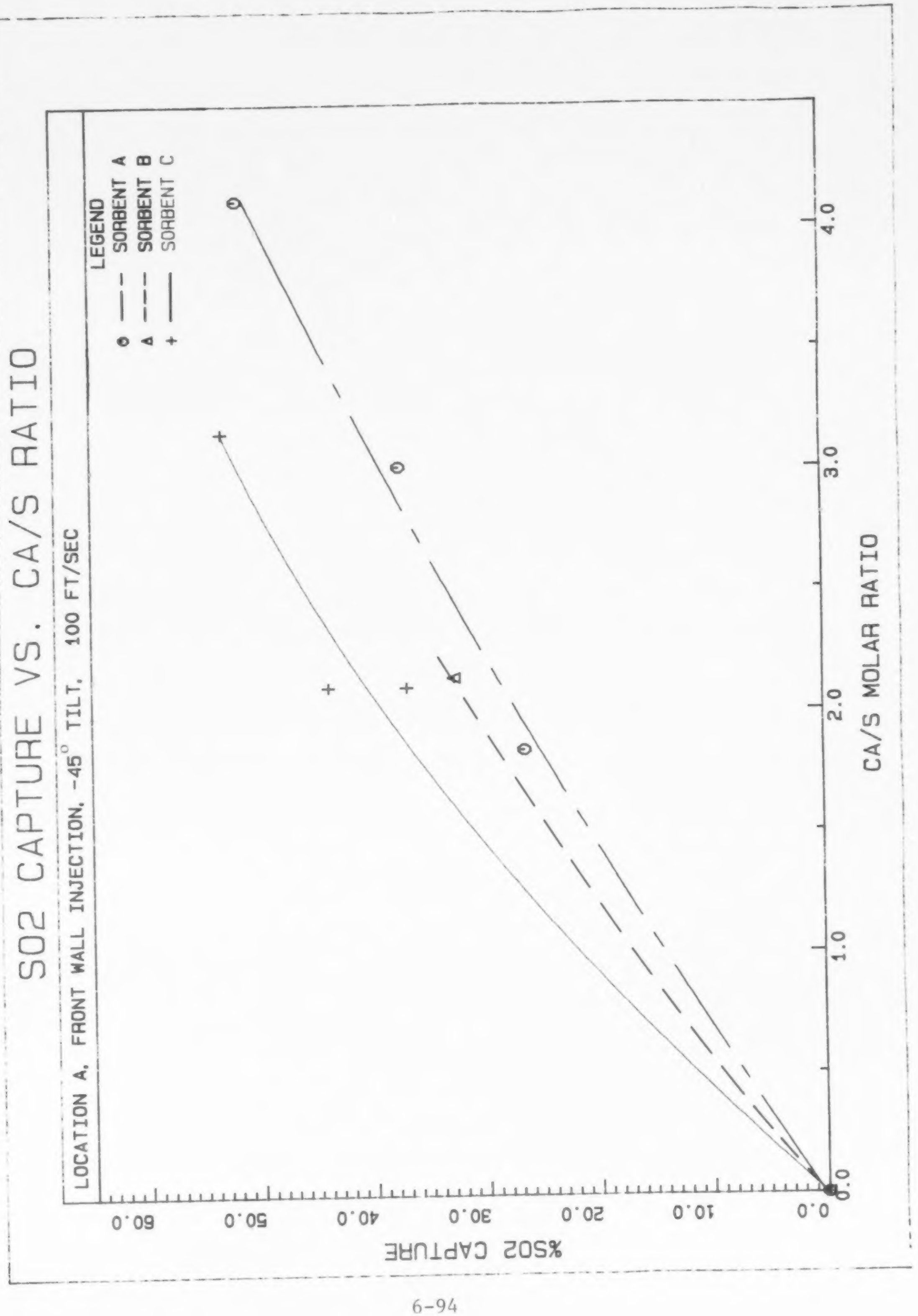
SO2 CAPTURE VS. CA/S RATIO
LOCATION A, FRONT WALL INJECTION, -45° TILT, 100 FT/SEC
LEGEND
⊙ —·— SORBENT A
△ — — SORBENT B
+ —— SORBENT C
%SO2 CAPTURE
0.0
10.0
20.0
30.0
40.0
50.0
60.0
CA/S MOLAR RATIO
0.0
1.0
2.0
3.0
4.0

low furnace injection position (Location D) and a greater degree of difference was obtained at the higher injection location (Location A). Specific differences in the percent SO_2 capture performance for sorbents were:

Sorbent A vs. B:

Sorbent B was better than A in % SO_2 capture by nine (9) to fifteen (15) percent (average of thirteen (13) percent) which equaled 3.5 to 4.0 percentage points of SO_2 capture (average of 3.8 percentage points). (i.e., SO_2 capture for A was 30%, SO_2 capture for B was 34% which equals 4 percentage points improvement or 13% improvement).

Sorbent B vs. C:

Sorbent C was better than B in % SO_2 capture by seven (7) to thirty (30) percent (average of eighteen (18) percent) which equaled 2 to 11 percentage points of SO_2 capture (average of 6 percentage points)

Sorbent A was untreated Black River hydrated lime, sorbent B was untreated Marblehead hydrated lime and sorbent C was treated Marblehead hydrated lime.

The relative SO_2 capture performances for sorbents A, B, and C correlate with the sorbent particle sizing. Sorbent C was the finest and had the best SO_2 capture performance. Sorbent A was the coarsests and had the poorest SO_2 capture performance. The magnitude by which the performance of sorbent C exceeded sorbents A and B, however, suggests that lignosulfonate treatment was an added benefit.

Injection location -- Figure 6-39 provides a comparison of front wall injection locations for sorbent A as a function of the calcium sulfur molar ratio (Ca/S). These tests were performed with four injectors at -45° tilt and injection at 100 ft/sec. At a Ca/S of 2:1 relatively poor SO_2 capture (less than 30%) was obtained for all locations. A trend of improved SO_2 capture with lower furnace locations was, however, also obtained. This result is consistent with the gas temperature distribution presented in Section 6.6.3.

Figure 6-39

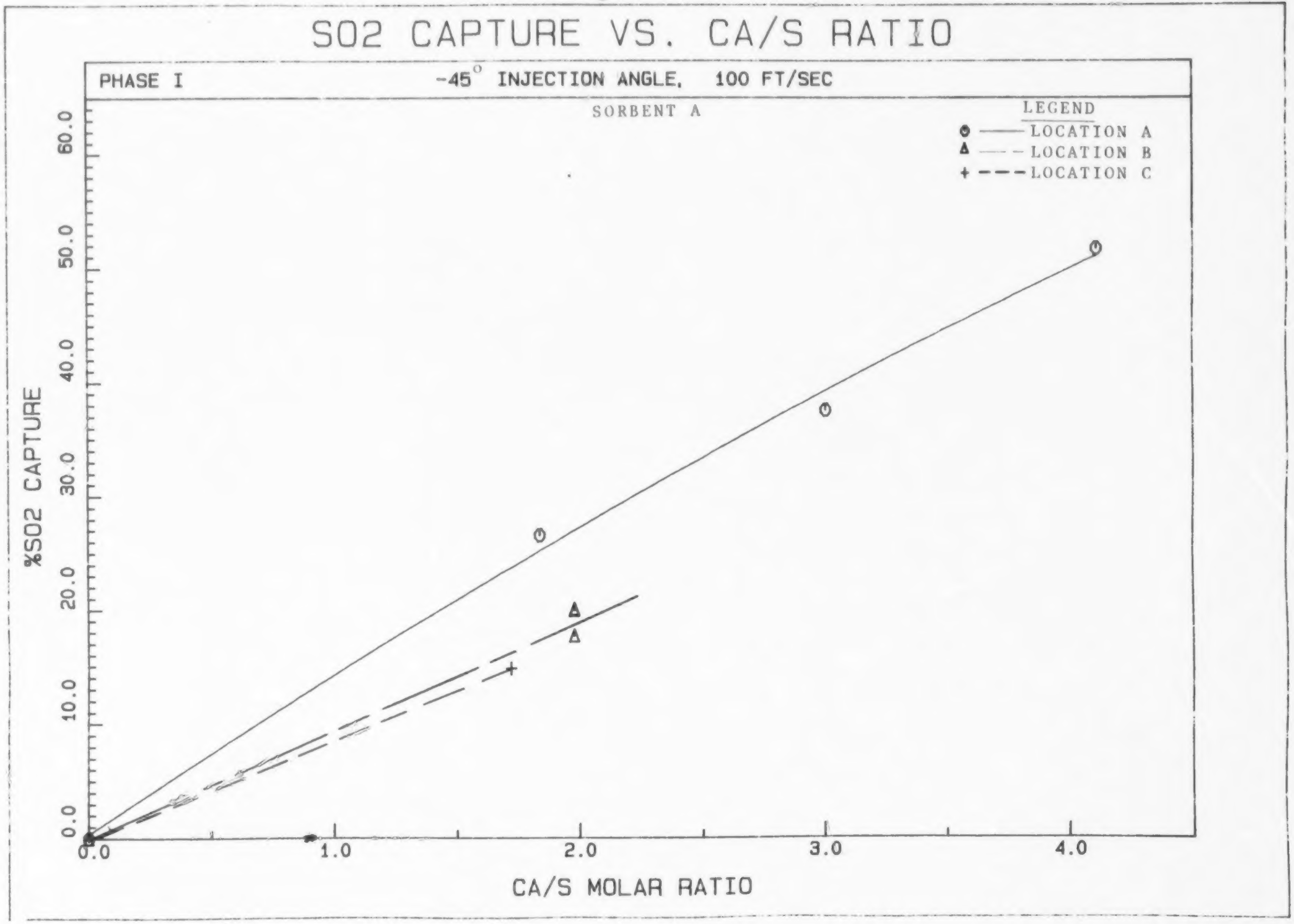
SO2 CAPTURE VS. CA/S RATIO
PHASE I
-45° INJECTION ANGLE, 100 FT/SEC
SORBENT A
LEGEND
LOCATION A
LOCATION B
LOCATION C
%SO2 CAPTURE
0.0
10.0
20.0
30.0
40.0
50.0
60.0
0.0
1.0
2.0
3.0
4.0
CA/S MOLAR RATIO

SO_2 capture data for Locations A, B, and C demonstrated improved performance with successively lower injection locations. On the basis of this data an even lower location was then tested (Location D on Figure 6-20). Figure 6-40 shows SO_2 capture data obtained at Location D as a function of Ca/S molar ratio for two different injector tilts (refer to Figure 6-19 for definition of level D injector tilts). This figure shows that at this location with upward tilt excellent SO_2 capture was obtained (~50%) at Ca/S = 2.0. However, at this location with downward injector tilt poor performance was obtained (~25% at Ca/S = 2.0). Thus an optimum injection location for sorbent C was identified which was below Location A and above Location D. Further data that follows will clarify this result. By comparison to Figure 6-29 one can see that the furnace gas temperatures in the region average from 2200°F to 2500°F. Below location D average furnace gas temperatures exceed 2500°F.

Injector tilt and injection velocity -- For a given furnace injection location, SO_2 capture performance varied with injector tilt and injection velocity. Figure 6-41 shows the SO_2 capture data obtained as a function of injector tilt for front wall injection Locations A, B, and C. The improvement in SO_2 capture performance with lower injection locations can again be seen. For Location A, downward injector tilt was much better than upward. This result may be explained on the basis of furnace gas temperatures. Furnace gas temperatures above Location A were less than 2100°F. Injection into such low gas temperatures should result in low SO_2 capture as witnessed by injection at Locations B and C. Upward injector tilt at Location A would have certainly caused sorbent to quickly penetrate to a low gas temperature region. Downward injector tilt at Location A would have resulted in much better mixing performance (discussed later in Figure 6-48) and would have exposed the sorbent to furnace gas temperatures of about 2300°F (average based on Figures 6-29 and 6-30).

Figure 6-41 also shows the lack of effect of injector tilt at Locations B and C. Cold flow studies showed little variation in mixing performance at Locations B and C for -20° vs. -45° tilt and since the furnace gas temperatures are unfavorably low in this region, it is not surprising that SO_2 capture was unaffected.

Figure 6-40

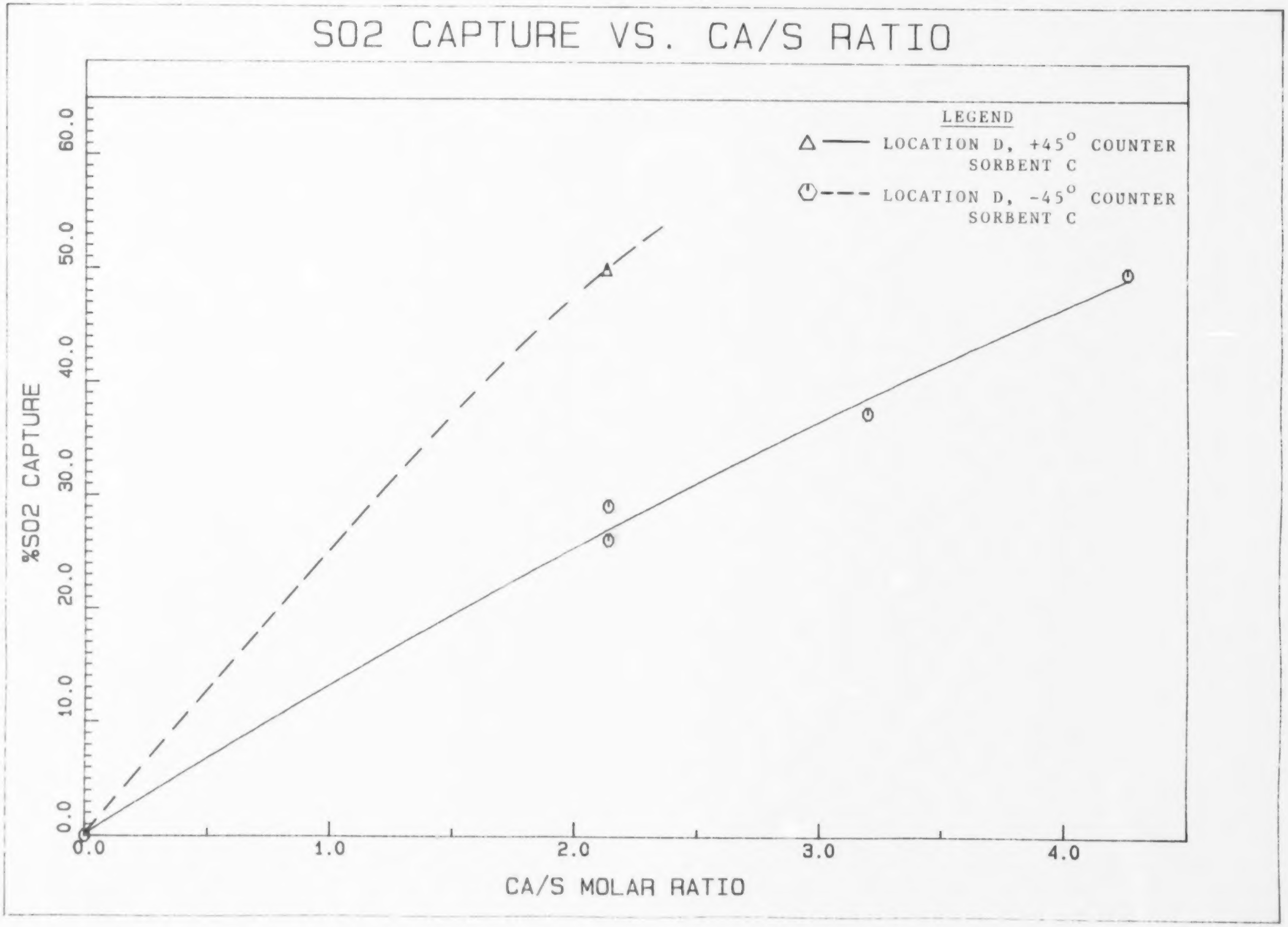
SO2 CAPTURE VS. CA/S RATIO
LEGEND
△—— LOCATION D, +45° COUNTER SORBENT C
○--- LOCATION D, -45° COUNTER SORBENT C
%SO2 CAPTURE
0.0
10.0
20.0
30.0
40.0
50.0
60.0
CA/S MOLAR RATIO
0.0
1.0
2.0
3.0
4.0

Figure 6-41

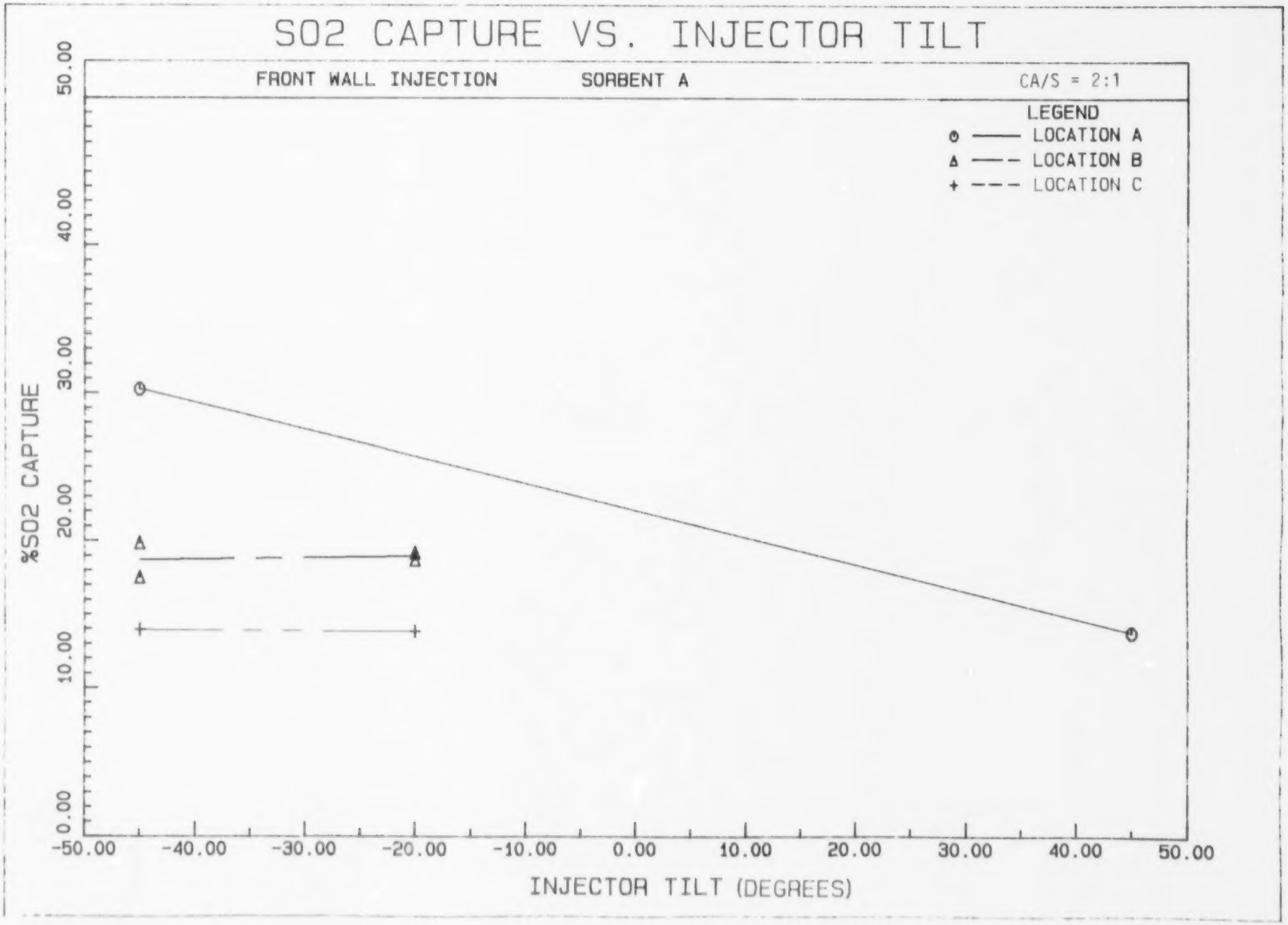
SO2 CAPTURE VS. INJECTOR TILT
FRONT WALL INJECTION
SORBENT A
CA/S = 2:1
LEGEND
LOCATION A
LOCATION B
LOCATION C
%SO2 CAPTURE
0.00
10.00
20.00
30.00
40.00
50.00
-50.00
-40.00
-30.00
-20.00
-10.00
0.00
10.00
20.00
30.00
40.00
50.00
INJECTOR TILT (DEGREES)

Figure 6-42 presents SO_2 capture results as a function of injection velocity for Locations B and C. These data show an optimum injection velocity of about 90 to 100 ft/sec. The optimum at 90 to 100 ft/sec suggests that for Locations B and C, lower injection velocity gives inadequate penetration, but very high velocities causes the sorbent to pass rapidly out the upper furnace into the convective pass where the gas temperatures are too low for the SO_2 capture reactions.

Extensive data on the effects of injector tilt and injection velocity was obtained for Location A. These data are presented in Figures 6-43 through 6-47. In several of these figures, data is given which compares Sorbents A, B, and C. In all cases the already discussed trend of relative SO_2 capture performance, being highest with Sorbent C and lowest with Sorbent A is observed.

Figures 6-43 and 6-44 show the effect of injector tilt at Location A. Figure 6-43 presents data with injection velocities ranging from 100-145 ft/sec. Figure 6-44 presents data with injection velocities ranging from 160-220 ft/sec. Interpreting these curves requires engineering judgement since there is incomplete data and as a result some inconsistencies can be extrapolated. However, it can be concluded from both figures that -90° tilt and +45° tilt are unfavorable while conversely, -45° and 0° tilt are favorable. Zero tilt may be slightly better than -45° tilt, although the linear curve fit for Sorbent A, shown in Figure 6-43 suggests that 0° tilt is poorer. This may be an erroneous conclusion because no actual data was obtained at the condition of zero tilt at Location A with Sorbent A. Furthermore that trend would be inconsistent with the data for Sorbents B and C.

Cold flow visualization studies support the trends of SO_2 capture at Location A as functions of both injection tilt and velocity. Figure 6-45 presents sketches of smoke tracer studies recorded on videotape. It can be seen that zero degree injector tilt gave good dispersion of the smoke tracer and -45° tilt was the most favorable condition for Location A based on cold flow mixing. Tilts of +45°, +20°, and -90° gave poor dispersion of the smoke tracer.

Figure 6-42

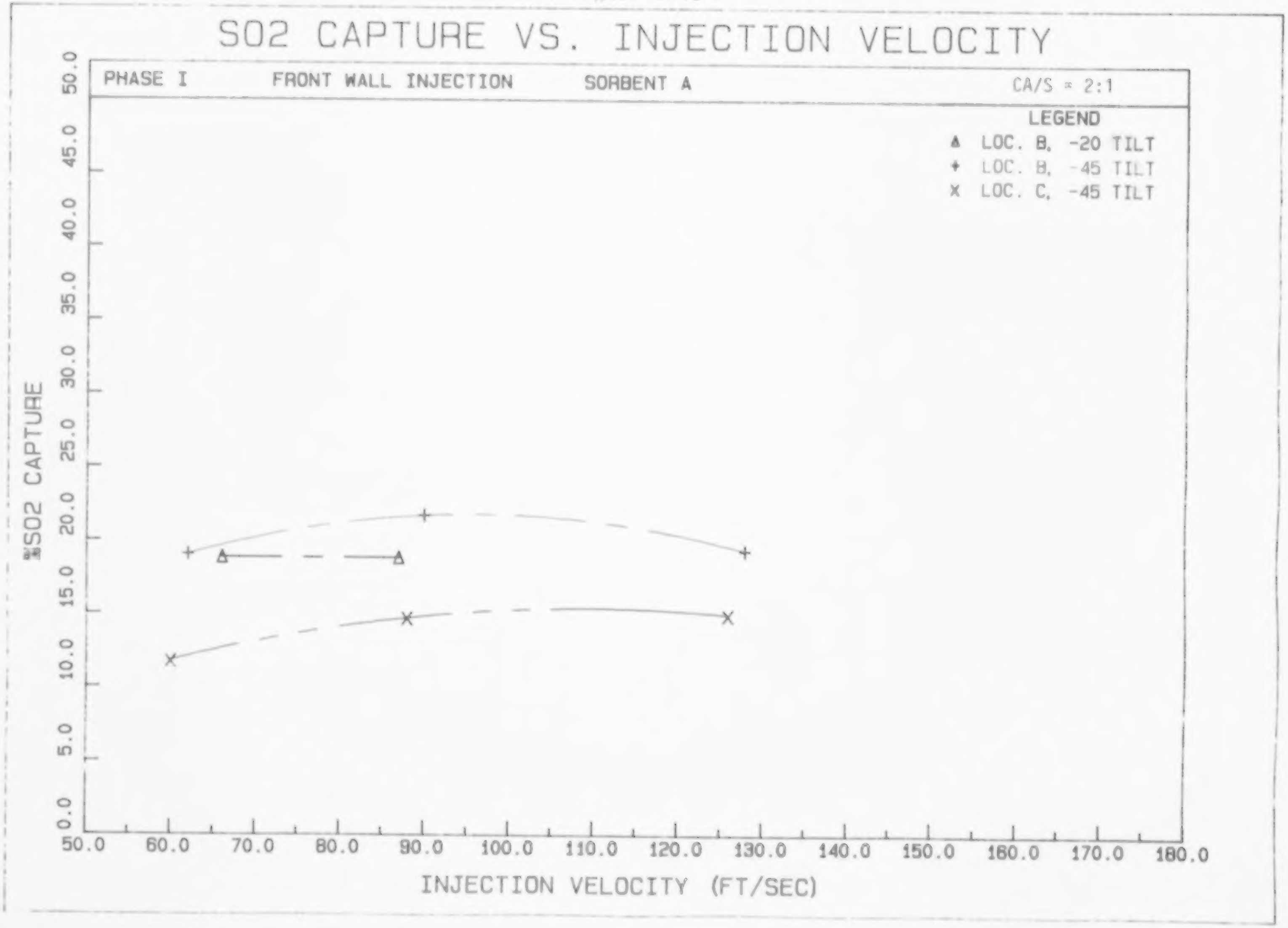
SO2 CAPTURE VS. INJECTION VELOCITY
PHASE I
FRONT WALL INJECTION
SORBENT A
CA/S = 2:1
LEGEND
▲ LOC. B, -20 TILT
+ LOC. B, -45 TILT
× LOC. C, -45 TILT
%SO2 CAPTURE
0.0
5.0
10.0
15.0
20.0
25.0
30.0
35.0
40.0
45.0
50.0
50.0
60.0
70.0
80.0
90.0
100.0
110.0
120.0
130.0
140.0
150.0
160.0
170.0
180.0
INJECTION VELOCITY (FT/SEC)

Figure 6-43

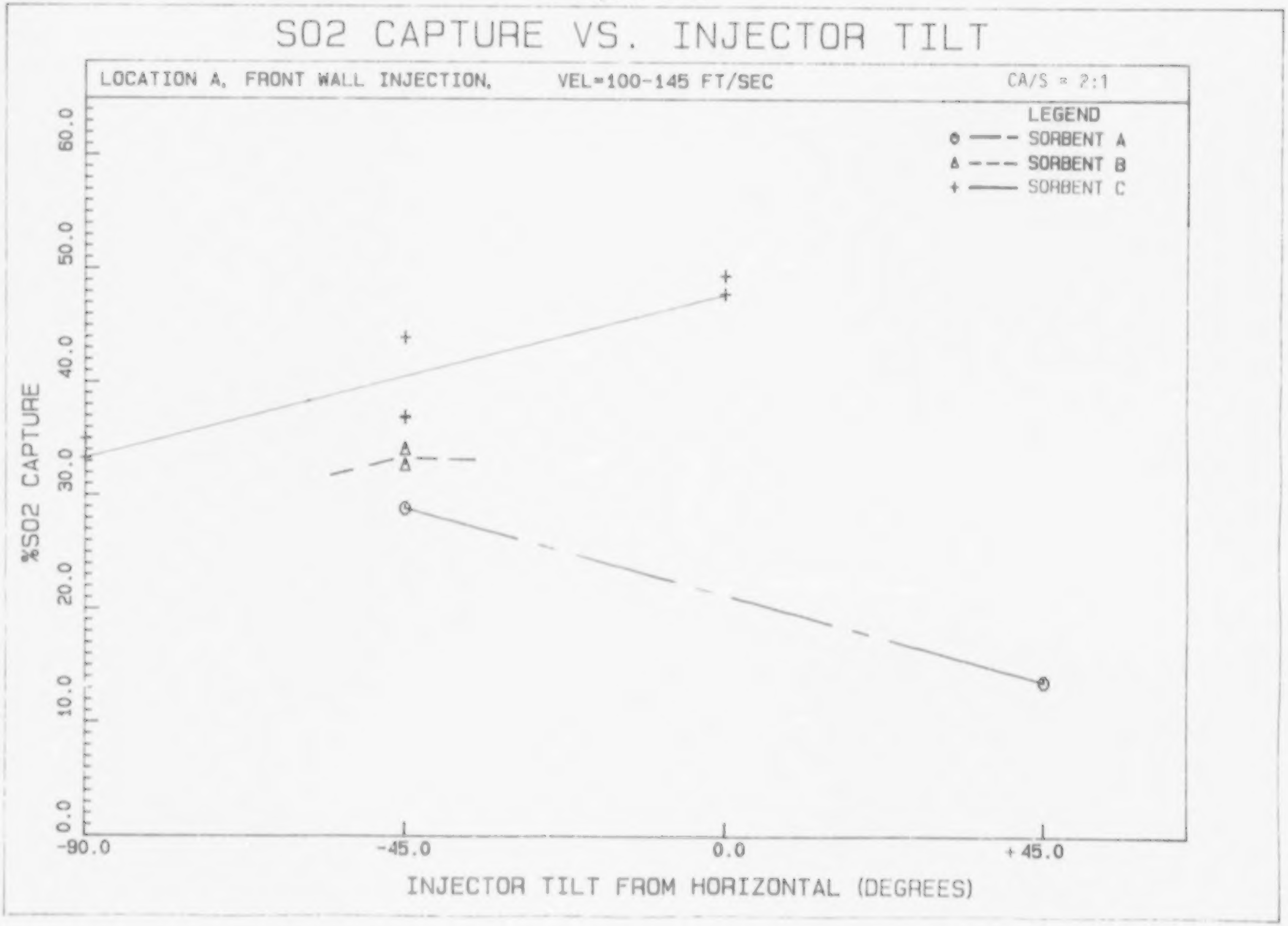
SO2 CAPTURE VS. INJECTOR TILT
LOCATION A, FRONT WALL INJECTION,
VEL=100-145 FT/SEC
CA/S = 2:1
LEGEND
SORBENT A
SORBENT B
SORBENT C
%SO2 CAPTURE
0.0
10.0
20.0
30.0
40.0
50.0
60.0
-90.0
-45.0
0.0
+45.0
INJECTOR TILT FROM HORIZONTAL (DEGREES)

Figure 6-44

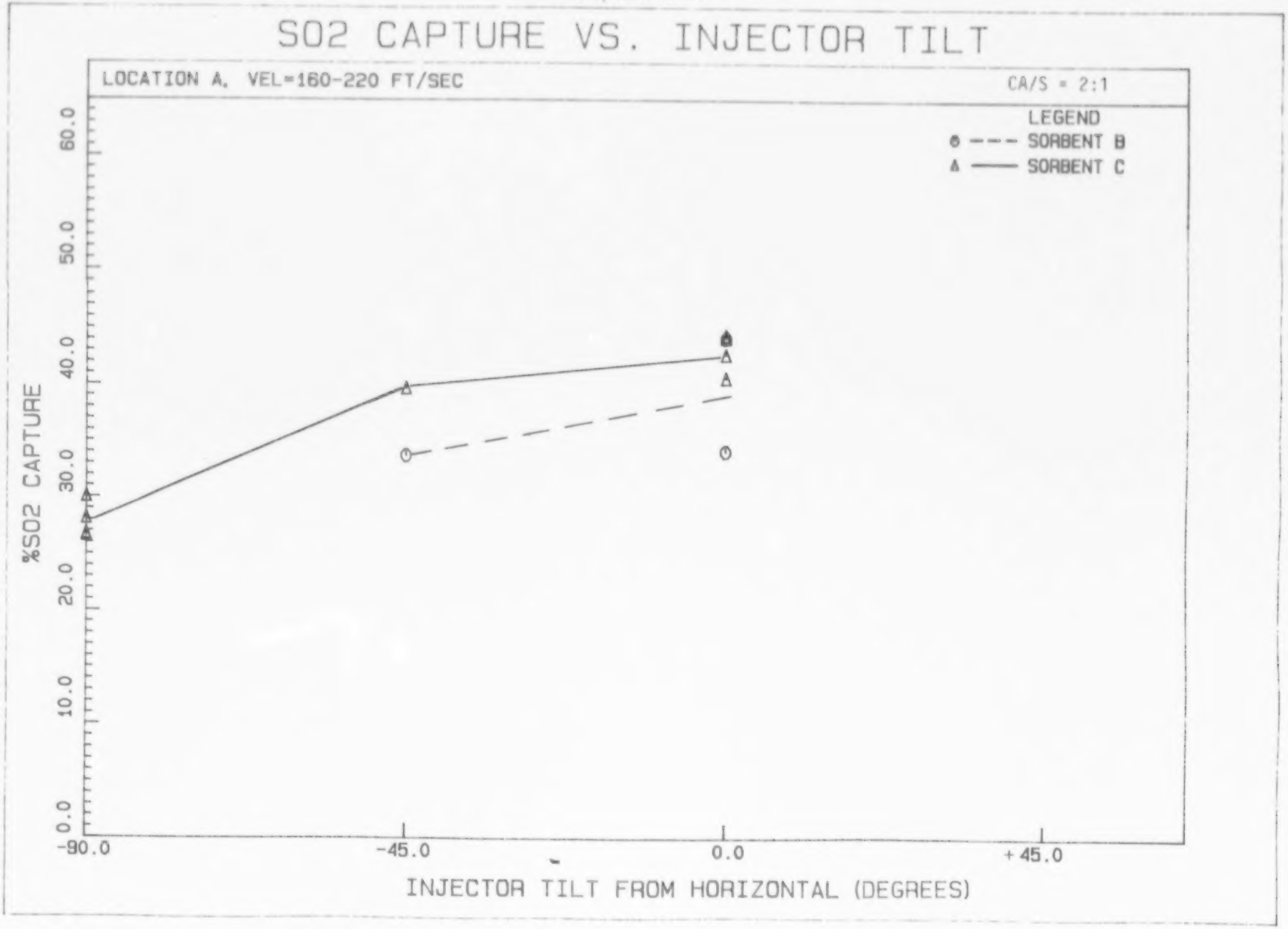
SO2 CAPTURE VS. INJECTOR TILT
LOCATION A, VEL=160-220 FT/SEC
CA/S = 2:1
LEGEND
SORBENT B
SORBENT C
%SO2 CAPTURE
0.0
10.0
20.0
30.0
40.0
50.0
60.0
-90.0
-45.0
0.0
+45.0
INJECTOR TILT FROM HORIZONTAL (DEGREES)

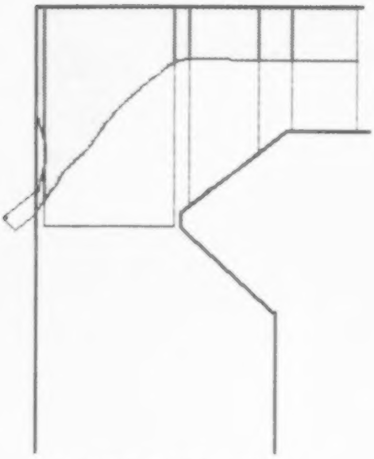

LOCATION A +45° TILT

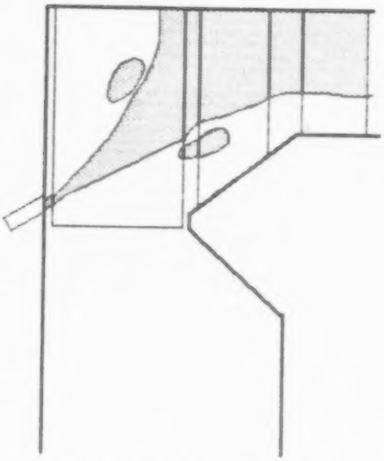

LOCATION A + 20°

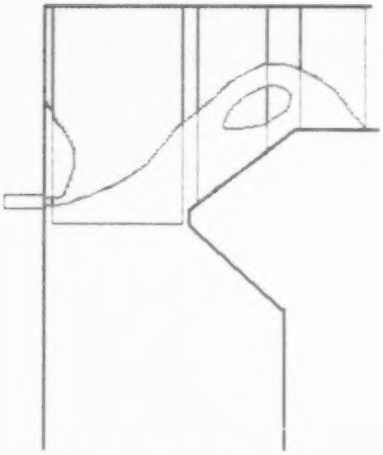

LOCATION A 0° TILT

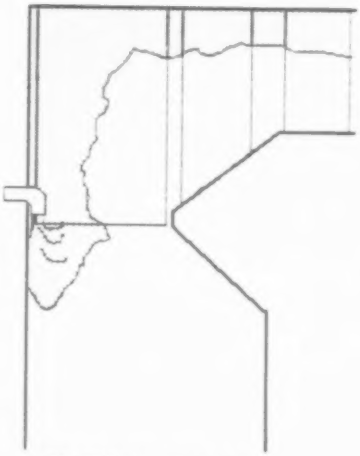

LOCATION A -90° TILT

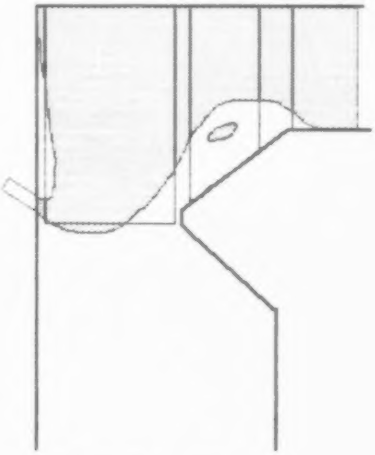

LOCATION A -45° TILT

Figure 6-45. Flow visualization results for Location A injection at various tilts.

Although cold flow mixing studies showed -45° injector tilt to be better than zero degree tilt, SO_2 capture data is the opposite. The reason may be the thermal environment of injection. Figures 6-46, 6-47, and 6-48 show that at location A, tradeoffs between the thermal environment of injection and the degree of sorbent dispersion result in differences in SO_2 capture levels. These figures present % SO_2 capture versus injection velocity at 0°, -90°, and -45° tilt respectively. Figure 6-46 (0°- tilt) shows that SO_2 capture clearly drops with increased injection velocity. Cold flow testing showed that at 0° tilt increased velocity helped penetration, but not dispersion. Increased velocity did not change the effective elevation of sorbent injection. Therefore the sorbent was exposed to the same furnace gas temperatures regardless of velocity and SO_2 capture dropped with injection velocity at 0° tilt as a result of diminished sorbent jet dispersion.

Figure 6-47 (-90° tilt) also shows that SO_2 capture dropped with increased injection velocity, and seems to level off at velocities between 150 and 200 ft/sec. Although -90° tilt was not tested during cold flow studies, the mixing patterns are speculated in Figure 6-45. Relatively poor dispersion performance is hypothesized, and it is likely that the effective elevation of sorbent injection was lowered with increased velocity. Therefore the SO_2 capture trend may be explained on the basis of exposure to excessive furnace gas temperatures. Above injection velocities of 150 ft/sec, the sorbent jet may penetrate within the lower furnace tangential flow field and improved mixing may offset excessive gas temperatures. Overall -90° injector tilt produced poor SO_2 capture, so the exact mechanisms suggested here are not critical.

Figure 6-48 (-45° tilt) shows essentially constant SO_2 removal regardless of injection velocity. Again this result is likely due to tradeoffs between the thermal environment of injection and the effectiveness of sorbent dispersion. Figure 6-45 presented smoke tracer results for location A with -45° injector tilt. This tilt produced the best sorbent dispersion at Location A. Increased injection velocity with -45° tilt appeared to enhance dispersion through increased turbulence levels. Increased injection velocity also lowered the effective elevation of injection and thus it exposed the

Figure 6-46

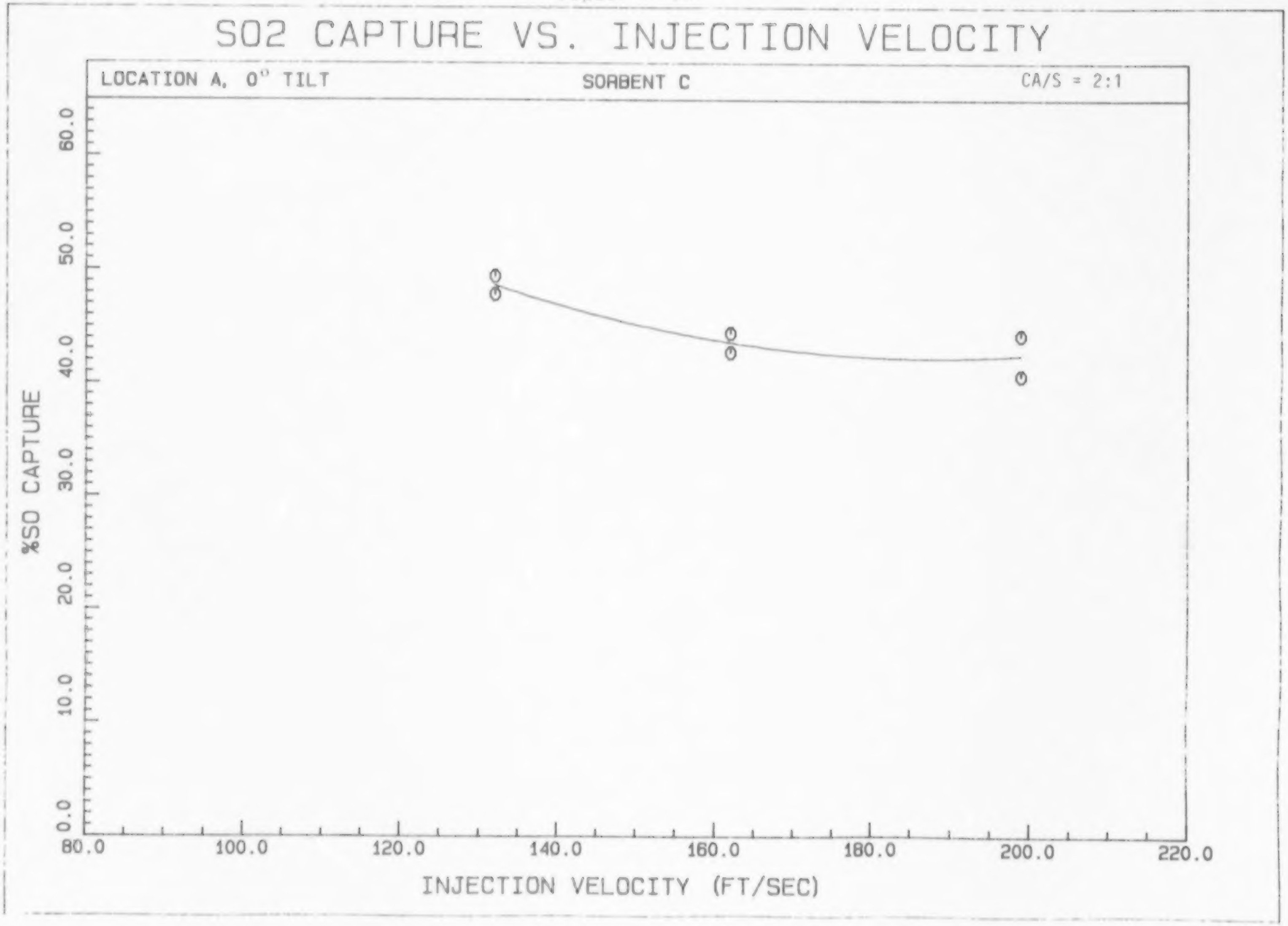
SO2 CAPTURE VS. INJECTION VELOCITY
LOCATION A, 0° TILT
SORBENT C
CA/S = 2:1
%SO CAPTURE
0.0
10.0
20.0
30.0
40.0
50.0
60.0
80.0
100.0
120.0
140.0
160.0
180.0
200.0
220.0
INJECTION VELOCITY (FT/SEC)

Figure 6-47

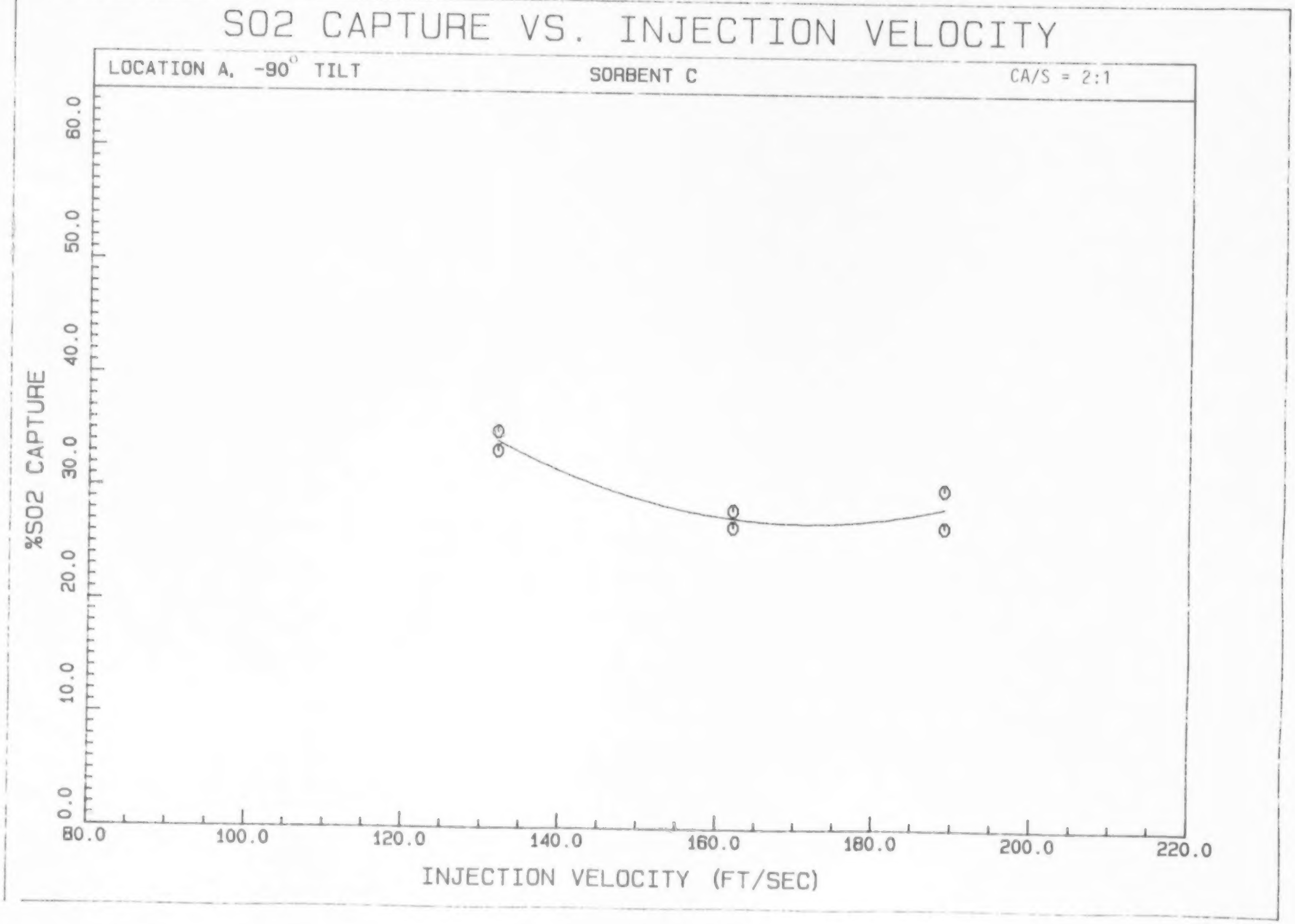
SO2 CAPTURE VS. INJECTION VELOCITY
LOCATION A, -90° TILT
SORBENT C
CA/S = 2:1
%SO2 CAPTURE
0.0
10.0
20.0
30.0
40.0
50.0
60.0
80.0
100.0
120.0
140.0
160.0
180.0
200.0
220.0
INJECTION VELOCITY (FT/SEC)

Figure 6-48

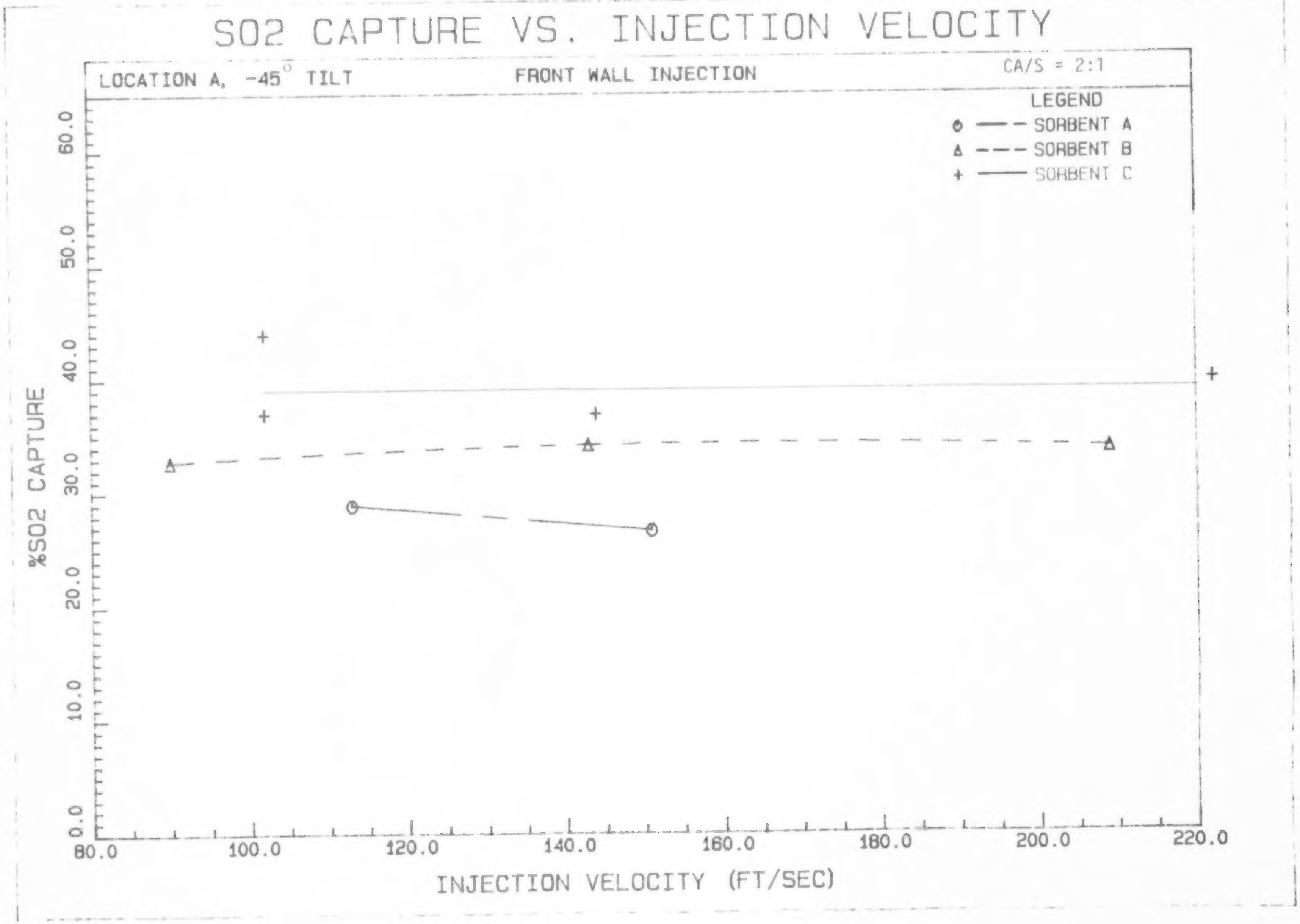
SO2 CAPTURE VS. INJECTION VELOCITY
LOCATION A, -45° TILT
FRONT WALL INJECTION
CA/S = 2:1
LEGEND
⊖ SORBENT A
△ SORBENT B
+ SORBENT C
%SO2 CAPTURE
0.0
10.0
20.0
30.0
40.0
50.0
60.0
80.0
100.0
120.0
140.0
160.0
180.0
200.0
220.0
INJECTION VELOCITY (FT/SEC)

sorbent to progressively higher injection temperatures. Therefore, the SO_2 capture trends presented in Figure 6-48 are believed due to a direct tradeoff between improved mixing versus increased furnace gas temperature at the point of injection.

On the basis of the lower than expected SO_2 capture efficiencies obtained at Location A and the measured furnace gas temperatures presented in Section 6.6.3, an injection location lower in the furnace (Location D on Figure 6-20) was also tested. At Location D, injectors were mounted in each of the four corners of the furnace and sorbent injection was into the furnace tangential flow field below the arch. Furthermore, cold flow mixing studies showed that Location D provided the best overall sorbent dispersion of all the sorbent injection locations studied.

Figures 6-49, 6-50, and 6-51 are sketches of the flow visualization results recorded by video for Location D with various injection tilts and injection velocities. These are plan views of smoke tracer dispersion as viewed from the furnace hopper. Figure 6-49 shows that counter-current injection (injection against the direction of the swirling furnace flow field) yielded better dispersion than co-current injection. Figure 6-50 shows that sorbent dispersion with counter-current injection was enhanced with increased injection velocity. Lastly, Figure 6-51 shows the effect of upward versus downward injector tilt with counter-current injection at Location D. From the standpoint of mixing, counter-current injection with -45° tilt was the most favorable condition at Location D.

Figures 6-52 and 6-53 present the SO_2 capture data obtained at Location D for various injection conditions. Figure 6-52 shows the effect of injector tilt. Injector tilt at Location D was defined in Figure 6-19. SO_2 capture gradually improved as injector tilt was varied from downward tilt (-45° counter) to upward tilt (+45°). This trend is opposite that of improved sorbent mixing and is due to furnace gas temperatures. As discussed in Section 6.6.3 and shown in Figure 6-30, furnace gas temperatures at Location D averaged about 2500°F. The average furnace gas temperature just two feet above Location D (at the bottom of the furnace arch) was 2350°F and five feet

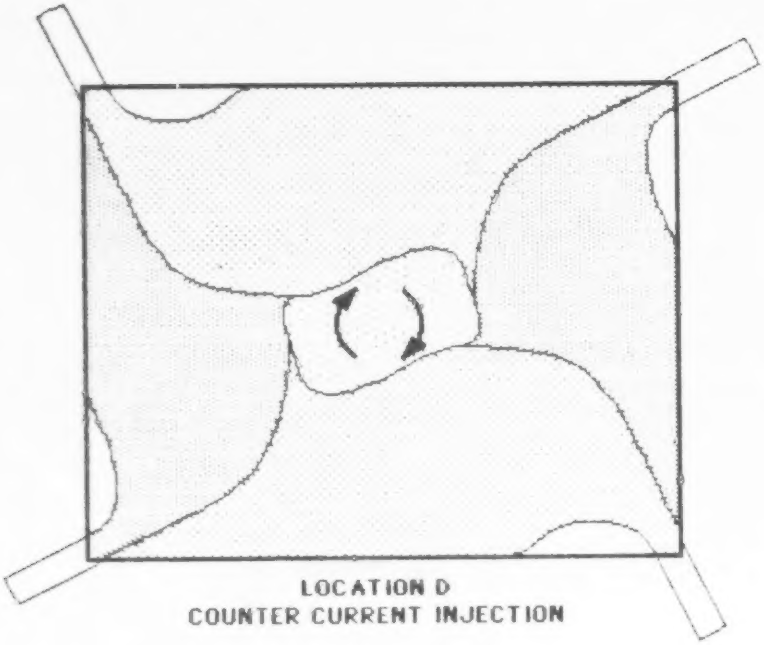

LOCATION D
COUNTER CURRENT INJECTION

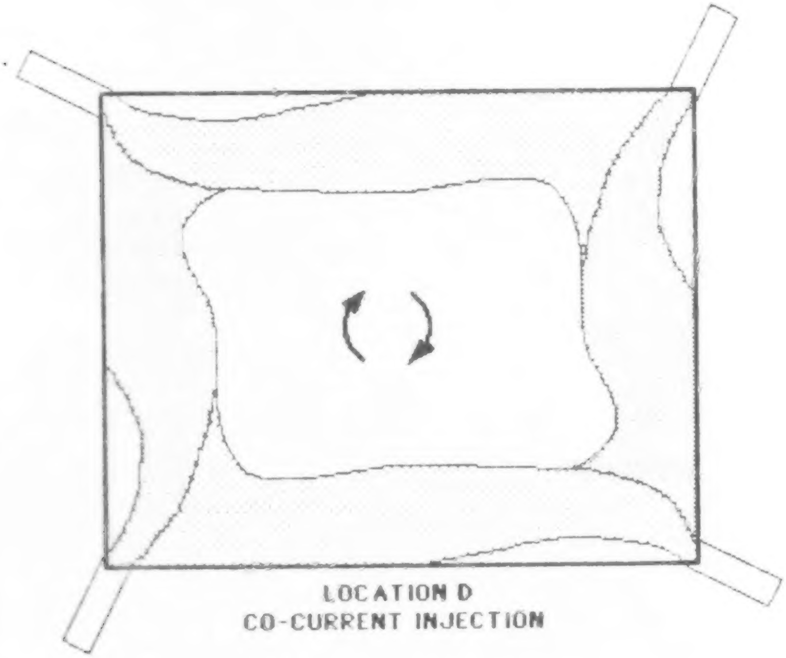

LOCATION D
CO-CURRENT INJECTION

Figure 6-49. Flow visualization results for Location D injection, counter-current vs. co-current injection.

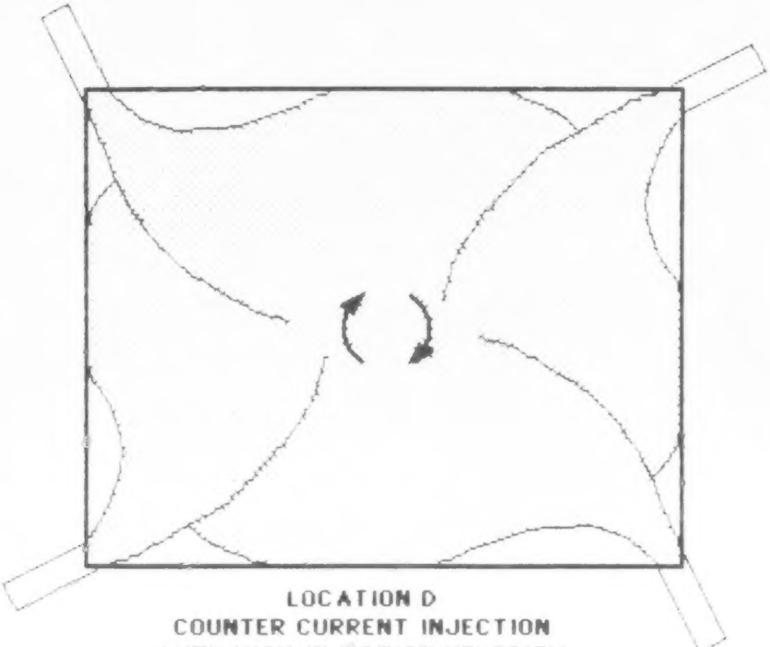

LOCATION D
COUNTER CURRENT INJECTION
WITH HIGH INJECTION VELOCITY

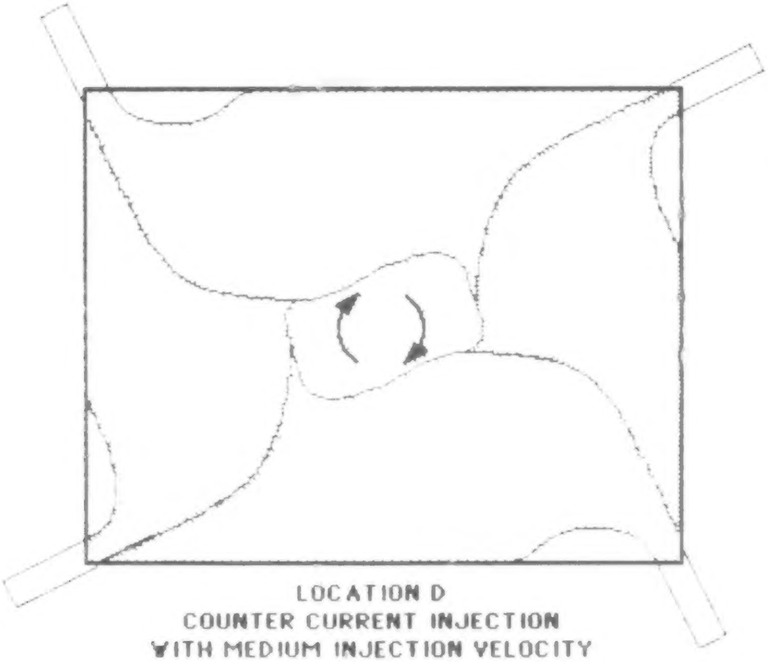

LOCATION D
COUNTER CURRENT INJECTION
WITH MEDIUM INJECTION VELOCITY

Figure 6-50. Flow visualization results for Location D injection as a function of injection velocity.

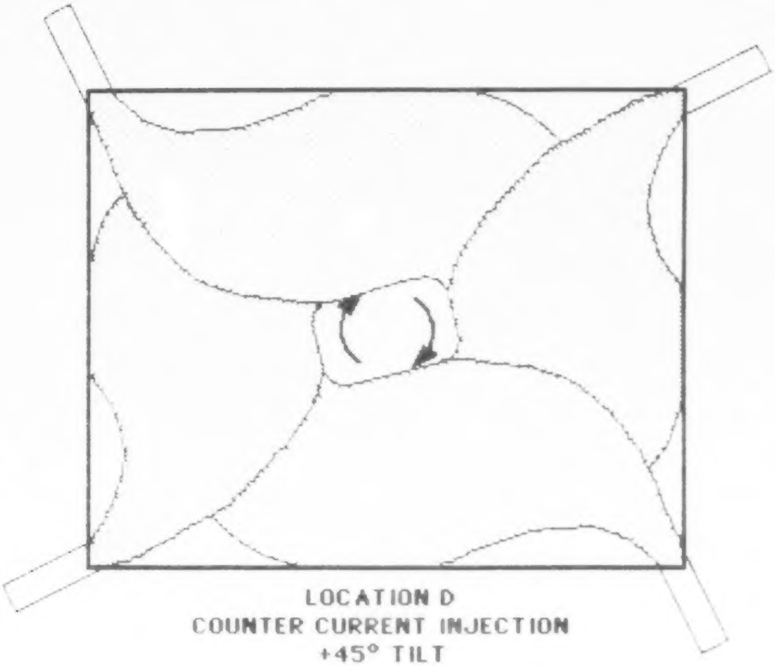

LOCATION D
COUNTER CURRENT INJECTION
+45° TILT

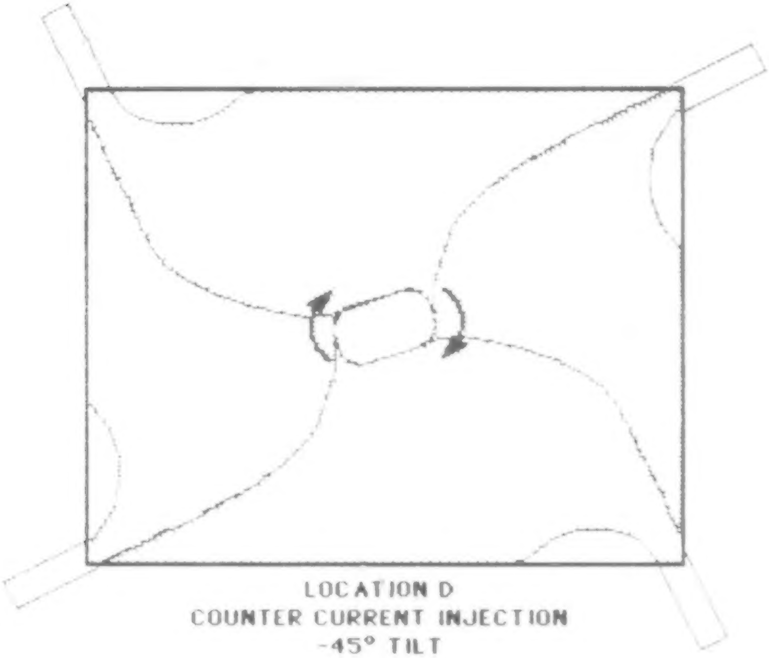

LOCATION D
COUNTER CURRENT INJECTION
-45° TILT

Figure 6-51. Flow visualization results for Location D injection as a function of injector tilt.

Figure 6-52

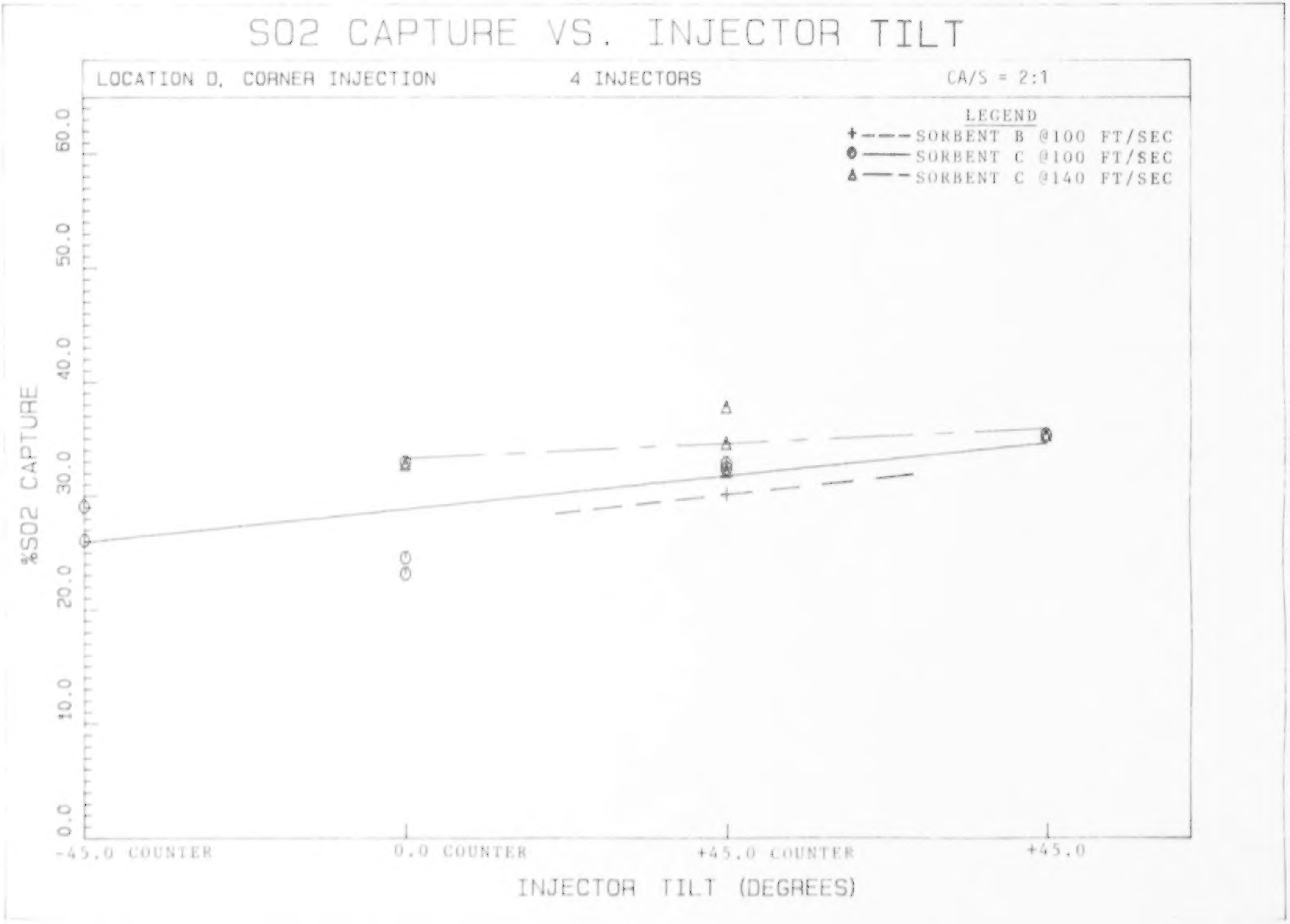
SO2 CAPTURE VS. INJECTOR TILT
LOCATION D, CORNER INJECTION
4 INJECTORS
CA/S = 2:1
LEGEND
SORBENT B @100 FT/SEC
SORBENT C @100 FT/SEC
SORBENT C @140 FT/SEC
%SO2 CAPTURE
0.0
10.0
20.0
30.0
40.0
50.0
60.0
-45.0 COUNTER
0.0 COUNTER
+45.0 COUNTER
+45.0
INJECTOR TILT (DEGREES)

Figure 6-53

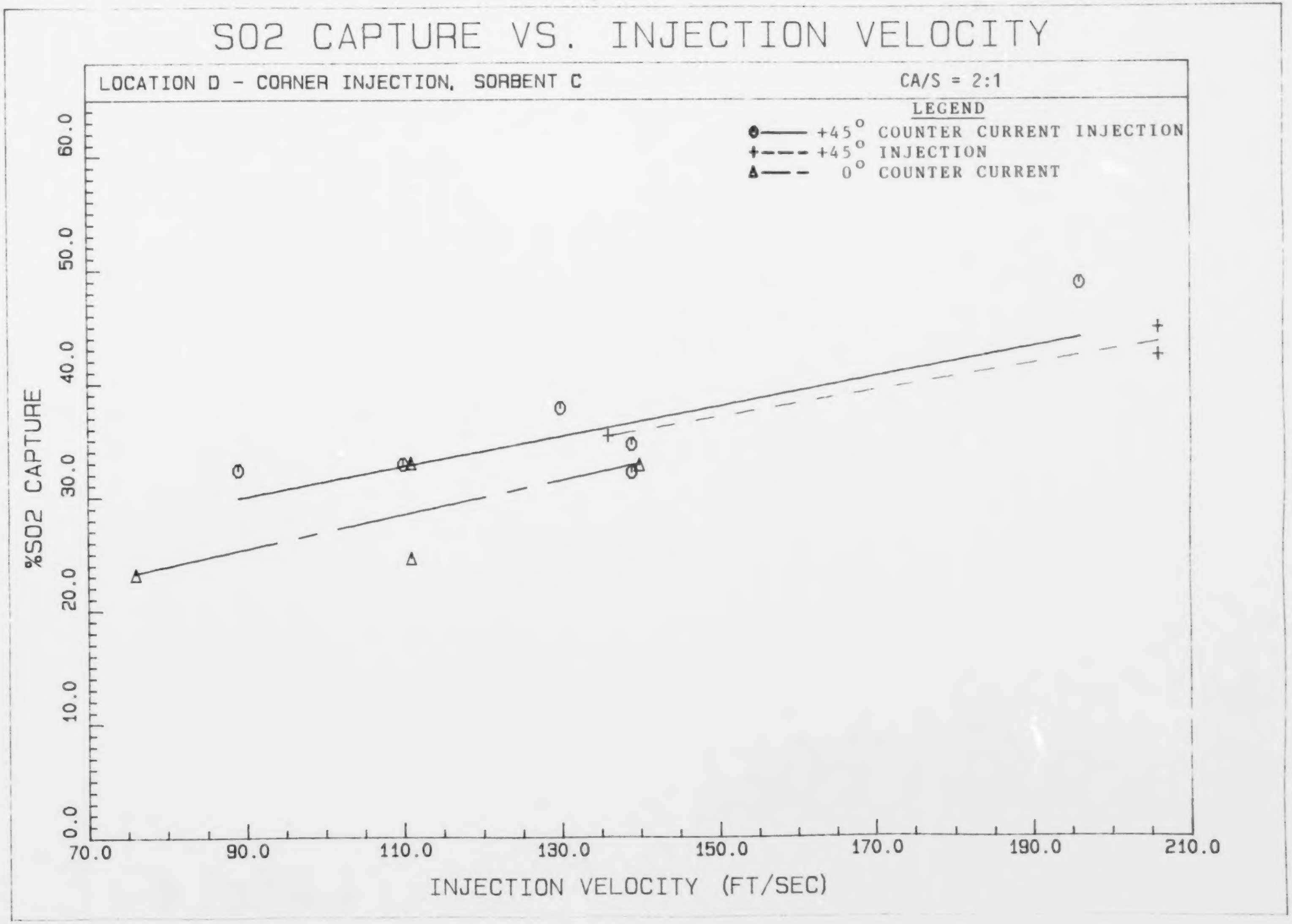
SO2 CAPTURE VS. INJECTION VELOCITY
LOCATION D - CORNER INJECTION, SORBENT C
CA/S = 2:1
LEGEND
+45° COUNTER CURRENT INJECTION
+45° INJECTION
0° COUNTER CURRENT
%SO2 CAPTURE
0.0
10.0
20.0
30.0
40.0
50.0
60.0
70.0
90.0
110.0
130.0
150.0
170.0
190.0
210.0
INJECTION VELOCITY (FT/SEC)

above Location D (at the centerline of the furnace arch or horizontal furnace outlet plane) it was 2200°F. Downward (-45° tilt) or horizontal (0° tilt) injection at Location D likely exposed the sorbent to excessive furnace gas temperatures (certainly greater than 2400°F). Upward injection (+45° countercurrent or +45°) produced sorbent jets which quickly penetrated into the more favorable furnace gas temperatures of 2350 - 2250°F. These data show that although Location D was actually lower than the ideal location, injector tilt could be used to compensate by changing the effective sorbent injection elevation.

Figure 6-53 shows SO_2 capture as a function of injection velocity for Location D. For all three injector tilts, SO_2 capture performance improved with increased injection velocity. This result is likely due to both enhanced mixing (as shown in Figure 6-50) and more rapid jet penetration into the more favorable furnace gas temperatures.

From the SO_2 capture results at Locations A and D with four injectors the following conclusions can be drawn; 1) downward tilt at Location A was best, and 2) upward tilt at Location D was best, therefore 3) the optimum sorbent injection location was between Locations A and D where the furnace gases ranged in temperature from 2400°F to 2200°F.

Number of injectors and carrier air flowrate -- Another approach for enhancing dispersion is to increase the number of injectors. This was studied by tests with six (6) and eight (8) injectors which combines sorbent injection at Locations A and D. Tests were also performed to study the effect of carrier air flow rate. Figures 6-54, 6-55, and 6-56 present the SO_2 capture results from these tests.

Figure 6-54 shows % SO_2 capture versus injection velocity for eight total injectors; four at Location A with -45° tilt, and four at Location D with +45° tilt. Three curves are presented which differ in the sorbent carrier air mass flow rate. The nominal carrier air mass flow was 2000 lbs/hr which equalled 5% of the total air. Higher airflows were also studied because cold flow testing showed that eight injectors resulted in poorer mixing performance than

Figure 6-54

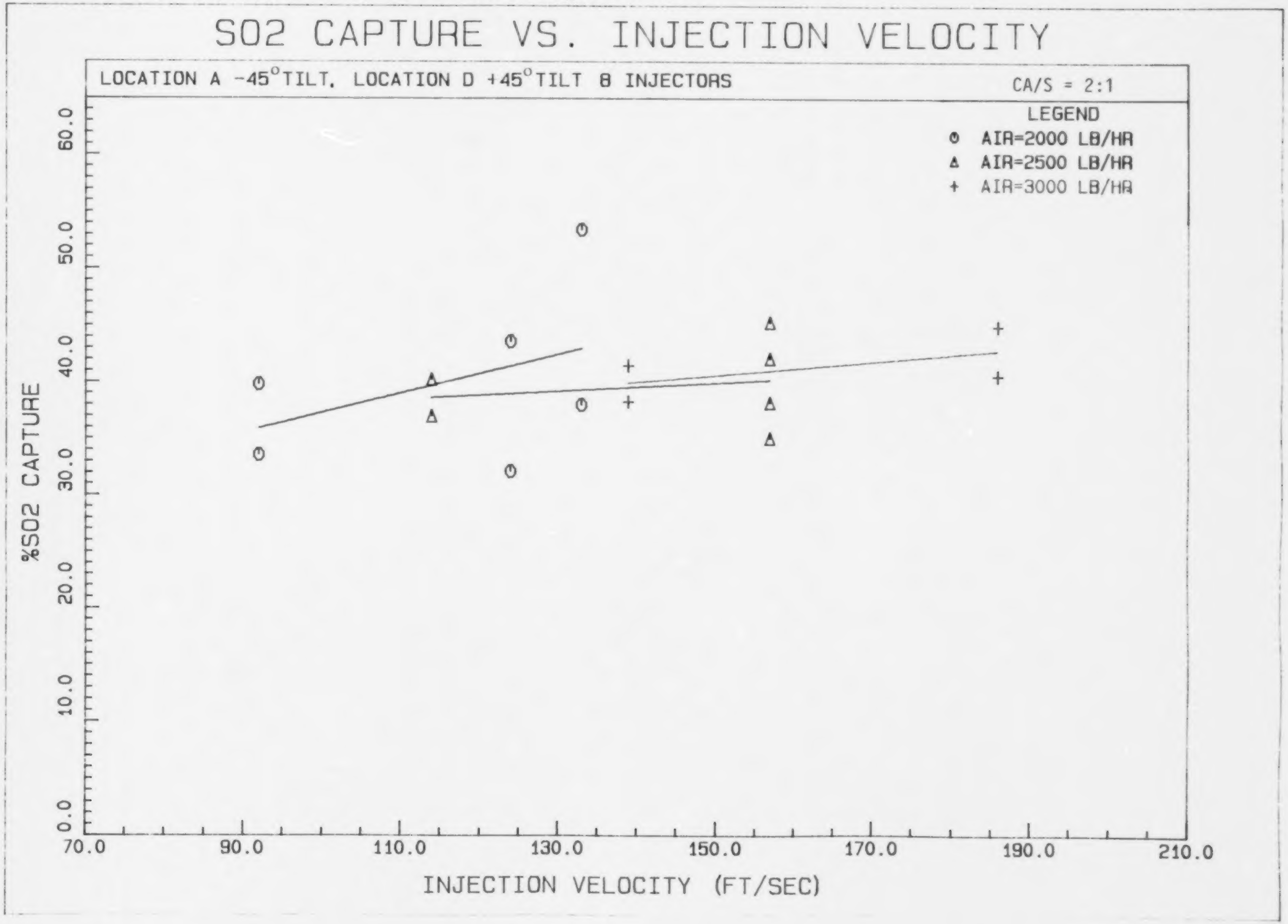
SO2 CAPTURE VS. INJECTION VELOCITY
LOCATION A -45°TILT, LOCATION D +45°TILT 8 INJECTORS
CA/S = 2:1
LEGEND
○ AIR=2000 LB/HR
△ AIR=2500 LB/HR
+ AIR=3000 LB/HR
%SO2 CAPTURE
0.0
10.0
20.0
30.0
40.0
50.0
60.0
70.0
90.0
110.0
130.0
150.0
170.0
190.0
210.0
INJECTION VELOCITY (FT/SEC)

Figure 6-55

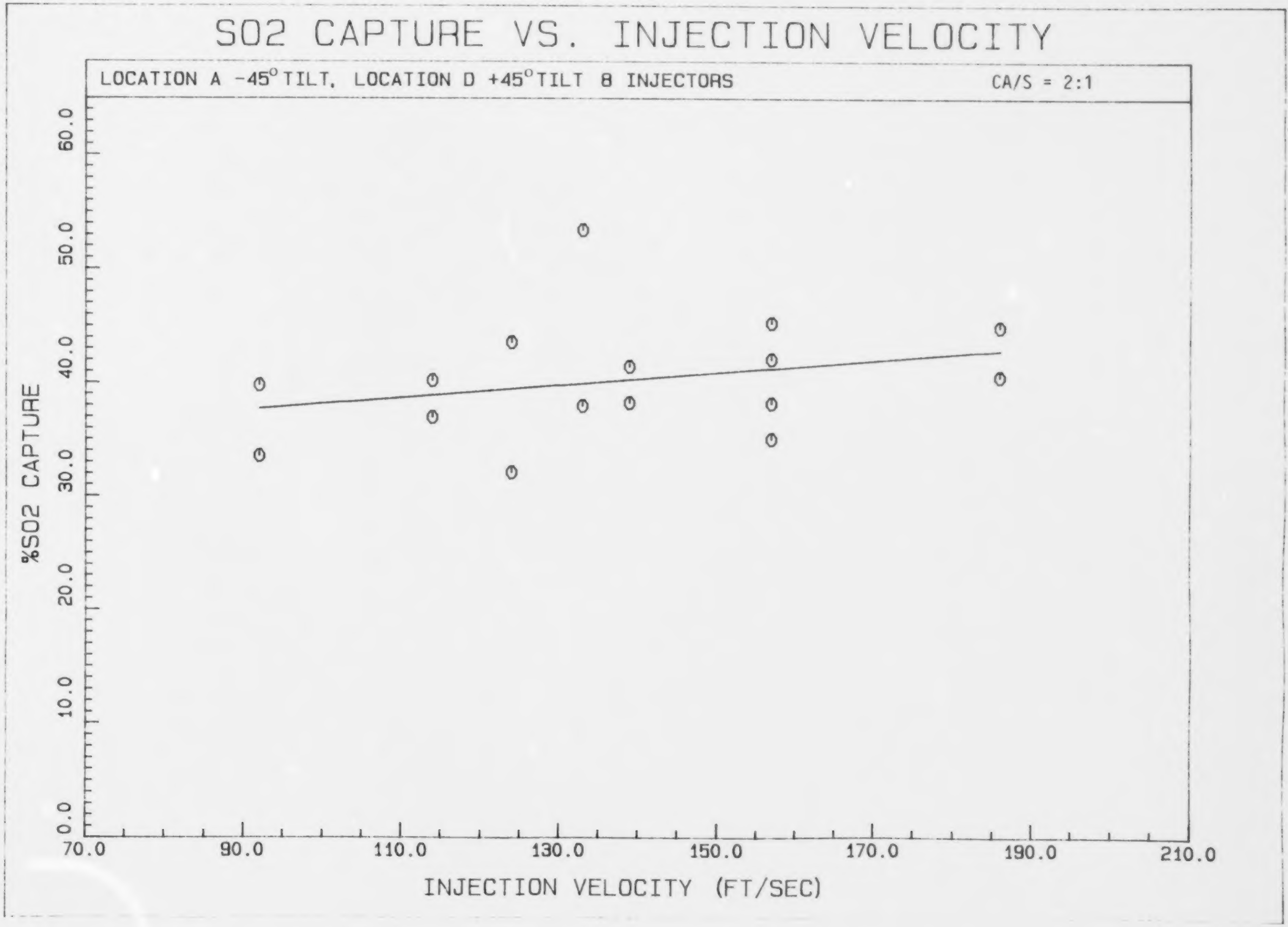
S02 CAPTURE VS. INJECTION VELOCITY
LOCATION A -45° TILT, LOCATION D +45° TILT 8 INJECTORS
CA/S = 2:1
%S02 CAPTURE
0.0
10.0
20.0
30.0
40.0
50.0
60.0
70.0
90.0
110.0
130.0
150.0
170.0
190.0
210.0
INJECTION VELOCITY (FT/SEC)

Figure 6-56

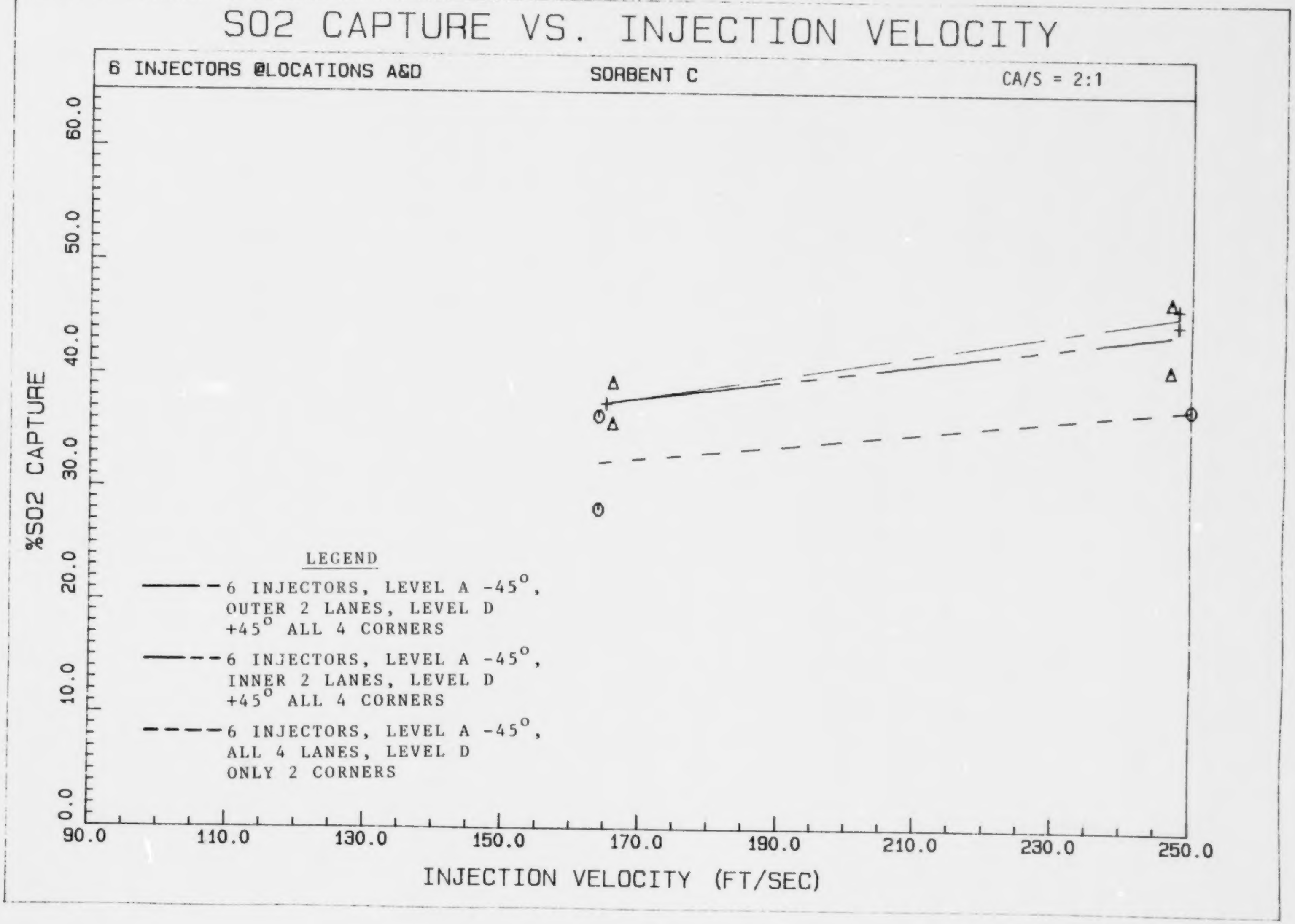
SO2 CAPTURE VS. INJECTION VELOCITY
6 INJECTORS @LOCATIONS A&D
SORBENT C
CA/S = 2:1
%SO2 CAPTURE
0.0
10.0
20.0
30.0
40.0
50.0
60.0
INJECTION VELOCITY (FT/SEC)
90.0
110.0
130.0
150.0
170.0
190.0
210.0
230.0
250.0
LEGEND
6 INJECTORS, LEVEL A -45°, OUTER 2 LANES, LEVEL D +45° ALL 4 CORNERS
6 INJECTORS, LEVEL A -45°, INNER 2 LANES, LEVEL D +45° ALL 4 CORNERS
6 INJECTORS, LEVEL A -45°, ALL 4 LANES, LEVEL D ONLY 2 CORNERS

four when injection velocity and carrier air mass flow were held constant. Figure 6-54 shows that regardless of carrier air flow rate, SO_2 capture improved with increased injection velocity. Here injection velocity was varied by changing injector nozzle diameter.

Figure 6-55 is a replot of the data in Figure 6-54 and reflects this observation. It can, therefore, be concluded that SO_2 capture was improved by increased injection velocity either if the velocity was increased by restricting nozzle diameter or by increasing the carrier air flow rate. Since SO_2 capture did not improve at Location A alone with increased velocity (Figure 6-47) but did at Location D alone (Figure 6-53), this result with eight (8) injectors must be attributed to Location D.

Figure 6-56 presents SO_2 capture data obtained with six (6) injectors for various combinations of the Location A and D injection ports. This figure shows that four (4) injectors at Location D and two (2) at Location A produced higher SO_2 capture than four (4) at Location A and two (2) at Location D. Differences in the placement of the two (2) injectors at Location A seemed to have little effect (i.e. injection into the outer two lanes between the superheater panels versus the inner two lanes). Injection at Location A was within the lanes between the superheater panels and once sorbent was injected within a lane little or no mixing occurred between material in adjacent lanes. Figure 6-56 shows again that SO_2 capture improved with increased sorbent injection velocity.

Figure 6-57 summarizes the SO_2 capture data obtained at Locations A and D with six (6) and eight (8) injectors and provides a comparison to Location D injection with four (4) injectors. At low injection velocities, (90 - 180 ft/sec), eight (8) injectors produced the highest SO_2 capture performance. Above 180 ft/sec, four (4) injectors produced the overall highest SO_2 capture. Six (6) injectors produced the poorest SO_2 capture and required high injection velocities.

Figure 6-57

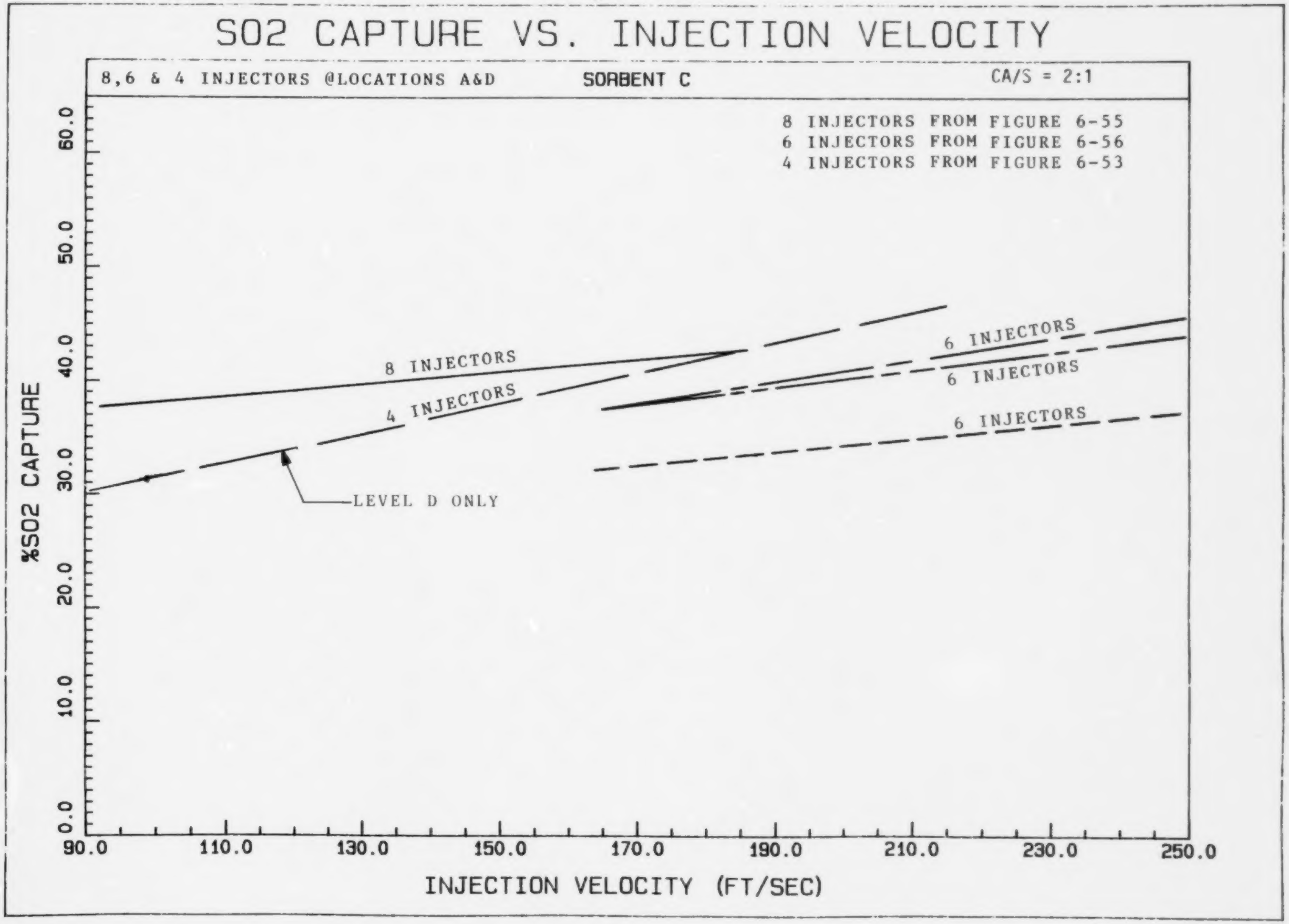
SO2 CAPTURE VS. INJECTION VELOCITY
8,6 & 4 INJECTORS @LOCATIONS A&D
SORBENT C
CA/S = 2:1
8 INJECTORS FROM FIGURE 6-55
6 INJECTORS FROM FIGURE 6-56
4 INJECTORS FROM FIGURE 6-53
8 INJECTORS
4 INJECTORS
6 INJECTORS
6 INJECTORS
6 INJECTORS
LEVEL D ONLY
%SO2 CAPTURE
0.0
10.0
20.0
30.0
40.0
50.0
60.0
90.0
110.0
130.0
150.0
170.0
190.0
210.0
230.0
250.0
INJECTION VELOCITY (FT/SEC)

6.7 SUMMARY OF COMBUSTION TEST RESULTS

The observations of the combustion test data are summarized as follows:

- Over one hundred and sixty (160) total tests were performed which include baseline conditions, sorbent injection over a range of Ca/S molar ratios, sorbent types, injector tilts, velocities, and locations, and repeat conditions.

- The BSF was found to be representative of a large utility boiler in terms of operation, volumetric heat release, gas time/temperature history, carbon burnout, and NO_x/SO_2 emissions.

- The BSF horizontal furnace outlet plane gas temperature (at the furnace arch) averaged 2200°F. The convective pass thermal quench rate was 500-600°F/sec.

- NO_x emissions ranged from 275 ppm to 375 ppm (corrected to 3% O_2), and increased with excess air. These emissions equal 0.30 to 0.40 lbs/MBtu. Minimization of NO_x emissions was beyond the scope of this investigation.

- Average baseline SO_2 emissions were 2150 ppm during Phase I and 2000 ppm during Phase II. This difference was due to fuel sulfur content.

- SO_2 capture varied with sorbent type. Typical SO_2 capture performance results at a calcium/sulfur molar ratio of 2:1 were as follows:

Sorbent A	25% - 30%
Sorbent B	30% - 40%
Sorbent C	35% - 50%

  Specific differences in the percent SO_2 capture performance for sorbents were:

Sorbent A vs. B:

Sorbent B was better than A in SO_2 capture by nine (9) to fifteen (15) percent (average of thirteen (13) percent).

Sorbent B vs. C:

Sorbent C was better than B in SO_2 capture by seven (7) to thirty (30) percent (average of eighteen (18) percent).

Sorbent A was untreated Black River hydrated lime, sorbent B was untreated Marblehead hydrated lime and sorbent C was treated Marblehead hydrated lime.

- The relative SO_2 capture performances of sorbents A, B, and C correlated with the sorbent particle sizing. Sorbent C was the finest and had the best SO_2 capture performance. Sorbent A was the coarsest and had the poorest SO_2 capture performance. The magnitude by which the performance of sorbent C exceeded sorbents A and B, suggests that lignosulfonate treatment may have enhanced SO_2 capture.

- Although most sorbent injection tests were run for a constant twenty (20) minute time interval, longer duration tests showed that SO_2 capture could be increased by 10 to 20 percent (or 4 to 10 percentage points) by extending the sorbent injection to one hour. This was due to deposition of reactive sorbent on heat transfer surfaces.

- With Sorbent C, SO_2 capture efficiency of up to 50% was obtained with a Ca/S molar ratio of 2:1 for selected test conditions.

- SO_2 capture was found to vary widely with the furnace gas temperature at the point of injection and with the sorbent jet penetration and dispersion characteristics observed in cold flow studies. These conditions were varied by the following sorbent injection parameters:

  - injection location
  - injection velocity
  - injector tilt
  - number of injectors
  - carrier air flowrate

- Optimum SO_2 capture efficiencies were obtained by a balance of appropriate furnace gas temperatures at the point of sorbent injection and mixing performance. Gas temperature had the dominant affect.

- Optimum SO_2 capture was obtained by injection into the region between Locations A and D where furnace gas temperatures ranged from 2250°F and 2350°F.

- Injection into the optimum region was accomplished by upward injection at Location D, or downward injection at Location A, and combinations thereof. Tilt, therefore, was demonstrated to be an effective approach to adjusting the effective location of sorbent injection for the purpose of optimizing SO_2 capture.

- At Location D, injection was into the swirling lower furnace flow field. Here increased injection velocity, by either injector nozzle diameter reduction or increased carrier air flow rate, improved SO_2 capture.

- Eight (8) sorbent injectors provided better SO_2 capture performance than four (4) injectors at lower injection velocities. The best SO_2 capture was, however, with four (4) injectors, although only at high injection velocities. Six (6) injectors produced poor SO_2 capture and required high injection velocities.

SECTION 7

SORBENT INJECTION SYSTEM DESIGN RECOMMENDATIONS

7.1 APPROACH

A procedure for designing sorbent injection system locations and injection methods for tangentially fired furnaces was developed by applying design guidelines, experimental methods, and computation methods described in Section 4, 5, and 6. The procedure involves a sequence of information collection, calculation, and experimental steps. In this procedure important design features of the specific application are identified including time/temperature profile, upper furnace geometry, and others. Several candidate injector designs are evaluated by an iterative process involving sorbent mixing performance evaluation and SO_2 capture performance evaluation. The primary method for evaluating sorbent mixing performance is cold-flow modeling using the methods described in Section 4. This physical modeling is supplemented by sorbent dispersion computation modeling to provide additional insight concerning the mixing process. Sulfur capture performance is calculated by the methods described in Section 5. By an iterative evaluation process optimized sorbent injector designs are recommended for both full-load and part-load operation of a specific tangentially fired utility unit. A step-by-step description of the sorbent injector design procedure is given in the next section.

7.2 DESCRIPTION OF THE DESIGN PROCEDURE

Step 1 - Establish Furnace Design and Operating Conditions

Specify and obtain the following data:

a. Name of the unit.

b. Maximum and minimum load.

c. Coal feed rate at maximum and minimum load.

d. Air flow rate at maximum and minimum load.

e. Coal ultimate, proximate, and ash elemental analyses.

f. Dimensioned side elevation drawing of the unit.

g. Time/temperature/furnace location data for the unit at maximum and minimum load.

Step 2 - Establish Sulfur Capture Performance Requirement and Sorbent Properties

Specify and obtain the following data:

a. Sulfur capture performance requirement.

b. Sorbent elemental analysis.

c. Sorbent particle size, porosity, and specific surface area.

d. Sulfur capture performance data for the design sorbent. The sulfur capture performance data may be available in several forms. The preferred form is SO_2 capture data vs. calcium/sulfur mole ratio for one or more quench rates obtained from a bench-scale or small pilot scale combustion test facility where the sorbent is well mixed at the beginning of the sulfur-capture window.

Step 3 - Establish Sorbent Injection Design Guidelines

Sorbent injection design guidelines were developed in Tasks A, B, and C and are detailed in Sections 4, 5, and 6 of this report. The most significant design guidelines for tangentially fired boilers are summarized here:

a. Effective mixing of sorbent can be obtained with injection through the front wall or with tangential injection.

b. Effective sorbent mixing can be obtained with pneumatic transport of sorbent with an airflow equal to five percent of the full-load furnace airflow. Greater airflow improved SO_2 capture for tangential injection. However, for commercial applications increased carrier airflow must be balanced against potential increase in overall furnace excess air.

c. Pneumatic sorbent injection counter to the furnace gas flow is more effective than injection in the same direction as the furnace gas flow.

d. When applied in combination with design guideline (b) above, an intermediate number of injector ports gives optimum mixing performance. For a fixed total injector air mass flow and injector air velocity, a fewer number of large size injectors gives deeper penetration of injection air and sorbent but a greater number of smaller injectors gives more complete dispersion. The optimum number of injectors for a particular furnace design can best be determined by a flow modeling study. This is discussed further below.

e. For injection through the front wall an intermediate injection air velocity is most effective. This velocity was 100 ft/sec at the BSF. The analogous velocity for commercial units can be calculated from scaling criteria given in Section 4.

f. For tangential injection, increasing velocity and carrier airflow both improved SO_2 capture. In commercial applications limitations on velocity and airflow will depend upon the constraints of the available air supply.

Step 4 - Establish Sorbent Injection Elevations

Several factors influence the selection of the sorbent injection elevations. The most important of these are the need to provide maximum residence time for sorbent mixing and chemical reaction and the need to avoid deactivation of sorbent. Excessively high gas temperature causes deactivation of the sorbent by sintering the porous reactive sites on and in the sorbent. Therefore, the optimum sorbent injection location is a balance between two conflicting requirements of a location lower in the furnace to maximize residence time and higher in the furnace to avoid excessively high gas temperature. Experience gained during Task C testing in the BSF has indicated that the optimum gas temperature at the injection location for tangentially fired furnaces with hydrated lime sorbent is between 2250 and 2350°F. The location corresponding to these temperatures is established by the time/temperature/furnace location data obtained in Step 1.

Normally, the optimum sorbent injection location will move down in the furnace at reduced load. Two methods for accommodating the part-load requirement are to provide a tilting mechanism so that the sorbent injection angle can be adjusted to follow load or to have multiple sorbent injection elevations. The preferred alternative depends upon the furnace turndown requirements, the degree to which the optimum location changes with load and the change in mixing effectiveness with changes in furnace load, injector location, and injector tilt.

In order to provide for part-load and full-load operation and to provide flexibility for optimization testing of candidate sorbent injection, several candidate sorbent injector elevations should be specified. Recommended elevations are those where the gas temperature is 2200, 2400, and 2600°F for full-load operation and where the gas temperature is 2200 °F at part load. Depending on the time/temperature profiles, the 2400 and 2600°F full-load locations may correspond to the 2200 and 2400°F part-load locations. If the locations do not work out in this way, design compromises should be specified based upon the full-load and part-load time/temperature profiles of the specific unit under study.

Other candidate sorbent injection designs will involve multiple levels of sorbent injectors. Since the same temperature zones are of interest for multiple levels of injectors as for a single level, the elevations selected above will also apply for multiple levels of injectors.

Step 5 - Select Sorbent Injector Peripheral Locations and Number of Injectors

The selection of injector locations for tangentially fired furnaces depends upon the specific furnace design. The presence or absence of the following furnace design features are particularly important for the selection of injector peripheral locations:

a. An arch (nose) separating the combustion zone from the superheater and reheater zones.

b. Top-supported heat transfer surface (panels) in units with an arch.

c. One to two foot deep superheater or reheater "minipanels" mounted from the front wall to the roof of units with an arch.

d. A center wall extending from the front wall to the rear wall in units either with or without an arch.

e. Separation between the front and rear pass sufficiently wide for installation of injectors on the rear corners or rear walls.

f. Other structural obstructions such as buckstays and gratings.

The optimum number of injector locations around the furnace periphery will be an intermediate number since too few a number of locations results in poor peripheral dispersion of sorbent and too large a number of injectors with a fixed carrier airflow results in inadequate penetration of the carrier air and sorbent into the furnace.

The design guidelines given in Step 3 indicate that effective sorbent mixing can be obtained in tangentially fired furnaces with injection either through the front wall or tangentially counter to the direction of the swirl of the gases in the furnace. As a further guideline, since the goal is uniform mixing, it is reasonable to position the injectors symmetrically if front-wall injection is used for a furnace without panels; and to position the injectors symmetrically between panels or between each second or third panel for a furnace with upper furnace panels.

By applying these guidelines, specify peripheral locations and the number of injectors for candidate sorbent injector designs. A dimensional sketch of injector locations is useful to identify the location of the injectors relative to other components of the furnace.

Step 6 - Specify Injector Size and Shape

In order to simplify engineering, construction, and operational considerations it is recommended that all injectors be of the same size. The total carrier air mass flow and carrier air velocity can be calculated from guidelines given in Step 3. The total number of injectors was specified in Step 5.

Two sorbent transport methods are under consideration for the Tangentially Fired LIMB Demonstration. In the first, the sorbent is picked up and transported from the sorbent feeder by the full flow of transport air. In the second the sorbent is transported from the sorbent feeder by a limited amount of transport air and the sorbent and transport air are mixed with the remainder of the sorbent carrier air at a location before the furnace. The selection between these systems has not yet been made. However, if the second method is used, the sorbent and transport air will be mixed with the remainder of the sorbent carrier air at a location where the sorbent and the total sorbent carrier air will be fully mixed before entering the furnace. Therefore, calculations specified below will be the same for either sorbent transport methods.

One final operating parameter, the carrier air temperature, must be specified. The furnace operates at essentially atmospheric pressure. After specifying the carrier air temperature, the carrier air density can be calculated by the gas law. After assembling these data, the area of each injector can be calculated by the following equation:

$$A = \frac{W}{\rho V n} \tag{7-1}$$

where A = area of each injector

W = total sorbent carrier air mass flow

ρ = sorbent carrier air density

V = carrier air velocity at the injector exit

n = number of injectors

After calculating the area of the injectors, the injector dimensions can be calculated when the shape is specified. Circular injectors were used in Tasks A and C. Square or rectangular injector ports may be used in utility units in order to satisfy injector tilt design requirements. Data reported by Sfeir (1976) and Krothapalli et al. (1981) shows that square and rectangular jets injected into a cross stream behave similar to circular jets of the same area at distances beyond eight (8) jet equivalent diamaters provided that the height to width ratio of a rectangle is between 0.7 to 1.4. Therefore, if the width of the nozzles is specified, the height can be calculated provided the height to width ratio is maintained within the above limits.

Higher or lower height to width aspect ratios may be specified to enhance dispersion. However, in this case jet penetration would be reduced.

Step 7 - Evaluate Mixing Performance of Candidate Injector Designs

Using the procedure outlined in Steps 4, 5 and 6 above, candidate sorbent injector designs, including injector elevation or elevations, number and size of injectors, peripheral locations, and carrier air operating condition, can be specified for the specific tangentially fired furnace application. If the application is similar to one where there is experience, eight to ten candidate designs should be considered. If the application is different from ones where there is experience, as many as twenty candidate designs should be used. Evaluate candidate designs by aerodynamic flow modeling using the methods described in Section 4. A scaled aerodynamic model should be constructed. Scale the injector geometry and sorbent carrier velocity for the model by methods described in Section 4. The test program should include velocity traversing to characterize the furnace aerodynamics, flow visualization, and detailed tracer concentration traversing for injector designs which show the best potential in the flow visualization tests. Conduct tests for conditions corresponding to both full-load and part-load operation.

Evaluate the results of the flow modeling tests to identify candidate designs which satisfy the sorbent mixing performance requirements. If none of the initial designs satisfy the mixing requirements, additional candidate designs should be selected. Steps 4, 5, and 6 should be repeated until two preliminary designs for full-load operation and two preliminary designs for part-load operation have been identified.

Step 8 - Calculate Estimated SO_2 Capture Performance

To evaluate the effectiveness of the injector designs identified in Step 7, estimate SO_2 capture performance for each candidate design using calculation methods described in Section 5. Estimate performance for a range of Ca/S molar ratios and for alternate sorbents if there is more than one sorbent of interest. Make SO_2 capture performance calculations for full-load and part-load furnace operation for candidate sorbent injector designs.

Step 9 - Finalize the Sorbent Injector Designs

Evaluate the results of the SO capture performance calculations. If the performance estimates satisfy the SO_2 capture performance requirements, the design procedure sequence is complete. If none of the designs satisfy the performance requirements, repeat Steps 4 through 8 until a satisfactory design or designs have been established.

7.3 SUMMARY

A procedure was described for specifying sorbent injection locations and methods for a full-scale demonstration of the sorbent injection process in a tangentially fired boiler. Mathematical modeling, design guidelines, and experimental verification gained within the program are applied in the sorbent injector design procedure. A step-by-step description of the procedure was given.

REFERENCES

Anderson, D. K., J. D. Bianca, and J. G. McGowan, "Recent Developments in the Physical Flow Modeling of Utility Scale Furnaces," paper presented at 1986 Joint Symposium Industrial Combustion Technologies, April 30, 1986, Chicago, Illinois.

Beer, J. M. and N. A. Chigier, Combustion Aerodynamics, John Wiley and Sons, Inc., New York 1972.

Beittel, R., S. J. Bortz, G. R. Offen, and D. C. Drehmel, "Effects of Injection Temperature and Quench Rate on Sorbent Utilization," Proc. 1986 Joint Symposium on Dry SO_2 and Simul. SO_2/NO_x Control Technol., Vol. 1, EPA-600/9-86-029a (NTIS No. PB87-120465), 19-1 (1986).

Boysan, F., W. H. Ayers, J. Swithenbank, and Z. Pan, "Three-Dimensional Model of Spray Combustion in Gas Turbine Combustors," J. Energy, Vol. 6, pp. 368-375, 1982.

Clark, J. P., A. Kokkinos, D. C. Borio, R. W. Koucky, and C. Y. Sun, "Boiler Design Criteria for Dry Sorbent SO_2 Control with Low-NO_x Burners," EPA-600/7-86-023 (NTIS PB 86-216-736) (1986).

Cole, J. A., J. C. Kramlich, W. R. Seeker, G. D. Silcox, G. H. Newton, D. J. Harrison, and D. W. Pershing, "Fundamental Studies of Sorbent Reactivity in Isothermal Reactors," Proc. 1986 Joint Symp. on Dry SO_2 and Simul. SO_2/NO_x Control Technol., Vol. 1, EPA-600/9-86-029a (NTIS No. PB87-120465), p. 16-1 (1986).

Collette, R. J., "1985 Update on NO_x Emission Control Technology at Combustion Engineering," Proc. 1985 Symposium on Stationary Combustion NO_x Control, Vol. 1, EPA-600/9-86-021a (NTIS No. PB86-225042), p. 9-1 (1986).

Feindel, R. and D. Gass, "Demonstration of Front End Alkali Injection and Combustion Modification Techniques at Boundary Dam G. S. Unit 4," Proc. 1986 Joint Symp. on Dry SO_2 and Simul. SO_2/NO_x Control Technol., Vol. 2, EPA-600/9-86-029b (NTIS No. PB87-120457), p. 46-1 (1986).

Gooch, J. P., E. B. Dismukes, R. Beittel, J. L. Thompson, and S. L. Rakes, "Sorbent Development and Production Studies," Proc. 1986 Joint Symp. on Dry SO_2 and Simul. SO_2/NO_x Control Technol., Vol. 1, EPA-600/9-86-029a (NTIS No. PB87-120465), p. 11-1 (1986).

Gullett, B. K. and J. C. Kramlich, "Fundamental Processes Involved in SO_2 Capture by Calcium-based Adsorbents," Proc. Fourth Annual Pittsburgh Coal Conference, p. 210 (1987).

Ivanov, Y.V., cited in Mohr, C.M., Incinerator Overfire Mixing Study, EPA APTD 1133 (NTIS PB210382), pp. IV-21, IV-25 through IV-31 (1972).

Kamotani, Y. and I. Greber, "Experiments on a Turbulent Jet in a Cross Flow," AIAA Journal, 10, No. 11, November 1972.

Kelly, J. T., et al., "Pilot Scale Development of a Low-NO_x Coal-Fired Tangential System," EPA-600/7-81-137 (NTIS PB81-242513), August 1981.

Kirchgessner, D. A., B. K. Gullett, and J. M. Lorrain," Physical Parameters Governing the Reactivity of $Ca(OH)_2$ with SO_2," Proc. 1986 Joint Symp. on Dry SO_2 and Simul. SO_2/NO_x Control Technol., Vol. 1, EPA-600/9-86-029a (NTIS No. PB87-120465), p. 8-1 (1986).

Kirchgessner, D. A. and J. M. Lorrain, "Lignosulfonate-Modified Calcium Hydroxide for Sulfur Dioxide Control," I. and E. C. Research, Vol. 26, p. 2397 (1987).

Kokkinos, A. and R. D. Lewis, "Field Evaluation of a Low-NO_x Firing System for Tangentially Coal-Fired Utility Boilers, EPA-600/7-85-018 (NTIS PB85-201093) (1985).

Koucky, R. W., D. K. Anderson, P. R. Thibeault, J. L. Marion, and C. C. Masser, "Sorbent Injector Design for Sulfur Oxides Control from Tangentially Fired Furnaces by Dry Sorbent Injection," Proc. 1986 Joint Symp. on Dry SO_2 and Simul. SO_2/NO_x Control Technol., Vol. 2, EPA-600/9-86-029b (NTIS No. PB87-120457), 23-1 (1986).

Krothapalli, A., D. Baganoff, and K. Karamcheti, "On the Mixing of a Rectangular Jet," J. Fluid Mech., Vol. 107, pp. 201-220 (1981).

Levy, J. M., J. H. Pohl, A. F. Sarofim, and Y. H. Song, "Combustion Research on the Fate of Fuel-Nitrogen under Conditions of Pulverized Coal Combustion," EPA-600/7-78-165 (NTIS PB286208) (1978).

Offen, G., "Status Report - Furnace Sorbent Injection," paper presented at 1985 ASME/IEEE Joint Power Generation Conference, Milwaukee, WI, October 23, 1985.

Overmoe, B. J., J. M. McCarthy, S. L. Chen, W. R. Seeker, and D. W. Pershing, "Reactivity Study of SO_2 Control with Atmospheric and Pressure Hydrated Sorbents," EPA-600/7-86-040 (NTIS No. PB87-129250) November 1986.

Patrick, M. A., "Experimental Investigation of Mixing and Flow in a Round Turbulent Jet Injected Perpendicularly into a Main Stream," J. Institute of Fuel, September 1967.

Rudinger, G., "Some Aspects of Gas-Particle Jets in a Cross Flow," ASME Paper 75-WA/HT-5, 1975.

Salzman, R. N. and S. H. Schwartz, "Experimental Study of Solid-Gas Jet Issuing into a Transverse Stream," J. of Fluids Engineering, 100, September 1978.

Sfeir, A. A., "The Velocity and Temperature Fields of Rectangular Jets," Int. J. Heat Mass Transfer, Vol. 19, pp. 1289-1297, (1976).

Shandorov, G. S., cited in Mohr, C. M., Incinerator Overfire Mixing Study, EPA APTD 1133 (NTIS PB210382), p. IV-21 (1972).

Singer, J. G., (Editor) Combustion Fossil Power Systems, Combustion Engineering, Inc., Windsor, CT, 1981.

Stern, R. D., "EPA's Program for Evaluation and Demonstration of Low-Cost Retrofit LIMB Technology," Proc. Fourth Annual Pittsburgh Coal Conference, p. 232 (1987).

Wendt, J. O. and O. E. Schulze, "On the Fate if Fuel Nitrogen During Coal Char Combustion," AIChE Journal, Vol. 22, 1976.

Zeldovich, Ya. B., P. Ya. Sadovnikov, and D. A. Frank-Kamenetskii, "Oxidation of Nitrogen in Combustion," Academy of Sciences of the USSR, Institute of Chemical Physics, Moscow - Leningrad, translated by M. Shelf, 1947, Scientific Research Staff, Ford Motor Co.

APPENDIX A

QUALITY ASSURANCE PROCEDURES

A.1 SUMMARY OF QUALITY ASSURANCE PROCEDURES

Quality assurance procedures for the program were conducted in accordance to EPA Air and Energy Engineering Research Laboratory (AEERL) Document (QA)-003/85, "AEERL Quality Assurance Procedures Manual for Contractors and Financial Assistance Recipients." The QA procedures conformed to a Category III program. The technical objectives of the program were to develop design criteria for injection of dry sorbents into tangentially fired furnaces for the control of sulfur oxides emissions. To achieve these objectives experimental testing was conducted in an aerodynamic cold-flow model and in a large Boiler Simulation Facility (BSF). Data acquisition throughout the program was of quality necessary to achieve the technical objectives of the program. There is no need to place any limitations or constraints on the use or applicability of the data in the report.

The original Quality Assurance Project Plan (QAPP) was transmitted to EPA on September 13, 1985. Conditional acceptance of the QAPP was received from the EPA on October 11, 1985 along with a request for certain additional information. This information was provided in an addendum transmittal to EPA on November 15, 1985. Final approval of the QAPP was received on December 10, 1985. No further changes were made to the QAPP. A detailed discussion of data quality is given in Section A.2.

An internal audit of the Boiler Simulation Facility (BSF) was conducted on April 7, 1987. The report of this internal audit and corrective action taken in response to the audit are documented in Section A.3. No external audits were conducted.

A.2 DISCUSSION OF DATA QUALITY

This section describes the routine quality assurance checks conducted during the tests performed in this research project and discusses the precision, accuracy, and completeness of the critical measurements made.

A.2.1 Continuous Gas Analysis

The continuous gas analyzers used in this project were:

CO_2 - Infrared Industries, Inc., Model 702D (method of analysis is by infrared absorption).

CO - Beckman, Model 864
(method of analysis is by infrared absorption).

O_2 - Teledyne Analytical Instruments, Model 326A
(method of analysis is by fuel cell).

NO_x - Thermo Electron, Series 10 Analyzer
(method of analysis is by electrical chemiluminescence)

SO_2 - DuPont Analytical Instrument, Inc.
Model 400 Photometric Analyzer
(method of analysis is by pulsed fluorescence).

All analyzers were calibrated several times a day during testing using compressed bottled calibration gases. The calibration gases used during the test program are listed in Table A-1. The best accuracy calibration gases available were obtained and used for this project. Procedures for instrument calibrations are discussed in detail in the Quality Assurance Project Plan (QAPP).

The precision and accuracy of each analyzer was determined by review of the analyzer strip chart records and the operator's log book which recorded the numerous daily calibrations performed during each test series. A record

TABLE A-1. CALIBRATION GASES

GAS (Grade)	TYPE	SUPPLIER	CYLINDER NO.	CONCENTRATION
NO-NO$_x$ (Certified)	2% of span	Matheson	AH043238	230 ppm
	2% of span	Matheson	11371	495 ppm
CO (Primary Standard)	5% of span (-)	Matheson	SX15685	92 ppm
	5% of span (±12 ppm)	Matheson	SX10596	298 ppm
CO$_2$ (Primary Standard)	1% of span (±.02%)	Matheson	AS10293	12.99%
	1% of span (-)	Matheson	WI35031	15.50%
O$_2$ (Primary Standard)	1% of span (±.02%)	Matheson	AH057010	2.29%
	1% of span (±.02%)	Matheson	73634	5.5%
	1% of span (±.02%)	Matheson	95931	5.0%
SO$_2$ (Certified)	2% of span (-)	Matheson	9725T	399 ppm
	2% of span (-)	Matheson	6643	955 ppm
	2% of span (±15 ppm)	Matheson	SX13954	1500 ppm
	2% of span (±20 ppm)	Matheson	SX10087	1996 ppm
Zero Air	-	Airco	H12599X	NA

Best available accuracy calibration gases were used. Primary standards for SO_2 and NO_x are not available.

of the calibration checks (i.e., calibration gas value vs. analyzer reading) prior to the zero and span adjustments for forty (40) cases yielded the following:

CO_2 analyzer:
accuracy +/- 0.58% of span
precision +/-2.15% of span
where, span = 13% CO_2 concentration calibration gas

CO analyzer:
accuracy +/-0.75% of span
precision +/-4.28% of span
where, span = 92 ppm CO concentration calibration gas

O_2 analyzer:
accuracy +/-0.07% of span
precision +/-2.44% of span
where, span = 5.5% O_2 concentration calibration gas

NO_x analyzer:
accuracy +/-0.58% of span
precision +/-2.80% of span
where, span = 495 ppm NO_x concentration calibration gas

SO_2 analyzer:
accuracy +/-0.11% of span
precision +/-1.75% of span
where, span = 1996 ppm SO_2 concentration calibration gas

Accuracy is defined as an average of calibration checks. Specifically:

$$\frac{\sum^{N} \frac{\text{Calibration Value - Actual Reading}}{\text{Calibration Value}} \times 100}{N}$$

where N = number of cases

Precision is defined by the standard deviation of calibration checks, specifically, the standard deviation for N measurements of:

((Calibration Value - Actual Reading)/Calibration Value) x 100

These accuracy and precision results are well within the QAPP objectives of +/-5% for each.

Most critical to this program was the determination of percent SO_2 capture by sorbent injection. This was calculated by three approaches: 1) by gas analysis measurements, 2) by mass balance of sulfur utilizing flyash samples, and, 3) by measurement of calcium utilization in flyash samples. These approaches were discussed in detail in Section 6.6.4.1 and will therefore not be repeated here, except to point out that independent measurement approaches correlated. Furthermore, an average of the value obtained by each method was determined for each test case and only the average value was used in plots presenting the effects of injector variables on SO_2 capture performance. Lastly, for most test cases, repeat tests were performed to verify repeatability and to improve measurement precision. By these steps (which included gas analysis calibrations already discussed) SO_2 capture efficiencies were determined as accurately as possible.

A.2.2 Laboratory Analyses

During this program laboratory analysis of coal, ash, and sorbent samples were performed primarily by ASTM procedures in C-E's KDL Analytical Laboratory. Accuracy and prevision of the measurements was established during analyses by daily laboratory calibration checks to standard reference materials and by submission of blind and split samples along with test samples by the KDL Project Manager. Daily calibration records are documented in laboratory log books maintained for each instrument and were audited by the C-E QA/QC Officer (see Section A.3). The results of blind standard reference samples are presented below. The standard reference materials (SRM) used in this program where:

For:	SRM Used
Proximate	1632B NBS
Ultimate	1632B NBS
HHV	1632B NBS
Size Distribution	<325 mesh (none available) >325 mesh (none available)
Ash	2689, 2690, 2691 NBS
Porosity	No Standard. Calibrate according to manufacturer.
Surface Area	Duke Scientific Alumina Standards #386, #389
Fusibility	No specific standard but use 1632 NBS for guide.

Comparison of blind sample analyses to these given by NBS for the SRM's for coal and ash composition are given in Table A-2 and for sorbent in Table A-3. Detailed analysis of ash constituents was beyond the needs of the test program although reported in Tables A-2 and A-3. Critical analyses were the ultimate for coal and flyash and the calcium content for flyash and sorbent. As can be seen good agreement between KDL laboratory analyses and NBS SRM's was obtained.

Ash fusibility precision data is shown in Table A-4. Although no NBS SRM exists for this analysis, C-E has established its own by use of NBS coal standard SRM #1632B.

Lastly, size distribution was measured and precision data of split samples is shown in Table A-5.

A.2.3 Aerodynamic Flow Modeling

During aerodynamic flow modeling, gas flow patterns and effectiveness of sorbent mixing were determined by a 5-hole pitot probe for velocity measurements and by a laser absorption spectrophotometer for methane tracer gas concentration distribution.

TABLE A-2. ANALYSES OF COAL AND ASH STANDARD REFERENCE MATERIALS

	CASE 1 3/30/87	CASE 2 4/13/87	AVERAGE	ACTUAL*
Proximate (wt. %):				
Moisture	0	0	0	0
Volatiles	36.0	37.1	36.6	35.4 ± 1.1
Fixed Carbon	57.3	56.1	56.7	**
Ash	6.7	6.8	6.75	6.79 ± 0.16
Total	100.0	100.0	-	**
HHV (Btu/lb):	13,890	13,845	13,868	14,005 ± 35
Ultimate (wt. %):				
Moisture	0	0	0	0
Hydrogen	5.2	5.2	5.2	5.07 ± 0.06
Carbon	78.6	78.6	78.6	78.11 ± 0.37
Sulfur	1.9	2.0	1.95	1.89 ± 0.06
Nitrogen	1.6	1.6	1.6	1.56 ± 0.07
Oxygen	6.0	5.8	5.9	**
Ash	6.7	6.8	6.75	6.79 ± 0.16
Total	100.0	100.0	-	
Ash Composition: (wt. % total sample)				
Silicon	3.12	3.20	3.16	3.00 ± 0.00
Aluminum	1.62	1.69	1.66	1.62 ± 0.04
Iron	1.11	1.11	1.11	1.09 ± 0.01
Calcium	0.26	0.24	0.25	0.29 ± 0.06
Magnesium	0.07	0.07	0.07	0.06 ± 0.005
Sodium	0.07	0.06	0.065	0.07 ± 0.085
Potassium	0.09	0.09	0.09	0.07 ± 0.005
Titanium	0.08	0.06	0.07	0.08 ± 0.005

(*) NBS SRM 16326

(**) Not determined by NBS

TABLE A-3. ANALYSES OF SORBENT STANDARD REFERENCE MATERIALS

	CASE 1 3/18/87	CASE 2 4/15/87	ACTUAL*
Silica (SiO_2)	5.3	-	4.92
Alumina (Al_2O_3)	1.2	-	1.12
Iron (Fe_2O_3)	0.6	-	0.75
Titania (TiO_2)	Trace	-	0.05
Manganese (MnO)	0.3	-	0.20
Calcium (CaO)	50.8	50.8	50.9
Strontium (SrO)	-	-	0.14
Magnesium (MgO)	0.3	0.2	0.36
Potassium (K_2O)	0.2	-	0.25
Phosphorus (P_2O_5)	-	-	0.08
Carbonate (CO_2)	-	-	40.4
Loss on ignition	37.1	-	41.1

(*) NBS SRM 16 Argillaceous limestone

TABLE A-4. ASH FUSIBILITY PRECISION DATA

NBS 1632 B COAL

ASHED ACCORDING TO ASTM D1857

PRECISION DATA (REDUCING ATMOSPHERE)

	---- RUN #1 ----		----RUN #2 ----	
	DAY 1	DAY 2	DAY 1	DAY 2
I.T., °F	1980	1980	1970	1970
S.T.	2140	2150	2130	2140
H.T.	2340	2340	2340	2340
F.T.	2380	2370	2380	2370

TABLE A-5. COAL SIEVING PRECISION EXAMPLE

KDL Sample No. 7-3059-C
EPA LIMB Test 7/17/86

Size	+16	+30	+50	+100	+200	+325	325x0
Amt.	Trace	.03	.21	1.76	5.91	6.77	35.32
%	Trace	.1	.4	3.5	11.8	13.5	70.7
Size	+16	+30	+50	+100	+200	+325	325x0
Amt.	Trace	.02	.14	1.69	5.96	6.79	35.40
%	Trace	Trace	.3	3.4	11.9	13.6	70.80
Size	+16	+30	+50	+100	+200	+325	325x0
Amt.	Trace	.02	.16	1.70	5.95	6.88	35.29
%	Trace	Trace	.3	3.4	11.9	13.8	70.6
Size	+16	+30	+50	+100	+200	+325	325x0
Amt.	Trace	.01	.14	1.71	5.97	6.86	35.31
%	Trace	Trace	.3	3.4	11.9	13.7	70.7
Ave. %	Trace	Trace	.33	3.43	11.88	13.65	70.70
Std. Diff.	0	0	.05	0.05	0.05	0.13	0.08

The equipment was calibrated before and routinely during each set of experiments. The results of an analysis of calibrations of the 5-hole pitot probe are as follows. Critical components of this system are a probe tip (calibrated by the manufacturer and prior to testing) and electronic manometers which measure specific pressures at the five holes on the pitot probe. Calibration of the manometers is required since these have the potential to drift in time. The probe itself is less critical because it can only go out of calibration if physically and visibly damaged. Ten manometer calibrations were performed with the following results:

Average of ((calibration - actual)/calibration) x 100 = +/-0.52%
Standard deviation of the same = +/-1.56%.

These results have a direct relationship to the accuracy and precision of velocity measurements and are well within the QAPP objective of +/-10%.

Methane concentration was also part of the aerodynamic measurements made during this program. This was determined by sampling within the flow model and by continuous measurement of the sample's methane gas concentration by a laser absorption spectrophotometer. This instrument, like the continuous gas analyzers used during combustion testing, was calibration checked both before and during testing by bottled calibration gases in the same range as that measured in testing. A Matheson certified calibration gas was utilized (947 ppm - Cylinder No. AS-10778). Analysis of seventeen (17) calibration cases yielded the following:

Average of ((calibration - actual)/calibration) x 100 = +/-1.1%
Standard deviation of same = +/-2.0%.

These measures of the accuracy and precision of the methane concentration calibrations are well within the QAPP objectives of +/-5% for each.

A.3 AUDITS AND CORRECTIVE ACTION

A technical system audit was conducted to evaluate the entire measuring system including record keeping, data handling, and lab analysis. The audit was performed on April 7, 1987 by P. Gingras, QA officer at the time of the audit. The audit reviewed the data collection techniques, instrumentation calibration and control, and the data acquisition logs. The following is a chronology of audit events conducted to support the objectives of the QA/QC plan.

The technical system audit checklist (Attachment 1) was used to audit the measuring systems. The following systems were reviewed: (1) Gas Analysis System, (2) Sampling System, (3) Conditioning System, (4) EPA-5 Sampling Train, (5) Sampling Collection, (6) Laboratory Sampling and Custody Procedures, (7) Analytical Lab, (8) Data Acquisition and Reduction, (9) Records and Miscellaneous Measuring Equipment.

The Corrective Action Report (Attachment 2) documents the areas of nonconformances. The area of nonconformance relates to the calibration control system.

The response by the Task Leader, J. Marion, to the Corrective Action Report is given in Attachment 3. The response details the specific corrective actions required to comply with the overall QA/QC project plan.

The follow-up to the System Audit to verify the implementation of the corrective action is given in Attachment 4. This review includes the verification of effective corrective action to the specified nonconformances. The final conclusion of the audit was that all nonconformances initially identified were effectively closed out and satisfactorily comply with the QA/QC plan.

ATTACHMENT 1

M. R. Gogineni
cc: R. W. Koucky
J. Marion

PAGE 1 OF 5

Date: 4-7-87

Prepared by: P.J. Gingras

TECHNICAL SYSTEMS AUDIT CHECKLIST
EPA CONTRACT NO. 68-02-12985

Scope: QA Project Plan - CE Contract No. 12985 & Addendum

1. Gas Analysis System

   a. Verify Configuration Figure 3.1.2

   The Gas Analysis System configuration is in accordance with figure 3.1.2.

   b. Verify Calibration of system in accordance with Para. 4.1.8.

   The system was calibrated in accordance with Para. 4.1.8. Reviewed Pre-Test Inspection Record dated 3/10/87. The inspection/calibration were performed by Gregg Cartier and accepted by J. Marion 4/6/87 and W. R. Hocking 3/11/87.

   c. Is the calibration procedure & checklist Appendix A available and in use?

   The calibration procedure and prepared checklist are available and in use.

   d. Are zero-span calibration checks documented on chart recordings?

   The zero-span calibration checks are noted in the checklist page 6 and on the strip chart recordings.

   e. Verify certification of gases: 1%, 2%

   All calibration gases are purchased from Matheson and are certified within the required limits. The certification of gases was verified by review of actual certification certificates or bottle tags. Verified: O_2 73634, AH057010. CO_2 - AS10293. SO_2 6643, 9725T. SO_2 SX 10087 and SX 13954 purchased on P.O. 1572345 1996 PPM +/- 20 PPM, and 1500 PPM respectively. No Nox S/N 11371 and AN043238.

2. Sampling System

   a. Verify configuration Figure 3.1.3.

      The Sampling System Configuration is in accordance with Figure 3.1.3.

   b. Verify calibration/function of temperature monitor and T.C.'s.

      The temperature monitor is tied into the computer system and is utilized as a process control indication only.

3. Conditioning System

   a. Verify configuration Figure 3.1.4.

      The Conditioning System Configuration is in accordance the Figure 3.1.4.

   b. Verify calibration of T.C.'s & instruments.

      The temperature devices in this system are tied into the computer system and are utilized as a process control indication only.

4. EPA-5 Sampling Train

   a. Verify configuration Figure 3.2.1.

      Unable to verify configuration during the audit as it had already been disassembled.

   b. Verify instrument & T.C. calibration.

      Verified calibration of Wet Test Meter: (Pre-Test) 3/12/87 by YUL, and (Post-Test) 3/19/87 YUL, Flowmeters #1 & #2 3/17/87. Corrected Flow Data for Meters #1 & #2 by WTM.

   c. Is the sampling procedure available and in use?

      The sampling procedure was available and in use. (Project Plan)

   d. Are field data sheets properly completed?

      The Field Data Sheets were properly completed. Reviewed sheets dated 3/18/87. Data was recorded approximately every 5 minutes.

4. EPA-5 Sampling Train (Con't)

e. Verify calibrations: Para. 3.2.5

Gas Meter ✓ Probe Nozzle ✓

Orifice ✓ Gas Meter Thermometers 3% ✓

Stack T.C. (1.5%) / Barometer ✓

Analytical Balance

O.K. Calibration by Northeast Balance Service 3/87 due 3/88. Calibration records were not available for review.

5. Sample Collection Para. 3.2.4

a. Verify sample identification: Test #, Date, Container #.

Verified identification of test samples in the analytical laboratory. The samples were identified by: KDL No. 7-1795-A, dated 3/19/87, time: 0600 sample point 13B, and KDL No. 7/1788-A, dated 3/18/87, time: 5:45 sample point 21A.

b. Is required data documented: Forms Fig. 3.2.3

The sample data was properly documented. Reviewed Field Data Sheets dated 3/18/87 and particulate sampling data sheet for Impinger Sets 1 & 2 and 3 & 4 dated 3/18/87.

6. Laboratory Sampling & Custody Procedures - Para. 3.4

a. Verify sample identification

Verified sample identification labels KDL No. 7/1785A., 13B. No. 7/1772C 21A, and No. 7-1775-C-1E.

b. Check KDL Log

Reviewed KDL Log. The log documented sample No. 7-1788 Proj. 900044 - Test No. 21A - Fly Ash sample and analysis requirements.

c. Are analytical request forms in use?

The analytical request forms were in use and properly filled out. Reviewed forms for test samples 6E, 1F, and 1E.

d. Are Lab. analysis report forms in use?

There were no lab analysis reports completed at the time of this audit. The forms were readily available for use.

e. Are blind/split samples submitted in accordance with Table -A1?.

Both blind and split samples were submitted for analysis. Reviewed the Project Manager's Log for blind sample KDL No. 7-1775C Test 1E (coal) sample #4, and split sample Test No's 21A and 21B.

7. Analytical Lab.

a. Verify calibration records for instruments in use (weekly).

Reviewed calibration notebooks for Leco Sulfur analyzer 1R33, and Leco CHN-600 and Perkin Elmer Carbon/Hydrogen/Nitrogen analyzers. The calibrations are performed utilizing NBS Standards and are usually checked on a daily basis.

b. Verify calibration procedures are available and in use.

ASTM/Manufacturers calibration and test procedures are readily available and in use.

c. Are analysis procedures in the immediate area?

Analysis procedures are available in the test areas.

8. Data Acquisition & Reduction

Reviewed particulate EPA method 5 data FM/system dated 4/1/87. Reviewed Baseline Test 1A data acquisition record dated 3/18.

9. Records

Records such as Test Logs, Laboratory Logs, Test Records, and Lab Reports were readily available for review and appear to be properly maintained by responsible personnel.

EQUIPMENT CALIBRATION

Miscellaneous:

1. Optical Pyrometer

   INST No. G-166 calibrated to gold wire std. monthly or as required. No record of calibration. —

2. Pitot Tube ✓

   Computerized calibration record B-1884-2 checked 3/3/86 and B-1996 checked 3/4/86.

3. Pressure Sensing System (Monthly) ✓

4. Manometer ✓

   Calibrated 2/26/87.

5. Diff. System Calibration (Precision D.C. Supply)

   Not readily available for review. —

6. Type 1015 Elec. Manometer

   Barocells calibrated 3/3/86.

Laboratory:

1. Teledyne Anal. Inst.-Model 326 CO
2. Beckman Model 864 (CO)
3. Infrared Ind. IR-702 (FPTF)
4. Dupont Model 400 (SO)
5. Thermo Electron Corp. (SO)

Test-Set-Up. Calibrated prior to test and during test as required.

General Comments:

The Technical Systems Audit was performed at KDL with the assistance of John Marion - Project Manager. there were no significant problems associated with the overall test program. The system for calibration of test equipment and associated records was found to be deficient in several areas and will require immediate Corrective Action. Reference CAR: KDL-EPA-001. *

Paul J. Gingras

P. J. Gingras
Q.A. Office

PJG:wr
(PJG001)

ATTACHMENT 2

COMBUSTION ENGINEERING

CORRECTIVE ACTION REPORT

cc: M.R. Gogineni
R.W. Koucky

CAR NO. KDL-EPA-001
DATE 4-13-87
*PAGE 1 OF 2

TO: J. Marion, Project Manager KDL Lab CEP 9005-0301	PO/MO/PSSPO CONTRACT 12985
FROM: P.J. Gingras, Q.A. Officer EPA Contract CEP 5072-EG06	OTHER: EPA-68-02-4224

Referenced document(s): Q.A. Project Plan, CE Contract 12985

Description of nonconformances: See attached.

Reported by P.J. Gingras

Title Q.A. Officer Date 4/13/87

This report requires prompt corrective action to resolve the nonconformance and to prevent recurrence. Please respond to the following questions and return to sender by 5/13/87

1. Action taken to resolve nonconformance
2. Action taken to prevent recurrence
3. Scheduled completion date ______ Signature ______

Title ______ Date ______

For GQA Department Use Only

Corrective Action Approved ☐ Disapproved ☐

Verification Follow-up Action Required Yes ☐ No ☐ (Explain)

COMMENTS:

GQA Representative Signature ______ Date ______

Closeout By ______ Date ______

*Use continuation sheet(s), if required

C-E 0012064 (Rev. 5/86)

During the Systems Audit performed at the KDL Labs, several nonconformances were noted in regard to the Calibration Control System which requires corrective action:

Analytical Lab:

1. Balances are calibrated and stickered but no documentation was in house from Northeast Balance Service to verify standards used or provide traceability to NBS.

2. EDTA Standard from LECO-1087-101. No Certification.

3. 100 MG Weight - No certification or Calibration Record.

Test Equipment:

1. Thermocouples, when required, should be calibrated within the temperature range of desired usage.

2. Measuring Instruments which impact on the quality of test data must be under calibration control.

Recommendations for Corrective Action:

1. Please review the Quality Plan and provide a listing of test and measuring devices which directly effect the quality of the data, and those devices which are essentially for system control/reference only.

2. Test and Measuring Equipment under Calibration Control should be identified with a calibration sticker or tag which is directly traceable to the Calibration Record Card or Certification.

3. Calibration records should address:

   (a) The Calibration Date - Due Date.
   (b) The standards used to perform the calibration.
   (c) The procedure used to perform the calibration.
   (d) The identify of the person who performed the calibration.

4. Calibration records must provide traceability to National Bureau of Standards, when possible.

PJG/sk
(CAR.txt)

Interoffice Correspondence

ATTACHMENT 3

MBUSTION ENGINEERING

TO: ✓ P.J. Gingras
QA/QC Officer
5072-EG06

DATE: June 18, 1987

FROM: J.L. Marion

CC: Distribution

LOCATION: KDL 9005-0301
Windsor
FS-87-67

SUBJECT: EPA 'T'-Fired LIMB Project
QA/QC Corrective Action Report

During your systems audit of KDL for Contract 12985, you identified several items requiring corrective action and documented these for M.R. Gogineni per our QA/QC project plan (Attachment A). Corrective action has been and is being taken on these items as detailed on the following pages. We are scheduled to run a final week of testing the week of July 12-18, 1987. Please let me know if there are any other steps required to comply with the QA/QC Project Plan than those discussed here.

John L. Marion
J.L. Marion

nfp

attachment

A) Analytical Lab

A.1. "Balances are calibrated and stickered but no documentation was in-house from Northeast Balance Service to verify standards used or (to) provide traceability to NBS (National Bureau of Standards)."

Documentation from Northeast Balance Service has been requested. Also, a set of NBS standard weights has been ordered.

A.2. "EDTA standard from LECO-1087-101. No Certification."

This is a calibration standard provided by LECO for C, H, N analysis and is not certified even by LECO when requested. NBS traceable standards from another source are being obtained to replace the LECO standards for future calibrations. NBS traceable coal samples are available in the Analytical Lab which are also used to verify the LECO Analyzer's accuracy with NBS traceability.

A.3. "100 MG Weight - No Certification or Calibration Record."

Please refer to reply on action item A.1.

B) Test Equipment

B.1. "Thermocouples, when required, should be calibrated within the temperature range of desired usage."

Agreed. This point refers to furnace stack temperature measurement required as part of EPA Method 5 Stack Sampling. This Tc was calibrated at and below temperatures of 212°F while its application is at temperatures exceeding 1000°F. KDL does not have equipment to calibrate Tc's at these high temperatures and therefore it requires an outside contract. Since EPA Method 5 Sampling will not be performed in the next and final week of testing on this project, no action will be taken to correct this item at this time.

B.2. "Measuring instruments which impact on the quality of test data must be calibration control"

We have made a concerted effort to calibrate all test instrumentation. Attachment B is a partial list of some sixty instruments calibrated before Phase I testing. However, instruments which must contractually be under calibration control are only those that affect the critical test measurements specified in Table 2 of our QA/QC project plan (Attachment C).

The following is a listing (in order) of measuring devices which directly affect the quality of the critical measurements outlined in Table 2 (Attachment C):

i. Gas Analysis System: O_2, CO, CO_2, SO_2, NO_x from BSF and FPTF

The gas analysis system (G.A.S.) for both the BSF and FPTF facilities is detailed in the QA/QC Plan. Please note, however, that the FPTF facility was an option to this contract which was not exercised, therefore references to FPTF equipment are not applicable.

The G.A.S. simplistically consists of a sample probe, a sample line, a conditioning system (dryer), and separate analyzers for each gas species measured. Each analyzer is calibrated with a certified calibration gas between every test. All other instrumentation (i.e., temperatures and pressures) in the G.A.S. are process-related. None of these readings is used in the determination of gas concentrations. Should these be grossly inaccurate they would affect the readings. However, analysis of results to date shows excellent agreement between gas analysis data and other operations data including stack solids analysis. Therefore no action will be taken to calibrate these instruments on this project.

ii. Particulate Sampling (EPA Method 5)

The following measurements have a direct impact on the quality of the data obtained with EPA Method 5:

a)	Stack temperature	calibrated 3/13/87
b)	Dry gas volumetric meter	calibrated 3/13/87
c)	Gas meter inlet temperature	not accessible
d)	Gas meter outlet temperature	not accessible
e)	Sample and moisture weights	Analytical Lab measurement-See A.1.

The following measurements do not have a direct impact on the quality of the data on this project:

a) Stack static pressure
b) Stack velocity pressure
c) Oven temperature
d) Probe temperature
e) Impinger outlet temperature
f) Orifice static pressure
g) Orifice delta pressure
h) System vacuum

As a step to reduce program costs, no Method 5 Sampling was performed during the previous test run, nor will any further Method 5 Sampling be performed on this project. Therefore, no action will be taken on these measurements.

iii. Analytical Lab (Ash Analysis, HHV, Size Distribution, Porosity, Surface Area, Ash Fusibility)

No action has been taken to identify secondary measurements which affect the quality of data in the Analytical Laboratory. The Analytical Lab uses NBS traceable standards for equipment calibration. Corrective actions on one of these standards and on analytical balances connected with these analyses are in progress as specified in reply A.1., A.2., and A.3.

iv. Methane Concentration and Velocity

No action has been taken on these measurements because they were required under Task A only, which was completed in 1986.

Interoffice Correspondence

ATTACHMENT 4

COMBUSTION ENGINEERING

J. Marion

cc: M.R. Goginini
R.W. Koucky

October 23, 1987

From: P.J. Gingras

Location: GQS 9374-EG06

Subject: Follow-up to Systems Audit Finding to verify implementation of corrective action.

Reference: EPA Contract No. 12985
Technical Systems Audit dated 4/7/87
Corrective Action Report No. KDL-EPA-001

A follow-up meeting was held with J. Marion-KDL Project Manager on October 22, 1987 to verify implementation of the corrective actions taken to correct the deficiencies noted during the Systems Audit.

During the meeting, a review was made of calibration records. Certifications for balances, gases, and secondary standards were on file and provided direct traceability to NBS.

As a result of this follow-up activity the referenced Corrective Action Report is considered to be closed.

Attached is a copy of the closed-out Corrective Action Report for your records.

I would like to thank both yourself and KDL personnel for the full cooperation received in corrected the system nonconformance.

Very truly yours,

Paul J. Gingras

P.J. Gingras
Q.A. Officer

PJG/st

COMBUSTION ENGINEERING

CORRECTIVE ACTION REPORT

cc: M.R. Gogineni
R.W. Koucky

CAR NO. KDL-EPA-001
DATE 4-13-87
*PAGE 1 OF 2

TO: J. Marion, Project Manager KDL Lab CEP 9005-0301	PO/MO/PSSPO CONTRACT 12985
FROM: P.J. Gingras, Q.A. Officer EPA Contract CEP 5072-EG06	OTHER: EPA-68-02-4224

Referenced document(s): Q.A. Project Plan, CE Contract 12985

Description of nonconformances: See attached.

Reported by P.J. Gingras
Title Q.A. Officer Date 4/13/87

This report requires prompt corrective action to resolve the nonconformance and to prevent recurrence. Please respond to the following questions and return to sender by 5/13/87

1. Action taken to resolve nonconformance : see attachments
2. Action taken to prevent recurrence : see attachments
3. Scheduled completion date 7/10/87 Signature John J. Marion

Title Sr. R&D Engineer (KDL Project Manager) Date 6/18/87

For GQA Department Use Only

Corrective Action Approved ☒ Disapproved ☐

Verification Follow-up Action Required Yes ☒ No ☐ (Explain)

COMMENTS: VERIFICATION FOLLOW-UP COMPLETED 10/22/87
REVIEWED CERTIFICATIONS FROM NORTHEAST BALANCE SERVICE DATED 3/27/87 AND 6/23/87. REVIEWED CERTIFICATIONS FROM MATHESON FOR CERTIFIED GASES, REVIEWED CERTIFICATION FROM GE DATED 8/13/86 FOR L&N RESISTOR BRIDGE.

GQA Representative Signature Paul J. Gingras Date 6/23/87

Closeout By Paul J. Gingras Date 10/22/87

*Use continuation sheet(s), if required

C-E 0012064 (Rev. 5/86)

During the Systems Audit performed at the KDL Labs, several nonconformances were noted in regard to the Calibration Control System which requires corrective action:

Analytical Lab:

1. Balances are calibrated and stickered but no documentation was in house from Northeast Balance Service to verify standards used or provide traceability to NBS.

2. EDTA Standard from LECO-1087-101. No Certification.

3. 100 MG Weight - No certification or Calibration Record.

Test Equipment:

1. Thermocouples, when required, should be calibrated within the temperature range of desired usage.

2. Measuring Instruments which impact on the quality of test data must be under calibration control.

Recommendations for Corrective Action:

1. Please review the Quality Plan and provide a listing of test and measuring devices which directly effect the quality of the data, and those devices which are essentially for system control/reference only.

2. Test and Measuring Equipment under Calibration Control should be identified with a calibration sticker or tag which is directly traceable to the Calibration Record Card or Certification.

3. Calibration records should address:

   (a) The Calibration Date - Due Date.
   (b) The standards used to perform the calibration.
   (c) The procedure used to perform the calibration.
   (d) The identify of ther person who performed the calibration.

4. Calibration records must provide traceability to National Bureau of Standards, when possible.

PJG/sk
(CAR.txt)